

Co-located with SPIE Security+Defence 2011

Technical Summaries

www.spie.org/ers

Conference Dates: 19-22 September 2011

Clarion Congress Hotel Prague Prague, Czech Republic

Connecting minds for global solutions

Contents

8174:	Remote Sensing for Agriculture, Ecosystems, and Hydrology2
8175:	Remote Sensing of the Ocean, Sea Ice, Coastal Waters, and Large Water Regions 2011
8176:	Sensors, Systems, and Next-Generation Satellites 55
8177:	Remote Sensing of Clouds and the Atmosphere 76
8178:	Optics in Atmospheric Propagation and Adaptive Systems
8179:	SAR Image Analysis, Modeling, and Techniques 96
8180:	Image and Signal Processing for Remote Sensing 113
8181:	Earth Resources and Environmental Remote Sensing/ GIS Applications
8182:	Lidar Technologies, Techniques, and Measurements for Atmospheric Remote Sensing
8183:	High-Performance Computing in Remote Sensing 170





Virgo

Monday-Wednesday 19-21 September 2011 Part of Proceedings of SPIE Vol. 8174 Remote Sensing for Agriculture, Ecosystems, and Hydrology XIII

8174-01, Session 1

Remote sensing of snow cover and snow water equivalent for the historic snowstorms in the Baltimore/Washington area during February 2010

J. L. Foster, D. K. Hall, G. A. Riggs, NASA Goddard Space Flight Ctr. (United States)

In February 2010, snowfall totals from two powerful east coast storms along the U.S. Atlantic seaboard approached 2 m. In this study, remotely sensed observations of snow depth and snow water equivalent (SWE) were examined during the snowfall events and throughout the period of time that snow remained covering the ground. The purpose of this paper is to determine the utility of passive microwave satellite sensors in making SWE measurements during (and following) major snowstorms over the relatively challenging Chesapeake Bay area; where snowfall often mixes with rain, snow cover is generally patchy and a true multi-layered snowpack is rarely established. The Advanced Microwave Scanning Radiometer (AMSR-E) onboard the Aqua satellite was used to assess snow water equivalent (SWE) and the Moderate Resolution Imaging Spectroradiometer (MODIS) sensor aboard the Terra satellite was employed to validate the snow cover extend derived from AMSR-E.

Though substantial snow depth and SWE were retrieved in the February storms, the algorithm performance was uneven due to the high variability of snowfall accumulation as well as to the complex surface features in the Baltimore/Washington area. In general, the AMSR-E algorithm we employed somewhat underestimated snow depth and SWE. On the two days having extremely heavy snowfalls (snow falling in temperatures not far from 0° C and at rates > 2.5 cm/ hour), February 6 and 10, SWE from AMSR-E was not retrieved. SWE retrievals from the AMSR-E measurements (algorithm) on February 6, near 0740 UTC, and on February 10, near 0716 UTC,) apparently failed during the passage of the snow storms because of the presence of liquid water within the storm clouds. On the days following these storms, icy surfaces within and on top of the snowpack resulted in an overestimation of SWE in southern portions of the study area, early in the month, and in northern portions of the study area later in the month.

This work has utility in the build-up to NASA's Global Precipitation Mission (GPM) and the European Space Agency (ESA CoREH20 Mission.

8174-02, Session 1

Snow evolution in Sierra Nevada (Spain) from an energy balance model validated with Landsat TM data

J. Herrero, Univ. de Granada (Spain); M. J. Polo, Univ. de Córdoba (Spain)

Sierra Nevada Mountains are the highest continental altitude in Spain. Located in the South, facing the Mediterranean Sea in less than 40 km distance, the high level of solar energy income along the year together with the extremely variable character of climate in such latitudes, make it necessary to use energy balance approaches to characterize the snow cover evolution. Wind and relative humidity becomes decisive factors in the evolution of the snow cover due to the high evaporation rates that can arise under favorable meteorological conditions. This work presents the enhanced capability of the combination of Landsat TM data with the simulation with an energy balance model to produce sequences of hourly high resolution maps of snow cover and depth distribution under variable meteorological conditions such as those found in Mediterranean mountainous watersheds. Despite the good agreement found between observed and predicted snow pixels, different examples of disagreement arose in the boundaries, most of them related to the temperature spatial pattern simulation together with the discrimination between rain and snowfall occurrence.

8174-03, Session 1

Characterization of snow pack over Pyrenees using remote sensed data for runoff modeling

L. Moreno, A. Reppucci, X. Banque, Starlab (Spain); M. J. Escorihuela, isardSAT (Spain); M. Aran, Applus Agroambiental, S.A. (Spain); R. Sanchez Diezma, HYDS (Spain)

Characterization of snow pack evolution is a key parameter for regions where water supply is mainly due to snow melt and runoff.

Main goal of the project "AGORA", partially founded by the Catalan government, is to study the impact of assimilating earth observed data in a water prediction numerical model. The site chosen for the study cover the Pyrenees area in Catalonia.

As first step an observation of the water balance terms, such as snow cover, snow water equivalent, changes in soil water content, have been done through extensive in situ campaigns in the area of study.

Collocated earth observed data from both passive, e.g. MERIS, MODIS, and active, e.g. ENVISAT-ASAR, ENVISAT-RA, sensors have been collected during the surveys. These measurements will be used to develop and validate algorithms for the characterization of the snow pack appropriately tuned for the area of interest.

The final phase of the project will evaluate the impact of assimilating remote sensing data into an hydrological model developed to cope with the significant weather changes in time and space in the area of study.

Preliminary results of the activity scheduled during the first year of the project will be highlighted. The importance of developing application based on remote sensed and in situ data will be discussed.

8174-04, Session 2

Local effects on the water balance in flood plains induced by dam filling in Mediterranean environments

C. Aguilar, M. J. Polo, Univ. de Córdoba (Spain)

Mediterranean mountainous watersheds present several unique aspects that influence dominant hydrological processes. The combination of flash floods and processes characterizing dry periods determine to a great extent the evolution of water flows. Urban development and the proliferation of intensive and irrigated subtropical agricultural products in the last years have led to high demands of water resources in the area. In these situations dams constitute the solution in order to guarantee water supply and control flash floods. Dams are known to modify in space and time the natural regimen of natural biogeochemical flows. However up to now, little has been said about the possible local effects on the ecosystem along the river banks upstream the dam.



In the Guadalfeo river watershed, southern Spain, elevations range from 3480 m to sea level in 70 km length in a 1300 km² area. The combination of such altitudinal gradients together with the large number of vegetation, landforms and soil types produces a complex mountainous territory with variable hydrological behaviour. In 2002, Rules dam started to function as a flood control structure and water supply for the coast. This work presents the effects of the dam filling on the water balance in flood plains. Thus, the influence of the enhanced soil moisture in the surroundings of the free surface of the reservoir on the vegetation cover status was analyzed and related to meteorological agents and topographic features, before and after the construction of the dam. To this purpose, meteorological, topographic, soil and land use data were collected and analyzed in the contributing area of the dam, together with Landsat TM images during the period 1984-2010 to derive NDVI values. Dry and wet years were combined in order to avoid interference of climatic sequences on the vegetation status. Principal Component Analysis was carried out in order to identify individual and combined interactions of meteorological and dam-derived effects. The results showed higher NDVI values (close to 20%) once the dam was filled and NDVI values in very dry years similar to the ones obtained in medium-wet years prior to the construction. Besides, the obtained values proved to be highly related to the distance from the free surface of water once the meteorological and topographic features were isolated. These results quantify the dam influence along the river banks and the superficial recharge effects in dry years.

8174-05, Session 2

The use of lidar derived high resolution DEM and intensity data to support urban flood modeling

M. D. Aktaruzzaman, Universitâtsbibliothek Kaiserslautern (Germany)

The modelling of urban flooding requires two types of input data namely topographic elevation data and surface roughness of different types of land cover. In recent years, the use of airborne LiDAR (Light detection and ranging) derived digital elevation model (DEM) has become a standard practice in order to model both the rural and the urban floodplains. However, the processing of large volume of LiDAR point data and subsequent feature extraction for a complex urban area still remain a challenge for the urban flood modellers. While the LiDAR derived elevation data serve as a basis for detecting above ground objects e.g., buildings, trees and boundary walls, the LiDAR intensity data provide substantial information on different types of urban land cover such as grassland, bare soil and paved surfaces. In this study, a LiDAR filtering algorithm is presented that is flexible in nature and able to detect not only buildings but also boundary walls, fences and hedges that guide and impact the surface flow of flood water. Besides, the potential use of LiDAR intensity data is described in combination with existing aerial image for separating different urban surfaces. Very often the high resolution aerial images (< 25 cm) have three wavebands namely red, green and blue (RGB). The use of only RGB wavebands is often incapable of identifying types of surface under the shadow. On the other hand, LiDAR intensity data can provide surface information independent from sunlight conditions. Thus the integration of aerial image and LiDAR intensity data can serve as a powerful approach for distinguishing land cover types in a complex urban scene. A pixelbased and an object-based image classification approach is performed for classifying different urban surface types and subsequently make a comparison of both the approaches. The filtering algorithm and surface classification techniques are applied to two study areas. The output results of the filtering algorithm closely correspond to the reality and the object-based image analysis technique outperforms the traditional pixel-based classification.

8174-06, Session 2

Tracking, sensing and predicting flood wave propagation using nomadic satellite communication systems and hydrodynamic models

R. Hostache, P. Matgen, L. Giustarini, Ctr. de Recherche Public - Gabriel Lippmann (Luxembourg)

The main objective of this study is to contribute to the development and the improvement of flood forecasting systems. Since hydrometric stations are often poorly distributed for monitoring the propagation of extreme flood waves, the study aims at evaluating the hydrometric value of the Global Navigation Satellite System (GNSS). Integrated with satellite telecommunication systems, drifting or anchored floaters equipped with navigation systems such as GPS and Galileo, enable the quasi-continuous measurement and near real-time transmission of water levels and flow velocities, from any point of the world. The presented study investigates the effect of assimilating GNSS-derived water level and flow velocity measurements into hydraulic models in order to reduce the predictive uncertainty.

To initiate such an analysis, synthetic experiments have been carried out. Experiments with a virtual nomadic flood wave tracking system (NFWTS) were used to define the technical specificities of the required system components. The objective consisted in setting target values in terms of accuracy and transmission rates for individual system components. Synthetic water stage observations were assimilated into an ensemble of hydrodynamic models whose upstream boundary conditions were produced using corrupted semidistributed hydrological models. The experiment was conducted with a hydrological-hydraulic model implemented over a 19 km reach of the Alzette River. A Particle Filter was used as an assimilation algorithm for integrating observation data into the hydrological-hydraulic models. Synthetic observations were generated by adding "white noise" to a so-called "truth" model. Different observation perturbation magnitudes, number of measurement sites and measurement locations were chosen in order to investigate the performance of the assimilation scheme as a function of uncertainty and spatio-temporal resolution of observations. The parameters of the virtual NFWTS are expected to enable the recovery of the "true" water surface line. The experiment helped to determine the optimal configuration of a NFWTS setup. The results of the experiment, although specific for the reach under investigation, highlighted general requirements for NFWTS deployments.

We conclude from our experiments that the performance of the assimilation depends on the absolute measurement accuracy. However, even more significantly, the reduction in predictive uncertainty depends on the number and locations of the floating sensors. In fact, the performance of a model is never homogeneous over the entire model domain. This means that when a model is locally biased, forcing the model to take over the observation values at a given site may improve the model at local level but create larger errors at many other cross sections. To solve the problem of local biases, the number of observation sites needs to be increased. This result confirms the advantages that drifting sensors have over fixed sensors.

8174-07, Session 2

River discharge estimation through MODIS data

A. Tarpanelli, L. Brocca, F. Melone, T. Moramarco, T. Lacava, M. Faruolo, N. Pergola, Consiglio Nazionale delle Ricerche (Italy); V. Tramutoli, Univ. degli Studi della Basilicata (Italy)

River discharge is an important quantity of the hydrologic cycle because it is essential for both scientific and operational applications related to water resources management and flood risk prevention. Streamflow measurements are sparsely and for local sites along natural channels and, hence, are not able to detect the complexity of variation in surface water systems adequately. Therefore, in recent years, the possibility to obtain river discharge estimates through remote sensing has become more and more of great interest. For large river basins, the use of satellite data derived by altimeter and microwave sensors, characterized by a daily temporal resolution, has proven to be a useful



tool to integrate or even increase the discharge monitoring. For smaller basins (<10000 km2), Synthetic Aperture Radars (SARs) have been usually employed for the indirect estimation of water elevation but their low temporal resolution (from a few days up to 30 days) might be considered not sufficient for many rivers characterized by high temporal variability of discharge.

On this basis, the capability of the Moderate Resolution Imaging Spectroradiometer (MODIS) for river discharge estimation is investigated here. MODIS is characterized by high frequency repeat coverage and moderate spatial resolutions (~250 m) thus having a significant potential for mapping flooded area extent and dynamics. Specifically, the Robust Satellite Technique (RST) approach has been applied to MODIS data acquired in the optical band considering the 11-year time-series collected from 2000 to 2010. These time-series are compared with water level observations carried out for several gauging stations located along the Upper Tiber River basin (drainage area of ~5300 km2) in Central Italy. Empirical relationships between satellite and in-situ time-series are investigated in order to develop a procedure allowing to estimate the water level (and potentially the discharge) based on remote sensing data.

8174-08, Session 2

Flood monitoring and warning over Huaihe River Basin in China using AMSR-E data

W. Zheng, National Satellite Meteorological Ctr. (China)

Huaihe River Basin is located in the middle eastern part of China, which extends about about 800km from east to west, and 500km from north to south. The basin is an area where flood and waterlogging disaster happened very frequently. The disaster has mad adverse impacts on the region's economic development.

Advanced Microwave Scanning Radiometer for Earth Observation System (AMSR-E) presents a potential for flood monitoring because of the ability of the microwave signal to penetrate through cloud and provide all-day data and because of its sensitivity to surface water. It can fast reveal large-scale flood patterns. Our study is restricted to the 37GHz frequencies because it is less affected by atmospheric effects than 21 or 85GHz channels and it's spatial resolution is higher than 6.9 to 22GHz channels.

The proposed approach is based on the polarized ratio index (PRI), which is computed by using AMSR-E data at 37GHz, vertically and horizontally polarized brightness temperature values. The spatial resolution of AMSR-E data is about 10km at 37GHz frequency. At this resolution, many water surfaces will generally be imaged as mixed pixel containing substantial fractions of water and land. So, PRI is a combination of different response generated by the water surface and the land surface. The PRI characterizing each surface type is weighed by its surface fraction. Water surface fraction is a crucial parameter in flood monitoring as it indicates the variation of water areas in both space and time. Consequently, we choose water surface fraction (WSF) method based on Linear Special Mixed Model.

The Huaihe River Basin was hit by severe heavy rains from June to October of 2003. The rise of water level in rivers, lakes and reservoirs caused a severe flood and waterlogging disaster. We utilize the WSF method to monitor the 2003's Huaihe River flood. Moderate Resolution Imaging Spectroradiometer (MODIS) data with 250-m spatial resolution are used to validate the WSF values. The 62 AMSR-E images are selected to calculate WSF and got the water area during the summer of 2003. The result showed the measured flood level and the water area derived from AMSR-E data similar trends, which demonstrates the potential of AMSR-E data for flood warning.

Comparing the flood extents derived from the WSF maps at different dates in flood seasons based on the 2002 to 2006 AMSR-E data sets, we find the flood-damaged areas' spatial and temporal variability. The result shows the WSF maps in flood seasons from 2002-2006 years. The red circles in the maps with higher WSF values reflect the higher flood levels in mainstream. It is worth noting that the forming of higher WSF (WSF>10%) zone in the buffer along the Huaihe River mainstream extending 50km south and 100km north may be used as an indicator for flood forecasting. These research results can indicate AMSR-E data might help with the flood warning over Huaihe River Basin.

Predicting soil erosion under land-use and climate changes using the revised universal soil loss equation (RUSLE)

S. Y. Park, C. G. Jin, C. U. Choi, Pukyong National Univ. (Korea, Republic of)

Soil erosion reduces crop productivity and water storage capacity, and, both directly and indirectly, causes water pollution. Loss of soil has become a problem worldwide, and as concerns about the environment grow, active research has begun regarding soil erosion and soil-preservation polices. This study analyzed the trend of soil loss in South Korea over a recent 30-year period and predicted future soil loss in 2020 using the revised universal soil loss equation (RUSLE). Digital elevation (DEM) data, detailed soil maps, and land cover maps were used as primary data, and geographic information system (GIS) and remote sensing (RS) techniques were applied to produce thematic maps, based on RUSLE factors. Using the frequency ratio (FR), analytic hierarchy process (AHP), and logistic regression (LR) approaches, land suitability index (LSI) maps were developed for 2020, considering the already established Environmental Conservation Value Assessment Map (ECVAM) for Korea. In the period 1975-2005, soil loss showed an increasing trend, from 22.92 ton/ha in 1975 to 23.51 ton/ha in 2005; the 2005 value represents a 0.59 ton/ha (2.58%) increase, compared with 1975 and is attributable to the increased area of grassland and bare land. Scenario 1 assumes that urban areas have a similar trend to that between 1975 and 2005 and that precipitation amount follows scenario A1B of the IPCC. In this case, the soil loss amount for LSI maps that account for the ECVAM should increase by 25.0~26.3% compared to 1975. In the case where the ECVAM is not considered, soil loss should increase by 27.7~31.8%. In Scenario 2, in which the urban area and precipitation follow the same trend as between 1975 and 2005, soil loss for LSI maps that consider the ECVAM will increase by 6.8%~7.9% compared to 1975. When the ECVAM is not considered, soil loss will increase by 9.1~12.6%. These results indicate that if urban areas are developed such that they damage areas of high value, as defined environmentally and legislatively, the amount of soil loss will increase, whereas if such areas are preserved, erosion will decrease slightly. Thus, when planning urban development, the environmental and legislative value of preservation should be considered to minimize erosion and allow for more sustainable development.

8174-10, Session 3

Perspectives of remote sensing of soil moisture for hydrological applications

L. Brocca, F. Melone, T. Moramarco, Consiglio Nazionale delle Ricerche (Italy); W. Wagner, Technische Univ. Wien (Austria)

Soil moisture is the core of the system controlling the hydrological interactions between soil, vegetation and climate forcing, thus playing a key role in governing the water and energy balance between land surface and atmosphere. Therefore, the monitoring of soil moisture represents an important issue for many scientific and operational applications in hydrology, meteorology, agriculture, to cite a few. Nowadays, remote sensing sensors operating in the microwave band are becoming readily available for measuring soil moisture spatial-temporal variability at a global scale with a nearly daily temporal resolution and a good accuracy. Thus, a great chance to improve hydrological predictions is offered based on the use of these new source of data within rainfall-runoff modelling.

In fact, it is well-known that a flood forecasting system based on a rainfall-runoff model strictly requires an accurate estimation of the initial state of the catchment wetness to achieve reliable flood predictions. However, the incorporation of remotely sensed soil moisture observations within rainfall-runoff modelling is not straightforward due to the different spatial and temporal scales of observations and modelled quantities and, mainly, to the thin soil layer depth investigated by satellite sensors. Moreover, rainfall-runoff models should be adapted to efficiently incorporate these new types of observations.

In this study, the soil moisture products derived from two different satellite microwave sensors, the Advanced SCATterometer (ASCAT) and the Advanced Microwave Scanning Radiometer (AMSR), are

8174-09, Session 3

tested in order to improve runoff prediction through a continuous and distributed rainfall-runoff model, named MISDc. Specifically, two different strategies for assimilating satellite-based soil moisture data within MISDc are considered, tied to the use of both the surface and the profile soil moisture products. The profile soil moisture is obtained through the application of an exponential filter thus obtaining the so-called Soil Wetness Index (SWI). By using both satellite sensors and strategies, the MISDc performance on flood estimation, with and without assimilation, is analyzed by using synthetic-twin and realdata assimilation experiments. Rainfall-runoff hourly data for different catchments (with drainage area ranging between 100 and 5000 km²) located across the Upper Tiber River Basin (central Italy) and in other European countries are used as case-study.

Results reveal that the ASCAT and AMSR soil moisture estimates can be conveniently used to improve runoff prediction in the study areas. Moreover, the use of the SWI product provides improvements higher than the direct application of the surface soil moisture one. These products become essential when the soil wetness conditions before a storm event are highly uncertain or unknown. These encouraging results reinforce the idea of assimilating the soil moisture products to improve flood forecasting also by using more detailed data assimilation approaches (e.g. the Ensemble Kalman Filter or the Particle Filter) and a large number of catchments in different regions worldwide.

8174-11, Session 3

Cosmo SkyMed announcement of opportunities projects: an overview of the first year results in the hydrology and land surface research fields

L. Dini, C. Benedetto, Agenzia Spaziale Italiana (Italy)

At the beginning of 2010, the Italian Space Agency (ASI) has started more then 150 project to exploit Cosmo/Skymed data. Twenty seven of them have been funded, while the remaining have been approved to receive Cosmo SkyMed (CSK®)data.

Many of these projects have focused in particular on the exploitation of the high spatial and temporal resolution, polarimetric X-Band CSK® data for land surface research and applications.

After more than one year of investigation a critical review and an analysis of the preliminary achieved results will be presented with the main goal to provide the community with a synthetic overview of the state of the art of the research in the exploitation of CSK® data in fields such as hydrology and land surface studies.

The covered topics will be in particular: soil parameter retrieval (e.g. moisture, roughness, correlation length, etc.), vegetation parameter retrieval (e.g. LAI, biomass, leaf water content, vegetation height, leaf angle distribution, etc.), snow parameter retrieval (mass of snow, snow water equivalent, etc.), land cover/land use.

For any of the above mentioned topics examples of the most innovative approaches and methodologies, the most interesting results and the most promising applications in fields like precision agriculture, forestry, drought and natural resource management will be shown.

Finally, a description of the expected future ASI activities (e.g. new Announcement of Opportunities, ASI internal projects, ASI research investments, etc.) in the land surface research field will be presented.

8174-12, Session 3

Interception modeling with vegetation time series derived from Landsat TM data

M. J. Polo, A. Díaz-Gutiérrez, Univ. de Córdoba (Spain); M. P. González-Dugo, Instituto de Investigación y Formación Agraria y Pesquera (Spain)

Interception of rainfall by the vegetation may constitute a significant fraction in the water budget at local and watershed scales, especially in Mediterranean areas. Different approaches can be found to model locally the interception fraction, but a distributed analysis requires time series of vegetation along the watershed for the study period, which includes both type of vegetation and ground cover fraction. In



heterogeneous watersheds, remote sensing is usually the only viable alternative to characterize medium to large size areas, but the high number of scenes necessary to capture the temporal variability during long periods, together with the sometimes extreme scarcity of data during the wet season, make it necessary to deal with a limited number of images and interpolate vegetation maps between consecutive dates.

This work presents an interception model for heterogeneous watersheds which combines an interception continuous simulation derived from previous work by Zheng et al. (2002) and a time series of ground vegetation cover fraction and type from Landsat TM data and vegetation inventories. A mountainous watershed in Southern Spain where a physical hydrological modelling had been previously calibrated was selected for this study. The dominant species distribution and their relevant characteristics regarding the interception process were analyzed from literature and digital cartography; the evolution of the vegetation ground cover fraction along the watershed during the study period (2002-2007) was produced by the application of a spectral mixture model analysis on the available scenes of Landsat TM images. This model was further calibrated by data collected during two field campaigns in selected areas in the watershed.

The vegetation time series produced allowed the identification of local areas where the interception fraction was significant enough, together with the quantification of the variability of vegetation cover along the year and between years along the watershed. The use of Landsat TM data provided us with a sufficiently high spatial resolution for the heterogeneity found along the watershed. Different areas were identified in terms of the significance of the interception potential losses, and these fractions were estimated on a daily basis throughout the study period, and aggregated to upper scales to be included in the water budget at watershed scales.

8174-13, Session 3

Hydrological water balance modelling of a poorly observed basin using RS techniques: Lake Manyara, East African Rift, Tanzania

D. M. Deus, Technische Univ. Bergakademie Freiberg (Germany) and Ardhi Univ. (Tanzania, United Republic of); R. Gloaguen, Technische Univ. Bergakademie Freiberg (Germany); P. Krause, Friedrich-Schiller-Univ. Jena (Germany)

Accurate hydrological water balance determination and simulation needs correct approximation of spatial and temporal distribution of water parameters. The general objective of the work presented here is to quantify the water balance in Lake Manyara basin and hence the key interest is on the hydrological aspects. The specific objectives of this study include in the first place, estimation of parameters for the hydrological cycle so as to identify where and when the great losses and gains occur. Second is the assessment and validation of the performance of J2000g water balance model in a poorly gauged semiarid tropical environment using a combination of multi-satellite remote sensing datasets and in-situ observations. The performance of a model in prediction depends on the setup and parameterization. J2000g model setup involves catchment and physical parameter discretization into hydrologic response units (HRUs). The model requires two types of input values at the initialisation: Temporally varying values, called "data" and temporally more or less constant values, called "parameters". For the first type, time series input mainly meteorological data, were provided. This includes absolute and relative air humidity, sunshine duration, maximum, mean and minimum temperature, wind speed, precipitation and observed runoff. For the second type, for every HRU, parameters related to land use/land cover like albedo, stomata conductance, maximum plant height (Hmax), leaf area index (LAI) and maximum rooting depth (RDmax): Soil type, hydrogeology and topographic specific parameters namely mean elevation, slope and aspect.

Remote sensing derived spatially distributed model inputs and outputs are found to be very useful in understanding the hydrologic behaviour of the basin. The study therefore presents the water balance model calibration and validation results. The spatial and temporal variability of the water balance components mainly precipitation (P), evapotranspiration (ET) and runoff (R) were quantified. In this study J2000g water balance model was calibrated manually by trial and error. The goodness-of-fit of the observed and simulated data sets were



evaluated based on a visual comparison and Nash-Sutcliffe coefficient to support the judgement. Since the basin is poorly monitored, the model was calibrated using daily discharge observations for a period of only two month and validated using simulated and observed ET on monthly timescale. Calibration and validation results at the daily and monthly timescale gave moderately satisfactory Nash-Sutcliffe coefficient of efficiency (CE) of 0.66 for calibration and Pearson correlation coefficient (R) of 0.82 for validation using simulated and observed ET. J2000g water balance model was found to be useful in the lake catchment and showed the potential to be used in poorly gauged catchments using satellite data. The water balance information obtained can be used for further analysis of the fluctuation of lake levels in relation to the effect of soil erosion, climate and land cover/ land use change as well as other different lake management and conservation scenarios.

8174-14, Session 3

Retrieving rainfall fields through tomographic processing applied to radiobase network signals

L. Facheris, Univ. degli Studi di Firenze (Italy); F. Cuccoli, Consorzio Nazionale Interuniversitario per le Telecomunicazioni (Italy); S. Gori, Univ. degli Studi di Firenze (Italy); L. Baldini, Istituto di Scienze dell'Atmosfera e del Clima (Italy)

The infrastructures of mobile communication systems (i.e., GSM, GPRS, UMTS) constitute a unique opportunity for low cost rainfall monitoring, since they can be exploited - especially in urban areas - to generate a high link-density tomographic network, with an enormous potential in terms of areal accuracy and time resolution. The number of possible microwave radio links of an urban radio base network (RBN) is much higher than the number of links that is generally sufficient to provide a good estimate of a specific attenuation map induced by rainfall. Furthermore, the frequencies of the channel services in Italy fall around 18, 23, and 38 GHz, allowing in theory multifrequency measurements that cover a wide range of rainfall intensities. However, the density and the crossings of the radio links can be highly irregular. Therefore, the situation is quite different with respect to the case of a dedicated radio link infrastructure conceived and built with the exclusive purpose of monitoring rainfall (e.g., in a narrow valley) where the tomographic procedure must be able to deal with the basic practical/economic limitations mentioned above. Evidently, the choice of an adequate tomographic processing procedure is fundamental.

We present here a new tomographic algorithm specifically developed for the typical problems caused by the topology of the urban RBN. The algorithm was tested on simulated specific attenuation (K) maps. Realistic K maps at a much better resolution than that achievable by the tomographic network were obtained based on polarimetric C-band reflectivity measurements gathered by the POLAR55 C radar. We ran simulations at 18, 23, and 38 GHz over the radar-derived K maps by applying the new tomographic algorithm to the current RBN of the town of Florence. The K maps were also used to simulate the power attenuation measurements along the RBN links.

We concentrated on the retrieval of the K maps, since the rainfall maps are obtained from them through well established K-R relationships, introducing a known error. The results provided by the simulation are extremely encouraging, showing an excellent reconstruction performance of the tomographic algorithm already when exploiting a fraction of the total number of possible links offered by the urban radio base network. Since it is also of interest to avoid to overcharge the tomographic algorithm with an input attenuation vector carrying more elements than needed to obtain a good estimate of the K field, we analyzed the degradation of the reconstruction performance when the number of links is reduced (according to a pre-defined strategy), trying to identify the minimum level of link density required to obtain sufficiently accurate reconstructions through the proposed tomographic procedure.

6

8174-15, Session 4

Damage estimation on agricultural crops by a flood

N. C. Silva, A. A. López-Caloca, J. L. Silván-Cárdenas, Ctr. de Investigación en Geografía y Geomática (Mexico)

Nowadays, due to climate change, disastrous and catastrophic events are happening frequently and unexpectedly, affecting valuable resources-both human and natural, in various regions of the planet. Currently, the water, being a source for life and motor of economical development, is also a cause of death and destruction, so it constitutes a hazard to prevent. Agricultural areas are one of the most critical areas to analyze, because they are exposed to damage by floods, and because the excess or lack of it, have been cause of land degradation.

Southeastern Mexico, particularly Tabasco's flatlands is always influenced by fluctuations and disturbance of the water resource; which unchained a severe flood in 2007 affecting more than 80% of Tabasco's territory. This disastrous flood event makes the start point to reconsider and to develop new flood protection techniques, so it was used as a case of study for testing a methodology for the estimation of direct damage looses on agricultural crops by a flood. We proposed an improvement of Support Vector Machines (SVM) for land cover classification of the SPOT-5 images data, which consists on integration of spatial and spectral information during the image analysis, through a segmentation classification procedure.

The spatial information is obtained using the watershed segmentation, a powerful image segmentation tool developed in mathematical morphology, which consists on partitioning the image into catchment basins, so each basin is associated with each minimum in the image (gradient). Typical watershed segmentation of image gradient tends to be over-segmented. In order to alleviate this, two approaches are considered: one is the thresholding of the gradient image; the other is the well known centroid linkage region growing algorithm which merges regions with certain statistical similarities.

After the image is segmented into regions, each pixel is assigned to one of the classes based on the spectral information by a machine learning algorithms (SVM) to locate the optimal boundaries between classes, using the majority voting within the regions obtained by the segmentation. The application of this method allowed an accurate delineation of agricultural lands on the study area.

In order to evaluate the impact of floodwater on agricultural crops, a radar data (RADARSAT-1), were used for both, delineating the flood boundary delineation and estimating water depth. These layers were overlaid on the land cover classification layer, so the yield damage at flooded crop was estimated using a depth damage function. The study quantified and evaluated the overall economic loss (tangible damage) from the impact of floodwater on agricultural crops which is essential to prepare for a disaster and facilitating good decision making at the local, regional, state, and national levels of government.

8174-16, Session 4

Evaluation of time-series and phenological indicators for land cover classification based on 10 year of MODIS data

F. Vuolo, Univ. für Bodenkultur Wien (Austria); K. Richter, Ludwig-Maximilians-Univ. München (Germany); M. Mattiuzzi, C. Atzberger, Univ. für Bodenkultur Wien (Austria)

The continuous monitoring of land surfaces from medium spatial resolution satellites provides input to a variety of mapping applications, including land use and land cover changes. Time series of the Normalized Difference Vegetation Index (NDVI) usually provide the basis to evaluate vegetation status and dynamics for such purposes. The utilisation of long time series and large scale data sets is nowadays facilitated by readily available and standardized (in time and space) products. Such global composites have a high potential for continuous and real time updating. However, land cover maps derived from regional to global scales are not revised as frequently as newly available observations and on such a regular basis.

In the context of defining a procedure for nearly real time land cover

mapping with seasonal updated products, this research examines the use of time-series and phenological indicators from MODIS NDVI for land cover mapping. Thus, 16-days NDVI composites from MODIS (MOD13Q1) covering the period from 2001 to the present were acquired from a region in Southern Italy (Campania) and from Lower Austria (Marchfeld region). The first part of the paper focuses on different filtering techniques. The newly proposed Whittaker smoother, a very fast algorithm giving continuous control over smoothness with only one parameter, was tested against the asymmetric Gaussian and double logistic functions as well as the Savitzky-Golay filter.

Subsequently metrics of vegetation dynamics such as minimum, maximum and timing of NDVI, start and end of the vegetation season were extracted from the cleaned time series of the 10 years. The performance of the different filtering procedures and phenological indicators were indirectly evaluated by using the capability of the cleaned time series to separate between different vegetation species.

For this purpose, regional land cover maps were available, based on the CORINE Land Cover (CLC) classification. Differences, drawbacks and advantages of the filtering techniques and metrics are finally discussed on the basis of the proposed quality indicators.

8174-17, Session 4

A multispectral multiplatform based change detection tool for vegetation disturbance on Irish peatlands

J. O'Connell, J. Connolly, N. M. Holden, Univ. College Dublin (Ireland)

In Ireland, maintenance of peatland Carbon (C) stock has taken on a renewed importance with articles 3.3 and 3.4 of the Kyoto Protocol / Marrakech Accords recognising soil organic carbon as a biosphere sink. Peatlands in Ireland cover approximately 20% of the land surface and accounts for between 53% (1071.13 Mt C) to 62% (1503 Mt C) of national soil carbon stock. Extensive anthropogenic disturbance to peatland habitats can have negative impacts on sequestration rates, and in extreme cases, can convert such habitats from net sinks to a net source's of C emissions.

Irish peatlands are spatially extensive and relatively inaccessible, therefore satellite based multispectral imagery is ideally suited to the monitoring peatland vegetation due to its high spatial and temporal resolution. However Ireland's extensive cloud cover means that over 78% of all optical based satellite imagery taken throughout the year is completely obscured. An alternative approach in a change detection study that requires a high temporal resolution is to use multiplatform data.

In this study satellite data from six different multispectral sensors (TM, SPOT 2, 4 and 5, IRS P6, Aster VNIR) were used in a change detection study of vegetation disturbance on Irish peatlands. All data was corrected for atmospheric scattering using dark object subtraction and converted from digital numbers to Enhanced Vegetation Index 2 (EVI2). Radiometric normalisation was performed using Temporally Invariant Clusters (TIC) and cross calibration applied using linear regression of radiometrically stable ground-based targets. Erdas Imagine's Spatial Modeller was used to create a change detection model using pixelto-pixel based subtraction with a Standard Deviation (SD) threshold. The model can be adjusted by altering the SD threshold as well as a pixel based clump function which was used to mask isolated pixels that may have occur due to local anomalies or mis-registration. Initial results after TIC normalisation show EVI2 cross platform correlation values (R²), regressed against a Landsat TM master image, of of 0.9346 for Aster VNIR, 0.9487 for IRS P6, 0.9246 for SPOT 4 and 0.9641 for SPOT 5. Change detection analysis of prior and post cross calibrated data reveled an average decrease of 15.4% in the area of detected change which was attributed to spectral and radiometric variability across platforms as opposed to actually vegetation change on the around.

Auxiliary data detailing type, date and extent of know disturbance events (e.g. burning, bog burst, afforestation, peat harvesting) is currently being used to train and validate the change detection model to ensure that SD and clump adjustment parameters are set to accurately detect vegetation disturbance on the ground. It is hoped that this change detection model, combined with other models which



have been created as part of this research for image pre-processing, will all be combined to form a tool/protocol for the quantification of vegetation disturbance on Irish peatlands.

8174-18, Session 4

Mapping peatland disturbance in Ireland: an object oriented approach

J. Connolly, N. M. Holden, Univ. College Dublin (Ireland)

Soil organic matter and soil Carbon (C) play a major role in the carbon cycle of the soil. The global soil carbon pool contains 1,500 gigatons (Gt). Peatlands contain large amounts of soil organic carbon. In a pristine state they sequester atmospheric carbon dioxide (CO2), however, when they are disturbed they emit it. In Ireland peatlands are extensive and cover between 14 and 20% of the national land area. They contain between 53% and 62% of the total national soil organic carbon. However, a large percentage of Irish peatlands are disturbed. The main types of disturbance that occur on Irish peatlands are drainage, forestry plantations, industrial and domestic extraction, burning and conversion to pasture. Most of these activities impact on the peatlands ability to sequester CO2. This has implications for Ireland's carbon budget and its Kyoto protocol and EU obligations.

The mapping of disturbed peatlands on a national basis is a difficult task. Peatlands are extensive and often quite inaccessible. Therefore mapping using satellite data can be useful. The CORINE 2000 landcover map was based on Landsat imagery in Ireland and included a classification for intact and exploited peat. This research uses satellite data from several platforms: IRS, Ikonos and Geoeye, to create a detailed map of peatland disturbance. The high resolution multispectral imagery allows the distinct geometric patterns and spectral signatures of disturbance to be seen and the data extracted from the images.

This method uses recent peat maps to examine the spatial extent of peatlands on the imagery. An object oriented approach is used in ArcGIS to extract the peatland disturbance. The process results in maps that depict the extent of intact and disturbed peatlands. Preliminary results from the study have shown that relatively detailed disturbance maps can be extracted. These maps will allow policy makers and environmental officers to make informed decisions about the use, conservation and restoration of peatlands in Ireland.

8174-19, Session 5

Unmanned aerial vehicle (UAV) operated spectral camera system for forest and agriculture applications

H. K. Saari, VTT Technical Research Ctr. of Finland (Finland); I. Pellikka, Univ. of Jyväskylä (Finland); L. Pesonen, MTT Agrifood Research Finland (Finland); S. Tuominen, Finnish Forest Research Institute (Finland); J. Heikkilä, Pineering Ltd. (Finland); C. Holmlund, J. H. Mäkynen, K. M. Ojala, T. Antila, VTT Technical Research Ctr. of Finland (Finland)

VTT Technical Research Centre of Finland has developed a Fabry-Perot Interferometer based hyperspectral imager compatible with the light weight UAV platforms. The concept of the hyperspectral imager has been published in the SPIE Proc. 7474, 7680 and 7668. In forest and agriculture applications the recording of multispectral images at a few wavelength bands is in most cases adequate. The possibility to calculate a digital elevation model of the forest area and crop fields provides possibility to estimate the biomass and perform forest inventory. The developed UAS spectral imaging system is capable of recording 5 Mpixel multispectral data in the wavelength range 500 - 900 nm at a resolution of 10 nm @ FWHM. The overlap between successive images is 60...70% which makes it possible to calculate the digital elevation model of the target area. The field of view of the system is 24 x 36 degrees and ground pixel size at 150 m flying altitude is around 3.5 cm. The UAS system will be tried in summer 2011 in Southern Finland for the forest and agricultural areas. The design, calibration and first forest and agriculture application results will be presented at the conference.

8174-20, Session 5

Automated object detection of climate tracers in remote-sensing data

L. Tyrallova, Univ. Potsdam (Germany)

Automated object detection in remote-sensing and image-based data as well as the statistical analyses of morphometric key parameters are valuable tools in the field of remote-sensing geomorphology. Both help to identify processes that are directly related to climatic boundary conditions. The automated detection of primary climate related landforms and the assessment of their change during three decades of remote sensing observations allow quantifying and finding predictors for the consequences of climate changes on a regional and global scale.

Our goal is to create approaches and concepts for catalogue-based object detection of landforms within a commercial GIS suite. Our intention is to transfer the workflow onto other climate-tracer landforms to enable operational use of the workflow above the conceptual level.

Landforms, that we consider being climate tracers, react to climate and its changes. However, only few landform types are suitable for automated object detection.

They have to fulfil a number of requirements. For example, the isolated landforms have to be detected, delineated, and morphometrically characterized using an object catalogue of appropriate criteria and significance levels of different criteria; pixel scales must be unambiguously represented in the data in order to test different sample sites.

In order to achieve this, we have chosen thermokarst depressions as initial landform type as it is known to be variable on a scale of years and it is a prime indicator of changes induced by climate variability. Thermokarst depressions are associated with frozen ground and periglacial environments and are formed and developed through permafrost degradation. Their shape is relatively simple making them primary test targets. They are often circular to elliptical in shape and occur in groups with a preferred long-axis direction. Their prime occurrences in Northern Siberia and Canada are different in geomorphology, which is a promising setting for spatial comparative analysis.

The inputs into the automated object detection process are multispectral and multitemporal remote-sensing data (e.g., RapidEye, Landsat) as well as terrain-model data. The crucial part of the processing framework is formed by an object catalogue and an employment of a well-defined decision tree on which the spatial analysis is based upon. Extraction of geomorphological parameters from terrain-models in combination with cell-based image-data calculations and spectral classifications form the core of the automated object detection. Output data of the spatial analysis enable identifying objects which represent isolated transient landforms as defined through vector-based delineations of positive detections. Object detection and extraction of key values allow to systematically and automatically derive quantitative information and spatial statistics over large areas and a large number of similar landform types.

The detection tools help to identify and assess landforms on an a-priori level. GIS-integrated automated detection tools will be available for a wide range of experts. Furthermore, object informations within a proper geospatial context will be useful for data exchange and ongoing studies. The detection process is less time-consuming and provides means to extract statistical parameters over large areas and timespans.

8174-21, Session 5

Novel applications of optical remote sensing in animal ecology

P. Lundin, M. Brydegaard, M. Liang, P. Samuelsson, L. Cocola, A. Runemark, H. Jayaweera, M. Wellenreuther, E. Svensson, C. Löfstedt, S. Åkesson, G. Somesfalean, S. Svanberg, Lund Univ. (Sweden)

Animal ecology is a research field which has always been dominated by remote sensing in the shape of visual observations. This is especially true for studies on flying animals like migrating birds of



which most information is gathered by the sound of their flight calls, wing beat signatures or their visual appearance.

When observing an animal in the field with, e.g., a pair of binoculars or a telescope, the visual information based on the shape and reflectance spectrum (color) of the animal is providing useful information which could be used for species and age classifications. However, except for the trichromatic vision of the observing person, little of the spectroscopic information of the collected electromagnetic radiation is traditionally used.

Recently we have tried to change this scenario by introducing a set of spectroscopic methods to the research field of animal ecology. The use of automated measurements systematically gather statistics. We have employed a LIF-LIDAR setup and marking methods to remotely find and classify different species of damselflies, flying over a river in south Sweden [1,2] with application in behavioral studies and migration between microhabitats. Another class of insects under study has been moths. Some moth species are known to cause large losses in agriculture of, e.g., rice crop, especially in Asia. Remote sensing studies of moth with the aid of LIF were performed in China with application for evaluating pheromone traps [3].

In connection to the studies of damselflies, fluorescence LIDAR trials were also performed on Starlings flying in an open field setting [4]. Both these studies were performed by a UV-laser, inducing species-specific fluorescence which was collected with a telescope and studied with a spectrometer or a multi-channel detector setup. The remote fluorescence studies on birds have been further explored in a campaign at the nature reserve of the Kullaberg sea shore cliff in the south-west of Sweden [5]. During this campaign, two additional techniques were also explored with the purpose of remotely classifying birds during nighttime, namely infrared and passive spectroscopy.

Infrared cameras have previously been used in bird migration studies, but possible spectral information has not been used. Gaining inspiration from in nature frequently observed structural colors found in the visible region, created by biologically produced nanometer sized structures, we use the fact that feathers largely are made up by micrometer sized structures to remotely obtain this structure by midinfrared studies. In short, two mid-IR spectral detection bands, one on each side of the CO2 absorption band at around 4.3 microns are used. The modulation of the ratio of the intensity in these bands during a wing beat cycle of the bird should hopefully be species dependent and thus help in the classification. We have developed methods for passive spectroscopy, in which, a fast fiber coupled spectrometer analyzes the signal from a telescope and observes the sun-induced light scattering from the birds or insects during daytime. We are currently looking into lunar and sun induced transmittance spectroscopy using tracking telescopes.

8174-22, Session 5

Methods and potentials for using satellite image classification in school lessons

K. Voss, H. Hodam, R. Goetzke, A. Rienow, Rheinische Friedrich-Wilhelms-Univ. Bonn (Germany)

The project "Remote Sensing in Schools" aims at finding ways to integrate Remote Sensing in secondary schools. The devised learning materials are digital and interactive learning applications which integrate a wide range of remote sensing techniques. In this study we present the potential of deriving thematic information from remote sensing images in secondary education.

Map generation is an important topic in geography classes in secondary school education. This also includes the question of how to derive thematic maps based on satellite imagery and, hence, presents a good opportunity to introduce satellite image classification to school education. Relying on mere visual interpretation would only scratch the surface of the possibilities offered by digital image data.

The heterogeneous pattern of grayscale and color values presented in satellite images constrains a purely visual quantitative and qualitative analysis. Not until the digital information contained in these patterns is generalized can the content be profoundly interpreted. Deriving thematic information through classification is therefore one of the main applications in digital image processing.

If the general topic of remote sensing is to be transferred into school



education, the integration of such methods is of utmost importance; but pupils will need simple analysis tools allowing them to derive land cover maps from satellite imagery.

This contribution presents ways of integrating the topic of "classification" into geography lessons. It is focused on methods reducing the procedure's complexity to an adequate level for the use in class. For this purpose, different classification tools have been created offering alternative ways for approaching the topic of "image classification".

8174-23, Session 6

Improvement of the triangle method for soil moisture evaluation by adding a third index: albedo or cellulose absorption index

J. Krapez, ONERA (France); A. Olioso, Institut National de la Recherche Agronomique (France)

Vegetation and soil temperatures have long been recognized as an indicator of water availability. Thermal sensors used for environment monitoring on board of satellite or airplane have a spatial resolution ranging from a few meter to a couple of kilometres. The consequence is that most pixels are a mixture of vegetation and bare soil. The radiance reaching the elementary detector is thus a combination of the radiance coming from the leaves and the radiance coming from the soil. For same soil water content, the brightness temperature may thus have different values depending on the vegetation fraction cover, the temperature and emissivity of soil and the temperature and emissivity of vegetation. When considering only the brightness temperature, one thus faces an underdetermined problem. A method proposed a few years ago consists in jointly analyzing the temperature and a vegetation index well correlated with the vegetation fraction cover. Such index could be the classical NDVI. One can also use SAVI or TSAVI which are less dependant on the spectral properties of the soil.

When plotting the two-dimensional distribution of temperature and vegetation index (T-VI) corresponding to an area with well distributed vegetation cover and moisture content, one gets a triangular of trapezoidal shape. Iso-moisture lines are then said to range between two plot edges: the dry edge and the wet edge.

The concept of exploiting T-VI only is however based on a simplified representation of the thermal and radiative properties of the soil/ vegetation structure and of the heat/mass transfers therein. A large number of parameters, in addition to soil moisture, are actually influencing the apparent soil/canopy temperature. Spreading the temperature distribution along only one dimension like the VI is indeed not enough for allowing an unambiguous determination of soil moisture.

We propose to improve the identifiability of soil moisture by introducing an additional observable parameter. We tried two different parameters: albedo and CAI (Cellulose Absorption Index). Albedo was chosen to separate areas according to the absorbed solar radiation whereas CAI was chosen to separate areas according to the fraction of senescent vegetation.

The aim of this study is to analyse the benefit of adding a third index to the classical T-VI empirical method for soil moisture mapping. The proposed procedures were applied on remote sensing data obtained during two airborne campaigns. When applying the classical triangle method for a series of field (wheat, alfalfa, vineyard, meadow, bare soil and ploughed soil), the correlation coefficient R2 between inferred moisture index and gravimetric moisture content is 0.61. It slightly diminishes to 0.56 when adding albedo to T-VI whereas it increases to 0.67 when adding CAI instead. Therefore adding albedo doesn't seem to provide a significant improvement, at least for present types of crops. The use of the Cellulose Absorption Index (CAI) seems to be more promising.

8174-24, Session 6

Energy balance modeling of agricultural areas by remote sensing

A. Andreu, M. P. González-Dugo, Instituto de Agricultura Sostenible (Spain); M. J. Polo, Univ. de Córdoba (Spain); F. L. M. Padilla, P. Gavilan, Instituto de Agricultura Sostenible (Spain)

The integrated water resource management required to face the water scarcity situation in semiarid regions relies on the ability to obtain accurate information about the use of water by crops and natural vegetation. Thermal remote sensing provides key data about the vegetation water status and helps to precisely determine its evapotranspiration. The integration of remotely sensed data into water and energy balance models helps to better estimate evapotranspiration under heterogeneous cropping and natural vegetation patterns, and it has broadened the field of application of these models from point to basin and regional scales.

In this work, we present an approach to estimate spatially distributed crop evapotranspiration using a series of Landsat TM and ETM+ satellite images combined with simulation modelling and ground-based measurements. A physically-based method for the energy budget partitioning based on the Two Source Model (Norman et al., 1995; Kustas and Norman, 1999) was applied over an agricultural watershed with irrigated crops in southern Spain. An integrated value of the latent heat flux over the day, more useful for most agricultural and hydrological applications, was obtained assuming that the evaporative fraction remains constant over the day.

Two growing seasons during 2008 and 2009 were analysed and the instantaneous surface energy fluxes and daily ET estimations were validated with field data from an eddy covariance system installed over a corn field during both campaigns. The results were also compared with that provided by a previously calibrated hydrological model in the study area corresponding to 2009.

The instantaneous fluxes of net radiation (Rn), soil heat flux (G), sensible heat flux (H) and latent heat flux (LE) were estimated for the time of satellite overpasses for each day of study. The comparison between instantaneous flux estimations and observations from the flux towers indicates a reasonable adjustment for convective fluxes (relative error 15-25%) and Rn (relative error 10%), and a greater dispersion of the soil heat flux (relative error 55%), highlighting the need to review G formulation under the study conditions. On a daytime basis, LE relative error is reduced to a 7%.

These results support a large scale application of the model as a first step for a decision-making tool for water resource planning and management. However, further validation over different crops is required.

8174-25, Session 6

On the use of MODIS fPAR and NDVI products for monitoring heterogeneous irrigated agriculture in western Uzbekistan

S. Fritsch, M. Machwitz, C. Conrad, S. W. Dech, Julius-Maximilians-Univ. Würzburg (Germany)

The fraction of photosynthetic active radiation (fPAR) intercepted by plants is a biophysical parameter that is important for global and regional vegetation studies. FPAR derived from MODIS data as well as vegetation indices are operationally available since 2000. Up to now there are few studies that explicitly deal with the accuracy of the MODIS fPAR product for arid and semi arid croplands. In this study the use of MODIS products (1km fPAR and 250m NDVI) for vegetation monitoring was investigated in a spatially heterogeneous irrigation system in western Uzbekistan. The first step was to validate the existing MODIS 1km fPAR product. For this purpose, high spatial resolution fPAR maps were developed using linear regression between in situ and time series data of the RapidEye sensors.

The data was aggregated and compared to MODIS fPAR composites for the growing season 2009. The comparison showed that both datasets were highly correlated but that the MODIS product overestimated fPAR based on RapidEye data. Furthermore, the results also indicated that the degree of correlation highly depends on the spatial heterogeneity of the MODIS pixels investigated. The lower the fraction of agricultural area per MODIS pixels, the lower was the relationship. The majority of MODIS pixels in the study region had an agricultural area of significantly less than 80%. Therefore, the use of the MODIS fPAR product is limited in this case. A viable alternative might be the use of higher resolution 250m products, which have been empirically calibrated.

As a second step the statistical relationships between the RapidEyebased high resolution fPAR maps and MODIS NDVI was investigated. The latter was derived from three different MODIS products: daily reflectances, 8-day reflectances and the 16-day NDVI product. Special attention was given to the analysis of the quality information included in the data. Good correlations were found between RapidEye fPAR and MODIS NDVI. This was mostly due to the overall high quality of the MODIS products in the study region. Differences in the degree of correlation between the different MODIS NDVIs were found and attributed to their corresponding production intervals. Analysis showed that MODIS pixels at the 250m scale were more homogeneous in terms of the fraction of agricultural area. Depending on the task, the found regression equations can therefore be used for regional agricultural studies that rely on fPAR as a key parameter as the 250m data better accounts for the spatial heterogeneity in the study area.

8174-26, Session 6

Comparing actual evapotranspiration and plant water potential on a vineyard

C. Cammalleri, G. Ciraolo, F. Colletti, G. La Loggia, A. Maltese, T. Santangelo, Univ. degli Studi di Palermo (Italy)

Agricultural water requirement in arid and semi-arid environments represents an important fraction of the total water consumption, suggesting the need of appropriate water management practices to sparingly use the resource. Furthermore the quality of some crops product, such as vineyards, is improved under a controlled amount of water stress. The latter is related, on a side, to actual evapotranspiration (ET) through water demand; on the other side, to plant water content through leaf water potential. Residual remote sensing-based energy balance approaches allow to estimate the spatial distribution of daily actual ET at plant scale, representing an useful tool to detect the spatial variability across different cultivars and even within each parcels. However, the connection between actual ET and leaf water potential, commonly used by farmers to plan irrigation supply, is not well studied, especially under water stress conditions. The actual ET derived from remote sensing data and measured by eddy covariance tower were analyzed together with water potential measured using a Scholander chamber; the analysis highlights that, under water stress conditions, daily actual ET is significantly inversely proportional to water potential. These results suggest the possibility to use remote sensing-based ET estimation as support for irrigation management at plot scale.

8174-27, Session 6

10

Estimating evapotranspiration of riparian vegetation using high resolution multispectral, thermal infrared and Lidar data

C. M. U. Neale, H. Geli, S. Taghvaeian, A. Masih, R. T. Pack, Utah State Univ. (United States); R. Simms, M. Baker, J. A. Milliken, S. O'Meara, A. J. Witherall, U.S. Bureau of Reclamation (United States)

High resolution airborne multispectral and thermal infrared imagery was acquired over the Mojave River, California with the Utah State University airborne remote sensing system integrated with the LASSI imaging Lidar also built and operated at USU. The data were acquired in pre-established mapping blocks over a 2 day period covering approximately 144 Km of the Mojave River floodplain and riparian zone, approximately 1500 meters in width. The multispectral imagery (green, red and near-infrared bands) was ortho-rectified using the



Lidar point cloud data in a direct geo-referencing technique. Thermal Infrared imagery was rectified to the multispectral ortho-mosaics. The lidar point cloud data was classified to separate ground surface returns from vegetation returns as well as structures such as buildings, bridges etc. One-meter DEM's were produced from the surface returns along with vegetation canopy height also at 1-meter grids.

Two surface energy balance models that use remote sensing inputs were applied to the high resolution imagery, namely the SEBAL and the Two Source Model. The model parameterizations were slightly modified to accept high resolution imagery (1-meter) as well as the lidar-based vegetation height product, which was used to estimate the aerodynamic roughness length. Both models produced very similar results in terms of latent heat fluxes (LE). Instantaneous LE values were extrapolated to daily evapotranspiration rates (ET) using the reference ET fraction, with data obtained from a local weather station. Seasonal rates were obtained by extrapolating the reference ET fraction species distribution and area were obtained from classification of the multispectral imagery.

Results showed that cottonwood and salt cedar (tamarisk) had the highest evapotranspiration rates followed by mesophytes, arundo, mesquite and desert shrubs. This research showed that high-resolution airborne multispectral and thermal infrared imagery integrated with precise full-waveform lidar data can be used to estimate evapotranspiration and water use by riparian vegetation.

8174-28, Session 7

Why confining to vegetation indices? Exploiting the potential of improved spectral observations

C. Atzberger, F. Vuolo, Univ. für Bodenkultur Wien (Austria); K. Richter, Ludwig-Maximilians-Univ. München (Germany); R. Darvishzadeh, Shahid Beheshti Univ. (Iran, Islamic Republic of)

Data sets derived from imaging spectrometers contain useful information for characterizing vegetation canopies which are not available from multi-spectral data sources. However, to fully use the information content of hyperspectral imagery, strategies have to be developed to account for the strong multi-collinearity in the data. The redundancy results from the fact that only a few variables effectively control the spectral variability is caused by only five variables: leaf area index (LAI), leaf angle distribution (ALA), soil brightness, leaf chlorophyll and leaf water content. This low dimensionality strongly contrasts with the often more than 100 spectral channels provided by modern field spectroradiometers and through imaging spectroscopy from air- and spaceborne platforms.

To deal with this data redundancy, four approaches will be presented and discussed. The first two approaches are of empirical-statistical nature, namely vegetation indices (VI) and partial least squares regression (PLS). Whereas VIs are the most traditional methods for variable retrieval from remote sensing data, PLS was developed in chemometrics for (spectroscopic) analysis of laboratory samples. With this technique, the spectral feature space is transformed in such a way that the resulting (latent) factors account for a maximum of the covariance with the target variable(s). The other two approaches belong to the physically based or hybrid methods, respectively, including radiative transfer models (RTM) combined with a look-up table (LUT) and predictive equations. By using RTMs, the interaction of the incoming electromagnetic radiation with the canopy elements and the underlying soil background is modeled based on physical laws.

Both approaches present specific advantages and disadvantages. In the case of RTM the available set of spectral-directional measurements is simultaneously used to derive the variables(s) of interest. The problem concerning data redundancy is relatively small and (white) noise is partly cancelled out. Problems with the physically based approach derive mainly from two sources: (1) difficulty of RTMs to correctly simulating (in the forward mode) the spectral signature of the canopy under study, and (2) the ill-posedness of the inverse problem due to counterbalancing effects, particularly strong between ALA, LAI and soil brightness. Moreover, appropriate weighting schemes for the spectral channels should be developed for the inversion procedures to avoid uncertainties and errors in the estimates.



With PLS very accurate (and cross-validated) models can be build whatever vegetation type is studied. However, models generally lack portability to different regions and/or growing seasons and between different sensors. A further shortcoming is the time consuming need for collecting reference data and the assumed linear relation between spectral inputs and the vegetation variables.

Benefits and drawbacks of these methodologies will be demonstrated using data acquired during a hyperspectral field campaign carried out in Sicily in 2010.

8174-29, Session 7

Goodness-of-fit measures: what do they tell about variable retrieval performance from Earth observation data

K. Richter, T. Hank, W. Mauser, Ludwig-Maximilians-Univ. München (Germany)

In view of the high number of ongoing and upcoming Earth observation missions, such as Proba-V, Sentinel families, EnMAP, Pleiades II, VEN μ S or DMC, there will be an increasing activity concerning the derivation of biophysical variables. One of the variables most relevant for many applications is the leaf area index (LAI), widely used in particular as input for process-based ecosystem modeling. A variety of methods has been developed for the quantification of LAI and other biophysical products from Earth Observation (EO) data, ranging from empirical-statistical to physically based approaches.

The capability of those models to predict the variables is usually evaluated by means of one or several goodness-of-fit measures. Many different of such statistical indices have been applied in studies dealing with LAI estimation. Among the most popular are the root mean square error (RMSE), relative RMSE (RRMSE), normalized RMSE (NRMSE), Pearson correlation coefficient (R), coefficient of determination (R²), mean bias error (MAE), relative percentage error as well as slope and intercept values. Hence, the greatest difficulty for the readers is the lack of comparability between the different models' accuracies, when different statistical indices are applied.

The objective of our study, therefore, is to provide an overview about the various statistical techniques employed for the quantitative assessment of LAI retrieval performance, being one of the key variables for vegetation monitoring. Furthermore, we aim to suggest an 'optimal statistical measure' not too sensitive to the magnitude of values, outliers or additive differences between observations and model predictions. For this purpose, a literature review is carried out, summarizing the statistical measures that have been used to quantitatively assess model performances, concentrating on the retrieval of LAI. Supported by some exemplary datasets, a range of statistical measures is applied and the results discussed regarding their information content and differences as a function of the heterogeneity of the LAI datasets.

Results show that most frequently used measures such as absolute RMSE or R² might not always be the most appropriate. Moreover, uncertainties connected to the simulations (and observations) should be quantified and illustrated in a suitable way. In conclusion we define possible standard statistic(s) to guarantee comparability of (LAI etc.) model prediction accuracies, enabling a better intercomparison of scientific results in the context of the high data availability associated with upcoming EO missions.

8174-30, Session 7

11

Use of MODIS data to map the growing season and biophysical parameters during the growing season in northern Norway and northern Finland

S. R. Karlsen, K. Høgda, Norut Tromsø (Norway); A. Tolvanen, Finnish Forest Research Institute (Finland); B. E. Johansen, Norut Tromsø (Norway)

The study area of northern Norway and northernmost Finland is an ecologically heterogeneous region in the arctic/alpine-boreal transition

area. Changes in the timing of the growing season (phenology) are among the most sensitive indicators of changes in temperatures in the northern areas. The aim of this project is to study the spectral properties of different ecosystems for improved mapping of the growing season, and then to extract biophysical parameters during the mapped growing season.

To map the growing season we use the MOD09A1 product, with 8-days composites, 500m resolution and 7-bands reflectance for the 2000 to 2010 period. In the calibration process, first every 8-day period were visually inspected for clouds. The noisiest 8-day periods were then replaced with mean values from the periods before and after. Then, the spectral bands, the NDVI and other indices curves were smoothed with the TIMESAT program. After the calibration we studied the spectral reflectance of different land cover types during the growing season close to phenological observation sites, this to identify which band combinations that best monitor the onset and end of the growing season. Finally, a combined pixel-specific threshold and decision rule-based mapping method was used to determine the onset and end of the growing season. In spring, NDVI map the onset of the growing season well. In autumn, indices based on combination of a band in the visible part with a band in the short-wave infrared part best map the end of the season. The results show large variations in the onset of growing season from year-to-year during the last 11 years. The resulting phenological maps can be used in a broad range of ecological and climate change studies. The next step is to extract biophysical parameters as LAI, NPP, and albedo during the growing season. The preliminary results indicate that the standard MODIS based products for LAI (the MOD15A2 product) and NPP (the MOD17A2 product) only have a weak correlation with field data.

8174-31, Session 7

Chlorophyll and soil effects on vegetation colorimetrical characteristics

R. H. Kancheva, D. Borisova, G. K. Georgiev, Solar-Terrestrial Influences Lab. (Bulgaria)

Vegetation state assessment is a priority of remote sensing monitoring where the development of efficient means for data analysis is one of the most essential issues. The importance of the issue is related to the ever-increasing amount of data provided by numerous sensors and the strong stress being put on the accuracy of the retrieved information. In vegetation monitoring reliable spectral indicators of plant condition and growth are to be used for reliable data interpretation. The use of multispectral and multitemporal remotely sensed data and the implementation of advanced data processing technologies result in the possibility of getting different information for solving problems related to natural vegetation preservation and agricultural land use. In agriculture remote sensing is applied for the assessment of plant development processes. Along with other databases provision, it is a tool that is used for retrieving agronomic variables in order to evaluate crop current state and make predictions. Modeling and forecasting algorithms can be developed on the base of explicit knowledge of vegetation covers spectral behavior under different growth conditions. The objective of this work is to investigate the relationship of plant colorimetrical characteristics with vegetation canopy fraction and chlorophyll content. Varying soil background (in terms of soil type and fraction) and plant senescence effects on crop color features were examined using field and green-house multispectral data. The colorimetric analysis included the estimation of the tristimulus values, the trichromatic coefficients, the excitation purity and the the dominant wavelength following the standard CIE methods. The obtained results indicate that plant colorimetrical features are statistically meaningful spectral indicators for quantitative crop assessment. Simple and multiple regression models were developed using colorimetrical and spectral ratio predictors.

8174-32, Session 7

Multispectral vegetative canopy parameter retrieval

C. C. Borel, D. J. Bunker, Air Force Institute of Technology (United States)

Recent research has shown that it is possible for hyper-spectral data to invert plant reflectance spectra and estimate nitrogen content, leaf water content, leaf structure, canopy leaf area index and, for sparse canopies, also soil reflectance. The capability of retrieving leaf water content and nitrogen content has important applications in determining the health of vegetation, e.g. plant growth status, disease mapping, quantitative drought assessment, nitrogen deficiency, plant vigor, yield, etc. However hyper-spectral sensors on satellites are still in the research state whereas commercial multi-spectral sensors such as DigitalGlobe's WorldView-2 provide routinely data for precision agriculture, forestry and environmental remote sensing are applications. Using 8 bands and the fine spatial resolution of 0.5 m (panchromatic) and 2 m (multispectral) individual trees can be readily resolved.

In this paper we adapt the PROSAIL leaf and canopy model for multi-spectral vegetative canopy retrieval. The PROSAIL 5 model is composed of the SAIL (Scattering by Arbitrary Inclined Leaves) vegetation radiative transfer model for the canopy structure and the reflectance model PROSPECT4/5 for the leaf reflectance. Working on a previous paper we observed that a limited number of adjacent bands covering just the visible and near infrared can retrieve the parameters through AMOEBA inversion as well, opening up the possibility that this method can be used to analyze multi-spectral WV-2 data. Thus it seems possible to create WV-2 specific inversions using 8 bands and apply them to imagery of various vegetation covered surfaces of agricultural and environmental interest. However a pixel-by-pixel inversion using AMOEBA is too complex and a simpler path using linear regression of the multi-spectral bands was chosen. This method has the advantage that it is possible to estimate the error for each estimated parameter. The retrieved regressions and statistical significance measures show that the 8 band spectral data is able to create useful vegetation parameter maps at high spatial resolution of 2 m ground sampling distance. A regression analysis for the 8 WV-2 bands shows that using simulated canopy reflectance spectra from PROSAIL 5 the leaf area index can be determined with medium accuracy. Average leaf angle, chlorophyll content and brown pigment content can be determined with lower accuracy. However, leaf mass, structure coefficient and carotenoid content have high uncertainty. Leaf water content and soil dryness are not retrievable. In contrast, the 4 band QuickBird sensor retrieves the leaf area index with medium accuracy and the average leaf angle with low accuracy.

In this paper we will use the same methodology and add two or more bands in the 1 to 2.5 micron region to determine (1) if the accuracy improves for the already retrievable parameters and (2) if more canopy parameters can be retrieved. In particular we will investigate band selections that would help retrieval of leaf water content.

8174-33, Session 7

Exploiting the DMC satellite constellation for applications in agriculture and forest monitoring

G. Holmes, P. Stephens, DMC International Imaging Ltd. (United Kingdom)

This paper presents examples of how a number of organisations are exploiting this powerful data source for applications such as precision farming, tropical forest monitoring, land cover mapping, illicit crop detection and agricultural statistics.

The DMC consists of a growing constellation of small satellites, each carrying a wide swath (650km) optical sensor. It is an international programme with joint campaigns being coordinated centrally by DMC



International Imaging (DMCii). All sensors in the constellation are rigorously calibrated to enable all satellites to be used interchangeably within any given campaign, and to enable quantitative biophysical information to be extracted from the data.

The constellation provides a daily global imaging capability at 22m-32m resolution in three Vis/NIR spectral bands. The capability to cover large areas on a regular basis enables a different approach a number of applications that are either difficult or impossible with other data sources, and examples will be presented.

8174-34, Session 7

Evaluation of remote sensing DMP product using five years of savanna biomass field measurements in Senegal

F. Nutini, M. Boschetti, P. A. Brivio, D. Stroppiana, Consiglio Nazionale delle Ricerche (Italy); E. Bartholome, European Commission Joint Research Ctr. (Italy); G. Bèye, Ctr. de Suivi Ecologique (Senegal)

This work was carried out in the framework of the Natural Resource Monitoring in Africa (NARMA) of EU FP7 Geoland-2 project as a contribution to the ECOWAS component (Economic Community Of West African States) of the AMESD (African Monitoring of the Environment for Sustainable Development) programme, in a region characterized by food insecurity and strong biomass production variability linked to climate variations.

The purpose of the present work is to evaluate the quality of Dry Matter Productivity (DMP), one of Earth Observation derived thematic products that are distributed to African partners via EUMETCast. For this objective a comparison has been carried out with field measurements of savannah biomass, herbaceous and shrubby leaves, acquired during five years (2005-2009) with the aim to test the utility and goodness of DMP in a semiarid environment.

Study area is situated in West Africa, a region characterized by several drought during last century, with a recovery of vegetation growth during recent 20 years. Despite this positive trend, food supply remains critical in meagre years as signalled by international agencies (FAO and USAID); this conditions reinvigorate the importance of the monitoring of natural resources.

The DMP product is a spatial estimation of dry matter (DM) expressed in kg per hectare, derived from SPOT-VGT data and provided at 1km spatial resolution every ten days. DMP is oriented towards crop monitoring and yield estimation and it is based on Monteith's model of radiation use efficiency (RUE).

The evaluation was carried out thanks to the Centre de Suivi Ecologique (CSE), the Senegalese partner of AMESD which provided the field biomass measurements for the present study. The dataset made available annual biomass production values for 33 ground sites and ancillary information on sites characteristic. In order to make comparable ground and satellite data, ten days DMP data have been processed to obtain the estimation of total biomass production during the rainy period (from July to October, JASO period). Correlation analysis has been conducted looking for goodness of DMP product and analyzing the influence of ecological characteristics such as pedology, floristic composition and land cover.

Absolute values of DMP estimates are comparable with measurements of total biomass collected in the field. Statistical analysis results showed a good correlation between herbaceous production and DMP, while no significative relation was found with shrubby leaves biomass, which represents an important component of edible rangeland biomass in the case of North Senegal study area. Moreover the analysis of the different ground measurements sites showed different relationships: possible reasons for this behaviour due to site characteristic are discussed.

The paper suggests an interpretation of the DMP product behaviour and analyse other environmental variables related to rangeland biomass production in order to better explain the variance of field sampling among the different years.

8174-35, Session 7

Hybridizing multi- and mono-source classifications for tropical rainforest mapping

R. Pouteau, B. Stoll, Univ. de la Polynésie Française (French Polynesia)

By offering a multidimensional description of objects on the Earth, the use of complementary remotely sensed data generally improves land cover classification. As United Nations General Assembly declares 2011 as the International Year of Forests, this study focuses on tropical rainforests at the species scale which is an interesting structurally complex model to classify, getting higher and higher interest. The potential of multi-source fusion to deal with this level of complexity is addressed.

This work is in the Moorea Biocode Project framework (see http:// mooreabiocode.org/) and concerns obviously the island of Moorea, French Polynesia (South Pacific). A Quickbird image and a StripMap TerraSAR-X serie of images were both acquired over the island. The Quickbird product is informing on morpho-anatomical and biochemical properties of the vegetation and is providing fine Gray-Level Cooccurrence Matrix (GLCM) analysis useful for species discrimination. On the other hand, the dual-polarized StripMap TerraSAR-X scenes we used are sensible to structural properties of rainforest and its humidity rate. This SAR source fills cloudy areas - frequent in tropical high volcanic islands - of the multispectral data. We also add GIS ancillary data extracted from a 5 m-resolution Digital Elevation Model (DEM), namely elevation, slope, aspect, windwardness and wetness. Support Vector Machine (SVM) is arguably one of the most successful statistical tools to weight such a numerous and heterogeneous data set.

Contrary to the classical global approach which combines the separate rule images of a priori mono-source SVM by another SVM, we propose to use the same fusion architecture but for classes in difficulty only. Classes accurately classified with a single source are expelled from fusion since we show that fusion can perform worst than monosource classification for some source-specific classes (e.g. the tree with a white crown Aleurites moluccana is very well classified with the Quickbird source only and the montane cloud forest as well with the DEM source only). Both SVM-based fusion schemes give very good results emphasizing their ability to deal with complex structures. When the difficulty threshold (α) we introduce is appropriated, our method slightly outperforms the classical global approach in term of accuracy and reduces by a factor 2 fusion processing time in our study case. This method can be used effectively to enhance accuracy and processing speed when analyzing the wealth of information available from remotely sensed products of a complex object such as tropical rainforests.

8174-36, Session 9

Evaluation of rededge spectral information for biotope mapping using RapidEye

M. Bindel, S. Hese, C. Berger, C. C. Schmullius, Friedrich-Schiller-Univ. Jena (Germany)

Mapping of Landscape Protection Areas with regard to user requirements for detailed land cover and biotope classes has been limited by the spatial and temporal resolution of Earth observation data. With the new spatial high resolution RapidEye data providing an additional channel in the rededge region potentially new possibilities for vegetation mapping should be investigated. The presented work is part of the ENVILAND-2 project, which focuses on the complementary use of RapidEye and TerraSAR-X data to derive land cover and biotope classes as needed by the environmental agencies. The goal is to semiautomatically update the corresponding maps by utilising more Earth observation data and less field work derived information.

The rededge spectral region located between the red and near infrared (NIR) wavelengths, has proven to held valuable information on vegetation type, age and condition. In this study the goal is to evaluate the rededge spectral information compared to the shorter and longer wavelength of the RapidEye sensor. This is done with regard to the classification capability of different land cover classes. Four RapidEye images were used covering two study sites: 1. Rostocker



Heide; (Special Area of Conservation (SAC, EC Habitats Directive)), Mecklenburg-Vorpommern and 2. Elsteraue (Landscape Protection Area) near Groitzsch, Sachsen. Both test sites are located in Germany. RapidEye data was atmospheric corrected and orthorectified. The spectral bands were analysed for redundant information by using regression and hypothesis testing. Other analysis focused on class separability issues. Tested classes are mainly different broadleaf and needleleaf forest and grassland classes. For the rededge band and for every class combination present in the study area different separability measurements like divergence or Bhattacharyya distance were computed. As result there are for every class a separability values. The separability values are provided for all spectral bands. A comparison of the values showed the applicability of the rededge for the classification. Furthermore a classification using the different spectral bands for every class was performed. This classification and the following accuracy assessment supplement the results of the separability analysis. Results have shown that additional rededge information leads to similar class separability and classification capabilities for vegetation classes as using red and NIR spectral information. Some specific classes can be classified with a higher accuracy by additional using the rededge information.

8174-37, Session 9

Estimation agricultural crops area by object based image analysis in Tabriz County, Iran

B. Feizizadeh, T. Blaschke, Univ. Salzburg (Austria)

Land use agricultural databases are an essential source of information for natural resource management and spatial variability in a crop field creates a need for precision agriculture. The maintenance of this type geo-databases is expensive and time consuming, and the updating rate must be high in order to make them useful. Currently economical and rapid means of identifying spatial variability is obtained through the use of remote sensing. While remote sensing has made enormous progress over recent years and a variety of sensors now deliver medium and high resolution data. Remote sensing methods and techniques have proved to be very useful for these applications. However, remote sensing imagery needs to be converted from raw information into tangible information that can be utilized in conjunction with other data sets, for example within Geographic Information Systems. To development of automatic feature extraction and object based classification methods can facilitate the progressive improvement of the updating tasks of spatial databases. This research proposes an Object Based Image Analysis (OBIA) based technique to classify agricultural crops, exploring information of satellite images of SPOT in Tabriz County Iran, which nowadays is one of the most important human habitations, industrial regions and agricultural activities in the East Azerbaijan province (North-Western Iran). Endeavours of our research to estimate agricultural crops area based on object-based classification techniques. OBIAs are used to relate the varying spectral response for different crop classes. The method recognizes different agricultural crops by analyzing their spectral profiles over a sequence of medium resolution satellite images. In our approach the spectral behaviour of each crop class is modelled by a specific OBIA. A segment-based classification is performed using the average spectral values of each image segment across an image sequence, which is subsequently submitted to the OBIAs of each crop class. The image segment is assigned to the crop class, whose corresponding OBIA delivers the highest probability of emitting the observed sequence of spectral values. In order to evaluate the classification results for the satellite imagery, the overall accuracy and Kappa coefficient were calculated. In a consecutive stage a geodatabase was created by calculating the geometric characteristics of each land use class and final results are presented.

8174-38, Session 9

Remote mapping of susceptible areas to soil salinity, based on hyperspectral and geochemical data in the southern part of Tunisia

M. Bouaziz, Technische Univ. Bergakademie Freiberg (Germany) and National School of Engineers of Sfax (Tunisia); R. Gloaguen, Technische Univ. Bergakademie Freiberg (Germany)

Monitoring and identification of encountered salinity can be undertaken by a variety of methods including remote sensing, geographic information system (GIS), airborne optical and radar, groundwater monitoring surveys. Spectral properties, supervised classification and salinity indices were used to discern salinization features and patterns from south-eastern Tunisian soils.

The electrical conductivity (EC) from 102 sites was determined (1:5 soil/water suspension method) to test the capability of each indicator to identify salt-affected areas, based on correlations between indicators and EC (ground-truthing). Ground points collections and acquired remote sensing data were carried out at the dry season period of 2010 (Jun and Jully). At this period the accumulation of salts at the surface is maximum, providing better conditions under which salt affected area are most easily detectable. Support Vector Machine, Maximum Likelihood and Minimum distance classifiers are used to map the different level of soil salinity classes. Data from the geochemical analysis and field work are used as input for these classifiers. A map representing the water table level in the region is generated from the ground water information collected. The ground water map shows the high susceptible area to soil salinity (i.e. High susceptibility regions occur with a water table level less than 3 m depth). This map is combined with map of irrigation area (high susceptible to salinity due to salty irrigation water) and used to provide the map of susceptibly to soil salinity.

The spectral capabilities of hyperspectral imagery for salinity mapping have been investigated. Pearson correlation between spectral bands and remote sensing indices and the EC measurements from ground truth was used.

RESULTS

14

The present study evaluated the scope of remote sensing indicator from Hyper-spectral data for the assessment and monitoring of salt affected area. The followed remote sensing methodology provided a reliable variety of indicators to address the widely spread complex problem of land degradation by salinity. The correlations found in this study are not so high but they reveal the level of contribution of various spectral indicators to predict salt affected areas in the South-east of Tunisia. The results showed that salt affected soils reflect more incident energy in the VIS and NIR. In addition, the combination of data from ground water depth, ground truth measurements (Electro-Conductivity) and the spatial distribution of irrigation area could be an efficient parameter to prepare a susceptible soil salinity map.

8174-39, Session 9

Multitemporal classification of agricultural crops in the Czech Republic

P. Stych, Charles Univ. in Prague (Czech Republic)

The aim of this study is to analyze seasonal developments concerning the state of vegetation using MERIS and Landsat data. Spectral characteristics of vegetation were observed in selected locations in the Czech Republic. Changes in vegetation, with a focus on forests and agricultural land, were examined. Spectral characteristics of vegetation were examined both by analyzing changes in reflectivity as well as by utilising vegetation indices. These results were used for classification of agricultural crops. Time series MERIS and Landsat images from April to September 2009 and 2010 were the primary input data.Calculating the selected vegetation indices was the next step. All operations were performed using the MERIS Vegetation Processor, NDVI Processor and MERIS FAPAR Processors in BEAM. The neuron networks method is involved in the Vegetation Processor algorithm and 11 MERIS spectral bands (excluding the 1st, 2nd, 11th and 15th bands) plus additional



data from the MERIS 1P product are used. Outputs consisted of LAI, fAPAR, fCover and LAIxCab indices. The NDVI Processor uses information from the 6th and 10th spectral bands. Phenological phases of vegetation, respectively the period of maturity can be determined from selected vegetation indices. Average reflectance and vegetation indices were calculated inside the masks in SW BEAM. The presented study investigates the possibilities of using MERIS high temporal and Landsat data to monitor the spectral characteristics of vegetation. High time resolution data offers the possibility of using all of these data to map agricultural land. For the year 2009 and 2010, detailed data for reference categories of maize, cereals, beet, oilseed rape, permanent grassland and hops was obtained by field investigation and information from LPIS. High time resolution data offers the possibility of using all of these data to map agricultural land. Fields in the Czech Republic have an average size of roughly 12 ha and can be as large as 300 ha. Therefore, the landscape structure is suitable for using the fusion MERIS and Landsat data. Crop classification from MERIS and Landsat was done in the Czech Republic.

8174-40, Session 10

Investigating agro-drought in the Lower Mekong Basin using MODIS NDVI and land surface temperature data

N. Son, C. Chen, C. Chen, National Central Univ. (Taiwan)

Agro-drought usually refers to the shortage of water for crop irrigation in a short period, creating serve impacts on crop production due to insufficient soil moisture. Over the last decades, this phenomenon has been concerned as a prevailing challenge for rice farmers in the Lower Mekong Basin (LMB), especially in the dry season (from November to April). The LMB includes four Southeast Asia countries in part: Laos, Thailand, Cambodia, and Vietnam. Thus, information on agro-drought is important for water management and planning in respect to food security in the region. The main objective of this study is to investigate the applicability of monthly MODIS normalized difference vegetation index (NDVI) and land surface temperature (LST) data for agro-drought monitoring from 2007 to 2010. The data was processed for the dry season because this period is usually suffered from droughts. A simple temperature vegetation difference index (TVDI) was used to estimate the surface soil moisture content. The monthly precipitation from TRMM (Tropical Rainfall Measuring Mission) data were collected and used for verification of the TVDI results. The results achieved by investigating the sensitivity between TVDI and TRMM precipitation data revealed good agreement between the two datasets. This indicated that the TVDI was declined during or after rain events indicating greater soil moisture content, but increased again later indicating less soil moisture content.

The results by analysis of TVDI showed that the moderate and serve droughts were spatially scattered over the region from November to March and backed to normal condition by the end of the dry season (April) with the onset of rainy season. The drought was found more serve and extensive in plains of Thailand and Cambodia. The larger area of serve drought was especially observed for the 2008-2009 dry seasons compared to that of 2007 and 2010. The results achieved from this study could be useful for crop production in terms of irrigation scheduling and water management.

8174-41, Session 10

Potentials of RapidEye time series for improved classification of crop rotations in heterogeneous agricultural landscapes: experiences from irrigation systems in Central Asia

C. Conrad, M. Machwitz, G. Schorcht, F. Loew, S. Fritsch, Julius-Maximilians-Univ. Würzburg (Germany); S. W. Dech, Deutsches Zentrum für Luft- und Raumfahrt e.V. (Germany) and Julius-Maximilians-Univ. Würzburg (Germany)

From the early beginning of Earth observations from space, remote sensing has become an important tool for the generation



of geoinformation supporting management of agricultural areas at different scales. Various agricultural parameters have been derived consisting of agricultural area extent, intensity of use, yield prediction, drought detection, evapotranspiration, water demand estimation (irrigation agriculture), bioenergy and straw potentials, and many more. For all of these parameters, the accurate classification of crops and crop rotation can be seen as basic prerequisite.

For accurate discriminations of crop types with multispectral remote sensing the optimum data selection usually depends on characteristics of the agroecosystem, field sizes, cropping patterns, seasonality, and the heterogeneity of the surrounding landscape. Especially, the tradeoff between geometric and temporal resolution hampered standardized and operational delineation of crops with acceptable accuracies. While phenologies can be mapped using time series, pixel sizes of moderate resolution available for time series exceed field sizes in many agricultural landscapes. Vice versa, geometric high resolution data often hardly capture all necessary crop phenological stages of the observed agroecosystem during classification. The RapidEye system launched in 2008 was expected to overcome these limitations.

This contribution summarizes experiences of classifying crops and crop rotations of different irrigation systems in Uzbekistan (Fergana Valley, Khorezm, Karakalpakstan) using multiple observations of 6.5 m RapidEye data. RapidEye data were partly supplemented with 30 m Landsat 5 TM acquisitions. Phenological developments of various crops (cotton, wheat, rice, wheat-rice, wheat-maize, sorghum, maize, alfalfa, mixture of trees and crops, trees, sunflowers, watermelons) were extracted from fields of different sizes and demonstrate the potential for crop monitoring in comparatively heterogeneous and fragmented agricultural systems. A two-step field based procedure for classifying crops and crop rotations in irrigation systems of Central Asia has been developed. First, field parcels were extracted by segmentation using SPOT 5 or ALOS PRISM data at a scale of 2.5 m or the RapidEye data. Second, a random forest was applied to multi-temporal spectral information aggregated at field level.

Overall classification accuracies ranged between 80.82% (RapidEye combined with Landsat) and 88.1% (RapidEye). In comparison to previous studies, the number of classes and hence the level of detail could be increased by the high resolution of RapidEye. However, not all time steps improved the classification accuracies. Testing the impact of single time steps on the classification accuracies resulted in a recommendation scheme for the acquisition dates and number of scenes most useful for valid crop distribution maps. As optimization, the integration of temporal features and texture parameters in the classification routine is suggested.

The results have been used in different projects for subsequent calculation of field water demands, simulations of irrigation water distribution, and modelling crop yields in Central Asian irrigation systems. The presented classification approach is assumed to be applicable to all agricultural systems in Central Asia (eight million ha irrigated land) and in many other semi-arid regions.

8174-42, Session 10

15

Spectral and agronomic indicators of crop yield

R. H. Kancheva, D. Borisova, G. K. Georgiev, Solar-Terrestrial Influences Lab. (Bulgaria)

Being recognized as a powerful tool in many scientific and application fields, remote sensing enters recently still wider into its application stage when the goal is to bring the up-to-now investigation results to an operational use. Agricultural monitoring is among the priorities of remote sensing observations supplying early information on the development and growth conditions of crops. Various approaches are implemented for crop behaviour assessment in order to provide objective, timely and quantitative yield forecasts at regional and national scale (agro-meteorological models, remote sensing methods, area estimates). On the other hand, continues the research to improve the reliability of the results by implying, for instance, different sampling strategies, different statistical data analysis and extrapolations, and different use of remote sensing data. In this paper we propose an algorithm for yield forecasting and predictions verification based on the following main steps: 1-development of inverse crop radiative

transfer models for estimation of crop state variables from radiometric data; 2-development of yield prediction models based on key crop state bioparameters and considering plant phenology; 3-current yield forecasting models from crop radiometric data; 4-yield forecast updates from time series radiometric data; 5-yield predictions verification from crop biophysical models.

8174-43, Session 10

Monitoring rice growing areas in the Lower Mekong subregion from MODIS satellite imagery

C. Chen, C. Chen, S. T. Nguyen, National Central Univ. (Taiwan)

Rice is a staple food crop and plays an important role in the economy of the Lower Mekong Subregion (LMS) countries. Rapid population growth in this region has caused increasing demand for food while environmental degradation continues. To balance between food needs and rice production while safeguarding the environment, a jurisdiction of rice crop monitoring framework is required. By using the information of rice crop monitoring, policymakers can draw up strategies to ensure security of the food supply and environment resource. This study aims at the applicability of time-series MODIS data for monitoring rice cultivation areas in the LMS during 2001 to 2010. Data processing involves three main steps: 1) constructing indices derived from timeseries MODIS indices: Normalized Difference Vegetation Index (NDVI), Land Surface Water Index (LSWI), and Normalized Difference Soil Index (NDSI); 2) Filtering time-series MODIS data; 3) developing a classification algorithm that uses smooth time series of MODIS-derived vegetation indices to discriminate rice fields from non-rice areas based on rice phenological profiles and surface moisture. The results validated with rice area statistics indicate the good agreement between the datasets at the subnational level. The information from the result is useful for rice production estimation, water irrigation scheduling and other environmental application.

8174-44, Session 10

Plastic covered vineyard extraction from airborne sensor data with an objectoriented approach

E. Tarantino, A. Aiello, Univ. degli Studi di Bari (Italy)

The Apulia Region is one of the most prone Italian area to soil alteration phenomena due to geographical and climatic conditions, surface karstic textures and morphology, hydrogeological balance changing and also to intense human activities.

In the last years, the widespread vineyard cultivation have showed negative consequences on the hydrogeological balance of the Apulia soils as well as the visual quality of rural landscape was significantly altered by an heavy diffusion of artificial coverings. The generalized coverage of vineyards with plastic sheets concentrates the rainfall along vineyard borders. This phenomenon precludes the soil wetting and the rainwater infiltration, and transforms the major part of the precipitation in runoff. The modified hydrogeological behavior of the surface makes floods much more common than a few years ago, especially in the Ionian side of the Apulia Region.

In order to monitor and manage this phenomenon, a detailed site mapping become essential. Plastic covered vineyard extraction from high spatial resolution imagery poses unique challenges that require new interpretation procedures.

Generally, extraction methods are chosen according to data availability and level of detail to achieve. National coverage true color aerial digital data sets with excellent spatial detail are routinely produced, such as every one or two years, for many countries. In multi-temporal analysis they can be compared with scanned historic aerial photography for assessing and predicting change based on long-term trends. However, in such data there is a loss of basic information due to occlusions, low contrast, lack of infrared and thermal information or disadvantageous perspective.

Traditional pixel-based supervised classification methods require the creation of training sets to include the different signatures of various features within the targets. Furthermore, with the increase of spatial resolution, single pixels no longer capture the characteristics of classification targets. Consequently, classification accuracy is reduced. Object-based image classification techniques overcome these difficulties by first segmenting the image into meaningful multipixel objects of various sizes, using both spectral properties and geometric attributes of pixel groups, such as scale, colour, smoothness and shape. Then the segments are assigned to classes using fuzzy methods and hierarchical decision key. Moreover, incorporation of additional or ancillary data sources (i.e. DSM and NIR/TIR) in the classification process may result in achievement of higher accuracy than utilizing a sensor data alone. The ancillary data from various sources may be available in different forms and contexts, and at different frequencies, time, and spatial domains.

In this study an object-based classification procedure from Very High Spatial Resolution (VHSR) true color aerial data is developed on a test area located between Ginosa and Palagiano (Apulia Region - Italy) in order to support the update of existing land use database aimed at plastic covered vineyard monitoring. Ancillary data sources, as the elevation information and the multispectral capability of satellite data, will be used to improve the accuracy of results.

8174-45, Session 11

Monitoring Mediterranean marine pollution using remote sensing and hydrodynamic modelling

F. Capodici, G. Ciraolo, Univ. degli Studi di Palermo (Italy); A. Drago, Univ. of Malta (Malta); G. La Loggia, A. Maltese, Univ. degli Studi di Palermo (Italy)

Human activities contaminate both coastal zone and open sea, even if in different ways, in terms of pollutants, ecosystems and recovery time. In particular offshore pollution of Mediterranean sea is mainly related to maritime traffic of oil accounting for a quarter of the global maritime traffic. Maritime traffic caused nearly 7% of the world oil accidents during the last 25 years, thus inducing serious biological impacts on both open sea and coastal zone habitats.

The paper firstly provides a general review of maritime pollution monitoring using integrated approaches of remote sensing and hydrodynamic modelling; focusing on the main results of the MAPRES project (Marine pollution monitoring and detection by aerial surveillance and satellite images) that synergistically coupled remote sensing and forecast modelling, to define cleanup measures and estimate environmental consequences. Secondly, the paper investigates oil spill detection using SAR images, and reports the first results of the "Monitoring of marine pollution due to oil slick", a "COSMO-SkyMed: - Progetti Scientifici" project. The research has been carried out using X-band SAR images provided by the Italian Space Agency (ASI). Finally, hydrodynamic simulations will be validated within the framework of CALYPSO (CALYPSO-HF Radar Monitoring System and Response against Marine Oil Spills in the Malta Channel) project, a PO 2007-2012 Italia-Malta project aiming to set up a permanent and fully operational HF radar observing system, to record (in real-time with hourly updates) surface currents within Malta channel. Collected data, combined with numerical models, will help to optimize intervention in case of oil slicks eventually occurring within an high traffic sea road, the marine space between Malta and Sicily.

8174-46, Session 11

16

Ecological study wetland vegetations in Ichkeul marshes (north of Tunisia) by using remote sensing techniques and and field obeservations

K. Zeineb, Univ. Paris-Est Marne-la-Vallée (France); Z. Lili, Institut National Agronomique Tunisie (Tunisia); B. Deffontaines, Univ. Paris-Est Marne-la-Vallée (United States); R. Caloz, Ecole Polytechnique Fédérale de Lausanne (Switzerland); M. J. Ellloumi, Agence Nationale de Protection de l'Environnement (Tunisia)



How to map and study carefully wetland vegetations influenced by salinity, pH, and immersion/emersion in coastal areas especially those submitted to major anthropic influences? Integrated numerical topographic-bathymetric data was then used to improve the object-oriented classification of an Aster (2007) multi-spectral imagery data covering the studied area of the Ichkeul marshes (North Tunisia). Such work is validated in the fields by botanic observations done along many transects.

The resulting classification was used to evaluate both ecological amplitude and ecological preferences of species. As, the eight classified vegetation communities differenciated in the lchkeul wetlands were studied by identify the ecological factors mostly influencing species distribution within a particular vegetation in order to evaluate both ecological amplitude and ecological preferences of species. Different ecological profiles were settled for three factors (altitude, pH and electrical conductivity) from a data set of 265 phytosociological field studied sites, and from measures, carried out in selected sites, for hydrochemical variables (pH and salinity).

By applying a statistic test to ecological profiles, the species significantly deviating from uniformity were detected.

More specifically for altitude, it is not possible to explain the shift considering the reduced elevation amplitude with correlation to the salinity in the whole area. Furthermore, dealing with pH, bolboshenus communities occurs in less basic habitats, probably due to the soil characteristics in lchkeul marshes.

8174-47, Session 11

Jellyfish prediction of occurrence from remote sensing data and a non-linear pattern recognition approach

A. Albajes-Eizagirre, M. Haneda, L. Romero, A. Soria-Frisch, Starlab (Spain); Q. Vanhellemont, Institut Royal des Sciences Naturelles de Belgique (Belgium)

Impact of jellyfish in human activities has been increasingly reported worldwide in the last years. Segments such as tourism, water sports and leisure, fisheries and aquaculture are commonly damaged when facing blooms of gelatinous zooplankton. Hence the prediction of the appearance and disappearance of jellyfish in our coasts, which is not understood from its biological point of view, has been approached as a classification problem, a set of potential ecological cues was selected to test their usefulness for prediction. Remote sensing data was used to describe environmental conditions that could support the occurrence of jellyfish blooms, with the aim of capturing physicalbiological interactions: forcing, coastal morphology, food availability, and water mass characteristics are some of the variables that seem to exert an effect on jellyfish accumulation on the shoreline, under specific spatial and temporal windows. A data-driven model based on computational intelligence techniques has been designed and implemented to predict jellyfish events on the beach area as a function of environmental conditions. Data from 2009 over the NW Mediterranean continental shelf have been used to train and test this prediction protocol. Standard level 2 products are used from MODIS (NASA OceanColor) and MERIS (ESA - FRS data). After application of the included level 2 flags and additional quality checks for turbid waters, the data products are reprojected to a standard grid, 1 Km and 250 m for MODIS and MERIS respectively. Adjacent overpasses are stitched together and if overlap occurs in the MODIS data, the best quality data is retained, based on viewing geometry. The procedure for designing the analysis system can be described as following. The aforementioned satellite data has been used as feature set for the performance evaluation. Ground truth has been extracted from visual observations by human agents on different beach sites along the Catalan area. After collecting the evaluation data set, a cross-fold validation is established for comparing the performance between different computational intelligence methodologies. The outperforming one in terms of its generalization capability has been selected for prediction recall. Different tests have been conducted in order to assess the prediction capability of the resulting system in

operational conditions. This includes taking into account several types of features with different distances in both the spatial and temporal domains with respect to prediction time and site. The implementation and performance evaluation results are detailed in the present communication together with the feature extraction from satellite data. To the best of our knowledge the developed application constitutes the first implementation of an automate system for the prediction of jellyfish appearance founded on remote sensing technologies. Moreover the results can be used in order to throw new light on the ecological procedures underlaying jellyfish appearance.

8174-48, Session 11

Characterizing the spectral signatures and optical properties of dams in Cyprus using field spectroradiometric measurements

D. G. Hadjimitsis, C. Papoutsa, Cyprus Univ. of Technology (Cyprus)

This paper presents the results obtaining for carrying out two years (2010-2011) field spectroradiometric measurements at Asprokremmos and Kourris Dams in Cyprus, the biggest dams in the Island. A GER-1500 field spectroradiometer was used to maesure the in-situ reflectance. During the spectroradiometric measurements Turbidity, Temperature and Chl-a were acquired so to provide a tool for analysing the retrieved spectral signatures. Apparent and inherent optical properties have been determined.

8174-49, Session 11

Development of Japanese inland water surface temperature database using ASTER thermal infrared imagery

H. Tonooka, M. Hirayama, Ibaraki Univ. (Japan)

Many water bodies like lakes and marshes are inhabited by many lives. For these lives, water temperature is an important environmental factor, because water temperature influences and regulates many chemical, physical and biological processes, including metabolic rates of aquatic organisms. Temperatures shift may cause to replace some species by others in an ecosystem, because the aquatic biota has an optimum temperature range for growth and reproduction. An increase of water temperature causes a decrease of oxygen solubility in water. Thus, water temperature monitoring for water bodies is important for water environment studies. In the case of Japan, water temperature is, however, not fully or never monitored for most of small water bodies except for some of major water bodies, partly because in-situ temperature measurements are not easy for small water bodies which are widely scattered and variously managed by individuals, companies, governments etc. We are therefore developing a Japanese inland water surface temperature database (JIWSTD) using thermal infrared (TIR) imagery observed by the Advanced Spaceborne Thermal Emission and Reflection Radiometer (ASTER) onboard the NASA's Terra satellite. The present paper involves the current status of the database, its system design, its water surface temperature retrieval algorithm, some validation results, and so on.

8174-50, Session 11

Preliminary work of mangrove ecosystem carbon stock mapping in small island using remote sensing: above and below ground carbon mapping on medium resolution satellite image

P. Wicaksono, H. Hartono, P. Danoedoro, Univ. Gadjah Mada (Indonesia); U. Nehren, L. Ribbe, Fachhochschule Köln (Germany)



Mangrove forest is an important ecosystem located on coastal area that provides various ecological and economical services. One of the service provided by mangrove forest is the ability to act as a long term carbon sink by sequestering CO2 from atmosphere through photosynthesis and carbon burial on the sediment. The carbon buried on mangrove sediment may persist for millennia before return to the atmosphere, and thus act as an effective long-term carbon sink. As a consequence, mangrove forest is very promising for the future climate change mitigation and adaptation strategy. Therefore, it is important to understand the distribution of carbon stored within mangrove forest in a spatial and temporal context. However, currently, the information about carbon dynamics in mangrove forest is limited due to the difficulties of having proper measurement and monitoring using field survey. In this work in progress, an effort to map carbon dynamics in mangrove forest is presented using remote sensing technology to overcome the handicap encountered by field survey. In this paper, the use of medium spatial resolution Landsat 5 TM, ASTER, and ALOS image is emphasized. These images are widely available and cover large portion of earth within one scene, and thus provide a cost and time effective way of mapping mangrove forest carbon dynamics. The mangrove ecosystem carbon dynamics considered here are above and below ground carbon stock of mangrove including the soil carbon stock. The relationship between measurable tree dimension and mangrove carbon stock is evaluated and the best surrogate variable is determined. Carbon stock value is determined from allometric equation developed for each mangrove species. For species without existing allometric equation, common allometric equation is used. Soil carbon stock is analyzed in the laboratory. From the field data, various image processing techniques including Principle Component Analysis (PCA), Linear Spectral Unmixing (LSU), Spectral Angle Mapper (SAM), and Vegetation Index are evaluated to find the best method to explain the variation in mangrove carbon dynamics using remote sensing data. Finally, the technique which produces significantly better result is used to produce map of mangrove forest carbon dynamics, which is spatially extensive and temporally repetitive.

8174-51, Poster Session

Multi-angle, multi-polarization backscatter model inversion for soil moisture estimation using Radarsat-2 data

A. Merzouki, H. McNairn, A. M. Pacheco, Agriculture and Agri-Food Canada (Canada)

Managing and mitigating risk to the agriculture sector requires information and knowledge to assess risk potential, implement risk reduction strategies, and deliver essential responses. The availability of water, in particular the amount of moisture held in the soil, presents a significant risk factor for this sector. Thus monitoring available soil moisture is important in the assessment of agricultural risk. Synthetic aperture radars (SARs) are sensitive to the dielectric properties of soils and are thus well suited to provide quantitative soil moisture estimates to support effective risk assessment and mitigation. With the launch of RADARSAT-2 in 2007, Agriculture and Agri-Food Canada (AAFC) began testing the potential of fully polarimetric SAR data to estimate surface soil moisture. For validation purposes, ground measurements over a test site in southern Manitoba have been collected since in spring of 2010, simultaneous with RADARSAT-2 data acquisitions.

It is well known that empirical and semi-empirical models require the derivation or adaptation of model coefficients to suit local conditions and this presents challenges for large area operational implementation. Physical models like IEM are more robust. In a preliminary sensitivity analysis, a better agreement was found between the calibrated IEM results and SAR-based backscatter coefficients compared to the original IEM results. The calibrated IEM also reduced the impact of variation in incidence angle on both the HH and VV backscatter coefficients. Inversion of the calibrated version of this model was implemented using a look up table (LUT) optimization. The LUT was generated by simulating HH and VV backscatter coefficients using a specific formulation of the optimum roughness correlation length. Two approaches were considered: the multi-polarization method where only measured backscatter coefficients were used within the inversion routine and the multi-angle method where image-derived backscatter coefficients from ascending/descending acquisitions were combined.



Of the two inversion configurations, results showed that the calibrated IEM was able to retrieve volumetric soil moisture with an improved accuracy when a hybrid (multi-angle + multi-polarization) inversion scheme is adopted.

8174-52, Poster Session

A diachronic analysis of estuarine turbidity due to a flood following an extreme rainfall event

G. Ciraolo, Univ. degli Studi di Palermo (Italy); A. Granata, Agenzia Regionale per la Protezione Ambientale (Italy); G. La Loggia, A. Maltese, Univ. degli Studi di Palermo (Italy)

Rivers bring to their mouths the higher concentration of sediments, occasionally, during floods following rainfall events of certain intensity and therefore characterized by long return period.

This paper deals with a qualitative assessment of coastal water and turbidity load in estuarine areas as a consequence of an intense rainfall event occurred in 2001 in the eastern part of Sicily.

Empirical relationship to map turbidity using remote sensing can be found in literature, however model parameters have to be calibrated by means of in situ measures obtained by intensive field campaigns. The algorithm used within this research was calibrated using field data acquired during three periods in 2008 (at the beginning of July, August and September).

The plumes caused by two rivers, the Simeto and Anapo, were analyzed spatially and temporally. The rivers belong to catchments characterized by different pedology and surface. It was proved that the turbidity plume at the estuary has a strict correlation with distance from river mouth, however it strongly depends on catchment characteristics.

Finally a multitemporal analysis of MODIS images, with 250 m spatial resolution, shown that nephelometric turbidity rises as the flow discharge reaches the gulf, than it sharply decreases to reach an asymptotic undisturbed value approximately after a decade. Due to their low spatial resolution, if compared with characteristic plume dimension, MODIS images having a spatial resolution of 1000 m were supposed not appropriate for this kind of application.

8174-53, Poster Session

Drought analysis in north China based on observed and satellite TRMM precipitation data

Y. Ren, Ctr. for Earth Observation and Digital Earth (China)

Precipitation shortage has become one of the severest problems in northern China. Henan, Anhui, Shanxi, Shandong, Hebei, Jiangsu and so on were suffering from the droughts from 2009.

In this paper, the spatial and temporal characteristics of drought in China are analyzed. Average monthly precipitation data of the selected 756 observation stations in Chinese mainland from January 1951 to February 2011 are spatial grid. Different interpolation methods were used and compared. Results show that mixed method, namely the combination of multiple regression and kriging interpolation method, is the best one for its high prediction accuracy verified by three validated stations. The new data are then analyzed by using the Empirical Orthogonal Function (EOF) method. The results reveal the space and time modes which represent the El-Nino, La-Nina and Drought in china.

The satellite TRMM data of sea surface average monthly precipitation from January 1998 to December 2010 over Pacific Ocean are also processed with the same method. The results reveal the space and time modes which represent the El-Nino, La-Nina and precipitation over Pacific Ocean.

8174-54, Poster Session

Landscape freeze-thaw monitoring using passive microwave remote sensing

L. Li, J. Shi, J. Du, Institute of Remote Sensing Applications (China)

Over one-third of the global land area undergoes a seasonal transition between predominantly frozen and nonfrozen conditions each year. Freeze/thaw transitions influence the thermal and hydraulic properties of the soil, which in turn have a significant impact on the surface energy and moisture balance, hence on weather and climate.

Satellite microwave remote sensing is well suited for Freeze/Thaw(F/T) monitoring due to its insensitivity to atmospheric contamination and solar illumination effects, and its strong sensitivity to the relationship between surface dielectric properties and predominantly frozen and thawed conditions. We investigated the utility of multi-frequency and dual polarization brightness temperature(TB) measurements from Advanced Microwave Scanning Radiometer-Earth Observing System (AMSR-E) to map regional patterns and daily variations in Landscape F/T cycles of Chinese region. We applied a temporal change classification algorithm based on a seasonal threshold scheme to classify daily F/T states from time series TB measurements, it has successfully used in the previous study. The ratio of 37GHz horizontal polarization TB (TBh) to corresponding vertical polarization TB (TBv) was used in the algorithm to eliminate the temperature effect, so it was mean the ratio of emissivity between them. Firstly the frozen and thawed reference states were calculated on a grid cell-by-cell basis by averaging AMSR-E TB ratio under air temperature defined frozen and thawed conditions, It occurred in January and July respectively. Secondly we defined a spatial and seasonal scale factor and defined threshold values similarly on a cell-by-cell basis. Finally we determined the F/T state according to the threshold values defined previously. Frozen soil areal extent and the duration of freeze/thaw process were investigated using the above frozen soil algorithm for the period from July 1, 2003 through June 30, 2004 over the Tibet Plateau. The MODIS LST and soil temperature from weather stations used to validate the results obtained from above algorithm.

8174-56, Poster Session

Use of imaging spectroscopy to assess different organic carbon fractions of agricultural soils

M. Vohland, M. Harbich, O. Schmidt, S. Thiele-Bruhn, Univ. Trier (Germany)

The site for this study is located in Rhineland-Palatinate, Germany ("Bitburger Gutland") and covers different geological substrates and agro-pedological zones (triassic sediments [sandstone, siltstone, limestone, dolomite, Keuper clays]). In total, 42 plots were sampled in the field; soil samples from the top horizon were analysed in the laboratory for total organic carbon (OC), hot water-extractable C (HWE-C) and microbial C (Cmic). Cmic and HWE-C showed significant correlations; HWE-C reflects fertilization, indicates fast turnover rates and thus allows a quantification of the decomposable, active organic matter fraction.

In parallel to the ground campaign, a data set of the HyMapTM airborne imaging sensor (Integrated Spectronics, Baulkham Hills, Australia) was acquired (27th of August 2009 near solar noon). These data covered the wavelength range between 0.45 and 2.48 µm with 125 spectral bands and a bandwidth of approximately 16 nm; in the overflight, a ground resolution of 4 m was realized.

After pre-processing (including atmospheric and cross-track illumination correction), HyMap spectra were used to calibrate OC, HWE-C and Cmic. As calibration method we used partial least squares regression (PLSR), as it allows a handling of large input spaces and noisy patterns. As calibration quality was poor for all three constituents (R² values were less than 0.5 for Cmic and HWE-C), we additionally combined PLSR with a genetic algorithm (GA) to pre-select an



optimum set of spectral features instead of using the full spectrum. A GA follows the strategy of a purely stochastic selection of an initial set of spectral variables, which then is optimised by considering many combinations of features and their interactions in many runs. At the end of all runs, the spectral variables (genes) of the fittest chromosomes are accepted for the final PLSR model.

With this approach, results improved considerably for all constituents in the cross-validation. With GA, the importance of the measured spectral variables for prediction can be assessed via the obtained selection frequencies. Thus, the resulting selection patterns were finally analysed and compared for the examined C fractions.

8174-57, Poster Session

Application of large footprint full GLAS waveform data on savanna vegetation

E. Khalefa, H. Balzter, Univ. of Leicester (United Kingdom)

Savannas cover approximately half of the African land surface and considered to be one of the most important, but least understood terrestrial ecosystems. Growing recognition of the importance of the structural component of savanna landscapes has highlighted the need to understand the spatial distribution and temporal dynamics of woody plant structural diversity. The relatively new Ice, Cloud and Elevation Satellite (ICESat) and its sole onboard instrument, the Geosciences Laser Altimeter System (GLAS) has been an active area of research in recent years, specifically in temperate and boreal forests, but been insufficiently explored for ecological research in savanna ecosystems. The main objective of this research is to assess the ability of ICESat/ GLAS LiDAR full waveforms to retrieve canopy structure over savanna vegetation landscapes in Kruger National Park in South Africa to understand the landscape dynamics which has great implications for land management. The Geoscience Laser Altimeter System (GLAS) instrument on ICESat provides various data products, of which GLA14 and GLA01 are of interest in this study. The GLA01 Level 1 product provides the transmitted and received waveform from the instrument, while the GLA14 Level 2 product is intended to represent the potential complexities of returns from land. The results showed that the GLAS waveform data provides reasonable prediction for the savanna structural characteristics such as vegetation height and density which are comparable to the results obtained from airborne LiDAR data and field measurements.

8174-58, Poster Session

19

An improvement of satellite-based algorithm for gross primary production estimation optimized over Korea

K. Pi, K. Han, I. Kim, S. Kim, M. Lee, Pukyong National Univ. (Korea, Republic of)

Monitoring the global gross primary production (GPP) is relevant to understanding the global carbon cycle and evaluating the effects of interannual climate variation on food and fiber production. GPP, the flux of carbon into ecosystems via photosynthetic assimilation, is an important variable in the global carbon cycle and a key process in land surface-atmosphere interactions. The Moderate-resolution Imaging Spectroradiometer (MODIS) is one of the primary global monitoring sensors. MODIS GPP has some of the problems that have been proven in several studies. Therefore this study was to solve the regional mismatch that occurs when using the MODIS GPP global product over Korea. To solve this problem, we estimated each of the GPP component variables separately to improve the GPP estimates. We compared our GPP estimates with validation GPP data to assess their accuracy. For all sites, the correlation was close with high significance (R2 = 0.8164, RMSE = 0.6126 g•C•m-2•d-1, bias = -0.0271 g•C•m-2•d-1). We also compared our results to those of other models. The component variables tended to be either over- or under-estimated when compared to those in other studies over the Korean peninsula, although the estimated GPP was better. The results of this study will likely improve carbon cycle modeling by capturing finer patterns with an integrated method of remote sensing.

8174-59, Poster Session

Assessment of tundra-taiga boundary changes using MODIS LAI data

M. Lee, K. Han, K. Pi, S. Kim, I. Kim, Pukyong National Univ. (Korea, Republic of)

Surface of the earth temperature of the earth caused phenomenon that rise and is global warming as greenhouse gas concentration into waiting by continuous discharge of greenhouse gas increases since passing industrial revolution. While gravity about climate fluctuation is risen worldwide, place that can diminish successively biggest surface of the earth change by global warming is high latitude area of polar regions. This study observed distribution of vegetation to confirm change of tundra-taiga boundary. Tundra-taiga boundary is used to observe the transfer of vegetation pattern because it is very sensitive to human activity, natural disturbances and climate change. The circumpolar tundra-taiga boundary could observe reaction about some change. Reaction and confirmation about climate change were definite than other place. This study used Leaf Area Index(LAI) 8-Day data in August from 2000 to 2009 that acquire from Terra satellite MODerate resolution Imaging Spectroradiometer(MODIS) sensor and used Köppen Climate Map, Global Land Cover 2000 for reference data. This study conducted analysis of spatial distribution in low density vegetated areas and inter-annual / zonal analysis for using the long period data of LAI. Change of LAI was confirmed by analysis based on boundary value of LAI in study area. Development of vegetation could be confirmed by area of grown vegetation(730,325km^2) than area of reduced vegetation(22,372km^2) in tundra climate. Also, area was increased with the latitude 64° N~66° N as the center and around the latitude 62° N through area analysis by latitude. Vegetation of tundra-taiga boundary was general increase from 2000 to 2009. While area of reduced vegetation was a little, area of vegetation growth and development was increased significantly.

8174-60, Poster Session

On the Influences of vegetation biomass on COSMO-Skymed X-band

F. Capodici, Univ. degli Studi di Napoli Federico II (Italy); G. Ciraolo, Univ. degli Studi di Palermo (Italy); G. D'Urso, Univ. degli Studi di Napoli Federico II (Italy); G. La Loggia, A. Maltese, Univ. degli Studi di Palermo (Italy)

The knowledge of spatial and temporal variability of land cover is important to manage water resources for yield forecasting, water stress prediction, irrigation water management and flood protection. Widely used algorithms based on optical data are reliable but the temporal resolution is dramactically reduced by cloud cover; in addition, often the spatial resolution is inadequate for operational uses in heterogeneous areas. On the other hand, algorithms to retrieve vegetation parameters based on Synthetic Aperture Radar (SAR) observations are not yet operational or not fully validated. New SAR missions (COSMO-Skymed and Terrasar-X) may represent a suitable source of data for operational uses due to the high spatial and temporal resolution, although X band is not optimal for agricultural and hydrological applications. This paper analyses the influence of the soil-vegetation variables (especially biomass indices) on X-band COSMO-Skymed SAR data using both Ping Pong and Spotlight products. The study is carried out over two different sites: the SELE plain (in the south-eastern part of Campania, Italy) mainly characterized by herbaceous and tree crops and the Campobello-Castelvetrano area (in the south-western part of Sicily, Italy) mainly covered by olive trees, vineyards and woods.

The sensitivity analysis is performed by comparing both in situ measures and Landsat 5, 7 derived products with COSMO-Skymed images acquired in May-June 2010 within the Italian Space Agency (ASI) COSMOLAND (Use of COSMO-SkyMed SAR data for LAND cover classification and surface parameters retrieval over agricultural sites) project. Results of sensitivity analysis address developing operational algorithms aiming to retrieve both soil moisture and vegetation biomass maps with this new data source characterized by high temporal and spatial resolution, working in the X band with dual or single polarization.



8174-61, Poster Session

Airborne spray drift measurement using passive collectors and lidar systems

E. Gregorio, Univ. de Lleida (Spain); F. Solanelles, Generalitat de Catalunya (Spain); F. Rocadenbosch, Univ. Politècnica de Catalunya (Spain); J. R. Rosell, R. Sanz, Univ. de Lleida (Spain)

Minimization of the risk associated with spray applications requires a proper understanding of the spray drift phenomenon. This fact has led over the years to the development of several techniques to measure the deposition on horizontal surfaces as well as the airborne spray profiles. Assessment of airborne spray drift is particularly difficult because this phenomenon is subject to variable micrometeorological conditions. However the monitoring of airborne drift has a great importance since it can be carried over long distances from its source. This paper reviews main sampling techniques currently used to asses the airborne spray drift, based on passive collectors and tracers. Theoretical principles that determine the efficiency of passive samplers are studied as well as the performance of different types of tracers. On the other hand, this paper shows new airborne spray drift assessment techniques based on lidar technology, reviewing its principle of operation as well as its practical application in several spray drift trials. In comparison with conventional methods, lidar systems allow real-time monitoring of airborne spray drift obtaining range-resolved images of the spray plume with a more reduced personnel and time consumption. Despite the advantages of lidar systems they have been used on a limited way because currently available instruments are expensive and require trained personnel for their operation. In addition, many of these systems are not eye-safe, which hinders their practical application in terrestrial spray drift studies (quasi-horizontal sounding). The future adoption of lidar technology for airborne spray drift studies will be subjected to the development of lidar instruments really adapted to this application.

8174-62, Poster Session

20

Spatial analysis of LST in relation to surface moisture and NDBI using landsat imagery in Cheongju city

S. I. Na, J. H. Park, J. K. Park, S. C. Beak, Chungbuk National Univ. (Korea, Republic of)

Landsat TM (thematic mapper) and ETM+ (enhanced thematic mapper plus) imagery, respectively acquired in 1991, 1994, 2000 and 2006, were utilized to assess urban area thermal characteristics in Cheongju, the city of Chungbuk province in Korea. As a key indicator for the evaluation of urban environments, sub-pixel surface moisture was mapped to quantitatively determine urban LULC extent and urban thermal pattern. In order to accurately estimate urban surface moisture, tasseled cap model (TCM) was utilized to generate the proportion of surface moisture. The converted image by TCM can be plotted on the three axes of Soil Brightness, Greenness of Vegetation and Wetness. Wetness was used as a main principle of moisture associated with significant characteristics of the surface. Urban thermal characteristic was analyzed by investigating the relationships between the LST and NDBI. NDBI was used to differentiate the LULC types by setting the appropriate threshold values. It is worth noting that NDBI may have different range of values for different land-use types, depending on the study areas and different conditions of development. And in this study we observed an increasing trend of intensity of UHI (represented by LST) from 1991 to 2006. Using this information, we can estimate how changes in LULC may have contributed to the change in regional temperature.

The results indicate surface moisture is an accurate indicator of UHI effects with strong linear relationships between LST and surface moisture in 1991, 1994, 2000 and 2006. Detailed analysis of relationships between LST and surface moisture shows that variations in surface temperature could be better accounted for by differences in impervious. This implies that surface moisture can be used to analyze temperature quantitatively for UHI studies validated by NDBI. And this suggests that surface moisture, combined with LST, and NDBI, can quantitatively describe the spatial distribution and temporal variation of urban thermal patterns and associated LULC conditions. We estimated the contribution to the net increase or decrease in temperature by each surface moisture category to the regional LST dynamics. It is concluded that urbanization has led to a significant LST increase, which conforms to the changes of the total contributions of surface moisture category.

8174-63, Poster Session

Development of land surface temperature retrieval algorithm from the first Korean geostationary satellite, COMS data

M. Suh, W. Park, J. Kang, Kongju National Univ. (Korea, Republic of)

Land surface temperature (LST) is a one of the most difficult surface variables to observe regularly due to the strong spatio-temporal variation. At present, satellites remote sensing data are regarded as the only available operational systems capable of collecting cost-effective LST data at spatial and temporal resolutions appropriate to modelling applications. In this study, we have developed two LST retrieval algorithms from COMS (Communication, Oceanic, and Atmospheric Satellite) data, the first geostationary multipurpose satellite of Korea which was launched on 27 June 2010. As in other algorithms, we made the synthetic LST data through the radiative transfer simulations under various atmospheric profiles (TIGR data), satellite zenith angle (SZA), spectral emissivity, and surface lapse rate conditions using MODTRAN 4. To consider the differences in the temperature profiles at the planetary boundary layer between day and night, we developed day/night LST algorithms separately based on the temperature profiles. To minimize the LST inconsistency at the boundary time and/or region caused by the two different LST algorithms (day/night algorithms), the final LST is recalculated by using the weighted sum of two LST estimated separately by the day and the night LST algorithms. And the weighting value is calculated by a function of solar zenith angle. The evaluation results showed that the weighted LST of day/night algorithm is more accurate than that of LST estimated by original algorithm algorithm although the improvement clearly dependent on the water vapor amount, $\Delta \epsilon$, SZA, and boundary layer profiles. The spectral emissivities of split-window channels were calculated using vegetation coverage method by using emissivity look up table and monthly MODIS NDVI data. The validation results using the co-located MODIS LST data showed that the quality of weighted LST by the day/night algorithm is significantly improved compared to that of LST estimated by the original algorithm.

8174-64, Poster Session

Satellite remote sensing data for heat waves assessment in urban areas

M. A. Zoran, National Institute of Research & Development for Optoelectronics (Romania)

Climate change and extreme climate events are the great environmental concerns facing mankind in the twenty first century. Surface temperatures are expected to continue to increase globally and major changes are likely to occur in the global hydrological and energy cycles.Extreme climate events like heat waves are a key manifestation of complex systems, in both the natural and human world.It was estimated that during last years regional surface warming caused the frequency, intensity and duration of heat waves to increase over Europe. During last period global warming was intensified because the global mean surface temperature has increased since the late 19th century.As urbanization has become an important contributor for global warming, Urban Heat Island (UHI) effect, will be sure to influence the regional climate, environment, and socioeconomic development. Much more, extreme climatic events as heat waves will amplify the UHI effect with severe urban ecosystem health consequences.

Remote sensing is a key to mesoscale modeling through specification of land cover distributions and creating spatial products of moisture, reflectance, and surface temperatures. Because the knowledge of urban surface energy budgets and urban heat islands is significant to assess urban climatology, global environmental change, and human-



environment interactions important for planning and management practices, is very important to study land surface temperatures and urban energy budget

characteristics using the technology of satellite remote sensing imagery.

The aim of this paper was to analyse from LANDSAT TM, ETM, MODIS and IKONOS satellite remote sensing images urban surface energy budgets and UHI effect for Bucharest urban area during heat waves events of 2003 and 2007, 2010 summers.

Satellite data have been selected to retrieve the urban biogeophysical parameters and brightness temperatures in relation with changes of land use/cover types over Bucharest urban area, Romania. The spatial distribution of heat islands has been changed from a mixed pattern, where bare land, semi-bare land and land under development were warmer than other surface types, to extensive UHI. Our analysis showed that higher temperature in the UHI was located with a scattered pattern, which was related to certain land-cover types. In order to analyze the relationship between UHI and land-cover changes, this study attempted to employ a quantitative approach in exploring the relationship between temperature and several indices, including different Normalized Difference Vegetation Index (NDVI). Spectral/ climatic modeling of extreme high temperature events in urban areas is providing a scientific base for heat wave hazard assessment. Heat waves events of 2003, 2007 and 2010 summers have been correlated with UHI effect for Bucharest urban area.

8174-65, Poster Session

Early warnings of Rhynchophorus ferrugineus infestation of Phoenix canariensis: a proximity thermal sensing approach

C. Cammalleri, Univ. degli Studi di Palermo (Italy); F. Capodici, Univ. degli Studi di Napoli Federico II (Italy); G. Ciraolo, G. Filardo, G. La Loggia, A. Maltese, Univ. degli Studi di Palermo (Italy)

Phoenix canariensis represents one of the most widespread ornamental plant within Mediterranean environment. However in last six years the infestation of a curculinoid coleopteron, namely the Rhynchophorus ferrugineus, caused an extensive decimation of these palms. Unfortunately damages caused by the insect are evident only in the advanced phase of the disease making futile to treat plant. Early warnings of this disease may represents the only way to setup efficient treatments to fight the coleopteron in trees where it takes over thus limiting the desease spreading in contiguous palms. This research aims to achieve the former result by processing: i) short and long-wave images of the crown acquired by a balloon platform in day-time, and ii) a time series of thermal images of the trunk recorded on the field in night-time. The research is based on the hypotheses that the disease causes a rise of radiative temperature of canopy as a consequence of changes of both evapotranspiration processes and crown shape due to damage to vascular tissue. Indeed, the infestation causes a local increase of temperature within trunk due to anaerobic fermentation processes within the palm, as it was proved by recording kinematic temperatures through two thermocouples inserted within the trunk close to focus cavity and in a healthy reference zone.

8174-67, Poster Session

21

Spatio-temporal variability analysis of the Douro River plume through MERIS data for one hydrological year

A. C. Teodoro, H. Almeida, Univ. do Porto (Portugal)

Estuarine outflow plumes are important coastal processes. Satellite ocean color observations of the optical properties of coastal surface waters can be used to distinguish plume water from ambient water masses, particularly based on increased concentrations of TSM in the plumes (Teodoro et al., 2009).

The main objective of this study was to analyse the spatial and

temporal variation of the Douro river plume (DRP) dimension, for one hydrological year, based on image segmentation of MERIS data and to modelling the plume dimension based on different environmental parameters that should be related to the DRP dimension. In this work, 107 MERIS scenes (level 2 data) from September 2008 to October 2009 were considered (data provided by ESA).

The adopted methodology consisted in the development and implementation of an algorithm based on region growing approach, to automatically select the region seed (S) and the threshold (T) values for each image. In this algorithm two options may be used to select the S and the T values. The first option consisted in assuming S as the centroid value and T as S/2, whereas the second option is based on assuming S as the mean value of the plume region and T as half the maximum. The second option led to better results, since its nature allows for a more realistic and accurate delineation of the plume.

In order to relate the DRP dimension with several environmental parameters, the Douro river discharges (at Crestuma dam), tide level and wind speed and direction values were computed. According to Teodoro et al., (2009) the parameter that most directly influences DRP dimension is river discharges at Crestuma dam. However, the relations found between the DRP dimension and river discharges considering all the data were not significant. Therefore, a seasonal study was performed, considering summer and winter periods separately. The best results were obtained for the winter period with a correlation coefficient of 0.45 (p-value=0.002) for the second segmentation option. No significant correlations (α =5%) were found regarding the summer period. The results found for the first segmentation option were identical, but less robust. It was verified a considerable increase of the correlation between the DRP and the river discharges after excluding the values of discharges rates less than 300 m3/s. The best results were obtained for second segmentation option with a correlation coefficient of 0.74 (p-value=0.001). The result for the first segmentation approach was similar (r=0.71; p-value=0.003). Therefore, the plume derived from MERIS data represents DRP only when the river flow exceeds a certain threshold. During low discharge, the remotely sensed plume results from other factors. This fact explains why lower correlation coefficient values were found considering all the data. Nevertheless, the segmentation approach applied in this work seems to be a valid method to estimate the plume size.

Teodoro, A.; Gonçalves, H.; Veloso-Gomes, F. & Gonçalves, J.A. (2009). Modelling of the Douro river plume size, obtained through image segmentation of MERIS data. IEEE Geoscience and Remote Sensing Letters, Vol. 6 (1), 87-91.

8174-68, Poster Session

The analysis about the characteristics of oil pollution and model of Yellow River delta

F. Yanguo, Y. Sun, China Univ. of Petroleum (China)

Abstract: Yellow River Delta is China's coastal areas of oil, natural gasrich region. China's second largest oil field - Shengli Oil Field locates here. The development of oil field provides the economic foundation for the local economic development and the industrialization of the coastal zone, but at the same time it also brought a number of environmental problems to soil, river, air and so on. In order to effectively combat these problems, it needs a series of research investigations. The traditional method of investigation and assessment is the ground field surveys, this method is time-consuming and effort-consuming. With advances in remote sensing technology, it is widely used satellite images to analyze and investigate the typical features. Nowadays, experts focus on how to renovate pollution, reduce damage pollution brought, but environmental restoration is on the premise of finding the polluted areas and determining their pollution levels.

In view of these series of problems, this study was aimed to use the study area's multi-temporal remote sensing image data, meteorological data, hydrological data, and the already collected oil, oil well location data of the area etc, adopt ENVI, ARCGIS software platforms; first confirm oil region range in remote sensing images based on the investigation, import oil Wells into images according to the obtained oil Wells geographical position data, then sift the oil Wells falling into oil region according to the scope of oil region. After that, we chose 4-5 sample points in each well around 40 meters range, it was just because crude oil pollutant presented mainly radial distribution with oil Wells as the center for a certain range. Then we obtained these sample points' spectral reflectance curves. Lots of indoor and outdoor

SPIE Remote Sensing

crude oil and soil spectral measurements showed that hydrocarbons have a series of obvious characteristic absorption valley in 1725nm, 1760nm, 2310 and 2360 wavelengths etc, while in 2300-2360 band have strong double valley shape. Through comparing these sample points characteristic wavelength and bands, we could analyze whether sample area exists spilled oil pollution, at the same time, we could predict the corresponding underground reservoirs target area. We could judge the spilled oil samples regional pollution levels based on the sample points characteristic wavelength and waves threshold settings.

Finally, we built remote sensing information model about soil oil pollutant concentration according to sample points' spectrum value in oil region and actual research. When establishing remote sensing information decoder model, it should be considered all sorts of relevant information. We should find out the main factors, factors influencing soil oil pollutant concentration include temperature, pollution emissions, rainfall, soil texture, distance sample points to the sources, etc.

We could get soil oil pollutant concentration model formulas according to the general formula of remote sensing information model, then we could forecast and general decide the other polluted areas pollution levels.

8174-69, Poster Session

A research on soil petroleum content hyperspectral model based on measured spectrum in Gudong oilfield

F. Yanguo, L. Zhang, China Univ. of Petroleum (China)

Abstract: ShengLi Oil field is the second largest oil field in China, which located in the Yellow River Delta. With the exploitation of oil, the area of the oil-contaminated soil is of 24 percent of the total area there. Ground crude oil is the most serious pollutant . Soil pollution will eventually bring harm to human health. We should detect and assess the oil pollution in soil, so as to minimize and reduce the petroleum pollution, which leads to the ecological environment damage and human health hazards. The detection of oil content in soil has the important practical significance in petroleum pollution prevention and control. Having used univariate prediction model to analyze the linear and nonlinear relationships between soil spectral characteristic parameters and petroleum content, based on indoor determination of soil samples hyperspectral reflectivity in GuDong oilfield. The result suggested that the correlation between the third line segment slope of envelope analysis and petroleum content was best, the cubic function of this paragraph slope was the best single variable estimation model. Further using stepwise regression analysis technology to modeling, the result suggested that the standard normal variable transform had the best effect in spectrum pretreatment. Having used transformation spectral to build multivariate regression model, the adjusted coefficient of determination of which was 0.826 , the total RMSE was 0.531, number of variables was small, which was the best forecasting model. This paper made use of hyperspectral data predicting the oil content, which provided a new effective idea about the detection of the soils polluted by petroleum.

8174-70, Poster Session

22

Change actors' analysis of vegetation degradation from remote sensing data in parts of Niger delta region

O. O. Fabiyi, Regional Ctr. for Training in Aerospace Surveys (Nigeria)

Studies on land use changes have shown that human activities inevitably result in medium to large scale changes in the ecosystem. These changes can be monitored in the short or long term small scale or large scale with the aid of remote sensing data. Several change actors are usually responsible for observed changes in vegetation cover of an area. While some of these actors are localized and intensive in impact, others are global and extensive. The paper attempted to identify the change actors in the short run causing identifiable changes in the vegetation cover in the Niger delta region as opposed to those changes due to climate change effects which are measurable in a longer interval.

The study utilized two-date satellite images of parts of Niger delta and other auxiliary data on oil activities in parts of Niger delta to examine the main change actors in the vegetation cover. The locations of small and medium human settlements were identified in the study area to represent the informal or non-corporate anthropogenic activities that impacts on vegetation quality(Large settlements were removed from the analysis as they introduced biases into the data). The location of Oil facilities such as oil well, platforms terminals and helipad were noted to identify major industrial oil related activities in the study area.

Normalized Differential vegetation indices were computed for the study area on the enhanced landSat images and the values were used to estimate vegetation richness or vegetal degradation. The Landsat images acquired in 2000 and 2006 were used in the NDVI computation.

The location of oil facilities were captured using the corresponding pixel they fall in and the bolean values were applied to both settlements and oil facilities. Geo-statistical analysis in the Raster data platform was performed. The correlation analysis was performed on the presence of oil facilities and the NDVI values on one hand while the presence of human settlements (Only small and medium settlements were considered) and the NDVI values were also correlated

The result showed that Informal human settlement development and other similar anthropogenic activities were responsible for major changes in the vegetation cover in the study area compare to oil related industrial activities in the oil rich region of Nigeria.

NGOs, and many environmentalist had in the past put the blame of vegetal degradation on industrial activities especially oil exploration in the Niger Delta region. The study however showed that oil activities have lower correlation (0.38) relationship with the vegetation loss while human settlement developments have high correlation (0.762) with the vegetation loss in the project area. The paper posited that changes in the vegetation occurring in the Niger delta are more from informal human activities than from the multinationals oil activities

8174-71, Poster Session

Applying remote sensing techniques to monitor mangrove changes in the Iranian coastal zone of Oman Gulf

A. Salehipour Milani, Geological Survey of Iran (Iran, Islamic Republic of)

Mangroves in Iran can be found in the tidal zones of the sea of Oman and of the Persian Gulf. These forests are composed mainly of Avicennia marina, which forms dense forest in the intertidal zones. Mangrove forests in many parts of the world are declining at an alarming rate possibly even more rapidly than inland tropical forests. The rate and causes of such changes are not known. The forests themselves are dynamic in nature and are undergoing constant changes due to both natural and anthropogenic forces. Application of remote sensing techniques for mangrove mapping and monitoring is increased and recognized for sustainable management of the resources to the country. This paper quantifies mangrove forest cover change in Iranian Coast of Oman Gulf from 1974 to 2008 using Landsat satellite images from Multispectral Scanner Landsat (MSS) (1976), Thematic Mapper (TM) (1989) , Enhanced Thematic Mapper plus (ETM+) (2000,2006) and IRS LISS III (2008)sensors. We used three image processing techniques: normalized differential vegetation index (NDVI). Change detection was applied and mangrove in the study area was found to have increased by about 43% from 1974 to 1999.

8174-72, Poster Session

Multitemporal spatial pattern analysis of Tulum's tropical coastal landscape

S. C. Ramirez-Forero, A. A. López-Caloca, J. L. Silván-Cárdenas, Ctr. de Investigación en Geografía y Geomática (Mexico)

Nowadays, the world faces a series of complex environmental and social changes that are altering the dynamical processes taking place



in it. The transformations of terrestrial ecosystems are considered as an important element of global change. Remote sensing can contribute to understanding short-time changes that take place in the ecosystem in order to support policies for sustainability.

The tropical coastal landscape of Tulum, Quintana Roo, Mexico has high ecological, economical, social and cultural values, as they provide environmental and tourism services at the global, national, regional and local level. The area of study has rock pool, forest, beach, archaeological zones, protected natural areas with enormous diversity and natural richness. The biosphere reserve of Sian Ka'an and the Mayan Ruins of Tulum are notable sites in this region. In recent years, the increase in tourism has promoted an expansion of hotel, transporationt and recreation infrastructures to provide all the services and facilities to visitors, thereby altering the complex landscape. The study of the temporal changes of spatial patterns is important to understand the environmental dynamics and to propose the future management of ecological area by the authorities.

This paper addresses a multi-temporal analysis of land cover changes from 1993 to 2000 in Tulum. The study used Thematic Mapper (TM) data acquired by Landsat-5. The landscape of the area is heterogeneous and presents random fragmentation patterns especially in the forested zone, which has been deforested for agriculture. Two complementary methodologies were applied for the analysis of changes in the landscape and definition of fragmentation patterns. First, the multi-temporal change detection study uses an Iteratively Multivariate Alteration Detection (MAD) algorithm to detect and localize environmental changes through time. The advantage of this method is the invariance under linear transformations of the original variables and focus on "difficult" observations in a change detection setting. Secondly, the area was classified with the Support Vector Machine (SVM) algorithm to generate the data needed to calculate the ecological value of landscape with some indices. This algorithm has a high sensitivity to detect spectral signatures in areas with complex patterns.

Preliminary results have provided indications on the ecological value of the landscape as well as its conservation status in the period of study. Specifically, the high fragmentation in the west side of the area indicates changes in the economical activities. These alter the natural connectivity of ecosystems in the region. The landscape value will be determined by means of the integration of different indicators under an exclusively ecological approach, like number and size of patch. The results will be provided to land managers for monitoring these complex ecosystems and for establishing new conservation measure of the area.

Further analysis of our multi-temporal data will be carried out in order to understand the dynamical process that is taking place in study area. This will allow local population to use and exploit the natural resources in a sustainable way.

8174-73, Poster Session

23

Identification of weeping love grass using hyperspectral imagery in the shore of the Kinu River, Japan

S. Lu, Northeast Normal Univ. (China); Y. Shimizu, J. Ishii, The Univ. of Tokyo (Japan)

Weeping love grass has become a well-established invasive species along the Kinu River, Japan and is now considered a problematic invasive weed species. We chose a study site where weeping love grass spread widely along the shore of mid and lower reaches of the Kinu River. The AISA (Airborne Imaging Spectrometer for Applications) hyperspectral imagery was acquired on 26 May 2004. The AISA collected images have 68 contiguous spectral bands, in the range from 398 to 984 nm. One pixel size was 1.5×1.5 m. In the field surveying, thirty five 5×5 m plots were established, and in each plot, three 1×1 m subplots were randomly chosen to measure the coverage of weeping love grass. The means from the three subplots were used to represent each 5×5 m plot.

Logistic regression models were used to predict the per-pixel probability of the occurrence of weeping love grass. Two types of input variables for the regression models were tried to entry into the logistic regression model. One was the original reflectance data (68 bands) and the other was the selected bands (18 bands) of the minimum noise fraction (MNF) transformation of hyperspectral data. No significant original reflectance band was selected by the logistic regression analysis for predicting the presence-absence of the weeping love grass, while a prediction of formula using MNF band 13 and 14 optimized the discrimination of weeping love grass from the other land cover types. This model was assessed by regressing the estimated probability of weeping love grass occurrence (p) against percent cover estimates from the inventory data. The value of the p (p=0.68) corresponding to 60% cover by weeping love grass which residual error was not high was identified and the pixels were classified as "weeping love grass" if their predicted value exceeded this threshold.

In the training samples, the user's and producer's accuracies for weeping love grass presence were 100% and 71.4% respectively, and the total accuracy for all the training samples was 92.0%. The kappa coefficient relative to the weeping love grass was 0.78. To estimate the prediction accuracy of the model, the remaining 10 inventory samples were assessed. The final classification distinguished weeping love grass from pseudo-absence pixels with user's and producer's accuracies of 100% and 66.7% respectively, and the total accuracy for all the testing samples was 90.0%. The kappa coefficient relative to the weeping love grass was 0.74. The process of the MNF has reduced the redundancy of the hyperspectral data, as well as extracted the useful information of the data. The information extraction of the MNF made it performed well in identifying the invasive weeping love grass.

The results indicated that the MNF transformed hyperspectral bands were more suitable than that of the original reflectance data to estimate the distribution of the invasive weeping love grass in the Shore of the Kinu River. The estimated distribution map of the weeping love grass would help the regional planning of the invaded vegetation removal and protecting the native plants.

8174-74, Poster Session

A statistical model for the selection of ground observations of solar radiation: an application in producing a five-year dataset of radiation maps on Italian territory through correction of MSG-derived data

L. Campo, F. Castelli, Univ. degli Studi di Firenze (Italy)

The incident solar radiation is one of the component of the land surface energy budget and constitutes an essential input for several applications, like hydrological balance models, agricultural planning and SVAT (Soil-Vegetation-ATmosphere) models. An accurate estimation of this variable on large areas requires a dense network of ground sensors and continuous knowledge of the cloud cover, that are rarely available. The information about the cloud cover can be obtained through remote sensing, that can provide reliable observations of this variable with spatial and temporal resolutions sufficient for the characterization of the solar radiation. In this work a simple algorithm is used in order to integrate the LSA-SAF (Land Surface Analysis Satellite Applications Facility) products of shortwave incident radiation obtained from MSG-SEVIRI imagery with ground radiometers observations. A statistical approach is followed in order to define a criterion for accept or reject the ground sensors observations. In this approach both the mean daily error between the ground measure and a theoretical radiation time series and the cloud cover measures from MSG imagery are modelized with probability distribution functions. The theoretical time series is obtained by correcting the astronomical radiation values by a reduction factor that takes into account the observed fraction of cloud cover. A conditional probability distribution of the radiation error given the cloud cover is built using a copula function; the Frank's Copula was selected for this application. Such conditional distribution is used for the ground sensors selection criterion. The analysis is used to produce a dataset of corrected solar radiation maps on the whole Italian territory for a period of 5 years (2005-2009). Discussion of the results of the analysis is provided.

8174-75, Poster Session

Ecosystem service value assessment by land use change in South Korea using remote sensing data and a geographic information system

Y. H. Jung, C. U. Choi, H. Ahn, Pukyong National Univ. (Korea, Republic of)

In South Korea, rapid industrialization and economic growth have led to serious problems including reduced open space, environmental degradation, traffic congestion, and urban sprawl. These problems have been exacerbated by the absence of effective conservation and governance, and have resulted in various social conflicts. In response to these challenges, we hope to achieve sustainable development through environmentally sound planning and management. Toward this goal, this study analyzed ecosystem service value (ESV) over the past 20 years using previously reported coefficients. In addition, using frequency ratios (FR), the analytical hierarchy process (AHP), and logistic regression (LR), we projected the land use distribution in 2020 according to the Environmental Conservation Value Assessment Map (ECVAM) and analyzed ESV based on land use changes. More than 60% of South Korea is covered by forest. Between 1985 and 2005, built-up areas had increased threefold. In the same time period, forest, grassland, and wetland areas decreased. Because of these trends, ESV decreased from 7,300~16,741 million USD to 6,525~15,658 million USD. By analyzing land use distribution with a land suitability index (LSI) map drawn according to the ECVAM, we determined that farmland, grassland, and bare land areas had declined by approximately 24.3%. The ESV of the 2020 land use/land cover (LULC) map was calculated by extrapolating from the 2005 LULC. The 2020 ÉCVAM LSI map showed a decrease of 89~594 million USD in ESV, while the 2020 LULC and LSI maps without ECVAM showed a decrease of 165~767 million USD. The results of this analysis indicate that environmentally sustainable systems and urban development must be applied to achieve sustainable development and environmental protection.

8174-76, Poster Session

The theory of shortwave infrared perpendicular water stress index and its application in soil moisture retrieval under full covered vegetation condition

H. Chen, H. Zhang, Henan Institute of Meteorological Science (China)

With the analysis of SWIR and NIR spectral space, and based on the Short Wave Perpendicular Water Stress Index (SPSI) of which was constructed by Abduwasit Ghulam. The SPSI was applied in the soil moisture retrieval during the growing period of wheat in April with full cover condition. The result showed there is a high correlation coefficient between SPSI and soil moisture in 0-30 cm, and has been tested that the SPSI has a potential in the soil moisture retrieval under full cover condition.

8174-77, Poster Session

Scaling from instantaneous remote-sensingbased latent heat flux to daytime integrated value with the help of SiB2

Y. Song, M. Ma, X. Li, X. Wang, Cold and Arid Regions Environmental and Engineering Research Institute (China)

Abstract: The sine function and the constant evaporative fraction (EF) method are commonly used in scaling from instantaneous Latent Heat Flux (LE) to Daytime Integrated Value. Jackson et al. (1983) related the ratio of instantaneous LE to daily value to the diurnal trend of solar irradiance with a sine equation. The sine function gives a good approximate of the change of diurnal solar irradiance from near sunrise



to sunset. The constant EF method assumed the EF to be constant during the daylight hours to determine regional daily evapotranspiration (ET) (Sugita and Brutsaert, 1991). Knowing the daytime available energy (Rn-G)d, and assuming that EF is constant during the daytime, daily estimate of ETd can therefore be obtained. The variability of conservation of EF on individual day is affected by complicated combination factors, such as weather conditions, soil moisture, topography, biophysical conditions, cloudiness and the advections of moisture and temperature directly contributed to the amount of variability of EF on a given day (Crago, 1996). Zhang and Lemeur (1995) compared the sine function with the constant EF method and concluded that both methods were accurate to estimate daily total ET for cloud-free days and recommended that the sine function was preferable for the purpose of estimating ET using remotely sensed data. However, both these two methods do not work well in cloudy days, and ignore ET in night. This research dealt with a daytime integration method with the help of Simple Biosphere Model, Version 2 (SiB2).

The field observations employed in this study were obtained at the Yingke (YK) oasis super-station, which includes an Automatic Meteorological Station (AMS), an eddy covariance (EC) system and a Soil Moisture and Temperature Measuring System (SMTMS). This station is located in the Heihe River Basin, the second largest inland river basin in China. The study used remotely sensed data, including a TM image and MODIS Leaf Area Index (LAI) products. In detail, the Landsat TM image, acquired on July 7, 2008, was involved in the LE estimation. This image was pre-processed using radiative, atmospheric and geometric correlations. The remotely sensed data and field observations employed in this study were derived from Watershed Allied Telemetry Experimental Research (WATER). Daily variations of EF in temporal and spatial scale would be detected by using SiB2. An instantaneous midday EF was calculated based on a remote-sensingbased estimation of surface energy budget. The invariance of daytime EF was examined using the instantaneous midday EF calculated from a remote-sensing-based estimation. The integration was carried out using the constant EF method in the intervals with a steady EF. Intervals with an inconsistent EF were picked up and ET in these intervals was integrated separately.

The truth validation of land Surface ET at satellite pixel scale was carried out using the measurement of eddy covariance (EC) system. The validation strategy considering the footprint of EC is reasonable at satellite pixel scale.

8174-78, Poster Session

Spatial distribution of carbon dioxide absorption and emission in Chungcheongbuk-do, South Korea using RS and GIS method

J. K. Park, S. I. Na, J. H. Park, Chungbuk National Univ. (Korea, Republic of)

The main objective of this study was to make and suggest carbon dioxide spatial distribution with absorption and emission using RS and GIS method. First, Topographic characteristics and environment information of Chungcheongbuk-do(after, Chungbuk) were extracted from Landsat satellite image, numerical map and DEM(Digital Elevation Model). The experimental site is located in the central part of South Korea. Carbon dioxide emission was estimated from statistics data of Chungbuk, TOE(Ton of Oil Equivalent) factor and CEF(Carbon Emission Factor). Stock map(forest type and age-class) and BEF(Biomass Expantion Factor) were used to estimate carbon dioxide absorption. Finally, carbon dioxide spatial distribution map was made by overlaying carbon dioxide absorption map and emission map.

The result of this study is that amount of carbon dioxide emission by energy consumption of chungbuk was 8,065,110 TCO2/year(Ton of Carbon dioxide) in 1999 and 13,275,370 TCO2/year in 2006. It had increased 73.6% for seven years. The percentage of carbon dioxide emission by energy consumption comprises 38.40% for petroleum, 51.46% for electric power and 10.14% for gas. Amount of carbon dioxide absorption by forest was 3,989,901 TCO2/year in 2006. The forest absorbed 30.12% of total emission. Forests play a major role in determining the current atmospheric concentration of carbon dioxide, as both sources of carbon dioxide following deforestation and sinks of carbon dioxide probably resulting from carbon dioxide stimulation



of forest photosynthesis. The results suggest that both the carbon sources and sinks in forests are significantly greater than previously thought.

This study was effective to understand carbon dioxide spatial characteristic of absorption and emission using RS/GIS. If carbon dioxide spatial distribution characteristic will be used for planes such as green land in urban area, land use, urban improvement and forestation business, it can get efficient effect on reduction of carbon dioxide emission.

8174-79, Poster Session

Physical satellite observation collocation algorithms in polar-geostationary observation integration system

H. Sun, Perot Systems Government Service (United States); W. W. Wolf, National Oceanic and Atmospheric Administration (United States); T. S. King, Perot Systems Government Service (United States); C. D. Barnet, M. D. Goldberg, National Oceanic and Atmospheric Administration (United States)

Satellite observation collocation algorithms are generally used to spatially match observations and/or products from different satellite observing systems. The spatially matched and integrated satellite datasets are wildly used in retrieval algorithms, satellite instrument inter-calibration and satellite observation validation. Instrument based physical collocation algorithms are developed in NOAA/NESDIS/STAR to support the development and validation of integrated satellite product processing systems. The algorithms are applied in two geostationary & polar satellite (GEO-LEO) integrated systems using IASI/SEVRI observations and AIRS/SEVIRI observations. These algorithms will also be applied in the future combined CrIS/GOES-R system.

The observed radiance of the remote sensing instrument is contributed by all the points within the effective field of view (EFOV) of the sensor. The weight of the individual point of the observation is the convolution product of the spatial response function (SRF) of instantaneous field of view (IFOV) and the integration time. The shape of the EFOV is defined by the IFOV shape and the scan pattern. This shape will be bias from circle (more like an ellipse) for most cases, especially for cross-scanning instruments at large scan angles. Physical satellite observation collocation algorithms collocate observations from different instrument basing on the instrument EFOV and regulate the observed radiance basing on the instrument effective spatial response function. By introducing the EFOV and EFOV SRF in collocation algorithms, the collocated observation will come from "same" physical targets.

The Integrated Polar-Geostationary Satellite system includes two basic processing steps: observation collocation and observation regulation.

Collocation: Observation collocation processing is to select the polar and geostationary pixels that are spatially collocated, temporally concurrent, and geometrically aligned. The collocation is accomplished using polar observation geo-location information and spatial response function information. The geostationary observation point is mapped to the polar observation spatial response matrix to get the weight of its contribution. The geostationary observation with non zero weight will be collocated. The EFOV SRF for different instruments will be generated separately.

Regulation : Collocated geostationary data are 'regulated' to the same physical target of the polar observation. This includes unification of the spatial characteristics of the observations in which the collocated geostationary data are averaged with the contribution weight applied. This unification may be applied to the spectral and temporal data information as well.

Geo-stationary satellite observations can ensure coverage with high temporal sampling and fairly high ground resolution, but with a lower signal-to-noise ratio and a lack of spectral resolution needed to obtain highly accurate atmosphere property retrievals. Polar satellites have a relatively high signal-to-noise ratio, high spectral resolution, and wide spectral coverage but they have a fairly poor temporal resolution. The Integrated Polar-Geostationary Observation System aims at a combined product of complementary specifications. In this paper, the algorithm details for IASI/SEVERI and AIRS/SEVIRI collocations are described and the results are presented.

25

8174-80, Poster Session

Remote sensing of key indicators of karst rocky desertification

Y. Yue, K. Wang, Institute of Subtropical Agriculture (China); B. Zhang, Q. Jiao, Ctr. for Earth Observation and Digital Earth (China); B. Liu, Nanjing Institute of Environmental Sciences (China); M. Zhang, Institute of Subtropical Agriculture (China)

Karst regions are typically ecological fragile zones constrained by geological setting. Karst rocky desertification is a process of land desertification associated with human disturbance of the fragile eco-geological setting of karst ecosystem. The fractional cover of vegetation (GV) and exposed bedrock are key indicators of the extent and degree of land degradation in karst regions. The main land cover of karst rocky desertification (vegetation, limestone soils, and carbonate rocks) are mixed-distributed and resulted in a high heterogeneous landscape with vegetation fragmentation and soil discontinuousness, rendering it was difficult to estimate the fractional cover of GV and exposed bedrock.

In this study, we suggested and compared new methodology for direct and objective estimation of key indicators of karst rocky desertification with hyperspectral and multispectral imagery. For hyperspectral remote sensing method, it used EO-1 Hyperion imagery to estimate the fractional cover of GV and exposed bedrock with the combination of karst rocky desertification synthesis index (KRDIS) and dimidiate pixel model that pre-segmented Hyperion with spectral similarity. For multispectral imagery, it employed EOS Terra ASTER imagery to extract the key indicators of karst rocky desertification with Lignin Cellulose Absorption Index (LCA) and dimidiate pixel model that presegmented ASTER with slipped windows of 35×35 pixels.

The results showed that the Hyperion estimated fractional covers of GV had good correlation with the field surveyed fractional covers and the R2 (coefficient of determination) and RMSE (root mean square error) for GV was 0.91 and 0.05, respectively; while for exposed bedrock was not so good, 0.53 and 0.11, respectively. It was due to that the KRDSI did not take the spectral differences of limestone and dolomite into consideration. It demonstrated that hyperspectral imagery was able to directly estimate the key ecological indicators of karst rocky desertification, which was in a heterogeneous landscape. As for the ASTER imagery, the results were not so accurate. The R2 and RMSE for GV were 0.61 and 0.10, and for exposed bedrock were 0.48 and 0.11, respectively. It indicated that multispectral imagery could not be used to effectively estimate the fractional cover of GV and exposed bedrock. It was due to the limits of multispectral bands to identify the spectra differences of ground objects under high heterogeneity of karst ecosystem. In addition, whatever hyperspectral or multispectral imagery, it should segment the imagery into relatively homogeneous subsets firstly to reduce the effects of heterogeneity of karst ecosystem.

Our study indicates that it could use hyperspectral imagery to directly and effectively estimate the fractional cover of GV and exposed bedrock in a heterogeneous landscape of karst ecosystem. The designed KRDSI should differentiate the spectral features of limestone and dolomite to improve the estimation of fractional cover of exposed bedrock.

8174-81, Poster Session

An insight of using remote sensing technique on water resources management

A. Farid, P. Mirhosseini, H. Gazerani, Ferdowsi Univ. of Mashhad (Iran, Islamic Republic of); A. Daneshvari, Islamic Azad Univ. (Iran, Islamic Republic of); A. M. Rafati Sokhangoo, L. Rafati Sokhangoo, Ferdowsi Univ. of Mashhad (Iran, Islamic Republic of)

Shortage of water is one of the most important factors which restricts the environment, the sustainable development, economics and politics. Desertification, species extinction and reduction of vegetation which appear due to the lack of water resources deteriorate the environmental conditions. In recent years, population growth especially



in the arid and semi-arid area leads to an overburden pressure on the water resources and even on the earth.

As we know, more reliable model related data is more accurate flood and runoff models will be. Therefore, we can prepare more authentic data via using remote sensing technique for measuring snow characteristics and rainfall rate. Additionally, the satellite images can roughly provide comprehensive information to illustrate the soil attributes, which will enhance irrigation planning through estimation of the actual crop evapotranspiration. In addition, to predict the drought conditions, the remote sensing method can be considered as an invaluable tool. Furthermore, using satellite data can be a valuable asset in the early stages of shallow stagnant groundwater areas detection and also modeling.

Since 1960, launching the first Earth Resources Technology Satellite(ERTS-1), scientists have utilized remote sensing data and satellite images to produce relevant maps and in the process of land modeling.

Using satellite images in natural resources as an information input has been known as a popular source in the field of environmental processes modeling. Accessing and availability of the remote sensing data from different sensors with various spatial, spectral and temporal resolutions has made remote sensing technique to the one of

the greatest information source in the study of large scale areas. Furthermore, remote sensing images which are captured by the aircrafts and satellites are one of the main important sources in the field of water resources management. Emerging new achievements in sensors technology facilitated collecting data in a wide range of spectral bands since more than two decades. In this paper, some of the main remote sensing applications are being discussed.

Finally, this paper is reviewed the use of satellite images in recent water resources management studies and also outline its possible key roles in the future research of remote sensing.

8174-82, Poster Session

A remote sensing technique for the assessment of stable interannual dynamical patterns of vegetation

M. Chernetskiy, A. P. Shevyrnogov, Institute of Biophysics (Russian Federation)

One of the tasks to be fulfilled to understand global changes in the functioning of the biosphere is the analysis of remote sensing data over the past 10-30 years. One of the challenges of analyzing such data is to distinguish between different biospheric changes and changes of catastrophic nature (deforestation, fires, insects, etc.). In turn, biospheric changes can be divided into those of stable and unstable dynamical patterns. Another problem is the level of automation of data analysis. That is, at present, most methods for land cover classification are based on the presence of a large amount of training samples. However, expert information that is needed for training samples is not always available, not always reliable and not always statistically significant.

The time series of various parameters of satellite imagery (NDVI/ EVI, temperature, NPP) during the growing season were considered in this work. This means that satellite images were considered not like a number of single scenes but like temporal sequences. Using time series enables estimating the integral phenological properties of vegetation. The basis of the developed technique is to use one of the methods of transformation of the multidimensional space in order to get the principal components. The technique is based on considering each dimension of the multidimensional space as satellite imagery for a specific date range. The technique automatically identifies spatial patterns of vegetation that are similar by phenology and growing conditions. Subsequent analysis allowed identification of the belonging of derived classes.

Thus, the technique of revealing the spatial distribution of different dynamical vegetation patterns based on the phenological characteristics has been developed. The technique is based on a transformation of the multidimensional space of states of vegetation. Based on the developed technique, areas were obtained with similar interannual trends.

26

8174-83, Poster Session

Research on spectral imaging technology for medical imaging and remote sensing

Y. Luo, Institute of Fluid Physics (China)

Multi-spectral and hyper-spectral analysis of rays reflected from the object's surface is expected to play an important role in biomedical imaging and remote sensing. The Liquid Crystal Tunable Filter has a capability of selecting the observing wavelength instantaneously with high spectral resolution and excellent imaging quality in visible and near-infrared spectrum band. Taking advantage of this filter we have developed an LCTF imaging spectrometer prototype instrument at the visible and near-infrared wavelength bands for such analysis.

This paper first presents the architecture of an imaging spectrometer prototype instrument using LCTFs which are sensitive to radiation in the 450 nm-1000 nm wavelength bands. The theoretical model of LCTF has been set up based on the optical interference theory and the electronic-controlled characteristics of nematic liquid crystal. The LCTF imaging spectrometer prototype instrument with high spectral resolution and perfect transmission are prepared through F-P type cavity combined with cascaded lyot-ohman LC cells, index matching and polarization diversity technology. The laboratory experiments have verified the excellent properties of the prototype instrument, including hyper-spectral resolution of less than 10 nm, continuous selection of the output wavelength. We have photographed the xianhai beaty spot locate in sichuan province using the LCTF imaging spectrometer prototype instrument at different altitude from 300 meters to 500 meters. Through the postprocess of the series hyper-spectral imaging, we can distingunish the different objects such as tree, farm and lake,etc. Simultaneously,we have developed the biomedical imaging to skin of different burn degree, and the clear spectral difference to different burn degree skin at 530 nm-580 nm wavebands are found.

To sum up, The feasibility of determining object characteristics based on the measurement of the spectrum characteristics of the reflected rays is also demonstrated. The applicability of the LCTF imaging spectrometer to medical diagnosis and remote sensing are summarized based on the results of above experiments.

8174-84, Poster Session

MODIS GPP product validation in Heihe River basin, China

X. Wang, M. Ma, X. Li, G. Huang, Y. Song, J. Tan, Z. Zhang, Cold and Arid Regions Environmental and Engineering Research Institute (China)

Gross Primary Production (GPP) is the sum of carbon absorbed by plant canopy. It is a key measurement of carbon mass flux in carbon cycle studies. It is generally estimated using models because it is difficult to measure GPP directly. With the development of remote sensing, a number of production efficiency model were developed to estimate seasonal and spatial dynamics of GPP, such as GLO-PEM, VPM, EC-LUE, MODIS-PSN. MODIS GPP product (MOD17A2) is global GPP dataset produced by the Land Processes Distributed Active Archive Center (LP DAAC). It is an 8-day cumulative GPP at 1-kilometer spatial resolution. It is validated with carbon flux data from Ameriflux in American, but it is still not widely validated in China. The objective of this study is to validate MODIS GPP product in Heihe River Basin which is located in Northwest China and analyze the reasons that result in bias to MODIS GPP product.

Eddy Covariance (EC) can directly measure carbon flux over a footprint. GPP over the footprint can be estimated with meteorological data and carbon flux data. GPP estimated with EC is comparable with that from remote sensing at spatial scale. Thus, it can be used to validate GPP estimated using remote sensing data. We collected data from three EC stations in Heihe River Basin: A'rou (AR) freeze/thaw observation station, Yingke (YK) oasis station and Linze (LZ) inland river basin observation station. Surface cover type at YK station and LZ station is maize, and alpine meadow at AR station. AR station is in the upper stream of Heihe River Basin; YK station and LZ station are in the middle stream of Heihe River Basin.

Through this study, we found that the MODIS GPP product greatly underestimated the GPP at the three stations. At AR station, it is



about 1/2 of GPP observed by EC, and 1/5 of GPP observed at YK and LZ station. The RMSE is up to 74gC/m2/8d. When we used Air temperature, VPD and PAR observed at the three stations, FPAR from MOD15 and maximum light use efficiency retrieved from EC data as inputs of MODIS-PSN, the result was improved greatly. The RMSE becomes 15.9 gC/m2/8d. The GPP predicted by MODIS-PSN was consistent with observed GPP.

The great bias in MOD17A2 mainly resulted from the $\epsilon 0$ and input meteorology data produce by DAO. The maximum light use efficiency ($\epsilon 0$) is the basis for the production efficiency models, and the accurate estimating of $\epsilon 0$ is one of key steps for using the production efficiency models to estimate GPP. In the MODIS GPP algorithm, the $\epsilon 0$ value of crop land and grass land is 0.68 gc/MJ (approximately 1.32 gc/MJ APAR), which was lower than the $\epsilon 0$ obtained from the flux tower data. $\epsilon 0$ is 1.6gc/MJ APAR for alpine meadow, 2.66gc/MJ APAR for maize.

8174-85, Poster Session

Validation of MODIS land surface temperature products using ground measurements in Heihe River Basin, China

W. Yu, M. Ma, X. Wang, Cold and Arid Regions Environmental and Engineering Research Institute (China)

Land surface temperature (LST) is a key variable in climatological and environmental studies. LST is also the core information of surface energy exchange, and has cruel influence on land surface processes. The Moderate Resolution Imaging Spectroradiometer (MODIS), onboard the NASA Terra and Aqua satellites in the Earth Observing System, can provide multiple LST products on the daily basis for LST monitoring. MODIS LST products have been validated in previous, but the reported accuracy cannot be applied to all the global scale. The objective of this study is to validate MODIS LST products in Heihe River Basin-a typical arid and semi-arid region, Northwest China. Then, through the accuracy analysis, we obtained the MODIS LST preliminary errors range in Heihe River Basin, and even could provide accuracy reference for various studies using MODIS LST products in Heihe River Basin.

The daily MODIS LST products (MOD/MYD11A1) from Terra and Aqua with 1 km spatial resolution during 2008 and 2009 were used for the LST validation in the Heihe River Basin. The quality assurance information of LST scientific data sets (SDS) was used to select the high quality LST data. The ground measurements used in this study were obtained from five metrological and hydrological flux observation stations, provided by the Watershed Allied Telemetry Experimental Research. In order to validate MODIS LST products, the groundmeasured LSTs were converted from surface upwelling longwave radiation based on Stefan-Boltzmann's law. Then base on thermal radioactive transfer theory, the upwelling longwave radiation at the surface level depends on LST, emissivity, and downwelling radiation

$Fu = \delta Tb4 = (1 - \epsilon) Fd + \epsilon \delta T4$

27

Where Fu [w/m2] is surface upwelling longwave radiation; Fd [w/m2] is surface downwelling longwave radiation; ϵ is broadband emissivity; δ is the Stefan-Boltzmann constant (5.67×10-8 Wm-2K-4); T[K] is LST, and Tb[K] is surface brightness temperature. In this study, the broadband emissivity for each site was derived from the vegetation spectra of ASTER Spectral Library. For vegetated sites, considering the usually unknown land surface emissivity, the validation data is limited to the grow season.

The preliminary results of validation from biases mean, absolute error (MAE) and root mean squared error (RMSE), show MOD/MYD11A1 LSTs match well with ground measurement in A'rou (AR) freeze/thaw observation station, Huazhaizi(HZZ) desert station and Yingke (YK) oasis station sites with biases less than 0.6K, MAE less than 2.8K, and RMSE less than 4K. In these sites MOD/MYD11A1 LSTs are a few Kelvin degrees lower than the ground-measured LSTs in average level and the fitting lines are close to the line MOD/MYD11A1 LSTs = Ground-Measured LSTs. In other two sites, MOD/MYD11A1 LSTs have been larger negative biases (2-5K), MAEs (3-6K), and RMSEs (4-7K). However, the accuracy at the two sites close to the well-known accuracy of satellite LST products (3-4K). MYD11A1 LSTs from Aqua have large biases, MAEs, and RMSEs than that of MOD11A1 LSTs from Terra in most cases. From the comparisons daytime and nighttime MOD/MYD11A1 with ground measured LSTs, the MAEs and RMSEs from daytime are larger than that from nighttime.

8174-86, Poster Session

Microwave radiometry of soil moisture in forested areas

A. A. Chukhlantsev, A. M. Shutko III, E. P. Novichikhin, Institute of Radio Engineering and Electronics (Russian Federation)

Forests are one of the most important objects of ecological monitoring. A change in the hydrological regime of forests due to unwise felling and deforestation leads to a serious violation of their functioning. To monitor the hydrological regime in the forested areas, microwave radiometry as the primary remote sensing tool can be used. Research of microwave radiation from vegetated lands and forested areas, particularly, is conducted in the IRE RAS during more than three decades. A review of the research is given in the paper.

Several algorithms for soil moisture retrieval from microwave radiometric data were tested. These are regression algorithms, forward model inversion algorithms, and neural networks algorithms. The forward model inversion to retrieve land surface parameters requires two main steps: selection of a forward model providing minimum model errors; selection of a method for inversion providing maximum accuracy of soil and vegetation parameters estimation at known errors of the model and measurements and their statistical properties. In the paper, both of these two main steps are discussed.

To determine the soil surface moisture with acceptable accuracy from microwave radiometric measurements at a single frequency, it is required to guarantee a low level of microwave attenuation in the vegetation layer. Besides, the transfer coefficient of the vegetation layer should be assigned a priory with accuracy not worse than 0.05-0.1. Results of our research distinctly show that in the decimeter part of the microwave spectrum (wavelength 15-20 cm) practically all types of vegetation canopies are semitransparent. This circumstance makes it possible to retrieve soil surface parameters from microwave radiometric measurements in the L-band when the soil is covered with agricultural vegetation or with not so dense forest. For the retrieval of more accurate soil-moisture values, more exact data on the vegetation water content (transfer coefficient) are required. These data can be obtained from ancillary remote sensors, particularly, from optical sensors. Particularly, a relation between vegetation optical depth and NDVI (or NDWI) was established by several researches.

The necessity of a priori knowledge of the transfer coefficient (or vegetation water content) in single frequency measurements can be removed by conducting multi-configuration measurements, particularly, by measurements at several frequencies, polarizations, and observation angles. However, someone should be careful choosing the number of configurations. Engaging into the number of measurements a configuration at which the brightness temperature is not sensitive to the soil moisture could produce great errors in retrieval of soil moisture from multi-configuration measurements. So the sensitivity analyses should precede the choice of the measuring configurations.

8174-87, Poster Session

Combining high and moderate resolution satellite data for pan-tropical forest carbon monitoring

H. Lu, G. Liu, Henan Univ. (China)

Tropical forests play a particular important role in the global carbon budget because they contain about as much carbon in their vegetation and soils as temperate-zone and boreal forests combined. Nowadays released carbon from deforestation activities in tropical region accounts for approximate 20% of global greenhouse gas (GHG) emissions every year, larger than the traffic sector - cars, trucks and buses etc. However such issue was not addressed in Kyoto Protocol, which is regarded as a first step towards a truly global emission reduction regime that would stabilize GHG concentration. As a result it is generally accepted that the demand for mitigation of global warming will not be met unless tropical forests are included in an international reduction framework. During COP15, Parties agreed that reducing emissions from deforestation and forest degradation and enhancing "removals of greenhouse gas emission by forests" (REDD+) in developing countries through positive incentives under the United



Nations Framework Convention on Climate Change (UNFCCC) was capable of dealing with global emissions.

Accurate and precise quantification of emissions from deforestation and forest degradation has become a key policy issue in light of recent developments relating REDD+ as a climate mitigation strategy. Conventional methods are not suitable for such monitoring. Large-scale and contemporary data products derived from high and moderate resolution satellite systems, such as TM and MODIS can help to assist these monitoring systems. Here we developed a vegetation mapping system that combines these free satellite images for pan-tropical forest carbon monitoring.

The result showed:

(1) The TM data with 30m resolution specially designed for pantropical vegetation information extraction is getting used operationally, especially combined with MODIS data with multispectral bands.

(2) Only one sensor data from MODIS or TM does not work well in extracting land use information because of the limitation of spatial resolution or spectral information. Compared with the single TM or MODIS image, image fusion can preserve the color information from multispectral image and the spatial details of TM. Vegetation texture, residential, road and water were identified easily. The present examination shows that the fused images, with accordance about over 80 percent with the ground truth, are best suited to extract deforestation information.

(3) TM and MODIS data is free on the Internet in comparison with other high spatial resolution remote sensing such as SPOT etc. This advantage gives developing countries in tropical region a chance to develop capacity in remote sensing technology with modest budget by themselves. This has the clear advantage of being closely linked to decision-makers in these countries.

(4) Land use map shows a rapid decrease in forest area with an average annual change rate of 2.28% during the period 2005-2009. Meanwhile total carbon storage shows a substantial decrease. The results concerning carbon emissions, 1,471.3 thousand metric tons CO2 for 2005-2009, present a large carbon reduction in recent years.

8174-88, Poster Session

28

Agricultural land use classification using RapidEye satellite data in South Korea

H. Kim, J. Yeom, Y. Kim, Korea Aerospace Research Institute (Korea, Republic of)

Global climate changes as well as abnormal climate phenomena have affected the agricultural environment on a great scale and there is a strong need for countermeasures by making full use of agriculture related information. In South Korea, agricultural lands are mostly operated by private farmers on a small parcel level so that seeding, crop dusting, and harvest period usually differ. Further, crop condition depends on the owner's farming skill. Therefore, it is difficult to gather information for taking an overview on a changing crop condition and to construct database necessary for disease management, production estimation and compensation measures on a regional or governmental level. For this purpose, remote sensing offers the technical possibility as an effective and inexpensive method to identify crop fields and to detect crop condition. However, because of high variability of spectral response according to crop species, growth stage, health condition, soil, water and microclimate, remote sensing in agriculture has so far been only applied to a limited extent. The new satellite mission RapidEye, developed in Germany and launched in 2008, offers a very fast revisit rate up to single day on the same area, which is a very important factor to cover nationwide data sets within a growing season and also in order to monitor rapidly changing crop condition. Also, a new spectral feature in RapidEye sensor, the Red Edge band (690-730 nm) is supposed to allow better estimation of the ground cover and chlorophyll content of the vegetation. In this study, we examine the applicability of high resolution RapidEye multispectral remote sensing data to detect rice fields and their growing condition. First, we investigate reflection values, band ratio indices, and standard difference indices to examine possible correlations between actual field condition and image data. Second, we develop an algorithm to classify rice fields using an object-based approach with eCognition Developer (version 8.0) by Trimble and Imagine (version 9.1) by ERDAS.

8174-89, Poster Session

Rational design of long-wave infrared band for application of the earth surface temperature observation

Y. Bao, Beijing Institute of Space Mechanics and Electricity (China)

The land surface temperature (LST) is very important in determining net radiation, evaportranspiration, and energy balance at the Earth's surface and assessing the status of crops and soils such as water requirement, land degradation. LST estimation from satellite radiance needs to take into account the nonblackness of natural surfaces, their heterogeneity at satellite pixel scale and disturbing effects introduced by the atmosphere. Rational band configuration and sensor performance requirements must also be determined. The paper (Caselles et al., 1996) have analyzed different atmospheric and emissivity correction algorithms and its results showed that the splitwindow technique that uses channels in the 10-12.5um region is the most suitable technique for deriving accurate LST estimates. However, if this spectral region is not technically accessible, the region of 8-10 um may be taken into account for LST estimation.

For argumentation of feasibility of LST retrieval using 8-10 um infrared band, this paper focuses on band design of long-wave infrared based on theory research. Basis of thermal infrared radiative transfer and atmospheric simulation, the paper analyses atmospheric effect on different long-wave infrared and obtain a preliminary selection of potential spectral channels. Several configurations of long-wave infrared spectral band were selected to perform in Split-Window algorithm and the relation of LST retrieval precision and error source were analyzed. Several sources of error must be identified to estimate the total error for LST. We have distinguished three independent error contributions: the error associated with the split-window method; the temperature error due to the emissivity uncertainty; and the radiometric noise error, due to the propagation of the noise equivalent difference of temperature (NEDT).

The analytical results show that the temperature error from splitwindow algorithm using 10-12.5um is about ± 0.89 K, while the temperature error using 8-10 um is about ± 1.13 K. So the results indicate the scheme of LST retrieval using 8-10 um long-wave infrared is feasibility in scope of needed retrieval precision.

8174-90, Poster Session

Assimilation of soil moisture retrieved from remote sensing in LPJ-DGVM

M. Ma, X. Wang, Cold and Arid Regions Environmental and Engineering Research Institute (China)

Combination of NDVI and surface temperature can provide information on soil moisture conditions at the surface. Based on this theory, a simplified land surface dryness index (Temperature-Vegetation Dryness Index, TVDI) was constructed by Sandholt in 2002. It is can be used to estimate land surface soil moisture temporal and spatial dynamics.

Process-based ecological models are effective tools to assess carbon and water exchanges between ecosystem and atmosphere from individual sites to large scales. LPJ-DGVM is one of widely used dynamic vegetation models. Comparing with land surface process model, water cycle in LPJ-DGVM is simplified. Irrigation is not accounted in LPJ-DGVM, so it can not correct simulate soil moisture dynamics in irrigated area. In our previous study, we found that Net Ecosystem Exchange (NEE) and Evapotranspiration (ET) simulated by LPJ-DGVM is sensitive to soil moisture.

Heihe River Basin is the second largest inland river basin in China. It is located between 97°24'-102°10' E and 37°41'-42°42' N and covers an area of approximately 128,900 km2. Irrigated farmland widely is distributed in the middle stream of Heihe River Basin. This must be accounted if simulate carbon and water exchange with LPJ-DGVM in this region. Model driving and validating data was from in situ observation at Yingke (YK) oasis station, which is in an area of irrigated farmland in the middle stream of Heihe River Basin. The YK station (E100°25', N38°51', 1519 m) was constructed in November 2007. During 2008 and 2009, the primary crop in the area was seed maize.



The observation variables included the following: wind speed and direction, air temperature and humidity, air pressure, rainfall, the four components of radiation, soil temperature and moisture profiles and Eddy Covariance.

In this study, TVDI was calculated with MODIS land surface temperature product and NDVI product. Based on TVDI, irrigation date and surface soil moisture were retrieved. Irrigating information of the pixel was gotten by combining the irrigation date of the pixel and irrigation material collected from local water authority. Then, take irrigation water as precipitation input of LPJ-DGVM, and assimilating surface soil moisture retrieved from remote sensing data. The data assimilation algorithm used in this work is Ensemble Kalman Filter (EnKF) which is a widely used sequential data assimilation algorithm in nonlinear system.

This data assimilation system can improve the NEE and ET prediction of LPJ-DGVM at this region and make up the deficiency in water cycle module of LPJ-DGVM by combining remote sensing data and irrigation data.

8174-91, Poster Session

A computer simulation model to compute the radiation transfer of mountainous regions

Y. Li, F. Zhao, BeiHang Univ. (China)

A Computer Simulation Model to Compute the Radiation Transfer of Mountainous regions

Yuguang Lia, Feng Zhaoa

Key Laboratory of Precision Opto-Mechatronics Technology, Ministry of Education, School of Instrument Science and Opto-Electronics Engineering, Beijing University of Aeronautics and Astronautics, Beijing, 100191, P. R. China

E-mail addresses: lyg433@sina.com (Yuguang Li)

The calculation of ground reflectance imagery from a satellite scene acquired over mountainous terrain is a challenging task. The radiometric signal recorded at the sensor depends on a number of factors such as sun angle, atmospheric conditions, surface cover type, and topography. The topographic effect produces a variation in the spectral radiances associated with a given cover type and causes problems in image classification and interpretation due to the increased variance for the same class. These effects are caused by complex radiative processes happened in the mountainous terrain and need to be considered before accurate classification of multispectral data from mountainous terrain can be achieved.

In this paper, a model of radiation transfer in heterogeneous media is designed and evaluated. This model implements the Monte Carlo ray-tracing techniques and is specifically dedicated to the study of light propagation in mountainous regions. The radiative processes between sun light and the objects within the mountainous region are realized by using forward Monte Carlo ray-tracing methods, i.e., from the energy source to the scene. The energy source is supposed to consist of direct solar radiation, and sky radiation (solar radiation scattered by atmosphere). Once the ray is generated from the energy source, the module is invoked to determine the object of the scene and the location that will interact with the ray. When a ray collides with an object of the scene, its trajectory is affected by the optical properties and the scattering function of the object. In this paper, we assume the objects in the scene are Lambertian surfaces. The trajectory of each ray is then tracked through the scene from interaction to interaction until the ray is absorbed or leaves the scene. By collecting the rays above the scene, the total BRF, single scattering contributions and multiple scattering contributions can be computed.

The performance of the model is evaluated through detailed comparisons with the well-established 3D computer simulation model: RGM (Radiosity-Graphics combined Model) based on the same scenes and identical spectral parameters. The statistics of these two models' BRF fitting results for several typical mountainous structures under same conditions confirms the good agreements: all the correlation coefficients are above 0.99.

At the last part of the paper, series of typical mountainous scenes are generated, upon which different solar sources and objects' optical parameters are given to use the newly developed computer model to analyse the physical mechanism of mountainous radiation transfer. The results show that the effects of the adjacent slopes are important

29

for deep valleys and they particularly affect shadowed pixels, and the topographic effect needs to be considered in mountainous terrain before accurate inferences from remotely sensed data can be made. The model introduced in this paper, can be used to evaluate the accuracy of various correction techniques for different topographic scenes and irradiance conditions.

8174-92, Poster Session

Mutual influence between climate and vegetation cover through satellite data in Egypt

M. A. El-Shirbeny, M. A. Aboelghar, S. M. Arafat, National Authority for Remote Sensing and Space Sciences (Egypt); A. M. El-Gindy, Ain Shams Univ. (Egypt)

No abstract available

8174-94, Poster Session

DEM densification based on SFS from single multispectral remote sensing image

C. Zhe, T. Sun, Wuhan Univ. (China)

Numerous geoscience applications need denser and more accurate Digital Elevation Model (DEM) data. Photogrammetry is considered as the main method of producing DEM, however, there are cases for which no aerial photography is available. Otherwise, conventional interpolation methods are mathematical processes which often have the over-smooth phenomenon, or couldn't fully take the real characteristics of the terrain detail into account. In order to overcome these shortcomings, a DEM densification method was constructed by using shape from shading based on spectral information from single highly spatial resolution satellite image.

In accordance with the idea of introducing shape from shading (SFS) into DEM interpolation by Rajabi, a modified method is put forward, which is under the condition of the unknown light source and heterogeneous region. Surface relative shape is reconstructed at first, and the second order edge-oriented image interpolation method is applied to build a high-resolution DEM grid.

The relationship among image pixel value, light source direction, surface normal and surface albedo is established, in which different type of land cover has different surface albedo. In order to calculate surface normal from single image, light source direction and surface albedo estimation should be done at first.

Supervised classification for multi-spectral image is implemented in this article, and surface albedo is estimated respectively using statistic information for each class number. Different albedo for different land cover could overcome the drawback of assuming uniform albedo for the imaging model. Light source direction is calculated using shading information along image contours and minimization approach for each land cover type is applied to solve the ill-posed problem existing in SFS method. Finally least-square based on second order edge-oriented image interpolation method is utilized in interpolation procedure using slope map calculated from SFS result.

The model was used in heterogeneous landscapes in Sichuan province of China. High-resolution multi-spectral image and high-resolution DEM grids data were matched at first. Then the DEM data were downsampled to sparse level. Both traditional processes, including leastsquare, spline, Kriging, optimal interpolation, and our method were done to make the DEM grid has the same space resolution with remote sensing image.

Results show that traditional methods have over-smoothing phenomenon in some sharp jump areas, while SFS can capture the dramatic ups and downs of the regional characteristics. When the density of DEM data becomes sparse, especially in the case of only a few control points, conventional interpolation methods can't establish the global area elevation, while three-dimensional reconstruction of single remote sensing image can overcome this problem and obtain the real details of the terrain .The method is very effective for the sparse grid DEM interpolation and offer a new way for DEM densification.



8174-95, Poster Session

Periodicity analysis of NDVI time series in Heihe River basin in China

H. Han, Anhui Agricultural Univ. (China); M. Ma, Cold and Arid Regions Environmental and Engineering Research Institute (China)

Vegetation indices (VI) play an important role in monitoring variations in vegetation. The normalized difference vegetation index (NDVI) is the most widely used VI. The use of NDVI data acquired with multiple satellite sensors has become a necessity in research fields such as agriculture, land-use and land-cover change and changes in the natural environment, where fast changes are taking place. A good understanding of these changes is a strong requirement of long-time-series monitoring researches (Gallo et al. 2005).

Two long time series NDVI dataset were used in this paper for the periodicity analysis. One is the VEGETATION 10-day composite (VGT-S10) NDVI data with a 1×1 km resolution, covering the period from April 1998 to December 2009. The other is the Global Inventory Modeling and Mapping Studies (GIMMS) Advanced Very High Resolution Radiometer (AVHRR) NDVI data with an 8×8 km resolution, covering the period from April 1982 to December 2006. First, these two NDVI dataset were compared and converted by using the method developed by (Song et al. 2010). Then, the extended GIMMS AVHRR NDVI data set during 1982 to 2009 was used in this paper.

A new method, Empirical Mode Decomposition (EMD) (Huang et al. 1998), has been used for analyzing the periodicities of the extended GIMMS NDVI dataset during 1982 to 2009 in Heihe River Basin in China.

Four typical land cover types (A'rou alpine-cold meadow, Guantan Picea crassifolia forest, Huazhaizi desert, Yingke oasis farmland) were selected for the periodicity analysis on the NDVI time series. The result show that: except the Guantan Picea crassifolia forest, the NDVI in Heihe River Basin show an increased trend from 1982 to 2009. At the same time, most of station shows 2-3a, 5-6a, and 12-13a periodicity. This phenomenon may be consistent with the climate factors periodicity such as precipitation and temperature. Several studies have successfully proved that the precipitation and temperature have 2-3a and 5-6a periodicity in Northwest China (Chen et al. 2001; Yang et al. 2005). These results point to the forceful correlation between NDVI and climate factors, periodic changes in climatic factors may lead to causes in NDVI change. On the other hand, the periodicity in climate factors are related to some possible physical processes such as the mutual action of sea and atmosphere, solar activities, and so on. For example, 2-3a periodicity is the most fundamental periodic changes of meteorological elements on earth, this is an extremely important law in the process of atmospheric circulation.however,5-6a periodicity is the vibration period of solar activity.

In addition, NDVI periodicity may also be affected by other factors: Large-scale climate events, characteristic of topography, and the impact of human activities for in instance, But the specific impact of the mechanism needs further analysis.

8174-96, Poster Session

30

Passive microwave radiance estimation by coupling a land surface emissivity model with CRTM

H. Pan, J. Shi, Institute of Remote Sensing Applications (China); H. Yang, China Meteorological Administration (China)

Microwave land surface emissivity can be used for several purposes including land surface characterization and atmospheric retrieval over land from satellite passive microwave observations. Land surface heterogeneities make passive microwave radiance simulation over land challengeable. This paper focuses on microwave emissivity retrieval and radiance simulation over snow-free land for AMSR-E sensor configurations.

Microwave land surface emissivity is spatially highly variable, being sensitive to many surface parameters (e.g. vegetation cover, soil moisture, surface roughness, standing water or snow), and depending on frequency, polarization and incident angle. Inputs are provided by a land surface model, i.e. the Global Land Data Assimilation System (GDAS), including parameters such as daily atmospheric temperature and humidity profiles, surface skin temperature, soil moisture, global vegetation types and fractions. As accurate atmosphere and surface parameters over globe are poorly known at present, Daily GDAS data can be a good option. Daily AMSR-E brightness temperature observations are required for comparison with estimated radiances.

In general, the land surface is represented as a three-layer medium above an irregular subsurface in Community Radiative Transfer Model (CRTM), which takes volumetric scattering of dense medium into consideration. Emissivities at the surface-air interface and lower boundary are derived from a rough surface emission Qp model to account for cross polarization and surface roughness effects. The Qp model has proved itself accurate for AMSR-E data. The emissivity of the three-layer medium is then achieved by calculating the radiative transfer equation using a two-stream approximation. Finally, supposing that atmosphere is plane-parallel, radiances on top of atmosphere can be generally estimated by CRTM.

Emissivities and radiances are simulated at AMSR-E frequencies from 6.9 to 36.5 GHz for both v- and h- polarizations. The results are then validated against satellite observations. Estimated radiances show good agreement with observations. Generally, better results are derived at v- rather than h- polarization for each frequency. The radiances display biases from measurements with root-mean-square error less than 20K and mean biases less than 10K. These biases are partially caused by the uncertainties of the surface and atmosphere properties, where uncertainties of soil moisture have a large impact on emissivity simulations. The biases may also be caused by the model deficiencies (e.g. roughness parameterization).

8174-97, Poster Session

A combined active/passive microwave remote sensing approach for soil moisture retrieval

S. Wu, China Meteorological Administration (China)

Soil moisture constitutes only about 0.005% of the global water resources, but it's important for hydrological and climate models as boundary conditions. Microwave remote sensing provides a monitoring technology for spatial distribution of soil moisture with all-time, all-weather features. At present, there are two main methods to monitor soil moisture using the microwave remote sensing: one is active microwave remote sensing method based on radar or scatterometer. This method has higher spatial resolution, and it has significant changes to surface roughness and vegetation structure, but it's complicated to do the data processing; the other is passive microwave remote sensing method based on radiometer, which has a high time resolution, and is more sensitive to soil moisture. Compared with the former method, it's easier to process the data, but it has a lower spatial resolution.

We can see that both active and passive microwave remote sensing ways to monitor soil moisture have their own advantages. In fact, due to the surface vegetation cover, soil surface roughness and topography and other factors, both space-borne radar and satellite radiometer ways are not able to obtain accurate soil moisture. Through the studies of active and passive microwave remote sensing, researchers gradually realized that the passive and active microwave ways in soil moisture retrieval have advantages and limitations respectively, whichever a combination of both will get a better resolution. The present studies in home and abroad have shown that the combination of active and passive microwave remote sensing ways can improve the accuracy of soil moisture. But no matter Lee or Narayan, they didn't take consideration of the surface roughness parameter which has critical effect to backscattering coefficient and brightness temperature; therefore, it will bring relatively large uncertainty to the result.

This study develops a new algorithm for estimating bare surface soil moisture using combined active / passive microwave remote sensing on the basis of TRMM (Tropical Rainfall Measuring Mission). Tropical Rainfall Measurement Mission was jointly launched by NASA and NASDA in 1997, whose main task was to observe the precipitation of the area in 40 $^{\circ}$ N-40 $^{\circ}$ S. It was equipped with active microwave radar sensors (PR) and passive sensor microwave imager (TMI). To accurately estimate bare surface soil moisture, precipitation radar (PR) and microwave imager (TMI) are simultaneously used for observation.

According to the frequency and incident angle setting of PR and TMI, we first need to establish a database which includes a large range of surface conditions; and then we use Advanced Integral Equation Model (AIEM) to calculate the backscattering coefficient and emissivity. Meanwhile, under the accuracy of resolution, we use a simplified theoretical model (GO model) and the semi-empirical physical model (Model) to redescribe the process of scattering and radiation. There are quite a lot of parameters effecting backscattering coefficient and emissivity, including soil moisture, surface root mean square height, correlation length, and the correlation function etc. Radar backscattering is strongly affected by the surface roughness, which includes the surface root mean square roughness height, surface correlation length and the correlation function we use. And emissivity is differently affected by the root mean square slope under different polarizations. In general, emissivity decreases with the root mean square slope increases in V polarization, and increases with the root mean square slope increases in H polarization.

For the GO model, we found that the backscattering coefficient is only related to the root mean square slope and soil moisture when the incident angle is fixed. And for Model, through the analysis, we found that there is a quite good relationship between parameter and root mean square slope. So here, root mean square slope is a parameter that both models shared. Because of its big influence to backscattering and emissivity, we need to throw it out during the process of the combination of GO model and model. The result we obtain from the combined model is the Fresnel reflection coefficient in the normal direction . It has a good relationship with the soil dielectric constant. In Dobson Model, there is a detailed description about Fresnel reflection coefficient and soil moisture. With the help of Dobson model and that we have obtained, we can get the soil moisture that we want.

The backscattering coefficient and emissivity data used in combined model is from TRMM/PR, TMI; with this data, we can obtain ; further, we get the soil moisture by the relationship of the two parameters-- and soil moisture. To validate the accuracy of the retrieval soil moisture, there is an experiment conducted in Tibet.

The soil moisture data which is used to validate the retrieval algorithm is from GAME-Tibet IOP98 Soil Moisture and Temperature Measuring System (SMTMS). There are 9 observing sites in SMTMS to validate soil moisture. Meanwhile, we use the SMTMS soil moisture data obtained by Time Domain Reflectometer (TDR) to do the validation. And the result shows the comparison of retrieval and measured results is very good.

Through the analysis, we can see that the retrieval and measured results in D66 is nearly close; and in MS3608, the measured result is a little higher than retrieval result; in MS3637, the retrieval result is a little higher than measured result.

According to the analysis of the simulation results, we found that this combined active and passive approach to retrieve the soil moisture improves the retrieval accuracy.

8174-98, Poster Session

31

Validation of AMSR-E soil moisture products in Xilinhot grassland

S. Wu, China Meteorological Administration (China)

Soil moisture is a primary product of Advanced Microwave Scanning Radiometer for EOS (AMSR-E) which onboard Aqua satellite. AMSR-E soil moisture product provides us global soil moisture dataset from 2002 to present. It is known to all that validation is a big problem in the use of satellite remote sensing soil moisture product. The instantaneous field of view (IFOV) of different channel of AMSR-E ranges from 10 km to 50 km. For the lower frequency which is more sensitive to soil moisture, IFOV is larger. This means that a single point of AMSR-E soil moisture product contain average soil moisture of hundreds of km2 land surface. The traditional soil moisture measurement only gives us a single point soil moisture measurement result which is not equal to large area soil moisture.

In this paper, we present an experiment to validate the soil moisture product of AMSR-E. The experiment was carried out from July 15, 2008 to September 30, 2008. 9. The location of the experiment is in Xilinhot grassland, Neimeng province, China. During the former period, we put 9 soil moisture and temperature measurement systems



(ECH2O) in an area of about 3kmx3km. We selected this area because it's a very typical area in the Xilinhot grassland, which contain most land cover types and terrain types in the grassland. For each point, 5 layers of soil moisture and temperature were measured by ECH2O. The 5 layers are 2cm, 5cm, 10cm, 20cm and 50cm respectively. Considering the penetration depth of AMSR-E, 2cm measurements were used to do the validation. The location of the 9 ECH2O is very dispersive and the elevations of them are very different. Measurement result shows that the main factor that affects the soil moisture distribution is elevation. In grassland, soil moisture in higher place is always smaller than that of lower place. Which means a single soil moisture measurement is not suit for the soil moisture used purpose.

Precipitation measurement was also done in this area during the experiment period. Result shows that the precipitation is more effective to the top layers soil moisture than the bottom layers. In our sites, only 2cm and 5cm layers are affected by the precipitation. Other layer didn't change much during the whole period.

The average soil moisture measurement result in this area during the experiment is 11.8cm3/cm3, while the soil moisture product of AMSR-E in this area shows that the average soil moisture during this period is 13.3cm3/cm3. The RMSE of them is 3.7cm3/cm3.

Result show that AMSR-E soil moisture product has a good accuracy in the grassland of north China.

8174-99, Poster Session

The phenological characterization of the semi-arid regions of China based on remote sensing, flux tower observations and terrestrial ecosystem model

H. Wang, M. Ma, Cold and Arid Regions Environmental and Engineering Research Institute (China)

The land surface phenology is a key indicator of ecosystem dynamics, it can affect the carbon and water fluxes of ecosystems. Generally, the effect of vegetation phenology on energy and CO2 fluxes is represented by prescribing leaf onset and offset times or the seasonal evolution of vegetation indices. Over the last few decades, numerous studies have used the time series of vegetation indices derived from remote sensing to characterize land surface phenology. Recently, the eddy flux towers offers a new tool for delineating land surface phenology through net ecosystem exchange (NEE) and gross primary production (GPP) of CO2. In order to simulate the carbon and water fluxes correctly, the terrestrial models generally use empirical formulations to estimate the timing of crucial phonological events like leaf- on/off dates only based on abiotic variables, especially temperature or growing degree-days (GDDs).

In this study, we discussed three methods to characterize the land surface phenology: the satellite observation approach and CO2 eddy covariance flux observation approach and the terrestrial ecosystem model approach. We evaluated three vegetation indices(Normalized Difference Vegetation Index(NDVI), Enhanced Vegetation Index(EVI), and Land Surface Water Index(LSWI)) and the leaf area index(LAI) derived from MODIS land products in relation to NEE and GPP data from three CO2 eddy flux tower sites in the semi-arid regions of northwest of China representing three vegetation types (temperate grassland, cropland and evergreen needleleaf forest). Also, we simulated the phenology using a ecosystem model(Integrated Biosphere Simulator(IBIS)), and perform the simulation of carbon and water fluxes by replacing the phenology model with remote sensing products. From the Terrestrial ecosystem model simulation, we discuss the effect of phenological characterization on ecosystem carbon and water dynamics.

These studies showed that we need to combine the different approaches together, in order to develop better understanding of land surface phenology. What is more, repalce the process of simulating LAI of IBIS by using satellite leaf area index can improve the simulation of carbon fluxes.



8174-102, Poster Session

Angular and polarization measurements of snow and bare soil microwave reflective and emissive characteristics by Kaband (37ghz), combined scatterometerradiometer

M. L. Grigoryan, A. K. Arakelyan, A. K. Hambaryan, A. A. Arakelyan, ECOSERV Remote Observation Ctr. Co. Ltd. (Armenia)

For unambiguous and accurate retrieval of land snow cover and soil moistures and classification of soil vegetation a wider set of independent measurements and a synergy of various sensors are welcomed. Since, microwave signals backscattered from and emitted by the soil surface are partially decorrelated from each other and in practice may be considered as independent variables, the synergetic application of microwave radar and radiometer observations represents special interests. For it successful implementation it is important and suitable to develop multi-band complex of polarimetric, combined radar-radiometer systems and to perform multi-frequency, polarimetric, microwave, active-passive combined measurements of snow, bare and vegetated soils under well controlled conditions. On the basis of the acquired data, it will be possible to validate and to improve reflective (scattering) and radiative transfer models, and to develop new methods and algorithms providing the possibility to reach high precision in snow and soil moistures retrieval. Unfortunately, at present time, similar investigations have been carried out only partially.

In this paper the results of simultaneous and spatially coincident measurements of snow and bare soil microwave reflective (radar backscattering coefficient) and emissive (brightness temperature) characteristics angular dependences at 37GHz will be represented.

The measurements were carried out from a stationary, quartercircle shaped measuring platform of 6.5m of radius built over the experimental soil area of sizes of 10m x 3m. The system ArtAr-37 set on the mobile buggy has smoothly moved along a quarter circle shaped path of the measuring platform. A drive mechanism of the buggy allows stop it at any point of the path along the platform and perform measurements under any angle of incidence from 0-800. The platform allows research angular dependences of microwave reflective and emissive characteristics of the same area of the observed surface. The measurements were curried out under various conditions of soil and snow moistures, snow depth (thickness), surface roughness parameters, snow, air and soil temperatures. In this paper a methodology of experiments' performance and field calibration of the measuring system and the measured results will be discussed too.

The main characteristics of ArtAr-37 system are:

Central frequency 37GHz (Ka-band)

Antenna - Beamwidth Horn - 7.2degree

Polarization of Radar Channel - "vv", "vh", "hh" and "hv"

Polarization of Radiometer channel - "v" and "h"

Radar pulse type and duration - A train of 8 pulses of 25ns each

Radar pulse power - 30mW

Radar receiver's bandwidth - ~40MHz

Radar receivers noise factor - ~2dB

32

Radiometric receiver's noises - ~3000K

Radar channel's sensitivity at 1s - ~0.1dB

Radiometer receivers bandwidth - ~ 1GHz

Radiometer Channel's sensitivity at 1s - ~0.3K

The principal peculiarities of the utilized device are its originality in spatio-temporally combining of functionality of microwave active-passive channels of observation, under the condition of short range sensing application of the system. The minimum operational range of the system's scatterometer is 4m, at a far zone condition of sensing.

8174-103, Poster Session

Trajectories of land use change in huangshui river basin based on CLUE-S model

J. Gu, Cold and Arid Regions Environmental and Engineering Research Institute (China); X. Gao, S. Feng, Qinghai Normal Univ. (China)

Land use change is characterized by a high diversity of change trajectories depending on the local conditions, regional context and external influences. However, the land use change model can be an effective tool to simulate the land use change in different land use scenarios. In this paper, we will use CLUE-S model to simulate the temporal and spatial change pattern of land use in Huangshui river basin and also compared with real land use condition based on Landsat TM to make further analysis.

Huangshui river basin is the study region here, which is the first branch of Yellow river basin and covers 16120km2. For CLUE-S model, we collected 1986, 1996, 2007 Landsat TM data and get land use map by visual interpretation. The soil type map, digital elevation model data and social-economic statistical data are also collected. Furthermore, rivers, roads and urban area are extracted respectively from the associated maps to form driving force maps to represent the corresponding driving factors. Slopes, aspects, and elevation are derived from the digital elevation model. All data are made on the GIS software using pixels of 100×100m as unit of observation.

CLUE-S model used here is developed by Peter H. Verburg in Wageningen University, which has been extensively implemented in China, Central America, and other region. Results obtained form the literatures show that the model and show an excellent grid-based, multi-scale land use change model.

In this study, we calculate the land use coefficient based on 1986 land use map and then make simulation of land use pattern of 2007 based on land use of 1996. Then we calculate the change pattern of land use map between 2007 simulation and 2007 reality by Kappa analysis. Kappa analysis method used here is for describing the agreement of accuracy between the remote sensing-derived classification map and the reference data as indicated by CLUE-S simulation. The region with good agreement between the simulation and reality is explained that the change is driving by the factors we select. On the contrary, the region with no-good agreement can not be explained by the current model factors. Then we make logistic regression analysis between the change quantity of driving factors and the land use in 2007.The land use change feature can be explored by setting different scenario simulation.

Results indicated that the scheme based on CLUE-S model and scenario analysis can be used to identify the main driving factors in real land use change.

8174-104, Poster Session

Estimation of water budget by remote sensing in Taihu basin, China

X. Zhao, Y. Liu, Nanjing Institute of Geography and Limnology (China)

An improved knowledge of the land surface hydrologic states and fluxes, and of their spatial and temporal variability across different scales, is an important goal in many hydrologic studies. Taihu Basin is located in the lower reach of the Yangtze River basin. Recently, severe pollution in Lake Taihu was frequently occurred, which has led to the need to evaluate transport pathways and the overall water balance of the basin. Evapotranspiration (ET) and precipitation are the key elements in water balance estimation that give scientifically sound information on water availability. Currently, satellite remote sensing is widely used for estimation of these two parameters. In this study, precipitation and ET from remote sensing and observing runoff are used to estimate annual variations in the water budget of the Taihu Lake Basin from 2005 to 2007. The Global Satellite Mapping of Precipitation (GSMaP) data was applied to estimate precipitation in spatial and temporal variability of the Taihu Basin. Before application, the GSMaP data was evaluated using ground gauge observations and

calibrated. The surface temperature-normalized difference vegetation index (Ts-NDVI) triangle method with topographic correction was used to estimate ET from MODIS datasets in this study. The evaporative fraction (EF), defined as the ratio of ET and available radiant energy, was estimated by the triangle method with topographic correction. And then, spatially distributed net radiation (Rn) maps were retrieved as an estimate of available energy to get both the spatial and temporal distribution maps of ET for clear sky days. Runoff was observed from hydrological station. The ET is the largest consumption in water budget components. For the whole basin, the ratio of ET/Rainfall is about 0.85-0.95 from 2005 to 2007, and it is about 1.2-1.4 for Lake Taihu. In general, the income terms of water balance in the basin including precipitation and inflow from Yangtze River should be equal to outgo terms including ET, outflow and water storage. But the income terms is mostly larger than outgo terms in Taihu Basin, the imbalance percentage is about 0.4-9.6% for the whole basin, and 0.5-3.7% for Taihu Lake. The largest uncertainties possibly come from ET estimation, and due in part to ignore annual variation of soil water contents. So it remains challenging to improve the results by assimilating evapotranspiration estimated from satellite-based measurements.

8174-105, Poster Session

Evaluation of MODIS and reanalysis atmospheric products for atmospheric correction in thermal infrared domain with ground measurements

L. Hua, Q. Liu, Y. Du, B. Zhong, Institute of Remote Sensing Applications (China)

The removal of the atmospheric perturbation introduced in the signal registered by remote sensing sensors is one of the key elements in order to obtain accurate geo/biophysical products for earth observation purposes. Accurate atmospheric correction requires the knowledge of vertical information for some meteorological variables, such as the availability of an atmospheric profile, which could be achieved by launching an atmospheric sounding. However, local soundings are not available in most cases, we need to use other sources of atmospheric profiles for accurate atmospheric correction. Since the main objective of atmospheric correction in thermal infrared (TIR) range is the retrieval of the land surface temperature (LST), we intend to assess the feasibility of using other external sources of atmospheric profiles for LST retrieval from remote sensing data.

In this paper, two atmospheric profiles sources were assessed. One is the MODIS atmospheric profiles product (MOD07), another is the National Center for Environmental Prediction (NCEP) operational global analysis data. LST retrievals from HJ-1B/IRS data after atmospheric correction using MOD07 and NCEP data were compared with ground measured temperatures obtained from a series of field campaigns in Hebei province, China, from May to September, 2010. Ground measurements were carried out over four land cover types which include bare soil, full-cover wheat, full-cover corn and water surface. Six days'measurements over water surface and three days' measurements over land were collected, respectively.

The results indicate that the LST derived from HJ-1B/IRS data by using MOD07 and NCEP profiles both showed good agreements with the ground LSTs, with RMSE equal to 1.31K and 1.53K, respectively. Therefore, it can be concluded that the different atmospheric profile sources are useful for accurate atmospheric correction when local soundings are not available.

8174-106, Poster Session

A radiosity-based model to compute the radiation transfer of soil surface

F. Zhao, Y. Li, BeiHang Univ. (China)

Soil surface, as the lower boundary under the atmosphere or the vegetation cover, plays an important role in the process of the mass, momentum, and energy exchange between them. Field and remote sensing observations have shown that the directional distribution of solar radiation scattered from the soil surface is generally anisotropic.



Physically based models that can accurately depict soil reflectance anisotropy have immediate applications to the interpretation of remotely sensed data, to the further development of plant canopy reflectance models, to the understanding of the surface energy balance, and to the remote determination of soil properties.

The intent of the work reported here was to develop and evaluate a radiosity-based analytical model for soil Bidirectional Reflectance Factor's distributions that depends primarily on a soil property that can be characterized in the filed, i.e., surface roughness. The model was specifically dedicated to the study of radiation transfer for the soil surface under tillage practices. The soil was abstracted as two dimensional U-shaped and V-shaped geometric structures with periodic macroscopic variations. The roughness of the simulated surfaces was expressed as a ratio of the height to the width for the U and V-shaped structures. The assumption was made that the shadowing of soil surface, simulated by U or V-shaped valleys, has a greater influence on the soil reflectance distribution than the scattering properties of basic soil particles of silt and clay. Another assumption was that the soil is a perfectly diffuse reflector at a microscopic level, which is a prerequisite for the application of the radiosity method. To calculate radiation exchange among the soil surfaces, view factors between them were computed. Then the radiosity equation, which describes the conservation of energy, for each surface was established and solved easily.

This raiosity-based analytical model was evaluated by a forward Monte Carlo ray-tracing model under the same structural scenes and identical spectral parameters. The statistics of these two models' BRF fitting results for several soil structures under the same conditions confirmed the good agreements: all the correlation coefficients are above 0.9.

By using the newly developed model, BRFs of several soil surface structures were simulated to analyse the influence of soil surface roughness of soils, illumination and viewing geometries on the soil bidirectional reflectance pattern. It shows that BRFs for the simulated soil surface shows a clear backscatter regime with the peak appearing at the solar position, namely the 'hotspot' effect. This model can be coupled with a row crop model as a lower boundary condition to characterize the soil reflectance anisotropy. Besides, considering its analytical nature, it can be inverted to retrieve the roughness and optical parameters of soil surface from the remote sensing data.

8174-107, Poster Session

Validation of the collection 5 MODIS LAI product by scaling-up method using in situ measurements

H. Xue, J. Wang, Beijing Normal Univ. (China)

The Moderate Resolution Imaging Spectroradiometer (MODIS) land science team produces a number of standard products, including leaf area index (LAI).LAI is very often a critical parameter in processbased models of vegetation canopy response to global environment change. This paper made an assessment of the Collection 5 MODIS LAI product (MCD15A2) using field sample data in agriculture areas. Ground measurements were collected in heterogeneous areas and homogeneous areas for validation of collection 5 MODIS LAI products. LAI was measured with the LAI-2000 plant canopy analyzer. In order to improve the accuracy and reliability of ground measurements, two independent LAI-2000 units were used to take simultaneous measurements. GPS locations were recorded at each measurement point.

LAI-2000 instrument measures effective LAI, but the value of collection 5 MODIS LAI products is true LAI. To obtain the true LAIs of ground measurements, the instrument reading should then be multiplied by a correction factor. The correction factor was regressed in representative quadrats. In these quadrats, effective LAI value was collected using LAI 2000 and true LAI value was collected using direct measurement. The MODIS data in the hierarchical data format (HDF) and sinusoidal projection were transformed to geographic tagged image file format (GeoTIFF) and to UTM/WGS84 projection using the MODIS Reprojection Tool. One of the major problems for validating MODIS LAI product using ground measurements is the scale mismatch between ground "point" measurements and the MODIS resolutions. The homogeneous area is so large that the ground "point" measurements was in direct comparison to the MODIS LAI. heterogeneous area, In heterogeneous areas, we need to transform field measurements to the

scale of MODIS due to scale effect caused by the heterogeneity of land surface. In this study, we performed the scale transformation through fractal dimension theory, which describes the spatial heterogeneity of land surfaces and hence can be used to resolve the scale effect caused by spatial heterogeneity.

The field data was related to 30-m resolution TM images using empirical methods to create reference LAI map. Fractal dimensions for each MODIS pixel were calculated using a differential box counting method based on reference LAI map. TM imagery was also used to create a general vegetation cover classification map. We calculated the LAI of MODIS pixel according to the classification map. Then LAI values were up-scaled to 1km for MODIS LAI product validation. The results showed that, in homogeneous areas, ground measured LAI is closed to MODIS LAI product, also ground measured LAI in every quadrat is quite similar. In heterogeneous areas, it's obvious that MODIS LAI is lower than ground measurements without scale corrected. Transformed to the scale of MODIS spatial resolution using the fractal dimension theory, the ground measurements of LAI is quite close to MODIS LAI. The fractal dimension theory can solve the scale problem caused by spatial heterogeneity quite well.

8174-108, Poster Session

Estimating chlorophyll content of in Populus euphratica leaves from hyperspectral vegetation indices

G. Jiapaer, W. Dong, S. Wang, X. Yang, Xinjiang Institute of Ecology and Geography (China)

Leaf chlorophyll content is a good indicator of vegetation photosynthesis activity, nutritional and stress state. Recent studies have shown that the feasibility of retrieval of chlorophyll content from hyperspectral vegetation indices composed by the reflectance of specific bands. In this paper, field-derived hyperspecral reflectance of the Populus euphratica leaves and chlorophyll content of in leaves at the lower reaches of the Tarim River were measured and studied. Based on the field-measured hyperspectral data, we construct new simple ratio spectral indexes(SR) and normalized difference spectral indexes(ND) composed of the pair wise combination of all the possible bands in the 350-2500nm region, compare theses new pigment indices with a set of published vegetation indices belonged to three classes, normalized difference vegetation index(NDVI), simple ratio (SR) index and the chlorophyll absorption ratio index (CARI,CARI). Our objective is to explore their potentials in estimating chlorophyll content of Populus. euphratica leave. The 126 leaves of Populus euphratica were sampled at different development stages, representing a wide range of pigment contents. The hyperspectral reflectance of leaves of Populus euphratica and the corresponding chlorophyll contents were measured. The R2 values are calculated to determine the best vegetation index and the best bands for deriving the Populus euphratica Chl with field hyperspectral data from the linear regression between the measured Chl of Populus euphratica and the vegetation indexes. The result indicated that the good indicators for estimating ChL concentration in Populus euphratica were SR and ND hyperspectral indices calculated in the red edge region and short wavelength region. Compared to the published indices, the new construct SR(750,705) and ND (750,705)indices are most appropriate for chlorophyll estimation for Populus euphratica with high correlation coefficients R2 of 0.84 and 0.87, respectively.

8174-109, Poster Session

Deriving water content from canopy equivalent water thickness using hyperspectral indices and neural network

Q. Yi, A. Bao, Xinjiang Institute of Ecology and Geography (China)

Drought is one of the major environmental disasters in the world. In recent years, the damage from droughts to the environment and economies of some countries was extensive, and the death toll of livestock and wildlife was unprecedented. Drought monitoring has been an important issue to policy makers and the science community.



It is possible to assess the severity of a drought by simplifying complex drought phenomena into a single drought index because its sensitivity to surface biophysical parameters, such as soil moisture, vegetation condition. Amount of water in vegetation indirectly reflect soil moisture condition, and is regarded as an important indication for drought severity. Together with other parameters, vegetation water content is an important property that can be investigated by using remotely sensed data.

The main parameters describing the amount of water at canopy in vegetation that usually investigated by remote sensing are canopy EWT and VWC. There is now an extensive literature which shows that leaf or canopy water content, measured as EWTcanopy may be estimated from remotely sensed vegetation indices; however, very few studies have explicitly examined relationships among remotely sensed vegetation indices and those two water parameters of cotton at canopy level.

Numerous methods have been developed to estimate water content from reflectance data collected at different scales; they mainly rely on empirical or physical approaches that use regression techniques with hyperspectral indices, and leaf and canopy radiative transfer models. Although estimating EWT or VWC through canopy rediative transfer models inversion represents an attractive alternative, current methods estimate water parameters from remotely sensed data rely upon empirical relationships between spectral vegetation indices and water parameters. Most previous approaches for vegetation water content estimation use linear regression technique. In recent years, quantitatively remote sensing of the vegetation biochemicals has been greatly improved by the use of multivariate statistical methods, particularly artificial neural networks (ANNs). Some comparison studies between regression statistical technique and neural networks have been carried out by many authors using various datasets. To date, however, the predictive ability of ANN for water content estimation has not been well compared.

This paper initially analyses the relationship between remote sensing indices and EWT, VWC, and then discusses the method for improving the accuracy in retrieving water parameters at leaf and canopy levels. The study was focused on three major areas: (i) the relationships between remote sensed drought indices (DI) and water parameters; (ii) the suitable vegetation indices and water parameters for estimation of water information; (iii) the proper models for water content deriving. The objective of this paper is to explore further potential of NIR, SWIR wavelengths to estimate FMC, EWTleaf, VWC and EWTcanopy using leaf and canopy hyperspectral reflectance, and compare the performance of LR method and ANN technique for vegetation water content deriving based on remote sensed drought indices.



Conference 8175: Remote Sensing of the Ocean, Sea Ice, Coastal Waters, and Large Water Regions 2011

Wednesday-Thursday 21-22 September 2011

Part of Proceedings of SPIE Vol. 8175 Remote Sensing of the Ocean, Sea Ice, Coastal Waters, and Large Water Regions 2011

8175-01, Session 1

Sea surface temperature and ocean colour (MODIS/AQUA) space and time variability in Indonesian Sea coral reef systems from 2002 to 2011

R. A. Polonia, Univ. de Aveiro (Portugal); M. P. Figueiredo, Univ. dos Açores (Portugal); D. F. R. Cleary, Univ. de Aveiro (Portugal); N. Voogd, Univ. Twente (Netherlands); A. M. Martins, Univ. dos Açores (Portugal)

Indonesian Seas are placed in the center of the "Coral Triangle". These are comprised of more than 90 000 km2 of coral reef systems with more than 500 species of reef-building corals within. Presently, some of these reef systems are already experiencing massive destruction caused by anthropogenic local-scale sources (e.g. overfishing, deforestation, runoff, sedimentation, eutrophication, pollution) and/ or natural climatic global-scale sources which can inflict acute and/ or chronic impacts on these ecosystems. Temperature, for example, can be considered the most important contributor to coral bleaching. Within the framework of the 3-year project "LESS CORAL" an effort is being made to assess the combination of impacts linked to the human settlement which can affect the reef ecosystems at different temporal and spatial scales. With this in mind, we selected two of the most inhabited conurbanizations of Indonesia: a) Jakarta: and b) Makassar. These are both high density coastal cities in a close association to a coral reef ecosystem. Makassar with 1.5 million of inhabitants (capital of South Sulawesi) has its coast surrounded by the Spermonde coral reef system. Jakarta holding a population of 12 million of inhabitants (capital city of Indonesia) is located close to the Kepulauan Seribu coral reef system.

For a first evaluation of the temporal and spatial variation of nearsurface phytoplankton concentrations (in mg m-3) and surface temperatures (in C) in these two regions, we use MODIS/AQUA satellite-derived Ocean Colour (OC, Chl a as a proxy for phytoplankton) and Sea Surface Temperature (SST) data for a period of 9,5 years (2002-2011), under the framework of project DETRA. The two regions Jakarta and Makassar are both shallow water regions and satellite imagery show mixed water types (I and II, depending on coast distance). Therefore, OC imagery may not reflect only Chl a concentrations but suspended organic/inorganic particulate matter, CDOM, etc. These results were then correlated with large-scale atmospheric climate indices, particularly with the Southern Oscillation Index (SOI), Dipole Mode Index (DMI), and the North Atlantic Oscillation Index (NAO). Seasons were classified as: 1) Intermediate Wet (Sep-Oct-Nov or "SON"; 2) Wet (Dec-Jan-Feb, or "DJF"; 3) Intermediate Dry (Mar-Apr-May, or "MAM"); and 4) Dry (Jun-Jul-Aug, or "JJA"). In general, preliminary results show that despite theoretically belonging to different seasons, the trimesters JJA and SON as well as, DJF and MAM have similar behaviour both in terms of SST and OC. Surface temperatures show an increasing trend over the years in both regions but in a more pronounced manner in Makassar. In terms of SST vs OC, a positive but not significant correlation was found in Jakarta, while in Makassar these two variables are significantly negative correlated. Comparison of satellite data with the atmospheric indices, show a significant negative correlation between OC and NAO in Jakarta, and a significantly negative correlation between OC and SOI in Makassar.

35

8175-02, Session 1

Bathymetry mapping and sea floor classification using multispectral satellite data and standardized physics based data processing

T. Heege, S. Ohlendorf, EOMAP GmbH & Co. KG (Germany); S. Cerdeira-Estrada, CONABIO (Mexico); H. T. Kobryn, Murdoch Univ. (Australia)

All satellite data were calibrated with respect to the standards provided by the satellite data provider. The resulting calibrated radiances were analysed on correctness using the EOMAP radiative transfer model. For this check, we MODIS satellite data are used, that are recorded within 2-3 hours difference to the satellite data record. MODIS is used as reference sensor to calculate independently and precisely the optical conditions in water and atmosphere close to the target area. These conditions are taken over homogeneous adjacent deep water areas, and used as input for the radiative transfer model to calculate the expected sensor radiances for the high resolution WV-2 satellite data. WV-2 radiances needed to be systematically reduced for all channels, in order to fit with the MODIS results and allow physics based processing of bathymetry and sea floor products.

The calibrated radiances of input imagery were corrected for the so called adjacency effect (increased radiance over water due to reflection of photons by the nearby land and their further scattering in the atmosphere). The adjacency processor calculates the land albedo from the satellite scene itself. The adjacency effect has a range of up to 50km. Therefore, land-water border lines outside the satellite image are accounted for by use of the EOMAP global land-water data base. Scenes with sunglitter impact is corrected for spatially highly resolved sensors such as WV-2. Intermediate and slight sunglitter noise is corrected with an adaptive spatial filter.

Coupled retrieval of atmospheric optical thickness and water constituents is performed by minimising the mean square deviation of modelled top-of-atmosphere radiances and those measured for all sensor channels. For modelling of radiances the fast finite element code for the solution of radiative transfer equation in atmospherewater system is applied. The results of modelling for a large set of atmospheric parameters and concentrations of water species were stored once in large databases on the server and extracted in the core memory in the process of minimisation. The optical properties of the atmosphere are obtained basing on the model of the atmosphere use in a well-known MODTRAN code (Abreu & Anderson, 1996). The calculation to the subsurface reflectance is just a transformation of sensor radiance to reflectance after the aerosol concentration is retrieved.

Seafloor and water depth calculation is performed using the WATCOR module . The transformation of subsurface reflectance to the sea floor albedo is based on the equations published by Albert and Mobley (2003). The unknown input value of depth is calculated iteratively in combination with the spectral un-mixing of the respective bottom reflectance. The final depth is assessed at the minimum value of the residual error.

The final step of the thematic processing classifies the bottom reflectance due to the spectral signature of different bottom types and biota using a cluster and classification approach.

The bathymetry and sea floor classification product is filtered with a adaptive spatial filter. Values below 1m remain unfiltered. The filter radius is increased with depth, with respect to the increasing product noise and decreasing sensitivity of the satellite signal to water depth.

The accuracy of the satellite based method depends on the optical conditions at the satellite data take, the sensitivity of the satellite sensor and the accuracy of the calibration. We analyzed several WordView-2 scenes, an QuickBird and IKONOS scene recorded at



coastal areas of Mexico, West-Australia, Indonesia and in the Persian Gulf. For validation of water depth, echosounding data were used at all sites. In dependendy on the in-water optical conditions, water depth between 8 and 25 meters are be retrieved with an accuracy of 8 to 20%.

8175-03, Session 1

In-orbit radiometric performance variations of geostationary ocean color imager

S. Lee, S. Cho, H. Han, E. Oh, J. Ryu, Y. Ahn, Korea Ocean Research & Development Institute (Korea, Republic of)

Geostationary Ocean Color Imager(GOCI), a payload of the Communication, Ocean and Meteorology Satellite(COMS), is the world's first ocean color observation satellite in geostationary orbit. It is launched at Kourou Space Center in French Guiana in June 2010. The detector array in GOCI is custom CMOS Image sensor about 2 Megapixels, featuring rectangular pixel size to compensate for the Earth oblique projection.

This satellite is being operated on geostationary orbit about 36,500km far from earth, hence it is more influenced by sun activities than the other on low Earth orbit. Especially, the detector is sensitive of heat and it can give rise to increasing the defective pixels. In this paper, radiometric performance variations have been analyzed to monitor the aging of GOCI.

GOCI observes the ocean of northeast Asia by dividing into 16 areas (slot). Each slot is imaged over the 8 spectral channels. And two dark images are acquired before and after a slot for calibration.

the offset values are calculated from the two additional images. One is the dark current offset depending on the integration time, called as 'O'. The other is 'F'. It is the fixed offset term independent of the integration time, generated from the entire electronic component including the detector. They are characterized through time series analysis from 17 July 2010 to 15 Mar 2011.

When launching the COMS, the averaged offset O and F are 0.0384 and 596.33 for all slot and pixels on 13 July 2010. Though sun activities occurred on 7-8 Oct 2010 and 4-6 Mar 2011, the values have few differences with the first. But a diurnal variation is found that the averaged O is increasing at noon when sun energy is strongest throughout the day. After then it is decreased. The variation range is 0.038 to 0.040. A correlation analysis will be conducted with sun energy and the temperature of detector.

8175-04, Session 1

36

Development of a remote sensing algorithm for Cyanobacterial phycocyanin pigment in the Baltic Sea using neural network approach

S. Riha, H. Krawczyk, Deutsches Zentrum für Luft- und Raumfahrt e.V. (Germany)

Water quality monitoring in the Baltic Sea is of high ecological importance for all its neighbouring countries. They are highly interested in a regular monitoring of water quality parameters of their regional zones. A special attention is paid to the occurrence and dissemination of algae blooms. Among the appearing blooms the possibly toxicological or harmful Cyanobacteria cultures are a special case of investigation, due to their specific optical properties and due to the negative influence on the ecological state of the aquatic system. Satellite remote sensing, with its high temporal and spatial resolution opportunities, allows the frequent observations of large areas of the Baltic Sea with special focus on its two seasonal algae blooms. For a better monitoring of the Cyanobacteria dominated summer blooms, adapted algorithms are needed which take into account the special optical properties of these blue-green algae. Chlorophyll-a standard algorithms fail in a correct recognition of these occurrences.

To significantly improve the opportunities of observation and propagation of the Cyanobacteria blooms, the Marine Remote Sensing group of DLR has started the development of a model based inversion algorithm that includes a four component bio-optical water model for Case2 waters, which extends the commonly calculated parameter set Chlorophyll, Suspended Matter and Gelbstoff with an additional parameter for the estimation of Phycocyanin absorption. It was necessary to carry out detailed optical laboratory measurements with different Cyanobacteria cultures, occurring in the Baltic Sea, for the generation of a specific bio-optical model.

The inversion of satellite remote sensing data is based on an artificial Neural Network technique. This is a model based multivariate nonlinear inversion approach. The specially designed Neural Network is trained with a comprehensive dataset of simulated reflectance values taking into account the laboratory obtained specific optical properties of these algae species, according to the wavelengths of MERIS VIS/ NIR bands. The input to the inversion neural network are atmospheric corrected (Level2) MERIS bottom of atmosphere reflectances as well as viewing geometries of the sensor from which the output maps for Chlorophyll concentration, Suspended Matter concentration, Gelbstoff absorption and Phycocyanin absorption are generated.

The Poster will demonstrate the theoretical basis and development of the algorithm together with a number of example results obtained from MERIS scenes in the Baltic Sea. Furthermore it will compare the Phycocyanin-algorithm to the standard DLR PCI algorithm based on the related inversion technique "Principal Component Analysis" and discusses the different inversion approaches.

8175-05, Session 1

Uncertainties assessment and satellite validation over 2 years time series of multispectral, hyperspectral and polarization measurements in coastal waters at Long Island Sound Coastal Observatory

S. Ahmed, T. Harmel, A. Gilerson, A. Tonizzo, S. Hlaing, The City College of New York (United States); A. Weidemann, R. Arnone, U.S. Naval Research Lab. (United States)

Optical remote sensing of coastal waters from space is a basic requirement for effective global monitoring of seawater quality and assessment of anthropogenic impacts. However, this task remains highly challenging because of the optical complexity of the atmosphere-water system in coastal areas. To support present and future multi- and hyper-spectral calibration/validation activities for the Ocean Color Radiometry (OCR) satellites, as well as the development of new measurements and retrieval techniques for coastal waters, City College of New York along with Naval Research Laboratory, Stennis, has established a scientifically comprehensive observational platform for coastal waters, the Long Island Sound Coastal Observatory (LISCO). In operation since October 2009, LISCO uniquely combines continuous multispectral water-leaving radiometric measurements, using SeaPRISM, as part of the NASA AERONET - Ocean Color Network, with coincident hyperspectral measurements using the HyperSAS detectors, which, in addition to hyperspectral radiometry of the water leaving radiance also measure its polarization properties. This paper discusses the results and comparisons that can be achieved using these combined measurement approaches.

LISCO results of multi- and hyperspectral data processing as well as data quality analysis are described and related uncertainties evaluated over a two-year time series of coincident data. Intercomparisons between HyperSAS and SeaPRISM data were been carried out, permitting quantification of the main sources of uncertainty as follows: (i) sun glint removal generates unbiased uncertainties of 2.5%, (ii) sky glint removal generates unbiased uncertainties of 6%, (iii) viewing angle dependence corrections improve the data intercomparison by reducing unbiased uncertainties by more than 1.5%, (iv) normalization of atmospheric effects generates 5% of the unbiased uncertainties and adds a significant bias. Ways of reducing these uncertainties are proposed. Based on these results a dedicated HyperSAS data quality process has been implemented. In addition, the strong correlations between both datasets (R2>0.96) demonstrate the efficiency of the above-water retrieval concept and that the collocated instrumentations constitutes an important aid to the above-water data quality analysis, which makes LISCO a key element of the AERONET-OC network. The three main OCR satellites, MERIS, MODIS and SeaWiFS, were



evaluated against LISCO datasets of quality-checked measurements by SeaPRISM and HYPERSAS. The adjacency effects affecting the satellite data were analyzed and found negligible. The remote sensing reflectances retrieved from satellite and in situ data were then compared. It should be noted that the same atmospheric correction algorithm (Ocean Color Reprocessing 2009) were applied to each satellite dataset. The quality flags (glint, cloud, high solar and viewing zenith angle, atmospheric correction failure) were applied to filter satellite data. These comparisons show satisfactory correlations (r>0.9 at 550nm) and consistencies (absolute percentage difference ~ 15% at 550nm). Similar validations are shown for the hyperspectral satellite missions, HICO. Finally, future applications of the LISCO site to monitor current and future ocean color multispectral (VIIRS, Sentinel...) are finally proposed.

8175-06, Session 2

Estimating errors in satellite retrievals of bio-optical properties due to incorrect aerosol model selection

S. C. McCarthy, R. W. Gould, Jr., C. Kearney, A. Lawson, J. Richman, U.S. Naval Research Lab. (United States)

We examine the impact of incorrect atmospheric correction, specifically incorrect aerosol model selection, on retrieval of bio-optical properties from satellite ocean color imagery. Uncertainties in retrievals of bio-optical properties (such as chlorophyll, absorption and backscattering coefficients) from satellite ocean color imagery are related to a variety of factors, including errors associated with sensor calibration, atmospheric correction, and the bio-optical inversion algorithms. In many cases, selection of an inappropriate or erroneous aerosol model during atmospheric correction can dominate the errors in the satellite estimation of the normalized water-leaving radiances (nLw), especially over turbid, coastal waters. Here, we focus on only the impact of incorrect aerosol model selection on the radiance estimates, through comparisons between satellite retrievals and in situ measurements from AERONET-OC (AErosol RObotic NETwork - Ocean Color) sampling platforms.

The main challenge in atmospheric correction is the estimation and removal of the path radiance from the top-of-atmosphere (TOA) radiance values recorded by the satellite sensor. The path radiance contains both Rayleigh and aerosol scattering components, and can contribute about 90% of the TOA radiance. In the current version of the NASA ocean color atmospheric correction processing code, there are 80 aerosol models to choose from to calculate spectral aerosol radiance. Based on the spectral slope of the aerosol reflectance in the NIR bands, the two most appropriate aerosol models (from the entire set of 80 models) are retrieved and used for estimation of the aerosol radiance in the visible wavelengths. The question is, are we appropriately selecting these aerosol models?

We have tested all 80 aerosol models individually with data sets collected from three AERONET-OC sites in 2010 (Venice, Martha's Vineyard, and Gulf of Mexico). First, we derive nLw, chlorophyll, and aerosol optical depth from MODIS 1km resolution imagery at the locations of the AERONET-OC sites, using the aerosol models selected automatically from the standard atmospheric correction scheme. We compare these satellite values to the AERONET measurements. We then reprocess the MODIS imagery using all 80 aerosol models and again compare the products to the AERONET measurements, to determine the "optimal" aerosol model for each individual scene. The optimal model is the aerosol model that yields nLw closest to the AERONET values. We determine the optimal aerosol model at a single wavelength and use that model for the remaining visible wavelengths. We also determine the optimal aerosol model at each MODIS wavelength to estimate uncertainties in the satellite-derived optical properties.

Our results indicate that, in many cases, an incorrect aerosol model is selected during standard, automated processing. By properly selecting the optimal aerosol model, we can significantly reduce the errors in the retrieved nLw values, thereby improving the downstream estimates of the bio-optical properties. Furthermore, our analyses will allow us to accurately estimate uncertainties in satellite-derived optical properties and examine temporal and spatial patterns for multiple data sets.

37

8175-07, Session 2

Estimating uncertainties in bio-optical products derived from satellite ocean color imagery using an ensemble approach

R. W. Gould, Jr., S. C. McCarthy, I. Shulman, E. Coelho, J. Richman, U.S. Naval Research Lab. (United States)

We propose a methodology to quantify errors and produce uncertainty maps for satellite-derived ocean color bio-optical products, similar to those that accompany model results, by examining uncertainties in satellite water-leaving radiances and bio-optical properties using ensemble simulations.

Uncertainties in retrievals of bio-optical properties (such as chlorophyll, absorption and backscattering coefficients) from satellite ocean color imagery are related to a variety of factors, including sensor calibration, atmospheric correction, and the bio-optical inversion algorithms. Errors propagate, amplify, and intertwine along the processing path, so it is important to understand how the errors cascade through each step of the analysis, to assess their impact and identify the main factors contributing to the uncertainties in the final products. Ensemble techniques have been used by the environmental numerical modeling community to propagate initialization, forcing, and algorithm error sources through-out the full simulation process. For example, when each ensemble member uses a different realization (e.g., initial field and/or algorithms), the ensemble spread (or variance) provides an indication of uncertainty, or confidence in the estimate or forecast. This work develops, evaluates, and extends these techniques to satellite ocean color data processing and estimation.

First, we study the impact of incorrect or degrading sensor calibration on the bio-optical retrievals. The on-orbit calibration of a sensor can differ significantly from the pre-launch laboratory calibration. In addition, the calibration can drift over time, due to degradation of spectral filters and other factors. In a series of experiments, we applied random and systematic noise to the top-of-atmosphere (TOA) sensor radiance measurements to simulate the effect of sensor calibration errors. We then propagated these adjusted radiance values through the remaining processing steps (atmospheric correction and bio-optical inversion) to assess the effects on bio-optical retrievals, by examining derived single-point and spatial error statistics.

Second, we study the impact of different parameter selections in the algorithms used to estimate bio-optical properties from ocean color imagery and coupled biophysical models.

Finally, we compare the overall uncertainty estimates (combining algorithm uncertainties and sensor calibrations) using optical data sets from multiple open-ocean and coastal locations, at different time periods, to assess consistency and examine regional and temporal differences in the uncertainty patterns. We outline these processes and present preliminary results for this approach.

8175-08, Session 2

Some insights of spectral optimization in ocean color inversion

Z. Lee, Mississippi State Univ. (United States); B. Franz, Science Systems and Applications, Inc. (United States); S. Shang, Xiamen Univ. (China); Q. Dong, Mississippi State Univ. (United States); R. Arnone, U.S. Naval Research Lab. (United States)

In the past decades various algorithms have been developed for the retrieval of water constituents from the measurement of ocean color radiometry, and one of the approaches is spectral optimization. This approach defines an error target (or error function) between the input remote sensing reflectance and the output remote sensing reflectance, with the latter modeled with a few variables that represent the optically active properties (such as the absorption coefficient of phytoplankton and the backscattering coefficient of particles). The values of the variables when the error reach a minimum (optimization is achieved) are considered the properties that form the input remote sensing reflectance; or in other words, the equations are solved numerically. The applications of this approach implicitly assume that the error is a monotonic function of the various variables. Here, with data from



numerical simulation and field measurements, we show the shape of the error surface, in a way to justify the possibility of finding a solution of the various variables. In addition, because the spectral properties could be modeled differently, impacts of such differences on the error surface as well as on the retrievals are also presented.

8175-09, Session 2

Measuring underwater polarization field from above-water hyperspectral instrumentation for water composition retrieval

T. Harmel, A. Tonizzo, A. Gilerson, The City College of New York (United States); J. Chowdhary, Columbia Univ. (United States); S. Hlaing, S. Ahmed, The City College of New York (United States)

Increasing efforts are devoted by the Ocean Color Radiometry community to explore the polarization features of the underwater light field in order to enhance possibilities for retrieving inherent optical properties (IOPs) of coastal waters. New instrumentations and data inversion algorithms are being developed to take into account the supplementary information contained in polarization data. However, estimating the Stokes vector components of the polarized water radiance from above water measurements is a challenging task, mainly because of their small magnitude and the strong contamination by the polarized sky light reflected from the sea surface. In this study, above-water measurements are used to assess the feasibility of such retrievals and their utility for retrieving IOPs.

The Long Island Sound Coastal Observational platform (LISCO) near Northport, NY, was established in October 2009 to support satellite data validation. In June 2010, three customized hyperspectral HyperSAS systems (HyperSAS-POL) were added to LISCO platform enabling polarization measurements. A data processing algorithm, which includes vector radiative transfer computations, was developed and used to remove the polarization signal due to sky light reflected from the sea surface (sky glint) and derive the underwater polarization field. The impact of the aerosol type and loading on the polarized sky glint was also addressed and the use of aerosol data from the collocated AERONET system was assessed. The spectral shape of the retrieved underwater degree of polarization was then evaluated against theoretical radiative transfer computations and in situ underwater measurements achieved in the vicinity of the platform. The importance of taking into account coincident aerosol measurements for deriving the underwater polarization has been established. The results confirmed the validity of the polarization measurements by the LISCO site, thus validating a continuous time series starting from the beginning of June 2010 to the present which can be used for retrievals of IOPs from polarization measurements.

8175-10, Session 3

38

Remote sensing as input and validation tool for oil spill drift modelling

B. Baschek, Bundesanstalt für Gewässerkunde (Germany); S. Dick, F. Janssen, Bundesamt für Seeschifffahrt und Hydrographie (Germany); C. Kübert, Bundesanstalt für Gewässerkunde (Germany); S. Massmann, Bundesamt für Seeschifffahrt und Hydrographie (Germany); M. Pape, M. Roers, Bundesanstalt für Gewässerkunde (Germany)

Remote sensing by satellite and aerial surveillance is used operationally and as a combined tool for detection and characterisation of maritime pollution caused by oil spills. In Germany, on behalf of the Central Command for Maritime Emergencies (CCME), two aircraft of the type Dornier 228 are used that are equipped with a multi-sensor system. Available sensors are a side looking airborne radar, an infrared and ultraviolet scanner, a three channel microwave radiometer and a laser fluorescence sensor. Besides, the CleanSeaNet Service of the European Maritime Safety Agency (EMSA) is used that provides based on the analysis of radar satellite images - a monitoring service for possible spills. By these means, important information is gained for direct monitoring and as a support for oil spill response.

This information is a valuable input for numerical models predicting the drift of the detected spills - as the operational model run by the Federal Maritime and Hydrographic Agency (BSH) does. A prototype will be presented that has been developed, validated and tested quasi operationally by the Federal Institute of Hydrology in cooperation with BSH as part of the German project DeMarine. DeMarine ended in spring 2011 and was a German, DLR funded gateway project to the European GMES programme. This prototype realises a partly automatic connection between remote sensing and drift modelling. Mainly location and distribution of a spill are converted into the input for the drift model. Together with auxiliary information this input data can be transferred over the internet to automatically start the drift model run.

In addition, a method for drift model validation was developed and applied using this prototype: Chains of several observations by satellite or aircraft of one individual spill are compared to the results of the drift prognosis started from the first observation.

8175-11, Session 3

Airborne imaging sensors for environmental monitoring and surveillance in support of oil spills and recovery efforts

C. R. Bostater, Jr., J. Jones, H. Frystacky, G. Coppin, F. Leavaux, Florida Institute of Technology (United States)

Airborne Imaging Systems provide rapid initial monitoring and surveillance coverage over broad areas for initial disaster assessments as well as during recovery. During post disaster monitoring they provide unique insight into needed as well as ongoing efforts as part of the recovery process as well as a means to report on small scale releases. A combination of hyperspectral imaging systems, mapping cameras, digital cameras as well as high definition video sensors provide a combined view that enhances knowledge provided by satellites and single sensor system views. High spatial resolution imagery provides unique opportunities when combined with hyperspectral imagery for assessing coastal shoreline features and manmade operations. Results are shown from various airborne imaging sensor systems in the northern Gulf of Mexico region.

8175-12, Session 3

SETHI and SYSIPHE: the two newgeneration airborne remote sensing systems

J. Bruyant, P. Dreuillet, P. Chervet, L. Rousset-Rouviere, ONERA (France)

This paper presents the new-generation airborne remote sensing systems SETHI and SYSIPHE, developed by ONERA, the French Aerospace Lab, and dedicated to environmental, scientific and security applications.

For more than 20 years Onera is involve in deep research, including airborne systems development and extensive experiment campaigns, in radar and optronic imaging dedicated to military applications.

Today, many scientists from climatologists to agronomists, need specific types of information that cannot be provided in full by conventional observation systems. Thanks to its experience, Onera offers them a solution to use the huge potential of multispectral and hybrid radar/optronic data to help them to solve complex problems.

The SETHI remote sensing system is more dedicated to provide high resolution radar-optronics images. This system based on a bizjet Falcon 20 is operational from 2 years in a radar configuration. Its optronics capability is under development, the first radar-optronics flight will be made in summer 2011.

The SYSIPHE system is the state of the art airborne system to collect hyperspectral data. Its development is made in European cooperation involving three countries : France, Norway and Germany.



The first section of the paper introduces the objectives of the projects and their general architecture.

The second section describes the sensors characteristics, the implementation onboard the platforms, the data processing chain and gives an overview of the projects planning.

The third section presents results of the first years of operation and especially two significant experimental campaigns, the first dedicated to biomass measurement using a low frequency radar band, the second one dedicated to change detection in an urban area.

Fig 1 : Cutaway view of a SETHI pod

Fig 2 : Tropical forest SAR image

8175-13, Session 3

Short gravity-capillary waves modulation due to long surface and internal wave: laboratory and field experiment

I. Sergievskaya, S. A. Ermakov, Institute of Applied Physics (Russian Federation)

Modulation of short wind gravity-capillary waves due to long and internal waves is analyzing using data of radar and optical spectrum analyzer. The modulation of Ka-band radar backscatter due to long surface and internal waves has been studied in laboratory experiments in presence of surfactant film (Oleic acid) of different surface concentrations. Experiments were carried out in the oval wind wave tank of the Institute of Applied Physics. Wind waves were generated at two different fetches (7m and 11 m), wind velocities were varied from about 2 m/s to 5 m/s. The wavelengths of long surface and internal waves were about 1 meter, the amplitudes were 0.25 - 0.5 cm. Different physical mechanisms are taken into account including geometrical effects (tilt and range modulation), modulation of film surface concentration and transformation of the wind field over the long wave profile when the modulation of surface waves was retrieved. A new effect, an increase of the surface wave modulation in slicks, has been revealed. The Modulation Transfer Function (MTF) was analysed for non-slick and slick zones, and it is shown that the MTF magnitude in slicks can be several times larger than in non-slick areas. The phase of MTF is also changed in slicks. The theoretical estimations demonstrated that the effect cannot be explained using only the below mentioned mechanisms. The behaviour of the MTF is assumed to be determined by the contribution of bound components of the short wind-wave spectrum. The effect of increasing of surface waves modulation in slick zones was also observed in field experiments. The Ka- and X- band radars and optical spectrum analyzer with comparative wavelengths were used. The modulation was studied on the clean and contaminated water in the field of long and internal waves. This work has been supported by the Russian Foundation of Basic Research (project 10-05-00101, 11-05-00295).

8175-14, Session 3

39

Development and testing of an improved optimal band selection methodology using hyperspectral, multispectral imagery and synthetic imagery for shoreline feature analysis

C. R. Bostater, Jr., F. Leavaux, G. Coppin, H. Frystacky, J. Jones, Florida Institute of Technology (United States); X. Neyt, Royal Belgian Military Academy (Belgium)

Hyperspectral Imagery acquired from littoral or near shore remote sensing platforms (fixed or mobile) are utilized in the selection of optimal bands for detecting beach and shoreline features such as weathered oil due to the recent oil spill in the Gulf of Mexico region. The optimal band selection technique builds upon a technique previously utilized to detect vegetation stress and species discrimination due to vegetative water stress in coastal scrub vegetation. The algorithm approach is based upon an extension of the Weber contrast and utilizes multiple targets and or backgrounds for discrimination of spectral features from acquired hyperspectral spectral libraries. The resulting optimal bands are applied to hyperspectral imagery obtained from sensors aboard small vessels, aircraft and fixed platforms. The resulting images are combined with simultaneously acquired high spatial resolution multispectral images in order to form hybrid synthetic spatial-spectral sharpened hyperspectral imagery for enhanced detection of targeted shoreline features. The approach is designed for rapid monitoring and environmental surveillance of estuarine, freshwater or coastal harbor shorelines using airborne platforms, small vessels as well as fixed in-situ observation platforms as demonstrated.

8175-15, Session 4

Potential impacts of the Deepwater Horizon oil spill on large pelagic fishes

S. Frias-Torres, Ocean Research & Conservation (United States); C. R. Bostater, Jr., Florida Institute of Technology (United States)

The Deepwater Horizon (DWH) oil spill released crude oil from a depth of ~1500 m at an estimated rate of 68,000 barrels per day into the Gulf of Mexico during 87 days, from 20 April to 15 July 2010.

We report here that the oil spill covered critical areas used by large pelagic fishes. In satellite images, surface oil was detected in 100% of the northernmost whale shark sighting area, in 32.8 % of the bluefin tuna spawning area and 38 % of the blue marlin larval area. No surface oil was detected in the swordfish spawning and larval area. Possible consequences in the pelagic ecosystems of the Gulf of Mexico may be profound ranging from impacts on endangered species recovery to fish stock management.

8175-16, Session 4

High spectral resolution imager for solar induced fluorescence observation

A. Barducci, V. Nardino, D. Guzzi, C. Lastri, P. Sandri, I. Pippi, P. Marcoionni, V. Raimondi, Istituto di Fisica Applicata Nello Carrara (Italy)

The increase of the radiometric accuracy and spectral resolution of the optical imagers for Earth observation allows more accurate measurements of the spectral features of natural surfaces. The utilization of high-resolution imagers is particularly interesting for airborne and satellite remote sensing, allowing the investigation of vegetation, waters, and soils, as well as a better characterization of the global change phenomena and their bio-chemical and geophysical aspects.

Determination of the solar-induced fluorescence of natural bodies by observing the in-filling of Fraunhofer lines is being adopted as a tool for the bio-chemical and bio-physical characterization of the vegetation. To this purpose, the option to perform such kind of measurements from airborne platforms is being addressed in several research programs.

Recent in-field observations gave evidence of the main requirements for an imaging spectrometer to be used for Sun-induced fluorescence measurements. Among them we recall the high spectral resolution and the fine radiometric accuracy needed in order to resolve the shape of the observed Fraunhofer lines with a high level of accuracy.

In this paper, some solutions for the design of a high spectral resolution push-broom imaging spectrometer for Sun-induced fluorescence measurements are analysed. The main constraints for the optical design are a spectral resolution better than 0.01 nm and a wide field of view. Due to the fine instrumental spectral resolution, bi- dimensional focal plane arrays characterized by high quantum efficiency, low readout noise, and high sensitivity are requested. Beside, the development of a lightweight instrument is a benefit for aerospace implementations of this technology.

First results coming laboratory measurements and optical simulations are presented and discussed taking into account their feasibility.



8175-17, Session 4

Airborne hydromapping and hydroconnect shallow water bathymetry: pioneering underwater insights

F. Steinbacher, Leopold-Franzens-Univ. Innsbruck (Austria)

Water is fundamentally interdisciplinary in nature as it places mankind at the heart of any management objective. To protect and enhance the quality of aquatic ecosystems or to state the problems of flood protection in a simple way shows that ambitious programmes are needed to guarantee the key requirements of human next to environmental aspects. A multi-disciplinary research covering hydraulic, hydromorphological, ecological and climate change relevant expertise is needed. This means that an implementation of programmes predicated on understanding the complex interactions between hydromorphological, physico-chemical, biological and human factors expressed in terms of water bodies' ecological status is needed. Therefore a major commitment must be given in developing new monitoring standards and a much better understanding of the biophysical linkages between anthropogenic pressures and their ecological response. This is seen as a precondition to the development of cost-effective and sustainable remediation of damaged ecosystems and to future-proof the likely adverse impacts associated with climate change which will impact water bodies in different regions in a myriad of ways. The role and impacts of spatial structuring, variability and scaling effects is evidenced and further focused on realising the potential of the technique of laser ranging by airborne hydromapping. Technical developments within the last two-and-a-half years were set-up to deliver a better understanding for eco-hydro-morphological processes by a high resolution airborne bathymetric LIDAR survey technology and the detection of new indicators and the deliverance of advanced or new methods, combined with models, tools, software and services. The work at the University of Innsbruck is focused on the investigation and critically evaluation of the airborne hydromapping technology, on modelling and on decision-support tools which must be robust, uncertainty-inclusive, and offer the scope for standardisation.

Airborne Hydromapping and the research concept of HydroConnect try to cover technical and monitoring aspects next to the understanding of complex interactions between hydromorphological, physico-chemical, biological and human factors expressed in terms of water bodies' ecological status. Biodiversity is directly related to environmental decline or enhancement. An up-to-date, spatial and integrative monitoring approach on the level of water bodies followed by an analysis on the ecological impact meets the requirements needed to handle the present and future demands of our water bodies.

Some major impacts of the Airborne Hydromapping technology and the HydroConnect concept can be sum up as:

- the implementation of a new and innovative monitoring methodology enables better ecological impact estimation and will lead to cost-effective remediation measures.
- a new sustainable way to monitor large areas of water bodies in a more economic and less time intensive way.
- the higher quality spatial data will allow investigation of interrelationships between the fields of impact which will offer a new sight on biodiversity connectivity's.
- fast monitoring methods and water body relevant factor investigation enable faster, better, more cost-orientated decisions on management of water bodies.
- the new technology releases financial and personal resources due to less cost and time consumption and offer the possibility of increased monitoring.
- the investigation of underlying mechanisms between morphology and the physical and ecological processes is currently limited by lack of high resolution and up-to-date data. Therefore a new spatial monitoring technique was needed.
- biological and hydro-morphological indicators, tools and models can be found in a multitude of new information based on the bathymetric data by full waveform analysis.
- the range of research sites means that, a water body related impact analysis can be performed for spatial structuring, variability and scaling effects with regard to physical and ecological aspects of habitats.

40

 the repetitive monitoring based on high resolution data offers the development of advanced habitat models. The high spatial resolution results in a high discrimination between habitat types. Furthermore it will offer an increased effectiveness and speed in habitat survey.

8175-18, Session 4

Calibration, collection, and correction of airborne hyperspectral and high spatial resolution multispectral imagery for advanced coastal shoreline assessments

C. R. Bostater, Jr., G. Coppin, F. Leavaux, Florida Institute of Technology (United States); X. Neyt, Royal Belgian Military Academy (Belgium); H. Frystacky, J. Jones, Florida Institute of Technology (United States)

Airborne hyperspectral pushbroom images are corrected for platform motions using multiple sensor inputs from GPS and inertial motion sensor inputs. The algorithms developed are applied to imagery acquired in the Gulf of Mexico and nearby shorelines that have been monitored for oil spill impacts and assessments. The pushbroom image correction algorithms allow for a sequentially assessment and correction of airborne hyperspectral imagery prior to image to image rectification and ground based georeferencing of images. Systematic errors are analyzed and results presented using an adaptive Kalman smoothing methodology in a stepwise correction process. Image analysis methods are presented that indicate the ability of the airborne sensor data from multiple airborne imaging system to help in the assessment of oil spill monitoring and environmental surveillance in littoral zones, beaches and coastal wetlands.

8175-19, Session 4

Mesoscale and submesoscale eddies on the sea shelf and their impact on oil spill spread

O. Y. Lavrova, Space Research Institute (Russian Federation); A. G. Kostianoy, P.P. Shirshov Institute of Oceanology (Russian Federation); A. Y. Strochkov, Space Research Institute (Russian Federation)

Mesoscale and submesoscale eddies play an important role for mixing, vertical transport, or biogeochemical processes. However, quantifying in an objective way the distribution of eddies, their characteristics and how they change interannually remains a challenge. A large number of factors and wide variety of natural conditions in the ocean explain inevitable knowledge gaps concerning formation, evolution and propagation of eddies. They are a difficult subject of investigation by traditional techniques because of their small sizes, non-stationary character, sporadic occurrence and short lifetimes. The usage of visual and infrared remote sensing data as supplement to satellite SAR data has evoked a considerable advance in the studies of these processes. Joint analysis of satellite data, meteorological and contact measurements allowed us to estimate contributions of various factors into the mechanisms of mesoscale and submesoscale eddies generation and their spatial distribution for different areas of the Black, Baltic and Caspian Seas.

On the other hand, operational knowledge of water circulation, derived from multisensor data, can be used to improve numerical forecasts of oil spill drift.

Operational combined analysis of multisensor satellite and metocean data from the region of the spill in the Gulf of Mexico has shown that oil spill drift forecast, when not solely surface film but raw oil spill is concerned, should take into consideration primarily mesoscale circulation in the region, rather than wind and wave data as most models do. This discovery was vividly demonstrated in the formation and drift forecast of a gigantic oil jet that formed 17 May and drifted 300 km southeastward. Our team succeeded not only to explain the reason for the jet formation but also to reliably forecast its drift. It was shown that the jet was formed as a result of spilt oil entrainment by a strong gigantic eddy dipole of overall transverse size of 300 km. The results of satellite data analysis gave no chance for the jet



to reach either western Florida or the Gulf Stream, because it had to be entrained by the cyclonic part of the eddy, disintegrated and dissipated, which was exactly what happened in reality.

This work was partly supported by Russian Foundation of Basic Research project # 10-05-00428.

8175-20, Session 4

UAV remote sensing hazard assessment in Zhouqu debris flow disaster

Q. Wen, F. Xu, S. Chen, National Disaster Reduction Ctr. of China (China)

On August 8, 2010 morning, a large debris flow occurred in Zhouqu County, Gannan Tibetan Autonomous Prefecture, Gansu Province, China, which has damaged Zhouqu County and its surrounding area seriously and brought a huge loss of personal property. An UAV and airplane were sent there after one day to acquire disaster area images; UAV image of 0.2 meter resolution and aerial remote sensing image of 1 meter resolution were acquired.

Firstly, NDRCC compared pre-disaster and post-disaster remote sensing images of disaster area, continually monitored disaster scope, the damage of transportation, housing, residents of settlements, terrain and so on, and preliminary analyzed and judged the damage condition and disaster trend.

Then according to the preliminary analysis results, NDRCC partitioned the coverage and affection area of debris flow into 2-level grids with each house as an unit in high-resolution UAV and airborne remote sensing images, and about 2457 girds were numbered. Hazard assessment expert group were sent to implement field investigation according each grid. The loss extent, building area, architectural construction, and actual pictures of each grid were sent back to interpretation experts in NDRCC and some other damage conditions were also verified.

The disaster scope and extent of loss were defined again Disaster area was partitioned into three parts: heavy area is 1.2 square meters, serious area is 0.2 square meters and minor damage area is 1.0 square meters.

NDRCC detailedly assessed the physical quantity of housing, roads, power facilities, communication facilities, water conservation facilities, municipal utilities and land resources in high resolution UAV and airborne remote sensing images, combined with local government reporting data implemented the direct economic losses assessment. It is worth to mention that some damage quantity which was ignored in field investigation was detected in remote sensing images such as submerse street trees, telegraph poles, smart street pavilions.

This is the first time that remote sensing images are integrated into the national catastrophe assessment flow of China as a major data source.

8175-36, Poster Session

41

Is the katabatic wind the forcing factor of Terra Nova Bay polynya events?

F. F. Parmiggiani, Istituto di Scienze dell'Atmosfera e del Clima (Italy)

The dynamics of Terra Nova Bay (TNB) winter polynya events have been investigated by means of Sea-Ice Concentration (SIC) maps derived from the observations of thepassive microwave sensor AMSR-E [1,2]; these maps are produced by the Institute of Environmental Physics of the University of Bremen and made available on a daily basis through its web site.

The formation and persistence of TNB polynya are thought to be due to the combined effect of katabatic winds, advecting eastward the new formed ice, and of the Drygalski Ice Tongue which inhibits northward ice drift into TNB.

To measure polynya extents, an image window covering the area of TNB, approximately from 74.5 to 75.5°S and from 163 to 167°E, was extracted from the whole Antarctic SIC data set. This image window, 20x20 pixel size, i.e. $125 \times 125 \text{ km}$, which almost exactly circumscribes the TNB polynya, is used for the computation of polynya area. On the basis of previous studies [1,2], it is assumed that a SIC pixel is "open

water" when its value goes below 70%; polynya area is then computed by multiplying the number of "open water" pixels by the area of one pixel (39.0625 km2).

As katabatic wind, blowing eastward down from the Presley Glacier, is considered the main forcing factor in the opening of the polynya, wind data from AWS Eneide station, located in the vicinity of the Italian Antarctic Base "Mario Zucchelli Staion" (74.8°S 164.18°E), were retrieved. Eneide station takes measurements of wind speed and direction and air temperature every hour; wind speed and direction were then composed in one single figure defined as "effective wind", i.e. the wind component pushing eastward or at 270°.

The correlation between effective wind and polynya extents was analyzed by means of the "running correlation coefficient" (RCC) function [3] which can reveal the consistency between the forcing factor of the polynya and its opening. RCC function demonstrates that water areas may correlate either positively or negatively with offshore winds. This main result will be analyzed and discussed.

REFERENCES

[1] Parmiggiani, F.,(2006) "Fluctuations of Terra Nova Bay polynya as observed by active (ASAR) and passive (AMSR-E) microwave radiometers", Int.J. Remote Sensing, vol. 27, 2459-2467.

[2] Parmiggiani, F.,(2011) "Multi-year measure of Terra Nova Bay winter polynya extents", Europ.Phys.J.Plus, in press.

[3] Zhao, J., Cao, Y., and Shi, J.,(2006) "Core region of Arctic Oscillation and the main atmospheric events impact on the Arctic", Geophys. Res. Lett., vol.33, L22708, doi:10.1029/2006GL027590.

8175-37, Poster Session

Analysis of submarine sand wave imaging by SAR in Taiwan Shoal

K. Fan, W. Huang, B. Fu, The Second Institute of Oceanography, SOA (China)

In this paper, submarine sand wave imaging by SAR in Taiwan shoal and their relationships with sea surface wind and sea surface current are discussed. A total of 69 synthetic aperture radar (SAR) images over 11 years between 1996 and 2006 are collected and 496 profiles of sand wave SAR images are used for the observations of sand wave SAR images. The sea surface wind estimated from NCEP/ QSCAT blended wind data and the sea surface current calculated form high-frequency (HF) radar system are utilized for the study on the observations of sand wave SAR images with the wind speed and current speed. The results show submarine sand waves in Taiwan Shoal are mainly distributed from 117.75°E to 118.70°E and 22.7°N to 23.35°N with a high percent of 72.2. About 91% of sand waves are observed by SAR under wind speed of 9 m/s while only 6% of sand waves are imaged above wind speed of 10 m/s. And under the adverse wind direction, the observed sand wave reaches its maximum, while the crosswind has its minimum. These support that low and middle wind speed and adverse wind direction are favorable for SAR imaging submarine sand waves, high wind speed and crosswind are unfavorable. The observations of sand wave SAR images reach its seasonal maximum with a percentage of 49 in summer and have its minimum in autumn with 8%, while spring and winter has percentage of 20 and 23 respectively. The comparisons for monthly mean sea surface wind speed and monthly mean sea surface current speed with observed sand waves also shows strong relationships, which are lower sea surface wind speeds and higher sea surface current speed, the higher probability of sand waves observed by SAR. This may indicate that the higher observation of the sand waves by SAR is partly due to wind speed and current speed.

8175-38, Poster Session

Automatic procedure for oceanic internal wave detection on SAR image

K. Fan, X. Yu, Linyi Univ. (China); W. Huang, B. Fu, The Second Institute of Oceanography, SOA (China)

Ocean internal waves are meso-scale phenomenon that travel within the interior ocean and change the ocean surface roughness. As



synthetic aperture radar (SAR) works in microwave and resonates with surface Bragg waves, so SAR has the ability of observing ocean internal waves and this has been realized for some time. And the ocean internal waves appear as elongated bright and dark features in SAR images, due to the interaction between the surface Bragg waves and the surface currents induced by the spatially varying ocean internal waves. Because of the influence of SAR noise and other factors, it will be disturbed when we use computer auto-detection technique to detect the oceanic internal wave. In this paper, an automatic procedure has been developed for detection of oceanic internal wave on satellite SAR images based on the nature of sea surface oceanic internal wave. The procedure includes the edge detection, edge tracking and the determination and presentation of sea surface oceanic internal wave. Examples of detection of the sea surface oceanic internal wave on SAR images by the procedure are illustrated. The results of the sea surface oceanic internal wave detection have been compared with the visual interpretation. It is shown that the procedure works well.

8175-39, Poster Session

Exploring nutrient dynamics in Tampa Bay via sea-land interactions using MODIS images and clustering analysis

N. Chang, Univ. of Central Florida (United States)

Excessive Total Nitrogen (TN) and Total Phosphorus (TP) levels in natural water systems have proven to cause high levels of algae production. The Tampa Bay estuary has four major river basins that flow into it transporting TN and TP from the outfalls of terrestrial wastewater treatment plants and agricultural runoff. The process of phytoplankton growth which consumes the excess TN and TP in the bay can also be related to the changing water quality levels in the bay system such as dissolved oxygen (DO), salinity, available nutrient concentration, pH, water temperature, and turbidity. It is imperative that TP and TN levels be monitored for their impacts on the Tampa Bay and its estuary region. Therefore, such an indirect phenomenon can be monitored by satellites imagery such as MODIS sensor in this study. A genetic programming (GP) model was produced utilizing MODIS data to show the change of TN levels in 2008. In-situ data were drawn from a local database to support the GP model calibration, validation, and verification with the aid of the MODIS data. The sea-land linkages between the terrestrial nutrient inputs and nutrient distribution in the bay were assessed by using a clustering analysis. The bay has been divided into five sub-bay areas which relate to the four river influxes. These spatial linkages reveal significant correlations between sea-land interactions at the seasonal scale. This distinction helps trace back to show the major terrestrial contributor of nutrient inputs to the bay with strong implications in water quality management strategies related to the essential control of terrestrial effluent discharge.

8175-41, Poster Session

42

Integrated remote sensing and GIS applications in coastal environmental management and control based on high resolution satellite imagery data

N. Najibi, Univ. of Tehran (Iran, Islamic Republic of)

Coastal areas where the waters of the seas meet the land are indeed unique places in our global environment. They are unique in a very real environment sense as sites for port and harbor facilities that capture the large monetary benefits associated with waterborne commerce and are highly valued and greatly attractive as sites for resorts and as vacation destinations. The combination of freshwater and salt water in coastal estuaries creates some of the most productive and richest habitats on earth; the resulting bounty in fishes and other marine life can be of great value to coastal nations. In many locations, the coastal topography formed over the millennia provides significant protection from hurricanes, typhoons, and other ocean related disturbances. But these values could diminish or even be lost, if they are not managed.

Pollution of coastal waters can greatly reduce the production of fish, as can degradation of coastal nursery grounds and other valuable wetland habitats. The storm protection afforded by fringing reefs and mangrove forests can be lost if the corals die or the mangroves removed. Inappropriate development and accompanying despoilment can reduce the attractiveness of the coastal environment, greatly affecting tourism potential. Even ports and harbors require active management if they are to remain productive and successful over the long term. Coastal ecosystem management is thus immensely important for the sustainable use, development and protection of the coastal and marine areas and resources. To achieve this, an understanding of the coastal processes management that influence the coastal environments and the ways in which they interact is necessary. It is advantageous to adopt a holistic or systematic approach for solving the coastal problems, since understanding the processes and products of interaction in coastal environments is very complicated. A careful assessment of changes that occur in the coastal environments and in coastal ecosystems forms a major milestone for effective coastal ecosystem management and leads to sustainable utilization of coastal resources. All these can be achieved only through the collection of accurate, reliable and comprehensive set of scientific data. High resolution satellite imagery remote sensing technologies in recent years has proved to be of great importance in acquiring data for effective resources management and control and hence could also be applied to coastal environment monitoring and management. Further, the application of GIS (Geospatial Information System) in analyzing the trends and estimating the changes that have occurred in different themes helps in management decision making process.

8175-42, Poster Session

SVR-based chlorophyll retrieval of case II waters in Bohai Sea

Z. Tao, Institute of Remote Sensing Applications (China)

In this paper, We developed a new algorithm base on Support Vector Regression (SVR) to generate more accurate Chlorophyll production because it can makes possible accurate retrieval result from small training samples.

we pick out 29 observed data in case II waters which collected in 2009 around Bohai sea, and used for SVR-based algorithm to retrieval Chlorophyll. In the experiment here, the library libsvm, a robust SVR library, is used to produce a direct regression, using Gaussian Radial Basis functions(RBFs). Now, most of the retrieval of Chlorophyll using Rrs always choose blue - green ratio method. So here,we use Rrs443, Rrs467, Rrs488 and Rrs555 as the input band,pickup various combination to generate the different regression result. After lots of experiment, finally we find that use Rrs443/ Rrs555 and Rrs488/ Rrs555 as the input regression data will get the better result.

Compare with MODIS standard algorithm and some other algorithm, SVM-based algorithm provides higher accurate and adaptability. MODIS Standard algorithm shows 2-4 times higher than the real value. Tangjunwu's algorithm which works well in the case II water of yellow sea shows the same order of magnitude with observed data but bad matching. Multiple regression also shows inhomogeneous matching. Then we check out the turbid water index (tindx) of the 29 observed data in the bohai sea and find that most of the tindx are over 1.2(the average tindx of the open sea is around 1). So we can get a conclusion that MODIS Standard algorithm base on the open sea area observed data and may not suit the turbid coastal waters; empirical model may have a good retrieval result but it also limited by sea area.

In this paper, we offer a effective algorithm for Chlorophyll retrieval in case II water. Though the retrieval of Chlorophyll incase II water maybe complicated and uncertainty, we can still find out different method to improve the precision .Here, we just use a few data to checkout our algorithm but it still illustrate SVR can be use in case II water Chlorophyll retrieval. Next, we will collect more observe data to continue our Research and find out Seasonal change will causes any affection to our algorithm.



8175-43, Poster Session

Development of clarity model for Caspian Sea using MERIS images

H. Taheri Shahraiyni, Tarbiat Modares Univ. (Iran, Islamic Republic of); H. Sharifi, Shahrood Univ. of Technology (Iran, Islamic Republic of); M. Sanaeifar, Islamic Azad Univ. (Iran, Islamic Republic of)

Secchi disc is often used to measure the clarity of water in oceans and lakes and it is one of the most important indicators for water clarity. Monitoring of water clarity in a aquatic system is vital because it is highly related to the influent of nutrients, soil erosion, grazing of algae by zooplanktons, seasonal algae succession, circulation of bottom sediments, population of zooplankton and abundance of floating algae. In this study, an empirical model for the modeling is developed for the monitoring of secchi disc depth (SD) in the Caspian sea using satellite images. The Caspian Sea is a land-locked endorheic sea situated between Asia and Europe. It is the largest inland water body in the world. It covers a surface area of about

371 000 km2 and reaches a maximum depth of about 1000 m. In situ measurements of secchi disc depth have been performed in the Caspian Sea between July and October 2005. The in situ water samples were taken during 25 one-day campaigns at different distances to the coast using a motor boat as sampling platform, covering the natural variability between the coastal and the open sea waters. The samplings were performed concurrent with MERIS imaging of the Caspian Sea. Totally 37 secchi depth data of Caspian sea were gathered. The database was divided to 25 and 12 data for training and testing of empirical models, respectively.

A total of 25 Level 1B and 25 Level 2 MERIS Full Resolution (300m*300 m) images acquired over the Caspian Sea between July and October 2005 were used in this study. The level 1b and level 2 data are containing of remote sensing reflectance (Rrs) data of TOA (Top Of Atmosphere) and BOA (Bottom Of Atmosphere), respectively. The relation between secchi depth and Rrs, logarithm of Rrs, ratio of Rrs data and logarithm of ratio of Rrs data in different wavelengths for TOA and BOA data were investigated and then the highest correlation coefficient between secchi depth and mentioned Rrs parameters were selected and some empirical models were developed using them. The model development performed using 25 training dataset and then the developed models were tested using 12 test data. The results showed that the modeling using BOA data can lead to better results than TOA. The best developed model using BOA data is as 1/SD=-0.138 +2.08*[Rrs(681nm)/Rrs(560nm)]. The mean percent absolute error and correlation coefficient of this model in test stage were 28% and 0.86, respectively.

8175-44, Poster Session

43

Quasistationary areas of surface chlorophyll concentration as an indicator of the hydrological structure of the ocean based on satellite data

A. P. Shevyrnogov, G. Vysotskaya, Institute of Biophysics (Russian Federation)

Continuous monitoring of phytopigment concentrations in the ocean by space-borne methods makes possible to estimate ecological condition of biocenoses in critical areas. Unlike land vegetation, hydrological processes largely determine phytoplankton dynamics, which may be either recurrent or random.

The types of chlorophyll concentration dynamics can manifest as zones quasistationary by seasonal chlorophyll dynamics, perennial variations of phytopigment concentrations, anomalous variations, etc., that makes possible revealing of hydrological structure of the ocean.

While large-scale and frequently occurring phenomena have been much studied, the seldom-occurring changes of small size may be of interest for analysis of long-term processes and rare natural variations. Along with this, the ability to reflect consequences of anthropogenous impact or natural ecological disasters on the ocean biota makes the anomalous variations ecologically essential. Civilization aspiring for steady development and preservation of the biosphere, must have the knowledge of spatial distribution, seasonal dynamics and anomalies of the primary production process on the planet. Satellite recordings of phytopigment dynamics can help efficiently estimate anthropogenous impact on natural complexes.

In the papers of the authors (Shevyrnogov A.P., Vysotskaya G.S., Gitelzon J.I. Quasistationary areas of chlorophyll concentration in the world ocean as observed satellite data. Adv. Space Res. Vol. 18, No. 7, pp. 129-132, 1996) existence of zones, which are quasi-stationary with similar seasonal dynamics of chlorophyll concentration at surface layer of ocean, was shown. Results were obtained on the base of processing of time series of satellite images SeaWiFS. It was shown that fronts and frontal zones coincide with dividing lines between quasi-stationary areas, especially in areas of large oceanic streams. Biota of surface oceanic layer is more stable in comparison with quickly changing surface temperature. It gives a possibility to circumvent influence of high-frequency component (for example, a diurnal cycle) in investigation of dynamics of spatial distribution of surface streams. In addition, an analyses of nonstable ocean productivity phenomena, stood out time series of satellite images, showed existence of areas with different types of instability in the all Global ocean. They are observed as adjacent nonstationary zones of different size, which are associated by different ways with known oceanic phenomena.

The deriving moving variance using the intersection of the frontal zone between the Labrador Current and Gulf Stream may be an example. Even though the seasonal progress of dynamics in chlorophyll concentration is different and so are the absolute chlorophyll concentrations, the variance on both sides of the frontal zone is small. The variance drastically in¬creases at the intersection of the interface between the waters with differ¬ent seasonal dynamics of chlorophyll concentration.

It is evident that dynamics of a spatial distribution of biological productivity can give an additional knowledge of complicated picture of surface oceanic layer hydrology.

8175-45, Poster Session

Is it possible to add total SWH of ocean waves to the Globwave SAR dataset?

J. Yang, The Second Institute of Oceanography, SOA (China)

The GlobWave project funded by the European Space Agency (ESA) is to serve the needs of satellite wave product users across the globe. It seeks to improve the uptake of satellite-derived wind-wave and swell data by the scientific, operational and commercial user community. The newly released GlobWave data contain synthetic aperture radar (SAR, from Envisat ASAR) and altimeter (from ERS-1/2, Envisat, GFO, Jason-1/2 etc.) wave data with collocated in situ measurements (from National Oceanographic Data Center, NODC, etc.). While the derived altimeter wave data consist of total significant wave height (SWH) of ocean waves (both wind-waves and swells), the derived SAR wave data only consist of swell SWH. In this paper, some preliminary studies on mapping swell SWH to total SWH are carried out by using regression analysis. Dominant wavelength, azimuth cutoff wavelength, and wind speed of ocean surface are used as influence factors. Data from 2006 to 2009 are used in the studies. The results are compared to both collocated altimeter data and in situ measurements. Some preliminary results show that the difference between SAR derived total SWH and buoy data has a mean deviation (MD) of 0.03m and a relative deviation (RD) of 1.25%. As a conclusion, it is possible to add total SWH of ocean waves to the Globwave SAR dataset.

8175-46, Poster Session

a bio-optical model for the retrieval of suspending particulate material concentration based on MERIS image

Y. Song, B. Zhang, J. Li, Q. Shen, Ctr. for Earth Observation and Digital Earth (China)

A bio-optical model for the concentration retrieval of suspending particulate material is developed based on the in situ measurements of spectral reflectance data and suspending particulate material concentration of the Bohai Sea in July, 2010. The model utilizes spectral information of a single band after 750nm and is proved reliable since the relative error is acceptable when comparing with the suspending particulate material concentration measured in laboratory. The result relatively accords with the in situ measurements while utilizing this model to retrieve suspending particulate material concentration based on a MERIS image acquired synchronously. The spatial distribution features of suspending particulate material concentration are analyzed based on the combination of the model and the weather data collected during the in situ measurement.

(1) The areas with the highest suspending particulate material concentration in the Bohai Sea are located near the estuary of Yellow River and the coastal parts of the Bohai Sea. The suspending particulate material concentration has a decreasing trend when the distance to the coast is increasing.

(2) The spatial features of suspending particulate material concentration are mainly affected by river runoff and the resuspension of particulate materials on the seabed caused by sea waves. Besides, strong wind is another key factor dramatically influence the spatial distribution of suspending particulate material content.

8175-47, Poster Session

Phytoplankton bloom and sea surface cooling induced by Category 5 Typhoon Megi in the South China Sea: direct multisatellite observations

X. Chen, The Second Institute of Oceanography, SOA (China) and Zhejiang Univ. (China); D. Pan, The Second Institute of Oceanography, SOA (China); X. He, The Second Institute of Oceanography, SOA (China) and Zhejiang Univ. (China); Y. Bai, D. Wang, The Second Institute of Oceanography, SOA (China)

Category 5 typhoon Megi was the most intense typhoon both in 2010 of the world and in the last 20 years of the western north Pacific, which caused a significant phytoplankton bloom in the northern part of the South China Sea (SCS). In this study, we investigated upper ocean responses to Typhoon Megi by using MODIS ocean color data, multi-satellite microwave data, typhoon data and in-situ ARGO profiles. The chlorophyll-a concentration increased about thirty times after typhoon passage comparing with the value in the same time of 2008, when there was almost no typhoon passing through SCS. With the relationship of wind stress curl and upwelling, we found that the speed of upwelling was over ten times during typhoon passage than pre-typhoon period. Moreover, the mixed layer deepened about 20m observed from in-situ ARGO profiles. So these reveal that the enhancement of chl-a concentration was triggered by strong vertical mixing and upwelling caused by typhoon. On the other hand, remarkable sea surface cooling (6-8C°) was observed mainly to the right side of typhoon track on 21 October. The time-serial microwave sea surface temperature (SST) images show that the cold water moved westward and this phenomenon lasted about half a month. The cooling response of the upper ocean was probably due to the slow moving speed of typhoon and the shallow depth of mixed layer along the typhoon track in the SCS. In addition, the pre-existing positive sea level anomaly in the SCS became negative during the typhoon period. The cooling region corresponded with the large decline of sea level anomaly.

8175-48, Poster Session

Relationship between the colored dissolved organic matter and dissolved organic carbon and the application on remote sensing in East China Sea

L. Qiong, Wuhan Univ. (China) and The Second Institute of Oceanography, SOA (China); Y. Bai, H. Huang, Q. Zhu, The Second Institute of Oceanography, SOA (China); C. Zhe, Wuhan Univ. (China)

Dissolved Organic Carbon (DOC) plays an essential role in global carbon cycle as it is the largest organic carbon reservoir in the ocean, especially in the coastal areas. Estimation of DOC concentration in the coastal ocean by satellite remote sensing can offer us a better understanding of coastal carbon cycle. Three cruises were conducted in the Changjiang River estuary and East China Sea (ECS) in the summer and autumn 2010 to collect DOC, colored dissolved organic matter (CDOM) and Chlorophyll a concentration samples. DOC concentration varied from 54 to 87.6µM in the shelf of East China Sea in the late autumn, while there are a high DOC concentration in the Changjiang River estuary by rich terrestrial organic matter input, with 73 to 210µM DOC in summer and 104 to 169µM DOC in autumn. The distribution of DOC mainly controlled by the hydrography since the relationship between DOC and sanity was significant in both East China Sea and Changjiang River estuary. The biological activity did not affect the concentration of DOC obviously with a weak relationship between DOC and Chl a. CDOM represents a fraction of dissolve organic matter with significant optical properties and can be used to reflect the mixing behavior in coastal oceans where fresh water blends with the sea water. The absorption coefficient of CDOM (355) decreased with the sanity increasing in the Changjiang River estuary (R2=0.938) and the shelf of East China Sea (R2=0.9045). CDOM and DOC were significantly correlated in Changjiang River estuary and ECS dominated largely by the Changjiang diluted water. Based on the relationship of CDOM and DOC, we estimated the DOC concentration of the surface in ECS from satellite-derived CDOM images. Some deviations induced by the biological effect and related marine DOC accumulation and degradation were discussed.

8175-49, Poster Session

Study on long-term characteristics of suspended sediments in Minjiang Estuary based on MODIS DATA

X. Xu, The Third Institute of Oceanography, SOA (China) and South China Sea Institute of Oceanology (China); J. Chen, The Third Institute of Oceanography, SOA (China); D. Pan, Z. Mao, X. Chen, The Second Institute of Oceanography, SOA (China)

Concentration of suspended sediment directly affects the optical properties such as transparency and water color, and aquatic environment as well. Understanding temporal and spatial distribution of concentration of suspended sediment is key point in coastal study, such as in international proposal of LOICZ, S2S, and RioMa. The paper selects the Minjiang Estuary, southeast coast of China as study area, and has established inversion mode of suspended sediment by coupling field data with water-leaving radiation from MODIS data in Minjiang Estuary. Monthly-averaged concentrations and seasonal changes of suspended sediment from 2002 to 2009 were calculated and analyzed by the mode, in the end, mechanism affecting variability of suspended sediment was discussed. The main results are as follows:(1) Normalized water-leaving radiance ratio (nlw667/nlw488) from MODIS data has high relativity with the field observed turbidity by regression equation of Y = 0.618X2 -5.720X + 18.94, in which Y is turbidity, X is nlw667/nlw488 and R2 is 0.716. (2)Suspended sediment in the Minjiang Estuary has obviously spatial and temporal distribution characteristics, that higher concentration of suspended sediment is in coastal water and decreases from shore to sea, and highest concentration happens in winter.(3) Most of the sediment in water in the Minjiang Estuary and adjacent areas is original from runoff water from the Minjiang River, the Minzhe Coastal Water and re-suspension from sea bed. In a word, concentration of suspended sediment is mainly controlled by volume of runoff, wind and hydrodynamics, including wave, tide and circulation. (4) Remote sensing may overcome shortcomings of traditional field investigation for suspended sediment study, which is based on observation stations, and always gets discrete data in temporal and spatial scale with low efficiency. However, Remote sensing has more virtues by it's capability with high efficiency to monitor the suspended sediment dynamically and relative continually in temporal and spatial scale, and may provides long term time-series and large area data for suspended sediment study.





8175-50, Poster Session

Optical absorption and scattering properties in the East China Sea

X. Zhang, X. He, The Second Institute of Oceanography, SOA (China)

The absorption and particulate backscattering coefficients are the basic parameters of the water inherent optical properties(IOPs), which are also the basic parameters for the development and validation of the semi-analysis models of the ocean color remote sensing. In this work, the absorption and backscattering coefficients in the East China Sea(ECS) were measured in the summer and winter of 2009 using the three in-situ optical instruments, including the WETLabs ac-s, ECO VSF3, and the HOBILabs HydroScat-6. Based on the in-situ measured data, the distribution of the absorption and backscattering coefficients in the ECS are analyzed. The results show that in the summer the water of absorption coefficient at 443nm (a(443nm), excluding the absorption of the pure sea water) in the surface layer is ranged from 0.022 to 0.067 m-1, and the particulate backscattering coefficient at 442nm(bbp(442nm), is between 0.00064 and 0.03274 m-1. As a whoole, both of the absorption and backscattering coefficients decrease with the offshore direction, and the high values located at the mouth of Changjiang River. In the winter, a(443nm) is between 0.051 and 0.887 m-1, and bbp(442nm) is ranged from 0.000639 to 0.14614 m-1 at the surface layer. The spatial distributions in winter are similar as the summer, with the high value in the coast and low value in the offshore. The absorption and backscattering coefficients in winter are significantly larger than the summer's, especially in coastal area near the mouth of Changjinang River, which maybe casued by the southward Fujian-Zhejiang coastal current occurring in winter. As the vertical profile distributions, we find that both of the absorption and backscattering coefficients present a layer structure, which caused by the stratification of the sea water in the summer; while in the winter, affected by the strong wind disturbing, both of the absorption and backscattering coefficients are thoroughly vertical mixing. To our knowledge, it is the first time giving the distribution of the absorption and backscattering coefficients in the East China Sea.

8175-51, Poster Session

45

Remote sensing of water basins using optical range: time images of water surface

V. I. Titov, Institute of Applied Physics (Russian Federation)

The paper is devoted to the development of optical method for investigation of surface waves using RTI images (images in range - time - intensity coordinates) constructed from optical sections of surface.

The high-speed optical system based on linear array of CCD photodiodes for registration RTI images of capillary waves using artificial illumination is created. The data on free and bounded capillary waves, surface wave's breaking derived with this system is presented. The joint laboratory experiments with optical system and X-band scatterometer were conducted and the scattering mechanisms for radio waves by the waved surface were investigated.

The technique for creating of large scale RTI images of sea surface under grazing angles was developed. The principles of using such technique for a ship or airplanes permitting to eliminate the influence of ship's or airplane's tossing are proposed. This system is useful for monitoring of coastal zones and inland waters.

Some examples of RTI images recording from sea and river shore for various wind conditions, sea state and for oil slicks are presented.

The damping of surface roughness in oil slicks were calculated taking into account shadowing of surface waves under grazing angles and the method for retrieval of sea surface wave characteristics is proposed.

The underwater processes and wind are displayed on water surface due to its influence on surface roughness. The method for registration of large scale features of near surface wind fields using its manifestations on water surface is presented and method for retrieval of wind speed from optical image of waved water surface is discussed.

8175-53, Poster Session

Research on sea surface wind field retrieval from SAR imagery along the Zhejiang coast

J. Chang, Ocean University of China (China); W. Huang, X. Lou, K. Fan, The Second Institute of Oceanography, SOA (China)

The high-resolution, all-weather capability of synthetic aperture radar (SAR) image has been used to estimate marine wind vector fields. Upwelling phenomenon along the Zhejiang Coast is prevalent in summer. It makes the sea surface smoother which results in the lower backscatter cross section in SAR imagery. So the sea surface wind retrieval from SAR imagery in upwelling region would be underestimated. In this study, with sea surface temperature (SST) and chlorophyll2-a derived from MODIS, the low backscatter feature in ENVISAT ASAR image is analyzed along the Zhejiang Coast. Also the CMOD4 algorithm is adopted to retrieve the sea surface wind speed, under using the wind directions from interpolated NCEP NCAR reanalysis data, which is the result of operational numerical atmospheric model of NOAA National Center for Environmental Prediction. The result shows that the wind speed is underestimated associated with the low backscatter cross section, which is caused by coastal upwelling. It is necessary to propose a method to correct wind speed. In the following processing, the wind speed retrieved from ASAR, which is not influenced by upwelling and high resolution meteorological forecasting data is obtained and analyzed. Based on above statistical method and the mean value sample method and et al., the correlation relationship between wind speed retrieved from SAR and high resolution meteorological forecasting data is analyzed. The result shows strong correlation. Then combining with high resolution meteorological forecasting data, the wind speed correction model is established at first time for the large-scale low backscatter SAR image, which is caused by upwelling. The relationship between wind speeds retrieved from SAR and high resolution meteorological forecasting data is fixed in a same region. So the accuracy of corrected wind speed is approximately same as the accuracy of wind speed retrieved from SAR, which is not influenced by upwelling. The retrieval accuracy of sea surface wind in upwelling region is improved by using above method.

Result shows that the corrected wind speed by high resolution meteorological forecasting data could improve the accuracy of SAR wind retrieval in upwelling region and it is necessary to establish a wind correction model for the wind speed retrieval in upwelling region, based on meteorological forecasts data and GMF mode.

8175-54, Poster Session

Status of the ocean carbon observing from space in China

D. Pan, Y. Bai, X. Chen, The Second Institute of Oceanography, SOA (China)

The advantaged routine ocean observation from space has pushed the satellite application to go widely in the oceanography study with deepened multi-discipline cooperation. In this talk, firstly, some progresses in the estimation of particle and dissolved carbon, and the partial pressure of aquatic CO2 (pCO2) will be present. Due to the highly dynamic and complex water mass interaction in the marginal sea, especial in the East China Sea, the semi-analytic algorithm of water inherent optical properties is promising than the traditional empirical algorithm. Characteristic and parameterization of regional inherent optical properties were figured out with the accumulating field measurements. The absorption and backscattering coefficient of particle and dissolve matter can be retrieved by the semi-analytic algorithms, and further, the particle and dissolve carbon can be estimated by the regional geochemical-optical models. Also, the salinity in the plume regions can be mapped through the good relationship between CDOM and salinity in the ECS which is affected by Changjiang diluted water. The semi-analytic method can be further applied to the satellite-retrieval of pCO2. Based on the analysis of factors and processes controlling the changes of pCO2, quantified models were built up to estimate the specific pCO2 variation caused by the separated factors. By adding up the contributions of specific pCO2 variation with major controlling factors, the total pCO2 variation can be mapped using the satellite-derived products. Finally, the



satellite programs and application systems development in China will be introduced with the focus on the carbon observation from space, and some suggestions will be put forward to the carbon observation and multi-discipline cooperation.

8175-55, Poster Session

HAB detection based on absorption and backscattering properties of phytoplankton

H. Lei, The Second Institute of Oceanography, SOA (China) and Zhejiang Univ. (China); D. Pan, Y. Bai, X. He, The Second Institute of Oceanography, SOA (China); X. Chen, The Second Institute of Oceanography, SOA (China) and Zhejiang Univ. (China)

The coastal area of East China Sea (ECS) suffers from the harmful algal blooms (HAB) frequently every year in the warm season. The most common causative phytoplankton algal species of HAB in the ECS in recent years are Prorocentrum donghaiense (dinoflagellates), Karenia mikimotoi (dinoflagellates which could produce hemolytic and ichthyotoxins) and Skeletonema costatum (diatom). The discrimination between the dinoflagellates and diatom HAB through ocean color remote sensing approach can add the knowledge of HAB events in ECS and help to the precaution. A series of in-situ measurement consisted of absorption coefficient, total scattering and particulate backscattering coefficient was conducted in the southern coast of Zhejiang Province in May and August 2009, and the estuary of Changjiang River in December 2010, which encountered two HAB events and a moderate bloom. The Inherent Optical Properties (IOPs) of the bloom waters have significant difference between phytoplankton species in absorption and backscattering properties. The chlorophyll a specific absorption coefficient ($a^*phy(\lambda)$) for the bloom patches (chlorophyll a concentration >6mg m3) differ greatly from the adjacent normal seawater, with the $a^*phy(\lambda)$ of bloom water lower than 0.03 m2 mg1 while the a*phy(λ) of the adjacent normal seawater is much higher (even up to 0.06 m2 mg1). Meanwhile, the backscattering coefficient at 6 wavelengths (420, 442, 470, 510, 590 and 700nm) is also remarkably lower for bloom waters (0.02 m1). The backscattering coefficient ratio (Rbp(λ)) is much lower for diatom bloom waters than for dinoflagellates types (0.01079 vs. 0.01227), because most cells of diatom species tend to link together in long chains, showing the much larger particulate size. A discrimination model based on IOPs is established, and several typical dinoflagellates and diatom bloom events including Prorocentrum donghaiense, Karenia mikimotoi and Skeletonema costatum in the ECS are picked out for testing with the ocean color remote sensing products from NASA, including the chlorophyll a concentration, particulate backscatter coefficient at 443nm (QAA), and phytoplankton absorption coefficient at 443nm (QAA). The result proves that the satellite-derived inherent optical properties can be used to HAB detection and the discrimination of HAB species from dinoflagellates and the diatom types in the ECS.

8175-56, Poster Session

46

The internal waves' distribution of whole South China Sea extracted from ENVISAT and ERS2 SAR images

J. Wang, Ocean Univ. of China (China)

Internal waves are waves that travel within the interior of ocean, and often observed in South China Sea. Some persons, like Liu, Hsu, Zhao, have studied internal waves in South China Sea. But all of their study focused on the northern South China Sea. In this paper, more than 700 SAR (ENVISAT and ERS2) images from 2005 to 2010, what cover the whole South China Sea, are used to extract internal waves. The internal waves' distribution maps of whole South China Sea will be given year by year from 2005 to 2010. And the statistical analysis shows that: 1) Internal waves not only occur in the northern South China Sea (between Luzon Strait and Hainan island), also occur along the Vietnamese coast and nearby Spratly islands. Most internal waves occur in the northern South China Sea, they generated in Luzon Strait and propagated westward across Dongsha island. Some internal waves turned into northwestward because of the continental shelf.

Along the Vietnamese coast, internal waves generated at the shelf by the tide from Luzon Strait. They propagated toward Vietnamese coast. Nearby Spratly islands, internal waves are influenced by Mekong river and continental shelf. They propagated toward southeast or southwest. Even in Borneo coast internal waves can be observed. 2) Internal waves are observed all year in the South China Sea, mostly during summer.

8175-57, Poster Session

In-orbit image performance simulation for GOCI of using integrated ray tracing technique

E. Oh, Korea Ocean Research & Development Institute (Korea, Republic of); S. Kim, Yonsei Univ. (Korea, Republic of); Y. Jeong, I&A Tech, Inc. (Korea, Republic of); S. Jeong, LG Innotek (Korea, Republic of); S. Cho, J. Ryu, Y. Ahn, Korea Ocean Research & Development Institute (Korea, Republic of)

Geostationary Ocean Color Imager(GOCI) is one of three payloads on board the Communication, Ocean, and Meteorological Satellite(COMS) launched 27th, June, 2010. For understanding GOCI imaging performance, we constructed the Integrated Ray Tracing model consisting of the Sun model as a light source, a target Earth model, and the GOCI optical system model. We then combined them in Monte Carlo based ray tracing computation. Light travels from the Sun and it is then reflected from the Earth section of roughly 2500km * 2500km in size around the Korea peninsula with 40km in spatial resolution. It is then fed into the instrument before reaching to the detector plane. Trial simulation runs for the GOCI imaging performance were focused onto GSD and MTF. First, we used two island targets of 10km and 73km in size. Their image parameters including GSD obtained from the GOCI measurement were compared to the ray tracing simulation results. Second, we investigated GOCI in-orbit MTF performance with the slanted knife edge method applied to an East coastline image of the Korea peninsula covering from 38.04°N, 128.40°E to 38.01°N, 128.43°E. The ray tracing simulation results showed 0.34 in MTF mean for near IR band image while the GOCI image obtained 9th Sep, 2010 and 15th Sep, 2010, were used to produce 0.34 at Nyquist frequency in MTF. This study results prove that the GOCI image performance is well within the target performance requirement, and that the IRT endto-end simulation technique introduced here can be applicable for high accuracy simulation of in-orbit performances of GOCI and of other earth observing satellite instruments.

8175-59, Poster Session

An extracting process of the retrieval coefficients for three frequency channel microwave radiometer

G. Zheng, The Second Institute of Oceanography, SOA (China)

Satellite microwave radiometers have been successfully developed to observe the state of sea surface and atmosphere on a global scale. This paper focuses on the retrieval coefficients of satellite microwave radiometers in the retrieval models for cloud liquid, wind speed, and wet troposphere path delay. The kind of microwave radiometers with three frequency channels, such as TOPEX/Poseidon microwave radiometer (TMR) and Jason-1 microwave radiometer (JMR), is discussed. The retrieval models of TMR and JMR are almost same, and achieve success to retrieve cloud liquid, wind speed, and wet troposphere path delay. In the retrieval models of wet troposphere path delay, which is used to correct the altimeter range errors induced by water vapor content, the retrieval coefficients are stratified with wind speed and initial estimate value of wet troposphere path delay. How to extract these retrieval coefficients from observation data is not discussed well in former literature. In this paper, a process of extracting these retrieval coefficients from the data of the bright temperature in the three frequency channels and relevant physical quantity is presented. The data of JMR are used to extract the retrieval coefficients and validate this extracting process. The cloud liquid, wind speed, and wet troposphere path delay data retrieved with the retrieval coefficients obtained through the extracting process in this



paper are compared with these data of JMR. The results show a good agreement. The further error analysis of this extracting process for the retrieval coefficients is important, and will be studied in our future work.

8175-60, Poster Session

Sea ice remote sensing using AMSR-E data: surface roughness and refractive index

I. Shin, J. Park, A. Suh, S. Hong, Korea Meteorological Administration (Korea, Republic of)

Sea ice is vital in understanding the surface energy budget, atmospheric circulation, clouds, fresh water, and global climate system. In general, the space-borne microwave remote sensing uses a large contrast in emissivity between sea ice and water to estimate the sea ice variability. The emission of the sea ice surfaces depend on the surface roughness and refractive index significantly, however, the measurement of sea ice surface roughness and refractive index are rarely published.

This study provides a unique method for retrieving the small-scale roughness and refractive index of sea ice in Polar Regions using the Advanced Microwave Scanning Radiometer for Earth Observing System (AMSR-E) data. In addition, this study exhibits the global trends of small-scale roughness and refractive index of the sea ice in Arctic and Antarctic using the AMSR-E level-3 25-km brightness temperature data from March 2003 to September 2009.

An approximate relationship between the polarized reflectivities for the specular surface (Hong approximation) is the core idea. In addition, a method to estimate the small-scale surface roughness was developed using the Hong approximation and the characteristics of rough surface emissivity near the Brewster angle at microwave frequencies.

The procedure in this study is as follows:

First, the rough surface emissivity is estimated using AMSR-E level 3 data. Second, the small-scale surface roughness is calculated. Third, the specular emissivity of sea ice is retrieved. Finally, the refractive index of each pixel of AMSR-E data is computed using a direct inversion of Fresnel equation.

The retrieved small-scale roughness and refractive index at AMSR-E 6.9 GHz channel exhibit good agreements with the measurements of sea ice surface small-scale roughness in the Baltic Sea and the known refractive index of ice and snow, respectively. The seasonal and annual trends of sea ice extent agreed with those observed in previous studies. The surface roughness shows the seasonal and annual downward trends. The refractive index exhibits the opposite trends. Consequently, this study supports that polar sea ice is melting due to climate change on the basis of the surface roughness and the refractive index.

8175-61, Poster Session

The use of MERIS fluorescence bands for red tides monitoring in the East China Sea

B. Tao, Z. Mao, The Second Institute of Oceanography, SOA (China)

The East China Sea suffers from the frequent occurrence of a variety of red tides, some of which often result in severe negative impacts to local marine ecosystems and economy. The development of algorithm for the detection and monitoring of red tides, using data from Medium Resolution Imaging Spectrometer (MERIS), are discussed. Coastal waters of East China Sea are typically highly scattering waters with very high concentration of sediment load. The traditional Fluorescence Line Height (FLH) determined with MERIS bands at 665, 682 and 705 nm, cannot discriminate between red tide waters and highly scattering waters. The interpretation of in-situ measured water-leaving radiance spectra above both waters was presented in this paper. And a radiative transfer model based on Matrix Operator techniques was used to study the impact on the Chlorophyll fluorescence signal of wavelength redistribution functions and other in-water substances such as gelbstoff and suspended matter. Based on the analysis of measured and simulated spectrums, the red-shift phenomenon is obviously observed above the red tide water. The fluorescence peak is observed to shift progressively from a centre wavelength of 683 nm

(clear and green water) to 705 nm (red tide waters), and in red tides waters the FLH at 709 nm is much higher than FLH at 681 nm. The red-shift phenomenon can be used to distinguish red tide waters from highly scattering waters. So in this paper, fluorescence line height at MERIS bands 681 nm (FLH681) and 709 nm (FLH709) are computed while MERIS band 665nm and 753 nm determine the baseline. The ratio of FLH709 to FLH681 is used as an index to detect the red tides. The results of operational red tide detection in the East China Sea have been presented.

8175-62, Poster Session

The preliminary analysis of Asian dust events impact on the concentration of chlorophyll a in the Yellow Sea

Q. Tu, Z. Hao, F. Gong, D. Pan, X. Chen, The Second Institute of Oceanography, SOA (China)

Asian dust contenting nutrients and microelements can transport to the East China Sea (ECS), even far to the North Pacific region, particularly during the spring season when the dust storm events are frequent and maximal from the inland Asia. The large quantities of dust deposition could affect the marine ecosystem significantly, especially on the phytoplankton populations. In this study, we first identify individual major dust storm events and to study its impact on the chlorophyll concentrations along the track of the dust storms using Moderate Resolution Imaging Spectroradiometer (MODIS) data (such as aerosol optical thick(AOT), the chlorophyll a(Chl-a), fluorescence line height (FLH), and normalized water leaving radiance data) over the Yellow Sea during 2006. It shows a chlorophyll blooming in the Yellow Sea(usually 10-30 mg/m3) after the dust events within a period of 2-7days. The QuikSCAT data and altimetry SSHA (based on one 10 day cycle from a composite of the TOPEX/Poseidon and JASON-1 altimetry data) maps are used to rule out the possibility that the observed bloom patch was fuelled by nutrients from beneath the surface of the ocean through wind mixing or upwelling. However, the AOT of dust regions usually overflow or failure for the MODIS AOT retrieval algorithm base on the cloud free sky, and the dust is usually taken as cloud. So we have to retrieve the AOT and particle sizes of dust over ocean and then estimate the dust deposition flux and to quantify the ocean biogeochemical response to Asian dust events.

8175-63, Poster Session

Satellite observation of upwelling along the Zhejiang Coast of the East China Sea during 2007-2009

X. Lou, The Second Institute of Oceanography, SOA (China)

Upwelling water carries nutrients from deeper layer to the surface layer and promotes the growth of planktons, and therefore studying upwelling in coastal waters is of great ecological and biological significance. In this article, we observed and analyzed the upwelling along the Zhejiang Coast of the East China Sea with EOS MODIS imagery. First, we selected and processed more than 180 sea surface temperature (SST) images taken by EOS MODIS from 2007 to 2009 in this study. In order to observe upwelling phenomena, we chose cloud-free SST images and then rectified them to a standard transverse Mercator projection. Secondly, based on the temperature characteristics of upwelling, a changeable-temperature-threshold approach was established and then was employed to measure the physical parameters of upwelling. Since the upwelling water is colder than the surface water that it displaces, the upwelling areas can be easily identified in the SST images with a certain temperature threshold. By applying this threshold method, for an upwelling region, the location, area and temperature can directly be measured from the SST images. Finally, the temporal and spatial distributions of upwelling along the Zhejiang Coast were analyzed by using statistical methods. The results show that the upwelling looks like a belt in shape, and distributes along the Zhejiang Coast running from south to northeast, and covers an area varied from 6000 to 20000 square kilometers. There exists obviously temperature difference between the upwelling regions and non-upwelling waters on its boundary. The average temperature of upwelling is in range of 25~28, and the temperature



difference between the upwelling regions and the surrounding waters is about 2~4. The upwelling appeared in June and developed itself to its strongest period in July and August, and then it weakened and vanished in later September. Three years of observational results also reveal that the upwelling along the Zhejiang Coast has short-time, seasonal and annual variability.

8175-64, Poster Session

The buoy-based reversion of regional thermocline integrated with satellite observed SST in the margins off the Changjiang Estuary

L. Liang, J. Chen, X. Chen, H. Huang, The Second Institute of Oceanography, SOA (China)

Hypoxia has been widely observed in estuarine area and some reports have focused on the East China Sea over the past few decades. With the increasing nutrient load from Changjiang (Yangtze) River, the third largest runoff in the world, a severe hypoxia zone was found. The mechanism of hypoxia formation adjacent to the Changjiang Estuary receives more and more attention from both scientists and managers. Maintenance of hypoxia is due to the large density stratification caused by the significant salinity difference between the fresh plume and salty water from Taiwan Strait. Hypoxia is formed by organic detritus decay. Consumption of oxygen in bottom waters is linked to biological oxygen demand fueled by organic matter from primary production in the nutrient-rich river plume. Hypoxia occurs when this consumption exceeds replenishment by diffusion, turbulent mixing or lateral advection of oxygenated water. The margins off the Changjiang are affected the most by summer hypoxia. Physical stratification plays an important role with the Changjiang shelf showing strong thermohaline stratification during summer. In this study, we discusses the relationship between hypoxia and the density stratification according to the surface temperature observed from satellite and time series of profile data obtained from hypoxia buoy, which was especially designed for hypoxia identification. We examined the occurrence of seasonal hypoxia in the bottom waters of river-dominated ocean margins off the Changjiang River and compared the stratification processes leading to the depletion of oxygen summer. A simulation for stratification was performed to calculate the seawater temperature vertical profile by integration reversion result of satellite SST and real time data from buoy sensor. By collecting the historical investigated data, we can construct the parametric structural model by the relationship of climatological background between surface and bottom temperature. Based on the parameterization of the layered structure of seawater temperature vertical profile, the simulation method can calculate the parameter distributions of stratification structure. When the real time outputs of SST and buoy-based profile are received, the parametric model figures a set of major characteristic parameters of each profile directly; sea surface temperature, mixed laver depth. thermocline bottom depth, thermocline temperature gradient, and thermocline bottom temperature. Hence, the approach achieves the goal of reconstructing the regional thermocline profile directly. The thermocline reflects the ocean temperature field's important physics characteristics, and can be used in analysis of the influence on the exchange of the oxygen.

8175-65, Poster Session

48

On possibility of remote sensing of algae bloom using its effect on short surface waves

S. A. Ermakov, I. Sergievskaya, I. Kapustin, Institute of Applied Physics (Russian Federation)

Intensive algae bloom is a serious threat for the ecology of inland waters and shelf areas. Satellite optical and IR systems widely used nowdays to monitor algae bloom areas, have strong limitations in their operation in the night time or for cloudy sky. A very effective allweather and day and night instrument of remote sensing of the Earth is microwave radars, in particular, satellite SAR. From the analyses of optical and radar images of the sea surface it was concluded in

the literature that zones of intensive algae bloom can be seen in radar imagery as areas of depressed radar backscatter. However, there were no quantitative characterization of algae bloom from radar observations, and the very physical mechanisms of radar backscatter depression were not understood. This paper is aimed to understand better the physics of the action of algae on radar backscattering and possibilities of quantitative characterization of algae bloom areas from radar observations. The influence of algae bloom on the damping of gravity-capillary wave was studied experimentally in field experiment on the Gorky Water Reservour and in laboratory. It was obtained that the intensity of X-band radar backscattering decreased with phytoplankton concentration in the upper water layer. Samples of phytoplankton from the upper water layer and of biogenic film from the water surface were collected nearly simultaneously and co-located with radar probing of surface waves. Concentrations of main phytoplankton constituents as well as total algae concentration and their variability in the studied area were measured. Laboratory studies of damping of gravity-capillary waves on the water samples with skimmed film and on clean (without plankton) water covered with the biogenic films were carried out, and an effective water viscosity and the film elasticity values were retrieved. It was concluded that the increased water viscosity and the film elasticity in the presence of algae were the main physical reasons of enhanced wave damping, the contributions of the two effects in total wave damping and correspondingly in radar backscatter depression appeared to be comparable to each other. Since both the effective viscosity and the film elasticity depend on algae concentration the latter can be estimated from measurements of radar backscatter.

8175-66, Poster Session

Remote estimation of chlorophyll-a using MERSI and MODIS images in Tai lake, China

X. Han, W. Zheng, National Satellite Meteorological Ctr. (China)

The Chlorophyll-a (Chl-a) concentrations in water is of great importance for the monitoring of water quality and ecosystem balance. Remote sensing offers a convenient and systematical tool for the observations of water at a long time scale. In this paper, we present a study of Chl-a estimation using the reflectance models derived both from the Medium Resolution Spectral Image (MERSI) onboard the newly launched FY-3A satellite and the Moderate Imaging Spectroradiometer (MODIS) onboard the AQUA platforms.

Validation study was conducted on 23 Nov. 2009 using in situ water quality measurements and satellite observations. Results demonstrated that both models provided reliable estimates of Chl-a concentrations with determination coefficients R2 of 0.72~0.79 (MOD2) and 0.52~0.76 (MOD3) for MERSI standard band settings. This accuracy is slightly better than that of the MODIS results with R2 of 0.65~0.69 and 0.43~0.70 for MOD2 and MOD3, respectively. Different from the original models, comparison analysis between models and sensors indicated that the blue and near infrared wave ranges are of potential use for Chl-a estimation. Besides, the broad reflectance obtained from the standard band settings of MERSI and MODIS sensors are also demonstrated to be workable in Chl-a estimation.

With respect to the specific application of models in Taihu lake, China, the higher spatial resolution of MERSI (250 m) may explain the better performance for both models compared to that of MODIS. The primary results of this paper demonstrated the reliability of MERSI and MODIS bands in providing the useful signals for the estimation of ChI-a. Secondly, the blue and near infrared bands are of more potentials in ChI-a estimation using both the two band and three band models and this will be helpful in development of future ChI-a models with satellite observations.

8175-68, Poster Session

Robust scanning scheme over lage area for airborne EO/IR camera

Y. Yoon, G. H. Yu, C. G. Noh, D. B. Song, ADD, Agency for Defense Development (Korea, Republic of)

Airborne EO/IR camera(EO/IR) is designed to obtain images of large area. Most of airborne cameras usually have two actuation axes(roll



and pitch) to stabilize LOS(line of sight) under angular disturbances as well as to point its LOS to desirable direction. This two-axes actuation structure makes LOS become vulnerable to angular rate disturbance around yaw(heading)axis of aircraft and allows camera to obtain images of only strip vicinity of target instead of rectangular coverage around the target in moderate pitch lead/lag angle direction. These shortcomings, however, can be supplemented through the implementation of proper LOS scanning scheme suggested in this paper.

Generation of pitch angular reference rate command considering predetermined trace of LOS projected on target(earth surface) can be applied to acquire rectangular-shaped image of the target area. Scanning commands for airborne cameras consist of three terms, which are constant scanning rate with respect to earth fixed target, angular rate induced by the translation of sensor frame with respect to the earth fixed target, and the earth craft rate. Unlike other similar airborne camera system where there is only roll component of constant scanning rate, EO/IR has pitch component additionally, which contributes to guarantee LOS tracks on target to be always perpendicular to the direction of aircraft advancement. The pitch constant scanning rate is determined by current pitch/roll angle, flight altitude, aircraft velocity and required roll constant scanning rate with constraint that aircraft should proceed along straight path. As a result, overall scan area around target always maintains rectangular shape regardless of pitch lead/lag angle. Also, product of rotation matrix around heading direction to the transformation matrix from LL(local level) to gimbal coordinates can prevent LOS from swaying under aircraft heading disturbances. Even though aircraft suffers angular disturbance around heading direction, GPS/INS equipped on EO/ IR can provide aircraft proceeding direction information in the form of linear velocity. Then comparison between the aircraft proceeding direction and heading information directly extracted from the GPS/ INS produces amount of heading angular disturbance inflicting aircraft followed by the matrix calculation already mentioned just before. Simulation results show that the new scanning scheme ensures robust scanning under heading angular disturbances.

This paper describes the new scanning scheme along with overall but brief version of system formation of EO/IR, including introduction to the simulation package which enables us to verify and assess effectiveness of the scanning scheme.

8175-71, Poster Session

Platforms oil spill monitoring by means of TerraSAR-X: North Sea-Gulf of Mexico comparisons

D. Velotto, S. Lehner, X. Li, Deutsches Zentrum für Luft- und Raumfahrt e.V. (Germany)

No abstract available

49

8175-21, Session 5

Testing the consistency between MODIS ocean colour data and in situ chlorophyll-a measurements within coastal waters of the Maltese Islands

A. Deidun, Univ. of Malta (Malta) and European Commission Joint Research Ctr. (Italy); A. Drago, A. Galea, J. Azzopardi, A. Gauci, Univ. of Malta (Malta); F. Melin, European Commission Joint Research Ctr. (Italy)

Despite numerous studies testing the degree of match-up between ocean colour and in situ chlorophyll data, the only attempt in the marine area of the Maltese Islands (Central Mediterranean) dates back almost 15 years and utilized the LANDSAT platform. The aim of this study is a first attempt at statistically validating ocean colour data derived from the MODIS platform through a limited number of in situ surface chlorophyll-a measurements, taken in April and September 2010, for a near-shore marine area off the north-east coastline of Malta. In situ chlorophyll values for the two monitored periods ranged from 0.118mg/m3 to 0.511mg/m3, whilst ocean colour values over

the December 2009-December 2010 period ranged from 0.040mg/ m3 to 1.370mg/m3. These values are consistent with those for an oligotrophic, Class/Type I water body. Log bias values indicate that the MODIS data set under-estimates the surface chlorophyll-a values, whilst RMSD, average absolute relative difference and r2 values suggest that the match-up between satellite and in situ values is only partly consistent. In fact RMSD values for the April and September match-ups were 0.25 and 0.69, respectively, with only the first value comparing well with values in the literature for other Mediterranean and global regions. This apparent lack of agreement might be attributed, at least partly, to the coastal nature of the marine area under scrutiny (located just 2km offshore), in view of the optical complexity of coastal waters. This work further discusses the relevance of the applied methodologies to the operational monitoring of the productivity of Maltese near-shore waters, pursuant to fulfilling specific obligations under the EU Water Framework Directive and Marine Strategy Framework Directive.

8175-23, Session 5

Estimation of the seasonal sea level variations in the Gulf of Cadiz (SW Iberian Peninsula) from in-situ measurements, satellite altimetry and numerical models

I. M. Laiz, J. Gómez-Enri, B. Tejedor, A. Aboitiz, P. Villares, Univ. de Cádiz (Spain)

Long time series (1997-2008) of altimetry data and four in-situ tide gauge records located in different ports have been analyzed to investigate the seasonal variability of sea level along the coast of the Gulf of Cadiz. The spectral analysis of the four sea level time series shows a clear dominance of the annual and semiannual signals. Thus, a harmonic model was used to analyze these signals both for the average seasonal cycles and on a yearly basis. Harmonic analysis shows that more than 95% of the average seasonal cycle is explained by the annual and semiannual components, with the amplitude of the mean annual component (4.5 to 5.8 cm) about twice that of the mean semiannual component (1.9 to 2.7 cm). Results show that the average seasonal cycle of sea level anomalies is very similar at the four coastal stations, with minimum values during winter (February) and maximum during autumn (late October - early November). The contribution of different forcings to the observed sea level variability has been examined using additional datasets such as atmospheric sea level pressure (modelled and measured in-situ), satellite Sea Surface Temperature, and wind and river discharge time series. Moreover, the contribution of direct atmospheric forcing for a section of the sea level time series (1997-2001) has also been explored using the output of a barotropic oceanographic model (HIPOCAS project) forced with wind and atmospheric pressure, revealing that the effect of wind can be negligible at seasonal time scales. When correcting the sea level time series for meteorological forcing the amplitude of the average semiannual signal reduces notably, suggesting a meteorological origin of the semiannual seasonal component in agreement with previous studies. Altimeter data shows a good agreement with in-situ observations. The geographical distribution of the annual component of the average seasonal cycle obtained from altimeter data shows an eastward amplification of the signal. Linear correlations were carried out between the observed mean sea level anomalies and North Atlantic Oscillation (NAO) indices. Negative low but significant correlations are obtained when using the full time series and increase when using only the autumn and winter months.

8175-24, Session 5

The full-scale investigations of the action of internal waves and inhomogeneous flows on the wind waves in the White Sea

V. V. Bakhanov, N. A. Bogatov, A. V. Ermoshkin, V. N. Lobanov, O. N. Kemarskaja, V. I. Titov, Institute of Applied Physics (Russian Federation)

The full-scale investigations of the action of internal waves and inhomogeneous flows on the wind waves and the near-water layer of



the atmosphere were carried out in the White Sea in 2009 - 2010 yr. Measurements were carried out from onboard of the scientific research vessel "Ekolog" (Institute of Northen Water Problems Karelian Research Centre of RAS). Depth finder Humminbird 798c was used for registering the bottom relief. Internal waves characteristics were determined by the shift of the sound-scattering layers, recorded by depth finder, and according to the data of ADCP WHS300Khz (RD Instruments). The characteristics of heterogeneous flows at the depths from 10 to 100 m were recorded by ADCP. The characteristics of surface wave in the wide frequency range were recorded: by digital radar measuring complex on the base of the ship radar Icom MR-1000, wavelength is 3.2 cm; by 3 cm scatterometer; by 8 mm scatterometer; by the two-dimensional optical spectral analyzer; by CCD rules. The parameters of the near-water layer of the atmosphere were recorded by the acoustic anemometer HS-50 (Gill Instrument) and by the ship meteorological station Furuno.

Hydrometeorological conditions during observations varied essentially. Wind speed varied from 0 to 15 m/s, speed of current from 0 to 1 m/s. Data about the field of flow during different phases of tide are received. Internal waves and their manifestations on the sea surface are registered. The special features of the flow of the powerful tidal current (to 1 m/s) around the secluded underwater elevation and the spatial structure of surface anomalies in the field of these two-dimensionalheterogeneous flows are analyzed. The correlation of radar signal with current speed in near-surface region is observed Data about a change in the characteristics of reflected from the sea surface radar signal in process of development of wind waves are received. The relation of the X-range HH-polarization radiation at grazing incidence angles, scattered by the sea surface to near surface wind speed and sea roughness state is studied in detail. The technique of determining the kinematic characteristics of sea surface roughness such as length, period, velocity of energy-carrying wave and its propagation direction by radar and optic data obtained from the ship is described. Experiments on procedure finalizing of the determination of subsurface flow speed according to the numerical data of radar measuring complex on the base of ship radar Icom MR-1000 are carried out.

This work was supported by the grant RFBR 08-05-00195, 07-05-00565, 07-05-12011, 07-05-10106, and 08-05-10047

8175-40, Session 5

50

Total suspended solids concentrations mapping by THEOS imagery over Penang Island, Malaysia

R. Asadpour, L. H. San, Univ. Sains Malaysia (Malaysia); S. Kakooei, Univ. Teknologi Petronas (Malaysia); S. Asadi Shekafti, Univ. Sains Malaysia (Malaysia)

This study focuses on utilizing the satellite remote sensing to monitor the total suspended sediment (TSS) over Penang Island. The data employed in this study includes 4 THEOS (Thailand Earth Observation System) images as well as the nearly simultaneous in-situ data from 11 observation stations on the sea. The study area is Penang Island, Malaysia which is situated within latitudes 50 24'13.75" N to 50 14' 10.75" N and longitudes 1000 20' 27.75" E to 1000 22' 30.75"E. Digital numbers for each band corresponding to the sea-truth data collected simultaneously with the digital image acquisition were determined for later use in the algorithm calibration analysis. Total suspended sediment concentrations (TSS) can be estimated by establishing an optical model that relates the TSS concentrations with the reflectance. The algorithm used was based on the reflectance model, which is a function of the inherent optical properties of water, and these in turn can be related to the concentration of the pollutants. The collected water samples were combined for algorithm calibration. The results of these estimations are validated using the in-situ data by the linear regression analysis, and the accuracies are measured by the correlation coefficients R2. This result showed that the simple linear algorithm was sufficiently accurate to generate TSS map over Penang Island, Malaysia.

8175-69, Session 5

Coastal zone monitoring using high resolution X-band SAR sensor of TerraSAR-X

X. Li, S. Lehner, A. Pleskachevsky, S. Brusch, Deutsches Zentrum für Luft- und Raumfahrt e.V. (Germany)

Synthetic Aperture Radar (SAR) has exhibited its advantages for monitoring coastal zones, e.g., surface wave, surface wind, bathymetry, morph-dynamics and so on, as SAR can provide twodimensional surface information independent on weather situation and sunlight conditions. Particularly after the launching of new-generation spaceborne SAR sensors, e.g., TerraSAR-X (TS-X), Cosmo-Skymed and Radarsat-2, SAR data with high spatial resolution up to 1 m can be acquired to provide finer sea surface field over coastal zones.

In coastal area, the sea state is highly variably as it experiences shoaling, refraction/diffraction, and dissipation caused by rapidly changing bathymetry. We use the high resolution TS-X data to investigate spatial variations of sea state parameters including two-dimensional wave spectrum and integral wave parameters zones. Some case studies, e.g., waves approach to Azores archipelago located in middle of North Atlantic; waves propagate over coral reef regions in western coast of Australian.

The operational numerical wave models, generally limited by the spatial resolution or the boundary conditions, cannot often resolve the fine structure of coastal wave field. Here we present the research that use wind field retrieved from TS-X data to force high resolution coastal wave model and implement successfully over the German Bight. The significant wave height obtained from the high resolution wave model agrees well with in situ measurement.

Another application of using TS-X data for monitoring coastal zones is to obtain high resolution bathymetry in near-shore regions. Cases studied near to Helgoland, an island located in the German Bight, and at Phillip port near to Melbourne are demonstrating the great potential of using TS-X for obtaining high resolution under water topography with high accuracy.

8175-25, Session 6

Bidirectional reflectance function in coastal waters: modeling and validation

A. Gilerson, S. Hlaing, T. Harmel, A. Tonizzo, The City College of New York (United States); R. Arnone, A. Weidemann, U.S. Naval Research Lab. (United States); S. Ahmed, The City College of New York (United States)

Validation of the ocean color satellites can be accomplished through matchups between satellite data and measurements of SeaPRISM instruments which are installed on oceanic platforms as part of the NASA AERONET - Ocean Color Network. Both satellite and SeaPRISM measurements need to be corrected for bidirectional reflectance effects described by a distribution function (BRDF) which depends on the sun incident and sensor azimuth and viewing angles as well as on water parameters. This BRDF correction is currently made using open ocean water assumptions. These are usually not valid in coastal waters, and can therefore create significant errors in BRDF estimations in coastal zones. In this work, synthetic datasets were simulated using the Hydrolight radiative transfer program with bio-optical models and water parameters typical of coastal waters, and for the whole range of possible incident, azimuth and viewing angles. A new BRDF model then was created as a set of lookup tables of coefficients for the second order polynomial relationships between remote sensing reflectance and backscattering albedos.

To evaluate this new model, we made use of measurements from the Long Island Sound Coastal Observatory (LISCO) developed by the City College of NY together with NRLSSC. LISCO has two radiometers: a multi-spectral SeaPRISM, which is a robotic instrument programmed to scan and measure sky and water radiances at an azimuth angle 90° from the direction of the sun and a hyperspectral HyperSAS instrument with two radiance sensors looking at the water and at the sky in the fixed position and oriented directly to the West. This unique combination and configuration of the two instruments (HyperSAS and



SeaPRISM) was then used for the validation and analysis of our new BRDF model for various sun, viewing and water conditions. Results showed a 10-15% improvement in the estimation of the remote sensing reflectances.

8175-26, Session 6

Oceanic response around the Yucatan Peninsula to the 2005 hurricanes from remote sensing

E. J. D'Sa, N. Tehrani, V. H. Rivera-Monroy, Louisiana State Univ. (United States)

In 2005, three hurricanes namely Emily, Stan and Wilma made landfall along the Yucatan Peninsula (YP) that impacted the coastal environment of the region. We study the effects of these hurricanes on the coastal and oceanic waters around the Yucatan Peninsula using multiple satellite sensor data such as winds from QuikSCAT, sea surface temperature (SST) from MODIS and bio-optical properties from the SeaWiFS ocean color sensor. QuikSCAT wind data revealed the hurricane paths along with typical changes in wind speed and direction that aided in better interpretation of the SST and ocean color data obtained before and after the hurricane passages. Hurricane Emily made landfall at Cozumel and Playa del Carmen on 18 July as a strong Category 4 hurricane and weakened as it crossed the YP. Tropical storm Stan made landfall on 2 October south of Tulum and weakened to a depression as it crossed the peninsula. Hurricane Wilma made landfall on 21 October in the northeastern YP as a powerful Category 4 hurricane emerging and moving northeastward in the Gulf of Mexico as a Category 2 hurricane. SST imagery before and following the passage of the hurricanes indicated variable extent of upper ocean cooling that depended on the hurricane track and its intensity. Greatest cooling occurred following Hurricane Emily while Stan caused a general decrease in SST around the YP waters. Hurricanes contribute to resuspension and transport of material from the coast to oceanic waters resulting in the fertilization of the marine waters. An examination of SeaWiFS ocean color data products such as chlorophyll concentrations and backscattering coefficients suggested an increase in organic and inorganic suspended particulate matter. While increase in phytoplankton chlorophyll biomass were observed in both nearshore and offshore waters following the hurricane passages, the optical backscattering coefficients in addition suggested increased concentrations of suspended sediments, likely due to resuspension mainly in nearshore waters. Hurricanes Emily and Wilma caused large increases in chlorophyll off the northeastern YP coast while Hurricane Stan caused the largest increase along the western coast of YP with no impact at landfall locations along the eastern coast of the YP. The use of multi-satellite data provided a greater understanding of the hurricane effects on the bio-optical properties of the YP.

8175-27, Session 6

51

Spaceborne infrared calibration source design: current challenges and future trends

R. D. Dewell, J. Reveles-Wilson, D. Smart, ABSL Space Products (United Kingdom)

Changes in climate can have real and immediate economic impacts. It is becoming more and more important therefore to accurately monitor the state of the surface of the Earth in order to predict longterm climate trends reliably. Climate is driven by the states of the land and sea and space provides a way of monitoring the surface of the Earth continuously. Changes can then be more ubiquitously trended instead of relying on disparate land-based sources of data. Spaceborne radiometry will continue to play a vital role in monitoring the temperatures of the sea and land. Long term trends can only be accurately determined by repeated measurements from space, and errors in measurements must be carefully budgeted. ABSL black body calibration sources, which have been providing ultra-stable thermal and optical references for space radiometry measurements for the last decade, enable surface measurements to high levels of accuracy. Integrated Infra-Red emissivity levels of 0.999 over the whole operating waveband (typically 3.5 to 14.5 microns) are not unusual and this can

only be achieved through thorough radiometric, mechanical, thermal and electronic design. In addition temperature uniformity; isolation from the surrounding thermal environment, and long-term stability must be achieved. Any deviations from the ideal must be factored into error budgets for the duration of the mission. With volume, mass and power consumption being at a premium in any space instrument and continuing to add challenges to calibration source designers, future sources will require lower long-term drift, consistent reference to international standards and the incorporation of consistent quality processes and procedures. This paper will summarise the latest design features of black body calibration sources for radiometry instruments and the performance challenges that will be faced in future remote sensing missions.

8175-28, Session 7

Generalized satellite image processing: eight years of ocean colour data for any region on earth

Q. Vanhellemont, B. Nechad, K. Ruddick, Institut Royal des Sciences Naturelles de Belgique (Belgium)

The JELLYFOR project aims to set up a jellyfish forecasting system based on in situ and remote sensing input data. Existing BELCOLOUR procedures were adapted to process a large number of MODIS and MERIS images in order to create a gridded dataset of chlorophyll a concentration (chl), of sea surface temperature (sst - MODIS only) and of total suspended matter concentration (tsm) for custom regions.

An eight-year period (01/01/2003 - 31/12/2010) of standard OceanColor MODIS Aqua L2 files from NASA and MERIS RR L2 files from ESA were processed for the three regions in the JELLYFOR project. The necessary datasets were imported and reprojected to a standard grid after quality control. The MODIS chlorophyll a dataset is known to be less reliable in turbid waters, therefore an additional quality control and masking is applied in these waters.

The methodology for extracting the datasets was created generically, so that a similar archive can readily be created for any region on earth. The tsm algorithm of Nechad et al. (2010) is specific to turbid waters and might provide inaccurate results for clearer waters. The algorithm, however, can be easily adapted when regional specific inherent optical properties (SIOPs) are available.

An incredible amount of information can be extracted from the archive, for example eight year time-series for every location within the region and monthly and climatological average maps. In a multi-year dataset of remotely sensed parameters, known oceanographic features are apparent. Using monthly composites and time-series, the inter-annual changes and the evolution throughout the year can be analysed. The archive can be used for a wide range of applications in marine biology, sediment transport, coastal management, etc.

A long-term remote sensing dataset is a useful tool for understanding the oceanography of any region, be it a well-studied or a relatively unknown one.

References

B. Nechad, K.G. Ruddick, Y. Park. 2010. Calibration and validation of a generic multisensor algorithm for mapping of total suspended matter in turbid waters, Remote Sensing of Environment 114: 854-866.

8175-29, Session 7

Remote sensing and in situ observations of marine slicks associated with inhomogeneous coastal currents

S. A. Ermakov, I. Kapustin, I. Sergievskaya, Institute of Applied Physics (Russian Federation)

Co-located simultaneous field observations and satellite radar imagery, as well as optical observations of marine banded slicks on the sea surface aimed to study the relation between the slicks and the structure of marine currents were carried out in the coastal zone of the Black Sea. Measurements of the current velocity profiles were performed from a motor boat with an acoustic Doppler current meter



(ADCP) Workhorse 600 kHz. Additionally, current velocities in the thin upper water layer (about 5 mm thickness) were measured using special floats when fixing their coordinates with GPS receivers. Samples of surfactant films inside/outside slick bands were collected using a net method. The surfactant films were reconstructed in laboratory conditions and their physical characteristics (the surface tension coefficient and the elasticity) were retrieved when studying the action of collected films on characteristics of gravity-capillary waves with a parametric wave method. The studied slicks were also detected in an Envisat SAR image.

It is obtained that the banded slicks are characterized by enhanced concentration of surface-active material, i.e. by accumulation of surfactants. The slicks bands are revealed to be oriented along the coastal stream currents (and approximately along the coastline). In accordance with theory the slicks are located in the areas of convergency of transverse (small) components of the stream currents in the upper water layer, these areas are connected to variations of the current velocity profiles due to the bottom topography structure.

Two case studies were investigated. The first one is when one slick band was observed and it was located in a zone where alongshore current merged with a current flow coming from the sea. The second case when two banded slicks were detected. The first band was in the zone where a weak nearshore south-eastward SE-current met strong eastward current. The second band corresponded to an upwelling which appeared when the deep (sub thermocline) current directed to the shore met the bottom slope.

One thus can conclude that the structure of coastal currents can be studied from remote sensing of slicks on the sea surface.

8175-30, Session 7

Spring snow surface water content fluctuations as a tool to extract sea ice structures

E. Hudier, D. Ramdenee, Univ. du Québec a Chicoutimi (Canada)

Sea ice morphological features are of major relevance to oceanic and general circulation models as well as navigation or oil and gas exploration. Beside their first order impact on drag coefficients, they create a horizontal heterogeneity of the dynamic and therefore thermodynamic conditions at the ice water interface which control ocean-ice-atmosphere fluxes. Synphetic Aperture Radars (SAR) with improved resolutions, up to 3 meters in the ultra-fine-mode of RADARSAT-2, offer potential tools to better describe the statistics of large roughness features at scales compatible with large scale models.

At spring, the increase of the water content in the snow makes it opaque to microwaves and, in turn, causes surface scattering to be the main contribution of radar images. As a consequence, the radar signal becomes mainly function of the surface small scale roughness and interface slope. The angular dependence of surface scattering creates conditions allowing a higher return from ice surfaces oriented perpendicularly to the SAR incident beam and on the contrary a reduced backscattering from other areas within the scene where forward scattering causes the beam energy to be scattered away from the antenna.

The availability of liquid water in the snow is the result of a shift in the thermodynamic balance of the snow and sea ice covers. At spring, with the irradiance and air temperature increasing, heat fluxes cause the ice and snow media temperature to rise up to the freezing point. Quickly the snow becomes isothermal and melt starts to absorb the excess heat as latent heat of fusion. During this period, the snow layer is a tri-phasic medium in which water changes state to balance radiations (short and long waves) and conductive heat fluxes variations. As a consequence, the surface layer of the snow cover is subject to a diurnal cycle of thaw during day time and refreeze at night which translates into a parallel diurnal cycle on snow wetness content.

We present results of a thermodynamic model that computes the overnight variability of the water content in an isothermal snow layer. Thin snow cover conditions found on pressure ridge ice blocks are simulated.

The energy balance forced by incoming L \downarrow and outgoing L \uparrow long-wave radiation, incident S \downarrow and reflected S \uparrow short-wave radiation and turbulent atmospheric heat flux Qatm is computed as a function of

52

snow surface orientation with relation (1) to an horizontal plane and (2) to the sun.

During the day, wetness content increases throughout the snow cover. Maximum wetness is observed in the top layer, where, once saturation is reached, free drainage is initiated. With thin snow conditions, saturation can reach the bottom layer and lateral drainage start. This situation is typical of ice blocks in ridges where icicles can be observed on some edges of tilted blocks. With a decrease of incident $S\downarrow$ simulating sunset we observe a parallel decrease of the melt, before freezing starts in the top layer. With latent heat available at the air-snow interface, the heat flux toward the atmosphere causes first an intense refreeze at the air-snow interface before cascading downward. This creates, a dry array of ice crystals on top of a nearly saturated snow layer.

8175-70, Session 7

Cross-comparison of ERS-2 and Metop-A scatterometers measurements using various methods

A. Elyouncha, X. Neyt, Royal Belgian Military Academy (Belgium)

ERS-2 and METOP-A scatterometers are very similar C-band radars. They measure constantly (ERS-2 since 1995 and METOP-A since 2006) the global normalized radar cross-section. This normalized radar cross-section, called backscatter or sigma naught, is used to determine the wind speed and direction over the ocean. Many other applications using the sigma naught have emerged. The best-known applications are vegetation, soil moisture and ice studies.

Long term studies need data acquired during several years, which requires continuity and stability of the instruments. Moreover, simultaneous assimilation of ERS-2 and METOP-A data requires consistency. Hence a cross-comparison of the measurements is essential.

The measurements performed over several distributed targets by the two scatterometers are cross-compared using four different methods. The result of this cross-comparison is a bias between the two instruments.

The main principle of these methods is a comparison of the measured backscatter and a simulated backscatter computed using a geophysical model.

The cross-calibration method applied on the backscatter measured over ocean is based on the CMOD5 wind model while the crosscalibration over sea ice is based on the C-band sea ice model. The bias between the two instruments is the difference between their deviance from the considered model. When the cross-comparison is performed over the rainforest this bias is the difference between the pairs of the geophysical parameter gamma naught. The fourth method is a direct comparison of collocated (in time, space, look angle and incidence angle) pairs of sigma naught.

In this paper, the four cross-comparison methods introduced above are presented and applied to ERS-2/scatt and METOP-A/ascat measurements.

Each method providing a given bias is characterized by it's variance.

Furthermore, the stability of the instruments is investigated by monitoring the measurements over long time period. The variance and the stability results are used to assess the methods and the instrument comparison.

8175-31, Session 8

Preparatory works for the altimeter calibration of the Sentinel-3 mission using the dedicated calibration site at Gavdos

S. P. Mertikas, A. Daskalakis, E. Koutroulis, A. Tripolitsiotis, Technical Univ. of Crete (Greece)

Satellite altimetry provides the means for monitoring sea-level and climate changes over regional and global scales with mm/yr accuracy. The importance of satellite altimetry in monitoring the complex



ocean-atmosphere system led to the approval of the Sentinel-3 ocean topography mission. Sentinel-3 is scheduled to be launched in 2013. This mission will incorporate new instruments and measuring modes that are expected to provide high-accuracy for the determination of sea level as well as ocean and land color, sea and land surface temperature with improved spatial and temporal coverage. Nevertheless, satellite altimeter measurements of homogenous quality and reliability have to be maintained over longer periods of time. Hence, the Sentinel-3 observations, such as sea-surface heights and sea-level anomaly fields, need to be continuously and independently connected in a common, reliable but also long-term manner. This can be achieved by satellite calibration using dedicated research infrastructures. These calibration facilities consistently and reliably determine (1) the absolute altimeter biases and bias drifts for each of these various satellite altimeters and (2) the relative bias among them.

A permanent calibration facility for satellite altimeters has been operating in Gavdos island, Greece as of 2004. This facility has already been successfully and continuously determined the OSTM/Jason-2 altimeter bias, since orbits are crossing over the island. Satellite atmospheric measurements (i.e., ionospheric and tropospheric delays) have been also calibrated against ground-based sensors on a routine basis.

This work presents the actions to be performed to calibrate and validate altimetric measurements of Sentinel-3. Effective incorporation of the existing Gavdos facility, the newly developed microwave transponder and any other sea surface calibration techniques will be presented as well.

8175-32, Session 8

Quasi-operational marine wind retrieval system based on satellite-based synthetic aperture radar information

V. Zabeline, Environment Canada (Canada)

The Meteorological Service of Canada (MSC), Environment Canada is leading the National SAR Winds pilot project (2009-2011) which is providing near-real-time delivery of marine wind measurements derived from space-borne synthetic aperture radars (SAR) to operational meteorologists and scientific community. The Wind Information Processing System (WIPS) for quasi-operational surface wind speed retrieval over Canadian and adjacent U.S. water has been implemented and continues to undergo development. The system operates with RADARSAT-1, RADARSAT-2, and ENVISAT satellite imagery with very high resolution (100 m), and is able to map wind speed distributions with better than 1 km resolution even in coastal zones where orographic impact on wind patterns is very pronounced.

Based on the successful regional project conducted during 2006-2008 in Pacific and Yukon Region, this Canadian Space Agency funded project extends the use of SAR Winds to all marine regions in Canada including the Arctic new service areas (METAREAs). In addition to facilitating evaluation and operational use of large quantities of this data by marine forecasters and other multidisciplinary science users, project objectives include determination of the optimum system architecture for a proposed on-going, operational processing and dissemination system, and recommendations regarding implementation of such a system. To this end, partnerships have been developed between all MSC Regions, the Canadian Meteorological Centre, and the Canadian Ice Service to ensure the project objectives are met. MSC science divisions in the regions, particularly the National Laboratories, are also participating along with all the regional Storm Prediction Centers and 3 National Weather Services forecast offices in the U.S. Communication tools have been established to encourage interaction and facilitate learning amongst users. Training of the end users is another integral component of the project. Note that a similar project is underway in the United States (NOAA).

This presentation will briefly review results of the project, describe activities and achieved objectives, and present examples showing benefits of the SAR Winds system and promising scientific advances which should lead to continuing improvements of SAR wind speed derived accuracy will also be touched upon.

8175-33, Session 8

Directional ocean wave spectra estimation based on the joint measurement from synthetic aperture radar and wave spectrometer

R. Lin, P. Delu, Z. Hao, Z. Mao, X. He, The Second Institute of Oceanography, SOA (China)

Synthetic aperture radar (SAR) can measure directional wave spectra based on a closed nonlinear integral transformation mapping relation. The according wave spectra retrieval algorithm has been developed but some limitations remain, like high wave number cut-off in azimuthal direction and the need for the first guess spectra. Wave spectrometer is a kind of satellite-based real aperture radar (RAR) operating at low incidence, which has a narrow beam and scans complete 360°by antenna rotation. It derives wave spectra by the simple linear relation between the wave spectra and the modulation spectra from the wave spectrometer. The linear coefficient can be estimated by the nadir beam or other external information. This paper proposes a method for the directional spectra estimation based on the joint measurement from synchronous SAR and wave spectrometer. Firstly, the modulation spectra are derived from the wave spectrometer, from which the relative wave spectra are constructed. Then the relative wave spectra are seen as the first guess spectra for the wave spectra retrieval of SAR image. Because it have the same pattern with the real wave spectra, although have different energy. Finally, we adjust the first guess spectra energy until the image spectra from the input wave spectra are identical to the adjusted one by multiplying a coefficient in the process of iteration. The last adjusted wave spectra are the retrieval. This paper makes use of the simulation to validate the joint measurement. The simulation compares the input spectra and the retrieved one in terms of peak wave direction, peak wavelength and significant wave height, which has a deviation of 120, 10 m and 0.3 m. respectively, in the simulation. Results show the retrieval errors don't differ significantly and the joint measurement for the wave spectra has the feasibility.

8175-34, Session 8

Multifrequency and multipolarization measurements of water surface radar cross section and brightness temperature angular dependences

A. K. Arakelyan, A. K. Hambaryan, A. A. Arakelyan, M. L. Grigoryan, ECOSERV Remote Observation Ctr. Co. Ltd. (Armenia)

Radiophysical methods and means of remote sensing, such as radars, Doppler-radars, radiometers and combined radar-radiometers have wide application for sea surface mapping and for remote retrieval of near sea surface wind and wave fields parameters, water temperature and salinity, sea ice and sea surface pollution properties, etc. To achieve high accuracy and unambiguity in retrieval of sea salinity, sea water and near sea surface air temperatures, wind speed and direction, sea wave force, sea ice thickness and melting time, in detection and classification of sea surface signatures and anomalous formations with natural and artificial origins, oil spills or spills of other surface active substances, precipitation quantity (clouds water content), snowfall and rainfall parameters a synergy data of various independent and differing techniques and measurements carried out under test-control, quasifield conditions is necessary.

In this paper the results of spatio-temporally collocated, multifrequency, multi-polarization, microwave active-passive measurements of water surface radar and radio thermal characteristics changes due to clouds and rain are presented. The results have been obtained during the measurements carried out in quasi-field conditions from the measuring complex built in Armenia under the framework of ISTC Projects A-872 and A-1524. The measurements were carried out at various polarizations by C-band (ArtAr-5.6), Ku-band (ArtAr-15) and Ka-band (ArtAr-37) combined scatterometric-radiometric systems developed and built by ECOSERV ROC under the framework of the above Projects. In the paper structural and operational features of the

Conference 8175: Remote Sensing of the Ocean, Sea Ice, Coastal Waters, and Large Water Regions 2011



utilized systems and the whole measuring complex will be considered and discussed as well.

The represented results show that radar contrasts related to hand perturbed water surface and rain perturbed water surface are practically equal for all frequencies and polarizations. Cloud's contribution in water surface (perturbed or smoothed) reflective characteristics is practically zero. Radiothermal contrasts due to hand perturbations of the water surface are higher than radiothermal contrasts due to rain perturbations of the water surface for all polarizations and frequencies. Cloud's emission has a high contribution in water surface brightness temperature at all polarizations and frequencies. The value of this contribution increases with the frequency independentily of the polarization.

8175-35, Session 8

Strategy for quality evaluation of OSCAT data

M. Gupta, Y. Desai, B. Kartikeyan, Space Applications Ctr. (India)

OSCAT is a "Ku" band pencil beam scatterometer, which is an active microwave radar operating at a frequency of 13.51 GHz onboard Oceansat-2. The major objective of this instrument is to derive wind velocity over the ocean surface, which is an important parameter for geophysical estimation. OSCAT has an onboard rotating antenna with inner beam HH polarized and outer beam VV polarized rotating at 20.5 rpm to scan the earth surface with a maximum swath of 1800 Km without any nadir gap. It provides day and night data, covering the entire globe in two days with a spatial resolution of 50 km x 50 km.

It specifically measures the backscattered power from the ocean surface from which backscattering coefficient (known as Sigma-0) is estimated. The behaviour of Sigmao-0 at different land masses like snow, soil, sea ice, vegetation canopies, mountains etc varies depending on the scattering phenomenon over the respective surface. Over the ocean surface Sigma-o is highly dependent on the wind speed and wind direction. Thus knowing Sigma-0 indirectly gives the wind velocity.

OSCAT provides data at footprint/slice, grid and global levels, which are called L-1, L-2 and L-3 respectively. This paper describes strategy to evaluate the quality of these datasets.



Monday-Thursday 19-22 September 2011 Part of Proceedings of SPIE Vol. 8176 Sensors, Systems, and Next-Generation Satellites XV

8176-01, Session 1

NASA Earth Science Flight Program Overview

S. P. Neeck, S. Volz, NASA Headquarters (United States)

NASA's Earth Science Division's (ESD) conducts pioneering work in Earth system science, the interdisciplinary view of Earth that explores the interaction among the atmosphere, oceans, ice sheets, land surface interior, and life itself that has enabled scientists to measure global and climate changes and to inform decisions by governments, organizations, and people in the United States and around the world. The ESD makes the data collected and results generated by its missions accessible to other agencies and organizations to improve the products and services they provide, including air quality indices, disaster management, agricultural yield projections, and aviation safety. In addition to four missions now in development and 14 currently operating on-orbit, the ESD is now developing the first tier of missions recommended by the 2007 Earth Science Decadal Survey and is conducting engineering studies and technology development for the second tier. Furthermore, NASA's ESD is planning implementation of a set of climate continuity missions to assure availability of key data sets needed for climate science and applications. These include a replacement for the Orbiting Carbon Observatory (OCO), OCO-2, planned for launch in 2013; refurbishment of the SAGE III atmospheric chemistry instrument to be hosted by the International Space Station (ISS) as early as 2014; and the Gravity Recovery and Climate Experiment Follow-On (GRACE FO) mission scheduled for launch in 2016. The new Earth Venture (EV) class of missions is a series of uncoupled, low to moderate cost, small to medium-sized, competitively selected, full orbital missions. Finally, ESD is developing on behalf of the National Oceanic and Atmospheric Administration (NOAA) the Jason-3 operational ocean altimetry satellite. An overview of plans and current status will be presented.

8176-02, Session 1

55

Launch and on-orbit checkout of Aquarius/ SAC-D Observatory: an international remote sensing satellite mission measuring sea surface salinity

A. Sen, Jet Propulsion Lab. (United States); D. Caruso,Comision Nacional de Actividades Espaciales (Argentina);D. Durham, Jet Propulsion Lab. (United States); C. Falcon,Comision Nacional de Actividades Espaciales (Argentina)

The Aquarius/SAC-D observatory is scheduled to launch in June 2011 from Vandenberg Air Force Base (VAFB), in California, USA. This mission is the fourth joint earth-observation endeavor between NASA and CONAE. The primary objective of the Aquarius/SAC-D mission is to investigate the links between global water cycle, ocean circulation and climate by measuring Sea Surface Salinity (SSS). Over the last year, the observatory successfully completed system level environmental and functional testing at INPE, Brazil and was transported to VAFB for launch operations. Launch preparations are currently underway involving the Delta II rocket. This paper will present the challenges of this mission, the system, the preparation of the spacecraft, instruments, testing, launch, in-orbit checkout and commissioning of this Observatory in space.

Keywords: International Sea surface salinity mission, SSS, global water cycle, microwave remote sensing, projects, climate studies, Aquarius/ SAC-D, Observatory, launch, in-orbit spacecraft checkout and commissioning, instrument performance, NASA, CONAE, ASI, CNES, CSA, AEB (INPE/LIT), INVAP. 8176-03, Session 1

The NASA NRC Decadal Survey HyspIRI Mission: Global Imaging Spectroscopy and Multi-Spectral Thermal Measurements for Critical Earth Science and Climate Variability Objectives

R. O. Green, Jet Propulsion Lab. (United States)

In 2007, the National Research Council of the U. S. National Academies released the Decadal Survey: Earth Science and Applications from Space with national imperatives of the next decade and beyond. One of the missions called for in the Decadal Survey is HyspIRI: "A hyperspectral sensor (e.g., FLORA) combined with a multispectral thermal sensor (e.g., SAVII) in low Earth orbit (LEO) is part of an integrated mission concept [described in Parts I and II] that is relevant to several panels, especially the climate variability panel."

A HyspIRI science study group was formed in 2008 to analyze the recommendations of the Decadal Survey and support the development of a robust mission concept. This group has developed a critical set of HyspIRI Earth science and climate variability objectives based upon the Decadal Survey report. These include: Ecosystem Measurement for Climate Feedback; Black Carbon/Dust Effects on Snow and Ice; Carbon Release from Biomass Burning; Evapotranspiration and Water Use and Availability; and Critical Volcanic Eruption Parameters. A suite of additional measurement specific science objectives were as well and are described in this paper.

All of these science objectives are achieved with the current HyspIRI mission concept that includes a wide-swath visible-to-short-wavelength-infrared range imaging spectrometer, a multi-spectral thermal imager, and a real-time subset processing and broadcast capability. In this paper the current HyspIRI mission concept is described including traceability to the full set of Decadal Survey Earth science and climate variability objectives.

8176-04, Session 1

Joint Polar Satellite System

T. G. Trenkle, NASA Goddard Space Flight Ctr. (United States); P. A. Driggers, SGT, Inc. (United States)

The Joint Polar Satellite System (JPSS) is a joint NOAA/NASA mission comprised of a series of polar orbiting weather and climate monitoring satellites which will fly in a sun-synchronous orbit, with a 13:30 equatorial crossing time. JPSS resulted from the decision to reconstitute the National Polar-orbiting Operational Environmental Satellite System (NPOESS) into two separate missions, one to be run by the Department of Defense and the other by NOAA. This decision was reached in early 2010, after numerous development issues caused a series of unacceptable delays in launching the NPOESS system. NPOESS was originally conceived to merge the civil Polar-orbiting Operational Environmental Satellite (POES) and Department of Defense (DOD) Defense Meteorological Satellite Program (DMSP) and the 2010 decision reverses this conception back to relatively independent civil and DOD polar environmental satellite programs.

This paper will describe the JPSS mission overview and timeline, along with the planned sensor complement and data products for the JPSS-1 and JPSS-2 missions. JPSS-1 is currently base-lined to fly an instrument complement of a visible infra-red imager, an infra-red sounder, a microwave sounder, an ozone mapper/profiler, and an earth radiometer. The paper will discuss the differences between these JPSS sensors and data products and the NPOESS predecessor and the legacy POES sensors. In addition, this paper will provide a brief status of the JPSS mission precursor, the NPOESS Preparatory Project (NPP), which is scheduled for launch by NASA in October 2011, as well as

the lessons learned from NPP/NPOESS and how these lessons will be applied to JPSS. The paper will conclude with a look ahead to future missions and sensors.

8176-05, Session 1

Preflight assessment of the cross-track infrared sounder (CrIS) performance

V. V. Zavyalov, C. S. Fish, G. E. Bingham, M. Esplin, M. Greenman, D. Scott, Utah State Univ. Research Foundation (United States)

The Cross-track Infrared Sounder (CrIS) is part of the Crosstrack Infrared and Microwave Sounding Suite (CrIMSS) instrument suite that will be used to produce accurate temperature, water vapor, and pressure profiles on the NPOESS Preparatory Project (NPP) and upcoming Joint Polar Satellite System (JPSS) operational missions. The NPP CrIS flight model has completed sensor qualification, characterization, and calibration and is now integrated with the NPP spacecraft in preparation for the launch. This presentation will review the CrIS performance during thermal vacuum tests including spacecraft integration test and provide a comparison to the AIRS and IASI heritage sensors that it is builds upon. The key test results that will be reported in this paper are Noise Equivalent Differential Noise (or NEdN), Radiometric Performance, and Spectral Accuracy. The CrIS sensor performance is outstanding and will meet the mission needs for the NPP /JPSS mission. NEdN is one of the key performance tests for the CrIS sensor. The overall NEdN performance for the CrIS for the LWIR, MWIR and SWIR spectral bands is excellent and comparable or exceed NEdN performance of AIRS and IASI. The Principal component Analysis (PCA) approach developed to estimate contribution of random and spectrally correlated noise components in the NEDN will be also discussed in this presentation.

8176-06, Session 2

Status of new and future ESA missions

R. Meynart, P. Silvestrin, European Space Research and Technology Ctr. (Netherlands)

No abstract available

56

8176-07, Session 2

Observation requirements for the second generation EUMETSAT polar system visible/ infrared imager (VII)

P. L. Phillips, P. Schlüssel, C. J. Accadia, European Organisation for the Exploitation of Meteorological Satellites (Germany); I. Zerfowski, Deutsches Zentrum für Luft- und Raumfahrt e.V. (Germany)

The EUMETSAT Polar System Second Generation (EPS-SG) will continue operational meteorological measurements from polar orbiting satellites in the mid-morning orbit in the 2020 timeframe. The Metop Second Generation (Metop-SG) satellites will carry a payload which is primarily dedicated to operational meteorology and climate monitoring. A core mission within this payload is an optical imager required to meet the imagery user needs for Numerical Weather Prediction (NWP), Nowcasting (NWC) and climate applications. As NWP progresses towards operation on higher spatial resolution grids, improved representation of atmospheric processes encompassing the whole Earth system will be required, hence the availability of observations of clouds and aerosols as well as surface parameters will play an increasing role in a skilful weather forecast. Imagery data will also be very important in Nowcasting (NWC) applications, particularly in polar regions where space-borne imagery from geostationary satellites are not available.

The EPS-SG Visible/Infrared Imager (VII) follows on from an important list of predecessors such as the Advanced Very High Resolution Radiometer (AVHRR) and the Moderate resolution Imaging Spectro-



radiometer (MODIS), and will fly in the mid-morning orbit of the Joint Polar System served by the JPSS (U.S. Joint Polar Satellite System) Visible Infrared Imager Radiometer Suite (VIIRS) for the other orbits. The VII will be fulfilled by the DLR METimage instrument; a crosspurpose medium resolution, multi-spectral optical imager, measuring the optical spectrum of radiation emitted and reflected by the Earth from a low-altitude sun synchronous orbit over a minimum swath width of 2800 km. The VII's spectral and radiometric performances and space-time resolution introduce novel observing capabilities that will enhance the observation potential. These enhanced capabilities along with the evolution of the VII observation requirements are discussed.

The generation of mission requirements has been supported substantially by the Post-EPS Mission Experts Team and the METimage Science Advisory Group. Their support is gratefully acknowledged.

8176-08, Session 2

PDR status for TROPOMI, the Sentinel 5 precursor instrument for air quality and climate observations

J. de Vries, R. Voors, Dutch Space B.V. (Netherlands); N. C. J. van der Valk, G. Otter, TNO Science and Industry (Netherlands); R. C. Snel, R. W. Hoogeveen, I. Aben, SRON Nationaal Instituut voor Ruimteonderzoek (Netherlands); Q. Kleipool, P. Veefkind, Koninklijk Nederlands Meteorologisch Instituut (Netherlands)

The Tropospheric Monitoring Instrument (TROPOMI) is being developed for launch in 2014 on ESA's Sentinel 5 Precursor satellite. TROPOMI is a passive sun backscatter spectrograph using the ultraviolet-to-SWIR wavelengths to have good sensitivity down to the surface. Together with its spatial resolution of 7 x 7 km2 it allows high quality observations of sources and sinks of air quality and climate related gases and aerosols. This spatial resolution results in a high fraction of cloud-free observations and is combined with a wide cross-flight swath to allow daily coverage of the complete Earth.

The instrument has as most direct predecessors OMI (Ozone Monitoring Instrument) on NASA's AURA satellite and SCIAMACHY on ESA's ENVISAT, where the push broom concept is derived from OMI and the SWIR observations from SCIAMACHY.

The UV to SWIR wavelength range is divided into the following bands: UV (270 - 320 nm) for the ozone profile and SO2 products, UV/VIS (320 - 500 nm) for O3, NO2, BrO, HCHO and OCIO total columns, NIR (675 - 775 nm) for clouds and H2O columns and SWIR (2305 - 2385 nm) for CH4 and CO columns and the HDO/H2O ratio.

This means that since earlier publications we have extended the UV channel to 320 nm where the wavelengths > 300 nm have the full spatial and spectral resolution whereas wavelengths below 300 nm have been adapted for the lower radiance levels for these wavelengths to best fit the O3 profile retrievals. This extension is beneficial for the SO2 column product because it can make use of the higher signal-to-noise and lower stray light levels found at the upper wavelength end of the UV channel as compared to the lower end of the UV/VIS channel.

The most challenging performance requirements for TROPOMI are on stray light for scenes with extreme contrast and on co-registration. In addition the signal-to-noise and dynamic range require state-of-the-art custom development of detectors and electronics. The paper will give an overview of the challenges and current performances.

The TROPOMI UVN module is funded by the Netherlands and the SWIR module and platform are provided via ESA. The instrument development is now a truly European programme with contributions from several countries.

8176-10, Session 3

PREMIER's imaging IR limb sounder

S. Kraft, J. C. Caron, J. Bezy, R. Meynart, J. Langen, B. Carnicero Dominguez, P. Silvestrin, European Space Research and Technology Ctr. (Netherlands)

The Imaging IR Limb Sounder (IRLS) is one of the two instruments

planned on board of the candidate Earth Explorer Core Mission PREMIER (Process Exploration through Measurements of Infrared and Millimetre-wave Emitted Radiation) presently under feasibility study by ESA. Emerging from recent enhanced detector and processing technologies IRLS shall, next to a millimetre-wave limb sounder, explore the benefits of three-dimensional limb sounding with embedded cloud imaging capability. Such 3d imaging technology is expected to open a new era of limb sounding that will allow detailed studies of the link between atmospheric composition and climate, since it will map simultaneously fields of temperature and many trace gases in the mid/upper troposphere and stratosphere across a large vertical and horizontal field of view. PREMIER shall fly in tandem formation looking backwards to METOP's swath and thereby explore the benefit of 3-dimensional information for meteorological/ environmental analyses and climate forcing investigations.

As currently planned and if implemented, IRLS will cover a total horizontal field of about 360 km and observe the LIMB at altitudes between 4 and 52 km. The vertical sampling distance will be well below 1 km. It will be run in two different exclusive modes to address scientific questions about atmospheric dynamics and chemistry at spectral resolutions of ~1.2 cm-1 and ~0.2 cm-1, respectively. In such configuration IRLS will be composed of an imaging array with about 2000 macro pixels, thereby allowing cloud imaging at sufficient spatial resolution.

We will present an overview of the instrument requirements as derived from the scientific requirements, the present status of the mission and its prospected performances, and we will give an overview of the currently identified technology needs and instrument predevelopments.

8176-11, Session 3

FIMAS: on the feasibility of a fluorescence imaging spectrometer to be flown on a small platform in tandem with Sentinel 3

S. Kraft, J. Bezy, R. Meynart, European Space Research and Technology Ctr. (Netherlands)

Resulting from a call for ideas for the 7th Earth Explorer mission, the Fluorescence Explorer (FLEX) mission [RD-1] was selected for assessment as one of the six Earth Explorer missions to be studied within Phase 0. After the review of the study outcome by the Earth Science Advisory Committee (ESAC), FLEX was not selected for Phase A study. Although not selected, the Earth Science Advisory Committee (ESAC) has expressed a clear recommendation to make an in-orbit demonstration of the measurement of vegetation fluorescence from space. Since FLEX involved four different instruments that would be required by an autonomous satellite to measure the chlorophyll fluorescence signal and to make the necessary atmospheric corrections, a new strategy has been proposed, which should make use of existing missions.

Such a proposal has been investigated for its feasibility and scientific return optimisation. The mission configuration would be realised by using data and products from Sentinel-3, which would be flying in tandem with a smaller satellite carrying a Fluorescence Imaging Spectrometer (FIMAS). ESA has implemented a parallel study with the aim to show the feasibility of FIMAS that could be realised as in-orbit demonstrator or possibly as a mission with reduced resource budget such as the coming Explorer 8 opportunity mission. In the frame of such a mission, it is expected that an affordable small platform will offer only limited resources for the instrument.

The two studies have identified and analysed suitable instrument concepts that should be compatible with a small platform. As a conclusion the imaging grating spectrometer concept was selected as the most suitable instrument concept [RD-2]. The studies have now further advanced and investigated by detailed analysis the expected resource allocation compromising at the same time as little as possible the scientific objectives and the instrument requirements. We will present the conceptual designs of the investigated instrument concepts and we will present some results of the performance analysis.

[RD-1] ESA SP 1313-4, Report for assessment of the Six Candidate Earth Explorer Core Missions, Nov. 2008



[RD-2] S. Kraft FIMAS - Feasibility study of a Fluorescence Imaging Spectrometer to be flown on a small platform in tandem with Sentinel 3, ICSO, Greece, 2010

8176-13, Session 3

Aalto-1: a hyperspectral earth observing nanosatellite

A. Näsilä, A. Hakkarainen, J. Praks, M. Hallikainen, Aalto Univ. School of Science and Technology (Finland); H. K. Saari, J. E. Antila, VTT Technical Research Ctr. of Finland (Finland); P. Janhunen, Finnish Meteorological Institute (Finland); R. Vainio, Univ. of Helsinki (Finland)

AALTO-1 - A HYPERSPECTRAL EARTH OBSERVING NANOSATELLITE

1. Introduction

Nanosatellites are quickly growing field in the Earth Observing technologies. Being agile and cost effective platform in the era of ever smaller instruments, is being seen as an answer how to cut costs of satellite programs and how to provide quick "from design to launch" capability. Also, being light weight in required resources provides universities and smaller private companies an opportunity to build their own satellites. Dozens student satellite programs give valuable hands-on experience to engineering students who then will carry their knowledge to industry.

Aalto-1 is a student nanosatellite program coordinated by Aalto University Department of Radio Science and Technology and supported by Aalto University Department of Automation and Systems Technology, Department of Communications and Networking and Department of Applied Mechanics. The satellite will carry 3 separate scientific instruments which are provided by a consortium formed with other Finnish universities, research institutes and private companies. [1]

This paper will present design of the satellite platform for the Aalto-1 mission and describe scientific goals and plans for the mission.

2. The satellite

Aalto-1 is based on 3U Cubesat design with dimensions 10 cm x 10 cm x 34 cm and weighs approximately 3 kilograms. The satellite is 3-axis stabilized and will have better than 1° pointing accuracy. Communications are provided by UHF/VHF-transreceiver and S-band transmitter for measurement data downlink. Aalto-1 will have also powerful on board computer system running Linux-based operating system which can be rebooted or reflashed during the mission in case of OS-malfunction.

The main goal of the mission is to operate successfully the hyperspectral imager made by VTT Finnish Technical Research Institute. The imager is based on a tunable Fabry-Perot interferometer, which is either a MEMS or a piezo-actuated device. It will be capable of taking 2D-images with 5-10 nm spectral resolution in wavelength range from 500 nm to 900 nm.

The second payload is the Compact Radiation Monitor (RADMON) designed and built by a consortium lead by University of Helsinki and University of Turku. The basic design of RADMON follows the design of the similar instrument in European Space Agency's BepiColombo mission [2]. RADMON will be more compact version suitable for nanosatellites and it will house new novel measurement electronics.

Aalto-1 is equipped also with novel de-orbiting device Electrostatic Plasma Brake. The concept was invented by P. Janhunen from Finnish Meteorological Institute to be used as a propulsion device in the interstellar space. Device uses special tether made from conductive wires welded together. The tether is unreeled from the device at end of the mission and charged electrically. Interaction between electric field surrounding the tether and the ionospheric plasma will create force which will slowly brake the satellite from its orbit. The first prototype of the device will be launched in the Estonian Estcube-mission. [3][4]

3. Conclusions

Despite the small size, the satellite is a fully fledged space instrument and it employs several scientific payloads and an experimental deorbiting device.



The Aalto-1 project is still in its early stage. The feasibility study of the satellite was made during the first half of 2010 and currently the project team works towards the preliminary design report completion in the middle of 2011. Building of the satellite will start in the third quarter of 2011 and the launch is targeted for the end of 2013.

4. References

[1] Praks, J., A. Kestilä, M. Komu, Z. Saleem, J. Jussila, A. Hakkarainen, A. Näsilä, M. Lankinen, K. Amzil, M. Hallikainen, Aalto-1: Multi-Payload, Remote Sensing Nanosatellite Mission, 1st IAA Conference on University Satellite missions and CubeSat Workshop, Rome, January 24-29, 2011.

[2] Huovelin, J., et al. Solar Intensity X-ray and particle Spectrometer (SIXS), Planet. Space Sci. 58, 96. 2010.

[3] Janhunen, P., Electrostatic plasma brake for deorbiting a satellite, J. Prop. Power, 26, 370-372, 2010.

[4] Janhunen, P., Electric sail for producing spacecraft propulsion, J. Prop. Power, 20, 763-764, 2004.

8176-14, Session 3

Spectropolarimeter for planetary exploration (SPEX): performance measurements with a prototype

R. Voors, Dutch Space B.V. (Netherlands); S. G. Moon, S. Hannemann, cosine Research B.V. (Netherlands); J. H. H. Rietjens, SRON Nationaal Instituut voor Ruimteonderzoek (Netherlands); G. van Harten, F. Snik, Utrecht Univ. (Netherlands); M. Smit, D. M. Stam, SRON Nationaal Instituut voor Ruimteonderzoek (Netherlands); C. U. Keller, Utrecht Univ. (Netherlands); E. C. Laan, A. L. Verlaan, W. A. Vliegenthart, TNO Science and Industry (Netherlands); R. ter Horst, R. Navarro, ASTRON (Netherlands); K. Wielenga, Mecon Engineering B.V. (Netherlands)

SPEX (Spectropolarimeter for Planetary Exploration) was developed in close cooperation between scientific institutes and space technological industries in the Netherlands. It is a spectropolarimeter with which it possible to measure microphysical properties of aerosols and cloud particles in planetary atmospheres. These particles are of crucial importance to the planet's radiation field and also play a role in chemical and dynamical processes.

SPEX utilizes a number of novel ideas. The key feature is that full linear spectropolarimetry can be performed without the use of moving parts, using an instrument of approximately 1-liter in volume. This is done by encoding the degree and angle of linear polarization (DoLP and AoLP) of the incoming light in a sinusoidal modulation of the intensity spectrum. The optical elements that are responsible for this are: an achromatic quarter-wave retarder, an athermal multiple-order retarder and a polarizing beam splitter at the entrance pupil.

Based on this principle, and after gaining experience from breadboard measurements using the same principle, a fully functional prototype was constructed. The functionality and the performance of the prototype were shown by laboratory tests as well as by blue sky measurements. The DoLP response can be measured to an accuracy of 10-4. The performance of the instrument was also modeled by an instrument simulator. The simulated results and the laboratory measurements show striking agreement.

SPEX would be a valuable addition to any mission that aims to study the composition and structure of planetary atmospheres, for example, missions to Mars, Venus, Jupiter, Saturn and Titan. In addition, on an Earth-orbiting satellite, SPEX could give unique information on particles in our own atmosphere.

58

8176-15, Session 4

Overview of Japanese Earth observation programs

H. Shimoda, Japan Aerospace Exploration Agency (Japan)

Six programs, i.e. TRMM, ADEOS2, ASTER, ALOS, GOSAT are going on in Japanese Earth Observation programs. PR on TRMM and ASTER on EOS-Terra are operating well except SWI channels of ASTER. ASTER SWI channels have stopped the operation because of a refrigerator failure in 2009. ADEOS2 was failed, but AMSR-E on Aqua is operating. ALOS carries three instruments, i.e., PRISM, AVNIR-2 and PALSAR. PRISM is a 3 line panchromatic push broom scanner with 2.5m IFOV. AVNIR-2 is a 4 channel multi spectral scanner with 10m IFOV. PALSAR is a full polarimetric active phased array SAR. The spacecraft is operating well as well as all the 3 sensors are operating well. GOSAT carries 2 instruments, i.e. a green house gas sensor (TANSO-FTS) and a cloud/aerosol imager (TANSO-CAI). TANSO-FTS is a Fourier transform spectrometer (FTS) and covers 0.76 to 15 µm region with 0.2 cm-1 resolution. TANSO-CAI is a 5 channel push broom scanner to observe aerosols and clouds. Both sensors are operating well. SMILES is now on JEM of ISS. SMILES is a sub-millimeter limb sounding instrument using super conducting mixer and measures stratospheric ozone and related compounds. Unfortunately, SMILES stopped its operation on 21, April, 2010. Next generation satellites will be launched in 2011-2014 timeframe. They are GCOM-W1, GCOM-C1, GPM core satellite, EarthCare, ALOS2 and ALOS3. GCOM-W1 will carry AMSR2. The orbit is A-train and has higher resolution than AMSR-E. GCOM-C1 will carry SGLI. SGLI has polarization channels. GCOM-W1 will be launched on 2011 and GCOM-C will be launched on 2014. GPM is a joint project with NASA and will carry two instruments. JAXA is developing DPR. DPR has Ka band channel in addition to Ku band channel. GPM will be launched on2013. Another project is EarthCare. It is a joint project with ESA and JAXA is going to provide CPR with NICT. EarthCare will be launched on 2013. ALOS F/O is composed by 2 satellites like GCOM. One is called ALOS-2 and will carry L-band SAR while the other is called ALOS-3 and will carry optical sensors.

8176-16, Session 4

Eleven years of ASTER onboard calibration

F. Sakuma, M. Kikuchi, N. Ohgi, Japan Resources Observation System and Space Utilization Organization (Japan); H. Inada, NEC TOSHIBA Space Systems, Ltd. (Japan); S. Akagi, Mitsubishi Electric Corp. (Japan); H. Ono, Fujitsu Ltd. (Japan)

ASTER is a high-resolution optical sensor for observing the Earth in a five-year mission on the Terra satellite launched in December1999. ASTER consists of three radiometers. VNIR has three bands in the visible and near-infrared region, SWIR has six bands in the shortwave infrared region, and TIR has five bands in the thermal infrared region. The onboard calibration devices of VNIR and SWIR were halogen lamps and photodiode monitors which were used once in forty-nine days. In orbit three bands of VNIR showed a rapid decrease in the output signal. The band 1, the shortest wavelength, decreased most to 70% in eleven years. The detector temperature of SWIR increased from 77 K to 130 K which caused the offset increase and somewhat response decrease. The temperature of the onboard blackbody of TIR remains at 270 K in the short-term calibration for the offset calibration, and is varied from 270 K to 340 K in the long term calibration for the offset and gain calibration once in forty-nine days. The long term calibration of the TIR showed a decrease in response after launch. The decrease was most remarkable at band 12 decreasing to 60% in eleven years. The cause of the decrease is considered as the contamination by the fuel or the outgas.



8176-17, Session 4

ALOS ("Daichi") Observation Results of the Great East Japan Earthquake in 2011.

M. Takahashi, M. Shimada, T. Tadono, Japan Aerospace Exploration Agency (Japan)

The Advanced Land Observation Satellite (ALOS) was successfully launched on January 24th, 2006, and it is well operating by Japan Aerospace Exploration Agency (JAXA) more than five years. ALOS is carrying on three instruments called PRISM, AVNIR-2, and PALSAR. The Great East Japan Earthquake was occurred at 5:46 on March 11, 2011 (UTC). The earthquake and tsunami caused severe damage in many cities, and more than 20 thousand people were killed and lost their homes. The JAXA has performed the emergency observation to monitor the state of the damage by the Panchromatic Remote-sensing Instrument for Stereo Mapping (PRISM) and the Advanced Visible and Near Infrared Radiometer type 2 (AVNIR-2) onboard the ALOS. In this presentation, we introduce several ALOS observation results of the 2011 M9.0 earthquake and tsunami, and of several inland earthquakes.

8176-18, Session 4

On-orbit Status of TANSO onboard GOSAT

H. Suto, M. Nakajima, A. Kuze, K. Shiomi, Japan Aerospace Exploration Agency (Japan)

To monitor the global column concentration of carbon dioxide (CO2) and methane (CH4) from space, the Greenhouse gases Observing SATellite (GOSAT) was launched on January 23, 2009. The Thermal And Near infrared Sensor for carbon Observation Fourier-Transform Spectrometer (TANSO-FTS) and Cloud and Aerosol Imager (TANSO-CAI) are onboard GOSAT to derive the precise amount of CO2 and CH4 in the earth's atmosphere. The first high spectral resolution SWIR spectra by TANSO-FTS and the image by TANSO-CAI were acquired on Feb. 7, 2009. TANSO has been continuously measuring CO2 and CH4 distributions globally every three days , and data distribution to the public has started from Feb. 16, 2010. During two years operation periods, the radiometric, geometric pointing accuracy and spectroscopic characterization of TANSO have been continuously conducted with updating the Level-1 processing algorithm. Time-series of radiometric, geometric and spectroscopic response function were determined and performed with on-orbit and vicarious calibrations. In the updated Level-1 processing, the newly developed correction algorithm for micro-vibration effects are operationally installed and improved the accuracy of medium gain condition. In this presentation, the detail of on-orbit characteristics and the current status of TANSO will be discussed.

8176-19, Session 5

59

Update of the GOSAT higher level product status 2.5 years after the launch

H. Watanabe, A. Yuki, K. Hayashi, F. Kawazoe, N. Kikuchi, F. Takahashi, T. Matsunaga, T. Yokota, National Institute for Environmental Studies (Japan)

After the 2.5 year operation of GOSAT (Greenhouse gases Observing SATellite), NIES GOSAT DHF (GOSAT Data Handling Facility of National Institute for Environmental Studies) has been producing CAI Level 1B and 1B+, FTS Level 2 SWIR (Column amount of CO2 and CH4), CAI Level 2 (Cloud Flag), FTS/ Level 3 products (Global Map of XCO2, XCH4,) and CAI/Level3 (Global radiance and global reflectance) , receiving FTS Level 1A/1B, and CAI Level 1A data from JAXA (FTS: Fourier Transform Spectrometer; CAI: Cloud and Aerosol Imager, JAXA: Japan Aerospace Exploration Agency). In addition, FTS Level 2 TIR, FTS Level 3 TIR, and Level 4A and 4B products (Emission/Absorption and 3D distribution)are newly released.

Since the FTS Level 2 SWIR data have been accumulated more than 2.5 years, global trend data can be seen, while the validation results show that there are negative bias of 2 to 3 % for CO2 and also negative bias of 1 to 2 % for CH4. A comparison with the results by different algorithms is also conducted.

All the distribution is through GOSAT User Interface Gateway (GUIG). The users include the researchers responding to the 3 Research Announcements and General Users. The number of the PIs exceeds 100, and that for general users, 1000.

8176-20, Session 5

Airborne flight campaign for GOSAT validation

D. Sakaizawa, S. Kawakami, M. Nakajima, Japan Aerospace Exploration Agency (Japan); T. Tanaka, M. Inoue, I. Morino, O. Uchino, National Institute for Environmental Studies (Japan)

Continuous validation of satellite observed data is important to qualify the long-term trends obtained from orbital measurements. To validate the satellite data, high-precision measurements from ground-based FTS, airborne in-situ instruments, and flask sampling devices provide more accurate carbon dioxide observations over restricted regions.

As part of the CAL/VAL activities of GOSAT, airborne flight campaigns were performed over Tsukuba and Hokkaido prefecture using groundbased FTS with a direct solar spectrum, airborne in-situ instruments and flask devices with vertical profiles of carbon dioxide mixing ratio, and a 1.57-um laser absorption sensor (LAS) with weighted column-averaged carbon dioxide density. Likewise, airborne measurement with a 1.57-um laser absorption sensor was conducted to detect the difference between urban areas and grasslands. Other specific topics are shown.

8176-21, Session 5

On orbit performance of radio spectrometers of Superconducting

Submillimeter-Wave Limb-Emission Sounder (JEM/SMILES)

S. Mizobuchi, Japan Aerospace Exploration Agency (Japan); H. Ozeki, K. Tamaki, Toho Univ. (Japan); K. Kikuchi, T. Nishibori, Japan Aerospace Exploration Agency (Japan); S. Ochiai, National Institute of Information and Communications Technology (Japan); M. Shiotani, Kyoto Univ. (Japan); C. Mitsuda, Fujitsu FIP Corp. (Japan)

SMILES is a project that observes vertical profiles of atmospheric minor constituents related with stratospheric and mesospheric chemical processes. SMILES adopts the acousto-optical spectrometer (AOS) as Radio Spectrometers for analyzing the atmospheric signal and detecting its power spectrum. The retrieved profiles contain some error originated from the response characteristics of AOS. The on-orbit properties of the instrument are necessary to be characterized and be modeled, in order to minimize the retrieval errors.

Spectrometer's response function is obtained with the input of a carrier signal. It has a characteristic shape in frequency. Any input spectra to the AOS are convoluted with this kind of frequency response function. With this frequency response function, we can estimate the influence of some strong emissions at neighbor frequencies on the emission profile of interest.

In our study, comb signals are used for evaluating the on-orbit response characteristics. The comb signals are originally used for frequency calibration of the spectrometer during atmospheric observation, which consists of a series of carrier signals with a frequency interval of 100 M Hz. Since only a few channels in AOS spectrum data contain information from each comb signal, it is slightly difficult to fully derive response characteristics by using only normal calibration data. Therefore, we have acquired special calibration data set at the beginning of this January.

We have derived the channel dependence and time series variation of the response characteristics by using both the normal calibration data and special data. As the first step of the analysis, we focus on the main lobe by approximating with a single Gaussian function. In the next step, we tried to derive the characteristics of main lobe response with better accuracy by taking into account the side lobe component.

In this presentation, the results of these analyses will be reported.



8176-22, Session 5

Measurement of chlorine species, HCl, HOCl, and CIO by ISS/JEM/SMILES

M. Suzuki, Japan Aerospace Exploration Agency (Japan); C. Mitsuda, C. Takahashi, Fujitsu FIP Corp. (Japan); N. Manago, Japan Aerospace Exploration Agency (Japan); K. Imai, Tome R&D Inc. (Japan); Y. Iwata, T. Sano, Japan Aerospace Exploration Agency (Japan); K. Takahashi, Kyoto Univ. (Japan); T. Imamura, H. Akiyohi, National Institute for Environmental Studies (Japan); H. Hayashi, Y. Naito, M. Shiotani, Kyoto Univ. (Japan)

Chemistry of the stratosphere is largely controlled by the catalytic photochemical reactions of CIOx (family of reactive chlorine containing species, CIO, CI, OCIO, etc), BrOx, HOx, and NOx. Especially the precise knowledge on the CIOx distribution in the stratosphere from satellite observation is important because it is necessary to assess the effectiveness of regulation to chlorine containing chemicals (CFCs et al), as well as to predict the stratospheric chemistry when the ozone layer will recover from anthropogenic loading of chlorine and how the stratospheric chlorine chemistry and greenhouse gases will cross-affects to discuss the climate prediction.

Superconducting Submillimeter-Wave Limb-Emission Sounder, SMILES, is the instrument to observe sub-mm wave atmospheric limb emission, which is onboard Japanese Experiment Module (JEM) "Kibo" of the International Space Station (ISS). SMILES has been jointly developed by Japan Space Exploration Agency (JAXA) and National Institute of Information and Communication Technology (NICT). SMILES program has two objectives; (1) engineering demonstration of sub-mm technology, Superconductor-Insulator-Superconductor (SIS) mixer which is mechanically cooled to 4K, in space, and (2) scientific observation of minor constituents, such as chlorine monoxide (CIO), in the middle atmosphere (stratosphere and mesosphere). SMILES was launched on Sep. 11, 2009 and it worked from Oct. 12 to Apr. 21, 2010 when a sub-system sub-mm local oscillator aborted operation. It is obvious that the SMILES has better sensitivity to species such as CIO at the middle atmosphere (30-40 km) due to strength of its 4 K cryogenic system. But to break the previous detection limit of CIO, it will be necessary to check whole process to derive CIO physical value; platform/instrument characteristics, algorithm, spectroscopy and other physical parameters.

This paper describes; characteristics of SMILES and its platform ISS, features of calibrated spectra, retrieval algorithm, and test retrieval results of HCI, and daytime and nighttime CIO, HOCI in the background atmosphere, and also discusses how appropriate the precision and accuracy of the operational Level 2 dataset. The chemical balance of chlorine species are also discussed with photolysis rate (with multiple scattering) and chemical kinetic constants.

8176-23, Session 5

60

Current status of level 2 product of Superconducting Submillimeter-Wave Limb-Emission Sounder (SMILES)

C. Mitsuda, Fujitsu FIP Corp. (Japan); M. Suzuki, Y. Iwata, N. Manago, Japan Aerospace Exploration Agency (Japan); Y. Naito, Kyoto Univ. (Japan); C. Takahashi, Fujitsu FIP Corp. (Japan); K. Imai, Tome R&D Inc. (Japan); E. Nishimoto, H. Hayashi, M. Shiotani, Kyoto Univ. (Japan); T. Sano, M. Takayanagi, Japan Aerospace Exploration Agency (Japan); H. Taniguchi, Fujitsu FIP Corp. (Japan)

In this presentation, we introduce latest SMILES product v2.0 status, which is primitive gain nonlinearity corrected.

The Superconductive Submillimeter-wave limb-Emission Sounder (SMILES), which is joint mission of JAXA (Japan Aerospace Exploration Agency) and NICT (National Institute of Information and Communications Technology), was attached to Japan Experiment Module of International Space Station on September 25, 2009 and had observed atmospheric submillimeter spectra for about half a years. SMILES has 4K-cooled superconducting mixers and had performed high sensitive observation. SMILES has 3 bands in 640 GHz band (band A: 624.32 - 625.52 GHz, band B: 625.12-626.32 GHz, band C: 649.12-650.32 GHz). However, SMILES observe only 2 bands simultaneously because of limited to 2 receivers.

Standard SMILES L2 products (O3, HCI, CIO, HNO3, CH3CN, HOCI, HO2, BrO and O3-isotopes on stratosphere) have been released 4 times. In v1.3, which was released this spring, major issues of 1.X series, like as antenna pointing problem, internal inconsistency of O3, HCI and temperature between band A and B, field interference flagging, were almost cleared.

However, it is suggested that receiver's gain nonlinearity, which is remaining issue in level 1B processing, may have big impact for products. Estimated error in current version 005 is up to 10 K and in noisy products like as BrO, HOCI might have +50%, -100% error around 30km, respectively. So, we will release primitive gain nonlinearity corrected version (v2.X series) as early as possible (this summer or autumn). Other planed updates are AOS response function correction which is estimated by comb signal in orbits, some spectral line parameter changes, and so on.

8176-24, Session 6

Status of GCOM-W1/AMSR2 development, algorithms, and products

T. Maeda, K. Imaoka, M. Kachi, H. Fujii, A. Shibata, K. Naoki, M. Kasahara, N. Ito, K. Nakagawa, Japan Aerospace Exploration Agency (Japan); T. Oki, Japan Aerospace Exploration Agency (Japan) and The Univ. of Tokyo (Japan)

The Global Change Observation Mission (GCOM) consists of two polar orbiting satellite observing systems, GCOM-W (Water) and GCOM-C (Climate), and three generations to achieve global and long-term monitoring of the Earth. GCOM-W1 is the first satellite of the GCOM-W series and scheduled to be launched in Japanese fiscal year 2011. The Advanced Microwave Scanning Radiometer-2 (AMSR2) will be the mission instrument of GCOM-W1. AMSR2 will extend the observation of currently ongoing AMSR-E on EOS Aqua platform. Development of GCOM-W1 and AMSR2 is progressing on schedule. Proto-flight test (PFT) of AMSR2 was completed and delivered to the GCOM-W1 satellite system. Currently, the GCOM-W1 system is under PFT at Tsukuba Space Center until summer 2011 before shipment to launch site, Tanegashima Space Center. Development of retrieval algorithms has been also progressing with the collaboration of the principal investigators. Based on the algorithm comparison results, at-launch standard algorithms were selected and implemented into the processing system. These algorithms will be validated and updated during the initial calibration and validation phase. As an instrument calibration activity, a deep space calibration maneuver is planned during the initial checkout phase, to confirm the consistency of cold sky calibration and intra-scan biases. Maintaining and expanding the validation sites are also ongoing activities. A flux tower observing instruments will be introduced into the Murray-Darling basin in Australia, where the validation of other soil moisture instruments (e.g., SMOS and SMAP) is planned.

8176-25, Session 6

Outline GCOM - C1 / SGLI science

Y. Honda, Chiba Univ. (Japan)

GCOM-C1 is to contribute to the understanding of the climate system, which aims to contribute to the understanding of carbon cycle and radiation budget in particular. Therefore, 52 products will generated in this mission. Those algorithms will being developed mainly by 35 PIs (Principal Investigators). In the summer of 2009, GCOM-C1 PI team has been formed. Experiences of ADEOS-II / GLI have been utilized in the development of many algorithms. Its experiences have been utilized in many verification methods, too. These things made it possible to streamline and shorten the project time. There were few products on land under ADEOS / GLI project. Therefore, algorithm development land for new approach was needed. In particular it is needed to develop new algorithms using the multi-angular observation data of SGLI. Multi-angular observation is one of SGLI Features.



8176-26, Session 6

Status of proto-flight test of the dualfrequency precipitation radar for the global precipitation measurement

T. Miura, M. Kojima, K. Furukawa, Y. Hyakusoku, Japan Aerospace Exploration Agency (Japan); T. Iguchi, H. Hanado, K. Nakagawa, National Institute of Information and Communications Technology (Japan); M. Okumura, NEC TOSHIBA Space Systems, Ltd. (Japan)

The Dual-frequency Precipitation Radar (DPR) on the Global Precipitation Measurement (GPM) core satellite is being developed by Japan Aerospace Exploration Agency (JAXA) and National Institute of Information and Communications Technology (NICT). The GPM is a follow-on mission of the Tropical Rainfall Measuring Mission (TRMM). The objectives of the GPM mission are to observe global precipitation more frequently and accurately than TRMM. The frequent precipitation measurement about every three hours will be achieved by some constellation satellites with microwave radiometers (MWRs) or microwave sounders (MWSs), which will be developed by various countries. The accurate measurement of precipitation in mid-high latitudes will be achieved by the DPR. The GPM core satellite is a joint product of National Aeronautics and Space Administration (NASA), JAXA and NICT. NASA is developing the satellite bus and the GPM microwave radiometer (GMI), and JAXA and NICT are developing the DPR. JAXA and NICT are developing the DPR through procurement. The contract for DPR is NEC TOSHIBA Space Systems, Ltd.

The configuration of precipitation measurement using an active radar and a passive radiometer is similar to TRMM. The major difference is that DPR is used in GPM instead of the precipitation radar (PR) in TRMM. The inclination of the core satellite is 65 degrees, and the flight altitude is about 407 km. The non-sun-synchronous circular orbit is necessary for measuring the diurnal change of rainfall similarly to TRMM. The DPR consists of two radars, which are Ku-band (13.6 GHz) precipitation radar (KuPR) and Ka-band (35.55 GHz) precipitation radar (KaPR). According to the different detectable dynamic ranges, The KaPR will detect snow and light rain, and the KuPR will detect heavy rain. In an effective dynamic range in both KuPR and KaPR, drop size distribution information and more accurate rainfall estimates will be provided by a dual-frequency algorithm.

The proto-flight test for DPR started in November 2010. The status of proto-flight test of DPR will be presented.

8176-27, Session 6

61

Development status of PALSAR-2 onboard ALOS-2

S. Suzuki, Y. Kankaku, Y. Osawa, Japan Aerospace Exploration Agency (Japan)

The Advanced Land Observing Satellite-2 (ALOS-2) will succeed to the radar mission of the ALOS "Daichi" which has been contributing to cartography, regional observation, disaster monitoring, and resources surveys for more than 5 years. ALOS has contributed to disater mistigation activities on "The 2011 off the Pacific coast of Tohoku Earthquake" occurred on March 11 in Japan such as emergency observations and deformation analysis by INSAR.

The state-of-the-art L-band Synthetic Aperture Radar (SAR) called PALSAR-2 onboard ALOS-2/PALSAR-2 will have enhanced performance compared to ALOS/PALSAR. PALSAR-2 has Spotlight mode (1 to 3 m) and Stripmap mode (3 to 10 m), while PALSAR has 10 m spatial resolution at best. Moreover, ScanSAR mode (nominal 14MHz bandwidth and 350km swath) is expanded to include 28MHz bandwidth for INSAR and to extend the wide swath of 490km for maritime observation.

The new technologies, such as maximum bandwidth allocation for L-band SAR, spotlight mode with Active Phased Array Antenna, high power efficiency device of GaN and chirp modulation technique, have been verified by testing the Engineering Model for PALSAR-2. The ALOS-2 is scheduled to be launched in 2013 by the H-IIA Launch Vehicle. The Critical Design of ALOS-2 including PALSAR-2 has been conducted since March, 2010. This paper describes the current development status of ALOS-2 and the brief results of the Engineering Model for PALSAR-2.

8176-28, Session 6

Outline of Advanced Land Observing Satellite-3 and its instruments

H. Imai, H. Katayama, Y. Hatooka, S. Suzuki, Y. Osawa, Japan Aerospace Exploration Agency (Japan)

The Advanced Land Observing Satellite (ALOS) "DAICHI" launched in January 2006 has been operated successfully on orbit for more than five years, delivering a huge number of high-resolution images and contributing to a variety of fields. The Japan Aerospace Exploration Agency (JAXA) is planning a satellite system including ALOS-2 and ALOS-3 for the ALOS follow-on program. ALOS-3 will succeed DAICHI's mission with enhanced capabilities.

The timely update of geographical information including topographic map, land use and vegetation is needed. Also disaster monitoring is becoming more important. ALOS-3 will be an optical observation satellite with wide and high-resolution observation capability by enhancing the technologies developed for DAICHI.

ALOS-3 will carry optical sensors and have a capability to collect high resolution (better than 1m) and wide swath (50 km) images with high geo-location accuracy without ground control points by utilizing the precise geo-location determination techniques developed for DAICHI. ALOS-3 will also produce precise digital surface models (DSMs) by stereo pair images acquired with two sets of telescope, which are necessary to produce orthophoto images. These capabilities are ideal for the large scale geographical information including elevation and land cover-map that will be used in many research areas and practical applications including disaster management support.

JAXA has been conducting the conceptual design for the spacecraft and the mission instruments for ALOS-3.

This paper introduces the outline of ALOS-3 and its onboard instruments.

8176-29, Session 6

Retrieval of spectral response functions for the hyperspectral sensor of HISUI (Hyperspectral Imager SUIte) by means of onboard calibration sources

K. Tatsumi, N. Ohgi, H. Harada, T. Kawanishi, F. Sakuma, Japan Resources Observation System and Space Utilization Organization (Japan); H. Inada, T. Kawashima, NEC TOSHIBA Space Systems, Ltd. (Japan); A. Iwasaki, The Univ. of Tokyo (Japan)

HISUI (Hyper-spectral Imager SUIte) which is the next Japanese earth observation project has been developed under the contract with NEDO and METI. HISUI is comprised of hyperspectral and multispectral sensors. The hyperspectral sensor is an imaging spectrometer with two separate spectral channels: one for the VNIR range from 400 to 970 nm and one for the SWIR range from 900 to 2500 nm. Spatial resolution is 30 m with spatial swath width of 30km. The spectral resolution will be better than 10nm in the VNIR and 12.5nm in the SWIR. The multispectral sensor has four VNIR spectral bands with spatial resolution of 5m and swath width of 90km. HISUI will be installed in ALOS-3 which is an earth observing satellite in the project formation phase by JAXA. It will be launched in FY 2015.

This paper is concerned with the retrieval of spectral response functions (SRFs) for the hyperspectral sensor. The center wavelength and bandwidth of spectral response functions of hyperspectral sensor may shift and broaden due to the characteristics of the spectrometer, the optics and the detector assembly. Therefore it is necessary to measure or estimate the deviation of the wavelength

SPIE Remote Sensing

and the bandwidth broadening of the SRFs. In this paper we describe the methods of retrieval of the SRF's parameters (Gaussian functions assumed) by means of onboard calibration sources and we show some simulation's results and the usefulness of this method.

8176-30, Session 6

EarthCARE/CPR design and its evaluation status

T. Kimura, H. Nakatsuka, K. Sato, Y. Seki, Y. Sakaide, K. Okada, J. Yamaguchi, Japan Aerospace Exploration Agency (Japan); N. Takahashi, Y. Ohno, H. Horie, National Institute of Information and Communications Technology (Japan)

EarthCARE is the joint mission between ESA and JAPAN to observe global profile of cloud and aerosol. The mission is expected to reveal aerosol and cloud interaction quantitatively, which is still most uncertain factor of numerical climate model, using Ultra Violet LIDAR and W-band Doppler Radar. It was named Cloud Profiling Radar and developed by JAXA and NICT in Japan. CPR is the first Radar to provide Doppler measurement of cloud particles up/down draft. Doppler measurement from space does have some difficulties. CPR design makes it possible by developing some key technologies. One of them is the Large W-band antenna with precise surface, of which diameter is 2.5 m. It was designed and manufactured already and measured by Near Field Measurement System. Another one is knowledge of instrument pointing, which produce large Doppler error due to the satellite speed. Other factors are suppressed using some optimization techniques, such as Variable Pulse Repetition Frequency.

Throughout all RF and electrical components tests, CPR system level test is undergoing in Japan. The presentation and paper will also include recent results of these tests.

8176-31, Session 7

Designing an in-flight airborne calibration site using experience from vicarious radiometric satellite calibration

S. Livens, W. Debruyn, S. Sterckx, I. Reusen, VITO NV (Belgium)

Laboratory calibration of electro-optical sensors can be performed very accurately. However the radiometric properties of the sensors can change in-flight, which makes it essential to perform regular in-flight verification. Only then quantitative mapping from airborne hyperspectral imagery can be achieved. Accurate radiometric verification and calibration can be established by performing in-flight measurements of calibration targets in the field of view of the airborne sensors. This assumes a good geometric characterization (knowledge of boresight angles) and the availability of an accurate digital terrain model.

A well equipped calibration site will serve the needs of these vicarious calibrations. If needed, vicarious measurements can serve as calibration data, replacing the pre-flight laboratory measurements. Initially the calibration site will be set up for the radiometric calibration of hyperspectral imaging sensors. Later, a geometric in-flight calibration component will be added. The design of a radiometric calibration target is closely linked to the calibration methods to be used. We borrow from expertise gained from developing the calibration system for the PROBA-V global vegetation monitoring satellite. This includes multiple independent vicarious calibration methods which make use of diverse natural on-ground targets.

The higher spatial resolution of the airborne systems has the advantage that targets can be much smaller which also makes it less time consuming to perform ground measurements simultaneously with the flight. On the other hand, adjacency effects can be much more important. The PROBA-V instrument has four spectral bands, whereas the targets which should also be useful for calibration of hyperspectral imagers. The calibration methods should work for any sensor characteristics within a similar spectral range, but unfortunately they do not yield sufficiently accurate results at all wavelengths. Thus additional artificial targets might need to cover this. We foresee to identify and design calibration targets in the Belgian Campine region, close to the home base of the sensors to be deployed. There a number interesting natural targets are present. Small water bodies (lakes) can be used as equivalent for oceans. The sandy lakesides offer similarly good equivalents for desert and salt lake sites.

Reflectance based calibration using ground measurements by wellcalibrated spectro-radiometers taken during the flight is applicable to both space borne and airborne systems. Most other methods need data about the aerosol contents, so they need to be derived from locally measured sun photometer data.

Using lakes to perform Rayleigh calibration would be very difficult, as this method relies on knowledge about organic material content, which is not available through models and costly to measure. Adapting Sun glint calibration depends less critically on water properties and thus is easier to adapt. The effect of waves in lakes is different from ocean waves and would need to be studied. The sandy regions can be used to perform the equivalent of desert calibration, provided a suitable BRDF reflectance model can be worked out. Besides reflectance based calibration, the PROBA-V calibration methods besides are unproven for use in airborne calibration, but the identification of suitable calibration targets can facilitate their investigation.

8176-32, Session 7

Principal component noise filtering for NAST-I radiometric calibration

J. Tian, NASA Langley Research Ctr. (United States); W. L. Smith, Sr., Hampton Univ. (United States) and Univ. of Wisconsin - Madison (United States)

The National Polar-orbiting Operational Environmental Satellite System (NPOESS) Airborne Sounder Testbed - Interferometer (NAST-I) instrument is a high-resolution scanning interferometer that measures emitted thermal radiation between 3.3 and 18 microns. The raw interferogram measurements are radiometrically and spectrally calibrated to produce radiance spectra, which are further processed to obtain temperature and water vapor profiles of the Earth's atmosphere via retrieval algorithms. NAST-I produces sounding data with 2 kilometer resolution (at nadir) across a 40 kilometer ground swath from a nominal altitude of 20 kilometers onboard a NASA ER-2 aircraft or similar coverage from the PROTEUS aircraft.

The NAST-I radiometric calibration is achieved using internal blackbody calibration references at ambient and hot temperatures. In this paper, we introduce a refined calibration technique that utilizes a principal component (PC) noise filter to compensate for instrument distortions and artifacts, therefore, further improve the absolute radiometric calibration accuracy. The calibration procedure is summarized in the following steps: the raw interferograms are partitioned into 30-minute segments for calibration application; a PC noise filtering algorithm is applied to hot blackbody (HBB) and ambient blackbody (ABB) spectra; using the filtered HBB and ABB data, the responsivity and offset coefficients are computed and applied to PC-filtered Earth scene spectra, which results in calibrated scene radiances.

To test the procedure and estimate the PC filter noise performance, we form dependent and independent test samples of calibration data by using odd and even sets of blackbody spectra. To determine the optimal number of eigenvectors, the PC filter algorithm is applied to both dependent and independent blackbody spectra with a varying number of eigenvectors. The responsivity and offset coefficients are computed from filtered dependent spectra, from which, we can predict the independent blackbody radiances. The total root-mean-square (RMS) error as a function of eigenvectors is evaluated by comparing the predicted blackbody radiances with ideal Planck radiances. The optimal number of PCs is selected so that the total RMS value is minimized. To see the filtering effect on the calibration noise performance, we examine four different scenarios: apply PC filtering to both dependent and independent datasets, apply PC filtering to dependent calibration data only, apply PC filtering to independent data only, and no PC filters. The independent scene radiances are predicted for each case and comparisons are made. The results show significant reduction in noise in the final calibrated radiances with the implementation of the PC filtering algorithm.



8176-33, Session 7

SWIR calibration of Spectralon reflectance factor

G. T. Georgiev, Sigma Space Corp. (United States); J. J.
Butler, NASA Goddard Space Flight Ctr. (United States); C.
C. Cooksey, National Institute of Standards and Technology (United States); L. Ding, Sigma Space Corp. (United States); K.
J. Thome, NASA Goddard Space Flight Ctr. (United States)

Satellite instruments operating in the reflective solar wavelength region require accurate and precise determination of the Bidirectional Reflectance Factor (BRF) of laboratory-based diffusers used in their pre-flight and post-flight calibrations. Such BRF determination is needed throughout the reflected-solar spectrum requiring extension of those data already existing at wavelengths less than 1000 nm. Spectralon diffusers are commonly used as a reflectance standard for bidirectional and hemispherical geometries. The Diffuser Calibration Facility at NASA's Goddard Space Flight Center is a secondary calibration facility after National Institute of Standards and Technology (NIST) for over two decades, and has provided numerous NASA projects with BRF data in the UV. Visible and the NIR spectral regions. Presented in this paper are measurements of BRF from 1470 nm to 1630 nm obtained using an indium gallium arsenide detector and tunable coherent light source in the Diffuser Calibration Facility. The sample was a 2 inch diameter, 99% white Spectralon target. The BRF results are discussed and compared to empirically generated data from a model based on NIST certified values of 6deg directionalhemispherical spectral reflectance factors from 900 nm to 2500 nm. Employing a new NIST capability for measuring bidirectional reflectance using a cooled, extended InGaAs detector, BRF calibration measurements of the same sample were also made with NIST's Spectral Tri-function Automated Reference Reflectometer (STARR) from 1470 nm to 1630 nm at incident angle of 0o and viewing angles of 40deg, 45deg, and 50deg. Although not compared to NIST, additional BRF data of the same sample is presented at number of incident and viewing angle geometries. The total combined uncertainty for BRF in SWIR range is less than 1%. These measurement capabilities will evolve into a BRF calibration service in SWIR region in support of NASA remote sensing missions.

8176-34, Session 7

63

Analysis of MetOp/HIRS instrument selfemission and its impact on on-orbit calibration

T. Chang, I. M. Systems Group, Inc. (United States); C. Cao, National Oceanic and Atmospheric Administration (United States)

Instrument self-emission and nonlinear response play important roles in radiometric calibration for satellite thermal infrared radiometers, and can affect the accuracy of Earth scene radiance retrieval if uncorrected. This paper presents the pre&post-launch self-emission models for infrared radiometers and analyzes the interrelationships between the instrument self-emission, detector nonlinearity, and calibrations intercept and slope variations using both MetOp/HIRS pre-launch and post-launch data. HIRS is a traditional cross-track line scanning radiometer in the infrared and visible spectrum, including infrared channels with 12 in the long wave (669-1529cm-1), and 7 in the short wave (2188-2657cm-1), and 1 visible channel. The channels are separated with beamsplitters and a rotating filter wheel assembly consisting of 20 spectral filters. The warm filters and other in-path components generate self-emission which becomes the majority of the total radiance falling on the detector.

The thermal-equilibrium condition in pre-launch thermal vacuum (TV) allows us to evaluate the self-emission using a simplified model. The correlation between the self-emission and the instrument temperature has been demonstrated and the self-emission level has been quantified by analyzing the correlation of the instrument nonlinear response with instrument temperature. It was found that the self-emission contributions at the detectors are in the range of 95% to 97%. Post-launch the instrument operates in a more complex thermal environment, and a more comprehensive model is developed

to analyze the self-emission and its impact on on-orbit calibration and Earth scene retrieval. The self-emission fluctuates with the instrument temperature and causes the variation in instrument response, including the variations of intercept and the instrument gain. The quantification of instrument self-emission can be achieved by analyzing the correlation of instrument nonlinear response with instrument temperature. The self-emission contributions are slightly higher than those in prelaunch and are estimated to be in the range of 96% to 99%. The differences in self-emission between pre-launch and post-launch is discussed.

The calibration of the HIRS infrared channels makes use of instrument responses to the views of the onboard internal calibration target (ICT) blackbody and cold deep space (DS), which is performed every 40 scan lines. The two-point calibration provides a slope and an intercept for each channel. The instrument self-emission variation makes both coefficients deviate from their calibration value, and if uncorrected, can lead to errors in Earth radiance retrieval. These variations have been quantified using on-orbit data and this investigation provides guideline for on-orbit calibration algorithm improvement. It was found that, for MetOp/HIRS infrared channels, the self-emission induced intercept variation impacts the calibration up to 1%, which is more than the effect from slope variation.

The self-emission models developed in this work can be applied to other thermal infrared radiometers and sounders. However, the impact on calibration and Earth scene retrieval varies with calibration technique and algorithm used. Potential applications of both prelaunch and post-launch self-emission models to other infrared radiometers and sounders, and the impact assessment in general, are discussed.

8176-35, Session 8

Aqua MODIS on-orbit calibration and performance (2002-2011)

X. Xiong, NASA Goddard Space Flight Ctr. (United States); W. Barnes, Univ. of Maryland, Baltimore County (United States); A. Angal, Science Systems and Applications, Inc. (United States)

Launched in 2002, Aqua MODIS has collected more than 9 years of global datasets for studies of various land, ocean, and atmospheric parameters and their changes over time. These geophysical parameters are derived from instrument radiometrically calibrated and geolocated reflectances and radiances in 36 spectral bands, covering wavelengths from visible (VIS) to long-wave infrared (LWIR). MODIS spectral bands are located on four focal plane assemblies (FPA). The reflective solar bands (RSB) are calibrated using both its solar and lunar observations and the thermal emissive bands (TEB) are calibrated using an on-board blackbody (BB). The changes in sensor spectral and spatial characteristics are regularly monitored by an on-board spectroradiometric calibration assembly (SRCA). In this paper, we present an update to Aqua MODIS on-orbit calibration and characterization activities and assess instrument long-term radiometric, spectral, and spatial performance. Specifically, we illustrate and discuss on-orbit changes in detector radiometric gains, spectral responses, and spatial registrations. New challenges to continuously maintain calibration and data quality and lessons learned from launch to present are also reported.

8176-36, Session 8

Terra MODIS band 27 electronic crosstalk: cause, impact, and mitigation

J. Sun, Sigma Space Corp. (United States); S. Madhavan, Science Systems and Applications, Inc. (United States); B. Wenny, Sigma Space Corp. (United States); X. Xiong, NASA Goddard Space Flight Ctr. (United States)

MODIS is one of the key sensors in the suite of remote sensing instruments in the Earth Observing System (EOS). MODIS on the Terra platform was launched into orbit in December of 1999 and has successfully completed eleven years of operation. MODIS has 36 spectral channels with wavelengths varying from 0.4 μ m to 14.4 μ m. The thermal channels in MODIS have a spectral range from 3.75 μ m to 14.24 μ m, with a native spatial resolution of 1 km. Over the eleven

years of mission lifetime, the sensor degradation has been carefully monitored using various On-Board Calibrators (OBC). In particular, the thermal channels are monitored using the on-board Black-Body (BB) which is traceable to NIST standards. MODIS also has a unique feature for calibration reference in terms of lunar irradiance. The lunar observations are periodically measured using the space view port and this allows another viable source for monitoring sensor performance. Based on the lunar observations, it was found that there was a possible signal leak for Band 27 from its neighboring bands located on the Long-Wave Infrared (LWIR) focal plane. Further investigations revealed a signal leak from Bands 28, 29 and 30. The magnitude of the leak is trended and correction coefficients are derived using the lunar observations. In this paper, we demonstrate the across-band signal leak in MODIS Band 27, its potential impact on the retrieved Brightness temperature (B.T.). Also, the paper explores a correction methodology to relieve the artifacts due to the across-band signal leak. Finally, the improvement in the Band 27 image quality is quantified.

8176-37, Session 8

Solar and lunar observation planning for Earth-observing sensor

J. Sun, Sigma Space Corp. (United States); X. Xiong, NASA Goddard Space Flight Ctr. (United States)

MODIS on-orbit calibration activities include the use of the onboard solar diffuser (SD) / SD stability monitor (SDSM) and regularly scheduled lunar observations for the refective solar bands (RSB) radiometric calibration. Normally, the SD door is closed when there is no SD/SDSM observation to avoid the unnecessary illumination of the sunlight on the SD, which causes the SD degradation. The SD is illuminated over a very short period of time when MODIS passes the terminator from night side to day side. To implement a SD/SDSM calibration, the SD door needs to be opened and the SDSM should be turned on during the short period of time when the SD is illuminated. A planning tool is needed to predict exact times for the SD door open/close and SDSM turn on/off for each SD/SDSM calibration. The tool is also needed for MODIS yaw maneuvers implemented for SD bi-direction reflectance factor (BRF) validation and SD screen vignetting function (VF) derivation. MODIS observes the Moon through its space view (SV). To increase the opportunity for the lunar observations and keep the lunar phase angle in a selected narrow range that minimizes the view geometric effect on the observed lunar irradiance, a spacecraft roll maneuver is implemented for MODIS lunar observations. A lunar observation planning tool is required to predict the time and roll angle needed for each lunar observation in the selected phase angle range. The tool is also needed to determine the phase angle range such that the MODIS can view the Moon in as many months as possible each year. To support MODIS instrument operation and calibration, we have developed a set of tools to address the need and successfully applied them to both Terra and Aqua MODIS. In this paper, we describe the design methodologies and implementation of the tools. The tools have also been modified to support VIIRS on-orbit solar and lunar calibration ..

8176-38, Session 8

64

Using the Moon to track MODIS reflective solar bands calibration stability

X. Xiong, NASA Goddard Space Flight Ctr. (United States); X. Geng, Sigma Space Corp. (United States); W. Barnes, Univ. of Maryland, Baltimore County (United States)

MODIS has 20 reflective solar bands (RSB) in the visible (VIS), near infrared (NIR), and short-wave infrared (SWIR) spectral regions (bands 1-19 and 26) and 16 thermal emissive bands (TEB) in the mid-wave infrared (MWIR) and long-wave infrared (LWIR) spectral regions (bands 20-25 and 27-36). The RSB are calibrated on-orbit by a solar diffuser (SD) and solar diffuser stability monitor (SDSM) system. In addition to SD/SDSM calibration events, near-monthly lunar observations are scheduled and implemented for both Terra and Aqua MODIS. A time series of normalized detector responses to the Moon allows its calibration stability to be monitored. The normalization is made to remove the differences due to lunar viewing geometries and Sun-



Moon-Satellite distances. Initially, this approach was only applied to MODIS bands (1-4 and 8-12) that do not saturate when viewing the Moon. In recent years, we have extended its applications to other RSB bands that contain saturated pixels. In this paper, we describe the methodology developed to use lunar observations to track MODIS RSB radiometric calibration stability and present their long-term lunar response trending results for both Terra and Aqua MODIS. Also discussed in the paper are advantages and limitations of this approach and its applications for other earth-observing sensors.

8176-39, Session 8

Alternative approach of response versus scan-angle (RVS) for MODIS reflective solar bands

H. Chen, Sigma Space Corp. (United States); X. Xiong, NASA Goddard Space Flight Ctr. (United States); J. Sun, A. Wu, Sigma Space Corp. (United States)

MODIS has 20 Reflective Solar Bands (RSB) with wavelengths from 0.41µm to 2.2µm. All RSB are normally calibrated on-orbit with onboard calibrators, including a Solar Diffuser (SD), a Solar Diffuser Stability Monitor (SDSM), and a Spectroradiometric Calibration Assembly (SRCA). MODIS has a Space View (SV) port used to provide a background reference for each scan data, and also a viewing path for possible lunar observations. It views the Earth surface, SV and onboard calibrators via a two sided scan mirror, whose reflectance depends on the angles of the incidence (AOI) as well as the wavelength of the incident light. Response versus Scan angle (RVS) is technically described as a dependence function of the scan mirror's reflectance over AOI frames. An initial RSB RVS was measured prelaunch for both Terra and Aqua MODIS. Their RVS on-orbit variations over time are monitored with calibration results of the SD, lunar and SRCA. Any on-orbit RVS is a variable function versus AOI frames. Algorithms have been developed to track the on-orbit RVS using the SD, Moon, and SRCA observations as well as the Earth View (EV) response mirror side (MS) ratios. The time-dependent RVS look-up tables (LUT) are derived for RSB calibrations in the MODIS Level 1B (L1B) algorithm. In this paper, an alternative approach has been proposed to monitor the onorbit RVS without using SD/SDSM data and any MS ratios. Essentially, one stable desert site of MODIS L1A data is chosen for this alternative study, in which an entire month granules on this desert site have been collected in month July each year. Detector monthly-averaged responses for each selected AOI for each band and MS are first fitted to a smooth fitting function over AOI frames in each year. Then, for different AOI frames interested, EV gain trending profiles can be generated by sampling the smooth functions and fitting these samples over time. A lunar gain profile is generated from lunar observations, and the same in the traditional RVS calculations. At any time interested, the sampled values from the EV and lunar trending profiles are fitted to a quadratic function with a constraint of the lunar sample. Using this calculation procedure and appropriate normalizations, MODIS on-orbit RVS can be efficiently derived from the EV and lunar view responses. Comparisons are conducted with Collection 6 (C6) RVS for both Aqua and Terra MODIS. For most RSB, the difference is less than 2%. However, for shorter wavelength bands especially in Terra MODIS, the difference is much larger than 5% in recent years.

8176-40, Session 9

MERIS calibration: 9th year in space

S. Delwart, European Space Agency Ctr. for Earth Observation (Italy); L. Bourg, ACRI-ST (France)

The calibration results from the MEdium Resolution Imaging Spectrometer (MERIS) over nine years of operation of will be presented. These will include radiometric and spectral calibration results using the on-board diffusers as well as results different vicarious methods.



8176-41, Session 9

Radiometric and geometric Scarab-Megha-Tropiques ground calibration

A. Rosak, T. L. Trémas, N. Karouche, L. Gillot, O. Simonella, Ctr. National d'Études Spatiales (France)

The Scarab-3 instrument, part of the Indian-French Megha-Tropiques mission, scheduled to be launched in 2011, is a radiometer dedicated to earth radiation budget. CNES is prime of the development of this instrument. Last year, CNES conducted the final integration of the instrument and the radiometric/geometric calibrations. The spectral calibration of the channels was performed by the LMD (Laboratoire de Meteorologie Dynamique).

Two main spectral bands are measured by this instrument: A shortwave (SW) channel (channel 2, $0.2-4\mu$ m) dedicated to solar fluxes and a Total (T) channel (channel 3, $0.2-200\mu$ m) for (total) fluxes combining the infra-red earth radiance and the albedo. The earth LW radiance is isolated by subtracting the SW channel to the Total channel. Thus is defined a 3rd (virtual) long wave (LW) channel.

To obtain a good radiometric accuracy in SW domain, a calibration campaign was conducted in collaboration with ONERA, in a dry enclosure, using a 1meter diameter integrating sphere.

Concerning the LW domain, a special attention has been paid on three main points in order to get a good radiometric accuracy: 1-LW calibration that was done in a vacuum chamber, with two reference blackbodies. 2- The ratio of the SW sensibility between channels 2&3, in order to subtract channel 2 to channel 3. That was measured during the SW calibration, in front of the integrating sphere. 3- Co-localization of these two channels, in order to insure that they aim exactly at the same area. This was measured in a dry enclosure, in front of a collimator, both in static and dynamic way.

After a brief sum up of the instrument, including improvements added since Scarab-2-Resurs, the results of the calibration and the coherence between data will be presented.

8176-42, Session 9

65

Radiometric traceability and providing continuity of the earth radiation budget climate data record, CERES FM-5 on the NPP observatory

K. J. Priestley, NASA Langley Research Ctr. (United States); S. Thomas, G. L. Smith, Science Systems and Applications, Inc. (United States)

In order to understand our climate, it is necessary to understand the energy flows which govern the movements and the temperatures of the atmosphere and oceans. The solar radiation absorbed by the Earth and its emission as outgoing longwave radiation (OLR) are the heat source and heat sink for this heat engine. The Clouds and Earth Radiant Energy System (CERES) Flight Model FM-1 and FM-2 sensors aboard the Terra (Barkstrom et al., 2000) and the FM-3 and -4 sensors aboard the Aqua spacecraft have provided the first CERES observed decadal Earth Radiation Climate Data Record (CDR). To assure continuity of this CDR the CERES FM-5 sensor will fly on the NPP spacecraft, scheduled for launch in October 2011.

In late 2006, the FM-5 sensor was removed form storage and completed abbreviated radiometric characterization tests to verify stability of performance. In 2008, the FM-5 sensor was assigned to the NPP mission, removed form storage and the mechanical, thermal and electrical interfaces modified for integration on the NPP mission, and again subjected to the full pre-launch radiometric characterization campaign. The FM-5 was integrated to the NPP spacecraft in 2008 and has since undergone environmental and performance testing at the spacecraft level.

NPP will be placed in an orbit with the same inclination but higher altitude as the Aqua spacecraft. The Early Orbit Validation & Calibration campaign will commence once NPP reaches the operational orbit. These tests will consist of exercising all operational modes of the sensor, characterizing scan angle dependent offsets, observing the onboard calibration sources to establish traceability to the pre-launch radiometric scale, as well as initiate the intercalibration opportunities with other CERES sensors which are operating on NASA's Terra and Aqua missions.

8176-43, Session 9

Improved traceability of the on-orbit CERES reflected solar measurements through enhanced ground calibration

K. J. Priestley, A. M. Bullock, NASA Langley Research Ctr. (United States); S. Thomas, Science Systems and Applications, Inc. (United States); H. C. Bitting, Northrup Grumman Aerospace Systems (United States)

The Clouds and the Earth's Radiant Energy System (CERES) Flight Model-6 (FM-6) instrument will fly on the Joint Polar Satellite System (JPSS) -1 spacecraft, which has a launch-readiness date of January, 2015. This mission will continue the critical Earth Radiation Budget Climate Data Record (CDR) begun by the Earth Radiation Budget Experiment (ERBE) instruments in the mid 1980's and continued by the CERES instruments currently flying or scheduled to fly on the EOS Terra, EOS Aqua, and NNPP spacecraft. Rigorous pre-launch ground calibration is performed on each CERES flight unit to achieve a 1-sigma absolute accuracy goal of 1% for reflected solar, and 0.5% for emitted thermal radiance observations. Any ground to flight or in-flight changes in radiometer response are monitored using a protocol employing both onboard and vicarious calibration sources and experiments. The largest single source of systematic error in the CERES Reflected Solar radiance observations is due to uncertainty in knowledge of the calibration of the Transfer Active Cavity Radiometer (TACR) used during the pre-launch, ground calibration experiment. To reduce this uncertainty, CERES is undertaking an effort to quantify the complete spectral response of the TACR's optics to NIST traceable standards from UV to IR. Further, to improve traceability of the on-orbit measurements of scenes with content in shorter-wavelength spectrum. additional short-wavelength sources will be used in the calibration. This manuscript quantifies the expected reduction in uncertainties gained for CERES Global All-sky reflected solar observations as well as for clear-ocean and overcast scene types following these enhancements.

8176-44, Session 10

Orthogonal transfer CCD for compensation of image distortion

R. L. Kendrick, Lockheed Martin Space Systems Co. (United States); S. T. Thurman, Lockheed Martin Coherent Technologies (United States)

Many line-scan remote sensing sensors utilize multiple stages of Time Delay and Integration (TDI) to enhance the final image Signal-to-Noise Ratio (SNR). The swath width of these systems can be limited by optical distortion, which causes nonlinear image scanning and results in image smear at the edge of the field-of-view. Newly developed orthogonal transfer CCD arrays, with the ability to shift pixel charges in any direction, can be used to compensate for optical distortion. In this paper we will present a wide field of view sensor based on this approach. Also, an orthogonal transfer CCD can be used to compensate for image smear caused by scene scan misregistration to the detector array, enabling system-attitude requirements to be relaxed or higher SNRs to be obtained with additional TDI stages.



8176-45, Session 10

Recent developments of multi-spectral filter assemblies for CCD, CMOS and bolometer

R. Le Goff, F. Tanguy, P. Fuss, B. Badoil, SODERN (France); P. Etcheto, Ctr. National d'Études Spatiales (France)

Multispectral channels are employed on many pushbroom optical sensors. A possible technology well suited for focal plane miniaturization is to assemble several sliced filter elements (so-called stripes), each corresponding to one spectral channel, and located close to the detectors.

The assembled filter is thus customized to fit detector size. These stripes are cut from a wafer using a two dimensional accurate process. For the baseline concept, elementary stripes are then cemented edgeto-edge to form a single substrate. The opaque epoxy used for the stripes assembly creates a light barrier between adjacent elements and thus provides an interesting solution for cross channel image suppression inside the filter.

This paper recalls the current SODERN's multispectral filter assemblies status. Since 2007 R&T activity, the feasibility and the performances have been demonstrated by breadboards and qualification models. The selection of SODERN for two current VNIR space programs consolidates its role as a leading supplier in this field. A complementary 2011 R&T study will demonstrate the performances of this technology for the TIR range and the integration on a bolometer.

8176-46, Session 10

66

Performances and reliability tests of AlGaN based focal plane array for deep-UV imaging

J. Reverchon, G. Lehoucq, Thales Research & Technology (France); J. Truffer, E. M. Costard, Alcatel-Thales III-V Lab. (France); E. Frayssinet, F. Semond, J. Duboz, Ctr. de Recherche sur l'Hétéro-Epitaxie et ses Applications (France); A. Giuliani, M. Refregiers, M. Idir, Synchrotron SOLEIL (France)

Some 2D imagers based on AlGaN materials have been developed in the framework of a CNES founded research program to sustain visible blind imagers devoted to solar physics. We have already presented several prototypes of focal plane arrays extending the range of detection from near UV to deep UV. It consists in an array of 320x256 pixels of Schottky photodiodes with a pitch of 30µm. AlGaN is grown on a silicon substrate instead of sapphire substrate only transparent down to 200nm. The use of honeycomb structure has straightened the membrane after hybridization, maintain membrane integrity but decrease the filling factor.

After a preliminary study to optimize substrate and AlGaN window layer elimination, 12 focal plane arrays have been fabricated in order to achieve aging and reliability tests based on thermal cycling. Technological analyses such as cross-section, profilometry, microscopy and electrical measurements are presented without presenting any aging effect.

We present here the final results with a complete evaluation of quantum efficiency on all the spectral range of interest. A large intrinsic absorption in AlGaN takes place in the 100nm range where the quantum efficiency decreases down to 1%. Several growth parameters were identified as a key component to avoid cracks in the epitaxial structure and surface electrical traps affecting the quantum efficiency.

Finally we will discuss new structure developed in the fast development of GaN family components that could avoid the use of honey comb inducing a strong selectivity in order to achieve a clean surface after substrate removal.

8176-47, Session 10

15 µm pixel-pitch VGA InGaAs module for very low background applications

A. Rouvie, O. Huet, J. Reverchon, J. Robo, J. Truffer, J. Decobert, E. M. Costard, P. Bois, Alcatel-Thales III-V Lab. (France)

Thanks to the low absorption coefficient of short infrared wavelengths and specific contrasts, SWIR imaging is an attractive technology for space applications such as astronomical or earth observation. To meet the needs of this applications field, detection module must demonstrate high uniformity, sensitivity and resolution combined with compactness.

Image sensors based on InGaAs photodiodes arrays present very low dark currents even at ambient temperature as high quality materials can be grown on InP substrate. Besides, the suppression of InP substrate after hybridization is a way to extend the detection range towards visible wavelengths. These properties result in the generation of sensitive, compact and multifunctional InGaAs detection modules.

In this paper, we describe the performances of an InGaAs module developed in the field of a French MoD program. The 640x512 array with a pitch of 15µm allows high resolution images. The excellent crystalline quality induces dark current densities as low as 10nA/cm2 at ambient temperature. The readout circuit is based on a capacitive trans-impedance readout circuit with correlated double sampling resulting in low readout noise figure in the range of 30 electrons. This compact module appears as a serious alternative to the existing technologies for low light level imaging in the [0.4µm-1.7µm] spectral range.

8176-48, Session 10

Performance and reliability of the 3000-pixel Proba-V SWIR sensor

J. L. Bentell, P. Verbeke, P. Deruytere, K. Vanhollebeke, T. Bocquet, J. P. Vermeiren, K. Van Der Zanden, P. J. Merken, B. Grietens, Xenics NV (Belgium)

We report on the results of the qualification tests of the InGaAs-based 3000 pixel long image sensor designed for the Proba-V mission. In particular, we present results from the reliability tests, including performance degradation after irradiation of the device with heavy ions, high and low energy protons and Co60 gamma rays. The dark current and responsivity degradation rate due to irradiation have been analyzed and found to be negligible for 10 krad of Co60 irradiation and mission acceptable for 1010cm-2 of 30 MeV protons, where the dark current increases approximately 10-fold and no bi- or tri-stable pixels were found after irradiation. Latch-up threshold and saturation cross sections of the custom xro3508 read-out integrated circuit developed for the project were analyzed by irradiation with both 190 MeV protons and heavy ions. No latchups were detected for proton irradiation, but a ~12 MeV LET latch-up threshold was found with a saturation cross section just under 1e-3 events cm2/device during the heavy ion irradiation.

8176-49, Session 11

Recent developments of CMOS image sensors for Earth observation applications

O. Saint-Pé, M. Bréart de Boisanger, F. Larnaudie, S. Guiry, E. Berdin, M. Tulet, EADS Astrium (France); P. Magnan, Institut Supérieur de l'Aéronautique et de l'Espace (France)

This paper will present new performances results obtained for detectors developed by EADS Astrium and ISAE/CIMI for on-going and future Earth Observation programs. After a short introduction recalling why CMOS Image Sensors (CIS) can be of strong interest for space optical instruments, the authors will describe the architectures and operations of devices currently in development for Earth Observation programs, with an emphasis on their advantages with respect to scientific CCDs. Corresponding results of electro-optics characterisation will then be discussed, including the description of some dedicated test facilities. Finally, the CIS perspectives for space applications for medium and long-term targets will be addressed

8176-50, Session 11

Hybrid backside illuminated CMOS image sensors possessing low cross-talk

P. Ramachandra Rao, K. De Munck, K. Minoglou, J. De Vos, D. Sabuncuoglu, P. De Moor, IMEC (Belgium)

Backside illuminated (BSI) hybrid CMOS image sensors possessing excellent spectral response(> 80% between 400nm-800nm) have been previously reported by us. Particularly challenging with BSI imagers is to combine such sensitivity, with low electrical inter-pixel cross-talk (or charge-dispersion). Employing thick bulk silicon (in BSI) to maximize red response results in large cross-talk especially for blue light.

In the first generation BSI devices, we used a non-optimal "stepped" epitaxial profile to increase the internal electric field. However, this electric field was too low to have a significant impact on cross-talk. Nevertheless, in parallel, the use of high aspect ratio (1:50) trenches to physically separate the pixels was explored. This resulted in a dramatic reduction of cross-talk (below the detection limit of the measurement method), but also in an overall attenuated response most pronounced in the shorter wavelength regions. We hypothesize that this was due to carrier recombination at the trench side-walls.

In the second generation of these imagers, we undertook the exercise of solving the cross-talk problem by a two-pronged approach: a) an optimized epitaxial substrate that was engineered to maximize the internal electric field b) high aspect ratio trenches (30 μ m deep) with carefully tailored sidewall passivation.

On these optimized starting materials, 1 Mpixel, 22.5 µm pitch hybrid diodes were processed at imec and hybridized on a dedicated CMOS readout. Cross-talk was characterized by single pixel illumination (using a laser spot) as well as slanted metal-shield edge technique. The results show that the proposed optimizations are effective in curtailing cross-talk without having a major impact on other sensor parameters. These results will be presented in detail in the full-paper.

8176-51, Session 11

67

Current status of the EarthCARE BBR detectors development

M. Allard, L. Martin, C. Proulx, J. Bouchard, E. Oulachgar, INO (Canada); J. Delderfield, D. Parker, Rutherford Appleton Lab. (United Kingdom); F. Châteauneuf, INO (Canada)

The Broadband Radiometer (BBR) is an instrument being developed for the ESA EarthCARE satellite. The BBR instrument objective is to provide measurements of the reflected short-wave (0.25-4.0 µm) and emitted long-wave (4.0-50 µm) top of the atmosphere (TOA) radiance over three along-track views (forward, nadir and backward). The instrument has three fixed telescopes, one for each view, each containing a broadband detector. The BBR instrument is led by SEA in the UK with RAL responsible for the BBR optics unit (OU) while EADS Astrium is the EarthCARE prime contractor. The BBR detectors consist of three dedicated assemblies under the responsibility of INO. The detectors development started in 2008 and led to the design and implementation of a new gold black deposition facility at INO, in parallel with the preliminary and detailed design phases of the detector assemblies. As of today, two breadboard models and one engineering model have been delivered to RAL. The Engineering Qualification Model manufacturing activities are on-going. This paper first provides a description of the detector design along with its principles of operation. The current status of the development is presented along with key performance parameters measured on the latest units.



8176-52, Session 11

SOFRADIR in space: an overview on the activity and on the main programs

P. Pidancier, P. Chorier, SOFRADIR (France)

Space activity at SOFRADIR has been build for years, growing and strengthening, by relying on 25 years of experience in development and production of 2nd and 3rd generation MCT infrared detectors, and through major space programs. Thanks to its capabilities and experience, Sofradir is now able to offer high reliability infrared detectors for space applications. These detectors cover various kinds of applications like hyperspectral observation, earth observations for meteorological or scientific purpose and science experiments. In this paper, a presentation of SOFRADIR main space programs and space products answering customer needs from visible up to VLWIR waveband will be made.

8176-53, Session 11

Sofradir hyperspectral detectors for space applications : latest results

Y. Nowicki-Bringuier, P. Pidancier, P. Chorier, SOFRADIR (France)

For many years, Sofradir continuously improves its offer regarding hyperspectral detectors. Thanks to its constantly enlarged offer, Sofradir is now able to cover a large range of needs for various kinds of applications.

In particular, in addition to the already available configurations for the Saturn (1000x256-30µm pitch) and Neptune detectors (500x256-30µm pitch), including cryo-coolers, Sofradir has recently developed a space qualified passive cooling version of the Saturn product. Complete validation and qualification of this product versus most of environmental constraints linked to space missions has been recently achieved, for both VISIR (0.4µm-2.5µm detection band) and SWIR (0.9µm-2.5µm detection band) configurations. This paper will present the latest qualification results obtained on this configuration as well as the strong heritage from which this kind of Focal Plane Array already benefits, which makes it a first choice product for Hyperspectral SWIR and VISIR demanding missions.

8176-54, Session 11

Ultra low dark current CdHgTe FPAs in the SWIR range at CEA and Sofradir

O. Gravrand, L. R. Mollard, O. Boulade, V. Moreau, Commissariat à l'Énergie Atomique (France); E. Sanson, SOFRADIR (France); G. L. Destéfanis, Commissariat à l'Énergie Atomique (France)

We report here first results carried out at CEA and Sofradir to build ultra low dark current focal plane arrays (FPA) in the short wave range (SWIR) for space applications. Those FPAs are dedicated to very low flux detection in the 2µm wavelength range. In this purpose, Sofradir has designed a source follower per detector readout circuit (ROIC), 384x288, 15µm pitch. This ROIC has been hybridized on different HgCdTe diode configurations processed at CEA-LETI and low flux characterisations have been carried out at CEA-SAP at low temperature (from 60 to 160K). Both p/n and n/p structures have been evaluated. The metallurgical nature of the absorbing layer is also examined and both molecular beam epitaxy and liquid phase epitaxy have been processed. Dark current measurements are discussed in comparison with previous results from the literature. State of the art dark currents are recorded for temperatures higher than 120K. At temperatures lower than 100K, the decrease in dark current saturates for both technologies. In this regime, currents as low as 0.3e/s/pixel are reported.

8176-55, Session 11

Infrared ROIC for very low flux and very low noise applications

B. Fièque, L. Martineau, E. Sanson, P. Chorier, SOFRADIR (France)

Sofradir is involved in the manufacturing of detectors which cover a large range of wavelengths in the infrared domain from SWIR up to VLWIR for different kind of applications. Thus, different types of ROIC architectures are needed to cover these various kind of applications and operating conditions.

As a major player of the infrared market, Sofradir has developed numerous ROIC with architectures enabling to answer most of the infrared applications in tactical, commercial and space domains.. Sofradir is now able to present a new detector (384x288 with a 15 µm pitch) especially designed for very low flux applications in the SWIR domain (as astronomy for example). This new ROIC has been developed and includes a SFD (Source Follower per Detectors) input stage enabling to achieve a high gain as well as a low readout noise and a vey low power consumption.

In this paper, we will describe the architecture and functionalities of this new detector. The expected performances will be presented as well. Then, electro-optical characterizations and results will be described. Finally, main applications of this kind of detectors will be presented.

8176-12, Poster Session

A new space instrumental concept for the measurements of CO2 concentration in the atmosphere

C. Buil, V. Pascal, J. Loesel, C. Pierangelo, L. Roucayrol, L. Tauziede, Ctr. National d'Études Spatiales (France)

Measuring the concentration of greenhouse gases from space is a current challenge. This measurement is achieved via a precise analysis of the signature of chemical gaseous species (CO2, CH4, CO, etc.) in the spectrum of the Earth's atmosphere. Two families of spectrometers are commonly used. The first family is based on the phenomena of interference between two radiation waves. The Infrared Atmospheric Sounding Interferometer (IASI), onboard the METOP satellite, is a good example of a fully-operational instrument of this kind. The second family is based on the use of dispersive optical components. These instruments must have high radiometric and spectral resolutions, in narrow spectral bands, in order to discriminate absorption lines from various atmospheric chemical species and to quantify their concentration. It is the case, for example, of the instrument onboard the OCO satellite.

Our analysis led us to define a new instrumental concept, based on a dispersive grating spectrometer, with the same quality level of performances but more compact and therefore less expensive.

After a description of such a spatial instrument, which uses a specific grating component, a preliminary assessment of performances will be presented, including the theoretical calculations and formula. A breadboard implementation of this specific grating allowed us to show the practicality of this concept and its capabilities. This preliminary design is encouraging and shows that such a spectrometer may be compatible with a micro-satellite platform. Some prospects of improvements are also considered.

8176-70, Poster Session

68

A geometric algorithm for space optical imaging system based on topological mapping relationship

Z. Zhang, Z. Feng, W. L. Min, Beijing Institute of Space Mechanics and Electricity (China)

Space optical imaging system is affected by vibration of satellite platform on orbit. The purpose of this paper is improving image quality,



through simulating space optical imaging system by topological mapping. First, the source of motion error is introduced. Errors induce to jitter directly in the line of sight. Second, this paper considers methodological and applied problems of choosing parameters and analyzing a topological mapping relationship between object and image plane coordinate. The topological mapping relationship could be expressed that some matrixes are multiplied. The transformation relationship is between the earth WG84 coordinate and camera's image plane coordinate. The transformation matrix contains elements of interior orientation and exterior orientation. The geometric distortion of pixel position is calculated on image plane. And we calculate the pixel point on the image plane from corresponding point on object plane. Through these points being interpolated on the image plane, we got a geometric distortion of frame image. The measurement accuracy of geometric distortion is sub-pixel scale. Third, multi-mode vibrations are demonstrated directly in the line of sight, such as high frequent jitter and low frequent vibration. Parameters are variables, including angular velocity, angular acceleration, frequency, amplitude and so on. Four, according to physical character of optical imaging system, imaging procedure of space TDI camera is simulated. The simulation experiment of space TDI camera imaging is based on three-axial orientation. Different images are simulated by changing number of TDI. For example, changing the attitude angle and pointing errors, motion frequency and angular acceleration, even the altitude, we got the geometric distorted image.

Finally, the simulated image is generated. The problem of error boundary condition is discussed, as well as simulation of space TDI camera imaging. Image quality will be obviously degraded, if pointing accuracy's error exceeds this boundary. The result is benefit to analyzing parameters of satellite platform and guiding design of remote sensor.

8176-75, Poster Session

Short term operation planning for Japanese future hyperspectral and multispectral senor: HISUI

K. Ogawa, Rakuno Gakuen Univ. (Japan); T. Matsunaga, S. Yamamoto, National Institute for Environmental Studies (Japan); O. Kashimura, T. Tachikawa, Earth Remote Sensing Data Analysis Ctr. (Japan); A. Iwasaki, The Univ. of Tokyo (Japan); S. Tsuchida, National Institute of Advanced Industrial Science and Technology (Japan); N. Ohgi, Japan Resources Observation System and Space Utilization Organization (Japan)

Hyperspectral Imager Suite (HISUI), Japanese future spaceborne hyperspectral mission, is planed to be launched in 2015 or later as one of instruments onboard JAXA's Advanced Land Observation Satellite 3 (ALOS-3). HISUI consist of a hyperspectral and a multispectral imager with 30 m and 5 m spatial resolution and 30 km and 90 km in swath, respectively. HISUI is expected to use in various application including oil/mineral resource exploitations, agricultural monitoring, environmental studies. However the instrument duty time limitation and the allocation of down-link resources of ALOS-3 will constrain observation planning. Various planing methodologies including use of weather forecasts for HISUI short-term operations to make efficient planing will be discussed.

8176-76, Poster Session

A study of calibration KOMPSAT-2 image by relative radiometric calibration

C. G. Jin, H. Y. Ahn, C. U. Choi, Pukyong National Univ. (Korea, Republic of); S. G. Lee, Korea Aerospace Research Institute (Korea, Republic of)

The purpose of this paper is to ensure the reliability of the standard images from KOMPSAT-2 and the various kinds of thematic information additionally generated by the images by means of empirical relative radiometric correction. For this purpose, it examines the similarity between wave-length bands of KOMPSAT-2 and Landsat-7 ETM+, gathers their images which are taken within 5 days earlier to perform

the ortho-rectification and the radiometric correction. And it performs the empirical relative radio correction in which a linear correlation is derived from radiance and then it is applied to the images from KOMPSAT-2. As a result, the wave-length similarity of the blue band is low: 0.52; that in other bands shows high rate of concordance: 0.82 or higher. And the RGB images expressed in radiance show little change between before and after correction. According to the calculation of the index of vegetation by using reflectivity, the correlation of the NDVI images in January 2008 increases from 0.004 before correction to 0.8964 after correction; that in November 2008 increases from 0.1717 before correction to 0.7964 after correction; the correlation of the SR in January 2008 images increases from 0.0357 before correction to 0.8876 after correction; that in November 2008 increases from 0.0003 to 0.8083. Thus, it is judged that using the images from Landsat-7 ETM+ for the relative radiometric correction of the images from KOMPSAT-2 can contribute to ensuring their reliability.

8176-77, Poster Session

Optical shutter for gating and defense of an optical sensors

P. A. Molchanov, Ampac Inc. (United States); V. M. Contarino, R Cubed, Inc. (United States); O. Asmolova, Ampac Inc. (United States)

Optical shutter is provides gating and protection for the high-sensitiv optical sensors from overexposures which can cause permanent damage or short term sensors sensitivity changes. The nanosecond optical shutter with aperture 2 square inches demonstrated of 86% transmission and 30 dB switching contrast in visible light range. Application of low molecular weight polymer dispersed liquid crystal (PDLC) material with combination of high-voltage (200-500V) pulses allows to decrease switching time up to 20-100 nsec. Applied pulse electric field was 10 V/µm. For applied PDLC the delay time approaches a constant value at higher electric fields, >10 V µm-1. Transition and delay times decrease with increasing temperature. The proposed optical shutter technique can replace for electrical gating, such as dynode gating within high sensitive PMTs, currently incorporated into LIDAR and gated satellites remote imaging systems. Optical shutter can eliminate signal distortion caused by mixing of gate and signal pulses in current LIDAR remote one-pixel or imaging systems. Proposed optical shutter universal and could be integrated into any standard one-pixel or imaging telescope design for all visible range.

8176-78, Poster Session

69

Earth observation mission operation of COMS during in-orbit test

Y. Cho, Korea Aerospace Research Institute (Korea, Republic of)

Communication Ocean Meteorological Satellite (COMS) for the hybrid mission of meteorological observation, ocean monitoring, and telecommunication service was launched onto Geostationary Earth Orbit on June 27, 2010 and it is currently under normal operation service after the In-Orbit Test (IOT) phase. The COMS is located on 128.2° East of the geostationary orbit. In order to perform the three missions, the COMS has 3 separate payloads, the meteorological imager (MI), the Geostationary Ocean Color Imager (GOCI), and the Kaband antenna. Each payload is dedicated to one of the three missions, respectively. The MI and GOCI perform the Earth observation mission of meteorological observation and ocean monitoring, respectively. During the IOT phase the functionality and the performance of many aspects of the COMS satellite and ground station have been checked through the Earth observation mission operation for the observation of the meteorological phenomenon over several areas of the Earth and the monitoring of marine environments around the Korean peninsula. The Earth observation mission operation of COMS during the IOT phase is introduced in terms of mission planning and mission operation characteristics for the missions of meteorological observation and ocean monitoring

The COMS Mission Planning Subsystem (MPS) is a part of the satellite operation system of COMS ground station. The MPS synthesizes



the user mission requests for 'meteorological observation and ocean monitoring' and the satellite orbit and attitude control mission, resolves conflicts between missions, and establish daily mission plan of the Earth observation and the satellite control. The function of the MPS, the mission scenarios characteristics of 'meteorological observation and ocean monitoring', daily mission planning during the IOT are described in the point of overview. Also, the mission operation capability of COMS is dealt with through statistical approach for the satellite image reception status which is the result of the mission operation of COMS during IOT.

8176-79, Poster Session

The concept of a multibeams delay/Doppler radar altimeter

S. Yang, H. Liu, Ctr. for Space Science and Applied Research (China)

Radar altimeter can map the global geoid with high precision, and measure ocean circulation. This paper presents a new concept of mutibeams delay/Doppler radar altimeter (MBDDA) which combines a liner array of nadir receivers and a nadir transmitter. The unfocused SAR and delay/Doppler technology are applied in the along track, and the array signal processing technology are applied in the cross track. After the unfocused SAR and delay/Doppler processing, there will be many fan-beams in along track. The nadir-pointing linear-array receivers along the cross track are used to form multi-fan-beams in the cross track direction by FFT and digital beam forming algorithm. The raw signal received by all receivers will first be processed in along track and the output results will be referred by across track processing. Then there will be many fan-beams in along track and some fan-beams in across track, which results in many footprints in the transmitter antenna illuminated area. Thus the area illuminated by the MBDDA could be divided into many small grids in along-track and cross-track. Thus it could support wide swath ocean measurement and both orthogonal components of the ocean surface slope. It has three main advantages, first of all: it is uses much more of the altimeter's radiated energy than does conventional radar altimeter and the delay/ Doppler radar altimeter, secondly it is relative generous requirement on attitude, third it has uniform cross section in one footprint. Therefore, it could work at a precision as high as that of a conventional radar altimeter, but with wider swath. The key innovation in this concept is that fan-beams form in both along track and across track, and range correction is applied in across track as in along track, and the cross track further processing refers the along track processing results. So that it could provide high precision within wide swath and it could provide height profile with high precision for left scene and right scene, respectively, and leave small footprints at far range as at near range. But the 3D-matrix store and processing of the raw data from receivers are much more complicated than a conventional radar altimeter and a delay/Doppler radar altimeter.

8176-80, Poster Session

Miniaturized spectral imager for Aalto-1 nanosatellite

R. M. Mannila, VTT Technical Research Ctr. of Finland (Finland); A. Näsilä, J. Praks, Aalto Univ. School of Science and Technology (Finland); H. K. Saari, J. E. Antila, VTT Technical Research Ctr. of Finland (Finland)

Aalto-1 is a 3U-cubesat project coordinated by Aalto University. The satellite, Aalto-1, will be mainly built by students as project assignments and thesis works. VTT Technical Research Centre of Finland will develop the main Earth observation payload, a miniaturized spectral imager, for the satellite. It is a novel highly miniaturized adjustable spectral imager. Mass of the spectral imager will be under 400 grams, and dimensions will be around 80 mm x 80 mm x 45 mm. The spectral imager is based on a tunable Fabry-Pérot interferometer (FPI) accompanied by a 5 Mpixel RGB CMOS image sensor. The FPI consists of two highly reflective surfaces separated by a tunable air gap and it is based either on a microelectromechanical (MEMS) or piezo-actuated structure. The MEMS FPI is a monolithic device, i.e. it is made entirely on one substrate in a batch process, without assembling

separate pieces together. The gap is adjusted by moving the upper mirror with electrostatic force, so there are no actual moving parts. Benefit of the MEMS FPI is a low mass. However, large aperture (4 mm) MEMS FPIs are currently under development, thus it is not known if their performance is adequate. The piezo-actuated FPI uses three piezo-actuators and is controlled in a closed capacitive feedback loop. The draw back of the piezo-actuated FPI is higher mass. However it has large aperture (in order of 10 mm), which enables shorter exposure time. Selection of the FPI type will be done after thorough evaluation. Depending on a selected FPI type, the spectral resolution of the imager is 5 - 12 nm (FWHM). The spectral range of the spectral imager is 500 - 800 nm.

8176-81, Poster Session

Image-based adaptive optics system with deformable mirror in small satellite remote sensing

N. Miyamura, The Univ. of Tokyo (Japan)

In small satellites remote sensing, high spatial resolution has to be achieved by a lightweight sensor. To realize these contrary requirements, adaptive optics system (AOS) is used. In remote sensing, it is difficult to use a reference point source unless the satellite controls its attitude toward a star, so image-based wavefront estimation method, phase diversity, is used. We propose to estimate wavefront aberration and calibration parameters of deformable mirror (DM) simultaneously.

In our AOS, a deformable mirror applies the phase diversity, and then corrects the wavefront aberrations. In a phase diversity wavefront sensing, the change in the wavefront caused by the DM is used as a priori information in solving the inverse problem. On the other hand, the influence function between the input voltage of the DM's actuator and the modulated wavefront depends on the composition and the alignment of the optics. The accurate calibration, therefore, is required. In conventional calibration method, a single actuator is displaced to measure the influence function. In our work, first the influence functions are formulated with unknown parameters. The unknown parameters in wavefront aberrations and influence functions are then estimated by using the input voltage as a priori information. Furthermore, the optimal input profile of the DM for phase diversity is investigated instead of displacing a single actuator for each measurement.

We constructed the AOS for laboratory test, and proved that the modulated wavefront by DM almost consists with the ideal one using a Shack-Hartmann wavefront sensor as a reference.

8176-82, Poster Session

70

A comparative study of relationship to solar radiation and extraction of vegetation: using Kompsat-2 and IKONOS image

H. Ahn, S. y. Park, C. U. Choi, Pukyong National Univ. (Korea, Republic of)

A satellite image, which periodically records the spectroscopic characteristics of objects, is used to calculate the vegetation index. However, it can have different results according to sensor calibration, the state of atmosphere, geometric relations between the sun, sensor and object, and a diversity of other factors. So although it is a image of the same area, if it was taken at a different time, it is difficult to expect the same value of DN(Digital Number). This paper converses DN values of KOMPSAT-2 and IKONOS, satellites with high resolution, into Reflectence value and then calculates NDVI and TCT-GVI. It uses the calculated vegetation index and classifies between vegetation areas and non-vegetation areas to conduct a comparative analysis of the rate of concordance. And it calculates the solar radiation to conduct a comparison of relations with the areas where vegetation is wrongly classified. The analysis reveals that the rate of concordance in the areas of vegetation is high: NDVI 85%, GVI 85.35%. It shows a similar rate of concordance in NDVI and GVI. And the solar radiation in all areas are : KOMPSAT-2 207.5w/m² and IKONOS 668.4w/m²; those in the wrongly classified areas are: KOMPSAT-2 128.2w/m² and



IKONOS 553.7w/m². The reason that the wrongly classified areas have less solar radiation is that they have a shadow area influenced by its topography, it is judged. In particular, in the winter, when the solar radiation are comparatively less, KOMPSAT-2 has difficulty extracting vegetation, not more than, which means, it is judged, that it is impossible to normally detect the Red band and the NIR band which are used for calculating vegetation index from a satellite image.

8176-56, Session 12

The atmospheric processes on climate and its changes (APOCC) initiative

M. Bergeron, Canadian Space Agency (Canada)

The Atmospheric Processes on Climate and its Changes (APOCC) Initiative

Following recommendations from the Canadian atmospheric science community as articulated by the CSA Space and Atmospheric Environment Advisory sub-committee and expressed in the document resulting from the Community Workshops in May and September 2005 entitled "A Vision of Atmospheric Sciences from the Next 10 years (2005-2010)", the Canadian Space Agency (CSA) issued, in 2007, a Request for Proposals (RFP) on The Atmospheric Processes on Climate and its Changes (APOCC). Innovative mission concepts were selected on the basis that they: Lead to new scientific understanding of atmospheric processes that regulate Earth's climate and thereby lead to reduced uncertainty in climate forecasts; Address questions of particular importance for northern latitudes or that otherwise benefit Canadians; Build on Canada's considerable experience and capacity in atmospheric science; Complement and are synergistic with planned international satellite missions.

The competitive process resulted in six concept studies namely: Mission for Climate and Atmospheric Pollution (MCAP), Miniature Earth Observing Satellite (MEOS), SnowSat, Solar Occultation for Atmospheric Research (SOAR), Stratosphere-Troposphere Exchange Processes (STEP) and Thin Ice Clouds in the Far InfraRed Experiment (TICFIRE). These micro/small satellites concepts, from numerous Canadian academic institutions and industrial teams, encompass a wide range of technologies and applications. MCAP proposes five nadir-viewing instruments (FTS, Correlation radiometer, solar reflectance spectrometer, multi-angle and an infrared imager) for atmospheric composition measurements (trace gases and aerosols) for climate process and air quality studies. MEOS proposes five miniaturized nadir-viewing instruments (one UV spectrometer; three VISNIR spectrometers; one imager) for measurement of greenhouse and other trace gases for study of terrestrial vegetation absorption and emission of tropospheric gases. SnowSat proposes a cloud/precipitation radar (dual frequency at 35 and 94 GHz) instrument to measure clouds, snowfall and light precipitation building on the CloudSat and EarthCARE experience. SOAR proposes three instruments in solar occultation (IR-FTS; UV-VISNIR spectrophotometer; imager) to provide the vertical profiles trace gases and aerosols. STEP proposes three limb-viewing instruments (limb spectrograph; spatial heterodyne system; radiometer) for the photochemistry, dynamics and radiative properties associated with the Upper Troposphere and Lower Stratosphere (UTLS). Finally, TICFIRE proposes a nadir and limb viewing instrument (radiometer and imager respectively) for the far infrared detection and measurements of radiation anomalies induced by thin ice clouds in polar regions in the upper troposphere.

Five of the six studies finished in autumn 2009, the last one ending in winter 2010. CSA is now in a position to, through dialogue with the atmospheric science community; assess the science merit, technical readiness, affordability, timing, partnerships and synergy of the mission concepts with other EO missions such as the Chemical and Aerosol Sounding Satellite (CASS) and the Stratospheric Wind Interferometer For Transport studies (SWIFT) missions. The foreseen way forward is to issue a series of support initiatives (Science or technological developments and demonstrations, detailed concept studies, risk mitigation analysis, ground infrastructure and data assimilation support) to develop those reformulated concepts that combine the best ideas in several affordable instrument contributions and Canadian spacecraft missions (\$30M, \$75M, \$120M CAN).

8176-57, Session 12

TICFIRE: a far infrared payload to monitor the evolution of thin ice clouds

J. Blanchet, Univ. du Québec à Montréal (Canada); A. Royer, Univ. de Sherbrooke (Canada); F. Châteauneuf, INO (Canada); P. Gauthier, Univ. du Québec à Montréal (Canada); N. T. O'Neill, Univ. de Sherbrooke (Canada); O. Pancrati, INO (Canada); L. Garand, Environment Canada (Canada)

The TICFIRE mission concept developed with the support of the Canadian Space Agency aims: 1) to improve measurements of watervapor concentration in the low limit, where cold regions are most sensitive and 2) to determine the contribution of Thin Ice Clouds (TIC) to the energy balance and the role of their microphysical properties on atmospheric cooling. TICFIRE is a process-oriented mission on a micro-satellite platform dedicated to observe key parameters of TIC forming in the cold regions of the Poles and globally, in the upper troposphere. It locates cloud top profiles at the limb and measures at nadir the corresponding upwelling radiance of the atmosphere directly in the thermal window and in the Far Infrared (FIR) spectrum over cold geographical regions, precisely where most of the atmospheric thermal cooling takes place. Due to technological limitations, the FIR spectrum (17 to 50 µm) is not regularly monitored by conventional sensors despite its major importance. This deficiency in key data also impacts operational weather forecasting. TICFIRE will provide on a global scale a needed contribution in calibrated radiance assimilation near the IR maximum emission to improve weather forecast. TICFIRE is therefore a science-driven mission with a strong operational component. The TICFIRE payload consists of two instruments; the main one being a Nadir-looking multiband radiometer based on uncooled microbolometer technology and covering a large spectral range from 7.9 μm to 50 $\mu m.$ The secondary one is an imager that performs Limb measurements and provides cloud vertical structure information. This paper presents the key payload requirements, the conceptual design, and the estimated performance of the TICFIRE payload. Current technology developments in support to the mission are also presented.

8176-58, Session 12

Image quality effects due to image plane sampling: experimental results

R. L. Kendrick, A. T. Cochrane, K. M. Schulz, R. M. Bell, Jr., E. H. Smith, Lockheed Martin Space Systems Co. (United States)

An imaging test bed has been constructed for exploring the design considerations for selecting the appropriate image sampling or Q for electro-optical earth imaging systems where Q is defined as (lambda * f/#) / pixel pitch. The test bed includes errors such as image smear and shot noise produced by atmospheric haze. The value of Q can be varied by either changing the focal length of the imaging system or by varying the imaging aperture diameter. All of these parameters are varied to understand the effects on image quality. In this paper we explore practical design considerations for selecting Q for an electro-optical earth imaging system. We find that for a fixed integration time the image quality is not reduced by using higher values of Q provided Q is less than 2. We also find that increasing Q by decreasing the imaging aperture diameter reduces the image quality dramatically as the scene illumination is reduced.

8176-59, Session 12

71

Architecting the future of 'operational' earth monitoring satellites based on matured climate modeling and replicating existing sensor capabilities within constellation efficiencies

D. B. Helmuth, Lockheed Martin Corp. (United States)

Understanding the earth's climate and collecting requisite signatures over the next 10, 20, 30 years is a shared mandate by many of the



world's governments. But there remains a daunting challenge to bridge scientific missions to 'operational' systems that truly support the demands of decision makers, scientific investigators and global users' requirements for trusted data. For this paper we will examine the required components of a modeling framework that together could perform an adjoined earth modeling demonstration and verification. Interrogating such a modeling capability in detail will help uncover the most efficient and sufficient set of critical climate parameters & metrics needed to systematic capture and attribute climate monitoring environmental records. This in turn would allow globally trusted algorithms to produce climate products that the world's governments can use to most accurately assess man's impacts on earth's climate and promote informed decisions sustaining the earth's ability to support life. This paper is a natural extension to two earlier papers from 2009 & 2010.

8176-60, Session 12

Development and fabrication of a hyperspectral, mirror based IR-telescope using ultra precise manufacturing and mounting techniques for a 'snap-in' system assembly

S. Risse, S. Scheiding, A. Gebhardt, C. Damm, Fraunhofer-Institut für Angewandte Optik und Feinmechanik (Germany); W. Holota, Holota Optics (Germany); R. Eberhardt, Fraunhofer-Institut für Angewandte Optik und Feinmechanik (Germany)

A growing number of multi- and hyper-spectral imaging devices such as telescopes and spectrometers are based on all reflective metal optics. The sophisticated requirements regarding the precise shape and alignment of the optical elements in the optical beam path have to be considered during design, manufacturing and metrology to reduce the efforts in the time consuming alignment of the mirrors.

The assembly and alignment of each mirror in an imaging optic has to fit a tight tolerance budget. Controlling the relative position of the optical elements with alignment steps with micrometer resolution respectively few arcseconds is mandatory for diffraction limited imaging performance. The demands on system quality rise with shorter application wavelength. The resulting expenditure is cost-intensive from economic view.

The presented paper summarizes the fabrication of an optical bench for a high resolution IR - Three Mirror Anastigmat Telescopes (TMA), whose design concept is based on ultra-precision fabrication techniques allowing an efficient and easy "Snap-In" alignment. Several optical surfaces are diamond machined in one and the same machine setup with a common coordinate system to achieve a high degree of optical quality and alignment precision. A novel hybrid manufacturing approach, which is a combination of diamond turning and diamond milling, is used to manufacture fiducials and mounting planes that reduce the adjustment expenditure significantly.

The optical function of the build TMA design demonstrator is an afocal imaging for a Limb-Sounder Instrument with a magnification of 4.5:1. Besides the design and manufacturing approach also the "snap-In" integration of the optical bench is presented. The imaging error is reduced to $\lambda/10$ @ 10 µm wavelength by a few targeting iteration steps with a manipulation of only one mirror sub-assembly in two degrees of freedom.

8176-61, Session 13

The design of a space-borne multispectral canopy lidar to estimate global carbon stock and gross primary productivity

E. Rumi, J. W. Jack, The Univ. of Edinburgh (United Kingdom); D. M. Henry, UK Astronomy Technology Ctr. (United Kingdom)

Understanding the dynamics of the global carbon cycle is one of the most challenging issues for the scientific community. The ability to measure the magnitude of terrestrial carbon sinks as well as monitoring the short and long term changes is vital for environmental decision



making. Forests form a significant part of the terrestrial bio-system and understanding the global carbon cycle, Above Ground Biomass (AGB) and Gross Primary Productivity (GPP) are critical parameters. Current estimates of AGB and GPP are not adequate to support models of the global carbon cycle and more accurate estimates would improve predictions of the future, and the likely behaviour of these sinks. Various vegetation indices have been proposed for the characterisation of forests like Normalised Difference Vegetation Index (NDVI) and Photochemical Reflectance Index (PRI), beside canopy height and canopy area. Both NDVI and PRI are obtained from a measure of reflectivity at specific wavelengths and have been estimated from passive measurements. The use of multi-spectral LiDAR to measure NDVI and PRI and their vertical distribution within the forest represents a significant improvement over current techniques. This paper describes an approach to the design of an advanced Multi-Spectral Canopy LiDAR, using four wavelengths for measuring the vertical profile of the canopy simultaneously. It is proposed that the instrument be placed on a satellite, orbiting the Earth on a Sun- synchronous polar orbit to provide samples on a rectangular grid at an approximate separation of 1km with a suitable revisit frequency. The systems engineering concept design will also be presented.

8176-62, Session 13

Realization of flight model of a stereoscopic imaging laser altimeter micropayload

S. G. Moon, S. Hannemann, M. Esposito, cosine Research B.V. (Netherlands)

The Stereoscopic Imaging Laser Altimeter (SILAT) is an integrated micropayload that has been developed by cosine Research with its partners in the Netherlands. The instrument, meant for planetary survey on small satellites under 100 kg or as a secondary payload on large satellites, is a combination of a compact High Resolution Camera (HRC) with a single photon counting Laser Altimeter (LAT) with a second camera for stereoscopic imaging capability. The LAT uses a miniaturized pulsed laser as a source and is able to detect a single returned photon reflected from the target using a Single Photon Avalanche Diode that shares the optical path and focal plane array of the HRC. The precision optics and control algorithms behind the LAT and HRC result in a surface profile with an altitude accuracy of 15 cm that is correlated for surface position with the HRC data. The stereoscopic imaging capability is provided by a second camera that is placed in SILAT's modular slot. This module is interchangeable via a mounting strategy that allows for flexibility in the role of SILAT. The integrated, miniaturized nature of the instrument results in a package that contains all three instruments but has a mass less than 8 kg and a power consumption below 13 W.

Each of the instruments in SILAT are based upon key technologies that enable the high performance of SILAT despite its small size and resource consumption. These technologies include: single point diamond turning of a Three Mirror Anastigmatic (TMA) telescope with three off-axis aspherical mirrors and corresponding alignment system; the microchip laser emitter; unique focal plane array including the Single Photon Avalanche Diode (SPAD) system; the algorithms to synchronize and analyze a single photon counting altimeter; integrated on-board electronics controlled via an FPGA; and a light, compact structure that preserves optical alignment in the presence of thermomechanical displacements.

Each of these key technologies are currently being developed, or have been completed within their own projects. The next step is to integrate these technologies onto a aircraft-compatible unit in preparation for an Earth Observation (EO) or planetary exploration mission. This paper will detail the integration effort by highlighting the methods and planning used to synergize the key technologies as well as touch upon the results of the individual development activities. The progress towards the flight campaign, anticipated for December 2011, will be detailed along with the expected performance. The focus of the performance results will be on the field performance of the laser altimeter and the integration of the instrument control algorithms. Current simulations show a high Signal to Noise Ratio (SNR) and high altimeter return rate and confidence probability. Furthermore, adjustments of the design in order to be accommodated on a small aircraft without compromising data quality will also be covered in order to give insight into the conduct of such a test campaign.

72

8176-63, Session 13

An update on the NAST-I airborne FTS

A. M. Larar, NASA Langley Research Ctr. (United States); W. L. Smith, Sr., Hampton Univ. (United States); D. K. Zhou, X. Liu, NASA Langley Research Ctr. (United States); L. Rochette, LR Tech (Canada); J. Tian, NASA Langley Research Ctr. (United States)

The NPOESS Airborne Sounder Testbed - Interferometer (NAST-I) is a well-proven airborne remote sensing system, which has flown in 18 previous field campaigns aboard the high altitude NASA ER-2, Northrop Grumman / Scaled Composites Proteus, and NASA WB-57 aircraft since initially being flight qualified in 1998. While originally developed to provide experimental observations needed to finalize specifications and test proposed designs and data processing algorithms for the Cross-track Infrared Sounder (CrIS) to fly on the National Polar-orbiting Operational Environmental Satellite System (NPOESS) Preparatory Project (NPP) and the Joint Polar Satellite System, JPSS (formerly NPOESS, prior to recent program restructuring), its unprecedented data quality and system characteristics have contributed to a variety of atmospheric research and measurement validation objectives. This presentation will provide a program overview and update, including a summary of measurement system capabilities, select scientific results, and recent refurbishment activities.

8176-64, Session 13

Space-based hyperspectral imaging spectroradiometer for coastal studies

J. J. Puschell, J. Silny, L. Cook, S. Champion, S. Schiller, D. La Komski, Raytheon Space & Airborne Systems (United States); N. Malone, Raytheon Vision Systems (United States); C. Davis, Oregon State Univ. (United States)

Resolving the complexity of coastal and estuarine waters requires high spatial resolution, hyperspectral imaging spectroradiometry. Hyperspectral measurements also provide capability for bathymetry in some coastal waters and for detailed cross calibration with other instruments in polar and geosynchronous orbit. This paper reports on recent design studies for a hyperspectral Coastal Imager (CI - pronounced "sea") that measures key data products from sun synchronous orbit. These products include water-leaving radiances in the near-ultraviolet, visible and near-infrared for separation of absorbing and scattering coastal water constituents and for calculation of chlorophyll fluorescence. In addition, CI measures spectral radiances in the near-infrared and shortwave infrared for atmospheric corrections and cloud radiances without saturation to enable more accurate removal of instrument stray light effects. CI provides contiguous spectral coverage from 380 to 1800 nm at 20 m spatial resolution at nadir across 5000+ km2 scenes with spectral sampling, radiometric sensitivity and calibration performance needed to meet the demanding requirements of coastal imaging. This paper presents a detailed design description for the CI including concepts of operation for data collection, calibration (radiometric, spectral and spatial), onboard processing and data transmission to Earth. Performance characteristics for the instrument and all major subsystems including the optics, focal plane assemblies, onboard calibration, onboard processing and thermal subsystem are presented along with performance predictions for instrument sensitivity and calibration. Initial estimates of size, mass and power are presented and preliminary spacecraft interface requirements for LOS stability and knowledge, torques, power and data rate are discussed.



8176-65, Session 14

Extreme hyperspectral imager using the new microslice technology

R. Content, S. Blake, C. Dunlop, R. Sharples, D. Donoghue, G. Talbot, P. Luke, D. Nandi, P. Carbonneau, T. Shanks, Durham Univ. (United Kingdom)

Extreme multiplex spectroscopy has exciting potential for Earth observation from space and airborne platforms. We propose a novel application of microlens image resampling optics to deliver unprecedented field-of-view sampling over multiple spectral channels simultaneously. Such an instrument will address spectral resolution and sensitivity limitations with currently available spaceborne instruments. The main advantages of our new Integrated Field Spectroscopy approach are: rapid survey speeds with options for multiple viewing geometries, high spatial resolution with no limitations due to scanning speed on a single overpass as with pushbroom techniques; high spectral resolution at fixed spatial resolution; longer exposures in staremode to allow higher SNR in finer pixels for radiometry; meteorology and atmospheric composition studies; signal strength which is particularly important for low reflectivity targets such as water and shallow marine environments; compact design using state-of-the-art sensors to reduce mass/volume requirements. High spectral resolution enables Earth Observation to characterise and quantify ecosystem and land and water-surface properties needed to understand biogeochemical processes and fluxes. Spectral fingerprinting is an established technique that has not been scaled-up to address whole Earth system processes; a good example of a key area of NERC science that would benefit is monitoring dissolved organic contents and other pollutants in rivers for freshwater conservation. The spectrograph is a field portable laboratory prototype developed with 2010 Seedcorn funding from the Centre for Earth Observation Instrumentation (CEOI). It uses the new concept of microslice integral field unit (IFU) first developed for astronomy. It delivers 10,000 spectra 180 pixel long simultaneously on the detector at a resolution of 6 nm over the 420 nm to 700 nm range. All the optics and the detector fit in a cylinder 35 mm in diameter and 280 mm long. A full scale instrument could deliver one million spectra or longer spectra, and much higher resolution. With far more spectra observed simultaneously, integration time can be made proportionally longer for the same data rate. Another innovation of the instrument is the use of the Foveon detector which directly measures the 3 RGB colours on each pixel. This permits to have longer overlapping spectra that can be separated since the overlapping parts are not of the same colour. The concept, design and test results in laboratory and in the field will be presented.

8176-66, Session 14

Update on the DMC constellation and next generation satellites

G. Holmes, P. Stephens, DMC International Imaging Ltd. (United Kingdom)

This paper presents an update on the Disaster Monitoring Constellation (DMC) including the current operational constellation of five satellites, the two new satellites due for launch in 2011 and a longer term outlook.

The DMC consists of a growing constellation of small satellites, each carrying a wide swath (650km) optical sensor. It is an international programme with joint campaigns being coordinated centrally by DMC International Imaging (DMCii). The original constellation provided a daily global imaging capability at 32m resolution in three Vis/NIR spectral bands, for applications requiring large area coverage and rapid repeat.

In 2009 two second generation 22m resolution satellites, UK-DMC 2 and Deimos-1, launched into the constellation, adding much more imaging capacity to the constellation as well as enhanced resolution. These satellites are now fully operational and example applications are presented in the paper. Together with the pre-existing satellites the constellation now has the capacity to deliver multitemporal monitoring at continental scale.

Two new DMC satellites are due for launch in Q2 2011: NigeriaSat-2 and NigeriaSat-X. These will bring the total number of operational DMC satellites to seven and moves the DMC constellation into the VHR domain. NigeriaSat-2 will deliver 2.5m PAN and 5m MS data in four VIS/NIR bands, as well as a 32m wide swath sensor (also with 4 bands). NigeriaSat-x is very similar to UK-DMC-2 and Deimos-1 and will add another 22m multispectral sensor to the constellation, providing further data continuity for the wide swath HR applications.

Looking further ahead, DMCii will launch a constellation of 1m resolution sensors in 2013, built by Surrey Satellite Technology Ltd (SSTL). These will open a new range of applications for the DMC constellation, such as security and cartography. During the same period DMCii will also be designing and building the next generation of wide swath sensors for enhanced agricultural and environmental applications.

8176-67, Session 14

Dubaisat-1 mission overview

A. Al Rais, Emirates Institution for Advanced Science and Technology (United Arab Emirates)

The Emirates Institution for Advanced Science and technology (EIAST) was founded in 2006 to inspire scientific innovation and foster technological advancement in the UAE through its various initiatives and programs. The Space Programme is the first initiative introduced by EIAST aiming at making the UAE an internationally recognized hub for advanced space systems and supporting the creation of a knowledge-based economy by leveraging the advances in the satellite systems. EIAST leading project and starting point in the space programme is DubaiSat-1 satellite mission. The satellite was designed and developed by Satrec Initiative - a pioneer satellite manufacturing company in South Korea, with a strong participation from EIAST engineers. DubaiSat-1 is a catalyst project and part of an in-depth know how and technology transfer program to convey advanced satellites technology to the UAE. The launch of the satellite was on July 29th 2009 onboard Dnepr rocket from Baikonur launch site. DubaiSat-1 observes the Earth at a Low Earth Orbit (LEO) with an altitude of 680 Km and generates high resolution optical images at 2.5m panchromatic (Pan) and 5m multispectral (MS) bands at red, green, blue and Near-infrared bands. These images provide variety of users and decision makers in the UAE with a valuable tool for a wide range of applications including infrastructure development, urban planning as well as environment monitoring and protection. DubaiSat-1 images are also used extensively to promote geosciences and remote sensing research in the region and support different scientific disciplines in private and academic sectors.

Since the launch, DubaiSat-1 has been entirely operated by EIAST team which is based in its ground station in Dubai. This task they have carried consistently while at the same time beginning work on DubaiSat-2. As DubaiSat-1 has been launched and providing its services, the engineers in EIAST and Satrec Initiative have already started the work on the second satellite mission; DubaiSat-2.

8176-68, Session 14

Optical configurations proposed for low cost Earth imaging payloads

M. Waqas, A. Jawed, F. Khan, The National Space Agency of Pakistan (Pakistan)

Evolution of satellite-based remote sensing plays a leading role in the socio-economic development and military domination of a country. Today people have more access in this competitive field of high resolution imagery on a scale never imagined before. In this race of space technology, third world countries have been left behind due to lack of their vision about space. The requirements of earth imaging systems are becoming more demanding in terms of accuracy and reliability day by day. Leading technology holders do not seem to be interested to share classified research with others to keep their monopoly and domination. Therefore, in order to become a member of the space fairing club, indigenous effort for the acquisition and development of space technology is a need of the hour. The purpose



of this paper is to present the optical designs of some high resolution payloads which can be indigenously developed in developing countries. The proposed designs are economical and meet the worldwide standards set for earth imaging payloads.

The optical payload drives all the system requirements of an earth imaging satellite. The first key requirement is the size of the optics that is capable to provide the desired ground sampling distance. The nominal aperture diameter of telescope is set near the minimum optics size to acquire ground resolution and is near the maximum that can be accommodated within limitations imposed by payload mass, size and cost. Another requirement is field of view coverage that fully illuminates the detector area and thus provides high quality images.

The optical performance of space-borne imaging system is limited by the effects of geometric and wave front aberrations. Two fundamental analysis tools discussed in this paper to measure the optical performance of the telescope design are the Modulation Transfer Function (MTF) and Spot Diagram. The MTF expresses the image quality of a system in quantitative terms. It is the ability of an optical system to reproduce object contrast in the resulting image. An important design requirement is to achieve an MTF larger than 50% at the Nyquist frequency in sagittal and tangential directions over entire field of view. On the other hand, the spot diagrams illustrate the airy disk diameter of the system.

For instruments launched by rockets, the weight and stability requirements are a major concern for optical performance of telescope, so a light weight and dimensionally stable construction should be employed. There is a trade-off between payload launch costs and payload mass; they vary in a linear proportion so it is important to reduce payload mass to a point where total cost is the minimum. For this reason the telescope optics and structure incorporate low coefficient of thermal expansion (CTE) materials.

This paper discusses a comparative analysis of high resolution cost effective payloads, on the basis of their performance as well as the feasibility of the design. The camera systems are capable to acquire panchromatic images in the range of 2 to 5m GSD. The system employs Three Mirror Anastigmatic (TMA) optical design qualifying for space borne imaging. The telescope is compact, light weight and offers high resolution. The design of the instrument involves implementation of innovative techniques to fulfill the requirement of excellent image quality over a wide field of view. The performance requirements are accomplished within a low budget. This paper describes the theoretical performance of optical design based on software realized simulation analysis.

8176-69, Session 14

74

Gain control strategy for multispectral camera

D. Wang, Y. Man, Beijing Institute of Space Mechanics and Electricity (China); X. Shi, Beijing Institute of Tracking and Telecommunication Technology (China)

Multispectral camera is the principal payload in China's first hazards mitigation satellite, which is designed for hazards monitoring, assessment, and management. However, the camera's dynamic range of scenery is not as wide as expected and partly influences imaging quality on-orbit. This paper analyzed the reason of this phenomenon, discussed potential solutions and proposed a strategy of on-orbit gain control. The key point of this strategy is to update the radiation property of imaging area dynamically, to narrow down the flux range and sufficiently employ system capability of quantification. Case study on an urban scene provided gains for different latitudes and seasons to generate a lookup table. These gains were used in simulation and compared with the present used gains. The result showed that the strategy could effectively improve dynamic range and imaging performance. This study can provide guidance for future camera design.

8176-71, Session 14

Study on modeling and simulation techniques based on the whole imaging chain of optical remote sensing

N. Ruan, H. Zhao, Y. Man, C. Xu, Beijing Institute of Space Mechanics and Electricity (China)

The reality of modeling is the precondition of space optical remote sensing image modeling and simulation, which plays a great importance on simulation accuracy. So the modeling of space optical remote sensing image should cover integrated composition and effect. The imaging chains include scenario, atmosphere, illumination, sensor, satellite platform, compression/ transmission/ decompression/, ground image processing and so on. The influences of signal, noise and MTF should also be considered in the modeling.

The models based on the composing and effects of the whole imaging chain were established. The simulation process is separated to three parts, the first part includes scenario, atmosphere and illumination, and the second part covers remote sensor, satellite, and the third part have compression/ transmission/ decompression/, ground image processing and so on. The 3D objects with geometry and material information are built, and atmosphere and illumination condition of imaging time are added, and then radiances are simulated by ray tracing. The second part simulates the process transforming radiance into DN values after quantifying, affecting by remote sensor and satellite. The third part is data transmission and correction by experimental and on-orbit data. The simulations were completed and images were presented on the paper, involving scenario of 0.3m to 10m resolution, images after the influence of atmosphere and illumination of different season and imaging time, remote sensor of visible and infrared light, different satellite platform, compress ratio from 1:4 to 1:16, different ground image restoration method. Based on the models and simulation results, the keys of space optical remote sensor modeling and simulation were sum up and presented on the paper, which will be reference for the simulation of the whole imaging chain of remote sensing in space.

8176-72, Session 15

Use of SAR data for hydro-morphological characterization in sub-Saharan Africa: a case study

F. Ciervo, C.U.G.RI. (Italy); G. Ruello, Univ. degli Studi di Napoli Federico II (Italy); Y. Koussoube, Univ. de Ouagadougou (Burkina Faso); M. N. Papa, Univ. degli Studi di Salerno (Italy); D. Riccio, Univ. degli Studi di Napoli Federico II (Italy)

The integrated management of the geographical information is a crucial requirement for an appropriate analysis of the hydrological problems on large-scale basin analysis. In literature, significant efforts have been made for linking of GIS-approaches and hydrological assessment models. Moreover, an increasing research of several scientific divisions has been dedicated to improve the use of information extracted from remotely sensed images with SAR interferometric techniques. The paper aims to provide the first results of a research project devoted to retrieve from satellite images physical information useful for calibrating hydrological models. In particular, the project intends to provide a hydrologic modelling support for water management decisions in critical climate zones combining use of hydrologic and remote sensing models. The study area is the district of Yatenga, northern Burkina Faso in the sub-Saharan belt of West Africa, where extreme climate conditions cause several problems: soil erosion, drought, floods. The data comes from the Italian Space Agency (ASI) Cosmo-Skymed program, which provide high resolution (1 meter) Synthetic Aperture Radar (SAR) images. Crucial peculiarity of the project is the use of open source software for data processing and hydrological modelling. In this research work the Soil and Water Assessment Tool (SWAT) model has been employed. SWAT is a basin scale, physically-based continuous distributed model developed to predict impacts of land use and water management. The paper shows the preliminary results of the project obtained by the processing of the first available high resolution SAR data. In particular, the first step is the realization of a Digital Elevation Model (DEM) obtained from the interferometric processing

Conference 8176: Sensors, Systems, and Next-Generation Satellites



of a couple of SAR images taken with 1 day of temporal shift. Through the DEM-processing the needed hydro-morphological basin attributes have been extracted. Significant features like drainage contribution areas and drainage direction have been produced from catchment morphometric attributes processing (elevation, slope, curvature) providing the needed drainage network information and rendering the stream morphometric shape. The sub-catchments delineation, the network-stream definition and the its hierarchical classification have been obtained to support a geomorphological rainfall-runoff model running. A satellite image sequence will contribute to the model calibration supporting the comparison of flooded areas during the rainy season with model results.

8176-73, Session 15

Application of satellite remote sensing techniques to flood risk assessment in Yialias catchment area in Cyprus

D. Alexakis, D. G. Hadjimitsis, A. Agapiou, K. Themistocleous, Cyprus Univ. of Technology (Cyprus); A. Retalis, National Observatory of Athens (Greece)

The increase of flood inundation occuring in different regions all over the world have enhanced the need for effective flood risk management. As floods frequency is increasing with a steady rate due to ever increasing human activities on physical floodplains there is a respectively increasing of financial destructive impact of floods. A flood can be determined as a mass of water that produces runoff on land that is not normally covered by water. However, earth observation techniques such as satellite remote sensing can contribute toward a more efficient flood risk mapping according to EU Directives of 2007/60.

This study strives to highlight the need of digital mapping of urban sprawl in a catchment area in Cyprus and the assessment of its contribution to flood risk. The Yialias river (Potamia catchment area -Nicosia, Cyprus) was selected as case study where devastating flash floods events took place at 2003 and 2009. In order to search the diachronic land cover regime of the study area multi-temporal satellite imagery was processed and analyzed (e.g Landsat TMETM+, ASTER, Quickbird, GeoEye, etc.). The land cover regime was examined in detail by using sophisticated post-processing classification algorithms such as Maximum Likelihood, Parallelepiped Algorithm, Minimum Distance, Spectral Angle and Isodata. In advance, object - based classification methodology was applied to Landsat and Aster satellite images to segment and classify urban areas expansion not only according to their spectral characteristics but also according to their geometry. A high precision Digital Elevation Model was constructed through extensive Laser Scanning and GPS survey at certain areas across Yialias river bed. Additionally, SAR data of different polarisation and resolution were used to search the flood dynamics of the study area. Morphometric parameters such as stream frequency, drainage density and elongation ratio were calculated in order to extract the basic watershed characteristics. In terms of the impacts of land use/cover on flooding, GIS were used to detect identifying trends, both visually and statistically, resulting from land use changes in a flood prone area such as Yialias. The results indicated that there is a considerable increase of urban areas cover during the period of the last 30 years. All these denoted that one of the main driving force of the increasing flood risk in catchment areas in Cyprus is generally associated to human activities.

The project is supported by the Cyprus Research Promotion Foundation.

75

8176-74, Session 15

Spatial and spatio-temporal remote-sensing image classification using support vector machines for fire monitoring

S. Rejichi, F. Chaabene, SUP'COM (Tunisia)

Forest protection against fire threat is a priority in many countries as a consequence to global warming. So, in this context comes this work which is a part of an FP7 European project named "FireSense". After detecting a wildfire, vegetation, as fire fuel, can control fire spread, hence the necessity to make a vegetation map.

The vegetation classification approach is based on Support Vector Machine (SVM) algorithm. The proposed technique deals with supervised vegetation classification problem by combining spatial, spectral and textual VHR satellite images (Quickbird) features in order to improve its capacity to recognize and classify vegetation areas since vegetation spectral responses are similar. To this, temporal and spatiotemporal vegetation classifications are also considered in order to take into account the temporal changes of vegetation areas and update fire propagation parameters estimation.

A low-pass filter based pansharpening is applied as a preprocessing step. It aims to increase the spatial resolution of the multispectral image while preserving the spectral information. The VHR panchromatic image is merged with the lower resolution spectral image in order to create a single VHR spectral one. This pansharpened HR image is considered from different points of view as we try to combine the spatial interaction within each channel by considering the ground spectral responses according to the different spectral bands, the interaction between spectral channels by using the NDVI index which best describes vegetation and the texture discriminating features by using Gabor wavelet decomposition. In practice, Gabor texture features are computed through the local energy around each pixel in order to reveal the texture structure in the image. These features, merged in a feature vector, are used as input to the SVM algorithm. It should be noted that many kernels are tested and Radial Basis Function (RBF) kernel is used and tested for several gamma values. Since an SVM is a supervised classifier, then given a set of training examples, each marked as belonging to a vegetation category, an SVM training algorithm builds a model. This optimized model is then used to classify the whole image.

The use of SVM algorithm is extended to the temporal classification in order to analyze the temporal behavior of vegetation areas according to seasons, urban extension, etc. As a first investigation, we extract, from optical satellite image time series, stable and changing areas. The SVM algorithm is combined with a dimension reduction technique (Principle Component Analysis or "PCA") in order to preserve the principal spectral information and therefore focus on temporal differences. One component spectral image is then obtained for each date of acquisition. Finally, SVM algorithm is applied on these temporal images. The learning step is performed using temporal training examples. For spatio-temporal time series images classification, an object-based approach which aims to build a Spatial-Object Temporal Adjacency Graph (SOTAG) according to overlaps or intersection, region characteristics like means and variance, is considered. Then, according to this graph, scene object evolution is analyzed.



Wednesday-Thursday 21-22 September 2011 Part of Proceedings of SPIE Vol. 8177 Remote Sensing of Clouds and the Atmosphere XVI

8177-01, Session 1

Wind speed and direction measurements for a backscatter lidar with the contour correlation analysis

S. Tomas, M. Sicard, A. Comeron, Univ. Politècnica de Catalunya (Spain)

Sensing of wind fields with backscatter lidars is an affordable alternative to the relatively complex hardware-solutions required for Doppler systems. The inhomogeneous structures in the ABL aerosol concentration in the atmospheric boundary layer are persistent enough to be carried by the wind for a sufficient observation time. The comparison of signals at different times or positions may estimate the wind velocity with the aid of correlation processing and analysis.

Here a novel method which analyzes the range-time correlation contours is presented and applied to the UPC lidar system measurements. The contour correlation analysis (CCA), uses the bidimensional auto-correlation obtained from the range-time lidar signal sensed for a certain line of sight. It retrieves the along line-ofsight (LOS) projected wind velocity -radial velocity- and the modulus of the wind vector (wind speed). The analysis is intended to be used on isotropic media and assuming the frozen atmosphere hypothesis.

This method differs from the known approaches of optimization for both time and range correlations. The optimization criteria are linked to tangency conditions in a theoretical elliptic contour. In case of low resolution in any of the lag dimensions, either range or time delays, tangency points are difficult to obtain, leading to high inaccuracies; alternative algorithms with a general analytic expression using a linear system are formulated.

Thus, using the implicit expression of the contour and the model of the correlation function, the radial velocity and modulus can be inverted. The inversion system can be overdetermined with the addition of more points of the same contour. There are two possible methods to determine the points of the contour: one is based on the admission of a tolerance in the contour level to get a sufficient number of points, otherwise, an alternative algorithm uses a principal component analysis to get the principal axes of the ellipse.

Finally, the method can be extended to retrieve the wind direction. For the horizontal vector it needs a second line of sight; in case of a nonnegligible mean vertical component, at least three non-coplanar lines of sight are required. The inversion is made solving a linear equation system, which retrieves the wind components along some defined coordinate system using the radial projections.

8177-02, Session 1

76

Wind speed and turbulence estimation for a backscatter lidar at a single line of sight

S. Tomas, M. Sicard, A. Comeron, Univ. Politècnica de Catalunya (Spain)

By means of combined spectral and correlation analysis, a backscatter lidar using a single line of sight (LOS) can measure the wind turbulence standard deviation and the mean wind speed. In contrast, Doppler systems are capable to obtain the turbulence estimation but only the radial- projected velocity, and therefore they require a scanning procedure to obtain the mean wind speed. The technique senses the motion of inhomogeneous aerosol concentration structures which are advected by the mean wind and diffused by the turbulent fluctuations by range-time correlations. Measurements with the elastic-Raman lidar of the Universitat Politècnica de Catalunya (UPC) has been tested.

The model of aerosol medium consists in an isotropic passive scalar field, not forced by any large scale wind shear. Thus, the mean wind field is stationary and horizontally invariant; their fluctuating part is treated as a space-time varying stochastic field whose components are statistically independent and gaussian, sharing the same variance. These conditions are the basis for a well-known model of space-time correlation with isotropic eddy diffusion.

The spectral analysis of the range-time correlation does a transform in the radial domain. The time-variant spectrum is split into three factors. Under certain conditions the wind variance is contained in a real term. Since the factors does not mix wind parameters, the wind turbulence can be estimated independently of the wind velocity in the spectrum modulus.

By mean of a contour correlation analysis, both the modulus and radial wind component can be retrieved. The CCA can be extended for an isotropic-turbulent wind. The CCA consists in the analysis of the level curves of the range-time correlation function. The method is easily applied to elliptic contours, but the presence of isotropic turbulence in the transport of aerosol inhomogeneities requires a second order approximation in the contour. By means of tangency conditions on the contour expression, it is demonstrated that: a) the radial velocity condition is always valid even in the isotropic-turbulent wind case, and b) the second order approximation on the contour is a ellipse with an additional term of square-velocity that is three times the wind variance (in isotropic turbulence) added to the square modulus of the wind velocity.

8177-03, Session 1

Tolerance of a field-widened Michelson interferometric spectral filter for application in a high spectral resolution lidar

D. Liu, C. Hostetler, NASA Langley Research Ctr. (United States); I. Miller, LightMachinery Inc. (Canada); A. Cook, J. Hair, NASA Langley Research Ctr. (United States)

High spectral resolution lidars (HSRLs) are becoming increasingly important in current aircraft and future space-based aerosol remote sensing applications. The HSRL technique relies on spectral discrimination between scattering from molecules and aerosol or cloud particles, and the spectral filter can be one of the most challenging problems in HSRL system. Atomic and molecular absorption filters have been used very successfully in HSRL instruments. These filters are robust, stable, and can achieve complete separation of Mie from Cabannes backscatter; however, absorption filters are lossy and gaseous absorption lines do not exist at many convenient laser wavelengths. Fabry-Perot interferometers are another option. They are simple and can be tuned to any wavelength, but are limited by acceptance angle. Field-widened Michelson interferometers overcome the deficiencies of the aforementioned filters: they perform well at relatively large off-axis angles, are nearly lossless, and can be built to any wavelength. A compact, monolithic field-widened Michelson interferometer is being developed as the spectral discrimination filter for an HSRL system at NASA Langley Research Center. The Michelson interferometer consists of a cubic beam splitter, a solid glass arm, and an air arm. The spacer that connects the beam splitter to the air arm mirror is designed to optimize thermal compensation such that the frequency of maximum interference can be tuned with great precision to the transmitted laser wavelength. In this paper, a comprehensive radiometric model for the field-widened Michelson interferometeric spectral filter is presented. The model incorporates the angular distribution and finite cross sectional area of the light source, reflectivity of all surfaces, losses by absorption, effects of scattering on surfaces, and lack of parallelism between the air-arm and solid arm, etc. The model is used to assess the performance of the interferometer in terms optical specifications, including etendue, wavefront error, beam splitter coating ratio, absorption losses, uniformity of the glass in the solid arm, etc. As such, the model is also a useful tool to evaluate performance budgets and set optical specifications for new designs of the same basic interferometer type. In this paper, the performance predicted by the model for the prototype field-widened Michelson interferometer is compared with measured results.



8177-04, Session 1

Adding confidence levels and error bars to mixing layer heights detected by ceilometer

C. Münkel, Vaisala GmbH (Germany); K. Schäfer, S. Emeis, Karlsruher Institut für Technologie (Germany)

Eye-safe lidar ceilometers are reliable tools for unattended boundary layer structure monitoring around the clock up to heights exceeding 2500 m. Comparison to temperature, humidity, and wind profiles reported by RASS, sodar, radio soundings, and weather mast in-situ sensors has confirmed their ability to detect convective or residual layers. In addition, ceilometers with a single lens optical design enable precise assessment of inversion layers and nocturnal stable layers below 200 m. This design has been chosen for the Vaisala Ceilometers CL31 and CL51.

Based on the gradient method, an automatic algorithm for online retrieval of boundary layer depth and additional residual structures has been developed that covers not only ideal boundary layer diurnal evolution, but all situations involving clouds, fog, and precipitation. This robust all weather algorithm is part of the Vaisala boundary layer reporting and analysis tool BL-VIEW. The data averaging intervals used depend on range and signal noise; detection thresholds vary with signal amplitude. All layer heights reported are accomponied by a quality index. In most cases the lowest of these layers is a good measure for the mixing layer height. The continuous knowledge of this atmospheric parameter is supporting the understanding of processes directing air quality.

The utility of mixing layer height values for air quality forecast could be increased if the current quality index would be enhanced by more significant parameters like confidence levels and error bars. Investigations in this direction have been carried out with data from a measuring campaign at Athens airport. Ceilometer profiles collected in Vantaa, Finland have been evaluated with the help of mixing layer height values derived from co-located radiosoundings. The basic principles and parameters used for mixing layer determination from both sounding methods are discussed.

8177-05, Session 1

77

Advanced methods and means to improve atmospheric lidar stability against sky background clutter

R. R. Agishev, Kazan State Technical Univ. (Russian Federation)

A problem of Lidar system adaptation to background radiation remains actual, although complex issues of influence of lidar parameters and its optical and electronic systems structure on the magnitude, dynamic and information content of received signals are widely covered in the related literature up to now. An impact of intensive background illumination on the lidar photodetectors leads to changes of optical receivers sensitivity, their overload and even paralysis. As a result, information on atmospheric optical parameters is distorted and can sometimes be completely lost.

Existing methods for solving the lidar equation are often oriented to computing of measurement results carried out after experiments. If there is a significant delay between experimental and algorithmic processing results, the operational efficiency of research falls off and, more importantly, it limits the lidar system's capability to be adapted to changes in atmospheric-optical situation and background noise conditions during the measurement sessions. In the report, we discuss the structure and functioning features of lidar instruments realizing a method of direct-acting electro-optical processing of backscattering signals and recovering of atmosphere scattering coefficient profile by simultaneity of anti-clutter and algorithmic processing of lidar signals.

At daytime, the accuracy of optical measurements can deteriorate among other things because a lidar signal's illumination from any range occupies only a part of the angular field of view (which is to be chosen for reasons to provide a specified range of atmospheric layers) and the background can occupy all the angular field of the receiving system, and therefore can overload a high-sensitive photodetector. In the report, we discuss a method of adaptation of the receiving optical system by tracking the spatial and temporal displacement of a pulsed scattering volume along the sounding path and by corresponding temporal adjustment of the lidar receiver's spatial filters.

Different methods to compress the amplitude range of optical receivers' output signals are often used in lidar. One of disadvantages of the traditional R2-compensation method is a low noise immunity due to overloading of the receiving-amplifying tract of lidar by sky background as well as a low precision of the photodetector gain control law being formed. The intense sky background leads to the photodetector's noise increasing and to decreasing the measurement accuracy of weak signals, in what connection their following quadratic amplification, in turn, leads to a significant increase of noise for signals coming from distant layers, etc. On the other hand, the practical implementation of various methods to narrow the amplitude range of optical receiver's output signals (i.e. methods of logarithmic processing, of square range compensation, of step-linear processing, etc.) encounters difficulties related to a need for labor-intensive and thorough preliminary measurements and adjustments of receiver's functional units, which creates complexity for lidarists and makes lidar equipment more expensive.

One of advanced ways of lidar signals' primary processing provides taking output signals of PMT from several intermediate dynodes and the anode. By automatic selecting of different dynodes and by adaptive controlling these dynode signals gain, at the receiver output it can be generated a signal, for example, affected to adjusting the amplitude over time in proportion to a current time square, or any other regulation law etc.

Another advanced method is a formation of adaptive light characteristic of a photodetector for significant increasing of the lidar noise immunity. This is achieved by an automatic selection of a channel of the multi-channel receiver that works with non-exceedance of the specified harmonic distortion, which is measured using an auxiliary pilot-signal. As a result, under intense background conditions an increased stability-against-clutter is provided as well as a greater functionality, lower sensitivity to the detector parameters' technological spread and a significant expansion of the linearly processed signals range.

8177-06, Session 1

Atmospheric aerosol characterization combining multi-wavelength Raman lidar and MAX-DOAS measurements in Gwanjgu

J. Chong, D. H. Shin, K. C. Kim, Gwangju Institute of Science and Technology (Korea, Republic of); K. Lee, Kyungil Univ. (Korea, Republic of); Y. J. Kim, Gwangju Institute of Science and Technology (Korea, Republic of)

Information on the vertical distribution and microphysical properties of atmospheric aerosol is important for understanding its transport characteristics as well as radiative effect. The GIST multi-wavelength (3 beta + 2 alfa +1 sigma) Raman lidar system can measure vertical profiles of optical properties of atmospheric aerosols such as extinction coefficients at 355 and 532nm, particle backscatter coefficients at 355, 532 and 1064 nm, and depolarization ratio at 532nm (Noh et al., 2007). In addition to the vertical distribution, microphysical properties of aerosol can be also retrieved by an inversion algorithm. The incomplete overlap between the telescope field-of-view and beam divergence of the transmitting laser significantly affects lidar measurement, resulting in higher uncertainty near the surface where atmospheric aerosols of interest are concentrated. Differential Optical Absorption Spectroscopy (DOAS) technique is applied as a complementary tool for the detection of atmospheric aerosols near the surface. The passive Multi-Axis DOAS (MAX-DOAS) technique uses scattered sunlight as a light source from several viewing directions. Recently developed aerosol retrieval algorithm based on O4 slant column densities (SCDs) measured at UV and visible wavelengths has been utilized to derive aerosol information (e.g., aerosol optical depth (AOD) and aerosol extinction coefficients (AECs)) in the lower troposphere. The aerosol extinction coefficient at 356 nm was retrieved for the 0-1 and 1-2 km layers based on the MAX-DOAS measurements using the retrieval algorithm. Groundbased measurements of tropospheric aerosol using multi-wavelength Raman lidar system and a mobile MAX-DOAS system were carried out at the Gwangju Institute of Science and Technology (GIST). To evaluate the performance of the integrated measurement system

(Lidar+MAX-DOAS), an aerosol retrieval method called GSTAR (GIST satellite aerosol retrieval) has been applied to compare the satellite AOD products with those based on the vertical profiles of extinction coefficients determined by lidar and MAX-DOAS measurements. Integrated measurements using a multi-wavelength Raman lidar and MAX-DOAS allow complete monitoring of atmospheric aerosols' vertical profiles for better estimation of their radiative effects on atmospheric environment change.

8177-07, Session 1

Comparison of continuous detection of mixing layer heights by ceilometer with radiosonde observations

K. Schäfer, S. Emeis, R. Forkel, M. Hoess, P. Suppan, Karlsruher Institut für Technologie (Germany); C. Münkel, Vaisala GmbH (Germany)

The mixing layer height (MLH) is an important factor which influences exchange processes of ground level emissions. The continuous knowledge of MLH is supporting the understanding of processes directing air quality. If the MLH is located near to the ground, which occurs mainly during winter and nighttime, air pollution can be high due to a strongly limited air mass dilution. Ceilometers CL31 (backscatter profiles at 910 nm) were applied to detect the MLH in Augsburg since 2006. Radiosonde data cannot be used alternatively because they do not provide sufficient information.

The Vaisala ceilometers LD40 and CL31 are operated which are eyesafe commercial lidar systems. Special software for these ceilometers provides routine retrievals of lower atmosphere layering from vertical profiles (vertical gradient) of laser backscatter density data. The performance of the ceilometers is sufficient to detect convective layer depths exceeding 2000 m and nocturnal stable layers down to 50 m. The radiosonde data from the station Oberschleissheim near Munich (about 50 km away from Augsburg city) are also used for MLH determination. A summer and a winter episode of MLH measurement results are investigated. The profile behaviour of relative humidity (strong decrease) and virtual potential temperature (inversion) of the radiosonde agree mostly well with the MLH indication from ceilometer laser backscatter density gradients. The remote sensing by ceilometers can fill the temporal gap of information between the two radiosonde profiles per day so that the daily course of the MLH is available.

8177-08, Session 1

78

Putting all CERES instruments (Terra/Aqua) on the same radiometric scale

Z. P. Szewczyk, Science Systems and Applications, Inc. (United States)

A CERES (Clouds and the Earth's Radiant Energy System) scanning radiometer is designed to measure accurately the solar radiation reflected, and thermal radiation emitted by the Earth. There are two CERES instruments aboard the Terra spacecraft (launched 2000), and two aboard the Aqua spacecraft (launched 2002). Since their launches, all instruments (except the FM4 on Aqua) have been collecting science data without any disruptions; hence, there is more than a decade long, continuous radiation budget dataset. Moreover, if we include 1998 data from a CERES instrument aboard TRMM satellite, CERES scanners have already produced more than 14 years of science data indispensable in the climate research.

Currently, a third edition of an instantaneous CERES science data product, referred to as the ERBE-like for the continuity with Earth budget missions before CERES instruments, is being processed. Since this product lays foundation for other products, the main goal of this new edition is to maintain the high accuracy of 1% and 0.5% for shortwave and longwave fluxes, respectively, as specified in the mission objectives. In order to meet this requirement throughout the mission, the new edition incorporates the newly derived gains and spectral response functions to compensate for observed spectral degradation of sensors. In addition to greatly improved consistency of each instrument response, the new edition also improves the consistency of measurements between CERES instruments by putting



them on the same radiometric scale. As we showed before (Szewczyk et al. 2010), FM1 is selected to be the climate instrument based on its overall performance. We have also put measurements of FM2 on the same radiometric scale as FM1 at the beginning of the mission (March 1, 2000). After the initial shift, measurements of both instruments, FM1 and FM2, are independent of each other.

The paper shows work associated with putting CERES instruments aboard Aqua on the same radiometric scale as Terra CERES specifically FM1. We follow the same strategy as for Terra CERES, namely, one time adjustement to Aqua CERES is made at the beginning of their mission in July of 2002. The strategy for deriving the initial shift for FM3 and FM4 is based on direct comparison of measurements in all three channels: shortwave, longwave and window. For comparison the selected data collected in July of 2002 are used. In addition to comparing instruments on the same platform, radiation budget instrument scanning experiment is used to compare FM4 and FM1 in July of 2002. This experiment was described in details in (Szewczyk, Smith, Priestley, 2004). The comparison data are collected by using a Programmable Azimuth Plane Scan (PAPS) mode, in which scan planes of instruments on different platforms are aligned with each other at nodes of their respective orbits. The Edition 3 of the ERBE-like data product, currently available for the Terra and Aqua instruments, incorporates the shift that makes the FM3 and FM4 response in all three channels consistent with FM1 at the beginning of the mission. Paper describes the data selection, analysis and interpretation of derived results and statistics.

8177-10, Session 2

Expected data quality from the upcoming OMPS/LP mission

D. F. Rault, NASA Langley Research Ctr. (United States)

The Ozone Mapper and Profiler Suite (OMPS) is scheduled to be launched in October 2011. The primary goal of the mission is to build up the Environmental Data Records (EDRs) for atmospheric ozone to allow the science community to better understand and quantify the rate of stratospheric ozone recovery. OMPS will make global measurements of the vertical, horizontal and temporal distribution of ozone in the Earth's atmosphere. OMPS is composed of three instruments, namely the Total Column Mapper (heritage: TOMS, OMI), the Nadir Profiler (heritage: SBUV) and the Limb Profiler (heritage: SOLSE/LORE, OSIRIS, SCIAMACHY, SAGE III).

The proposed paper will be concerned with the OMPS Limb Profiler (OMPS/LP), and more specifically will the quality of products (ozone, stratospheric aerosol, NO2, cloud height) expected from the sensor. Numerical experiments with synthetic radiance data for whole orbits (corresponding to Winter/Summer solstice and Equinox) have shown that sensitivity to ozone/aerosol varies significantly along the orbit as the solar illumination (zenith and azimuth) changes and the Single Scattering Angle (SSA) transitions from backscatter (Southernmost part of the orbit) to forward scatter (Northernmost part of the orbit). Consequently, the quality of the OMPS/LP retrieval products (accuracy, precision, vertical resolution, height registration) varies significantly along the orbit. Alternative retrieval methods for the OMPS/LP will also be reviewed, such as: Spectral Fitting (SF), Direct Optimal Estimation (DOE) and Two-Dimensional (2D).

8177-11, Session 2

Ozone vertical profiles in the upper troposphere and stratosphere from the OMPS limb sensor

A. J. Fleig, PITA Analytic Science (United States); D. F. Rault, NASA Langley Research Ctr. (United States)

Scheduled for launch in October 2011, the NPOESS Preparatory Project mission includes an Ozone Mapping and Profiler Suite (OMPS) composed of two nadir looking sensors and a limb viewing sensor. The primary limb product is a 1.5 km vertical resolution ozone profile from cloud top to 60 km with an along-track spacing of 1 deg latitude. Secondary products include stratospheric aerosol vertical distribution, cloud top height and NO2 vertical profiles. We will describe the OMPS sensor specifications, orbital characteristics, and time line, illustrate sensor expected performance accuracy and precision, describe the planned validation effort and describe plans for data release.

8177-13, Session 2

Fast atmospheric correction algorithm based on the darkest pixel approach for retrieving the aerosol optical thickness: comparison with in-situ AOT measurements

D. G. Hadjimitsis, K. Themistocleous, Cyprus Univ. of Technology (Cyprus)

This paper presents an overview of a fast atmospheric correction algorithm developed at MATLAB based on the RT equation basics and the darkest pixel approach. The task is to retrieve the aerosol optical thickness (AOT) from the application of this atmospheric correction. The effectiveness of this algorithm is performed by comparing the AOT values from the algorithm with those measured in-situ both from MICROTOPS hand-held sun photometer and the CIMEL sunphotometer (AERONET).

8177-14, Session 2

Ultraspectral sounding retrieval error budget and estimation

D. K. Zhou, A. M. Larar, X. Liu, NASA Langley Research Ctr. (United States); W. L. Smith, Jr., Hampton Univ. (United States); L. Strow, Univ. of Maryland, Baltimore County (United States); P. Yang, Texas A&M Univ. (United States); N. S. Pougatchev, Jet Propulsion Lab. (United States)

The ultraspectral infrared radiances obtained from satellite observations provide atmospheric, surface, and/or cloud information. The intent of the measurement of the thermodynamic state is the initialization of weather and climate models. Great effort has been given to retrieving these atmospheric, surface, and/or cloud properties using advanced retrieval algorithms developed with fast radiative transfer models (RTMs) including cloud effects. Validation through inter-comparison between retrievals and other "coincident" measurements (e.g., radiosonde, Raman Lidar) has been done with dedicated field campaigns and matchup sounding analysis. We have developed a consistency analysis scheme through RTM forward and inverse calculations to estimate error in terms of bias and standard deviation of difference, contributed by ill-posed retrieval, instrument random noise, and the discrepancy between the RTM retrievalsimulated and measured radiances. The error budget and estimation has been investigated in both radiance and retrieved geophysical parameter domains. Initial investigation is demonstrated using the measurements of the Infrared Atmospheric Sounding Interferometer (IASI) on the METOP-A satellite during the Joint Airborne IASI Validation Experiment (JAIVEx) April to May 2007.

8177-15, Session 2

79

Optical properties of biomass burning aerosols during Russian forest fire events in 2010

I. Sano, S. Mukai, M. Nakata, Kinki Univ. (Japan); B. N. Holben, NASA Goddard Space Flight Ctr. (United States); N. Kikuchi, National Institute for Environmental Studies (Japan)

Modeling of optical properties of carbonaceous aerosols is an urgent work for aerosols research as well as climate study. This work intends to develop an algorithm for retrieving aerosol information based on the combined use of CAI (Cloud aerosol imager) on GOSAT satellite and POLDER (Polarization and directionality of Earth's reflectances) on PARASOL. The CAI measures the total intensity at 0.38, 0.67, 0.87 and 1.6 μ m. A near UV measurement at 0.38 μ m has an advantage for



detecting the absorbing aerosols, such as carbonaceous as well as dust aerosols. On the contrary, the POLDER gives us with the multi directional polarization information at 0.67 and 0.87 μ m. Polarization information is useful to retrieve the aerosol over land because the polarized reflectance by surface is much smaller than total intensity.

Our algorithm is mainly based on the radiative transfer calculations in the atmosphere involving various kinds of aerosols. This algorithm has been examined for Russian forest fire events in summer of 2010. As results, aerosol optical thickness (AOT) and single scattering albedo (SSA) at a wavelength 0.55 µm are retrieved. AOT takes the values of ~2 over the region and larger than ~5 over the plume. The particle size information is also retrieved as Angstrom exponent value which shows existence of small particles in the plume. The retrieved single scattering albedo indicates lower value (~0.85), especially the edge of plume takes lower values than those at the plume core. This fact might suggest the changing of particle property by water vapor uptake with transportation. Retrieved results are partially validated with ground based measurements (AERONET).

8177-16, Session 2

Mueller matrix for preferably oriented ice crystal particles of cirrus clouds

A. V. Burnashov, V.E. Zuev Institute of Atmospheric Optics (Russian Federation)

Mueller matrices for ice crystals horizontally oriented are calculated with a code ("facet-tracing") based on the geometric optics. The main physical regularities inherent to the scattering matrices are discussed. For hexagonal plates the bright optical phenomena like forward peak,sundog, parhelion 120 degrees and peak 150 degrees (it is caused by the abovementioned specific manifestation of the total internal reflection in trajectories with high order of collisions) are quantified by their weight coefficients that are tabulated as functions of both incident angles and particle aspect ratios. For hexagonal columns (Parry and 2D-orientation) the mostly bright halos are tabuleted also. Dependence of the scattered intensity on azimuth scattering angles is studied in details.

Using modified Mueller matrix it is shown that degree of polarization of the scattered light can be a qualitative criterion of number of photon trajectories that contribute effectively to the scattered light.

The inverse scattering problem of retrieving aspect ratios of the horizontally oriented hexagonal ice plates from polarization of the scattered light in the bistatic sounding scheme has been proposed and discussed. It is shown that matrix element M44 of sundog is most sensible in the case of incident angle 34-36 degrees.

For the preferably oriented in horizontal plane ice crystal particles

weight coefficients of main halos are calculated and tabulated also. Uniform and normal distributions of flutter with maximum dimension of 1-5 degrees are considered.

8177-17, Session 2

The successive scattering in radiative transfer theory and its application for aerosol retrieval

S. Mukai, T. Yokomae, I. Sano, M. Nakata, Kinki Univ. (Japan)

Retrieval of atmospheric aerosol characteristics from satellite data, i.e. aerosol remote sensing, is based on the theory of light scattering by small particles. In usual, the standard radiative transfer problem which gets the reflection and transmission from the atmosphere in a case of finite optical thickness is available. The aerosol properties are estimated by comparing satellite measurements with the numerical values of radiation simulations in the Earth-atmosphere-surface model.

In this work, the large scale events loading of too much aerosols are focused. The aerosol events frequently occur due to the unstable climate and/or global warming tendency. It is known that large scaleforest fire damages the Earth environment as biomass burning and emission of carbonaceous particles. It is also known that the heavy soil dust is transported from the China continent to Japan on westerly winds, and provides us with severe damages on the social life and/or



human health. Therefore the work to analyze such aerosol events as dust storm or biomass burning plume with multispectral satellite data is earnestly desired and very useful in practice.

Our aerosol retrieval work is divided into three parts as: multiple light scattering calculations, aerosol model simulations and satellite data analysis. The aerosol modeling is compiled from the accumulated measurements during more than ten years provided with the world wide aerosol monitoring network (AERONET). New code of radiative transfer simulation in the case of strong aerosol events is made with the successive order of scattering method for infinite atmosphere, and then practically examined with MODIS data.

8177-18, Session 2

A method for determination of the nitrogen dioxide content in the atmospheric boundary layer basing on zenith spectral observations

O. V. Postylyakov, A. Elokhov, V. Ivanov, A.M. Obukhov Institute of Atmospheric Physics (Russian Federation)

Nitrogen dioxide (NO2) is one of key components of the chemistry of Earth's atmosphere. Reactions with its participation lead, in particular, to increase the content of surface ozone and the formation of nitric acid with following acid rain. Anthropogenic sources of NO2 produce about 2/3 of the total emissions of this impurity. NO2 content in the atmospheric boundary layer (ABL) over major cities may exceed the natural background by orders of magnitude. To organize monitoring of the impurity, a method of estimating NO2 integral content in ABL is proposed.

A new method is based on measurements of the spectrum of the scattered solar radiation coming from the zenith during daytime and twilight period near 450 nm. Developed method uses DOAS technique to determine NO2 slant columns. Usage of twilight measurement allows retrieving accurately stratospheric NO2 content. Calculation of air mass factors is performed by radiative transfer model MCC++ for interpretation of ABL NO2 column. Effects of the major factors, affecting the accuracy of the estimation, such as aerosol, clouds and albedo of the underlying surface, are analyzed. It is shown that in cloudless condition and with the cloud lower boundary located above the near-surface layer of NO2, the determination of the integral ABL content is possible with an error of 15-25%.

Developed method is used at two observational points located in Moscow as well as at Zvenigorod Scientific Station located at 60 km to the west from Moscow beginning from 2008. Nitrogen dioxide contents have significant time variation from background value (5*10^14 mol/ cm^2) to high value 4*10^17 mol/cm^2. Results on the integral NO2 content in ABL are presented including observation during extremely hot summer with a lot of fires of 2011.

8177-36, Poster Session

80

An atmospheric correction method for typical grassland: take Xilinguole league, Inner Mongolia as example

L. Guo, J. Wang, Beijing Normal Univ. (China)

The atmospheric correction is the key step in data original processing of remote sensing imagery research. It is necessary and valuable to execute the atmospheric correction work before the application. The paper use Landset-5 TM image data and take improved many dark objects atmospheric correction method which derives from radiation transmission theory, using selected typical dark object pixels of the typical research region of Inner Mongolia grassland area, to execute the correction work by calculating the dark object pixels radiation transmission process and do the separately classified three sub-areas calculation in order to restore the corrected image data to composite with the just much more accurate image data. According to the correction work the atmosphere is much approach to the real state: the corrected TM data reflectance compared with the validation data it fit much better both with the water and vegetation spectrometer measured value and TM bands standard reflectance, the improved vegetation index initialed from the corrected TM band 3 and 4 data expressed by the samples calculate window's maximum and minimum value interval, the visualization effect of false color image fused by TM band 4,3and 2 also be enhanced after the correction work which expressed by the certain confuse and detail features can be distinguished. It is clear that the corrected retrieved land surface reflectance is much better and can provide the improved accuracy; it also provides some valuable references information for the further typical grassland environment element mechanism and application research work.

8177-37, Poster Session

Application of short-range lidar in windshear alerting

P. W. Chan, Hong Kong Observatory (Hong Kong, China)

A number of windshear/turbulence signatures are identified from the radial velocity data from the short-range LIDAR. Deviation of the measured radial velocity from the background wind is called the velocity fluctuation. Moreover, EDR are calculated. The performance of the various parameters is studied with reference to the pilot reports, by using the ROC curve.

8177-38, Poster Session

Application of lidar-based F-factor in windshear alerting

P. W. Chan, Hong Kong Observatory (Hong Kong, China)

F factor (windshear hazard factor) is calculated based on the LIDAR's headwind data. The performance of F factor in alerting low level windshear is studied based on the pilot reports. ROC curve is used in the alertnig, namely, striking the balance between alert duration and hit rate of pilot windshear reports.

8177-39, Poster Session

A new false color composite technique for dust enhancement and point source determination in Middle East

K. Karimi, Shahrood Univ. of Technology (Iran, Islamic Republic of); H. Taheri Shahraiyni, Tarbiat Modares Univ. (Iran, Islamic Republic of); M. Habibi Nokhandan, Islamic Republic of Iran Meteorological Organization (Iran, Islamic Republic of); N. Hafezi Moghaddas, Shahrood Univ. of Technology (Iran, Islamic Republic of); M. Sanaeifar, Islamic Azad Univ. (Iran, Islamic Republic of)

Dust storms are natural events and are common in the parts of world with dry land areas. Periods of severe and widespread drought can increase the number of dust storms, particularly during the summer months. Dust storms reduce air quality and may have adverse effects on health, particularly for people who already have breathing-related problems. In these days, the dust storm is one of major environmental disasters in the Middle East. The dust storm happens in the Middle East with very high frequency. It is vital to study on the dust storms in the Middle East. The first step toward the study on dust storm is the enhancement of dust storm and identification of the point sources. Remote sensing is an appropriate tool for these investigations. Many different dust indices have been developed for the dust identification from remotely sensed images. In this study, a new false color composite method is developed for the enhancement of dust and determination of the point sources of dust storms in Middle East using the dust indices

In this study, MODIS images were utilized as the remotely sensed images. MODIS images have been used successfully for dust storm detection. 28 MODIS-Level 1b images from 2008 to 2009 were selected from the archive of Iranian Space Agency and received. The software package for the image processing was ILWIS 3.7 (Integrated

Land and Water Information System). The different famous dust indices were developed using the MODIS images. These indices were BTD3132 (Brightness Temperature Difference in band number 31 and 32), BTD2931 (Brightness Temperature Difference in band number 31 and 32), NDDI (Normalized Difference Dust Index) and D (Roskovensky and Liou, 2005). Different false color composite maps were generated using these Indices, bands 3 and band 4 of MODIS images. Then the performance of different color composite map was evaluated using visual interpretation. Then using the selected color composite method, the point sources in 28 MODIS images were identified and then all of the identified point sources were combined in GIS environment.

The visual interpretation of the generated False Color Composite maps demonstrated that the best combination for dust identification is the utilizing of D, BTD3132 and NDDI indices as the Red, Green and Blue bands of color composite map, respectively. Using this color composite method, about 420 point sources were extracted of 28 MODIS images and point sources map was generated. The point sources map showed that about 39.2, 23, 14.5, 13.8, 5.7 and 3.7 percent of the point sources of dust storms have been located in Iraq, Syria, Saudi Arabia, Iran, Jordan and Turkey territories, respectively.

8177-40, Poster Session

The estimate of the cloud attenuation factor when retrieving insolation from MTSAT-1R data

J. Yeom, H. O. Kim, Y. Kim, Korea Aerospace Research Institute (Korea, Republic of)

Solar surface insolation (SSI) represents how much solar radiance reaches the Earth's surface in a specified area and is an important parameter in various fields such as surface energy research, meteorology, and climate change. This study calculated insolation using Multi-functional Transport Satellite (MTSAT-1R) data with a simplified cloud factor over Northeast Asia. For SSI retrieval from the geostationary satellite data, the physical model of Kawamura was modified to improve insolation estimation by considering various atmospheric constituents, such as Rayleigh scattering, water vapor, ozone, aerosols, and clouds. For more accurate atmospheric parameterization, satellite-based atmospheric constituents were used instead of constant values when estimating insolation. Cloud effects are a key problem in insolation estimation because of their complicated optical characteristics and high temporal and spatial variation. The accuracy of insolation data from satellites depends on how well cloud attenuation as a function of geostationary channel and angle can be inferred. This study used a simplified cloud factor that depends on the reflectance and solar zenith angle. Empirical criteria to select reference data for fitting to the ground station data were applied to suggest simplified cloud factor methods. Insolation estimated using the cloud factor was compared with results of the unmodified physical model and with observations by ground-based pyranometers located in the Korean peninsula. The modified model results show far better agreement with ground truth data compared to estimates using the conventional method under overcast conditions.

8177-42, Poster Session

The tropical cyclone intensity estimation based on MODIS data

Z. Hao, F. Gong, Q. Tu, D. Pan, X. Chen, The Second Institute of Oceanography, SOA (China)

Knowledge of tropical cyclone intensity is good for pre-analysis on its development and its possible damage. It is the lack of observations in situ and the drawback of numerical model that make the remotely sensing from space be a means for tropical cyclone study. In this paper, a preliminary study on estimating tropical cyclone intensity by using MODIS (Moderate Resolution Imaging Spectroradiometer) data is present. The tropical storm 0922 Nida is as an instance for this study and the maximum wind speed in the cyclone is used to an index of cyclone intensity. Typhoon often occurs on summer over the western pacific. The tropical storm is an approximately axisymmetric vortex, which is very nearly in a state of hydrostatic and gradient



wind balance. Based on the bulk of the vortex is neutral to slantwise moist convection, the maximum gradient wind is estimated from the sea surface temperature, cloud top temperature and the change in saturation moist static energy at cloud top altitude from the eyewall to the outer region, which mainly depends on the cloud top temperature and height. The cloud-top height and cloud-top temperature in tropical storm region, which are two key parameters for estimating tropical cyclone intensity, is firstly obtained from MODIS observations. The retrieved cloud-top height is compared and validated with the CloudSat radar observations, which just cross the neighborhood of the 0922 storm center. According to a physically based framework, the maximum wind speed is estimated approximately from the background sea surface temperature, cloud-top temperature and cloud-top height. A simple result indicates that the technique for estimating cyclone intensity from MODIS observation is feasible. On the other hand, the future applications and some potential uncertainties on means are needed to be on second thoughts and discussed.

8177-44, Poster Session

Physically based radar simulator for measurements of precipitation with polarimetric and spaceborne radar

T. Kobayashi, K. Masuda, Meteorological Research Institute (Japan)

The cloud feedback problem is one of the largest uncertainties in climate studies. Clouds have mutual relations to precipitation. Precipitation is generated from cloud droplets by condensation and coalescence, which in turn generates cloud droplets by breakup and removes clouds. Thus, precipitation controls cloud amounts. Detailed observations of precipitation are, therefore, essential for better understanding of the cloud-precipitation interaction to reduce the uncertainties.

A radar is a powerful tool for measurement of precipitation. Recently, polarimetric radar is widely used because it can measure the size of raindrops to some degree and therefore measures rainfall rate more accurately than the conventional weather radar. A space-borne radar is also widely used in precipitation studies. The Tropical Rainfall Measuring Mission (TRMM) satellite has been continuously monitoring precipitation on a global scale since the launch in November, 1977. Following the TRMM, the Global Precipitation Mission (GPM) is scheduled to launch in 2013. The polarimetric radar and the GPM will provide useful data but there remain some issues to be studied. For polarimetric radar, the received signals depend on the microphysical properties of precipitation like size, shape, orientation etc. of raindrops in a complicated way. The GPM will equip the Dualfrequency Precipitation Radar (DPR) which operates at two frequencies of 14 and 35 GHz. The radar operated at 35 GHz is more sensitive to small raindrops than the radar at 14GHz but may have suffer multiple scattering effects.

To develop a robust algorithm for more accurate measurements of precipitation from those radars, we should evaluate how microphysical properties of precipitation link to the received signals with polarimetric and to the multiple scattering contributions in the space-borne radar. We have developed a generalized radar simulator for polarimetric and space-borne radar (GPASS). This is a physicallybased simulator in which the scattering properties of cloud and raindrops are calculated by using radio wave scattering theory. Thus we can make detailed study how the radar signals varie with microphysical properties of precipitation by using the simulator. We will present detail of the simulator and dependence of polarimetric radar observals and multiple scattering effects on space-borne radar signals on various microphysical properties.



8177-45, Poster Session

Retrieval of aerosol optical depth from synergy of the SEVIRI (MSG) and ground-based observations

O. Zawadzka, Univ. of Warsaw (Poland) and Div. of Physics and Radiochemistry, Faculty of Chemistry (Poland); K. M. Markowicz, Univ. of Warsaw (Poland)

The Spinning Enhanced Visible Infrared Radiometer (SEVIRI) instrument on board Meteosat Second Generation (MSG) offers new capabilities to monitor aerosol loading over land at high temporal and spatial resolution. However, in order to retrieve aerosol optical properties with good accuracy a proper estimate of the angular distribution of radiance reflected by a surface is necessary. This function is quantified by the Bi-directional Reflectance Distribution Function (BRDF). We propose algorithm to derived value of surface reflectance for vegetation from synergy of the satellite and ground-based observations. In order to find suitable BRDF model we carried out a comparison of three BRDF models: Roujean (Roujean, 1992), Ross-Li (Maignan, 2004) and Rahman-Pinty-Verstraete (Rahman, 1993). Each of these models is parameterised by three parameters. To estimate these parameters we use the SEVIRI data and ground observations of the aerosol optical properties performed by the multi spectral sun photometer during a "clear-sky" day (no clouds, low aerosol content in the atmosphere). The first step provide three parameters of the BRDF models based on the cost function minimization. Among those evaluated the best model appear to be the non-linear Rahman-Pinty-Verstraete (RPV) model. Retrieved surface BRDF was validated with ground observation of the surface reflectance and compared with MODIS data. Assuming that surface reflectance at SEVIRI resolution change slowly with time we use the retrieved BRDF to calculate aerosol optical depth for several days (second step). For both steps we use Second Simulation of a Satellite Signal in the Solar Spectrum (6S) radiative transfer model to simulate top of the atmosphere reflectance.

The research for this paper was in part supported by the EU through the European Social Fund, contract number UDA-POKL.04.01.01-00-072/09-00 and by the Polish Ministry of Higher Education and ScienceGrants 1276/B/P01/2010/38.

Rahman, H., Pinty, B., & Verstraete, M.M. (1993). Coupled Surface-Armosphere Reflectance (CSAR) Model 1. Model description and invertion on synthetic data. Journal of Geophysical Research, 98(11), 20779-20789.

Roujean, J.L., Leroy, M., & Deschamps, P.Y. (1992). A bidirectional reflectance model of the Earth's surface for the correction of the remote sensing data. Journal of Geophysical Research, 97(18), 20455-20468.

Maignan, F., Breon, F.-M., & Lacaze, R. (2004). Bidirectional reflectance of Earth targets: Evaluation of analytical models using a large set of spaceborne measurements with emphasis on the hot spot. Remote Sensing of Environment, 90, 210-220.

8177-47, Poster Session

82

Evaluation of observed and pre-simulated passive microwave signatures over tropical oceans

E. Seo, Kongju National Univ. (Korea, Republic of); M. Biggerstaff, The Univ. of Oklahoma (United States)

Successful performance in Bayesian rain retrieval algorithms is greatly affected by the similarity of brightness temperatures (TBs) between observation and predefined databases. To assess the suitability of predefined databases to observations, this study simulated three observational cases using a cloud resolving model and compared the simulated TBs to observed TBs over four selected tropical oceans using EOF analysis of attenuation and scattering indices. Dominant EOF patterns of the radiation indices for the predefined databases exhibit overproduction of large-sized ice-phase hydrometeors for a given rain content in comparison to the observations. More rigorous comparisons were done with respect to the frequency distribution of EOF coefficients in EOF space, indicating that there are both underrepresentations and overrepresentations in spatial match

between manifolds of the predefined and observed databases and poor alignment in the frequency distribution between observed and simulated clouds structures. This partial poor match in the distributions can be a critical issue in Bayesian-type retrieval algorithms. Choosing both a simulation with proper environmental conditions and taking into account observed regional variability across the oceans seem to be equivalently important in retrievals involving shallow-to-moderately tall convective clouds with modest rain contents and little scattering signatures. Deep convective clouds with higher rain contents and pronounced scattering signatures, on the other hand, are better represented in the simulations and the observations. In non-convective clouds, improving microphysical parameterizations leading to stratiform rain appears to be required.

8177-48, Poster Session

Estimation of particulate matter from simulations and measurements

M. Nakata, T. Fujito, M. Yonemitsu, I. Sano, S. Mukai, Kinki Univ. (Japan)

The particulate matter is a typical indicator of small particles in the atmosphere. They distribution in Asia is complicated due to the increasing emissions of sulfuric, nitric, carbonaceous and other aerosols in association with economic growth. Anthropogenic small aerosols dominate the air over urban areas because of local emissions by diesel vehicles and industries. In addition to providing impacts on climate and environment, these small particles can bring adverse effects on human health. Then an accurate estimation of particulate matter is an urgent subject. We set up SPM sampler (SPM-613D, Kimoto Electric, Japan) attached to our AERONET (Aerosol Robotics Network) station in urban city of Higashi-Osaka in Japan. The SPM sampler provides particle information about the concentrations of various SPMs (e.g., PM10 and PM2.5) separately. The AEROENT program is world wide ground based sun-photometric observation networks by NASA and provides the spectral information about aerosol optical thickness (AOT) and Ångström exponent. The data are kept processed and updated by the standard AERONET processing system. Simultaneous measurements show that a linear correlation definitely exists between AOT and PM2.5. These results indicate that particulate matter can be estimated from AOT. However AOT represents integrated values of column aerosol amount retrieved from optical property, while particulate matter concentration presents in-situ aerosol loading on the surface. Then simple way using linear correlation brings the discrepancy between observed and estimated particulate matter. In this work, we use the vertical profile of atmospheric aerosols and meteorological data based on numerical simulations and ground measurements to reduce the discrepancy. Our improved method will be useful for retrieving particulate matter from satellite measurements.

8177-49, Poster Session

Satellite measurements, surface measurements, and model simulations of NO2 and SO2 columns over East Asia

S. Lee, C. Song, J. Lee, W. J. Choi, D. R. Kim, S. Y. Kim, J. S. Hong, Y. Hong, National Institute of Environmental Research (Korea, Republic of)

To assess the validity of satellite data and to evaluate the longrange transport of atmospheric trace gases over East Asia, satellite measurements of NO2 and SO2 from Ozone Monitoring Instrument (OMI) are compared with surface measurements and model results from Community Multiscale Air Quality (CMAQ). The increasing use of satellite data in the air quality application has improved the performance of air quality model. In this study, temporal and spatial variations of NO2 and CO2 column amounts from OMI are compared with those from CMAQ simulation and surface measurements. Also, long-range transboundary transport of NO2 and SO2 are analyzed using OMI data and model results. The analysis results showed that both satellite measurements and model results of NO2 and SO2 showed similar monthly and seasonal variations with higher concentration in winter than in summer and NO2 showed better



SO2 due to the uncertainties and limitations in the retrieval of SO2 concentrations from satellite measurements. Also, the results showed that satellite measurements were higher than modeling results in both urban (Seoul) and background (Taean) region. Concentrations from model were very low in summer due to the excessive washout by rain in the model. However, it needs more analysis to better understand model processes and the effectiveness of satellite measurements. The temporal and spatial analysis of satellite data made it possible to monitor distribution, emission source, and long-range transport of pollutants over wide area.

8177-50, Poster Session

Evaluation of long-range transport of greenhouse gases using satellite data from GOSAT and surface measurements

C. Song, J. Lee, W. J. Choi, D. R. Kim, S. Y. Kim, J. S. Hong, S. Lee, Y. Hong, National Institute of Environmental Research (Korea, Republic of)

Carbon exchange between Earth's system components such as biosphere, atmosphere, and hydrosphere is important to determine CO2 concentrations in the atmosphere. Since the increase of CO2 and other greenhouse gases in atmospheric concentration has been found to be the main cause of global warming, a better understanding on the carbon cycle and the human contribution is highly necessary to predict resulting changes in Earth's climate. The increasing consumption of fossil fuel in the northeast Asia due to the rapid economic development in China directly links to the emission of greenhouse gases in the atmosphere. Korea and Japan is mainly affected by the transboundary pollutants and climate changing substances from China because of the downwind of westerly. In this study, the temporal and spatial distribution of greenhouse gases was analyzed to assess the effect of long-range transport using data obtained from Greenhouse gases Observing Satellite (GOSAT). Satellite data from GOSAT were compared with ground-based measurements to validate satellite data. Also, the origin of transported greenhouse gases was analyzed using back trajectory model. The analysis from surface measurements showed that 40% of high concentration of CO2 is affected by the long-range transport and 38% is affected by the local effect. High concentration occurred more frequently during spring and summer than autumn because available number of data during spring and summer is larger than autumn and it is clearer atmosphere in autumn than other season in Korea. High concentration of CO2 affected by long-range transport occurred when northerly or northwesterly prevailed and wind speed was high.

8177-51, Poster Session

83

An auto-detection algorithm for Asian dust aerosols over China seas based on satellite observations and model simulations

Z. Hao, Q. Tu, F. Gong, Z. Mao, X. Chen, The Second Institute of Oceanography, SOA (China)

Asian dust storms, which often occur on spring, can long range transport and pass through the China Seas. During this process, it makes some impact on marine ecology and region climate. In this paper, the optical and thermal properties of Asian dust aerosols are firstly presented by combining the satellite observations and radiance transfer model simulations. By compare, the reflectance of dust aerosols over ocean at the visible $0.47 \mu m \ 0.86 \mu m,$ and the near-infrared 1.64µm have some significant features, it satisfies R0.47<R1.64<R0.86 for strong dust aerosol over ocean, the weak dust aerosol meets R1.64<R0.86<R0.47, and the dust reflectance may be from 0.1 to 0.3. At the thermal atmospheric windows bands 8.5, 11 and 12 μ m, for cloud and clear water region, the brightness temperature at $12\mu m$ is highest and the temperature at $11\mu m$ is close to 12µm. However, for dust aerosols, the brightness temperature at 12µm is much greater than those at 8.5µm and 11µm. The brightness temperature difference between 8.5 μm and 11 μm is small and the lower is the difference, the stronger is the dust aerosol. Based on those visible and thermal characteristics, an auto-detection algorithm for dust aerosols over ocean is designed and is conducted for some cases. It can identify the strong and the weak dust regions well and it is nice to study the dust properties deeply.

8177-52, Poster Session

Retrieval of the aerosol and atmospheric boundary layer structure over mountain valley by ceilometer (Sofia, Bulgaria)

N. Kolev, I. Grigorov, T. Evgenieva, D. Stoyanov, Institute of Electronics (Bulgaria); E. Donev, D. Ivanov, Sofia Univ. "St. Kliment Ohridski" (Bulgaria); G. Kolarov, I. Kolev, Institute of Electronics (Bulgaria)

In the recent years, the investigation of the atmospheric aerosol optical characteristics in-situ and by remote sensing from ground and space has significantly extended. The reason for increased interest is the influence of the aerosol on radiation budget of the Sun-Atmosphere-Earth system. In spite of high number of investigations, there are still a lot of uncertainties regarding temporal and spatial distribution of the atmospheric aerosol. Studies carry out in global, regional and local scale by means of: satellites (TOMS, MODIS, CALIPSO and LiTE); networks based on passive and active remote sensing devices (EARLINET, AERONET and SKYNET) and separated sets of apparatuses.

Recently, attempts are made to use ceilometers as CT25K and CL31 (Vaisala) to determine the atmospheric boundary layer (ABL) height. The use of up-to-date ceilometers (designed mainly to determine the height of cloud base in regions of airports) to determine the ABL height is quite perspective. These devices work 24 hours in automatic mode regardless of meteorological conditions, different seasons and regions. The low cost in comparison with classical type of lidars (as aerosol or Raman lidars), usually used for this purpose, is also of significance.

In the present paper the results from two-year measurements by ceilometer CHM-15k (Jenoptic) will be presented. The experiments are carried out in an urban area located in a mountain valley (Sofia). Part of the results is compared with results obtained by lidars operating in analog and photon counting modes for specific periods of simultaneous work. In the analysis of the results obtained, the data from two meteorological station located at two different heights of the valley are also taken into account. HYSPLIT back trajectory model data and satellite data from CALIPSO are also used.

8177-53, Poster Session

Lidar determination of the atmospheric boundary layer height over Sofia, Bulgaria

N. Kolev, T. Evgenieva, Institute of Electronics (Bulgaria); E. Donev, Sofia Univ. "St. Kliment Ohridski" (Bulgaria); R. Nenchev, I. Kolev, Institute of Electronics (Bulgaria)

The atmospheric boundary layer height can be determined with high time and spatial resolutions using lidars. That height defines the volume in which various pollutants spread, especially over an urban area in a mountain valley. Any particular volume of the atmosphere can be observed at the desired period of time (e.g during a period of a day, week or more) using ground based remote sensing means. This work aims at following of the seasonal variations of the mixing layer (ML) height over a mountain valley over different years.

In the present paper the experimental lidar data taken during different seasons in 2005, 2006 and the beginning of 2007 are shown.

The dynamic of the different layers development during various seasons is determined. To determine the stable, residual and the mixing layer heights two methods are used, namely, the minimum of the second derivative of the S function and that of the mean square deviation. The applicability of those methods in investigations performed during different seasons is also determined.

On the basis of three-year lidar studies, experimentally determined histograms of heights of the three main layers in the atmospheric boundary layer are presented. The time interval of the stable and residual layers destruction and the mixing layer formation are



determined and their behavior during different seasons is followed. For the purpose certain days in spring, summer, autumn and winter are chosen.

The presented experimental results can be summarized as follows: (i) the two methods have different applicability during different seasons; (ii) the method of the second derivative of the S function of the lidar signal is more reliable in winter and spring; (iii) the method of the mean square deviation might be used during all four seasons (excluding the cases of very homogeneous mixing layer).

In conclusion it should be noted that during the all seasons (except for the winter) two different types of ML, regarding the height reached and the manner of development, are observed: ML reaching low height with gradual increase in height during the day and ML reaching high height with two stages of development - slow in the beginning and rapid at the end of the experiment.

8177-54, Poster Session

Aerosols optical and physical characteristics at transports on Central Asia from various sources on multiwavelength lidar data

B. Chen, L. Sverdlik, S. Imashev, Kyrgyz-Russian Slavic University, Lidar Station Teplokluchenka (Kyrgyzstan); P. Solomon, US EPA, Office of Research & Development (United States); J. Lantz, US EPA, Office of Radiation and Indoor Air (United States); J. Schauer, University of Wisconsin-Madison, Civil and Environmental Engineering Department (United States); M. Shafer, University of Wisconsin-Madison, Environmental Chemistry and Technology Program (United States); M. Artamonova, Institute of Atmospheric Physics, RAS (Russian Federation); G. Carmichael, University of Iowa, Department of Chemical & Biochemical Engineering (United States)

The set of lidar profiles of tropospheric aerosol characteristics in Central Tian-Shan during the period between July 2008 and June 2009 is analyzed and discussed. The annual cycle of measurements showed significant contribution of dust aerosol in total aerosol optical depth (AOD). So, estimation of average AOD at λ =532 nm varied from 0.20 at long-range transport up to 0.37 at transboundary transport. Seasonal analysis showed that for planetary boundary layer (PBL) in the region has the height limits of lower than 2 km in winter and 3.5 km in summer with average values of 1.5 0.5 and 3.0 0.8 km, the values of AOD equal to 0.08 and 0.16, respectively are characteristic. During the summer period the average value of integral aerosol backscattering coefficient 1.2 0.58 (10-3 sr-1) exceeds the similar data for winter 0.38 0.28 (10-3 sr-1). Aerosol particles of organic component (fine fraction with soot impurity - elemental carbon and sulphates) and mineral coarse fraction which is mainly dust prevail in PBL layer. Above PBL layer - dust particles with impurity of small particles in the form of sulphates. In whole the basic part of aerosol particles forming optical characteristics, is concentrated in PBL layer above which, as a rule, spectral backscattering coefficients sharply decrease with height.

Models of optical and microphysical characteristics of aerosol in PBL at regional transport of pollution to the Central Asia, and model of optical and microphysical characteristics of aerosol in layers of pollution transport from various sources above PBL layer in free troposphere are presented.

8177-55, Poster Session

ESYROLidar system developments for troposphere monitoring of aerosols and clouds properties

O. Tudose, M. Cazacu, Univ. Alexandru Ioan Cuza (Romania) and SC EnviroScopY SRL (Romania); A. Timofte, Univ. Alexandru Ioan Cuza (Romania) and Regional Forecast Ctr. Bacau (Romania); I. Balin, SC EnviroScopY SRL (Romania) and EnviroScopY SA (Switzerland)

Targeting the remote sensing low cost, up-gradable and modular tools development for monitoring relevant atmospheric parameters processes in whole troposphere (250 m to 12-15 Km altitude), a new mini LIDAR system, i.e. ESYROLIDAR, dedicated for tropospheric aerosols and clouds high temporal (minutes) and spatial resolutions (meters) monitoring have been developed and tested.

The up-gradable configuration of ESYROLIDAR is based on: a multi -wavelengths (1064, 532 and 355 nm) powerful (200, 100 and 45 mJ/ pulse) and relatively high variable repetition rate (up to 30 Hz) Nd: YAG pulsed laser, a large Newtonian telescope (40 cm diameter of collector mirror) and a new opto-mechanics detection module built in an original "eye geometry" consideration. The firsts tests and measurements were performed at the site of Science and Technology Park TehnopolIS (lasi city located on the north-eastern region of Romania), using a basic configuration with a 532 nm elastic detection with depolarization study module. Different types of clouds up to 12 km in daylight are highlighted from this first measurement. These profiles obtained with ESYROLIDAR system were confirmed by satellite imagery. Measurements and tests made in other recent campaigns for 355 nm elastic channel are also presented.

The ability of the new LIDAR system to determine the height of planetary boundary layer (PBL) determined from the LIDAR signals, as well as the aerosols load and optical parameters (extinction and backscatter) and the evaluation of atmospheric dynamics at high spatial-temporal resolutions are demonstrated.

This paper presents the ESYROLIDAR basic configuration with its two VIS elastic channels (532 nm, parallel and cross). The first measurements made with the UV (355 nm - interchangeable channel) and VIS (532 nm) elastic channels are illustrated by typical examples.

The ESYROLIDAR advantages of low divergence, relatively high repetition rate and coaxial UV-VIS-NIR emission were so here demonstrated and the present challenges are: a new robust more automatized alignment system and to add more detection channels i.e. Raman H2O water vapor at 407 nm. This system is the base of the ROmanian LIdar NETwork (ROLINET).

8177-19, Session 3

On a relation between particle size distribution and mixing layer height

K. Schäfer, S. Emeis, M. Hoess, P. Suppan, Karlsruher Institut für Technologie (Germany); J. Cyrys, M. Pitz, Helmholtz Zentrum München GmbH (Germany); C. Muenkel, Vaisala GmbH (Germany)

Ceilometers are applied to detect layering of the lower atmosphere continuously. This is necessary because not only wind speeds and directions but also atmospheric layering and especially the mixing layer height (MLH) influence exchange processes of ground level emissions. It will be discussed how the ceilometer monitoring information is influenced by the particle size distribution which is detected near the ground.

The information about atmospheric layering is continuously monitored by uninterrupted remote sensing measurements with the Vaisala ceilometers LD40 and CL31 which are eye-safe commercial lidar systems. Special software for these ceilometers provides routine retrievals of lower atmosphere layering from vertical profiles of laser backscatter data. The monitoring air pollution network is operated by the Bavarian State Agency of Environment (LfU) for in situ concentration measurements of PM10 and gaseous air pollutants. The meteorological data are collected by the monitoring station of the LfU



at the southern edge of Augsburg and at the airport at the northern edge of Augsburg by the German National Meteorological Service (DWD). Particle size distributions (PSD) are measured at the aerosol measurement station in the center of Augsburg by the Cooperative Health Research in the Region of Augsburg (KORA).

The two intensive measurement periods during the winter 2006/2007 and 2007/2008 are studied. The weather situations are characterized, the meteorological influences upon air pollutant concentrations like wind speed and wind direction are studied and the correlations of ceilometer backscatter densities and MLH with PSD are determined.

8177-20, Session 3

Detection of the temporal and spatial structure of a volcanic plume by groundbased remote sensing

K. Schäfer, S. Emeis, P. Suppan, Karlsruher Institut für Technologie (Germany); C. Münkel, Vaisala GmbH (Germany)

CL31 ceilometers (backscatter profiles at 910 nm) have been applied to detect the Eyjafjallajökull volcanic plume after the eruption on 14 April 2011. Ceilometer backscatter intensities in Augsburg showed a layer of strongly enhanced backscatter above the planetary boundary layer (PBL) only on 17 April until 13:00. From 02:00 until 13:00, the volcanic plume subsided and was finally mixed into the PBL where its clear signature finally disappeared. From 17:00 until mid-night, a structured layer in the upper part of the PBL became visible and is interpreted as a remnant of the formerly confined plume layer above a stable lower atmosphere. The ceilometer observations further indicate that there was a defined upper boundary of the PBL and the lower atmosphere was well mixed on 17 April from 13:00 until 17:00 up to about 1500 m a.g.l., i.e. the vertical extension of the PBL was relatively large. Entrainment of volcanic material into the PBL must be assumed in this phase, but a corresponding signal on the nearsurface air composition at Augsburg was not detectable due to strong dilution and high background concentrations. On 19 April, the situation became different: Due to convection, the distinct separation of the PBL and the free troposphere above disappeared. During the following night, a stable near-surface layer and a residual second layer were formed. Such meteorological conditions favoured the enrichment of air pollutants near surface level, as seen during the night from 19 April to . 20 April.

8177-21, Session 3

85

Remote sensing of aerosol properties during CARES

E. I. Kassianov, J. Barnard, M. Pekour, C. Flynn, Pacific Northwest National Lab. (United States); R. Ferrare, NASA Langley Research Ctr. (United States)

Clear-sky aerosol intensive optical properties, such as single-scattering albedo (SSA), and asymmetry parameter (AP), are very difficult to retrieve accurately from remote sensing for locations where aerosol optical depth (AOD) is quite small (~0.1 at 500 nm). During the Carbonaceous Aerosol and Radiative Effects Study (CARES), which took place in the Sacramento, California, USA area from June 1-28, 2010, very small AODs were observed. Data collected during CARES provides an excellent opportunity to study the uncertainties of retrieved aerosol intensive properties during clean conditions, as well as the aerosol properties themselves. In particular, column aerosol properties (AOD, SSA, ASP and size distribution) are retrieved from data provided by ground-based Multifilter Rotating Shadowband Radiometers (MFRSRs) and the CIMEL sun photometer, and the robustness of the MFRSR- and CIMEL-based aerosol retrievals is examined using corresponding in situ measurements from ground- and aircraft-based instrumentation. The analysis of the remote sensing retrievals shows substantial diurnal and day-to-day changes of the retrieved aerosol microphysical (e.g., size distribution), and consequently optical properties (AOD, SSA and ASP). These changes and related issues of potential aerosol sources (e.g., several events with observed biomass burning) will be discussed.

8177-22, Session 3

Assessment of MODIS aerosol optical depth over oceans using 1-year data from maritime aerosol network

E. I. Kassianov, D. Chand, M. Wang, Pacific Northwest National Lab. (United States)

Oceans cover about 70% of the Earth surface and are well-known source of marine aerosol, which in conjunction with anthropogenic aerosol (pollution and biomass burning) and dust transported from remote terrestrial origins can influence the climate system substantially. This influence depends on aerosol optical depth (AOD) and global inventories of marine AOD are available mostly from satellite observations, such as the Collection 5 Moderate Resolution Imaging Spectroradiometer (MODIS) AOD product. The attempts to estimate uncertainties of the satellite maritime aerosol retrievals provided a powerful stimulus for the development of the Maritime Aerosol Network (MAN) as a component of AERONET (Smirnov et al., 2011). The MAN includes AODs from direct sun measurements offered by hand-held sunphotometers within the spectral range of 340-1020 nm. The MANbased data set combines measurements collected during completed (2006-2010) and ongoing (2011) cruises. We apply the most recent (2010) level 2.0 MAN-based AODs for assessment those from two MODIS sensors aboard Terra and Aqua satellites with morning (10:30 local time) and afternoon (13:30 local time) equatorial crossing times, respectively. To compare correctly the MAN- and MODIS-based AODs (550 nm), considerable attention was given to match ship tracks and satellite overpasses both temporally and spatially. Overall, analysis of collocated and coincident satellite and shipboard data reveals capabilities of two MODIS sensors to capture the strong spatial and temporal variations of AOD quite well, although a better agreement between the MAN- and MODIS-based AODs is observed for Aqua instrument. Application of satellite and shipboard data for evaluation of global model predictions of aerosol loadings over oceans will be also considered.

Smirnov, A. and co-authors, 2011: Maritime Aerosol Network as a component of AERONET - first results and comparison with global aerosol models and satellite retrievals, Atmos. Meas. Tech. Discuss., 4, 1-32.

8177-23, Session 3

To analyze the effects of mixing with soot aggregates on retrieving dust properties for satellite observations in Asia

T. Lin, National Central Univ. (Taiwan); Y. Ping, Texas A&M Univ. (United States)

Severe Asian dust storms tend to produce large quantities of dust aerosols which can contribute episodically to the regional or global aerosol load. Meanwhile, long range transport leads dust particles to internally/externally mix with the ambient aerosols such as soot particles naturally. The physicochemical characteristics of dust particles thus are dramatically altered after mixing with soot aggregates. Therefore, the investigation on the optical properties of mineral dust along with their pathway causes a significant topic for understanding the impacts of Asian dust storm on regional air quality, environment and climate. But the previous researches regarding to the optical properties of dust/soot mixture for satellite remote sensing are scarce. Consequently, the objective of this study is to simulate the effects of mixing with soot aggregates on the optical properties of dust particles for MODIS spectral bands (0.412, 0.470 and 0.650 mm) based on the well developed models for dust particles and soot aggregates.

For the mineral dust modeling, theoretical simulations based on the laboratory measurements suggest nonspherical shape for more accurate single scattering properties of dust particles than the spherical counterpart. Recently, a tri-axial ellipsoidal model by introducing the third morphological freedom to improve the symmetry of spheroids has been developed and showed in good agreement for the retrievals of dust optical properties from remote sensing measurements and ground based observations. As for the aggregation of soot aerosols, the scattering properties of fractal aggregates can be well obtained with the Rayleigh-Debye-Gans (RDG), T-matrix,

SPIE Remote Sensing

superposition T-matrix method and Generalized Multiple Mie (GMM) methods.

Although the scattering phase functions of dust/soot mixtures (external mix) are almost the same as the pure dust's counterparts (less than 0.4% in difference) due to the extreme distinction in scattering cross section, but the differences in single scattering albedo (SSA) are obvious (about 3% in difference) because of the strong light absorption of soot aggregates. Thus the apparent reflectance observed at TOA (top of atmosphere) would be altered by the variances in SSA and scattering phase function. For example, the mean relative difference of from pure dust are about 3% and 8% at 0.470 mm, respectively, when aerosol optical depth (AOD) and soot mixing weight are assumed to be 1.0 and 10%. The preliminary results show that the AOD (aerosol optical depth) retrievals of dust particles will be underestimated while the SSA (single scattering albedo) will be overestimated when neglecting the combination of soot aggregates. The simulations also suggest that simultaneously retrieve AOD and SSA based on the apparent reflectance may induce large uncertainty for the dust/soot mixtures.

8177-24, Session 3

A study on aerosol-cloud interaction inferred from MODIS satellite data in urban regions

Y. He, B. Gross, The City College of New York (United States)

Aerosols directly interact with solar radiation via scattering and absorbing sunlight. Aerosols also have important impact on cloud formation by acting as the cloud condensation nuclei (CCN) in the atmosphere. The aerosol indirect effect indicates that increasing aerosol particle number concentration correlates to decreasing cloud droplet size and increasing cloud reflectivity. However, the relationship between aerosols and clouds remains uncertain in urban regions due to complicated and unique aerosol and cloud properties. Three 1 degree by 1 degree regions centered at New York, Los Angles, and Osaka respectively were selected for this study. These three regions are all heavily populated. Therefore, anthropogenic aerosols are of the main aerosol sources. The relationship was mainly investigated between aerosol optical depth (AOD) and cloud droplet number concentration. Two different methods were applied to infer cloud droplet number concentration. Four years (January 2006 to December 2009) of Moderate Resolution Imaging Spectroradiometer (MODIS) level 2 cloud product were used to derive cloud droplet number concentration in each region from cloud effective radius and optical thickness. Fine mode AOD and coarse mode AOD were derived from the MODIS level 2 aerosol product. The results show seasonal variations of AOD and cloud droplet number concentration in all three regions. However, the correlation between AOD and cloud droplet number concentration is at most ambiguous. In Los Angles region, the correlation between AOD and cloud droplet number concentration is positive. The correlation between AOD and cloud droplet number concentration shows to be negative in New York and Osaka regions though. The cloud droplet number concentration seems to favor the coarse mode AOD. These results indicate the need for further study in decoupling the composition of aerosols and cloud properties.

8177-25, Session 3

86

Application of a multifilter shadowband radiometer and microwave radiometer for ground based evaluation of aerosol-cloud interactions

B. Gross, L. Cordero, J. He, B. Madhalvan, F. Moshary, S. Ahmed, The City College of New York (United States)

The quantification of the first direct aerosol cloud interaction mechanism requires simultaneous observations of cloud water drop properties as well as aerosol properties below the cloud. The simultaneous measurement of both these properties is very difficult from space borne systems and efforts to develop ground remote sensing measurements are critical. To measure the cloud properties, we make use of an approach which combines a Microwave radiometer and a MFRSR radiometer for simultaneous Cloud Optical Depth (COD) and Liquid Water Path (LWP) from a Passive Multispectral Microwave Radiometer (MWR) . From these measurements, effective droplet diameter can be estimated assuming the homogeneity of the cloud. Unfortunately, for thin clouds, COD measurements from the MFRSR are often underestimated due to strong forward scattering of radiation in the solar aureole region which is blocked and therefore not contained within the MFRSR diffuse measurements. However, by suitable calculation, we can estimate the fractional radiation within the shadow region as a function of cloud properties directly and find that for COD > 2 and solar zenith angles < 60, the standard MFRSR correction can be applied with errors < 1%.

From this result, we develop multidimensional sensitivity studies to quantify the sensitivity of cloud optical depth to various atmospheric and surface based uncertainties including instrumentation sensitivity of the MWR LWP, the aerosol microphysical and optical depth statistics and the effects of relative humidity on aerosol properties and surface albedo uncertainty. In this way, we estimate the main limitation to be the modification of the aerosol models to RH which if not taken into account can lead to errors in the COD $\sim 25\%$.

In addition, we develop an approach based on NN to retrieve the properties of aerosols based solely on multispectral extinction data based on training against full aeronet microphysical retrievals using Level 2 Inversions. We find that not only can the fine / coarse mode fraction be retrieved but SSA and particle number can be estimated. These properties together with lidar profiles below cloud base result in more directly applicable aerosol properties which can be used to better quantify aerosol effects on clouds. Preliminary data matchups for simultaneous cloud and aerosol retrieval are presented.

8177-26, Session 3

Capabilities and limitations of MISR aerosol retrievals in dust-laden conditions

O. V. Kalashnikova, Jet Propulsion Lab. (United States); M. Garay, Raytheon Co. (United States); R. Kahn, NASA Goddard Space Flight Ctr. (United States); D. Diner, J. Martonchik, Jet Propulsion Lab. (United States)

Multiangle remote sensing, in particular from the Multi-angle Imaging SpectroRadiometer (MISR) instrument on the Terra satellite, provides a unique source of data for studying dust emission and transport. MISR's multiple view angles allow the retrieval of aerosol properties over bright surfaces and such retrievals have been shown to be sensitive to the non-sphericity of dust aerosols over both land and water. In addition, MISR provides stereographic views of thick aerosol plumes, allowing heights and instantaneous winds to be derived at spatial resolutions on the order of 1 km.

We use the 10+ year aerosol data record of aerosol optical depth (AOD), aerosol optical properties, and dust plume heights and wind speeds in and downwind of large dust source regions to demonstrate MISR's unique strengths and assess potential biases in the current retrievals under dust-laden conditions, in the context of a satellite-based dust climatology.

Consistent with previous studies, MISR retrievals both near dust sources and in mid-range dust transport regions tend to overestimate instantaneous AOD in the low AOD range and underestimate it in the high AOD range compared to ground-based AERONET supphotometer retrievals. Even so, the MISR inter-annual and seasonal AOD patterns reproduce those at AERONET stations near Saharan and Asian dust sources, and are in agreement with independent meteorological surface observations. As such, MISR provides a useful record of such temporal patterns that is often temporally and spatially more extensive than those available from ground-based observations. Comparisons of MISR with MODIS Deep Blue and OMI data demonstrate similar anomalies, seasonal cycles, and AOT multi-year spatial patterns in dust source regions, although some discrepancies, especially under heavy dust loading, are observed and factors likely to contribute to this issue will be discussed.

MISR non-spherical aerosol fraction shows seasonal peaks consistent with the annual dust climatology in Asia. The seasonal cycle of MISR absorbing-particle AOD also agrees well with OMI aerosol index (AI) downwind of source regions. This suggests that MISR small and non-spherical fractions can be used to separate dust from pollution aerosols, particularly in the long-range transport regions. Finally, we will demonstrate MISR's capabilities to simultaneously retrieve dust plume heights and winds over deserts using the MISR iNteractive eXplorer (MINX) software tool. These retrievals have been used to derive dust plume climatologies for both the Bodélé region in northern Africa and the Taklamakan dust source region in Asia.

8177-27, Session 3

The effect of ozone and aerosol on the surface erythemal UV radiation

J. Lee, C. Song, W. J. Choi, D. R. Kim, S. Y. Kim, S. Lee, Y. Hong, National Institute of Environmental Research (Korea, Republic of)

Surface UV radiation affects the atmospheric circulation and climate by changing atmospheric thermal state through the absorption of energy by ozone. Also, UV radiation plays an important role in the photodissociation and atmospheric chemistry. Surface UV radiation is affected by various factors such as solar zenith angle, clouds, surface albedo, and aerosol as well as ozone. The effect of ozone on the surface UV radiation has been explored in many studies due the decrease of ozone layer and the increase of ozone hole over the polar regions. However, the effect of aerosol on the surface UV radiation is not well known. Not only the increase of surface UV radiation due to the decrease of ozone but also the decrease of surface UV radiation due to the increase of aerosol by anthropogenic activities should be considered for the better understand of variations of surface UV radiation. In this study, we estimated the effect of ozone and aerosol on the surface UV radiation using ozone, aerosol, and surface erythemal UV radiation data obtained from Ozone Monitoring Instrument (OMI). First, we compared satellite measurements with surface measurements to validate satellite data. The two measurements showed similar results for ozone and aerosol but surface measurements of UV radiation was larger than those of satellite measurements. The effect of ozone and aerosol on the surface UV radiation was analyzed using Radiative Aplification Factor (RAF). The RAF for ozone was 0.97~1.49 with solar zenith angle. Only clear-sky pixel data were used and solar zenith angle and total column amount of ozone were fixed to evaluate the effect of aerosol on the surface UV radiation. Also, RAF for aerosol was assessed with the single scattering albedo (SSA) of aerosols. The result showed that RAF for aerosol with smaller SSA (0.90). RAF for aerosol was 0.01 ~ 0.08 which is relatively small compared to that for ozone. However, it needs to consider the effect of aerosol as well as ozone for the better understand of characteristics of surface erythemal UV radiation because aerosol optical depth can change very rapidly in a short period of time while total column ozone does not change very much.

8177-28, Session 4

Detection of convective cells with a potential to produce local heavy rainfalls by a C-band polarimetric radar

A. Adachi, T. Kobayashi, H. Yamauchi, S. Onogi, Meteorological Research Institute (Japan)

Local heavy rainfalls in urban area are drawing attention in Japan recently, because quite a number of people have been injured or even died due to flush floods associated with local heavy convective rainfalls. Since convective cells do not always produce heavy rainfall, it is important to distinguish convective cells that have a potential to produce local heavy rainfalls from others in the observation field. Horizontal distributions of rainfall have been estimated from conventional weather radar observations using the so-called Z-R relationship. Although this relationship is relatively accurate for stratiform rain events, this method is unreliable for convective ones, which produce heavy precipitations.

Since large raindrops (D >3 mm) are found only in heavy rain (R > 50 mm/h, e.g. Pruppacher and Klett, 2010) the existence of large raindrops in clouds can be a good precursor to heavy precipitation events. Detection of large raindrops aloft could provide people several minutes to prepare for the events including to leave away from



riverbeds before the arrival of flush floods associated with the heavy precipitation.

Recent studies have shown that the dual-polarimetric radars are capable to provide particle size information on hydrometeors. Variables obtained by the dual-pol radars include the differential reflectivity (Zdr), which is expected to increase with the raindrop size. We especially focused on the Zdr observed with the C-band dual-pol radar in the present study because it is more sensitive to large raindrops than does radars operating at other frequency bands due to the Mie scattering resonance effect, which is supported by our simulation. In addition, our simulation also shows that the Zdr measured with C-band radar is the most sensitive to the raindrop with the diameter of about 6 mm; raindrops with the diameter within or more than 7-8 mm often break up into small raindrops while falling in the air and could not contribute to heavy precipitation on the ground. Therefore, the Zdr measured with C-band radar is suitable to detect large raindrops aloft that could produce heavy rainfall.

In the present study, we analyzed a local heavy rainfall event that occurred on 7 July 2010 using the MRI C-band polarimetric radar data as a case study. After an attenuation correction with the differential propagation phase (Phai-dp), a large Zdr region was clearly analyzed aloft about 10 minutes prior to the local heavy rainfall on the ground. On the other hand, enhanced Zdr regions were not formed aloft in the convective cells that did not produce heavy rainfalls. These results suggest that Zdr observed with C-band dual-pol radar can be a good index to detect heavy precipitation events in advance.

8177-29, Session 4

Atmospheric sounding from the joint polar satellite system

X. Liu, A. M. Larar, D. K. Zhou, NASA Langley Research Ctr. (United States)

The Joint Polar Satellite System (JPSS) and the NPOESS Preparatory Project (NPP) missions will fly a Cross-track Infrared Sounder (CrIS). The EUMETSAT Infrared Atmospheric Sounding Interferometer (IASI) was launched on 19 October 2006. These hyperspectral satellite sounders can provide abundant information on atmospheric and surface properties. In order to retrieve atmospheric temperature, water, and trace gas vertical profiles from these high spectral resolution data, one has to account for cloud contributions to the top of atmospheric (TOA) radiance spectra. We will discuss two methods for dealing with clouds: cloud-clearing and cloud retrieval. The cloud-clearing method is used by the AIRS level 2 data processing algorithm and by the JPSS Cross-track Infrared and Microwave Sounder Suite (CrIMSS) algorithm. At NASA Langley Research Center (LaRC), we have developed a retrieval algorithm, which explicitly retrieves cloud properties together with other parameters such as atmospheric temperature, moisture, and trace gases profiles, surface skin temperature and emissivity. We will present results of testing the CrIMSS Environmental Data Record (EDR) operational algorithm and the LaRC method using IASI satellite data.

8177-30, Session 4

A multispectral spatio-temporal approach for cloud screening of remotely sensed images

G. Vivone, R. Restaino, R. Conte, M. Longo, P. Addesso, Univ. degli Studi di Salerno (Italy)

Information extraction from remotely sensed images acquired in the visible and near-infrared (VNIR) frequency range strongly depends on an accurate cloud pixel screening. Indeed, many remote sensing applications require a preliminary cloud detection phase to obtain profitable results.

In the visible wavelength band $(0.4\mu m - 0.8\mu m)$ clouds and snow exhibit a very high reflectance, that allows for an accurate separation from the other classes. In this ambit we recently proposed a novel spatio-temporal Maximum A Posteriori Probability - Markov Random Field (MAP-MRF) approach [1]. The latter relies upon on the modification of the a priori probability for taking into account the



information inferable from the previous images. In particular a penalty term for the cloudiness test was constructed by predicting the position of the cloud masses in the current image by a Multi Target Tracking (MTT) algorithm based on Random Sets Theory or, alternatively, by a region matching technique.

On the other hand classification of pixels as cloud against snow represents a harder problem that can be conveniently tackled by exploiting the information contained in other frequency bands. Several multispectral and hyperspectral methods have been proposed in the literature, based on multiple threshold tests [2], as well as on Support Vector Machines (SVM) classifiers [3].

In this paper we propose to integrate the potential of the MAP-MRF methodology with the multispectral approach for augmenting the capability of the algorithm to detect cloudy pixels. In particular the proposed technique combine information from some SEVIRI sensor channels (in particular the channels 0.64 µm, 1.6 µm, 3.9 µm, 7.3 µm and 10.8 µm) with the classification obtained by the MAP-MRF method in the 0.8 µm channel in order to discriminate between snowy and cloudy pixels.

The validation is performed on challenging images of Alps mountains acquired by the SEVIRI sensor during winter months. Results point out that significant improvements are achieved respect to existing methods. In particular we highlight a more precise classification at the cloud borders and a considerable reduction of unsolicited holes inside the cloud masses.

[1] P. Addesso, R.Conte, M. Longo, R. Restaino, G. Vivone, MAP-MRF Cloud Detection Based on PHD Filtering, IEEE Geoscience and Remote Sensing Symposium (IGARSS), 1-5 August 2011, Sendai, Japan, accepted.

[2] M. S. De Ruyter de Wildt, G. Seiz, and A. Gruen, "Operational snow mapping using multitemporal meteosat seviri imagery," Remote Sens. Environ., vol. 109(1) pp. 29-41, 2007.

[3] G. Camps-Valls, L. Gómez-Chova, J. Calpe-Maravilla, J. D. Martín-Guerrero, E. Soria-Olivas, L. Alonso-Chordá, and J. Moreno, "Robust Support Vector Method for Hyperspectral Data Classification and Knowledge Discovery", IEEE Trans. Geosci. Remote Sens., vol. 42(7), pp. 1530-1542, 2004.

8177-31, Session 4

88

Adaptive cloud cover estimation using a thermal imaging camera

A. Wormald, M. D. O'Toole, A. Sandford, Campbell Scientific Ltd. (United Kingdom); D. Kerr, J. M. Coupland, Loughborough Univ. (United Kingdom)

Airports and meteorological observatories require accurate measurement of cloud cover to warn pilots of adverse conditions, and to assist in forecasting. We present a system which uses a LWIR (long wave infra red) camera to determine cloud cover automatically in up to three different layers.

This system uses the environmental lapse rate as defined by the International Civil Aviation Organization to estimate temperatures and hence height of clouds directly above the camera. An empirically determined formula is used initially to compensate for absorption and emission of the atmosphere at lower values of elevation, where the long path length between the camera and a cloud causes significant contribution by water vapour to the measured radiation. A mean shift algorithm is applied to cluster the cloud data into different layers, giving an initial report of cloud cover. This is then updated and refined by tracking individual clouds across the sky using continuously adaptive mean shift and amending the temperature correction factor to ensure that the clouds travel in a flat trajectory.

The resulting system is able to give measurements of cloud cover in oktas at different heights as required by the METAR reports generated at airports, and can also provide more detailed cloud distribution data for research.

8177-32, Session 4

Automatic cloud coverage assessment of Formosat-2 image

K. Hsu, National Space Organization (Taiwan)

Formosat-2 satellite equips with the high-spatial-resolution (2m ground sampling distance) remote sensing instrument. It has been being operated on the daily-revisiting mission orbit by National Space organization (NSPO) of Taiwan since May 21 2004. NSPO has also serving as one of the ground receiving stations for daily processing the received Formosat-2 image. The cloud coverage assessment of Formosat-2 image for NSPO Image Processing System generally consists of two major steps. Firstly, an un-supervised K-means method (Liu, 2004) is used for automatically estimating the percentage of cloud coverage from Formosat-2 image. Secondly, manual estimation of cloud coverage from Formosat-2 image is processed by operators' visual examination. Apparently, a more accurate Automatic Cloud Coverage Assessment (ACCA) method certainly increases the efficiency of processing step 2 with a good prediction of cloud coverage. In this paper, by taking the advantages of two-stages method (Chang et al, 2006) and two-pass filtering method (Irish, 2000), we present an modified Formosat-2 ACCA method which considered four steps: un-supervised K-means, threshold segmentation, region growing and reflective pixels filtering methods. Therefore, we statistically derive a set of threshold values and growing scheme for threshold segmentation and region growing method, respectively. Moreover, we examine all the threshold values of filters 1, 5, and 6 which are proposed by Irish for reflective pixels filtering method. Basically, different filter was designed not only for identifying the cloudy pixels, but also eliminating pixels of highly reflective vegetation. Furthermore, manual estimation was done in order to check the experimental results qualitatively and quantitatively. From preliminary results, we improve the results using un-supervised K-means method alone, especially for the images with low percentage (10%) of cloud coverage. Additional study and analysis of using current proposed method of simulated Formosat-5 images will also be briefly reported in the upcoming conference.

8177-33, Session 4

Multi-summer climatology of cumuli at SGP site: vertical structure

L. K. Berg, E. I. Kassianov, Pacific Northwest National Lab. (United States)

Compared to other cloud types, fair-weather cumuli (FWC) are relatively small in size and have large variations over time/space. As a result, their properties are poorly captured by current largescale numerical models of the atmosphere. Since these small-scale variations are very difficult to monitor and describe accurately, the improvement of models is hampered, at least in part, by the lack of appropriate observational constraints, including FWC statistics. We started the development of these statistics using data from a 96-GHz cloud radar, Micropulse Lidar, and 915-MHz radar wind profiler deployed at the U.S. Department of Energy Atmospheric Radiation Measurement (ARM) Southern Great Plains (SGP) Site located in north-central Oklahoma, USA (Berg and Kassianov, 2008). The original version of the developed statistics involves 5-summer climatology (2000-2004) of the vertically integrated cloud fraction and cloud-chord length, which is a horizontal length scale representative of the FWC. An updated version includes the vertical distributions of cloud fraction and cloud-chord length obtained for 10 summers (2000-2009) with relatively high (0.09 km) vertical resolution. In this presentation we will outline the updated version and discuss its potential benefits for improved model evaluations.

Berg, L.K., and E.I. Kassianov, 2008: Temporal variability of fair-weather cumulus statistics at the ARM SGP site, Journal of Climate, 21, 3344-3358.



8177-34, Session 4

Cloud droplet size retrievals from polarized reflectance measurements by the research scanning polarimeter

M. D. Alexandrov, B. Cairns, NASA Goddard Institute for Space Studies (United States); C. Emde, Ludwig-Maximilians-Univ. München (Germany); B. van Diedenhoven, A. Ackerman, NASA Goddard Institute for Space Studies (United States)

We present an algorithm for retrieval of cloud droplet size distribution parameters (effective radius and variance) from the Research Scanning Polarimeter (RSP) measurements. The RSP is an airborne prototype for the Aerosol Polarimetery Sensor (APS), which was on-board of the NASA Glory satellite. The RSP measures I, Q, and U components of the Stokes vector in 9 spectral channels with center wavelengths ranging from 410 to 2250 nm. The total and polarized reflectances are then derived from these Stokes parameters. The RSP is a push-broom sensor scanning along the aircraft track within 60 degrees from nadir and making samples at 0.8 degree intervals. The data from the actual RSP scans is aggregated into "virtual" scans, each consisting of all reflectances from a single point on the ground or at the cloud top.

While currently operational remote sensing of cloud optical properties (based on the multi-spectral measurements by e.g., MODIS) is affected by uncertainties due to 3D nature of radiation fields (not accounted for in the 1D radiative transfer models used), retrievals from polarized reflectance measurements in rainbow region (by e.g., POLDER) avoid these uncertainties, since the rainbow shape is dominated by single scattering of light by cloud particles. These retrievals have no surface albedo issues, and are independent of the optical depth down to unity (i.e. work for common low water path clouds). They can also be combined with lidar-derived extinctions at the cloud top in order to compute the number concentration of cloud droplets.

For cloud droplet size retrievals we utilize the scattering angle dependences of the polarized reflectances in 410, 865, and 2250 nm spectral channels. Our technique is focused on the sharply defined structure (rainbow) in the polarized reflectances of clouds observed in the scattering angle range between 135 and 165 degrees. We fit the measured polarized reflectances by linear combinations of the appropriate phase matrix element (computed using Mie theory for a grid of effective radius and variance values), and a term linear in scattering angle. The empirical coefficients of this combination account for contributions from cloud multiple scattering, molecular atmosphere, aerosols, and ground surface. We demonstrate on simulated data that this parameterization allows for adequate separation of cloud single scattering from other factors providing high accuracy retrievals. Our algorithm was tested on realistic cloud radiation fields simulated using the vector doubling/adding code (plane-parallel case) and the 3D radiative transfer model MYSTIC (Monte Carlo code for phYSically correct Tracing of photons In Cloudy atmospheres). The latter model was applied to cloud field obtained from large-eddy simulations based on measurements from the Rain in Cumulus over the Ocean (RICO) project.

We present the results of application of the described algorithm to the datasets from two recent field campaigns: the Coastal Stratocumulus Imposed Perturbation Experiment (CSTRIPE, 2003) and the Routine AVP CLOWD Optical Radiative Observations (RACORO, 2009). Our retrievals were compared with the correlative in situ measurements of cloud droplet sizes performed during these two campaigns.

8177-35, Session 4

89

Correlation and causal relationship between GPS water vapor measurements and rainfall intensities in a tropical region (Tahiti Island)

J. Serafini, L. Sichoix, J. Barriot, Univ. de la Polynésie Française (French Polynesia)

We present the approach to remote sensing of water vapor based on the Global Positioning System (GPS) and we show the shortterm causal relationship between GPS water vapor measurements and rainfall intensities in a tropical region subject to severe climatic changes like Tahiti island. Signals propagating from GPS satellites to ground-based GPS receivers are delayed by atmospheric water vapor.

We processed a nine years time series (from Oct. 2000 to Oct. 2009) of this zenith wet delay (ZWD) and associated precipitable water from the permanent GPS station THTI (Geodesy Observatory of Tahiti) and a corresponding time series of the precipitations from the pluviometer of the Matatia valley (5 km South East from the GPS receiver).

Daily GPS data were obtained (including zenith total delay (ZTD) and associated North and East gradients) by applying the Precise Point Positioning strategy of the GIPSY-OASIS II package w.r.t. IGS final products (Bar-Sever et al., 2003). We used the Saastamoinen model (Saastamoinen, 1973) to extract the delay hydrostatic part. Given surface meteorological measurements, the resulting wet delay can be transformed into an estimate of the precipitable water overlying the receiver (Bevis et al., 1994).

The precipitation dataset consisted of daily and sub-daily rainfall gauge measurements spanning the same decade provided by the 'Direction de l'Equipement (GEGDP) and MeteoFrance (French Polynesia).

We demonstrate that the best cross-modeling of the time-series is obtained by combining a seasonal signal (from a least squares fit with outlier rejection) with a bivariate cross-regression of the deseasonalized time series over a short time span.



Tuesday 20 September 2011

Part of Proceedings of SPIE Vol. 8178 Optics in Atmospheric Propagation and Adaptive Systems XIV

8178-01, Session 1

Seasonal trends and nightly fluctuations of SWIR airglow irradiance

D. C. Dayton, J. Gonglewski, M. M. Myers, J. Allen, R. V. Nolasco, Applied Technology Associates (United States)

Airglow luminescence in the SWIR region due to upper atmospheric recombination of solar excited molecules is a well accepted phenomenon. While the intensity appears broadly uniform over the whole sky hemisphere, we are interested in variations in four areas: 1) fine periodic features known as gravity waves, 2) broad patterns across the whole sky, 3) temporal variations in the hemispheric mean irradiance over the course of the night, and 4) long term seasonal variations in the mean irradiance. An experiment is described and results presented covering a full year of high resolution hemispheric SWIR irradiance images. An automated gimbal views 45 hemispheric positions, using 30 second durations, and repeats approximately every half hour through out the night. The gimbal holds co-mounted and bore-sighted visible and SWIR cameras. Accompanying those cameras are ground truth sensors including an additional SWIR camera, PVS-14 night vision system both focused at the horizon and a radiometer to measure the amount of energy being absorbed on the ground. Measuring airglow with respect to spatial, temporal, and seasonal variations will facilitate understanding its behavior and possible benefits, such as night vision and predicting upper atmosphere turbulence.

8178-02, Session 1

SWIR air glow imaging for detection of mesospheric gravity waves

D. C. Dayton, J. Allen, Applied Technology Associates (United States); J. Gonglewski, M. M. Myers, Air Force Research Lab. (United States); R. V. Nolasco, Applied Technology Associates (United States)

It is well known that luminance from photo-chemical reactions of hydroxyl ions in the upper atmosphere (~85 km altitude) produces a significant amount of night time radiation in the short wave infra-red (SWIR) band between 0.9 and 1.7µm wave length. The phenomenon, often referred to as air glow or sky glow, has been demonstrated as an effective illumination source for passive low light level night time imaging applications. It addition it has been shown that observation of the spatial and temporal variations of the illumination can be used to characterize atmospheric tidal wave actions in the sky glow region. These spatio-temporal variations manifest themselves as traveling wave patterns whose period and velocity and direction are related to the wind velocity at 85 km as well as the turbulence induced by atmospheric vertical instabilities. In this paper we present analysis methods to extract information about mesospheric air flow from the air glow gravity wave images.

8178-03, Session 1

Investigations of SNR for a short-wave infrared intensity interferometer

D. C. Dayton, Applied Technology Associates (United States); J. Murray-Krezan, J. Gonglewski, Air Force Research Lab. (United States)

Intensity interferometery holds tremendous potential for remote sensing of space objects. Whereas spatial resolution of imagery obtained from earth-based observatories is typically limited by both the size of the primary mirror and atmospheric effects, intensity interferometers (IIs) are relatively unaffected by atmospheric distortions and their effective apertures can be substantially larger than is practical for traditional observatories. Most intensity interferometer measurements have been performed in the visible region due to wellknown issues of poor signal to noise ratios and the performance of detectors in the visible spectral bands. In fact the short-wave infrared (SWIR) spectral band is relatively unexplored for II applications.

In this paper we explore the measurement signal to noise ratio (SNR) for a notional SWIR intensity interferometer. Our study goes beyond the most basic SNR equations of II, and analyzes atmospheric effects, sky backgrounds, and detector characteristics-considering the current state-of-the-art for experiments in the short-wave infrared spectral region.

8178-04, Session 1

Validation of the background simulation model MATISSE: comparing results with MODIS satellite images.

K. Stein, C. Schweitzer, N. Wendelstein, Fraunhofer-Institut für Optronik, Systemtechnik und Bildauswertung (Germany); L. Labarre, ONERA (France)

Generally available satellite images, e. g. from the MODIS sensor, provide data in spectral bands, which are suitable for remote sensing applications and earth surface observations. However, for some applications different bands as well as specific cloud formations for a certain region may be of interest, thus making the simulation of background data essential. Therefore, the software MATISSE ("Advanced Modeling of the Earth for Environment and Scenes Simulation") proved to be the appropriate tool. MATISSE is an infrared background scene generator developed by ONERA for computing natural background spectral radiance images including atmosphere, sea, land and high and low altitude clouds. In order to validate the model, comparisons with MODIS satellite data have been carried out using images in available spectral bands. The investigations comprised selected surface structures like sea, desert, lowland (dry) and highlands (humid). Furthermore, different standard cloud types have been tested. In general, the results on radiance images show a good correlation between original MODIS image and the MATISSEsimulation.

This paper focuses on comparing results between simulated MATISSE radiance images and the MODIS observations. Based on this, possible sources of error and the limits of the model are discussed.

8178-05, Session 1

Multiresolution infrared optical properties for Gaussian sea surfaces: comparison against the MIRAMER campaign measurements in solar glint configurations

S. Fauqueux, S. Langlois, C. Malherbe, K. Caillault, L. Labarre, ONERA (France)

A model of multiresolution sea surface optical property in the infrared has been developed and implemented in the natural background scene generator MATISSE-v2.0. It takes into account spatial variability ranging from 1-meter scale to large scale variability and belongs to the class of methods which estimates a statistical average of local properties. The main characteristic of our method, accounting for multiresolution in the sensor field of view, is the use of nonzero centered Gaussian probability density function. The statistical

properties of the slopes observed by one pixel of the sensor are estimated through a two-scale model combining sub-pixel scale statistics with over scale surface generation. Multiple reflections are neglected but shadowing and hiding effects are modeled through monostatic and bistatic shadowing functions.

This kind of model has intensively been investigated in the low resolution case, but extension to middle and high resolution cases leads to specific problem. The law of conservation of energy for any resolution and the convergence of the optical properties from high to low resolution case when surface size increases have been checked. Optical properties are in good agreement with the ones obtained by a reference model, based on the numerical simulation of all scales of the rough sea surface, from gravity to capillary waves: the general shape and amplitude are well retried except for grazing angles, where the influence of inner and mutual multiple reflections and adjacent shadowing in the high and low resolution cases has still to be investigated.

To improve our model validation from an experimental point of view, we face it against images of sea surface background signatures, collected during the MIRAMER field campaign (Mediterrenean sea, 2008). Various kinds of scenarios were defined and realised. We focus on Atalante on-board measurements (extremely grazing angles) and solar glint configurations, especially on sunrise and sunset. Environmental measurements such as wind speed and direction, aerosols visibility, atmospheric profile and sea temperature are used as input parameters of the modelling. The sun glint extension and average radiance vertical profile are well retrieved. Nevertheless, our model does not perform the entire variability of measured radiance: rare but higher values are not carried out by the model. Using a non-official sub-meter version of the code, the granularity of the simulated and measured images are visually similar.

8178-06, Session 1

On the characterization of IR signature of small surface crafts

D. Dion, Jr., Defence Research and Development Canada, Valcartier (Canada); V. Tremblay, AEREX avionique inc. (Canada)

Small surface crafts (SSC) like Zodiac and Rigid Haul Inflated Boat (RHIB) can represent real threats to large ships. The deadly attack of USS Cole by terrorists on a RHIB a decade ago was a trajic demonstration of what can happen. Better knowledge of the SSC signature in the IR and visible wavelengths is still required today to develop high-performance detection techniques. The signature of SSC heading toward you is complex to characterize as it is usually dominated by elements generated by the boat interaction with the environment (e.g. foam, wakes, solar reflections against de SSC, etc.). In the presentation, SSC detection is discussed and the significance of the various signature elements are assessed and compared using measurements in the mid- and long-wave IR bands.

8178-07, Session 2

91

Marine boundary layer investigations in the False Bay, supported by optical refraction and scintillation measurements

A. N. de Jong, TNO Defence, Security and Safety (Netherlands)

The knowledge on the marine boundary layer is of importance for the prediction of the image quality obtained from long range targets. One property of the boundary layer, that can be studied rather easily is the vertical temperature profile. This profile can be compared with the profile, as predicted by the generally accepted Monin-Obukhov (M-O) similarity theory, which is applied in the EOSTAR model. This model also predicts the atmospheric turbulence profile, for which a validation can be done by means of scintillation measurements. Along these lines we explored the data from the year-round FATMOSE experiment, arranged over the False Bay (South-Africa). Because of the large amount of refraction and scintillation data, supported by extensive data from local weather stations, we could select the conditions for which the M-O theory is valid and determine the particular conditions where



this theory is failing. In the paper samples of predictions (including raytracings in non-homogeneous conditions) and measurements along the 15.7 km path are shown.

8178-08, Session 2

Stability and height dependant variations of the structure function parameters in the lower atmospheric boundary layer investigated from measurements of the long-term experiment VERTURM (vertical turbulence measurements)

D. Sprung, P. Grossmann, E. Sucher, K. Weiss-Wrana, K. Stein, Fraunhofer-Institut für Optronik, Systemtechnik und Bildauswertung (Germany)

Operation and design of electro-optical systems are affected by atmospheric optical turbulence quantified by the refractive index parameter Cn². Regarding wave propagation in the visible and infrared, Cn² is a function of height, dependant on temperature, pressure, and the structure temperature function parameter CT². The longterm experiment VERTURM (vertical turbulence measurements) was designed to characterize the vertical variations of optical turbulence up to 250 m in the lower atmospheric boundary layer for a moderate typical central European climate. Since May 2009 two independent measurement systems have been operated in a flat pasture site in north-western Germany. In the atmospheric surface layer at a tall tower sonic anemometer measurements are performed on four discrete heights between 4 and 64 m providing information about atmospheric stability and turbulence. CT² is derived. From 50 to 250 m a SODAR-RASS system (Sound Detection and Ranging - Radio acoustic sounding system) yields every half an hour profiles of CT². Additional direct measurements of Cn² have been performed near the ground using a laser scintillometer. First results of the 3 measurement systems are presented. Vertical profiles and stability dependence are analysed in respect of Monin-Obukhov-similarity theory (MOST). Differences in the measurement systems and the expected height variations are discussed.

8178-09, Session 2

Ground-based solar astrometric measurements during the PICARD mission

A. Irbah, M. Meftah, Ctr. National de la Recherche Scientifique (France); T. Corbard, Observatoire de la Côte d'Azur (France); R. Ikhlef, Ctr. de Recherche en Astronomie, Astrophysique et Géophysique (Algeria); F. Morand, P. Assus, Observatoire de la Côte d'Azur (France); M. Fodil, Ctr. de Recherche en Astronomie, Astrophysique et Géophysique (Algeria); M. Lin, P. Lesueur, G. Poiet, Lab. Atmosphères, Milieux, Observations Spatiales (France); C. Renaud, Observatoire de la Côte d'Azur (France)

PICARD is a space mission developed mainly to study the geometry of the Sun. The satellite was launched in June 2010. The PICARD mission has a ground program which is based at the Calern Observatory (Observatoire de la Côte d'Azur). It will allow recording simultaneous solar images from ground. Astrometric observations of the Sun using ground-based telescopes need however an accurate modelling of optical effects induced by atmospheric turbulence. Previous works have revealed a dependence of the Sun radius measurements with the observation conditions (Fried's parameter, atmospheric correlation time(s) ...). The ground instruments consist in SODISM II, replica of the PICARD space instrument and MISOLFA, a generalized daytime seeing monitor. MISOLFA will allow us to analyze atmospheric turbulence optical effects on measurements performed by SODISM II. It will give estimations of the coherence parameters characterizing wave-fronts degraded by the atmospheric turbulence (Fried's parameter, size of the isoplanatic patch, the spatial coherence outer scale and atmospheric correlation times). The monitor will also estimate optical turbulence profiles. MISOLFA is founded on the observation of Angle-of-Arrival

(AA) fluctuations. This paper will give an overview of the ground based instruments of PICARD. Some results obtained from observations performed at Calern observatory in 2011 will be then presented.

8178-10, Session 2

Coherence of Bessel beams propagating in turbulent media

I. P. Lukin, V.E. Zuev Institute of Atmospheric Optics (Russian Federation)

In this article the coherence of Bessel beams in the turbulent atmosphere are analyzed. The problem analysis is based on the solution of the equation for the mutual coherence function (the second-order field moment) of a Bessel beam of optical radiation. For mean irradiance of a Bessel beam the condition which can be considered as quantitative criterion of possibility of formation of the given beam in a turbulent atmosphere is derived. The features of coherence of Bessel beams in the turbulent medium in comparison with the similar characteristic of plane wave and spherical wave are in detail studied. Let's investigate the Bessel optical beam formation in the turbulent medium, large-scale in comparison with the wavelength of optical radiation. The scale of the modulus of the complex degree of coherence of a Bessel beam from a difference of cross-section coordinates allows calculating an estimation of the spatial coherence radius of optical radiation in a random inhomogeneous medium. Results of numerical calculations of the modulus of the complex degree of coherence of a Bessel beam on its optical axis show to the sensitivity of a functional form of the given characteristic to level of fluctuations in a turbulent atmosphere. At low levels of fluctuations in a turbulent atmosphere the coherence in a Bessel beam higher, than in a plane wave, but lower, than in spherical wave, nevertheless in this case the modulus of the complex degree of coherence of a Bessel beam is closer to the same characteristic of a plane wave. At high levels of fluctuations in a turbulent atmosphere the modulus of the complex degree of coherence of a Bessel beam becomes closer to the similar characteristic of a spherical wave. For extremely low levels of fluctuations in a turbulent atmosphere the dependence of the modulus of the complex degree of coherence of a Bessel beam from difference of cross-section coordinate demonstrates oscillating character. At high levels of fluctuations in the turbulent medium the modulus of the complex degree of coherence of a Bessel beam is described by the one-scale curve close to square-law exponent, and practically with small difference from the modulus of the complex degree of coherence of a spherical wave.

8178-11, Session 2

92

Statistical properties of density fluctuations in the atmosphere

F. V. Shugaev, L. S. Shtemenko, O. I. Dokukina, O. A. Nikolaeva, T. A. Petrova, O. A. Solenaya, Lomonosov Moscow State Univ. (Russian Federation)

The full system of the Navier- Stokes equations is used in order to analyze the spectrum of density turbulent fluctuations on the basis of parametrix method (Section 1). As known, the fundamental solution to those equations is an oscillatory one. An unsteady flow is investigated near vortical structures (vortex rings and vortex tubes). As shown, the frequency spectrum depends on the flow characteristics. Explicit expressions are obtained for oscillation frequency in various points of the flow. As far as we use an iterative technique, we compare the results of the successive iterations (up to the third one). The numerical procedure which reduce differential equations to integral ones allows us to reveal fine patterns of the flow. The temporal evolution of the frequency spectrum is analyzed for decaying turbulence. We introduce source-like terms in the right-hand side of the Navier-Stokes system while studying oscillatory solutions that do not decay. We take into account experimental data on beam propagation in the atmosphere. As a result, data are presented on the frequency spectrum of turbulent fluctuations depending on the size of eddies and their intensity.

These data allow us to analyze the characteristics of the Gaussian beam propagation through the turbulent atmosphere with the aid



of the parabolic equation method (Section 2). Numerical results are presented.

The theory of laser schlieren technique is set forth in Section 3. A general case of 3D flow is considered. We suppose turbulence to be homogeneous and isotropic. The problem is reduced to the Fredholm equation of the first kind. Numerical procedure is described. Experimental data are given on grid turbulence in a shock tube.

8178-12, Session 3

Increase of correction efficiency of turbulent distortions in AOS on basis of measurements by the Shack-Hartmann wave-front sensor

V. P. Lukin, L. V. Antoshkin, L. N. Lavrinova, V. V. Lavrinov, V.E. Zuev Institute of Atmospheric Optics (Russian Federation)

Increase of correction efficiency of turbulent distortions in AOS on basis of measurements by the Shack-Hartmann wave-front sensor Àntoshkin L.V., Lavrinov V.V., Lavrinova L.N., *Lukin V.P.

*Tomsk State University, Tomsk, Russia

V.E. Zuev Institute of Atmospheric Optics SB RAS, Tomsk, Russia, lukin@iao.ru

The propagation of laser radiation through atmosphere is accompanied by change of light field under influence of turbulence and presents the casual process. To correction of turbulent distortions are applied the adaptive optical systems (AOS) including the Shack-Hartmann wave-front sensor and the flexible mirror. In plane of image registration by sensor are placed the video camera as the receiver. The video cameras constructed on the basis of CDD and CMOS technologies differ with characteristics of photosensitivity and noise. It is executed the comparison analysis of errors at definition of coordinate centroids by Shack-Hartmann sensor for optical beams with various distributions of the intensity for given types of video cameras.

For working with not bright astronomical objects is necessary to increase the time of information accumulation (exposition). The volume of accumulation time influences on the accuracy of the working of adaptive optical system. It are examined the regime of the instantaneous set and the regime of frames accumulation. The regime of frames accumulation proves the necessity of the advancing adaptive correction.

Adaptive system including the Shack-Hartmann wave front sensor and the flexible mirror provides the correction of the distortions which have been defined in the previous time but these distortions change to the time of their correction by system. The analysis of the turbulence during time interval allows to make the forecast of turbulent distortions in future time and to use it bringing the amendment in phase distribution. The quality growth of adaptive correction may be reached also by preparation of mirror surface on basis of the forecast of wave front surface in following time on turbulence parameters and on the cross forming of wind speed which have been defined on basis of previous measurements of Shack-Hartmann wave-front sensor. It are presented the ways of realization of advancing adaptive correction on the basis of sensor measurements.

8178-13, Session 3

Free space propagation of wide band light pulses

O. V. Tikhomirova, V.E. Zuev Institute of Atmospheric Optics (Russian Federation)

Progress in the development of laser systems generating the optical pulses of femtosecond and shorter duration calls attention to issues related to the spatial-temporal transformation of the shape of the pulses propagating in free space. However, as a rule, propagation of such pulses is analyzed under an assumption (explicit and implicit) that the pulse spectrum is narrow band of frequencies. As the spectrum width increases with pulse shortening the calculations in the narrow-band signal approximation can lead to unacceptably large errors and unphysical results (Porras M.A. Phys. Review E. 1998. V.58. P.1086

[1]; Peng R., Fan D. Opt. Communications. 2005. V.246. P. 241 [2]). In [1, 2] the broadbandness effect on pulse propagation was studied for the mode of the far zone of beam diffraction and izodiffraction for completely coherent radiation. This paper presents the results of investigation of propagation of the broadband pulses unrestricted on the diffraction mode of a beam. It is shown that the signal broadbandness can be ignored in analysis until the durations for the coherent-time pulse. An extreme case of propagation of the deltapulse with an unlimited radiation spectrum is considered. It is obtained that the delta-pulse beam of collimated radiation does not undergo diffraction. There is no diffraction also when focusing of the delta-pulse radiation; the beam becomes singular in the area of focus, its intensity at the focal point increases indefinitely.

8178-14, Session 3

Applications of adaptive optics in coherent laser array techniques

Y. Zheng, F. Shen, X. Li, Institute of Optics and Electronics (China)

The coherent laser array (CLA) has been proposed and extensively implemented in applications such as transceivers of free space optical communications (FSOC) and coherent beam combination of master oscillator power amplifiers (MOPAs-CBC). Comparing with the also usable monolithic schemes in which a large single beam is often applied, the arrayed lasers appears to be more preponderant, because, it could not only enhance the diffraction limit via filling more beamlets rather than expanding the diameter of emergent pupil with difficulty, but also suppress the dynamic phase distortions via individual correction of each sub-aperture. Therefore, the CLA concept would be very beneficial to enhance the quality and intensity concentration of far-field. In CLA experiments, the phasing techniques are the key point and main challenge. Until now, a variety of approaches has been proposed and actualized to do this job, such as the heterodynedetection, self-synchronous & self-reference, multi-dithering, algorithm control, etc. They only aim at the in-phase locking so as to maximize the power concentration of far-field. As we know, the propagation property of CLA is under the control of its initial phase distribution. Therefore, if the phase in each aperture could be arbitrarily controlled, some novel CLA applications would be developed. For example, the inertia-free beam steering in the optical phased array antenna (OPAA). The realization of arbitrary phasing in CLA is a main goal of our work.

Currently, lots of CLA experiments are fiber-laser-seeded because the phasing is usually implemented by fiber-based modulators, such as the LiNbO3 crystal and the fiber-wrapped PZT element. A limitation is that they can only provide piston modulation. However, while the turbulence is strong, the phase errors may vary over the finite diameter of the beamlets, tip-tilt corrections will also be needed. For this reason, we've innovatively introduced the adaptive optics (AO) in CLA field. The best feature of AO is embodied by its particular phase modulator (PM), an active segmented mirror (ASM). Comparing with the fiberbased PMs, the ASM mainly possesses three advantages: first, it could simultaneously implement both piston and tip-tilt modulations, and thus it is more powerful and competent for the corrections of higher orders phase aberrations; second, it could spatially steer the beamlets, and thus the fiber laser won't be the only option for seed source, various choices, such as the solid laser, gas laser, diode laser, etc. may also be usable; third, the ASM could endure high power laser and be suited to different wavelength, therefore, it could be directly equipped at the system's output end. Generally, by use of ASM, the applications of CLA could be extended to a wider domain. One potential technique would be the projection system of high power solid laser array. Some other usages, such as the optical phased array antenna (OPAA), master oscillator power amplifier (MOPA), spatial beam shaping, etc. could also be developed based on AO.

The preliminary investigations of these attractive concepts have been experimentally accomplished in our seven-channel laser array testbed. A hexagonal pyramid is employed to align seven spatial beamlets into a dense array with 0.625 fill factor, and a custom-made ASM is equipped behind to provide proper modulations. There are three main achievements of our experimet:

1. we have accomplished the in-phasing control of CLA via SPGD algorithm. The atmospheric turbulence, simulated by an electric heater, has been well corrected. The work in this part demonstrates the usage of AO in coherent beam combination.

93



2. We have proposed a novel piston detection method based on the zero-order interference fringe (ZOIF) phenomenon, and further realized the arbitrary phasing of laser array. In this experiment, the proper scanning of far-filed has been carried out. The work demonstrates the beam steering in OPAA could be implemented by AO.

3. The experimental generation of the dark hollow beam has been accomplished. This work demonstrates the CLA would be a promising technique for beam shaping.

8178-15, Session 3

Study of turbulent supersonic flow based on the optical and acoustic measurements

V. A. Banakh, D. A. Marakasov, R. S. Tsvyk, V.E. Zuev Institute of Atmospheric Optics (Russian Federation)

Aircraft and missiles moving in the atmosphere with supersonic velocities form air flows of a complicated spatial structure, in which compression shocks of different configurations and intensities arise. Since an air flow is strongly spatially inhomogeneous, the air density in the flow experiences random pulsations much exceeding turbulent pulsations of the air density in the atmosphere. Mean characteristics of supersonic flows are investigated rather well both theoretically and experimentally, but characteristic properties of turbulence in a supersonic flow are studied insufficiently.

In this research field, intensity fluctuations of the laser beam passed through a model plane layer of a turbulent flow and the beam propagating through a jet of a jet engine have been studied experimentally ((Joia et al, 1997, 1995) and (Dmitriev et al, 2004, Sirazetdinov et al, 2001), respectively). However, these results (Joia et al, 1997, 1995, Dmitriev et al, 2004, Sirazetdinov et al, 2001) correspond to subsonic velocities of studied flows, and for their interpretation it is sufficient to use the results of the theory of incompressible fluid mechanics (Monin & Yaglom, 1971, 1975) and optical radiation propagation in such turbulent media (Gurvich et al, 1976, Zuev et al, 1988). In case of supersonic flows, for the interpretation of measured results, it is necessary to take into account not only temperature fluctuations, but also pressure fluctuations, as well as the strong spatial inhomogeneity of the flow. In recent years, the theoretical papers were published, in which the authors undertook attempts to construct an electrooptical model of parameter fluctuations in compressible gas flows (Offer Pade, 2001, 2003, 2004, 2005). However, the results obtained can be considered only as an initial stage of the study of radiation propagation in supersonic flows. In (Offer Pade, 2001, 2003, 2004, 2005), only the variance of phase fluctuations of an optical wave passed through a supersonic flow was calculated and the variance of gas density fluctuations in a flow was estimated. The calculations were based on the Fluent Dynamic 6 turbulence model.

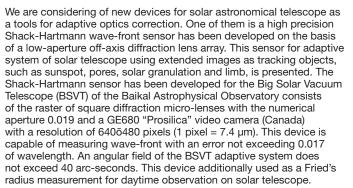
The existing theoretical models of turbulence of compressible flows can be found, in particular, in (Yoshizawa, 1995, Smits & Dussauge, 1996, Canuto, 1997). However, in this field there is no versatile model similar to the case of developed turbulence of incompressible flows (Monin & Yaglom, 1971, 1975).

The talk presents the review of the results of both experimental and theoretical studies of optical turbulence in supersonic flows performed by authors. The experiments on laser beam propagation through supersonic flows were conducted in T-326 and T-313 wind tunnels of the Institute of Theoretical and Applied Mechanics of the Siberian Branch of the Russian Academy of Sciences. The built theory of laser beam propagation through a supersonic flow was based on dynamical models of the Fluent 6.0 software. The transport equations for calculation of turbulent parameters were selected according to the k-e ring model.

8178-16, Session 4

Development of adaptive optics devices for solar telescope

V. P. Lukin, L. V. Antoshkin, N. N. Botugina, O. N. Emaleev, P. A. Konyaev, E. A. Kopylov, V.E. Zuev Institute of Atmospheric Optics (Russian Federation)



The second device is image quality analyser. Efficiency of the adaptive optical in system of the imaging is valued by quality of the updated image. For analysis quality images on output of BSVT is designed hardware-program complex, in composition which enters the optical system of the carrying the image from the second focus (f = 25,7i) BSVT in plane of the registrations, video camera GE680 with Ethernet channel of the issue to video information in computer and specialized software package. Due to efficient algorithm of the parallel processing signal analyzer can work the real-time to registrations of the image. The frequency of the frames of the video camera depends on time of the exposures. Time to exposures of the frame is adjusted within the range of from 30 ìêñ up to 10 ìñ. The maximum velocity of work under the real-time registrations is 200 frames per second.

8178-17, Session 4

94

Compensating aberrations of a 6 inch concave membrane mirror

I. Buske, Deutsches Zentrum für Luft- und Raumfahrt e.V. (Germany); P. Becker, RheinAhrCampus Remagen (Germany)

Large telescope apertures (>10 m) are currently the limiting factor of photon collecting applications like remote sensing LIDAR or deep space laser communication. Typical imaging applications are earth observation telescopes from GEO orbit and astronomy in the NIR spectrum. To be compatible with current launch capabilities general requirements for all spaceborne telescopes with large apertures are lightweight (< 3 kg/m²) deployable mirrors. Membrane mirrors are ideally suited for large optics with an inherent low mass to area ratio. Different investigations are done to build primary mirrors based on reflective membranes, where very large structures are possible with acceptable optical quality.

Our membrane mirror demonstrator consists of a 6" nitrocellulose pellicle. The membrane is pre-stressed and coated with a silver layer including anti-oxide layer. The mass to area ratio (~5 kg/m²) was measured including the ring carrier. To realize a concave shape a small difference of pressure (0.2 mbar) between the front and the back side of the membrane sheet was applied. The focal length can be easily shifted by controlling the pressure to realign the image plane. Primarily distortions of astigmatism and spherical aberrations were measured. The drawbacks of sensitivity of large membranes to acoustic disturbance, to ambient pressure and temperature, and the variable optical quality will be presented.

The characterization of the membrane mirror regarding its optical performance was investigated under normal ambient conditions. The measurement setup consisted of a near field wavefront sensor and a far field camera. An initial wavefront distortion of PV 26 μ m and RMS 5 μ m over 80% of the 6 inch aperture was measured.

The distorted wavefront generated by the lightweight membrane mirror can be corrected up to a certain degree using a wavefront correction element in the internal optical path. This active element should be able to create low order deformations comparable to the aberrations of the lightweight membrane mirror. Therefore we chose a deformable membrane mirror to compensate the major part of the wavefront error. Slight defocusing of the lightweight membrane mirror did not affect the type and strength of the wavefront aberrations. A wavefront sensor-less aberration correction can be used to compensate the slowly varying wavefront distortions. The figure of merit (FoM) control signal was defined by a power-in-the-bucket measurement, where the diameter of the bucket (30 μ m) was determined by the diameter of the



diffraction limited Airy disc. An iterative optimization routine based on an evolutionary algorithm search algorithm was developed to increase the figure of merit value relative to the initial condition.

As a typical result, this iterative method evaluated 30 x 30 adaptive mirror states which consumed 72 seconds totally. After the optimization the far field spot showed a high intensity spot comparable with an Airy function intensity distribution. Due to the setup only the center part of the Gaussian measurement laser beam has an impact of the aberrations of the lightweight membrane mirror. The wavefront was reconstructed over a reduced aperture of 90 mm to fit the calculated PSF with the camera far field intensity distribution. The corresponding wavefront distortions were compensated to PV 2.5 μ m and RMS 0.4 μ m.

8178-18, Session 4

New phasor reconstruction for speckle imaging

G. C. Dente, GCD Associates (United States); M. L. Tilton, Boeing-SVS, Inc. (United States)

We will develop and then compare object spectrum phasor reconstruction results for several speckle imaging approaches. Each phasor reconstruction algorithm results from minimizing a very naturally defined weighted-least-squares error function. Once we pick a phasor-based error function, the remaining steps in our algorithms are developed by setting the error function variation, with respect to each phasor element, to zero. The resulting coupled nonlinear equations for the minimum error phasor array are then solved iteratively. In the applications, we will specifically compare and contrast three implementations: 1) Knox-Thompson; 2) bispectrum, using only two bispectrum planes; 3) bispectrum, using four bispectrum planes. In each application of the three approaches, we first calculate the modulus of the object spectrum using a Wiener-Helstrom filter to remove the speckle transfer function. The methods then differ only in their object spectrum phasor reconstructions. In the simulations, we will implement all three methods on a simple object at low photonper-frame light levels. Next, we will apply the methods to a complex extended object. Although we develop and minimize error functions for three specific speckle methods, the approach readily generalizes to other cases.

We emphasize that our algorithms directly solve for the phasor array that minimizes a phasor-based error function. Once we have selected the error function, our converged solution for the phasor array represents a true minimum for this error function; no further improvements in the phasor array reconstruction are possible. For these reasons, these new algorithms should outperform methods in current use.

8178-19, Session 4

Compensating atmospheric distortions of point sources and extended objects through an adaptive iterative procedure

C. Scheifling, G. Marchi, Fraunhofer-Institut für Optronik, Systemtechnik und Bildauswertung (Germany)

In this paper we introduce a technique to correct turbulence which relies on the combined use of a deformable mirror controlled by a Stochastic Parallel Gradient Descent (SPGD) algorithm and an image quality measurement. This correction procedure differs from the conventional adaptive optics technique in the sense that the compensation for the aberrations will be done without using any information about the wavefront.

Depending on the correction to be done different quantities, modified by the atmospheric turbulence could be used as image quality parameter. In an iterative process the image quality will be evaluated and used to drive and modify the shape of the deformable mirror correspondingly.

This procedure is now being tested both for the correction of extended as well as point source objects. In our experiment tests two types of deformable mirrors (DM) are being used. The first DM is a membrane



mirror which has 37 actuators with a maximum stroke of 1.5 $\mu m,$ 15 mm diameter and a bandwidth of 500 Hz and will be used for correcting extended objects. The second DM is a bimorph one and is used for the experiment with the laser beam.

In order to enhance the speed capability of the SPGD algorithm by the correction of extended objects a parallel computing architecture CUDA (Compute Unified Device Architecture) will be taken into account. Preliminary results are presented.

8178-20, Session 4

Software-based turbulence mitigation of short exposure image data with motion detection and background segmentation

C. S. Huebner, Fraunhofer-Institut für Optronik, Systemtechnik und Bildauswertung (Germany)

The degree of image degradation due to atmospheric turbulence is particularly severe when imaging over long horizontal paths since the turbulence is strongest close to the ground. The most pronounced effects include image blurring and image dancing and in case of strong turbulence image distortion as well. To mitigate these effects a number of methods from the field of image processing have been proposed most of which aim exclusively at the restoration of static scenes. But there is also an increasing interest in advancing turbulence mitigation to encompass moving objects as well. Therefore, in this paper a procedure is described that employs block matching for the segmentation of static scene elements and moving objects such that image restoration can be carried out for both separately. This way motion blurring is taken into account in addition to atmospheric blurring, effectively reducing motion artefacts and improving the overall restoration result. Motion-compensated averaging with subsequent blind deconvolution is used for the actual image restoration.

8178-21, Poster Session

95

Coherent beam combining of collimated fiber array based on target-in-the-loop technique

X. Li, C. Geng, X. Zhang, C. Rao, Institute of Optics and Electronics (China)

Coherent beam combining (CBC) of fiber array is a promising way to generate high power and high quality laser beams. Target-in-theloop (TIL) technique might be an effective way to ensure atmosphere propagation compensation without wavefront sensors. In lots of current CBC systems, achieving phase-locking state among beamlets is the only consideration, where LiNbO3 phase modulators are widely used for piston-type error correction. In fact, laser beam propagation through atmosphere generates tip/tilt-type phase errors, which drop CBC effects seriously.

In this paper, we present very recent research work about CBC of collimated fiber array using TIL technique at the Key Lab on Adaptive Optics (KLAO), CAS. A novel Adaptive Fiber Optics Collimator (AFOC) composed of phase-locking module and tip/tilt control module was developed and tested at KLAO. It is showed that the performance of this kind of AFOC can be used for CBC. An experiment setup of CBC with AFOCs was established, include the a fiber source, a fiber splitter, three collimated AFOCs, a imaging lens with long focus length, a target screen at focal point, and an imaging sensor in local point to measure scatting light from target screen. Feedback control is realized using stochastic parallel gradient descent (SPGD) algorithm. The CBC based on TIL with piston and tip/tilt correction simultaneously is demonstrated. And the beam pointing to locate or sweep position of combined spot on target was achieved through TIL technique too. Although the experiment in this paper is performed in short distance and indoor only, the goal of our research is achieve multi-element CBC for long-distance transmission in atmosphere.

8178-22, Poster Session

A novel wavefront sensing technique for high speed atmospheric measurement based on digital micromirror device

P. Yang, S. Wang, Institute of Optics and Electronics (China); M. Ao, Univ. of Electronic Science and Technology of China (China); B. Xu, Institute of Optics and Electronics (China)

We propose a novel wavefront sensing technique based on the principle of binary-aberration-mode filtering and detection. Rather than using the Zernike polynomials, the orthogonal binary two-dimensional Walsh functions are transferred to circular mode-field-fitted Walsh functions and used to expand the wavefront aberrations. A Digital Micromirror Device (DMD) which can provide a modulation rate over 30 kHz is employed as an intensity spatial light modulator (SLM). It generates each of the intensity modulation patterns prescribed by the mode-field-fitted Walsh functions to modulate the intensity of the incident wavefront before it is focused to impinge on a singlemode optical fiber. The single-mode optical fiber, as a spatial mode filter, supports only fundamental binary aberration mode whose field distribution must be approximated by the Gaussian distribution. A detector collects the amount of the light intensity after each modulation. By building the relationship between the light intensity and the binary-aberration-mode coefficients, the coefficients can be calculated. This technique turns the complex two-dimensional wavefront sensing into simple intensity detection. Therefore, many constrains, such as low response frequency and weak far-infrared detection capability of most array devices can be easily avoided just by adopting a single photo detector such as a photodiode. Thus, this technique is especially suitable for weak and far-infrared light detection. The results demonstrate that the wavefront reconstruction with the binary aberration modes has a high precision. The RMS of residual wavefront aberrations decreases from 1 down to 0.05. The measurement frequency can achieve 1 kHz. We also find that the light intensity inhomogeneity has no obvious effect on the results. Thanks to these advantages, the technique can easily satisfy the demands of many atmospheric measurements and has a promise application in atmospheric fields.



Wednesday-Thursday 21-22 September 2011 Part of Proceedings of SPIE Vol. 8179 SAR Image Analysis, Modeling, and Techniques XI

8179-01, Session 1

Sentinel-1A and Sentinel-1B CSAR status

P. Snoeij, M. Brown, M. W. J. Davidson, B. Rommen, N. Floury, European Space Research and Technology Ctr. (Netherlands); D. Geudtner, Canadian Space Agency (Canada); R. Torres, European Space Research and Technology Ctr. (Netherlands)

The ESA Sentinels constitute the first series of operational satellites responding to the Earth Observation needs of the EU-ESA Global Monitoring for Environment and Security programme. The GMES space component relies on existing and planned space assets as well as on new complementary developments by ESA. In particular, as part of the GMES space component, ESA is currently undertaking the development of the Sentinels mission families. Each Sentinel is based on a constellation of 2 satellites in the same orbital plane. This configuration allows to fulfil the revisit and coverage requirements and to provide a robust and affordable operational service. The launch of the 2nd satellite is scheduled 18 months after the launch of the 1st spacecraft of the constellation. The lifetime of the individual satellite is specified as 7 years, with consumables allowing mission extension up to 12 years. The lifecycle of the space segment is planned to be in the order of 15-20 years. The strategy for Sentinel procurement and replacement over this period is being elaborated, but will likely result in a need for 4-5 satellites of each type if the desired robustness for the service that GMES will provide is to be achieved.

This paper will describe the operational and observational capabilities of the Sentinel-1 mission based on the user requirements, including potential emergency requests. An example of a pre-defined mission timeline for each and every cycle will be given.

Sentinel-1 is designed to work largely in a pre-programmed conflictfree operation imaging all global landmasses, coastal zones, shipping routes in full resolution and covering the global ocean with imagettes. This way reliability of service consistent with the demand of operational services can be achieved and a consistent long-term data archive built for applications based on long time series. Sentinel-1 revisit and coverage are dramatically improved with respect to ERS-1/2 and ASAR. The two-satellite constellation offers six days exact repeat and the conflict-free operations based on a main operational mode allow exploiting every single data take. In the framework of international interoperability agreements the effective revisit and coverage performance could be further improved by access to the planned Canadian SAR Constellation.

User service requirements are defined in terms of data availability, coverage & revisit, timeliness and characteristics of data products. To deal with user requirements for both high and medium resolution data traditional SAR system designs include different operational modes that either optimize the spatial resolution (at the expense of the swath, hence the coverage) or the swath width (at the expense of the resolution). Taking account of data access through GMES to complementary national very high-resolution SAR missions (TerraSAR-X by DLR/Astrium GmbH, Cosmo-SkyMed by ASI) Sentinel-1 has been designed to address primarily medium resolution applications having a main mode of operation that features a wide swath (250 km) and a medium resolution (5 m x 20 m). As the operation follows a pre-programmed conflict-free scenario there is no need to make data acquisition requests for this mode. This Interferometric Wide Swath Mode operates for a maximum of 25 minutes per orbit. The remaining time the instrument operates over the open ocean in the Wave Mode providing sampled images of 20 x 20 km at 100 km along the orbit with low data rate and 5 x 5 meter spatial resolution. It is expected that Sentinel-1A be launched in 2013 and Sentinel-1B about 18 months later.

The main mission product of Sentinel-1 is a dependable data flow day-and-night under all weather conditions following a systematic, pre-programmed and conflict-free operational scenario with data dissemination in near-real time. In its main operational mode the interferometric wide swath mode operating 25 % of the time (corresponding to 25 minutes operation time per orbit) it provides complete global coverage of all land surfaces, sea ice, coastal zones

96

and North Atlantic shipping routes at least once per 12 days for each of the two satellites. For high priority areas such as Europe, Canada and the Northern Atlantic revisit frequencies can be achieved ranging from 4 to 2 days per satellite depending on latitude. Special effort is made to support rapid mapping for emergency response services. Global average response time is largely defined by orbit configuration and swath width and amounts to about 5 days for a single satellite and 2.5 days for the 2 - satellite constellation. The actual performance depends on latitude, worst at the equator, best at high latitude. Over the open ocean, except the North Atlantic, data are collected in the wave mode operating all the time. This provides images of 20 by 20 km separated by 100 km for use in data assimilation in global wave models. In order to satisfy the service requirements for Sentinel-1 geographic coverage and temporal re-visit, 2 satellites (Sentinel-1A and 1B) are required.

This paper will present the current status of the satellite and instrument development and will discuss a potential operational scenario for both satellites.

8179-02, Session 1

Comparison of L and C band polarimetric SAR data for the retrieval of soil moisture in the Alps

L. Pasolli, L. Bruzzone, Univ. degli Studi di Trento (Italy); C. Notarnicola, EURAC research (Italy)

The SOFIA project (ESA AO-6280), supported by the Province of Bolzano in the framework of the IRKIS project, aims at investigating the possibility of estimating important biophysical variables in the Alpine area by using advanced state of the art retrieval methods in combination with new generation satellite polarimetric SAR data. Among the others, an important parameter of interest is the soil moisture content. The knowledge on the spatial and temporal distribution of soil moisture has indeed important implications in many application domains, such as flood and landslide prediction, climate change analysis and natural resource management.

Soil moisture retrieval is typically a challenging task, due to the nonlinearity of the relationship between input features (extracted from the microwave signal) and the desired target parameter. In addition to this, one has to take into account the sensitivity of the SAR signal to various target properties (e.g., soil roughness and vegetation coverage) and the influence of topography and land use heterogeneity, especially in mountain areas [1]. All these factors introduce further ambiguity in the SAR signal and thus increase the complexity of the retrieval process. In order to overcome these effects, one may resort on multi-frequency and multi-polarization acquisitions over the scene of interest [2], [3]. Up to now, however, very limited effort has been devoted to the investigation of these strategies for the estimation of soil parameters in mountain environments, thus pointing out the necessity of further research.

As a first analysis in this direction, in a previous contribution we investigated the effectiveness of fully polarimetric RADARSAT2 C-band SAR data for the retrieval of soil moisture in the Alpine area [4]. The retrieval process was carried out by means of an advanced state of the art regression method (the Support Vector Regression) and the integration of additional information on the investigated area obtained from ancillary data (i.e., digital elevation model and optical remote sensing data). The achieved results in the investigated area were promising and pointed out that with the proposed algorithm it was possible to achieve satisfactory estimates of the target parameter in terms of both quantitative accuracy and capability to reproduce the local spatial patterns.

With the aim to further improve our knowledge and analysis on the retrieval of soil moisture content in the Alpine area, in this paper we move the attention on the exploitation of L-band SAR data. The interest in this kind of data is motivated by the fact that several research activities carried out in the past have demonstrated that

sensors operating in the low frequency portion of the microwave spectrum (P- to L-band) are particularly suitable to measure the moisture of a soil layer. Again, however, no investigations are proposed in the specific case of mountainous landscapes. In more detail, our analysis aims at: 1) assessing the effectiveness of the proposed retrieval algorithm with different satellite SAR data, namely the L-band data; 2) comparing the estimates obtained with the use of C- and L-band SAR imagery, in order to understand common patterns and eventually discrepances due to the different penetration capability of the signals; and 3) understanding the feasibility of a synergic use of L and C band SAR data (when both available) for improving the retrieval of soil moisture in Alpine areas.

The experimental analysis will be carried out with the use of polarimetric RADARSAT2 (C-band) and ALOS PalSAR (L-band) SAR data. The test site is a small Alpine catchment located in the Mazia valley, Alto Adige, Italy. This area is mainly covered by grassland and has also some forest stands. It is particularly suitable for the analysis thanks to the well representative topographyc, climatic and soil conditions. In addition to this, the valley is well known since object of several research activities and numerous and reliable field reference data are available. A thorough description of the experiments and results will be provided in the final paper.

References

[1] Ulaby, F.T., Moore, R.K., and Fung, A.K., 1986. Microwave Remote Sensing: Active and Passive, vol. II. Norwood, MA: Artech House.

[2] Notarnicola, C., and Posa, F., 2006. "Combination of X, C and L band for retrieval of surface parameters," in Proc. SPIE vol. 6746.

[3] Paloscia, S., Palombini, P., Pettinato, S., and Santi, E., 2008. "A comparison of algorithms for retrieving soil moisture from ENVISAT/ ASAR images," IEEE Transaction on Geoscience and Remote Sensing, vol. 46, no. 10, pp. 3274-3284.

[4] Pasolli, L., Notarnicola, C., Bruzzone, L., Bertoldi, G., Della Chiesa, S., Hell, V., Niedrist, G., Tappeiner, U., Zebisch, M., Del Frate, F., and Vaglio Laurin, G., "Estimation of soil moisture in an alpine catchment with RADARSAT2 images", Applied and Environmental Soil Science, in press.

8179-03, Session 1

Soil moisture mapping using Sentinel 1 images: the proposed approach and its preliminary validation carried out in view of an operational product

S. Paloscia, Istituto di Fisica Applicata Nello Carrara (Italy); N. Pierdicca, Univ. degli Studi di Roma La Sapienza (Italy); C. Notarnicola, EURAC research (Italy); G. Pace, Advanced Computer Systems S.p.A. (Italy); S. Pettinato, Istituto di Fisica Applicata Nello Carrara (Italy); L. Pulvirenti, Univ. degli Studi di Roma La Sapienza (Italy); A. Reppucci, Starlab (Spain); E. Santi, Istituto di Fisica Applicata Nello Carrara (Italy)

A quantitative and accurate estimate of SMC on a global scale is always tricky since local measurements of SMC are strongly affected by spatial variability, besides being time consuming and expensive. In the last decades, a plethora of spatially distributed hydrological models and local scale numerical weather prediction models have been successfully exploited at a range of scales from small catchments to the globe; however, accurate spatial prediction of soil moisture requires proper account for the variability of soil characteristics and climate forcing, and an accurate assessment cannot be made without adequately spatially distributed soil moisture measurements at the scale of interest.

The possibility of measuring SMC on a large scale from satellite sensors, with complete and frequent coverage of the Earth's surface is, therefore, extremely attractive. However, the retrieval of soil parameters from radar measurements is a typically ill-posed problem, because, in general, more than one combination of soil parameters (SMC, roughness, vegetation cover, etc.) has the same electromagnetic response.

At present, most SAR systems onboard remote sensing satellites (e.g., ERS-2, RADARSAT, and Environmental Satellite (ENVISAT)) operate only at the C-band, which is not the best band for retrieving SMC.



At this frequency, this objective is, in fact, still challenging since the effects of surface roughness and, above all, vegetation cover on the backscattering coefficient are high. Therefore, an estimate of spatial variations of moisture with the accuracy required by many applications is still problematic, even when using some a priori knowledge of the meteorological conditions, soil properties, and surface cover, together with correcting procedures for the effects of soil roughness and vegetation. Much better results can be obtained if one's interest lies in measuring temporal variations over a relatively wide area, where the average characteristics of roughness and vegetation cover remain almost unaltered. The aforementioned considerations suggest that multitemporal approaches for retrieving SMC at regional scales from C-band SAR time series can successfully account for surface roughness effects and, to some extent, for low vegetation cover (≤ 1 kg/m2 of the biomass).

The inversion of analytical electromagnetic models (e.g., the Integral Equation Model (IEM) is, generally, a complicated procedure. However, once the forward models have been validated, inversion algorithms that are based on several techniques and make use of single- or multifrequency or multipolarization radar measurements can be developed.

An effective use of the SMC product to be generated from Sentinel 1 data requires an algorithm able to process operationally in near real time and deliver the product to the GMES services within 3 hours from observations. A procedure based on Neural Networks offers the best compromise between retrieval accuracy and processing time. The specific characteristic of the radar (e.g., ground resolutions, incidence angle and polarization mode) must be accounted for when building a suitable training set, taking advantage from real measurements and forward model simulations.

Nonetheless, the frequent revisit time achieved by the Sentinel 1 suggests, as discussed before, to take advantage from a multitemporal approach, whose design can be performed in the frame of Bayes theory of parameter estimation. The multitemporal approach shall be considered an alternative solution for applications with relaxed temporal requirements, but presumably better accuracy, especially for single polarization data which implies an highly ill-posed inversion problem.

The proposed approach to develop an operational SMC product from Sentinel 1 is depicted in this paper. An algorithm based on a NN approach is supposed to be run in quasi real-time, while a multitemporal algorithm runs in parallel to provide a benchmark in terms of accuracy. to support applications with relaxed timeliness requirements and provide a test.

8179-04, Session 1

Effects of SAR resolution on forest backscattering including topography

L. Villard, T. Le Toan, Ctr. d'Etudes Spatiales de la Biosphère (France)

1- INTRODUCTION

At low frequencies such as the P band, the underlying topography over forested regions come mostly with important distortions regarding the backscattered intensity. These distortions makes therefore more difficult the analysis of the link between the backscattering coefficient and geophysical information such as forest biomass. This paper addresses the impact of the ground slopes on the polarimetric SAR observables by means of electromagnetic (EM) simulations and especially in the case where various three dimensional slopes are present within the same resolution cell - in other words when the correlation length of slopes is lower than the pixel size. Indeed if the case of constant slopes have been widely treated in the literature - concerning the geometrical corrections or the EM effects on the dominant scattering mechanisms - the way of these effects are mitigated when the slopes vary rises many questions and is also often encountered, especially for wide resolution SAR. Actually, this issue has been emphasized in our analysis of the P-band airborne data from the TropiSAR campaign over some tropical forest test site in French Guyana. Although its resolution is only 1 meter, we seek the degraded one of about 50 meter in the framework of the performance analysis of the candidate BIOMASS sateliite mission, currently under investigations at ESA (European Space Agency).

2- ELECTROMAGNETIC SIMULATIONS TO ASSESS THE SAR



OBSERVABLES MAIN CHANGES

Generally, our model MIPERS (Multisatic Interferometric & Polarimetric Electromagnetic model for Remote Sensing) has been designed to simulate Pol-InSAR observables and therefore uses a coherent (especially to preserve the interferometric phase) and a descriptive approach. As far as topography is concerned, the scene geometry takes on particular importance.

3. ANALYSIS OF TROPISAR DATA : IMPACT OF A LOWER RESOLUTION ON POLARIMETRIC MEASURES

Two important test sites have been overflown during the TropiSAR campaign. For both, more than 20 plots have been studied and characterize with respect to their biomass. On top of these in-situ measurements, LIDAR airborne data have been acquired and provide us a 1 meter resolution digital elevation model (DEM), from which the 3D characterization of slopes can be derived. Degrading the spatial resolution from 1 to about 50 meter (using multilook averaging), the effect of the resolution loss can be interestingly appreciated, especially regarding polarimetric indicators such as the polarization degree of those derived from the standard polarimetric decomposition. For instance, we show that the slope information from polarimetry can not be retrieved in view of these mitigation effects as well as the $\boldsymbol{\beta}$ orientation angle resulting from the Cloude-Pottier decomposition. The backscattered intensities are shown to be more robust, which enables us to introduce new indicators to assess the topography effects with larger SAR resolution.

8179-05, Session 2

98

Integration of X-SAR observations with data of other remote sensing techniques: preliminary results achieved with Cosmo/ SkyMed announcement of opportunity projects

F. Vespe, Agenzia Spaziale Italiana (Italy); L. Baldini, Istituto di Scienze dell'Atmosfera e del Clima (Italy); G. Celidonio, Telespazio S.p.A. (Italy); C. Notarnicola, EURAC research (Italy); P. Pampaloni, Istituto di Fisica Applicata Nello Carrara (Italy); C. Prati, The ICT Institute Politecnico di Milano (Italy)

The Italian Space Agency is funding 27 scientific projects in the framework of Cosmo/Skymed program (hereafter CSK) . A subset of them are focusing on the improvements of the quality and quantity of information which can be extracted from X-SAR data if integrated with other independent techniques like GPS or SAR imagery in L and C bands. The GPS observations, namely zenith total delays estimated by means of GPS ground stations, could be helpful to estimate the troposphere bias to remove from IN-SAR imagery. Another contribution of GPS could be the improvements of the orbits of Cosmo/SkyMed satellites. In particular the GPS navigation data of the CSK satellites could serve to improve the atmospheric drag models acting on them. The integration of SAR data in L and C bands on the other hand are helpful to investigate land hydrogeology parameters as well as to improve global precipitation observations. The combined use of L, C and X SAR data with different penetration depth could give profiles of land surface properties, especially in forest and snow/ice-packs. For what concern the use of X-SAR imagery for rain precipitation monitoring, particular attention will be paid to its polarimetric properties that we plan to determine aligning the CSK observations with those obtained with ground L and C radars. Anyway the study goals, the approaches proposed, the test sites identified and the external data selected for the development and validation will be described for each project. Particular attention will be paid to single the advantages that the research activities can benefit from the added potentials of CSK system: the more frequent revisiting time and the higher resolution capabilities.

8179-06, Session 2

Analysys of snow changes in alpine regions with X-band data: electromagnetic analysis and snow cover mapping

B. Ventura, C. Notarnicola, T. Schellenberger, M. Zebisch, EURAC research (Italy); R. Ratti, V. Maddalena, L. Tampellini, Carlo Gavazzi Space S.p.A. (Italy)

This paper addresses two main topics related to snow changes and variability in alpine regions: the possibility to infer information on the electromagnetic response of the snow by using the X-band data and to define a snow cover mapping technique based on the difference in backscattering from snow-free surfaces and those covered by wet snow.

The different sensitivity with respect to the various snow conditions is analyzed by considering images collected by COSMO-SkyMed SAR in the framework of the project "SNOX - Snow cover and glacier monitoring in alpine areas with X-band data" funded by the Italian Space Agency. Stripmap PingPong mode, dual polarizations VV-VH images have been acquired on the test site, located in South Tyrol (Northern Italy). Two seasonal periods have been chosen for the analysis: winter season, from November 2010 to February 2011, when the snow physical parameters are characterized by a short-term variation; melting season, from March to May, when the increasing temperature determines rapid changes of the snow on the physical and morphological point of view.

The backscattering response of two different electromagnetic modeling approaches, IEM and Oh model has been analyzed taking into account both the in-situ data collected during the field campaigns carried out in contemporary with COSMO-SkyMed overpasses, and those measured by snow stations. Comparisons between model predictions and measured backscattering coefficients show a good agreement when considering both periods. In order to complete this analysis with other sensor responses, the same methodology has been applied on TERRASAR-X and ASAR images acquired in similar conditions over the same test sites, in particular when images close to the COSMO-SkyMed radar passes are available.

Regarding snow cover mapping, an analysis has been carried out to define a methodology in order to identify and monitor the snow cover area with COSMO-SkyMed images. Based on the difference in backscattering behavior between snow covered and snow free areas, an algorithm has been implemented. The results of the most suitable filtering techniques which allow a clearer distinction of distribution of backscattering coefficients for snow and no-snow areas are discussed. The derived snow maps are presented along with a preliminary quantitative validation analysis obtained through the use of optical images (LANDSAT and SPOT images).

8179-07, Session 2

Use of high resolution SAR data for the monitoring of water resources in Burkina Faso

F. Ciervo, C.U.G.RI. (Italy); G. Di Martino, A. Iodice, Univ. degli Studi di Napoli Federico II (Italy); Y. Koussoube, Univ. de Ouagadougou (Burkina Faso); M. N. Papa, Univ. degli Studi di Salerno (Italy); D. Riccio, G. Ruello, I. Zinno, Univ. degli Studi di Napoli Federico II (Italy)

In this paper we present the preliminary results of a research project devoted to exploit high resolution SAR data for calibrating an appropriate hydrological model. The project is tailored to the scenario of semi-arid regions, characterized by the alternation of rainy and dry seasons with extreme climate conditions. Floods and droughts follow one another with dramatic consequences for the agriculture and the people life. In this scenario, an appropriate water resources integrated management would improve the land productivity and would mitigate the people living conditions. We focus our attention to the Yatenga region in northern Burkina Faso, a Sahelian country struck by a long period of drought from 1970 to 2000.



We present the implementation of a processing chain developed to extract physical information from Cosmo-Skymed data. Most of the processing is performed via open source software. During the project we intend to extract a digital elevation model of the observed area, in order to identify the presence of surface water and to calibrate hydrological models for the impacts prevision of future water management policies [1].

In this paper, major emphasis will be placed on the development of innovative techniques devoted to monitor flooded areas during the rainy season. Direct and inverse models recently developed [2] will be applied to this case study. The whole processing chain is based on fractal models. In particular, for surface description purposes, we use an fBm model, a regular stochastic model defined in terms of two parameters. Such an easy and reliable model allows the expression of the surface spectrum by means of a linear relation in a log-log plane. A relation between image and surface spectrum is also found in order to extract the surface fractal parameters from the SAR images.

The use of fractal techniques allows the monitoring of the water resources in the observed basins. In particular, we implement innovative techniques based on the analysis of the spectral behaviour of the intensity image for identifying the evolution of the observed basins and to monitor the presence of flooded areas during the rainy season. In the final presentation we will also present the hydromorphological watershed characterization based on DEM-processing describing the first processed results of hydrological catchment response.

The obtained results are presented in the frame of a geographic information system, in order to obtain value added maps easily readable for non-expert users.

[1] Arnold JG, Williams JR, Srinivasan R, King KW. 1996. Soil and Water Assessment Tool, Users' Manual. USDA Agriculture Research Service, Blackland Research Center, Texas Agricultural Experiment Station: TX.

[2] G. Di Martino, A. Iodice, D. Riccio, G. Ruello, "A Novel Approach for Disaster Monitoring: Fractal Models and Tools", IEEE Geosci. Remote Sens., vol. 45, pp. 1559-1570, 2007.

8179-08, Session 2

99

An image acquisition planning tool for optimizing information content in image data of spaceborne SAR systems

H. Anglberger, S. Tailhades, H. Suess, Deutsches Zentrum für Luft- und Raumfahrt e.V. (Germany)

In contrast to remote sensing with optical sensors, synthetic aperture radar (SAR) satellites require a slant imaging geometry for image acquisition. This fact and because SAR systems operate their sensors actively emphasize, that the resulting shadowing effects can have crucial influence on the information content of the image product. Additionally, information retrieval is aggravated by layover effects, where e.g. signatures of target objects superimpose with clutter information. Especially for security applications, the prediction of the expected information content and the calculation of layover and shadow regions during mission planning could greatly improve the image product.

To optimize imaging geometry parameters for the image acquisition of a SAR sensor a tool will be presented in this paper, that performs simulation techniques for finding layover and shadow regions in a given complex target scene. Through the simulation of different imaging geometries an optimization of information content can be achieved. The input for this software tool is given through a roughly modeled 3D target scene and up to date state vectors of the space borne SAR system. A high precision orbit propagator predicts the satellite's track and through this, possible imaging geometries for the acquisition of the wanted target region are provided. By using powerful SAR simulation techniques, layover and shadow effects for these imaging parameters can be calculated in real time. In this way the image operator can be assisted in mission planning by analyzing these layover and shadow maps for an optimal information retrieval of the target scene.

The paper briefly presents the underlying simulation concepts for orbit propagation and SAR signature analysis. Afterwards, the overall procedure is described in detail and the methods are verified by applying them to TerraSAR-X system parameters and image data.

8179-09, Session JS1

SAR-based sea traffic monitoring: a reliable approach for maritime surveillance

A. Renga, Univ. degli Studi di Napoli Federico II (Italy); M. D. Graziano, M. D'Errico, Seconda Univ. degli Studi di Napoli (Italy); A. Moccia, A. Cecchini, Univ. degli Studi di Napoli Federico II (Italy)

Maritime surveillance problems are drawing the attention of multiple institutional actors. National and international security agencies are interesting in matters like maritime traffic security, maritime pollution control, monitoring migration flows and detection of illegal fishing activities. In this concern the European Maritime and Safety Agency (EMSA) is going to integrate its services to provide vessel traffic monitoring information using geographical information service (GIS) to improve the capability to detect illegal oil spills and to indentify responsibilities. Furthermore maritime security is also under consideration by European Space Agency (ESA) in the framework of the European crisis response architectures (Del Monte et al., International Astronautical Congress, 2010) to comply with different issues: counter piracy actions, tanker accident monitoring, rescue support in the Artic region. In addition, in January 2010 the kick-off of the BlueMassMed pilot project was held, granted by the European Commission, which aims at increasing the cooperation for maritime surveillance in the Mediterranean Sea, including surveillance of illegal immigration, illicit trafficking, environmental pollution and reinforcement of the Search and Rescue efforts. Up until now, different options have been considered for vessel monitoring, ranging from transponders located onboard the vessels, such as the AIS, to optical imagery. However the achieved results by those methodologies in real scenarios (Margarit et al., IEEE Trans. on Geosc. and Remote Sens, 2007) have shown that, although there are a number of commercial systems available on the market today, none of these systems is really mature, e.g. there is no fully automated operational system providing accurate, reliable near-real time monitoring information. The major problem of all these systems still is that they are not capable to accurately detect ships at every sea state and to separate ships from other artificial offshore objects with a high accuracy. The SAR instrument can be a valuable solution since it is able to monitor wide areas with high spatial resolution almost independently from weather conditions and both day and night time. However, in spite of significant research activity focused on ship detection and motion estimation, to date, there are no efficient and robust algorithms that can routinely provide useful detection of ship and estimates of the speed and heading of detected ships (Dragosevic et al., IEEE Geosc. and Remote Sens. Letters, 2008). This paper deals with ship monitoring, i.e. ship detection, classification and motion estimation, algorithms based on SAR data. Satellite imaging is a good way to identify ships but, characterized by large swaths, it is likely that the imaged scenes contain a large number of ships, with the vast majority, hopefully, performing legal activities. Therefore, the imaging system needs a supporting system which identifies legal ships and limits the number of potential alarms to be further monitored by patrol boats or aircrafts. Specifically the work focuses on maritime surveillance by using COSMO/SkyMed constellation, also adequately integrated by AIS information to individuate innovative and reliable SAR-based products for sea traffic monitoring. The developed approach is finally validated using different combinations of both simulated and real-world AIS and COSMOSkyMed data takes.

8179-10, Session JS1

A novel paradigm for urban environment characterization using ascending and descending terrasar-x data

E. Angiuli, G. Trianni, European Commission Joint Research Ctr. (Italy); P. Gamba, Univ. degli Studi di Pavia (Italy)

The combined use of better spatial resolution (up to 1 meter) satellite data provided by the new generation of VHR SAR sensors, Terrasar-X and Cosmo-Skymed, and of high performance machines allows us to process massive datasets more efficiently and quickly than ever before. This also implies that now we can monitor regularly and more

in depth the changes of the pattern in the human settlement landscape anywhere in the world. The benefits of this new ability are vast and vary from identifying, monitoring and thereby understanding human settlement vulnerabilities in a variety of contexts, from climate change responses to disaster risk reduction and improved post-disaster relief.

Therefore, innovative approaches are essential for a better assessment and a finer description of such areas. Synthetic Aperture Radar (SAR) imagery has become increasingly popular as some of its properties are favourable to optical imagery. The SAR signal is very sensitive to the geometry, orientation and material of the buildings; even though all that is usually considered as a drawback when using a single scene, it can become an advantage using different acquisitions. In that case SAR backscattering can be used to interpret not only the geometry of the man-made structures but also their spatial/topological relationships.

The dataset used in this study is composed of 2 different acquisitions over the city of Pavia, situated in northern Italy; the images have been acquired in HH polarization on the February 8, 2008 in ascending mode and on the February 12, 2008 in descending mode.

In this work, we propose a new paradigm for urban structures characterization exploiting the geometric and statistical properties of the objects backscattering.

The methodology is based on a semi-automatic segmentation method and on a statistical analysis by means of morphological and textural techniques [1, 2, 3]. This analysis should enable us to model and specify the spatial arrangement of the detected structures.

In this study we have investigated the potentialities of the joint use of images acquired in ascending and descending mode. The data have been analysed and processed individually and jointly and the results of the different processing steps are reported and discussed. Among the results, it has been proved that the joint use of the information extracted from the two different acquisition pass, leads to a more accurate and detailed representation of the urban environment descriptors.

REFERENCES

[1] M. Pesaresi, A. Gerhardinger, and F. Kayitakire, "A robust builtup area presence index by anisotropic rotation-invariant textural measure", IEEE Journal of Selected Topics in Applied Earth Observations and Remote Sensing, Vol. 1, No. 3, pp. 180-192, 2008.

[2] P. Gamba, M. Pesaresi, K. Molch, A. Gerhardinger, and G. Lisini, "Anisotropic rotation invariant built-up presence index: applications to SAR data", in Proc. IGARSS'08, Boston, MA, July 2008.

[3] F. Dell'Acqua, and P. Gamba: "Texture-based characterization of urban environments on satellite SAR images", IEEE Trans. on Geoscience and Remote Sensing, Vol. 41, n. 1, pp. 153-159, Jan. 2003.

8179-36, Session JS1

An experimental study on ship detection based on the fixed-point polarimetric whitening filter

D. Tao, Univ of Tromsø (Norway); C. Brekke, S. N. Anfinsen, Univ. of Tromsø (Norway)

This work investigates the behavior of the Fixed-Point Polarimetric Whitening Filter (FP-PWF) with respect to ship detection based on polarimetric Synthetic Aperture Radar (SAR) imagery. The purposes of this work are: (i) to investigate new distribution models for FP-PWF output that incorporate texture, (ii) to examine Method of Log Cumulants (MoLC) for shape parameter estimation associated with texture, and (iii) to assess the impact of the improved modeling and estimation on the discrepancy between specified and observed false alarm rate. Experiments are performed on simulated data sets.

The Polarimetric Whitening Filter (PWF) algorithm [1] processes the quad polarimetric Single Look Complex (SLC) SAR data into full-resolution pixel intensities, and provides effective speckle reduction. In a previous study [2], the FP-PWF was proposed as a modification of the original PWF. In brief, the original PWF includes the complex multivariate Gaussian distributed scattering vector and the sample mean estimator for the covariance matrix which is Wishart distributed. The distribution of the original PWF output is then a linear transformation of the F-distribution. In the FP-PWF, the sample mean covariance matrix estimator is replaced with the fixed



point (FP) estimator, which is asymptotically Wishart distributed also when the scattering vector has a non-Gaussian distribution [3]. The non-Gaussian scattering vector can be modeled as the product of a complex multivariate Gaussian vector representing the speckle and a texture variable representing spatial variability of the reflectivity, which is known to be an appropriate model for sea clutter. When texture variable is Gamma distributed or inverse Gamma distributed, the scattering vector becomes multivariate K-distributed or multivariate G0-distributed. Using Mellin Kind Statistics [4,5], new statistical models for the FP-PWF output can now be derived as a compound Gamma-F distribution and a compound inverse Gamma-F distribution, with the texture variable represented as Gamma and inverse Gamma distribution respectively. In this work, the goodness of fit of the compound F-distribution models are tested.

To the compound distribution models for the FP-PWF output, MoLC is applied to estimate the shape parameter [4,5]. The classical Method of Fractional Moments (MoFM) shape parameter estimator is involved as a reference in a comparison study. The MoLC shape parameter estimator is expected to provide better estimation accuracy (smaller bias and lower variance). The estimated parameters are applied by the cumulative distribution function of the FP-PWF output and affect the performance of the constant false alarm rate (CFAR) detector. In practice, there is an inevitable deviation between the specified false alarm rate and the observed false alarm rate, because of the inherent uncertainty in the parameter estimations. To compare the specified false alarm rate versus the observed false alarm rate, Monte Carlo simulations are performed with different statistical models and different shape parameter estimators. These simulations quantify the impact of the improved modeling and parameter estimation.

Reference:

[1] Novak, L. M., Burl, M. C., Irving, W. W., Optimal Polarimetric Processing for Enhanced Target Detection, IEEE Transactions on Aerospace and Electronic Systems, vol. 29, no. 1, 1993

[2] Anfinsen, S.N., Tao, D., and Brekke, C., Improved target detection in polarimetric SAR images by use of Mellin kind statistics, Proc. POLinSAR 2011, Frascati, Italy, 4 pp., 24-28 January, 2011

[3] Pascal, F., Forster, P., Ovarlez, J.-P., and Larzabal, P., Performance Analysis of Covariance Matrix Estimates in Impulsive Noise, IEEE Trans. Signal Proc., vol. 56, no. 6, 2206-2217, June 2008

[4] Nicolas, J.-M., Introduction aux statistiques de deuxi'eme esp'ece: applications des logs-moments et des logs-cumulants `a l'analyse des lois d'images radar, Traitement du Signal, vol. 19, no. 3, pp. 139-167, 2002

[5] Anfinsen, S.N., On the supremacy of Logging, Proc. POLinSAR 2011, Frascati, Italy, 8 pp., 24-28 January, 2011

8179-37, Session JS1

A radar target DB construction method using 3D scattering centers

J. H. Yoo, C. H. Kim, D. Y. Chae, K. Kwon, Agency for Defense Development (Korea, Republic of)

There can be several types of radar target database (DB) depending on the purpose for using them and the technical levels the constructors have. The simplest form of databases would be the one composed of complex Radar Cross Section (RCS) over frequencies, polarizations, and angles. A one-step advanced DB could be made from 3-dimensional scattering centers of targets [1]. The database of 3D scattering centers is obtained by signal processing the target RCSs over frequencies and angle apertures in azimuth and elevation directions via Matrix Pencil (MP), Estimation of Signal Parameters via Rotational Invariance Techniques (ESPRIT) or other superresolution techniques to get 3 dimensional positions and magnitudes of the scattering centers [2][3][4]. The scattering center database is different from the simple RCS value database in that it can be used to synthesize various radar signature datasets of a target such as High Resolution Range Profiles (HRRP) and Inverse Synthetic Aperture Radar (ISAR) images. It is also very useful from the point that changes of the received signal in a sensor can be modeled when the target is located within the near-field range, which happens when we do end game simulations.

Target RCS for scattering center extraction can be obtained not only by measurements but also by Computational Electromagnetics (CEM)



using target Computer-Aided Design (CAD) models. In this paper, a method to obtain target CAD models from the real targets to be used for the construction of a scattering center database of radar targets is proposed and a consideration to decide the appropriate collection of RCS data sets is also described. 3D CAD models of the targets can be come by the modification of their design drawings which were used to build the targets, but those drawings are not available in many cases. Therefore, a method to make a geometric model from the real target is needed. A 3D measuring instrument by contact is a viable tool when the target size is around a meter. When the target is larger than that, target shapes can be measured by a laser scanner [5]. This shape data will be used as the basis to form a CAD model of the target. With the CAD model obtained as described above, RCS values of the target are predicted over a series of frequencies and angle apertures, which will be processed to be transformed into scattering centers.

When the database is constructed from those scattering centers, a criterion on how many sets of scattering centers are needed in azimuth and elevation angle directions should be determined. If one set of scattering centers is needed every 1 degree, then the size of database would be huge because it has to have 359 sets of scattering centers for one fixed elevation angle at one kind of frequency band and one polarization. On the other hand, if the sets of scattering centers are obtained coarsely like every 30 or 50 degrees, then the size of our database can be smaller but the database will not be able to provide the detailed characteristics of the target. Consequently, the CAD model of an air-target is utilized for the test to infer the criterion on the frequency of scattering center sets for the optimal database construction, where RCS data sets from every 5, 10, 15 and 20 degrees over the whole azimuth angles are calculated to be used for the scattering center extraction and then RCS values are reconstructed from those sets of scattering centers to compare with the original RCS values of the target which are calculated every 0.2 degrees. Correlation coefficient and maximum/average difference techniques were used as the analysis methods. As can be expected, the results show that the smaller the sampling distance or the higher the frequency of collecting scattering center sets we have, the better match between the original RCS and the reconstructed RCS of a target could be obtained. There were also a few cases where scattering center sets from 10 degrees gap or 15 degrees gap showed a better match depending on the analysis method being used, which requires more inspection on the accuracy of CAD models, CEM tool used, and scattering center extraction algorithm.

[1] S. H. W. Simpson, P. Galloway, M. Harman, "Applications of EpsilonTM: A Radar Signature Prediction and Analysis Tool", International Radar Symposium, IRS 1998, Munich Germany

[2] D. Andersh, J. Moore, S. Kosanovich, D. Kapp, R. Bhalla, R. Kipp, T. Courtney, A. Nolan, F. German, J. Cook, and J. Hughes, "Xpatch 4: The next generation in high frequency electromagnetic modeling and simulation software", International Radar Conference, IRS 2008

[3] Y. Hua, E. Baqai, Y. Zhu, D. Heilbronn, "Imaging of Point Scatterers from Step-Frequency ISAR Data", IEEE Transactions on AES, vol.29, no.1, pp195~205, 1993

[4] Andre Quinquis, Emanuel Radoi, Felix-Costinel Totir, "Some Radar Imagery Results Using Superresolution Techniques", IEEE Transactions on AP, vol.52, no.5, pp1230~1244, 2004

[5] Frank Chen, Gordon M. Brown, Mumin Song, "Overview of threedimensional shape measurement using optical methods," Optical Engineering, vol. 39, no. 1, pp. 10~22, 2000

8179-11, Session JS2

An unsupervised method for quality assessment of despeckling: an evaluation on COSMO-SkyMed data

B. Aiazzi, Istituto di Fisica Applicata Nello Carrara (Italy); L. Alparone, F. Argenti, Univ. degli Studi di Firenze (Italy); S. Baronti, Istituto di Fisica Applicata Nello Carrara (Italy); T. Bianchi, A. Lapini, Univ. degli Studi di Firenze (Italy)

The quality of despeckling is generally measured by corrupting a test image by means of synthetic noise with speckle statistics and computing a distance metrics between the original noise free and the filtered noisy image. Unfortunately this approach is correct only for scenes where speckle is fully developed, i.e. there is a large number

of independent scattering elements within the smallest area that can be imaged by the instrument. In the presence of natural textures, e.g., forests, and of man-made structures, e.g., roads together with buildings, the fully developed speckle model no longer holds. As a limit case, a persistent scatterer produces an almost deterministic image, without any speckle.

Since despeckling filters should be optimized on true SAR images, the problem arises of how to evaluate the quality of despeckling; in other words, the fidelity of the despeckled image to a hypothetically noise free SAR observation. In the literature, this goal has been accomplished by taking the ratio of the original to the despeckled image, i.e. by extracting the noise that has been removed, and by matching its statistics (e.g. mean, variance, correlation, skewness) to the nominal ones of speckle on suitable manually chosen regions of interest (ROI), where speckle is assumed to be fully developed.

Goal of this paper is the development and evaluation of a fully automatic method for quality assessment of despeckled SAR images. The rationale of the new approach is that any structural perturbation introduced by despeckling, e.g. a local bias of mean or the blur of a sharp edge or the suppression of a point target, may be regarded as the introduction of a new structure, or the suppression of an existing one. Conversely, plain removal of random noise does not changes the structures in the image.

Implementation of the new approach is performed on the twodimensional scatterplot between estimators (e.g. 5x5 sliding averages) of the filtered and unfiltered image, or equivalently on the bivariate distribution obtained after binning. An ideally optimal filter would yield a scatterplot constituted by the superposition of several clusters, corresponding to classes encountered in the image. The ensemble of clusters is aligned along the diagonal of the first quadrant and spread across the plane far apart from the diagonal, where, however, all centers of clusters lie. The presence of filtering impairments produce secondary clusters that may be significantly far apart from the diagonal. Under this perspective, a measure of the accuracy of despeckling for each pixel may be formulated in the following way. For each point in the scatterplot, corresponding to one pixel in the original and in the filtered image, apply the mean shift algorithm to attract the scatterpoint towards its dominant cluster. Il the final position of the point is on the diagonal, the corresponding pixel in the image has been perfectly filtered. If the scatterpoint is attracted by a secondary cluster not lying on the diagonal, filtering was inaccurate. A measure of such inaccuracy is given in terms of the position and population of the attracting cluster, by using information theoretic concepts. A fast implementation is obtained by preliminarily binning the scatterplot and by applying the mean shift algorithm to the central scatterpoint of each bin.

Results on true SAR images (COSMO-SkyMed) will be presented. Bayesian estimators (LMMSE, MAP) operating in the undecimated wavelet domain have been coupled with segment-based processing (Bianchi et al., IEEE TGARS, 2008). Quality measurements of despeckled SAR images carried out by means of the proposed method highlight the benefits of segmented MAP filtering.

8179-12, Session JS2

Basis for optronic ScanSAR processing

L. Marchese, P. Bourqui, S. Turgeon, INO (Canada); B. Harnish, M. Suess, European Space Research and Technology Ctr. (Netherlands); F. Châteauneuf, A. Bergeron, INO (Canada)

ScanSAR is an important imaging mode of operation for SAR systems. It allows extended range coverage albeit at the expense of azimuth resolution. Compared to stripmap, ScanSAR is used more for large swath coverage for mapping and monitoring over a wide area. Applications are numerous and include boreal forest mapping, wetland mapping and soil moisture monitoring.

From its very nature, ScanSAR produces large amounts of data, resulting in long processing times precluding instantaneous access to the images. In previous work, an optronic processor prototype designed for fast processing of stripmap-mode data from the ENVISAT/ASAR instrument was constructed and images were successfully processed in real-time. Given the ultra-fast processing and upsampling capabilities of the optronic SAR processor, it would make a perfect candidate for a real-time ScanSAR processor. ScanSAR processing, however does significantly differ from stripmap



SAR processing due to the multiple range-swath azimuth-burst format type of data generated. The main challenge for optronic implementation of ScanSAR lies scientifically, in the comprehension of the physical parameters substantiating the processor operation and technically, in proper handling, processing and combining each of the burst sections to produce the final image.

The goal of the present work was thus to explore the possibility of processing ScanSAR data optronicaly. Tests were performed with simulated and artificially bursted ASAR stripmap data demonstrating that reconstruction of ScanSAR data using the optronic SAR processor is feasible. This paper describes specifically how the data control and handling of ScanSAR data is performed to make it compatible with the optronic processor that was specifically designed for stripmap processing. As well, the ScanSAR is generated optronically are presented.

8179-38, Session JS2

Comparison of using single- or multipolarimetric TerraSAR-X images for segmentation and classification of manmade maritime objects

M. Teutsch, G. Saur, Fraunhofer-Institut für Optronik, Systemtechnik und Bildauswertung (Germany)

Spaceborne SAR imagery offers high capability for wide-ranging maritime surveillance. SAR image processing can be used especially in situations, where AIS (Automatic Identification System) data is not available such as for small ships, which don't need to send AIS, in case AIS sender dysfunction, or intentionally switched off AIS due to potential criminal activities. Therefore, maritime objects have to be detected and optional information such as size, orientation, or object/ ship class is desired. With StripMap (SM) mode of TerraSAR-X satellite, quite high resolution of 3x3 meters per pixel can be achieved while still covering an area of 30x100 kilometers per image. Thus, it is possible to go beyond object detection towards segmentation, structure analysis, size and orientation estimation, and classification.

In recent research work, we proposed a SAR processing chain consisting of preprocessing, detection, segmentation and classification for single-polarimetric (HH) TerraSAR-X StripMap images to finally assign detection hypotheses to class "clutter", "non-ship", "unstructured ship", or "ship of structure x" (paper accepted for IGARSS 2011). A basic CFAR-like algorithm is used for initial detection of object hypotheses tending to accept false positives rather than producing false negatives. Thus, true objects are unlikely to get lost in an early processing stage, but false positives can be rejected later after more information was extracted. Segmentation is done using Local Binary Pattern (LBP) to extract object contours on the one hand, and perform a statistical structural analysis of an object hypothesis on the other. Together with Histograms of Oriented Gradients (HOG), good estimation of object size and orientation is possible even for object hypotheses strongly affected by speckle noise and typical SAR data distortion. For classification, three cascaded Support Vector Machines (SVM) are used to separate between clutter and man-made objects in the first, non-ships and ships in the second, and unstructured ship and different ship structures in the third classification cascade-level. In training stage, an automatic feature selection module evaluates and selects features coming from a big feature database. This database includes several hundred features such as texture, gradient, structure or LBP features. For each SVM a specific feature vector is set up consisting of features with highest separability for the specific classification task. The processing and classification results are promising

In this work, we extend the existing processing chain and are now able to handle dual- (HH, VV) and quad-polarimetric (HH, HV, VH, VV) TerraSAR-X data. With the possibility of better noise suppression using the different polarizations, we try to improve both the segmentation and the classification process. Automatic feature selection for the SVMs is applied to all polarizations to allow potentially mixed feature vectors in each classification cascade-level. In several experiments, we will investigate the potential benefit for both segmentation and classification. Precision of size and orientation estimation as well as correct classification rates will be calculated individually for single-, dual-, and quad-polarization and compared to each other. Furthermore, we will find out, if specific feature classes are suitable for specific polarizations.

8179-39, Session JS2

A new SAR image classification using compressive sensing on manifold

B. Hou, X. Cheng, S. Wang, L. Jiao, Xidian Univ. (China)

Compressive Sensing (CS) theory shows that we can reconstruct sparse or compressible signals from a small set of random-projection measurements. The utility of CS for signal reconstruction motivates the study of its latent capacity in other applications.

This paper proposes a new method for SAR image classification based on compressive sensing on manifold, which operates directly on the compressed random measurements of SAR images without reconstructing the images. The core idea of our method is that the compressive measurements of SAR images in one class can be modeled by a Mixture of Factor Analyzers (MFA) which fits to each class data very well by probabilistic formulation, and then SAR image classificaton is performed based on Bayes decision rule. We use the fact that the set of compressive measurements of SAR images in one class forms a nonlinear manifold and can be modeled as a finite mixture of Gaussians. We use nonparametric statistical methods to infer an appropriate number of mixture components for a given compressive measurements set, as well as the associated ranks of the covariance matrices.

The proposed compressive classification method have two parts including training and testing. First, the compressive measurements of each class are modeled so that the probability density function of compressive measurements of each class can be learned from the MFA as the prior distribution. Second, SAR image classification is performed based on the Bayes decision rule. Finally, we demonstrate the effectiveness of the proposed method in MSTAR dataset using limited random-projection measurements. The proposed method has reached a high classification rate with reasonable time cost even when the number of compressive measurements is far less than the dimensionality of the original images.

8179-26, Poster Session

Moving target imaging by both Ka-band and Ku-band high-resolution radars

Y. Zhang, W. Zhai, X. Zhang, X. Shi, X. Gu, i. Jiang, Ctr. for Space Science and Applied Research (China)

Ground moving target experiment with ground-based radar is a very useful, necessary, and cost-effective work for development of radar system. By conducting this kind of experiment, we can test the key and important components or subcomponents with real data on one hand, and test and improve the signal processing algorithms on another hand. In this paper, we introduce our experimental work on testing wide-band transmitters and receivers developed for Kaband and Ku-band radar systems, as well as the signal processing algorithms. A city light-railway train is selected as the imaged target. The wide-band transmitters and receivers are designed based on the stepped-frequency chirp signal (SFCS). The bandwidth of subchirp is 120MHz, and the frequency step is 100MHz. Up to 20 subchirps are used to synthesize wide-band signal with bandwidth larger than 2GHz. Both Ka-band and Ku-band high-resolution radar images are obtained, which show that Ka-band images are much clear than that of Ku-band as we expect. There are two reasons to explaining this, one reason is due to the electromagnetic scattering of train itself are different for Ka-band and Ku-band frequencies, and the other reason is due to the interactions, i.e. multi-reflection or multi-scattering between the train and the side metal fences are different. For Ka-band, both dechirping receiver and matched filtering receiver are implemented, while only matched filtering receiver is implemented for Ku-band right now. By comparing the radar image of dechirping receiver and the image of matched filtering receiver, we find that the former is better than the later. The reason is due to the motion-induced errors were different for the two cases, and the error of dechirping case was smaller because the echoes were coherently combined in time-domain, and the error of matched filtering case was bigger because the echoes were coherently combined in frequency-domain.

The imaged train has six compartments (including two locomotives), and each compartment has three same-sized windows and four samesized doors, as well as two ventilators of air-conditioner on both ends.



Both Ka-band and Ku-band images clearly showed the six-section structure, especially the ventilators were very well indicated. The range resolution was estimated to be as fine as less than 10cm through analyzing near ideal point-target response, and the azimuth resolution was theoretically estimated to be less than 7cm.

The correction algorithm for the phase and amplitude imbalances for SFCS, the applications of the Super-SVA technique and the compressive sensing reconstruction to experimental data are also presented.

8179-27, Poster Session

Distinguishing ability analysis of compressed sensing radar imaging based on information theory model

H. Jiang, Institute of Electronics (China) and Graduate Univ. of Chinese Academy of Sciences (China); B. Zhang, Y. Lin, W. Hong, Y. Wu, Institute of Electronics (China)

Radar imaging is a candidate tool in many military and civilian applications, including target identification, aircraft traffic control and air/space surveillance. In conventional radar imaging system, the resolutions depend on the bandwidth of the transmit signal and the Doppler bandwidth of the system. With the increasing resolution requirements of radar system, the sampling rates based on the framework of Shannon's sampling theorem are higher and higher, and thus radar signal acquisition and processing are more and more difficult. Overcoming these drawbacks become new challenges.

Since radar image is a map of the spatial distribution of the reflectivity function of stationary targets and terrain, many radar images can be sparse or compressible in some representation such as those from wavelet or complex wavelet transform. The recently introduced theory of compressed sensing (CS) or compressive sampling indicates that an unknown sparse signal can be exactly recovered from very limited number of measurements by solving a convex optimization problem with high probability [1]. Based on rigid mathematics, CS has attracted many attentions in radar applications recently. A compressed sensing radar sketch is proposed in [2], and in [3] which states that the targets' location can be determined by CS techniques with better resolution. Some other CS radar works have also been done [4], [5]. Among these works, no theoretical criterion to judge of the performance of CS radar is given.

The main contribution of this paper is the analysis of the information content contained in the CS radar echoes and the distinguishing abilities of the CS radar image. The information content contained in the echoes is analyzed by simplifying the information transmission channel as a parallel Gaussian channel, by theoretical analyzed the information content of the channel, the relationship among the signal-to-noise ratio (SNR) of the echo signal, the number of required samples, the length of the sparse targets and the distinguishing level of the radar image is gotten. Based on the result, the distinguishing ability of CS radar image is introduced and some of its properties are also gotten. Real IECAS advanced scanning two-dimensional railway observation (ASTRO) data experiment validates the conclusions.

Reference

[1] D. Donoho, "Compressed sensing," IEEE Trans. Inform. Theory, vol. 52, no. 4, pp. 1289-1306, Apr. 2006.

[2] R.G. Baraniuk and P. Steeghs, "Compressive radar imaging," IEEE Radar Conference, Boston, MA, USA, Apr.17-20, pp. 128-133, 2007.

[3] Y. S. Yoon and M. G. Amin. "Compressed sensing technique for highresolution radar imaging," Proc. SPIE, SPIE Signal Process, Sensor Fusion and Target Recognition XVII, 2008, 6968, pp. 69681A-69681A-10

[4] Joachim H.G. Ender, "On compressive sensing applied to radar," Signal Processing, vol. 90, pp. 1402-1414, 2010.

[5] Vishal M. Patel, Glenn R. Easley, Jr. Dennis M. Healy, and Rama Chellappa, "Compressed synthetic aperture radar," IEEE J. Sel. Top. Sig. Process., vol. 4, no. 2, pp. 244-254, Apr. 2010.

8179-28, Poster Session

SAR image despeckling by matching pursuit of subband coherent structures using a library of wavelet bases

Y. S. Bekhtin, Ryazan State Radioengineering Univ. (Russian Federation); A. A. Bryantsev, Ryazan State Radio Engineering Univ. (Russian Federation)

The new despeckling method based on matching pursuit of subband coherent structures of a wavelet-decomposed SAR image is suggested. In this paper, coherent structures are such components of an input SAR image that provide with speckle removing and when the maximal correlation between the best nonlinear approximations of the image and the given wavelet basis is achieved. The iterative pursuit of coherent structures within each subband is organized as an adaptive thresholding of arranged wavelet coefficients (sorted by descend of its absolute values) using the best wavelet basis chosen from the library of bases. The choice of the best wavelet basis depends on the kind of the cost function which has been formed as an entropy function taking into consideration the type of thresholding (hard or soft). The final processed image is formed as the cumulative sum of the pseudo images corresponding each subband and computed by applying of inverse wavelet transform to extracted coherent structures on each iteration. The results of computer modeling and comparison with few well-known despeckling procedures have shown the superb quality of the proposed method in the sense of different criteria as MSE, PSNR, SSIM, etc. The suggested method contains routine procedures and, therefore can be recommended for passive processing of SAR images, especially when the statistical properties of speckle are unknown.

8179-29, Poster Session

Efficient and accurate algorithm for the evaluation of Kirchhoff scattering from fractal surfaces

A. lodice, Univ. degli Studi di Napoli Federico II (Italy); S. Perna, Univ. degli Studi di Napoli Parthenope (Italy)

Scattering from a natural surface modeled by a fractional Brownian motion (fBm) two-dimensional process [1] can be evaluated by using the Kirchhoff approximation if proper conditions are satisfied by surface parameters [2]. This evaluation leads to a scattering integral that can be computed via two different asymptotic series expansions [2], whose behavior has been recently deeply investigated with the aim of finding suitable truncation criteria to compute, with a controlled absolute error, the field scattered by a fractal fBm surface [3].

Based on those results, in this paper truncation criteria are provided to compute aforementioned series with a controlled relative error instead of an absolute one. According to such an analysis, an algorithm is provided, which allows to automatically decide which of the two series, if any, can be used, and how it can be properly truncated for efficient and effective, that is, with a controlled relative error, computation of the field scattered by natural surfaces. With this respect, key-parameters to be considered are the Hurst coefficient H, that is only related to surface geometry (its roughness), the S parameters, that is related on both surface geometry (namely, its rms slope evaluated at the electromagnetic wavelength scale) and illumination (frequency and incident and scattering directions), the employed computer numbering format, and the required relative accuracy. It turns out that by using the standard IEEE double-precision numbering format, a relative accuracy of 10^-3 can be achieved for any value of H and S; however, even by using the single-precision format, a relative accuracy as high as 10^-5 can be achieved for most of the H and S values: in fact, only values of S of the order of unity are excluded. In addition, it turns out that very few terms of the series need to be computed to reach the desired relative accuracy, except that for values of S of the order of unity, and that computation of the scattering integral via the considered asymptotic series expansions is more efficient compared to direct numerical integration.

Finally, to illustrate its practical applicability, the proposed algorithm is employed to generate a Synthetic Aperture Radar (SAR) reflectivity map to be used within a SAR simulation scheme [4].



References

[1] B.B. Mandelbrot, The Fractal Geometry of Nature, New York: W.H.Freeman & C., 1983.

[2] G. Franceschetti, A. lodice, M. Migliaccio, D. Riccio, "Scattering from natural rough surfaces modelled by fractional Brownian motion two-dimensional processes", IEEE Trans. Antennas Propagat., vol.47, no.9, pp. 1405-1415, 1999.

[3] S. Perna, A. Iodice, "On the Use of Series Expansions for Kirchhoff Diffractals", IEEE Trans. Antennas Propagat., vol. 59, no.2, pp.595-610, 2011.

[4] G. Franceschetti, M. Migliaccio, D. Riccio, G. Schirinzi, "SARAS: a SAR raw signal simulator", IEEE Trans. Geosci. Remote Sens., vol.30, pp.110-123, 1992.

8179-30, Poster Session

Oil platform investigation by multitemporal SAR remote sensing image

C. Peng, The Second Institute of Oceanography, SOA (China)

Off-shore oil rig is an important facility of oil production in South China Sea. It has a similar back scatter character with ships in SAR image of scan model. We present a method of oil platform investigation using multi-temporal SAR remote sensing image in this paper. Firstly, we use a ship detection means to find the point target in the SAR imagery. The ship detection means is a CFAR detector. Secondly, an identifier is employed to choose the no-oil platform targets. These targets are different from oil rig obviously in shape and other features. Thirdly, we build a model of relevant matching to find the same point target in multi-temporal SAR remote sensing images. If a point target keeps the same position in multi-temporal SAR imagery, we will regard it as an oil platform. Then, we use about one hundred of SAR imagery to find the oil platform of South China Sea.

8179-31, Poster Session

Polarization scattering characteristics of some ships using polarimetric SAR images

J. Wang, Ocean Univ. of China (China)

Polarization scattering information has a potential application for ship classification and identification in SAR images. This paper investigates in the polarization scattering of several types of ships like hospital ship, LPD (Landing Platform Dock) ship, container ship and oil tanker.

The research steps are as follows: (1) Ships are detected by using a ship detection method in UAVSAR images, and the profiles of ships are obtained by using edge detection together with mathematical morphological approach. (2) The scattering characteristics of every ship's pixel is got by using decomposition methods such as Pauli decomposition, SDH (Sphere-Dihedral-Helix) decomposition, SDBV (Surface-Double Bounce-Volume) decomposition, Moriyama decomposition, four component decomposition, and Cameron decomposition. (3) Integration of scattering types of every pixel is done by voting mechanism because possible different scattering types exist by using different decomposition methods. The scatterings are fused to four scattering types: sphere scattering, diplane scattering, volume scattering and other scattering. Then the polarization scattering information of ships has been got.

It is shown that the main scatterings of hospital ship are sphere and diplane scattering, main scattering of LPD ship is sphere scattering, main scatterings of container ship are sphere and volume scattering, main scatterings of oil tanker are diplane and volume scattering. And it's also show that main scattering of the ship's apron and flat is sphere scattering, main scattering of the ship's bridge or superstructure is diplane or volume scattering.

So it is known that different types of ships have different polarization scattering information. This is useful for ship classification and ship classification.

8179-32, Poster Session

Application of sparse array and MIMO in near range microwave imaging

Y. Qi, Y. Wang, W. Tan, W. Hong, Institute of Electronics (China)

Near range microwave imaging can obtain information of shape, structure and scattering properties of detected targets. And it has advantages of penetrating, security and high resolution comparing with other imaging techniques such as visible light, infrared light and X-ray. Thus, near range microwave imaging systems have broad application prospects in the field of concealed weapon detection, biomedical imaging, nondestructive testing, three dimensional digital imaging, etc.

Near range imaging systems can reconstruct a three dimensional (3D) image of the detected targets with the amplitude and phase information collected. And an array consisting of a large number of antenna elements is usually utilized in these systems for fast data collection. To reduce the number of array elements and channels, this paper applies the techniques of sparse array and MIMO to near range microwave imaging.

Firstly, near range imaging systems usually adopt a planar aperture which consists of a real aperture and a synthetic aperture to from 3D imaging geometry. However, the purpose of the paper mainly is to verify the imaging ability of sparse array, so it mainly analyzes the two-dimensional imaging geometry formed by arranging sparse array in real aperture direction and transmitting broadband signals in range direction.

Secondly, based on the analysis of the relationship between MIMO and convolution principle, the paper develops a method to arrange sparse array which can reduce system complexity as well as ensure the quality of the resulting imagery. In detail, when MIMO applied to antenna array, the array can generate virtual phase centers by designing transceiver channels, which will reduce the number of antenna elements in array direction. And by choosing proper transceiver channels on the basis of convolution principle, appropriate sparse array can be designed to be equivalent to a full array. Then, the paper compares the results of the method with ones of existing methods such as brute-force method and simulate annealing algorithm.

Meanwhile, according to the designed sparse array and transceiver channels, echo model is established. Then, the paper deduces the resolution and algorithm for near range imaging mode.

Finally, the paper verifies the imaging capabilities of the techniques of MIMO and sparse array through numerical simulation.

8179-33, Poster Session

Comparison between ALOS PALSAR backscatter and AVNIR-2 NDVI on stem volume of mountainous forest

C. Kim, M. Hong, Kookmin Univ. (Korea, Republic of)

ALOS data have provided useful information on forest cover and biomass since 2006. Unfortunately, topographic effects influence illumination and shadow conditions of terrain so that accuracy statements of the biomass derived from ALOS data (i.e., both AVNIR-2 and PALSAR) are confused with ground truth data. The aforementioned reason has led to the initiation of this research to determine if ALOS data can be used both to estimate the stem volume and to monitor the canopy of forest in mountainous area.

In this paper, the NDVIs derived from AVNIR-2 data are analyzed for geometric illumination conditions influenced by topography (i.e., slope, aspect and elevation) and shadows (solar elevation and azimuth angle). This paper deals also with the problem of different backscattered sigma-nought $\delta 0$ values on the similar stem volume of the stands in PALSAR fine beam dual (FBD) horizontal / horizontal (HH) and horizontal / vertical (HV) polarization intensity data.

PALSAR data were obtained on 11th June 2010 and AVNIR data acquired on 12th June 2007. The study site is situated in 1111ha Kwangneung Experiment Forest, 127° 12' 05" North in latitude and 37° 70' 50" - 37° 81' 32" East in longitude, which is located of 39km east of Seoul.

Vegetation of the site characterized by brown forest soil and temperate climate, is composed of coniferous, deciduous, and mixed forest.



It can be noted that HV intensities are higher than HH intensities on the same stem volume regardless directionality. The variations of sigma-nought $\delta 0$ values caused by topographic effects can obscure real variations in stem volume. The regression model based on the above mentioned intensities and NDVIs would improve stem volume estimation in composite of HV/HH/HV.

In addition, digital forest map was useful for delineating composite of $\ensuremath{\mathsf{HV/HH}}\xspace$ /HV/HV.

8179-34, Poster Session

SAR image post-processing for the estimation of fractal parameters

D. Riccio, I. Zinno, G. Di Martino, G. Ruello, Univ. degli Studi di Napoli Federico II (Italy)

The new generation of Synthetic Aperture Radar (SAR) sensors has marked a huge increase in the resolution of microwave images of the Earth and other solar system planets. Therefore, new models, techniques and tools are required to adequately deal with this new available data. Concerning SAR images of natural areas, until now it was only possible to identify macroscopic topological features of the observed areas, roughly distinguishing them from urban ones. With the new available data, the extraction of meaningful stochastic parameters relevant to the roughness and to the shape of the observed surface, is now in order. In this paper we present an innovative technique for the analysis and interpretation of SAR images of natural areas. It consists in an electromagnetic post-processing of the image that provides value added information, with a precise physical meaning, of the scene under survey. The rationale of such a processing is based on the inversion of the complete direct model, that links stochastic parameters which describe a natural surface to the stochastic parameters of the relevant SAR image, developed by the authors [1]. This model uses reliable geometrical, electromagnetic and radar models. The observed natural surface is modeled as a fractal two-dimensional stochastic process; such a process is completely described via two independent parameters: the fractal dimension D and the increment standard deviation s [m^1-H]. These are the key parameters to be estimated from the SAR image.

It has been demonstrated by the authors that, in an appropriate range of spatial frequencies, the Power Spectral Density (PSD) of a range cut of a SAR Image of a natural scene presents, in the hypothesis of small slope regime of the surface, a power-law behavior [1]. Consequently, in a log(wavenumbers)-log(|spectrum|) plane, the spectrum has a linear behavior with a slope related to the fractal dimension and an amplitude proportional to the s of the scene under survey. Our SAR image processing is based on the implementation of linear regression techniques on the range spectrum of homogeneous areas of the SAR image: the maps of the point by point fractal dimension and of the point by point normalized s of the observed scene are provided. In particular, the implemented algorithm consists in a sliding window that scours the whole image selecting, at each iteration, the small image portion for the local fractal parameters extraction. For each iteration, in the corresponding window, range cuts - sufficiently spaced one from each other to be considered uncorrelated - are selected. Then, the evaluation of the spectra of these cuts is performed using the Capon estimator [3]. Finally, these spectra are averaged and a linear regression is performed on this mean PSD. The so retrieved fractal parameters values provide the final fractal map of the imaged surface.

Full details, along with applications to SAR data, and, for the first time, to the SAR images of Titan, the Saturno's moon explored by the Cassini-Huygens mission, will be provided in the final version of the paper and during the conference presentation.

References

[1] Di Martino, G., Iodice, A., Riccio, D., Ruello, G., Zinno, I., "The effects of acquisition geometry on SAR images of natural scenes", Proceedings of the Radar Conference 2009, Rome, Sept. 30 2009-Oct. 2 2009, pp. 541 - 544.

[2] G. Franceschetti, D. Riccio, Scattering, Natural Surfaces and Fractals. Academic Press, Burlington (MA), USA, 2007.

[3] T. Austin, A. W. England, G. H. Wakefield, "Special problems in the estimation of power-law spectra as applied to topographical modeling", IEEE Trans. Geosci. Remote Sens., vol. 32, no. 4, pp. 928-939, July 1994.

8179-35, Poster Session

Retrieval of soil surface parameters via a polarimetric two-scale model in hilly or mountainous areas

A. lodice, A. Natale, D. Riccio, Univ. degli Studi di Napoli Federico II (Italy)

In recent years there has been a growing development of applications that require the massive knowledge of ground physical parameters (i.e., the soil dielectric constant, the vegetation biomass index, the soil moisture content, the surface roughness and so on). Since remote sensing is the best tool to get data pertinent to extended scenes in a comparatively short time, then it is undoubtedly useful to develop reliable techniques to retrieve ground physical parameters from remote sensing data.

In order to meet this aim, recently we proposed a Polarimetric Two-Scale Model (PTSM) [1-2], able to retrieve the surface roughness, the ground permittivity and the soil moisture content by processing polarimetric Synthetic Aperture Radar (SAR) data.

In our model, a bare soil surface belonging to a (multi-looked) SAR resolution cell is described as composed of large-scale variations on which a small-scale roughness is superimposed; then we employ a two-scale model for the scattering surface. In particular, the large scale roughness is locally treated by replacing the surface with a slightly rough tilted facet. Notice that in [1-2] the facet's slopes along azimuth and range directions are modeled as independent and identically distributed zero-mean, sigmasquare-variance Gaussian variables. As a consequence of the facet's random tilt, a random rotation of the local incidence plane around the line of sight and a random variation of the local incidence angle occur: unlike other similar existing models, in [1-2] we account for both these effects to analytically evaluate the overall normalized radar cross sections (NRCS). This is achieved by averaging the facets' NRCS over the random facets' slopes. Inversion of this direct model leads us to retrieve the large-scale roughness and the soil moisture content (or the ground permittivity) using the co-pol/cross-pol method, see [1-2]. However, due to the assumption that large-scale roughness slopes have zero mean, the method described in [1-2] can be only applied to flat areas, with no significant topography. In this paper we remove this simplifying assumption, so that our retrieval algorithm can be applied to get the parameters of interest even on hilly or mountainous areas. In particular, by using an available Digital Elevation Model (DEM) of the observed scene, for each (multi-looked) SAR resolution cell, surface slopes along range and azimuth directions are computed, and these are used as mean values of the facets' slopes in our model. Polarimetric NRCS expressions of [1-2] are accordingly modified and employed in the inversion procedure. Examples of application of the method are presented to verify that it is possible to provide reliable retrieval maps even on wide and morphologically heterogeneous areas.

[1] A. lodice, A. Natale, D. Riccio, "Retrieval of Soil Surface Parameters via a Polarimetric Two-Scale Model", in print on IEEE Trans. Geosci. Remote Sens.

[2] A. lodice, A. Natale, D. Riccio, "A Polarimetric Two-Scale Model for the Soil Moisture Content Retrieval", in Proceedings of the International Geoscience and Remote Sensing Symposium IGARSS2010, pp. 1265-1268,Honolulu (Hawaii), 2010.

8179-36, Poster Session

Japan-Touhoku Earthquake : ALOS/PALSAR observations for flooding area by tsunamis

N. Kawano, Japan Aerospace Exploration Agency (Japan)

A terrible earthquake with 9.0 magnitude struke on Touhoku region, Japan at 14:46 (local time) on 11 March 2011, big tsunamis attacked about 20 - 60 minutes later to the Touhoku, which reached 6 - 7 km from coasts at most. Tsumanis caused huge damege along the coast, and flooding area by Tsunamis remained for about 2 weeks at longest. Phased array type L-band Synthetic Aperture Radar(PALSAR) boarded on Advanced Land Observing Satellite(ALOS) operated by Japan Aerospace Exploration Agency(JAXA) made emergency observations on 13, 14, 16, 17, 18, 19, and 21 March.

SPIE Remote Sensing

Comparison these "post disaster" images with "pre disaster", sigmanaught of post disaster in such flooding area is generally smaller than those of pre disaster due to flooding.

This presentation will discuss effective algorithm to estimate flooding area and show variations of flooding area.

8179-39, Poster Session

Neural networks algorithms for Oil spill detection using TerraSAR-X satellite data

R. G. Avezzano, Univ. degli Studi di Roma Tor Vergata (Italy); M. Soccorsi, D. Velotto, Deutsches Zentrum für Luft- und Raumfahrt e.V. (Germany); F. Del Frate, Univ. degli Studi di Roma Tor Vergata (Italy); S. Lehner, Deutsches Zentrum für Luft- und Raumfahrt e.V. (Germany)

Ocean oil slicks dampen the Bragg waves (wavelength of a few cm) on the ocean surface and reduce the radar backscatter coefficient. This results in dark regions or spots in satellite SAR images making them an important tool in oil spill monitoring also due to its wide area coverage and day and night all-weather capabilities.

However, the increased amount of available SAR images involves a growing workload on the operators at analysis centres. In addition, even if the operators go through extensive training to learn manual oil spill detection, they can provide different and subjective response. Hence, the upgrade and improvements of algorithms for automatic detection that can help in screening the images and prioritising the alarms are of great benefit.

In this paper we present the potentialities of TerraSAR-X data and Neural Network algorithms for detection of oil spills. The new German radar satellite TerraSAR-X provides X-band radar images of the entire planet with a resolution of up to 1m and can be very effective in the monitoring of coastal areas to prevent sea pollution. An artificial neural network (NN) may be viewed as a mathematical model composed of many nonlinear computational elements, named neurons, operating in parallel and massively connected by links characterized by different weights. This particular structure makes neural networks very stable and robust when there are sensible input variations. For this study, multilayer perceptrons (MPL) have been considered, which have been found to have a suited topology for classification and inversion problems. The network input is a vector containing the values of a set of features characterizing an oil spill candidate. The output gives the probability for the candidate to be a real oil spill.

The classification performance has been evaluated on a data set of about 50 TerraSAR-X images containing more than 150 examples of oil spills and lookalikes. After image radiometric calibration, dedicated procedures to extract the features from the dark object have been designed. These features consider the geometry of the dark object in terms of its extension and of its shape, as well as the physical behavior in terms of the characteristics of the backscattering intensity of the pixels belonging to the object and to the background. The preliminary classification results are satisfactory with an overall detection accuracy above 80%.

8179-40, Poster Session

Numerical weather prediction models and SAR interferometry: synergic use for meteorological and INSAR applications

N. Pierdicca, Univ. degli Studi di Roma La Sapienza (Italy); F. Rocca, Politecnico di Milano (Italy); D. Perissin, Institute of Space and Earth Information Science (China); R. Ferretti, Univ. degli Studi dell'Aguila (Italy); E. Pichelli, Univ degli Studi Dell'Aguila (Italy); B. Rommen, European Space Research and Technology Ctr. (Netherlands); N. Cimini, Istituto di Metodologie per l'Analisi Ambientale (Italy)

Spaceborne Interferometric Synthetic Aperture Radar (InSAR) is a well established technique useful in many land applications, such as tectonic movements, landslide monitoring and digital elevation model extraction. InSAR is based on the measurement of the

difference in phase of the signal backscattered by each land surface element observed from different points and/or at different times. The atmosphere, particularly due to the high water vapour spatial and temporal variability, introduces an unknown delay in the signal propagation. This effect might be also exploited, so as InSAR could become a tool for high-resolution water vapour retrieval. The ingestion of the latter into weather prediction models is very promising, since water vapour is one of the most significant constituents of the atmosphere, and its state change is responsible for cloud and precipitation and its interaction with radiation is a crucial factor in climate variation. Yet water vapour remains one of the most poorly characterized meteorological parameters. Improving knowledge of the water vapour field is needed for a variety of atmospheric applications and for studying the propagation of microwaves as well.

This paper is related to the ESA project METAWAVE (Mitigation of Electromagnetic Transmission errors induced by Atmospheric WAter Vapour Effects), where the above mentioned problematic was deeply investigated by a large team composed of SAR experts, meteorologists and atmospheric remote sensing experts. The main objective of the project was to develop a method to provide valuable information on the water vapour field at a suitable resolution to mitigate its effect on SAR interferograms. Nonetheless, a first attempt was made to exploit the availability of a sequence of Atmospheric Phase Screen (APS) maps for meteorological purposes. The APS maps were derived by processing a sequence of ASAR interferometric overpasses using the Permanent Scatterer (PS) technique developed by Polytechnic of Milan. In the frame of such project, the local circulation in the urban area of Rome was studied using the high-resolution Mesoscale Model (MM5) developed by PSU/NCAR. It is a well established Numerical Weather Prediction (NWP) fully compressible non-hydrostatic models, which allows for reaching resolution in the order of 1 km or even better. As far as the possibility to use InSAR APS into NWP models is concerned, a major difficulty is associated to the differential nature of the APS data (in time and space). APS's provide an insuperable high resolution mapping of the atmospheric path delay anomaly (i.e., differences in time and space) over points over the earth surface which remain steady in time, but they do not furnish absolute values. This difficulty can be overcome by relating on external information providing suitable climatological values, in order to provide the reference atmospheric signal associated to the master SAR image of the interferometric stack which cannot be known using SAR data only. Basically, we are incorporating the information on the water vapour field coming from global scale systems (such as ECMWF analysis), generally used as input for mesoscale or local scale meteorological forecasts, with the differential information at high spatial resolution provided by InSAR. In other words, in this work it is attempted to merge the low range of the spatial frequency spectrum of the vapour field provided by global NWP systems, with the high range of the spectrum provided by InSAR. Although this is probably one of the first and very preliminary attempt to exploit APS into NWP, based on the test we performed for the area of Rome, there are promising indications it may become another way to exploit InSAR multipass interferometry, like the one that will be feasible after the launch of Sentinel 1. The assimilation of the high resolution maps derived by the combination of ECMWF and APS data into MM5 produced small but significant effects on the NWP predictions. The impact is expected to become even more relevant by using the new generation of NWP models working at higher resolution, like the Weather Research & Forecasting Model (WRF). The work has demonstrated this is a promising way to use InSAR multipass technique characterised by a good revisit time, like the one made feasible by the Sentinel 1 mission, for atmospheric applications.

8179-41, Poster Session

Exploring constraints and benefits of PSI technique for landslide detection and monitoring from space

C. Iasio, S. Schneiderbauer, EURAC research (Italy); V. Mair, C. Strada, Provincia Autonoma di Bolzano Alto Adige (Italy)

The Persistent Scatterer Interferometry (PSI) technique as advanced interferometric analysis method is advantageous for tracking displacements over large areas and long time periods overcoming some of the constraints possessed by differential interferometry (DinSAR) techniques. It has the potential to cost-efficiently support the improvement of landslide inventories in quality and timeliness as well



as to increase monitoring frequency of known surface displacements if additional geological and geomorphological knowledge is integrated.

Recently the most often exploited family of SAR sensors operating in L- or C-Band (ENVISAT, ERS, JERS and RADARSAT) have been complemented by X-Band satellites (TerraSAR-X, COSMOSkyMed). X-Band SAR data are currently tested for their usefulness to be exploited by PSI techniques, counterbalancing their advantage of higher spatial and temporal resolution against the potentially problematic shorter wave length.

Recently the PSI technique gained relevance, particularly in remote and dangerous areas, where the implementation of traditional ground based measurements is too difficult or too expensive. Therefore, it is slowly evolving from a purely scientific application to an operational service, particularly appealing for public administrations responsible for the management of geo-physical hazards and landscape management. This new interest requires deeper understanding and better communication of potentials and limitations of the PSI methodology, the various SAR sensors as well as of the ranges of displacement rate for that it can be applied in a reliable way.

Within the scope of the GMES (Global Monitoring for Environment and Security) Fast Track Service SAFER, namely for test case South Tyrol the results of the PS analysis of 253 SAR scenes (ERS; ENVISAT and RADARSAT) are investigated in order to update the existing landslide inventory of the Province of Bolzano in Northern Italy. Due to the large amount of available scenes and new statistical methods for PS detection the data volume to be managed for adding value to the raw PS data is huge. Complex filters and classifiers based on terrain morphology, geology and other parameters are applied in order reduce the data amount, to eliminate errors and to allow for extracting most relevant surface movements.

The second project, LAWINA, is funded by the Italian Space Agency (ASI) deals with the monitoring of active slow moving landslides by means of COSMO SkyMed X-band. The research aims to assess:

- the capability and the convenience to use this high resolution data for monitoring surface movements in a non-urban area with scarce back-scattering objects;
- to assess the feasibility to integrate GPS and PS for high spatial and temporal resolution monitoring in order to reduce overall costs and to allow for monitoring processes in remote areas.

To implement and test this experimental methodology, a very well documented landslide is needed, with several ground control points, wide extension and good accessibility. For this purpose Corvara landslide in the Dolomites has been selected. The Corvara landslide area is used as ski slope in winter and represents one of the main tourist centres in the Alta Badia valley in the Dolomites threatening road, infrastructure and buildings close to the Corvara village. A preliminary feasibility study on persistent scatterers available in the test site, showed a critical scarcity of features on the moving sectors of the landslide. To improve the distribution of back-scattering features capable for X-band, a composite database with ancillary and historic data has been implemented in order to use adequate criteria for the location of artificial corner reflectors. The result of this methodology is finally validated and powered by a deformation model calculated on GPS and PS data separately, in order to compare and verify the hypothesis if the SAR-based measurements oriented along the LoS are able to describe the same dynamics detected by ground based measurements.

8179-42, Poster Session

Squint mode SAR raw data generation for moving ship on the ocean

D. Guijie, BeiHang Univ (China); X. Xu, BeiHang Univ. (China)

A procedure for synthetic aperture radar (SAR) raw data generation for moving ship on the ocean is proposed. It combines the raw data simulation of the ocean background and the moving ship. The raw data of the ocean and the ship are simulated under the uniform coordinate system according to the same simulation parameters, respectively. The relative geometry relationship between the ship and ocean background together with the ship's motion is defined in the uniform reference coordinate system. The desired SAR signal is obtained by vector summation.

For the ocean SAR raw data simulation, the dynamics and time-variant

reflectivity function are taken into account based on the distributed surface (DS) model. Firstly, one frame static ocean reflectivity function is calculated taking account the electromagnetic characteristics of the ocean. Then, a SAR raw signal simulation algorithm with time-domain integration along range dimension is adopted, to generate the raw signal of the static ocean reflectivity map. In the end, the time-variant characteristics of ocean wave is described by means of interpolation through the dispersion relationship. Compared with the traditional ocean SAR raw data simulator, the raw signal model is extended to squint mode SAR, and an efficient and accuracy raw signal simulation algorithm is presented for large squint SAR.

For the ship raw data simulation, this paper established the SAR raw signal model of the moving ship. The ship's six degrees of freedom movement (heave, surge, sway, yaw, roll, pitch) introduced by the time-varying ocean waves as well as the translation of the ship on sea surface are considered. The accurate SAR raw signal simulation algorithm in time domain is adopted for the moving ship.

The final SAR raw data for moving ship on the ocean is generated by vector summation in data domain.

In order to validate the proposed techniques, four kinds of SAR raw data are generated according to the ship's motion. Then the generated raw data is processed by SAR and ISAR imaging algorithm, respectively. The results demonstrate the validity and applicability of the proposed techniques.

8179-43, Poster Session

Evaluation of geometric accuracy and the features of TanDEM-X

T. Nonaka, K. Imai, T. Hiramatsu, PASCO Corp. (Japan)

TanDEM-X, the second TerraSAR-X series of satellite, was launched on 21 June, 2010. The specifications of TanDEM-X have similarities with TerraSAR-X, and its significant mission is to generate a global Digital Elevation Model (DEM) of unprecedented quality, accuracy, and coverage. The created homogeneous DEM will be released for the Earth's entire land surface in 2014. Based on this background, the knowledge acquisition for the accurate geometric accuracies of these satellites are critical for various users. Our study team has evaluated and reported the geometric accuracy of TerraSAR-X in previous papers, and revealed that the accuracy of the orthorectified product with corrected geometric distortion is better than 1m.

The current study evaluated the geometric accuracy of TanDEM-X twice in-situ by simultaneous observations using several corner reflectors. We set the reflectors on the flat ground, and measured the position of the reflectors before and after the satellite pass using GPS and achieved the accuracies within several centimeters. We utilized orthorectified product, and the correction of the geometric distortion was performed applying SRTM DEM with 90m pixel spacing. We used global SRTM DEM for the correction of our processing system for the prospect of actual operation for our commercial business.

The results indicated that the geometric tendency of TanDEM-X is almost similar with TerraSAR-X. We also evaluated the features for correcting the geometric distortion by examining the relationships between the geometric accuracy and incidence angle of the satellites. Then it showed that the geometric accuracy became better when the incidence angle is shallower. This evaluation revealed that we can actually acquire the outputs predicted by the theoretical morel.

The latest series of our conducted studies specify the high geometric accuracies as well as the reliability of the specifications of both TerraSAR-X and TanDEM-X, the newest commercially available SAR satellites.

8179-13, Session 3

Preliminary results of Cosmo/SkyMed announcement of opportunity projects about marine monitoring

F. Nirchio, Agenzia Spaziale Italiana (Italy)

The Italian Space Agency at the beginning of 2010 has started more then 150 project to exploit Cosmo/Skymed data. Twenty seven of

them have been financed, while the remaining have been approved to receive Cosmo/Skymed data. Some of these projects are relevant to sea monitoring or intend to develop applications pertinent to the marine or coastal environment. After one year of investigation some preliminary results are already available and will be presented in the paper. The subjects covered are relevant to coastal monitoring, in particular to the automatic extraction of the coastal line, the ship detection or metallic floating object detection, with the use of ISAR technique. Oil spill detection is another issue of special interest in the marine contest. For what concern the environmental condition there are some results about the wind and current estimation. For any theme it will be presented the study goals, the approach proposed, the test site identified and the external data selected for the development and validation. Particular attention will be paid to put in evidence the peculiarities of Cosmo/SkyMed features in the research activities, manly the frequent revisiting time and the high resolution capabilities.

8179-14, Session 3

The Gulf of Mexico oil rig accident: analysis by different SAR satellite images

F. Del Frate, A. Giacomini, D. Latini, D. Solimini, Univ. degli Studi di Roma Tor Vergata (Italy); W. J. Emery, Univ. of Colorado (United States)

The Gulf of Mexico oil spill is the largest accidental marine oil spill in the history of oil industry. After the explosion on the Deepwater Horizon semi-submersible Mobile Offshore Drilling Unit occurred, on April 20, 2010, it was estimated that 8,400 m3 of oil per day were escaping from the well until it was capped, on July 15. The spill caused extensive damage to marine and wildlife habitats as well as to the Gulf's fishing and tourism industries.

Microwaves are commonly used for remote sensing of ocean oil pollution. SAR images are not appreciably affected by the atmosphere except for heavy rainfall events and data can be acquired equally well in day or night. An oil film on the sea surface damps the short gravito-capillary waves due to the increased viscosity of the top layer, thus reducing the backscattered energy and hence yielding darker areas in the SAR image.

This contribution presents an analysis of the Gulf of Mexico oil spill event based on different satellite SAR images. The oil slicks were imaged at C- and X-bands by ENVISAT ASAR, TerraSAR-X, and COSMO-SkyMed sensors both at distant and close acquisition times. Two kinds

of analyses have been carried out based on the three sets of spaceborne SAR images. On one hand, the features of the backscattering coefficient inside the slick have been studied at the two radar frequencies and at different polarizations. On the other hand, the performance of automatic neural network algorithms for oil spill segmentation has been evaluated. In particular, Pulse Couple Neural Network (PCNN) algorithms, a relatively new technique based on the computational implementation of the mechanisms underlying the visual cortex of small mammals, have been considered for this purpose.

We report on the results obtained using different SAR bands, polarizations and spatial resolutions. In detail, the results of the analysis of the X-band SAR (TerraSAR-X and COSMO-SkyMed) images will be compared with those obtained from the C-band (ENVISAT) over the same areas and on the same days. We also show results obtained from COSMO-SkyMed images acquired at both VV and HH polarizations over the same areas and on the same days.

8179-15, Session 3

Oil detection in Radarsat-2 quadpolarization imagery: implications for ScanSAR performance

A. Cheng, R. De Abreu, Canadian Ice Service (Canada); P. Vachon, J. Wolfe, Defence Research and Development Canada (Canada)

Along with its mandate to monitor coastal ice conditions, Environment Canada's Canadian Ice Service (CIS) is also responsible for the daily



monitoring of Canadian coastal waters for the presence of oil-based pollution and potential oil sources (e.g. ships). The Integrated Satellite Tracking of Pollution (ISTOP) program uses RADARSAT-2 data to vector pollution surveillance assets to areas where oil discharges/ spills are suspected in support of enforcement and/or cleanup efforts. Both automated and visual detection techniques are used to identify potential pollution and source targets.

RADARSAT-2's new imaging capabilities and ground system promises significant improvement's in ISTOP's ability to detect and report on oil pollution. Of specific interest is the potential of dual polarization ScanSAR data acquired with VV polarization to improve the detection of oil pollution compared to data acquired with HH polarization, and with VH polarization to concurrently detect ship targets.

CIS and Defence R&D Canada - Ottawa are carrying out a joint project sponsored by the Canadian Space Agency's Government Related Initiatives Program to recommend RADARSAT-2 modes for maritime surveillance. ISTOP is a key maritime application, but it is difficult to obtain imagery with multiple polarizations over oil spills. As such, we have focussed on natural oil seeps where naturally occurring oil is consistently found on the ocean. To date, we have acquired a set of 12 RADARSAT-2 quad polarization (HH, HV, VV, VH) images off the Coal Oil Point Seep Field located near Santa Barbara, California. We have evaluated ocean backscatter suppression as a function of polarization. Although acquired at higher resolution than ScanSAR data, the observed results will be applicable to ScanSAR data and will be used to make mode recommendations to meet operational ISTOP requirements.

8179-16, Session 3

Multifractal analysis of oil slicks on SAR images

R. Coscione, G. Di Martino, A. Iodice, D. Riccio, G. Ruello, Univ. degli Studi di Napoli Federico II (Italy)

Synthetic Aperture Radar (SAR) systems offer incredible capability for earth observation and specifically for sea monitoring, which could, at least in principle, fill the lack of in-situ pollution surveys of seas and coasts and offer the ability to monitor oil slick occurrences. Nevertheless, the well known ambiguity problem of SAR images due to so called look-alikes (natural phenomena whose signature on the radar image is very similar to that of oil slicks), is a great limitation for this kind of applications. In order to cope with the ambiguity problem, postprocessing steps have to be performed on the original images.

In this paper we present a technique for the analysis of low intensity patches on SAR oceanic amplitude images. The proposed technique, which is based on multifractal analysis [1] of the edges of dark areas (here called regions of interest, ROI), can be used to identify oil slicks generated by moving ships. The core idea is that different physicalchemical interactions of oil slicks and look-alikes with the sea surface, imply different multifractal features for the edges of the ROIs on the acquired images. In particular, with regard to oil slicks generated by moving ships, mutlifractal features are involved by concurrent turbulent phenomena acting at different magnitude scales, i.e., ship movement, that determines typical elongated shape of related oil slick, sea turbulence due to ship's engines, as well as natural sea turbulence. Conversely, look-alikes due to lack of wind present a shape that is related to the wind turbulent behavior, implying a mono-fractal feature of ROIs' edges. Moreover, oil slicks not generated by moving ships, or slicks which stay on the sea surface for a long time, present a shape dictated essentially by sea turbulence, implying a monofractal feature of ROIs' edges, as well. Accordingly, we propose to perform a multifractal analysis on ROIs' edges, which consists in the estimation of their multifractal spectrum and in the evaluation of the "dispersion area" of this spectrum. The proposed procedure is tested on simulated SAR images, obtained by a two-step simulation scheme. First, a combination of deterministic and stochastic models (the latter based on fractional Brownian motion, fBm) are used to describe the contour of oil slicks and look-alikes [2]. Then these contours are given as input to a SAR simulator [3] able to provide simulated SAR images relevant to sea surfaces covered by slicks of different nature. On these simulated images the above mentioned multifractal analysis is applied. Methods and results are extensively discussed. In particular, the box-counting method is adopted for the evaluation of the multifractal parameters and a study on the choice of boxes dimension range is also performed, emphasizing the critical role of this processing step.

Conference 8179: SAR Image Analysis, Modeling, and Techniques



First results seem to indicate that the observation of multifractal spectra is useful in order to distinguish between oil slicks generated by moving ships from other kinds of slicks, even when these phenomena have the same degree of irregularity and an estimation of the classical fractal dimension is not suitable for discrimination purposes. References

[1] K. Falconer, Fractal Geometry: Mathematical Foundations and Applications, John Wiley & Sons, Ltd., 2003.

[2] A. Danisi, G. Di Martino, A. Iodice, D. Riccio, G. Ruello, M. Tello, J.J. Mallorqui and C. Lopez-Martinez, "SAR Simulation of Ocean Scenes Covered by Oil Slicks with Arbitrary Shapes", Proceedings IGARSS 2007, Barcelona (Spain), July 2007, pp. 1314-1317.

[3] G. Franceschetti, A. Iodice, D. Riccio, G. Ruello, R. Siviero, "SAR Raw Signal Simulation of Oil Slicks in Ocean Environments", IEEE Transactions on Geoscience and Remote Sensing, Vol. 40, n. 9, pp. 1935-1949, Sept. 2002.

8179-17, Session 4

Flood detection using COSMO-SkyMed data through a joint use of electromagnetic scattering models and mathematical morphology

L. Pulvirenti, N. Pierdicca, Univ. degli Studi di Roma La Sapienza (Italy); M. Chini, Istituto Nazionale di Geofisica e Vulcanologia (Italy); L. Guerriero, Univ. degli Studi di Roma Tor Vergata (Italy)

Floods are considered the most frequent natural disasters of the world and the most costly in terms of casualties as well. Mapping floods extension is important to determine the damages and for relief efforts. Several studies proved the potentiality of spaceborne Synthetic Aperture Radar (SAR) for flood mapping. The synoptic view, the capability to operate in almost all-weather conditions and both during daytime and nighttime, which are distinctive requirements for managing this kind of events, are the key features of this sensor. Moreover, the new very high spatial resolution SAR systems allow carrying out a fairly accurate delineation of the flood extent. However, the temporal repetitiveness of SAR measurements was a critical issue for their operational use, so far. To overcome this problem, the availability of images provided by a constellation of satellite radars can be exploited, in order to reduce the revisit time. The COSMO-SkyMed (COnstellation of small Satellites for Mediterranean basin Observation) mission offers a unique opportunity to obtain a large amount of daily acquired images, characterized by high spatial and radiometric resolutions.

An approach to deal with flood mapping using SAR data based on the outputs of well-established electromagnetic scattering models, an advanced image segmentation technique based on the mathematical morphology, and a fuzzy-rule-based classification method is proposed in this work. The approach includes also the use of ancillary data, such as a land cover map and a digital elevation model. The latter allows integrating simple hydraulic considerations into the classifier.

The study has been carried out within the framework of a project, named OPERA, funded by the Italian Space agency, whose final user is the Italian Civil Protection. OPERA aims at assessing the utility of Earth Observation techniques into an operational flood management system. Throughout the year 2010, several activations of OPERA were requested by the Italian Civil Protection, owing to several flood events happened in various countries (i.e., not only in Italy, but also in Pakistan, Thailand and Albania). A number of high-resolution Cosmo-SkyMed images were collected to observe the areas involved in the aforementioned flood events. More recently, the flood occurred in Australia (January 2011) and the inundations caused by the Japanese tsunami of March 11, 2011 were monitored through Cosmo-SkyMed as well.

Cosmo-SkyMed data have been processed by a pair of prototype algorithms implementing the proposed approach either using the fuzzy logic to perform a pixel-based classification, or based on a combined use of electromagnetic scattering models and image segmentation to carry out an object-based classification. The results of the applications of these algorithms on some of the aforesaid Cosmo-SkyMed data will be presented. Multi-temporal maps of flooded areas will be shown to highlight the capability of Cosmo-SkyMed to monitor the time evolution of flood events.

This work has been supported by the Italian Space Agency (ASI) under contract No. I/048/07/0

8179-18, Session 4

Detection of fault creep around NAF by InSAR time series analysis using PALSAR data

T. Deguchi, Nittetsu Mining Consultants Co., Ltd. (Japan)

North Anatolian Fault (NAF) has several records of a huge earthquake occurrence in the last one century, which is well-known as a risky active fault. Some signs indicating a creep displacement could be observed on the Ismetpasa segment. It is reported so far that the San Andreas fault in California, the Longitudinal Valley fault in Taiwan and the Valley Fault System in Metro Manila also exhibit fault creep. The fault with creep deformation is aseismic and never generate the large scale earthquakes. But the scale and rate of fault creep are important factors to watch the fault behavior and to understand the cycle of earthquake.

The purpose of this study is to investigate the distribution of spatial and temporal change on the ground motion due to fault creep in the surrounding of the Ismetpasa. DInSAR is capable to catch a subtle land displacement less than a centimeter and observe a wide area at a high spatial resolution. We applied InSAR time series analysis using PALSAR data in order to measure long-term ground deformation from 2007 until 2011. As a result, the land deformation that the northern part of the fault have slipped to east at a rate of 9 mm/year in line of sight was obviously detected. In addition, it became clear that the fault creep along the NAF extended 35 km in east to west direction.

8179-19, Session 4

A new neural networks scheme for automatic seismic source analysis from DInSAR data

M. Picchiani, F. Del Frate, G. Schiavon, Univ. degli Studi di Roma Tor Vergata (Italy); S. Stramondo, Istituto Nazionale di Geofisica e Vulcanologia (Italy)

Differential Interferometry techniques has been successfully applied to measure the surface displacement field caused by earthquakes. The coseismic deformation pattern mapped by an interferogram is the expression of an active fault at depth, so the fringe features somehow refer to the geometry and slip of the fault generating the seism. On the other hand information contained in the interferogram might not be easy to handle and an appropriate pre-processing stage can be recommended before the actual inversion, retrieving the fault parameters from the differential interferogram. The input redundancy reduction, aiming at extracting the most useful features contained in the interferogram, is even more crucial if the retrieval is performed by a neural network algorithm [1]. A network with fewer inputs has fewer adaptive parameters to be determined, which need a smaller training set to be properly constrained. This leads to a network with improved generalization properties providing smoother mappings. In addition, a network with fewer weights may be faster to train. All these benefits make the reduction in the dimension of the input data a recommended procedure in many NNs applications [2].

In this work we present a new scheme where the estimation of the fault parameters is obtained by chaining two different neural networks architectures: in the first one a dimensionality reduction is performed by the so called Auto-Associative Neural Networks (AANN) [3]. In the second stage the final inversion is carried out with a more standard MLP (Multi-Layer Perceptron) network [4]. The AANN architecture is characterized by a symmetrical topology in which the output layer is equal to the input layer and an internal "bottleneck" layer is included. The network is trained to perform the identity mapping between inputs and output. Since the bottleneck layer is smaller than the output, its nodes must represent or encode the information in the inputs for the subsequent layers to reconstruct the input.

Conference 8179: SAR Image Analysis, Modeling, and Techniques



The application of the proposed methodology has been validated with a set of experimental data obtained from different sensors, for three diverse events. In particular the earthquake occurred in Abruzzi region (Italy, April 2009) has been considered, using Cosmo SkyMed and TerraSar-X data. While the two events occurred in New Zealand near the city of Christchurch (4th September 2010 and 22nd February 2010) has been analyzed using ALOS PALSAR data.

[1] Stramondo S., Del Frate F., Picchiani M. and Schiavon G., 2011. Seismic Source Quantitative Parameters Retrieval from InSAR Data and Neural Networks, IEEE Transactions on Geoscience and Remote Sensing; doi:10.1109/TGRS.2010.2050776.

[2] Bishop, C. M.; 1995. Neural Networks for Pattern Recognition, Oxford University Press.

[3] Kramer M. A., 1991. Nonlinear principal component analysis using autoassociative neural networks, J. Amer. Inst. Chem. Eng. (AIChE), Vol. 37, pp. 233-243.

[4] F. Del Frate, G. Schiavon, 1998. A combined natural orthogonal functions/neural network technique for the radiometric estimation of atmospheric profiles, Radio Sci., vol. 33, n. 2, 405-410.

8179-20, Session 4

Preliminary analysis of a correlation between ground deformations and rainfall: the lvancich landslide, central Italy

F. Ardizzone, M. Rossi, G. Fornaro, R. Lanari, M. Manunta, Consiglio Nazionale delle Ricerche (Italy); A. C. Mondini, Consiglio Nazionale delle Ricerche (Italy) and Univ. degli Studi di Perugia (Italy); G. Zeni, F. Guzzetti, Consiglio Nazionale delle Ricerche (Italy)

We present the results of a preliminary comparison between ground deformation time series obtained usingthe SBAS-DInSAR technique in the period 1992 - 2010 and daily rainfall records, in the area of the Ivancich landslide, Assisi, central Italy.We investigate the ground deformationsexploitingfull-resolution analysis results obtained from the multi-temporal Differential Synthetic Aperture Radar Interferometry (DInSAR) technology applied to ascending and descending SAR data acquired by: (i) the European Remote Sensing (ERS-1/2) satellitesfrom 1992 to 2000, and (ii) the Envisat-ASARsatellitefrom 2003 to 2010. Wethen comparedthedeformation time series to the daily rainfall record for a representative rainfall station in the study area. Results are used to investigate the relationships between landslide surface movements and seasonal rainfall.

8179-21, Session 4

Comparative analyses of multi-frequency PSI ground deformation measurements

J. R. Sabater, J. Duro, D. Albiol, F. N. Koudogbo, Altamira Information (Spain)

In recent years many new developments have been made in the field of SAR image analysis. The wider diversity in available SAR imagery allows now to cover a wider range of applications in the domain of risk management and damage assessment.

The work that we propose is based on the analysis of differences in ground deformation measurements extracted from the analysis of data stacks acquired at different frequencies. The overall aim of the project is the definitions of criteria that could help in the selection of the appropriate SAR sensor for the each different type of region of interest. Key factors may be the geographic localization and the land cover type.

During the study, particular emphasis is placed on the study of the impact of the atmospheric artifacts at the different wavelengths, on the analysis of the achieved density of PS and finally on the capacity to detect and monitor fast and slow rate motions.

The first topic of the study deals with the conditions of wave propagation at the different frequencies. As noticed from image analysis, absorption and disturbance that undergoes the signal during its propagation can significantly impair on the quality of the SAR images, and thus on the ground deformation measurements. Moreover the use of frequencies above 3GHz minimizes ionospheric impact on propagation, while tropospheric effects are increased at those wavelengths. The impact of those effects will be observed and compared at the different frequencies.

The second theme of the study will conduct to a review and a redefinition of the criteria for the selection of those measurement points, depending on the frequency and the area of interest.

Finally the last part of the study focus on a better definition of how to exploit the L-band SAR data intrinsic capability to detect faster ground movements without ambiguities.

Sites of interest are identified in urban and rural zones, where stacks of datasets acquired by different sensors (TerraSAR-X, Cosmo SkyMed, Envisat ASAR, Radarsat-2 and/or ALOS) over overlapping periods are available. The processing will be done using the PSI processing chain developed by Altamira and qualified in the framework of the GSE ESA project Terrafirma called Stable Points Network interferometric Process.

8179-22, Session 5

Dedicated SAR simulation tools for ATR and scene analysis

H. Hammer, K. Schulz, Fraunhofer-Institut für Optronik, Systemtechnik und Bildauswertung (Germany)

With the advent of new high-resolution SAR satellites such as TerraSAR-X and Radarsat-2 the availability of SAR images for a wide range of applications has increased during the last years, including disaster management, arctic ice monitoring, building reconstruction from interferometric image pairs and even small scale deformation detection using the Permanent Scatterers technique on time series of satellite SAR imagery. Yet, the interpretation of SAR images for both human image analysts and computerized applications remains a challenging task. For many applications, SAR simulation can be a helpful tool. The basic simulator concept pursued at Fraunhofer IOSB, was presented at SPIE Europe 2009 in Berlin. Since then, the simulation has developed in several, sometimes contrary directions. These include the simulation of very large scenes at high resolution for purposes of scene analysis. The handling of large amounts of data always leads to a trade-off between calculation time and memory consumption, which ideally both should be low. Another direction is the use of simulated target chips for classification, which needs a very precise simulation of small objects with many facets, and a high flexibility of the simulation to model actual sensors as closely as possible. Since these tasks cannot be met by one single simulation software, a simulator suite was developed. In this paper, the different approaches for the simulation of large scenes at high resolution and for the calculation of training data for classification are presented and sample images, both for large scenes and for small objects for classification, are shown.

8179-23, Session 5

Target detection by change for SAR imagery

C. J. Willis, BAE Systems (United Kingdom)

Change detection provides a powerful means for the initial detection of small target objects. However, speckle effects mean this type of approach can be difficult to apply to Synthetic Aperture Radar (SAR) imagery. This paper examines two methods for object detection using change between a registered pair of SAR images and compares their performance when applied to a complex scene.

The techniques discussed are designed to detect change covering small areas ranging in size from a few to perhaps a few hundred pixels. The techniques considered are: the ratio of pixels, combined into small region detections, and; the ratio of variances, calculated from corresponding small regions in each image. Both techniques are implemented within a moving window framework to cover the whole scene, and both can use detected imagery. The pixel ratio based method is a straightforward approach with a correspondingly simple statistical interpretation. This scheme provides a good performance over a wide range of different image types, and a good baseline by which to consider the performance of the alternative approach. The

Conference 8179: SAR Image Analysis, Modeling, and Techniques



variance ratio method exploits the observation that, in SAR imagery at least, the pixels of man-made target objects in particular tend to show a more spiky speckle structure than those of natural clutter regions. The spikiness is captured, to some extent, by the variance operator and can be compared by taking the ratio of these measurements.

Ideally any test statistic should be characterized by a known statistical distribution such that formal tests of a null hypothesis might be carried out. Here the null hypothesis corresponds to no change, and knowledge of the distribution of the test statistic enables the implementation of a Constant False-Alarm Rate (CFAR) detection process. The analysis carried out herein considers the distribution of the ratio statistics under realistic operating parameterisations for target detection in SAR imagery. A property of the F-distribution is used to derive a bi-directional change detector such that changes associated with both the appearance and disappearance of objects can be treated.

Results are presented for a registered, high-resolution, X-band airborne SAR image pair collected over a short time interval. This pair of images cover an airfield and surrounding infrastructure. Unfortunately formal ground truth documenting exactly what changes have taken place is not available. However, colour composites provide an interpretable change image for human analysis and show a small number of easily identified differences between the imaging passes. Results are presented for the two change detection schemes in the form of detection maps and as composite detection maps for comparison. Both techniques are shown to give good results over the regions of identified change. However, the simple ratio is found to be considerably more sensitive to image speckle than the ratio of variances, typically leading to a higher false alarm rate for this approach.

8179-24, Session 5

Microwave remote sensing of natural stratifications

P. Imperatore, A. Iodice, D. Riccio, Univ. degli Studi di Napoli Federico II (Italy)

The response of natural stratification to electromagnetic wave has received much attention in last decades, since its crucial role played in the remote sensing arena. In this context, when the superficial structure of the Earth, whose formation is inherently layered, is concerned, the most general scheme that can be adopted includes the characterization of (piecewise) layered random media. Moreover, a key issue in remote sensing of Earth and other Planets is to reveal the content under the surface illuminated by the sensors. Accordingly, modeling electromagnetic scattering from complex 3-D layered media, including interfacial roughness, is of paramount interest in the microwave remote sensing context. In fact, the natural stratified media are definitely constituted by corrugated interfaces, each one exhibiting a certain amount of roughness, whereas the flatness is an idealization which does not occur in natural media

For such a purpose, a quantitative mathematical analysis of wave propagation in three-dimensional layered rough media is fundamental in understanding intriguing scattering phenomena in such structures, especially in the perspective of remote sensing applications. Recently, a systematic formulation has been introduced to deal with the analysis of a layered structure with an arbitrary number of rough interfaces. Specifically, the results of the Boundary Perturbation Theory (BPT) [1]-[5] lead to polarimetric, formally symmetric and physical revealing closed form analytical solutions. Indeed, this theoretical body of result enables the deep understanding of the involved physics mechanisms: the way in which the character of the local scattering processes emerges is dictated by the nature of the structural filter action, which is inherently governed by the series of coherent interactions with the medium boundaries. Strictly speaking, this is to say that a functional decomposition of the BPT global scattering solution in terms of basic single-scattering local processes is rigorously established [4].

The comprehensive scattering model based on the BPT, which maintains the formal consistence with all the previously existing simplified perturbative models, methodologically permits to analyze the bi-static scattering patterns of 3D multilayered rough media. The aim of this paper is to systematically show how polarimetric models obtainable in powerful BPT framework can be successfully applied to several situations of interest, emphasizing its wide relevance in

111

the remote sensing applications scenario. In particular, a proper characterization of the relevant interfacial roughness is adopted resorting to the fractal geometry; numerical examples are then presented with reference to representative of several situations of interest.

References

[1] P. Imperatore, A. Iodice and D. Riccio (2010). Electromagnetic Models for Remote Sensing of Layered Rough Media, Geoscience and Remote Sensing New Achievements, P. Imperatore and D. Riccio (Ed.), ISBN: 978-953-7619-97-8, InTech.

[2] G. Franceschetti, P. Imperatore, A. Iodice, D. Riccio, and G. Ruello, "Scattering from Layered Structures with one Rough Interface: A Unified Formulation of Perturbative Solutions", IEEE Trans. Geosci. Remote Sens., vol.46, no.6, pp.1634-1643, June 2008.

[3] P. Imperatore, A. Iodice, D. Riccio, "Electromagnetic Wave Scattering from Layered Structures with an Arbitrary Number of Rough Interfaces", IEEE Trans. Geosci. Remote Sens., vol.47, no.4, pp.1056-1072, April 2009.

[4] P. Imperatore, A. Iodice, D. Riccio, "Physical Meaning of Perturbative Solutions for Scattering From and Through Multilayered Structures with Rough Interfaces" IEEE Trans. Antennas and Propag., vol.58, no.8, pp.2710-2724, Aug. 2010.

[5] P. Imperatore, A. Iodice, D. Riccio, "Boundary Perturbation Theory for Scattering in Layered Rough Structures", in Passive Microwave Components and Antennas (Edited by V. Zhurbenko), INTECH Publisher, April 2010, pp. 1-25.

8179-25, Session 5

Multiple reflections in SAR images of business districts

D. Riccio, D. Di Leo, Univ. degli Studi di Napoli Federico II (Italy)

Multiple Reflections in SAR images of Business Districts Daniela Di Leo, Daniele Riccio

ABSTRACT

University of Napoli Federico II, Via Claudio 21, 80125, Napoli, Italy {daniele.riccio}@unina.it

The last generation of satellites is characterized by very small geometric resolution that complicates the interpretation of the corresponding SAR images: thus let growing the interest of unveiling some less evident features once not visible with the previous generation of spaceborne SARs. Within this framework we want to relate these features to the constituent of urban areas via a reliable electromagnetic model: in particular our attention is placed on the urban areas characterized by tall and/or closely spaced buildings, complicated by the presence of buildings with different form and materials, presenting windows, balconies and roofs, and possibly vehicles on the roads. All these constituents may lead to the "multiple reflections" phenomenon.

We consider for multiple reflections the interaction between different buildings, indeed we overcome the "electromagnetically isolated model" presented in [1,2] and introduce a set of conditions, as function of the distance between two subsequent buildings, to verify the occurrence of multiple reflections. Their individuation help us in the interpretation of a SAR image because some of these contributes can superimpose in the same resolution cell; this paper also provides the theory to eventually delete the multiple reflections detected on the SAR image and explain some less observable phenomenon.

We use a deterministic approach to relate the radar response to the characteristics of man-made structures and so the multiple reflections are expressed in a closed form in terms of the radar parameters (frequency, resolutions...) also introducing an electromagnetic description (dielectric constant of the wall and terrain surrounding the buildings) of the scene. We underline as the use of a closed form expression for the radar response lead to solve an inverse problem and retrieve some scene parameters. The employed approach requires a geometric description of the scene under test and lead to locate the multiple reflections of any order (from the double to N-th fold reflections) on the SAR slant range-azimuth plane. We develop a simulation code to verify the conditions found and locate the multiple

Conference 8179: SAR Image Analysis, Modeling, and Techniques



reflections with their correct value of amplitude on a selected reference system.

The described approach is applied on an actual case of an urban area characterized by regular buildings and we present the results by comparing the actual COSMO/Skymed and TerraSAR-X image at our disposal with our simulated images.

REFERENCES

[1] G.Franceschetti, A.Iodice, D.Riccio, "A Canonical Problem in Electromagnetic Backscattering from Buildings", IEEE Transactions on Geoscience and Remote Sensing, GE-40, 1787-1801, ago.2002.

[2] G.Franceschetti, A.Iodice, D.Riccio, G.Ruello, "SAR Raw Signal Simulation for Urban Structures", IEEE Transactions on Geoscience and Remote Sensing, GE-41, 1986-1995, set.2003.



Monday-Wednesday 19-21 September 2011 Part of Proceedings of SPIE Vol. 8180 Image and Signal Processing for Remote Sensing XVII

8180-01, Session 1

Multispectral pansharpening based on pixel modulation: state of the art and new results

B. Aiazzi, Istituto di Fisica Applicata Nello Carrara (Italy); L. Alparone, Univ. degli Studi di Firenze (Italy); S. Baronti, Istituto di Fisica Applicata Nello Carrara (Italy); A. Garzelli, Univ. degli Studi di Siena (Italy); M. Selva, Istituto di Fisica Applicata Nello Carrara (Italy)

Pan-sharpening is a branch of data fusion, more specifically of image fusion, that is receiving an ever increasing attention from the remote sensing community. New-generation space-borne imaging sensors operating in a variety of ground scales and spectral bands provide huge volumes of data having complementary spatial and spectral resolutions. Constraints on the signal to noise ratio (SNR) impose that the spatial resolution must be lower, if the desired spectral resolution is larger. Conversely, the highest spatial resolution is obtained whenever no spectral diversity is required. The trade-off of spectral and spatial resolution makes it desirable to perform a spatial enhancement of the lower resolution of the data-set having a higher ground resolution, but a lower spectral resolution; as a limit case, constituted by a unique panchromatic image (Pan) bearing no spectral information.

To pursue this goal, an extensive number of methods have been proposed in the literature over the last two decades. Most of them follow a general protocol, that can be summarized in the following two key points:

1) extract high-resolution geometrical information of the scene, not present in the MS image, from the Pan image;

2) incorporate such spatial details into the low-resolution MS bands, interpolated to the spatial scale of the Pan image, by properly modelling the relationships between the MS bands and the Pan image.

Among pansharpening methods, a large number rely on the radiative transfer model to produce a spatial detail vector, to be injected into the multispectral pixel vector, that is parallel to the latter. In this way, the smooth resampled MS image is pixel-by-pixel modulated through the sharp Pan image, thereby retaining its original spectral characteristics. Brovey transform method (Gillespie, 1987), HPM (Showengerdt, 1997), AWL (Nunez et al., 1999), SFIM (Liu, 2000), SDM (Aiazzi et al., 2003), and AWLP (Otazu et al., 2005) are only some examples of fusion methods based on pixel modulation. The main drawback of all such methods is that the constraint on spectral angle does not guarantee high spatial quality of pansharpened products. Same spectral angle as the resampled originals means that no distortion in color hues may occur. However, distortion in both intensity and saturation is likely to occur with Brovey transform, in saturation only with HPM, AWL, SFIM, SDM and AWLP. Therefore, the spatial quality of fusion products can be improved if some adjustment of the detail vector is devised.

In this paper, the characteristics of pansharpening methods based on modulation will be investigated. It is found that all the above methods significantly benefit, both visually and numerically, from setting a constraint also on the modulus of the detail vector, by means of a damping factor. Experiments on VHR MS+Pan data sets from different instruments highlight that such factor is always lower than one and depends on the instrument as well as on the landscape. Instead of a trial-and-error optimization, the value of the damping factor can be determined by minimizing some measurement of spatial distortion of fusion products. Sample values are reported for several instruments and types of land cover.

8180-02, Session 1

A new geometric invariant to match regions within remote sensing images of different modalities

C. Palmann, S. Mavromatis, J. Sequeira, Univ. de la Méditerranée (France)

The use of several images of various modalities has been proved to be quite useful for solving problems arising in many different applications of remote sensing. The main reason is that each image of a given modality conveys its own part of specific information, which can be integrated into a single model in order to improve our knowledge on a given area. With the large amount of available data, any task of integration must be performed automatically. At the very first stage of an automated integration process, a rather direct problem arises : given a region of interest within a first image, the question is to find out its equivalent within a second image acquired over the same scene but with a different modality. This problem is difficult because the decision to match two regions must rely on the common part of information supported by the two images, even if their modalities are quite different. This is the problem that we wish to address in this communication.

Knowing that targets can have various expressions in the images when they are "viewed" with sensors of different natures, our first purpose is to define what could be used as a common information between remote sensing images, independently of their modalities. Our discussion is focused on the physical processes involved in the construction of remote sensing images : we demonstrate that the only possible common information between any modalities is supported by the location of remarkable events, which are related to interfaces that occur between medium of different properties. These interfaces give rise to linear features that are likely to appear in different images at the same time. Nevertheless, these linear features are often extracted with various qualities and reliabilities, and they need to be represented into an unified manner. We propose to do it thanks to a set of primitives, each of them representing a local orientation.

Then our second purpose is to use the particular knowledge presented in the first part of this communication, in order to tackle our problem : finding out pairs of regions from images of different modalities. Given two candidate regions from two images, we demonstrate that it is possible to quantify their degree of similarity, thanks to the orientation distributions of the primitives they contain. Thus, according to their degree of similarity, the best N pairs of regions are obtained by a simple sorting process. The measure of similarity defined in this communication has the property of being invariant to the following transformations : translation, rotation and scaling ; this makes our method suitable for most of the situations that can be encountered in remote sensing. Moreover, attention has been paid about practical issues that must be taken into account in order to insure the effectiveness of our method.

Finally, we present several results on images of different modalities ; as we can see in the example below, a registration process could be initialized with the paired regions between the two images.

8180-03, Session 1

The automated procedure for detection of IDP's dwellings using VHR satellite imagery

M. Jenerowicz, Space Research Ctr. (Poland); T. Kemper, European Commission Joint Research Ctr. (Italy)

Internal displacement results from armed conflict, violence and human rights violation within a given administrative unit. A common reason of displacement is also inter-communal conflict caused by limited

access to natural resources, or by social and economic factors. In crisis situations the aim of the relief organizations is to gather the IDPs in camps thus allowing more focused humanitarian assistance. The proper location, the infrastructure and the type of shelters inside such camps are supposed to guarantee of IDPs security and wellbeing.

An efficient and comprehensive support in humanitarian crisis response and sometimes the only independent information source in the analysis of refugee and IDP camps are Very High Resolution (VHR) satellite imagery. The reliable procedures can support humanitarian relief agencies by providing rapidly a wide range of information in complex terrain situation. Furthermore, the last generation of VHR imagery, with a ground pixel size of meter and sub-meter with increased spectral fidelity, may be used to obtain an effective knowledge of population estimations and camp structure analysis based on automated dwellings extraction. So far, some studies have been done in order to highlight the advantage and importance of IDP and refugee camp's analyses based on VHR satellite data (S. Giada et al. 2003; M. Jenerowicz et al. 2010; T. Kemper et al. 2010).

This paper presents the results obtained by implementation of complex image processing algorithm for the estimation of dwellings structures in Darfur's IDP Camps, Sudan, based on Very High Resolution multispectral satellite imagery.

The automated method consists of accurately selected processing steps. At the preprocessing stage, in order to delimit the area of investigation, images has been segmented into contiguous regions based on texture properties.

The preliminary analysis involved the specific characterization of extracted structures. Based on VHR satellite imagery the visual interpretation and the granulometry-based features selection has been carried out in order to provide criteria for distinguishing different types of structures, build object-oriented ontology and thus construct the semantic network.

The quantification of dwellings number has been provided by application of Mathematical Morphology techniques (P. Soille, 2003). First, an area opening and an area closing is used to suppress all dark and bright objects, respectively, whose area is below a given threshold value. These objects can then be revealed by computing the difference between the original and the transformed images, considering at the final stage a given size criterion. Due to the similarity of spectral response from dwellings' roofs made of straw and surrounding in IDP Camps it is of grate importance to use a combination of information provided from wide multispectral range. First, the data fusion algorithm has been selected in order to provide an input for photogrammetric image analysis. The structural element used to probe image in hitor-miss transform consists of the pixels of the objects of interest and the pixels of a shadow cast by dwellings described in a function of the solar azimuth and elevation angle. This approach is dedicated to determine additional characteristics for the IDP dwellings extraction.

The results of analysis proved to be satisfactory for the roofs extraction and thereby for supporting the humanitarian relief agencies. The additional multispectral information used in analysis clearly improves the accuracy of dwellings detection. The Mathematical Morphology techniques are suitable for features extraction in VHR satellite imagery. Furthermore, the potential of Mathematical Morphology approach is evidenced due to its reliable results, easy application and low cost. If actively implemented, these approaches can provide important information that is necessary to confirm or measure the population number, enable decision making as a response of IDPs needs.

8180-04, Session 1

Applying modulation transfer function in high resolution image fusion

X. P. Zhang, The Second Institute of Oceanography, SOA (China); Y. Jia, Wuhan Univ. (China); D. Pan, The Second Institute of Oceanography, SOA (China); S. Jia, The First Surveying and Mapping Institute of Zhejiang (China); J. Chen, X. Chen, The Second Institute of Oceanography, SOA (China)

As an important technique in information processing and applications of remote sensing, image-fusion has made a great contribution to military and civil applications in national economy, agriculture, forestry, water conservancy and other application fields. However, existing fusion techniques are still less effective in very high-resolution



image fusion, and image spectrum distortion is the main problem. In this paper, a high frequency modulation fusion method based on modulation transfer function (MTF) filters is proposed to improve spectral quality of high-resolution fusion images such as GeoEye-1, Ikonos and Quickbird. Firstly, two dimensional modulation transfer function (MTF) filters are obtained from original GeoEye-1, Ikonos and Quickbird images respectively. Secondly, MTF filters are used to degrade original GeoEye-1, Ikonos and Quickbird images spatially, and initial multi-spectral and pan images in the degraded version are derived. Thirdly, high frequency modulation fusion parameters based on MTF-filters are performed under the minimum mean square error criterion. Finally, fusion images in the degraded version with spatial resolution of original multi-spectral images and the real scale with spatial resolution of Pan images are produced. Specifically, MTF-filters design is the key in the proposed algorithm. For one thing, several edges with proper angle are selected to obtain the average MTF value using the Edge method, and Gauss Fitting is applied to modify attained one-dimension MTF curves from original GeoEye-1, Ikonos and Quickbird images respectively. For another, the two dimensional MTF matrix is derived based on one-dimension MTF by transposition. Objective assessment indicators of entropy, root mean square error, difference index, average gradient, correlation coefficient and ERGAS are applied to the final fusion evulation along with subjective estimation. The results show that the proposed method performs well for GeoEye-1, Ikonos and Quickbird images fusion in terms of preservation of spectral information and spatial resolution compared to methods of weighted high-pass filtering, Gram-Schmidt and MTF general image fusion framework (MTF-GIF).

8180-05, Session 2

Application of multispectral color enhancement for remote sensing

N. Hashimoto, Y. Murakami, M. Yamaguchi, N. Ohyama, K. Uto, Y. Kosugi, Tokyo Institute of Technology (Japan)

Spectral imaging, which has more than 3 color channels, is useful for remote sensing, color reproduction, image analysis and so on. Since spectral features, which cannot be seen in RGB images, are included in them, many methods to visualize their spectral features have been developed. Previously, we proposed a multispectral color enhancement method [1], which can enhance the spectral features in multispectral images without changing the average color distribution, as the natural color of the object is sometimes important. On the other hand, hyperspectral images are often used in remote sensing for spectral classification, discrimination of species, vegetation analysis and etc. The proposed enhancement method is effective even for hyperspectral images. If we can find the meaningful spectral features in them, those features might be applied to novel indices for remote sensing. We applied the enhancement method to hyperspectral images of a rice paddy and trees, and analyzed them for remote sensing application.

In the enhancement method, the difference between the original image and its low-order approximation by KL transform is employed. This difference is weighted by multiplying the matrix and then overlaid to the original image. In the proposed method, the user can specify both the spectral band to extract the spectral feature and the color to be visualized, respectively. The enhancement result is visualized with the color assigned by the user.

In the experiment, we used the images which captured a rice paddy and trees. They were 101 band images sampled at 5 nm intervals through 400-900 nm. In the rice paddy image, the spectral feature, which could distinguish between crops and weeds, was seen at 800 nm. We might use such features, which cannot be observed in RGB images, for new vegetation indices. In the tree image, we aimed to find the spectral feature which can differentiate the tree species between oak and beech. In the result, the beech was enhanced at 705 nm and this spectral feature may be able to discriminate them. Furthermore, the spectral feature depending on the condition in the same species also could be seen at 695 nm. This result indicates that these spectral features might be utilized for indices to detect tree diseases.

In this paper, we applied multispectral color enhancement to hyperspectral images for remote sensing and could find the spectral features which might be useful to discriminate different species or regions with different conditions in the same species. It is considered that these spectral features found in this time might be utilized to



novel indices or other application for remote sensing. As a future work, we investigate the relationship between these results and physical meanings.

[1] N. Hashimoto et. al., Proc. IS&T CGIV, pp. 282-288, 2010.

8180-06, Session 2

Automated texture mapping of 3D models

A. Pelagotti, Istituto Nazionale di Ottica (Italy); F. Uccheddu, F. Picchioni, Univ. degli Studi di Firenze (Italy)

The texture mapping process is generally intended as the mapping of colour information onto the 3D data, i.e. on clouds of points or triangles (mesh). Depending on the device used, it is not always possible to simultaneously acquire the texture and the 3D model, and sometimes the texture obtained during 3D data acquisition does not have the required characteristics. This can be because of, i.e., low resolution or because it is required to texture a model with images different from RGB photos, such as, e.g, multispetral/multimodal images (IR, Xrays, UV fluorescence).

Texturing is currently a time consuming operation, which is mostly performed in a manual or semi-automated manner. Nevertheless, the visualization of a 3D model with a specific texturing is often the main, if not the only, product of interest of many application fields.

In case of detailed and complex 3D models, direct texturing of 3D point clouds allows a faster visualization, however, in case of meshed data, homologues points between the 3D mesh and the 2D image to-be-mapped mostly need an interactive procedure to be identify, since, to date, no automated and reliable approaches are available for all cases. Indeed the identification of homologues points between 2D and 3D data is a hard task, much more complex than image to image, or geometry to geometry registration. Furthermore, in applications involving infrared or multispectral images, it is generally quite challenging to identify common features between 2D and 3D data. Recently, we published the results of a first method of automatic texturing [1]. We present in this paper a new and improved technique, which increases the process automation.

Given a 3D model and a texture image related to a part of it, the developed method consists of the following steps:

1. automated generation of a set of images which are the depth-map images of the 3D model as seen from different points of view. Since in the 3D space the possible points of view are infinite, the exhaustive search of all the depth maps is not feasible. However we consider the 3D model (or the selected part of it which is under examination) as inscribed in a sphere. The start configuration for the possible viewpoints is a polyhedron inscribed in such sphere. All iteration step lay on the surface of the polyhedron a depth map is computed. Each depth-map image retains an intrinsic correspondence between depthmap pixels and the corresponding vertices of the model;

2. automated evaluation of the depth-map image, among the ones generated, which shows the best correspondence with the given texture, using a similarity measure based on mutual information between depth-map image and texture image. Once a viewpoint, and the corresponding depth map is selected, the polyhedron is then subdivided, increasing the number of its faces, generating new depthmaps form more view-points in the neighbourhood of the previous one. The evaluation procedure is then repeated until a high similarity is reached.

3. automated registration of the depth-map image with the texture (which may be rectified) using a maximization of the mutual information criterion (other robust automated registration methods may also be successfully applied);

4. automated texturing of the part of the model corresponding to the depth-map image.

This entire procedure can then be repeated for each available texture image.

The results that we present, demonstrate how this method provides a reliable solution for a fully automatic texture mapping technique in a finite number of iterations.

[1] Pelagotti, A. Del Mastio, F. Uccheddu and F. Remondino, "Automated Multispectral Texture Mapping of 3D Models", In Proceedings of 17th European Signal Processing Conference EUSIPCO 2009, August 24-28, 2009, Glasgow, Scotland

8180-07, Session 2

Radiometric correction of RapidEye imagery using the on-orbit side-slither method

C. Anderson, D. Naughton, A. Brunn, M. Thiele, RapidEye AG (Germany)

RapidEye AG is a commercial provider of geo-spatial information products and customized solutions derived from Earth observation image data. The source of this data is the RapidEye constellation that consists of five low-earth-orbit imaging satellites. This paper describes the rationale, methods and results of a relative radiometric correction campaign that was conducted between March and April 2011 using the side-slither technique.

Raw image data from any remote sensing electro-optical sensor contains spatial variations due to different pixel gain and bias terms. These variations in pixel responsivity lead to streaking and banding in images which is unique to the particular sensor. Several radiometrically uniform terrestrial scene types that included desert, ice field and rain forest were imaged with a Rapid Eye sensor that was positioned in a ninety-degree yaw orbital configuration. In so doing each imaging pixel was forced to view the same strip of ground and was therefore exposed to the same target radiance. This maneuver allows a flat-field to be produced and the relative response of each pixel to be evaluated for the same radiance input to the sensor.

The outcomes of this campaign provided several image sets of differing brightness that were used to calculate relative pixel gains in order to improve the relative calibration and correction of the spatial variations found in the raw image data. Pixel biases were derived from images using the same RapidEye sensor taken over the Pacific Ocean on ascending node passes at night on new-moon events. The relative gains computed from the side-slither images coupled with the biases derived from the night time images provided the correction parameters.

The results of this campaign were compared to standard processing techniques for the calculation of pixel parameters and demonstrated an improvement in the spatial uniformity associated with RapidEye sensor raw image data. The maneuver, data processing methods and the spatial non-uniformity correction levels achieved with the technique are described.

8180-08, Session 2

Metrological performances of smart structures based on Bragg grating sensors

E. de Cais, M. Borotto, M. Belloli, A. Bernasconi, S. Manzoni, Politecnico di Milano (Italy)

The fiber optic Bragg grating sensors (FBGS) have been recently introduced: they present a photo-record grating on the fiber itself, which allows the reflection of a certain wavelength of the imput light spectrum. The applied strain is estimated based on changes of the reflected wavelength.

One of the possible applications that has prompted us to study this type of sensors is the ability to create dynamometric structures based on carbon fiber: these kinds of structures are lightweight, strong and can be used, for example, in the wind tunnel where these characteristics are fundamental.

It is also possible to construct adhesive patches made of composite material: FBGS can be glued to a structure (a metal or a composite one) to determinate the applied strain field.

The metrological characteristics of FBGS have been tested and compared to strain gages ones, which represent the actual reference measurement systems.

It was decided to integrate the measurement system directly into a composite material, having achieved good results during the static and dynamic tests. We made carbon fiber specimens (two for traction and two for flexion tests) with FBGS integrated into them. The results were surprising: the integration of "nude" fiber optic sensor did not cause damage or deterioration in the quality of measurement, the signal noise was maintained at baseline levels and response to dynamic stress was definitely comparable to that offered by electrical strain gauges. The various solutions to compensate for thermal effects have offered



several information for analysis and the basis for a future use of these sensors for static or semi-static tests.

It was also possible to find out the amount of residual strains and the real temperature in the neighborhood of the sensor analyzing the changes in wavelength during the curing cycle: there are no other ways to determinate these parameters.

For this study, we used an unidirectional carbon fiber to avoid the creation of a double-pick reflection of the fiber bragg gratin sensor: the analysis of the whole spectrum shows that was an appropriate choice.

The possibility to integrate FBG sensors in a material that provides these features opens up new frontiers: it is possible to gain advantage in the construction of dynamometers for use in wind tunnel, characterized by high stiffness combined with limited weights, or even create adhesive patches to be applied to water craft to monitor the strains.

8180-09, Session 2

The null space method of deblurring problem solution

Y. Bunyak, InnoVinn (Ukraine); R. Kvetnyy, Vinnitsa National Technical Univ. (Ukraine); P. A. Molchanov, Ampac Inc. (United States) and Vinnitsya National Technical Univ. (Ukraine) and InnoVinn (Ukraine); O. Sofina, Vinnitsa National Technical Univ. (Ukraine)

Visualization of remotely measured data may be under influence of medium penetration, sensor vibration or defocusing. Such images have to be reconstructed by procedure of deblurring. The procedure includes estimation of the point spread function (PSF) and synthesis of the deconvolution operator.

Lane & Bates theorem has shown that if any blurred image is found as convolution of the PSF and original image then there is a zero-sheet which distinguishes zeros sets of characteristic polynomials of the PSF and original image. The general approach to zero-sheet separation is based on finding combinations of some mutually dependent zeros which create singularity of a Vandermonde like matrix.

The characteristic polynomials can be evaluated by autoregressive (AR) and moving average model of measured data matrix. The AR polynomial includes zeros sets of the PSF and original image polynomials, therefore the problem consists in choosin a method of zeros separation.

Pai & Bovik proposed the null space (NS) method: if there are some PSF (more then two) and corresponding to them measured images and their AR operators of convolution type then the right side NS of the combined operator is the sought original image.

The NS vector may be presented by AR model operator eigenvectors which correspond to least eigenvalues. The NS vector is the lexicographical presentation of original image matrix and so the NS approach is appropriate to relatively small images reconstruction. Estimation of the PSF and deblurring operator is the best choice in a case of large image.

Since original image can be defined as NS of the AR operator the PSF can be defined as the NS of conjugated AR operator. It was proven the lemma: the left side null space of the AR operator is the lexicographical presentation of the PSF on condition the AR parameters are common for original and blurred images.

The found PSF was used for deconvolution operator evaluation by least squares and Wiener spectral methods. The proposed NS method needs in single blurred image of arbitrary size. The deblurring of degraded by different degree of light speckle, defocusing, vibration and haze images shows effectiveness and simplicity of the method.

8180-10, Session 3

Kernel methods in remote sensing data processing: tricks of the trade

G. Camps-Valls, Univ. de València (Spain)

No abstract available

8180-11, Session 3

Active versus semisupervised learning paradigm for the classification of remote sensing images

C. Persello, L. Bruzzone, Univ. degli Studi di Trento (Italy)

Machine learning techniques have been widely used in the past decades for the analysis and classification of remote sensing (RS) data. In this framework, in the recent years, support vector machines (SVMs) and kernel methods have gained increasing attention in the RS community, and nowadays are becoming state-of-the-art techniques. The development of machine learning methodologies has been followed by a parallel development of novel concepts and paradigms that have gained some relevance also in the RS community, e.g., semisupervised and active learning methods. Automatic classification of RS images is typically performed by using supervised classification techniques, which require the availability of labeled samples for training the supervised algorithm. However, the collection of labeled samples is usually time consuming and costly. The amount and the quality of the available training samples are fundamental for obtaining accurate classification maps. Nonetheless, in many real world problems the available training samples are not enough for an adequate learning of the classifier. Thus, in order to enrich the information given as input to the supervised learning algorithm and to improve classification accuracy, semisupervised learning (SSL) techniques have been proposed, which jointly exploit labeled and unlabeled samples in the training of the classifier. SSL approaches based on SVMs have been successfully applied to the classification of multispectral and hyperspectral data, where the ratio between the number of training samples and the number of available spectral channels is small [1]-[2]. An alternative approach for improving the learning of the classifier is active learning (AL). This paradigm consists in iteratively expand the original training set according to an interactive process that involves a supervisor, which is able to assign the correct label to any queried sample. This approach results very effective in different application domains for optimizing the definition of the training set, and has been recently applied also to the classification of RS images [3]-[4]. In AL: i) the learning process repeatedly queries available unlabeled samples to select the ones that are expected to be the most informative for an effective learning of the classifier, ii) the supervisor (e.g., the user) labels the selected samples interacting with the system, and iii) the learner update the classification rule by retraining with the updated training set. In this way, the unnecessary and redundant labeling of non-informative samples is avoided, greatly reducing the labeling cost and time. Moreover, AL allows one to reduce the computational complexity of the training phase.

AL and SSL share common theoretical aspects and properties, and plays around similar concepts exploited from two different perspective. In this paper, we present a theoretical analysis on the two considered approaches in relation to the classification of RS images. Moreover, we present experimental comparisons that aim at identifying the advantages and disadvantages of AL and SSL methods, and also try to point out the boundary condition on the applicability of these methods both in terms of available labeled samples and reliability of classification results. The experimental analysis is carried out on both toy examples and on real RS data. Different kernel-based active and semisupervised learning methods are considered in the experiments. Limits and potentials of both approaches are critically analyzed in the light of possible applications to different RS scenarios characterized by different kinds of data and classification problems.

REFERENCES

[1] L. Bruzzone, M. Chi, M. Marconcini, "A Novel Transductive SVM for the Semisupervised Classification of Remote-Sensing Images,"IEEE Transactions on Geoscience and Remote Sensing, Vol. 44, No. 11, pp. 3363-3373, 2006.

[2] L. Gomez-Chova, G. Camp-Valls, J. Munoz-Mari, J. Calpe, "Semisupervised Image Classification with Laplacian Support Vector Machines," IEEE Geoscience and Remote Sensing Letters, Vol. 5, No. 3, pp.336-340, July 2008.

[3] P. Mitra, B. U. Shankar, and S. K. Pal, "Segmentation of multispectral remote sensing images using active support vector machines," Pattern Recognition Letters, Vol. 25, No. 9, pp. 1067-1074, Jul. 2004. [4] B. Demir, C. Persello, L.Bruzzone, "Batch-Mode Active-Learning Methods for the Interactive Classification of Remote Sensing Images," IEEE Transactions on Geoscience and Remote Sensing, Vol. 49, No.3, pp. 1014-1031, March 2011.

8180-12, Session 3

Selection of samples for active labeling in semi-supervised hyperspectral pixel classification

O. Rajadell, Univ. Jaume I (Spain) and AIDO Inst Tecnológico de Óptica Color e Imagen (Spain); V. C. Dinh, R. P. W. Duin, Technische Univ. Delft (Netherlands); P. García-Sevilla, Univ. Jaume I (Spain)

Many approaches have been given to pixel classification in satellite imaging, most of them from a supervised point of view. In such a case, a training set is picked at random among all labelled samples in the dataset. Here, we describe a semi-supervised pixel classification scheme for hyperspectral satellite images aimed at reducing the expert participation while improving previous results obtained by other classification schemes. One of the problems in semi-supervised land classification tasks for hyperspectral satellite images lies in improving classification results using a very reduced set of labelled pixels to train the system. It is known that the more labelled data the system is provided with, the better results it may obtain. However, providing larger amounts of labelled data is expensive in terms of expert participation. Our scheme includes a previous non-supervised band selection step followed by a non-supervised search of highly representative samples in the image. These most suitable samples are given to the expert to be labelled and a classification process is performed using them for training. Because the most representative samples are selected, a smaller number of them is needed to depict the labelled classes of the database. In this way, the classification keeps the results in the same range of the ones obtained by previous schemes but using fewer labelled data, that is, minimizing the supervised process.

A previous work based in this classification scheme has been recently presented with fairly good results. In that work, the selection of samples is based on a mode-seek clustering that selects the modes with higher densities. As a result of the clustering, an unsupervised division of the samples in clusters is obtained. This mode seek is based on densities and the nearest neighbor rule. Therefore, each cluster defines a local density maximum surrounded by samples in a neighborhood defined by a distance rule. The local maxima densities are called modes of their clusters and they are very suitable for representing a considerable amount of samples when using a knn-classifier. Here we reduce the number of descriptive samples used even more by using a space-density criterion after the modeseek clustering. Also, we explore low densities for detecting, in a non-supervised way, the higher amount of different classes in a sixteen-class problem. The set of modes obtained stands very well for a high amount of samples of different labelled classes and when used together with a knn-classifier performs as well as a traditional random pick scheme where much more labelled samples and more complex classifiers were needed. As for the features used in both the clustering and the classification process, they can be carried out over the spectral features selected by the previous step or over spectralspatial features derived from Gabor filters. The differences between the localization of the modes in the image space will be discussed in both cases and the classification performances will be compared.

8180-13, Session 3

An active transfer learning technique driven by change detection for classification of temporal series of images

B. Demir, F. Bovolo, L. Bruzzone, Univ. degli Studi di Trento (Italy)

This abstract presents a novel active transfer learning technique for updating land-cover maps by classifying a temporal series of remote



sensing images (i.e., images acquired on the same area at different times). In real applications, land-cover maps can be updated by direct supervised classification of each image of the temporal series. Such an approach requires the availability of ground truth information for all the available temporal images in order to train the classifier. However, the collection of suitable training samples is time consuming and expensive. To deal with this problem, transfer learning (TL) [1] and active learning (AL) [2] approaches have been proposed in the literature. TL methods define strategies that use the information derived from images previously acquired on the area of interest (i.e., early observations) to classify new acquisitions. AL methods iteratively expand the training set size by automatically selecting the most informative samples among unlabeled ones. In this last case, human experts are requested to assign labels to a small optimal number of samples identified by the classification algorithm.

In this work, we propose a novel active transfer learning (ATL) technique for land-cover map updating, which is driven by change detection. The basic assumption in the proposed technique is that that no training samples are available for the current image to be classified, but they are given for earlier observations. Thus, the problem can be modeled in the context of domain adaptation [1]. In order to automatically classify the remote-sensing image for which training data are not available, a 4-step procedure is proposed. In the first step unsupervised change detection is applied to the image for which training data are available and to the image to classify (for which a training set is not available). Here, unsupervised change detection is performed according to the polar change vector analysis (CVA) technique [3]. Such a technique allows one to distinguish: i) changed from unchanged pixels; and ii) land-cover transitions from each other among changed pixels. In the second step, class labels of detected unchanged pixels are transferred from the initial training set to a new training set associated with the image to be classified (label propagation Step), whereas labels of training samples that fall in changed areas (which are not more reliable because changed) are not transferred. As we do not know which labels changed pixels may assume in the image to be classified, such samples are highly uncertain. They may either belong to: i) a new classes appeared in the new acquisitions, or ii) an already existing class that experienced a spatial shift. Accordingly, changed pixels result to be the most uncertain with respect to the classification process of the new image. Following this observation, the third step of the proposed method applies AL with a mechanism of priority. At the early iterations, the pool for AL is made up only of changed pixels. For each detected landcover transition the most uncertain samples are selected and labeled (Priority Active-Learning Step). After a given number of iterations, the priority is removed. Thus, the fourth step applies AL including all (changed and unchanged) unlabeled samples in the pool (Standard Active-Learning Step). Here, AL is performed based on the wellknown uncertainty entropy measure [2]. The proposed strategy allows one to enrich the training set with samples that may belong to new unknown classes and are therefore highly critical and informative with respect to the considered problem. This is done at the first iterations of the AL process leading to a fast improvement of the classification performance.

Experimental results show the effectiveness of the proposed ATL approach driven by unsupervised change detection for land-cover maps updating. These results will be presented in the full paper. REFERENCES

[1] L. Bruzzone, M. Marconcini, "Domain Adaptation Problems: a DASVM Classification Technique and a Circular Validation Strategy," IEEE Trans. Pattern Analysis and Machine Intelligence, vol. 32, no. 5, pp. 770-787, 2010.

[2] D. Tuia, F. Ratle, F. Pacifici, M. Kanevski, and W. J. Emery, "Active Learning methods for remote sensing image classification," IEEE Transactions on Geoscience and Remote Sensing, vol. 47, no. 7, pp. 2218-2232, July 2009.

[3] F. Bovolo, L. Bruzzone, "A Theoretical Framework for Unsupervised Change Detection Based on Change Vector Analysis in the Polar Domain," IEEE Transactions on Geoscience and Remote Sensing, vol. 45, No.1, pp. 218-236, Jan. 2007.

8180-14, Session 4

Transfer component analysis for domain adaptation in image classification

G. Matasci, M. Volpi, Univ. de Lausanne (Switzerland); D. Tuia, Univ de València (Spain); M. Kanevski, Univ. de Lausanne (Switzerland)

In remote sensing image classification the ground truth collection process can be very demanding. Therefore, when classifying series of similar images in a supervised way, the possibility to reuse labeled samples from a first acquisition is very appealing. Particularly, the ability to adapt a classifier built on an image, the source domain, to a new scene without needing any labeled data from the second image, the target domain, is of remarkable interest (Bruzzone and Marconcini, 2009). Similarly, such an approach is helpful when dealing with partial ground truth data covering a small and moderately representative subset of the image only. In the pattern recognition/machine learning community, this field of investigation is known as domain adaptation (Quinonero et al., 2009).

In the present paper we study the possibility to project both domains to a common feature space minimizing the difference between them. We refer to this family of techniques as feature-representation-transfer methods (Pan et al., 2010). After the proper joint mapping of the samples belonging to the two domains based on these newly extracted components, a model trained exclusively on the source image can be used for the predictions on the target image. Originally proposed by Pan et al. (2011), this approach named Transfer Component Analysis (TCA) is founded on the minimization of the distance between probability distributions of the two domains as measured by the Maximum Mean Discrepancy (MMD) criterion (Borgwardt et al., 2006). Such a measure is based on the evaluation of the distance between the means of the samples of the different domains when mapped in a common Reproducing Kernel Hilbert Space (RKHS).

The TCA approach can be resumed in the two following main steps:

- Build the kernel matrix K encoding the similarities between samples from both domains (stacked source and target samples). Using K and through the kernel trick, empirically compute the MMD distance between the domains and find a transformation matrix W minimizing such a quantity. This matrix is obtained by keeping the m leading eigenvectors of the solution of a trace optimization problem (Pan et al., 2011).
- By means of W, perform a low-dimensional embedding of the samples in a latent subspace where distribution differences are reduced. Train a SVM classifier on the mapped source labeled samples and subsequently use it to classify the target image embedded in the same subspace. Therefore, the approach does not require any user intervention (labeling) on the target image to be classified.

Experiments have been carried out on a 1.3 m spatial resolution hyperspectral image acquired by the ROSIS sensor over the city of Pavia, Italy (Licciardi et al., 2009). Different subsets of the image showing variations in the signature of the 4 considered ground cover classes have been used as source and target domains. When testing on the target image, significant improvements over the application of the classification model trained using unmapped source pixels only have been observed by using TCA. Since the proposed approach aims at reducing the distance between domains, it also showed a superior performance when compared to non-linear feature extraction techniques such as kernel PCA.

REFERENCES

[1] Bruzzone, L. and Marconcini, M., Toward the automatic updating of land-cover maps by a domainad aptation SVM classifier and a circular validation strategy, IEEE Transactions on Geoscience and Remote Sensing 47(4), 1108-1122 (2009).

[2] Quinonero-Candela, J., Sugiyama, M., Schwaighofer, A., and Lawrence, N. D., Dataset Shift in Machine Learning, MIT Press (2009).

[3] Pan, S. J. and Yang, Q., A Survey on Transfer Learning, IEEE Transactions on Knowledge and Data Engineering 22, 1345-1359 (2010).

[4] Pan, S. J., Tsang, I., Kwok, J. T., and Yang, Q., Domain Adaptation via Transfer Component Analysis, IEEE Transactions on Neural Networks 22, 199-210 (2011).



[5] Borgwardt, K. M., Gretton, A., Rasch, M. J., Kriegel, H.-P., Schlkopf, B., and Smola, A. J., Integrating structured biological data by Kernel Maximum Mean Discrepancy, Bioinformatics 22 (14), e49-e57 (2006).

[6] Licciardi, G., Pacifici, F., Tuia, D., Prasad, S., West, T., Giacco, F., Thiel, C., Inglada, J., Christophe, E.,

Chanussot, J., and Gamba, P., Decision Fusion for the Classification of Hyperspectral Data: Outcome of the 2008 GRS-S Data Fusion Contest, IEEE Transactions on Geoscience and Remote Sensing, 47(11), 3857-3865 (2009).

8180-15, Session 4

A novel approach to targeted land-cover classification

D. Fernández-Prieto, M. Marconcini, ESRIN (Italy)

In several application domains (e.g., agriculture, forestry, spatial planning, ecosystem monitoring, disaster management, habitat mapping, etc.), the ultimate operational objective of land-cover classification is actually limited to the identification of only one or few specific land-cover classes of interest (i.e., "targeted classes"), disregarding all the other potential classes present in the area under analysis, which could be completely unknown to an operator.

This type of problems (hereinafter referred to as "targeted land-cover classification") could be effectively solved by traditional supervised techniques provided that full and exhaustive ground-truth information (including samples from all the land-cover classes characterizing the area of interest) is available. Nevertheless, such a requirement is seldom satisfied and presents several practical limitations, both in terms of time and economic cost that may render this task difficult to achieve in most real-life cases.

However, the possibility of performing an effective targeted classification only using ground-truth samples available for the classes of interest would represent a significant advantage. Indeed, the collection of labeled samples for a single or few specific classes is certainly simpler and cheaper (e.g., a trained operator could even accomplish it by photo-interpretation). In this paper, we address such a challenging issue and propose a novel technique capable of solving targeted classification problems by exploiting the ground truth available only for the classes of interest, while providing accuracies comparable to those of traditional fully-supervised methods.

The rationale of the proposed technique is based on the observation that, according to Parzen density estimation, the probability density function (PDF) of an image can be always approximated by a mixture of suitable kernel functions. In particular, we consider circularly symmetric Gaussian kernels, whose parameters (i.e., centers and variances) are initialized using the k-means clustering algorithm, whereas final estimates are obtained by using the Expectation-Maximization (EM) algorithm. Once modeled the PDF of the entire image, for each of the targeted classes of interest we estimate the corresponding conditional PDF by properly weighting the resulting set of kernels. Indeed, the PDF of the whole image is itself a mixture density both of targeted classes of interest and the "unknown class" corresponding to all the other land-cover classes characterizing the investigated area for which no ground truth is available. Weights are determined for each targeted class by using the EM algorithm over the available training samples. Finally, each pixel of the image is associated with one of the considered targeted classes or the "unknown class" by minimizing a suitable energy function through an iterative procedure based on Markov Random Fields (MRF). Due to its non-parametric nature, the proposed approach can also be applied to address multi-sensor problems.

An extensive experimental analysis and cross-comparisons with both traditional fully supervised methods and one-class classification techniques (i.e., specifically designed for handling the particular case of a single class of interest) on different multi-sensor datasets (derived from PROBA CHRIS, Envisat ASAR and SPOT-4 HRVIR data) confirmed the effectiveness and the reliability of the proposed technique and its superiority with respect to state-of-the-art approaches.

8180-16, Session 4

Texture-based approach for shadow detection and classification improvement: metropolitan area case study, Spain

B. I. Z. Alhaddad, J. Roca Cladera, M. C. Burns, Univ. Politècnica de Catalunya (Spain)

This paper proposes an algorithm to search the shadow areas caused by buildings which are very common in satellite imagery of urban areas. The proposed searching algorithm uses the fast Fourier transform- FFT and computes correlation in frequency domain. We search the threshold for correlation which is appropriate to obtain the shadow areas which do not include the scattered small dark areas. One Spot 5 scenes acquired over the Metropolitan Areas was giving the pre-final result of the classification area are employ in the previous chapter. The construction elements such as buildings and industries area tend to align in some dominant direction in a small area and posses geometric regularity. Therefore, their shadows also align following these dominant directions in a small area in spite of the acquisition condition. The error of classification area caused by similar reflection (wave length) of different element inside the satellite image such as urban area and irrigated land. The promising results from this analysis prove that shadow-base information could be used as a potential cue for automated detection and correct of classification error process. Experimental results show this method is valid to extract shadow areas from the satellite imagery.

8180-17, Session 4

Large database coconut field classification by data mining on high-resolution lkonos images

E. Desmier, F. Flouvat, Univ. de la Nouvelle-Calédonie (New Caledonia); B. Stoll, Univ. de la Polynésie Française (French Polynesia); N. Selmaoui, Univ. de la Nouvelle-Calédonie (New Caledonia)

Supervised classification of satellite images is a commonly used technique in Remote Sensing. It allows producing classification thematic maps by using a training set, most often determined by experts in the field. ROI (Region Of Interest) are manually created on each image in order to statistically characterize class set. When a large number of images with high resolution occurs, manual creation of ROI for each image can be very time and money consuming. Other classification techniques must be applied Such as Data Mining techniques.

In our case, we aim to map coconut fields in a complete Tuamotu (French Polynesia archipelago) Ikonos image database. As a reference, the database consists in about 306 high-resolution Ikonos satellite imageries (0.80 m) covering 59 atolls (over 150 GB of data). These images were taken at different times and acquired with different weather and illumination conditions. A complete ground truth mission is unrealistic, it would be cost expensive, and some atolls are inaccessible. In addition, extracting several ROI per image and per class is a tedious work. The Different classes considered are: vegetation, water (sea), coral reef, ... representing at least 7 classes. More over, only three RGB channels represent these images, the Infra Red is unfortunately lacking.

The aim of this work is to propose a semi-automatic data mining method, able to detect coconut field regions on these 306 images. The proposed method involves two steps :

 First step consists in creating a set of ROIs per group of images, acquired under same conditions. To determine those groups, we use a clustering method on metadata (using for instance sun position, time, ...) with an additional parameters set, calculated automatically from each histogram image. The idea is to reduce the human involvement by creating semi-automatically ROI by class of images



 Second step is the supervised classification itself based on decision tree method where we have, for classification, a set of objects corresponding to pixels of images. The extracted ROIs are destined to be used as a basic training set. We first construct a tree using the three RGB components, and then we consider the binary codes of these components. This decomposition will allow the improvement of our results. Indeed, each component (R, G and B) is encoded on 11 bits, we then obtain 33 binary attributes.

The validation of our process is obtained by comparing our results, for three atoll images, to other results from a method proposed by [1] and using image analysis. We also compare results of biologists ground truth mission.

[1] R. Teina, D. Béréziat, B. Stoll, S. Chabrier. "Toward a Global Tuamotu Archipelago Coconut Trees Sensing using High Resolution Optical Data". In IEEE International Geoscience & Remote Sensing Symposium IGARSS'08. 2008. Boston, Massachusetts, U.S.A

8180-18, Session 4

Evaluation of textural features for multispectral images

U. Bayram, G. Can, Middle East Technical Univ. (Turkey)

To gain some perspective on useful textural features, we have brought together state-of-art textural features in recent literature, yet to be applied in remote sensing field, as well as presenting a comparison with traditional ones. Therefore we selected most commonly used textural features in remote sensing that are grey-level co-occurrence matrix (GLCM) [1] and Gabor features [7,8,9]. Other selected features are local binary patterns (LBP) [2], edge orientation features extracted after applying steerable filter [2, 4], and histogram of oriented gradients (HOG) features [5]. Color histogram feature [2] is also used and compared. Since most of these features are histogram-based, we have compared performance of bin-by-bin comparison with a histogram comparison method named as diffusion distance method [6]. During obtaining performance of each feature, k-nearest neighbor classification method (K-NN) is applied.

In this work, we studied on multispectral images that have 4m resolution. Target classes are urban field, water field, forest and bare land. Experiments are window-based. Window sizes are selected by considering to get representative histograms for features like LBP.

For GLCM features, energy, contrast and homogeneity features are calculated in four directions (0, 45, 90, 135). Images are filtered with Gabor filters in 4 scales 8 directions, then mean and variance of resulting texture is calculated and added to feature vector. For HOG, we followed instructions in [5]. For LBP, edge orientation and color histogram features, implementation details are followed from [2, 3].

In this work, we evaluate performances of various features for remote sensing image classification. For each feature vector, features are extracted from each band and concatenated. According to Figure 1, Gabor feature seems to be most discriminative. For forest class, best performance is obtained from color histogram feature. By considering each bin as a separate feature, k-NN classifier is applied. In this case, water class could not be found. When diffusion distance is used, result improves for all classes and water class seems to be found successfully.

As expected, HOG feature, which depends on gradient calculation, fails to detect homogeneous water areas. Yet, it gives promising results for forest, urban and some soil areas.

Although LBP feature seems to fail detecting any class, edge orientation feature detects some forest, urban and water areas accurately.

In order to see performance of each band separately, features are extracted and tested. According to these results, separate band features might give better cues for accurate classification rather than features of four bands concatenated.

Although Gabor and GLCM features seem to separate well in PCA, test results do not seem that promising. Instead of k-NN classifier, SVM might have given more accurate results for these features. Moreover, panchromatic images might be better for comparison of textural features.

8180-19, Session 5

Spectral-spatial classification of polarimetric SAR data using morphological profiles

P. R. Marpu, Univ. of Iceland (Iceland); K. Chen, National Central Univ. (Taiwan); J. A. Benediktsson, Univ. of Iceland (Iceland)

Morphological profiles (MPs) have been successfully used as tools to combine spectral and spatial information for classification of remote sensing data [1-5]. However, the previous applications have been limited to the multi-/ hyper-spectral data analysis. In this study, we extend the use of morphological profiles for classifying polarimetric synthetic aperture radar (POLSAR) data. An MP of a gray-level image (or a feature) is a sequence generated with the morphological opening by reconstruction and closing by reconstruction operations, using structuring elements of increasing size. An extended morphological profile (EMP) is constructed by stacking the MPs built using different features.

The POLSAR data provides a wealth of information regarding the scattering phenomenon in a pixel. Several types of features can be derived using the scattering vector. Some examples of the features include the amplitude of the linear polarizations, the real and imaginary parts of the off-diagonal elements of the covariance matrix [6], correlation between HH and VV polarizations, phase difference between HH and VV polarizations, cross-polarization ratio, co-polarization ratio, depolarization ratio [7] and also the features derived from various decomposition methods such as eigenvalue decomposition of the coherence matrix [8], Freeman and Durden decomposition [9], Yamaguchi decomposition [10], etc. In this work, we first try building MPs with the elements of the covariance matrix and the features derived from the eigenvalue decomposition method. The resulting EMP is used for supervised classification of the images using a support vector machine (SVM) classifier. Experiments will also be done in the future to use other features and decomposition methods to construct EMPs.

References:

1. J. A. Benediktsson, M. Pesaresi, and K. Arnason, "Classification and feature extraction for remote sensing images from urban areas based on morphological transformations," IEEE Trans. Geosci. Remote Sens., vol. 41, no. 9, pp. 1940-1949, September 2003.

2. J. A. Benediktsson, J. A. Palmason, and J. R. Sveinsson, "Classification of Hyperspectral Data From Urban Areas Based on Extended Morphological Profiles," IEEE Trans. Geosci. Remote Sens., vol. 43, no. 3, pp. 480-490, Mar. 2005.

3. M. Fauvel, J. Chanussot, J. A. Benediktsson, and J. R. Sveinsson, "Spectral and spatial classification of hyperspectral data using SVMs and morphological profiles," IEEE Trans. Geosci. Remote Sens., vol. 46, no. 10, pp. 3804-3814, Oct. 2008.

4. M. Pesaresi and J. A. Benediktsson, "A new approach for the morphological segmentation of high-resolution satellite imagery," IEEE Trans. Geosci. Remote Sens., vol. 39, no. 2, pp. 309-320, February 2001.

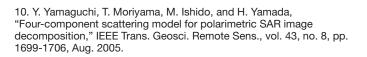
5. A. Plaza, P. Martinez, J. Plaza, and R. Perez, Dimensionality reduction and classification of hyperspectral image data using sequences of extended morphological transformations," IEEE Trans. Geosci. Remote Sens., vol. 43, no. 3, pp. 466-479, 2005.

6. Chia-Tang Chen; Kun-Shan Chen; Jong-Sen Lee; , "The use of fully polarimetric information for the fuzzy neural classification of SAR images," Geoscience and Remote Sensing, IEEE Transactions on , vol.41, no.9, pp. 2089- 2100, Sept. 2003.

7. Tongyuan Zou, Wen Yang, Dengxin Dai, and Hong Sun, "Polarimetric SAR Image Classification Using Multifeatures Combination and Extremely Randomized Clustering Forests," EURASIP Journal on Advances in Signal Processing, vol. 2010, Article ID 465612, 9 pages, 2010.

8. S. R. Cloude and E. Pottier, "A review of target decomposition theorems in radar polarimetry," IEEE Trans. Geosci. Remote Sens., vol. 34, no. 2, pp. 498-518, Mar. 1996.

9. A. Freeman and S. L. Durden, "A three-component scattering model for polarimetric SAR data," IEEE Trans. Geosci. Remote Sens., vol. 36, no. 3, pp. 936-973, May 1998.



Remote Sensina

8180-21, Session 5

An efficient approach for multi-temporal hyperspectral images interpretation based on high order tensor

S. Hemissi III, I. R. Farah, K. Saheb Ettabaa, Ecole Nationale des Sciences de l'Informatique (Tunisia); B. Soulaiman, TELECOM Bretagne (France)

Multi-temporal hyperspectral images are fundamental appliances for the worldwide assessment and monitoring of natural resources. Such tools allow a better description of the seasonal dynamics for land cover types. Thus, the temporal variation can provide an insight in the remote sensing studies. However, the use of this kind of images over highly heterogeneous areas might be practically unsuitable since that number of land cover types will be present in each pixel. This will lead to the so-called mixed pixel problem.

The main objective of this paper is to propose a novel approach for multi-temporal hyperspectral data interpretation based on multi-linear algebra and high-order tensor. It provides a robust framework for change analysis and multi-temporal endmembers extraction. Input dataset can be arranged from images which are taken at different acquisition times and having different temporal/spectral resolutions.

We introduce a novel approach for multi-temporal data interpretation based on multi-linear algebra and high-order tensor. Therefore, rather than using matrices for multi-dimensional analysis, the data is processed using the multi-way PARAFAC (PARallel FACtor analysis) model which is a decomposition of higher-order tensors in rank-1 terms.

The PARAFAC model overcomes the indeterminacies related to the linear mixing model. Thus, it is unnecessary to impose constraints such as statistical independence. Moreover, uniqueness is ensured with PARAFAC over ICA techniques. In a multi-linear decomposition of hyperspectral data, the multi-temporal data set can be transformed into a set of spatial independent components by taking linear combinations of multi-temporal endmembers. The analysis of the abundance fractions vector has also allowed us to better understand the nature and the trajectory of change.

8180-22, Session 5

Temporal interpolation and image fusion for improved land-cover maps

J. Inglada, Ctr. d'Etudes Spatiales de la Biosphère (France)

In the coming years, several optical space-borne systems with high resolution, high temporal frequency revisit and constant viewing angles will be launched: Venµs, Sentinel-2, LDCM. Formosat-2 is already providing this kind of data, but with low spectral resolution (4 spectral bands covering blue, green, red and near infrared). The availability of these data opens the opportunity for the development of new applications which require to closely monitor the temporal trajectory of the characteristics of land surfaces.

However, due to cloud cover and even to some rapid changes, a higher temporal resolution may be needed for some applications. One of the ways to improve the temporal resolution for these satellites is to merge their data with higher temporal resolution systems. For now, these other systems will fatally have a lower spatial resolution or a limited field of view.

Past research works have developed fusion approaches for using the synergy between HR resolution and mid- to low-resolution images. One of the conclusions of these works was that the resolution ratio between the images to fuse need to be not too far apart and that the spectral bands had to be very similar between the HR and the LR images. Therefore, combinations like SPOT-HRV and SPOT-Végétation were not suited because of the resolution ratio. And combinations like SPOT-HRV (or Landsat TM) and ENVISAT/MERIS were not appropriate

because of the differences in spectral sensitivities. The case of MODIS was even more complex, since bands are available with different ground sampling distances (GSD): 2 bands at 250 m., 5 at 500 m and the rest at 1 km.

In the coming years, the Proba-V mission and after that the Sentinel-3 family of satellites will offer improved and consistent spatial resolutions with respect to SPOT-Végétation and MODIS, as well as spectral sensitivities similar to those of some of the bands of Sentinel-2 and Landsat, for instance.

The goal of our work in this field is to assess the usefulness of this techniques for the joint use of Proba-V/Sentinel-3 data and Venus/ Sentinel-2/Landsat images for land-cover monitoring. As a result of the proposed work, one can expect an algorithm for the generation of land-cover maps and time profiles of surface reflectances with a spatial resolution of 10 to 30 m. with an update frequency of about 10 days.

8180-23, Session 6

An endmember extraction strategy for geometrical methods based on spectral-spatial information

M. Beauchemin, Natural Resources Canada (Canada)

A strategy for endmember extraction is presented. It has been preliminarily developed to mitigate the computationally intractable number of combinations problem involved in solving the optimization process associated to the class of endmember extraction techniques that depends on initialization. The proposed approach comprises two steps. The goal of the first step is to create two pools of spectra, one containing potential endmember candidates and the other one representing spectra that are unquestionably convex combination (mixed spectra). The second step exploits a sub-optimal subset search method, recently introduced elsewhere in the literature, to determine the best endmember combination. In the first step, vector order statistics is used to identify a medoid spectrum within nonoverlapping spatial windows that probe the entire image. The metric used to compute the medoid was originally designed for image database retrieval and combines both angle and magnitude of a pair of vectors. Each medoid spectrum that is too similar to all other spectra in a local window is discarded from the subset. This ensures that the medoid subset resides well within the convex hull of the whole dataset. Endmember extraction based on the iterative error analysis algorithm is then performed on the medoid subset to identify a set of medoid endmembers. The latter are subsequently used to spectrally unmix the original (entire) dataset. Spectra that are outside the simplex defined by the medoid enbmembers represent the pool of potential endmembers. Medoid spectra inside the simplex (inliers) constitute the mixed spectra pool. The inlier/outlier status of each spectrum of the original dataset is derived from conditions on their computed unmixing fraction values. Clustering analysis is next performed on the endmemder pool of candidates to produce a set of exemplars (homogeneous spectra bundles) that is referred to as the representative endmember pool. Spectral screening is applied on the inliers set to eliminate redundancy and this set is referred to the representative mixed spectra pool. In the second step, the oscillating feature subset search algorithm is adopted to identify the endmember combination that best reconstruct, in the least squares sense, the spectra in the joint representative pools. A second-pass algorithm is also proposed to improve the overall spectra reconstruction error by enlarging the inliers data set with spectra (new exemplars) that were poorly fitted in the first pass, and then re-performing the oscillating feature subset search. Results of the proposed strategy are presented for synthetic and real hyperspectral data.

8180-24, Session 6

Content-based hyperspectral image retrieval using spectral unmixing

A. J. Plaza, Univ. de Extremadura (Spain)

The purpose of content-based image retrieval (CBIR) is to retrieve, from real data stored in a database, information that is relevant to a query. A major challenge for the development of efficient CBIR systems in the context of hyperspectral remote sensing applications is how to deal



with the extremely large volumes of data produced by current Earthobserving (EO) imaging spectrometers. The data resulting from EO campaigns often comprises many Gigabytes per flight. When multiple instruments or timelines are combined, this leads to the collection of massive amounts of data coming from heterogeneous sources, and these data sets need to be effectively stored, managed, shared and retrieved. Furthermore, the growth in size and number of hyperspectral data archives demands more sophisticated search capabilities to allow users to locate and reuse data acquired in the past. Nowadays, it is estimated that a large fraction of collected hyperspectral data sets are never used but simply stored in a database, whereas these data already available in hyperspectral archives can be readily used in different application contexts or for different purposes than those that motivated the initial data collection, provided that effective CBIR mechanisms are in place to properly retrieve the data.

In this paper we propose new strategies to effectively retrieve hyperspectral image data sets from large image repositories. The combination of information from various sensors, and the combination with additional auxiliary experimental data (spectral and associated metadata) is supported by defining, developing and establishing procedures for this purpose based on spectral unmixing concepts. Spectral unmixing is a very important task for hyperspectral data exploitation since the spectral signatures collected in natural environments are invariably a mixture of the pure signatures of the various materials found within the spatial extent of the ground instantaneous field view of the imaging instrument. As a result, unmixing aims at inferring such pure spectral signatures, called endmembers, and the material fractions, called fractional abundances, at each pixel of the scene. In this work, we use the information provided by spectral unmixing (i.e. the spectral endmembers and their corresponding abundances in the scene) as effective metadata to develop a new CBIR system that can assist users in the task of efficiently searching hyperspectral image instances in large data repositories

The proposed innovative approach is experimentally validated using a collection of 154 hyperspectral data sets (comprising seven full flightlines) gathered by NASA using the Airborne Visible Infra-Red Imaging Spectrometer (AVIRIS) over the World Trade Center (WTC) area in New York City during the last two weeks of September, 2001, only a few days after the terrorist attacks that collapsed the two main towers and other buildings in the WTC complex. Our results indicate that the proposed system, which has been efficiently implemented in parallel, can efficiently retrieve hyperspectral images from a complex image database. The proposed system is expected to increase the value of the data acquired by airborne/satellite hyperspectral imaging instruments, and to improve the end-user services available in hyperspectral image databases.

8180-25, Session 6

Endmember detection in marine environment with oil spill event

C. Andreou, V. Karathanassi, National Technical Univ. of Athens (Greece)

Oil spill events are a crucial environmental issue. Detection of oil spills is important for both oil exploration and environmental protection. Hyperspectral remote sensing relies on the spectral information provided by numerous and spectrally narrow bands, and significantly contributes to the recognition of various components and properties of materials and objects. Spectral signatures of different oil types are very useful, since they may serve as endmembers in unmixing and classification models. In this paper, investigation concerning the potentiality of hyperspectral imagery for oil spill detection is performed for different oil type. Towards this direction, an oil spectral library resulting from spectral measurements of artificial oil spills in marine environment was conducted. Spectral measurements were acquired with spectro-radiometer GER1500 under sunny conditions. Samples of 5 different oil types were gathered from a Greek refinery. Among them, three were crude oils, one was heavy fuel oil, one was marine residual fuel oil, and one was light petroleum product.

For comparison reasons, same quantity of oil was used for each sample and spectral measurements were implemented for all the weathering states. Measurements of the reflectance of clear sea were also conducted.



Endmember extraction algorithms based on geometrical approach assume that the measured spectra can be expressed as a linear combination of the spectral signatures of linear independent materials (endmembers) presented in the mixed pixel. Oil spectral signatures will be examined whether they can be served as endmembers. This will be accomplished by testifying the linear independence and measure the correlation among them.

Synthetic hyperspectral images based on the relevant oil spectral library will be created. These images will simulate an oil spill event in marine environment. The oil spill and its spread on the sea surface will be presented in the image. In these images, targets will represent oils of various types and thickness. Endmember extraction methods will be applied on the synthetic images for evaluating their effectiveness for detecting oil spill events occurred from different oil types. For this purpose, several simplex-based endmember extraction methods have already been developed, such as sequential maximum angle convex cone (SMACC), vertex component analysis (VCA), n-findr (N-FINDR), automated target generation process (ATGP). All of them look for linearly independent and uncorrelated targets using different approaches, such as constrained unmixing method, convex cone analysis, maximization of the hyperspectral space volume and orthogonal subspace-based method, respectively.

8180-26, Session 6

Illumination and shadow compensation of hyperspectral images using a digital surface model and nonlinear least squares estimation

O. Friman, G. Tolt, J. Ahlberg, Swedish Defence Research Agency (Sweden)

The measured spectra in hyperspectral images from satellite or airborne platforms vary significantly depending on the lighting conditions at the imaged surface, e.g., shadow versus non-shadow. This complicates automated image analysis and object classification. In this work, a Digital Surface Model (DSM) and a spectral model is used to estimate different components of the incident light at a surface. These light components can subsequently be used to predict how a measured spectrum would look like under different lighting conditions.

The DSM used in this work is a height map of objects such as buildings, from which three geometry-related parameters can extracted at each pixel: the surface normal, the fraction of the sky that is visible, and the fraction of direct sunlight that hits the surface. For example, in shadow areas there is no direct sunlight, and close to a high building wall half the sky is blocked, thereby reducing the irradiance of the reflected skylight on the surface.

The latter two parameters can be found using ray casting algorithms. To find the direct sunlight fraction, the angle of the sun at the time of the image acquisition must also be known.

For an airborne hyperspectral sensor, the two major light components influencing the measurement are the direct sunlight and the typically bluish skylight. With the geometric parameters estimated from the DSM, the relative strengths of these light components in each pixel can be determined. Specifically, if pixels of the same material class, but under different lighting conditions, can be identified in the image, a non-linear least squares problem can be formulated to estimate the unknown direct sunlight spectrum, the skylight spectrum, and the reflectance spectrum of the material. The geometric parameters discussed above enter as known variables and the hyperspectral measurements for each pixel as the observations to which the residual squared errors are to be minimized. Note that we assume that the sunlight spectrum and the skylight spectrum are uniform across the scene, so that they can be used for subsequent processing of all pixels.

Based on all the spectral and geometrical parameters computed above, one can predict what a measured spectrum would look like if it were acquired under a different lighting condition. For example, it is possible to predict how a spectrum from a shadow area would look if it instead were illuminated by direct sunlight, or vice versa, i.e., a shadow correction. Another example is to simulate an image in which the direct sunlight hits all surfaces with an incident angle of zero degrees, to, for example, correct for slanted roofs in an urban environment. Results are demonstrated using a hyperspectral data set with 24 bands in the wavelength range 381.9 nm to 1040.4 nm. The images were acquired from an altitude of about 750 m and the pixel resolution is 0.5 m. A DSM with 0.25 m resolution was created from LIDAR 3D data acquired simultaneously with the hyperspectral data.

8180-27, Session 6

Spatial/spectral area-wise analysis for the classification of hyperspectral data

R. Guillaume, V. Achard, A. Alakian, ONERA (France); J. Fort, Univ. Paris Descartes (France)

In this paper, we propose an innovative classification method dedicated to hyperspectral images which uses both spectral information (Principal Component Analysis bands, Minimum Noise Fraction bands) and spatial information (textural features and segmentation). The process includes a segmentation as a a preprocessing step, a spatial/spectral features calculation step and finally an area-wise classification.

The segmentation is based on the works of Yining Deng and Feng Jing. They have developed respectively two criteria called J-image and H-image which allow to minimize the risks of over-segmentation by considering the homogeneity of an area at a textural level as well as a spectral level. These two criteria are calculated with a sliding window, respectively from a K-means classification result or from the data itself. Several scales of neighborhood are studied, resulting on a set of segmentation maps finally merged together using an agglomerative method. The segmentation step in itself is realized through a region growing method which detects initial seeds using both global and local information.

This segmentation method is expected to be used on multispectral data but we adapted it to hyperspectral imagery through reduction dimension methods. Then, we used it as a pre-processing for an area-wise classification. The first step of this new classification method consists in calculating several textural (Haralick's feature and texture spectra) and spectral (MNF or PCA bands) features for each area of the segmentation map. A vectorial classification is then performed either with a gaussian mixture model (unsupervised) or a support vector machine algorithm (supervised).

Our methods have been applied on two data sets. The first one is a semi-synthetic data set composed of six types of textural patches and built from a Rosis image of Oberpfaffen Hofen. The second one is an AVIRIS data set taken over the Indian Pine test site in northwest Indiana. The results of the algorithms have been compared with those obtained with the pixel-wise version of the classification methods. The improvement of classification performances, due to the coupling of spatial and spectral information is clearly demonstrated.

8180-28, Session 7

Sparse principal component analysis in hyperspectral change detection

A. A. Nielsen, R. Larsen, Technical Univ. of Denmark (Denmark)

This contribution deals with change detection by means of sparse principal component analysis (PCA) of simple differences of calibrated, bi-temporal HyMap data covering a small agricultural area near Lake Waging-Taching in Bavaria, Germany. HyMap is an airborne, hyperspectral instrument which records 126 spectral bands covering most of the wavelength region from 438 to 2,483 nm with 15-20 nm spacing. Data are acquired at 30 June 2003 8:43 UTC and 4 August 2003 10:23 UTC. The data at the two time points are radiometrically calibrated and orthorectified using GPS/IMU measurements, a DEM and ground control points. Changes detected over the five weeks are due to growth of the main crop types such as maize, barley and wheat. On pastures, which are constantly being grazed, in forest stands and in the lake to the south, no change is observed. Furthermore, both solar elevation and azimuth have changed which gives rise to edge effects where abrupt height differences on the ground occur.

A plot of percentage explained variance (PEV) shows that abrupt changes in PEV occur at around 80, 55 and (to a lesser extent) 15 nonzero elements. Hence we calculate and inspect leading sparse

principal component loadings (eigenvectors) and scores for 100, 80, 55 and 15 nonzero elements. Results show that if we retain only 15 nonzero loadings (out of 126) in the sparse PCA the resulting change scores appear visually very similar although the loadings are very different from their usual non-sparse counterparts. The choice of three wavelength regions as being most important for change detection demonstrates the feature selection capability of sparse PCA.

8180-29, Session 7

Change detection over Sokolov open-pit mine areas, Czech Republic, using multitemporal HyMAP data (2009-2010)

E. Ben-Dor, Tel Aviv Univ. (Israel)

Two HyMap images acquired over the same lignite open pit mining site in Sokolov, Czech Republic, during the summers of 2009 and 2010 (12 months apart), were investigated in this study. The site selected for this research is one of the three test sites (besides one in South Africa and another one in Kirgizstan) where research is being carried on within the framework of the EO-Miners FP7 Project (, http://www.eo-miners. eu). The goal of EO-MINERS is to "integrate new and existing Earth Observation tools to improve best practice in mining activities and to reduce the mining related environmental and societal footprint". Accordingly, the main objective of the current study was to develop hyperspectral-based means for detecting small spectral changes and relate them to possible degradation or reclamation indicators of the area under investigation. To ensure significant detection of small spectral changes, both temporal images were very carefully corrected to reflectance units using several different atmospheric correction approaches. Thus intensive spectroradiometric ground measurements to ensure calibration and validation aspects have been done during both over flights. The performance of these corrections was assessed using Quality Indicators (developed under a different FP7 project -EUFAR, (http://www.eufar.net) and the best corrected (reflectance) images were selected for further work. This approach allows directly the designation of those pixels that should be excluded for further analysis or that will be associated with a comparable weak accuracy respectively. The reflectance images were used as an input to apply change-detection algorithms, and indices for small and reliable spectral changes were then developed and applied on a pixel-bypixel basis. Using field spectroscopy and ground truth measurements on both overpasses' dates, it was possible to explain the results and allocate spatial kinetic processes of the environmental changes during the 12-month period of time. We found, for instance, that significant spectral changes are capable of revealing mineral processes, vegetation occurrences and soil formation long before these are apparent to the naked eye. Further study in this direction is being conducted under the above mentioned initiative in order to extend this approach to other mining areas worldwide. The present research is being undertaken within the framework of the FP7 Project (EO-MINERS, Grant Agreement n° 244242), and the grant n° 205/09/1989 funded by the Czech Science Foundation.

8180-30, Session 7

Urban land cover change of Olomouc city using Landsat images

M. Marjanovic, J. Harbula, J. Burian, J. Mirijovsky, Palack? Univ. Olomouc (Czech Republic); V. Kopacková, Czech Geological Survey (Czech Republic)

This research concentrates on mapping the land cover change in urban and sub-urban environments of Olomouc city in Czech Republic. The changes are tracked across a wide time span, from 1986 to 2009, by sequences of Landsat 5 TM images. For each sequence, identical image processing procedures were undertaken, in order to obtain consistent land cover maps of Olomouc. The processing thus came down to a classification problem. Among some standard pixel-based classification routines, we considered an approach that is somewhat hybrid, by introducing image segmentation (object-based classification) first, and then proceeding with a selection of pixel-based classifiers in supervised and unsupervised mode. The parameters of



the model with the highest accuracy in the test areas were adopted and applied to all image sets. Obtained land cover map of each set, i.e. each time sequence, was generalized to depict only the basic cover types of Olomouc city and its surroundings, i.e. classes involved urban areas, bare soil, vegetation, and water bodies (similarly as in Level 1 CORINE classification system for instance). These classes were subsequently cross-correlated among different time sequences and analyzed for temporal and spatial trends of change. Expectedly, the highest rates of change were noticed between the oldest dated and the most recent land cover map, although temporal rates of change fluctuate within the span. One spatial scenario is very typical, and suggests that the spatial change of urban areas are progressive, and developed on behalf of bare soil classes, which are presumably arable lands. Such plot simultaneously points to the pertinent problem in development of the city, and the ultimate practicality of this research is directed toward awaking of city's suburbanization problematic.

8180-31, Session 7

Analyzing SAR Image time series through change detection measures

S. Hachicha, F. Chaabane, SUP'COM (Tunisia)

Synthetic Aperture Radar (SAR) data enables direct observation of land surface at repetitive intervals and therefore allows temporal detection and monitoring of land changes.

In the literature, several approaches have been proposed for SAR change detection between two images. These methods can be classified in two classes: approaches based on pixel intensity and approaches based on local statistics.

All these techniques are designed for comparison between only two SAR images. Not many works were concerned to the change detection and monitoring over a times series of SAR images.

In this paper, we are interested in SAR change detection and monitoring through the analysis of a time series of SAR images covering the same region. The aim of this work is to consider the radiometric information and to characterize the change by its temporal signature and evolution. Then the investigation concerns the identification of the changes and their monitoring using a temporal classification.

The proposed technique suggests an original strategy for changes temporal classification using the behavior of the change detection measures between each SAR image and a constructed reference image. The proposed approach follows these main steps:

1. As a preprocessing step, we apply a spatio-temporal adaptive filtering of the SAR sequence.

2. Construction of the reference image which represents an intermediate state throughout the SAR time series.

3. Identification of the changes between the generated reference image and each filtered SAR image using the combination between change detection indicators.

4. Change detection map generation according to time series clustering of the previous step result.

As SAR images are inherently affected by the speckle which can be described as a multiplicative noise, the first step concerns a spatial and temporal adaptive filter which aims to reduce the speckle noise and to maximize the discrimination capability between the unchanged and the changed classes. The considered filter is based on the same scheme as the Non-Local Means filter by substituting the Euclidean distance with a similarity criterion adapted to speckle noise.

The second step is related to the reference image calculation. The reference image corresponds to the most stable state of the temporal patches for a given pixel. That's why it is considered as an intermediate image throughout the time sequence series.

Then the change detection measures are combined using an evidential and paradoxical reasoning in order to detect temporal changes between the generated reference image and each SAR image.

The last step concerns the temporal changes classification which is not straightforward, since time series contain a combination of seasonal, gradual and abrupt changes as explained above. Thus, we propose a generic change classification approach for time series change images based on SVM classification algorithm. This step allows the generation of a temporal map describing the spatial areas



according to their temporal behavior which can be very interesting in many applications.

The proposed approach was applied first on synthetic data which simulate most of the categories of the temporal changes and then validated in terms of probabilities of good detection and false alarms. We are now investigating the application of this approach on a set of 25 ENVISAT SAR images covering the region of Tunis City which is a developing region touched by several kinds of changes.

8180-32, Session 8

Lidar-based measurement of surface roughness features of single tree crowns

M. Kolditz, P. Krahwinkler, J. Roßmann, RWTH Aachen (Germany)

In remote sensing data, such as multispectral images and LIDAR height and intensity data, trees have a low interspecies variability. On the other hand they show a high variability within the tree species because of climatic variables like light, water and soil conditions, and different tree ages. Therefore, specific features that distinguish between unique properties of two tree species are required for a single tree based genera classification. Common approaches often use parameters describing the spectral differences between the classes and are already used in national forest inventories for example in Finland. To further improve classification results, the suitability of seven surface roughness features of objects, representing single tree crown regions or parts thereof, is studied.

The algorithms developed to provide roughness features can be validated and prototyped in a Virtual Forest testbed. The features are extracted from a normalized digital surface model with a resolution of 0.4m per pixel. The test area is located in north-west Germany and has an area of 240km². Within this test area more than 4000 single trees of eleven different species and additionally 200 buildings are available as reference data. As buildings usually have height values greater than zero in digital surface models, classification algorithms using the height as criterion to find tree objects, tend to take a building for a tree. To evaluate the results, the tree genera are divided in deciduous and coniferous trees and furthermore in seven categories - spruce, douglas fir, pine, larch, beech, oak and other broadleaved trees.

As deciduous trees generally have a smoother tree crown surface than coniferous trees, features describing the roughness of the tree crown's surface can be used to discriminate different tree species. Technical standards define several parameters to describe surface properties. These roughness features are evaluated in the context of single tree crowns. All of these features are based on the deviation of the height values of the tree crown to its mean height. Using previously segmented crown regions, the following features can be calculated: the arithmetic mean deviation, the root mean square deviation, the ten point height of irregularities, the total height, the skewness and the kurtosis. As an additional feature the relationship between the crown's surface area and its occupied ground area is used.

The evaluation results of these features regarding the discrimination of tree species on different levels - eleven single tree species, seven tree classes, deciduous and coniferous - and also towards discrimination of trees from buildings will be presented. As a measure for the separability of two classes Fisher's discriminant ratio J is used. It is defined as the ratio between the squared norm of the difference of the means and the sum of their variances. A large value of J corresponds to a high discriminative power of the corresponding feature. The evaluated features are incorporated into a tree species classification approach. Their contribution to the classification is analyzed and the results will be presented.

8180-33, Session 8

Dynamic and data-driven classification for polarimetric SAR images

S. Uhlmann, S. Kiranyaz, Tampere Univ. of Technology (Finland); T. Ince, Izmir Univ of Economics (Turkey); M. Gabbouj, Tampere Univ. of Technology (Finland)

Supervised methods for Synthetic Aperture Radar (SAR) image Land Use and Land Cover (LULC) classification proposed so far are only useful for static applications where a fixed set of features is applied to a particular SAR image dataset. Thus, it cannot be used for a new SAR dataset, even though it bears some similar terrain classes; and hence a new classifier has to be created and re-trained from scratch. Furthermore, the classifier cannot cope with new features, which can improve the discrimination power and hence the classification performance.

In this paper, we, therefore, introduce the application of the Collection of a Network of Binary Classifiers (CNBC) framework [1] for dynamic and scalable SAR terrain classification, where our main goal is to create a generic classifier for a collection of SAR images, which have a common data acquisition scheme and similar terrain classes. This is achieved by an adaptive and data-driven classification scheme applying incremental evolution sessions when new data is available in form of SAR images and their user-provided ground truth. The CNBC can support varying and large set of SAR features among which it optimally selects, weights and fuses the most discriminative ones for a particular class. Each SAR terrain class is devoted to a unique NBC, which encapsulates a set of evolutionary Binary Classifiers (BCs) discriminating the class with a distinctive feature set. Moreover, with each incremental evolution session, new classes/features can be introduced which signals the CNBC to create new corresponding NBCs and BCs within to adapt and scale dynamically to the necessary change.

During each incremental evolution session, existing NBCs are incrementally evolved only if they cannot accurately classify (or discriminate) the latest training data of the new emerging classes. In that, an empirical threshold level (e.g. 95%) is used to determine the level of classification accuracy required for the new training data encountered. This can in turn be a significant advantage when the current CNBC is used to classify multiple SAR images with similar terrain classes since no or only minimal (incremental) evolution sessions are needed to adapt it to a new classification problem while using the previously acquired knowledge. In this work, the recently proposed multi-dimensional Particle Swarm Optimization [2] is used for evolving feed-forward Artificial Neural Networks (ANN) that are used as the BC type.

We demonstrate our proposed classification approach over several medium and high-resolution NASA/JPL AIRSAR images within the San Francisco, San Diego and Long Beach area applying various polarimetric decompositions such as Yamaguchi [3] and van Zyl [4]. We evaluate and compare the computational complexity and classification accuracy using the USGS National Land Cover Dataset 1992 & 2001 [5] against static ANNs with fixed configurations. As CNBC classification accuracy can compete and even surpass them, the computational complexity of CNBC is significantly lower as the CNBC body supports high parallelization making it applicable to grid/ cloud computing.

References

[1] S. Kiranyaz, M. Gabbouj, J. Pulkkinen, T. Ince, K. Meissner, "Network of Evolutionary Binary Classifiers for Classification and Retrieval in Macroinvertebrate Databases", Proc. of IEEE ICIP, pp. 225-2260, 2010.

[2] S. Kiranyaz, T. Ince, A. Yildirim, M. Gabbouj, "Evolutionary Artificial Neural Networks by Multi-Dimensional Particle Swarm Optimization", Neural Networks, vol. 22, pp.1448-1462, 2009.

[3] Y. Yamaguchi, Y. Yajima, H. Yamada, "A four-component decomposition of POLSAR images based on the coherency matrix", IEEE Geoscience and Remote Sensing Letters, vol.3, no.3, pp.292-296, 2006.

[4] J.J. van Zyl, K. Yunjin, M. Arii, M "Requirements for Model-based Polarimetric Decompositions" IEEE IGARSS 2008, vol.5, pp.417-420, 2008.

[5] US Gelogical Survey Land Cover Institue http://landcover.usgs.gov/ index.php (accessed 21.3.2011)



Performance evaluation for blind methods of noise characteristic estimation for TerraSAR-X images

V. V. Lukin, D. V. Fevralev, N. N. Ponomarenko, S. K. Abramov, National Aerospace Univ. (Ukraine); K. Egiazarian, Tampere Univ. of Technology (Finland); B. Vozel, K. Chehdi, Univ. de Rennes 1 (France)

Since images formed by different systems are often noisy, this makes desirable to carry out estimation of noise characteristics before filtering or other operations of image pre-processing. Earlier we have proposed several methods for fully automatic (blind) estimation of noise characteristics [1-4]. These methods serve as a basis for a procedure consisting of the following steps. First, it is determined is noise i.i.d. or spatially correlated. For this purpose, it is possible to estimate mode R of the histogram of ratios of noise variance local estimates in spatial and spectral domain. R close to unity means that noise is practically i.i.d whilst larger R values (>1.05) relate to spatially correlated noise. Then, at next step, noise variance is to be estimated in the former case. In the latter one, it is also required to evaluate noise spatial spectrum.

The goal of this paper is to evaluate performance of the aforementioned methods for real life data. In this sense, TerraSAR-X data is a good choice since this spaceborne system produces images with fully developed speckle that fits well basic theoretical assumptions concerning its statistical properties. Then, deviations of the blind estimates are mainly due to the peculiarities of the considered techniques and their parameter setting and partly due to the influence of image content. Thus, we have selected 12 equal size (512x512 pixels) fragments from Rosenheim and Uluru images from TerraSAR-X database available for free use.

First, the values of R have been obtained. They are within the limits from 1.05 till 1.1 showing that noise is spatially correlated. Second, estimates of multiplicative noise variance have been obtained for different sizes of blocks (from 5x5 till 9x9 pixels). They are within the limits 0.25...0.34, i.e. quite close to the theoretical value 0.273 for amplitude SAR images with Rayleigh distributed speckle. Blind estimates are larger for images with more complex structure (larger percentage of blocks in textural and heterogeneous image regions) and/or if block size is larger. It is shown that confident conclusions can be drawn if the obtained estimates for different images or method parameters differ between each other by about 0.01.

Next, spatial spectrum of noise is evaluated in DCT domain. It is demonstrated that the obtained blind estimates do not differ a lot from each other for different considered image fragments and they are close enough to estimates obtained for manually selected homogeneous image regions.

The obtained estimates are exploited in DCT based filtering with frequency dependent thresholds proportional to local mean or median in each block. The use of frequency dependent thresholds is shown to provide about 2 dB improvement of noise suppression efficiency in homogeneous image regions compared to conventional (frequency independent) DCT filtering. Meanwhile, for better edge-detail-texture preservation, preliminary detection of such fragments is desirable. Then, slightly less thresholds are to be used in these regions to partly alleviate specific artifacts that can appear in the neighborhoods of sharp discontinuities.

Many examples of data obtained for aforementioned operations of real-life data processing will be presented in the final paper. REFERENCES

1. V. Lukin, N. Ponomarenko, K. Egiazarian, J. Astola, Adaptive DCTbased filtering of images corrupted by spatially correlated noise, Proceedings of SPIE Conference Image Processing: Algorithms and Systems VI, SPIE 6812, 12 p., 2008.

2. Lukin V., Fevralev D., Ponomarenko N., Abramov S., Pogrebnyak O., Egiazarian K., Astola J., Discrete cosine transform-based local adaptive filtering of images corrupted by nonstationary noise, Electronic Imaging Journal, 19(2), 1, April-June 2010, 15 p.



3. V. Lukin, S. Abramov, B. Vozel, K. Chehdi, J. Astola, Segmentationbased method for blind evaluation of noise variance in images, SPIE Journal on Applied Remote Sensing, Vol. 2, Aug. 2008, 15 p. (open access paper)

4. N.N. Ponomarenko, V.V. Lukin, K.O. Egiazarian, J.T. Astola, A method for blind estimation of spatially correlated noise characteristics, Proceedings of SPIE Conference Image Processing: Algorithms and Systems VII, San Jose, USA, 2010, 12 p.

8180-09, Session JS1

SAR-based sea traffic monitoring: a reliable approach for maritime surveillance

A. Renga, Univ. degli Studi di Napoli Federico II (Italy); M. D. Graziano, M. D'Errico, Seconda Univ. degli Studi di Napoli (Italy); A. Moccia, A. Cecchini, Univ. degli Studi di Napoli Federico II (Italy)

Maritime surveillance problems are drawing the attention of multiple institutional actors. National and international security agencies are interesting in matters like maritime traffic security, maritime pollution control, monitoring migration flows and detection of illegal fishing activities. In this concern the European Maritime and Safety Agency (EMSA) is going to integrate its services to provide vessel traffic monitoring information using geographical information service (GIS) to improve the capability to detect illegal oil spills and to indentify responsibilities. Furthermore maritime security is also under consideration by European Space Agency (ESA) in the framework of the European crisis response architectures (Del Monte et al., International Astronautical Congress, 2010) to comply with different issues: counter piracy actions, tanker accident monitoring, rescue support in the Artic region. In addition, in January 2010 the kick-off of the BlueMassMed pilot project was held, granted by the European Commission, which aims at increasing the cooperation for maritime surveillance in the Mediterranean Sea, including surveillance of illegal immigration, illicit trafficking, environmental pollution and reinforcement of the Search and Rescue efforts. Up until now, different options have been considered for vessel monitoring, ranging from transponders located onboard the vessels, such as the AIS, to optical imagery. However the achieved results by those methodologies in real scenarios (Margarit et al., IEEE Trans. on Geosc. and Remote Sens, 2007) have shown that, although there are a number of commercial systems available on the market today, none of these systems is really mature, e.g. there is no fully automated operational system providing accurate, reliable near-real time monitoring information. The major problem of all these systems still is that they are not capable to accurately detect ships at every sea state and to separate ships from other artificial offshore objects with a high accuracy. The SAR instrument can be a valuable solution since it is able to monitor wide areas with high spatial resolution almost independently from weather conditions and both day and night time. However, in spite of significant research activity focused on ship detection and motion estimation, to date, there are no efficient and robust algorithms that can routinely provide useful detection of ship and estimates of the speed and heading of detected ships (Dragosevic et al., IEEE Geosc. and Remote Sens. Letters, 2008). This paper deals with ship monitoring, i.e. ship detection, classification and motion estimation, algorithms based on SAR data. Satellite imaging is a good way to identify ships but, characterized by large swaths, it is likely that the imaged scenes contain a large number of ships, with the vast majority, hopefully, performing legal activities. Therefore, the imaging system needs a supporting system which identifies legal ships and limits the number of potential alarms to be further monitored by patrol boats or aircrafts. Specifically the work focuses on maritime surveillance by using COSMO/SkyMed constellation, also adequately integrated by AIS information to individuate innovative and reliable SAR-based products for sea traffic monitoring. The developed approach is finally validated using different combinations of both simulated and real-world AIS and COSMOSkyMed data takes.

8180-10, Session JS1

A novel paradigm for urban environment characterization using ascending and descending terrasar-x data

E. Angiuli, G. Trianni, European Commission Joint Research Ctr. (Italy); P. Gamba, Univ. degli Studi di Pavia (Italy)

The combined use of better spatial resolution (up to 1 meter) satellite data provided by the new generation of VHR SAR sensors, Terrasar-X and Cosmo-Skymed, and of high performance machines allows us to process massive datasets more efficiently and quickly than ever before. This also implies that now we can monitor regularly and more in depth the changes of the pattern in the human settlement landscape anywhere in the world. The benefits of this new ability are vast and vary from identifying, monitoring and thereby understanding human settlement vulnerabilities in a variety of contexts, from climate change responses to disaster risk reduction and improved post-disaster relief.

Therefore, innovative approaches are essential for a better assessment and a finer description of such areas. Synthetic Aperture Radar (SAR) imagery has become increasingly popular as some of its properties are favourable to optical imagery. The SAR signal is very sensitive to the geometry, orientation and material of the buildings; even though all that is usually considered as a drawback when using a single scene, it can become an advantage using different acquisitions. In that case SAR backscattering can be used to interpret not only the geometry of the man-made structures but also their spatial/topological relationships.

The dataset used in this study is composed of 2 different acquisitions over the city of Pavia, situated in northern Italy; the images have been acquired in HH polarization on the February 8, 2008 in ascending mode and on the February 12, 2008 in descending mode.

In this work, we propose a new paradigm for urban structures characterization exploiting the geometric and statistical properties of the objects backscattering.

The methodology is based on a semi-automatic segmentation method and on a statistical analysis by means of morphological and textural techniques [1, 2, 3]. This analysis should enable us to model and specify the spatial arrangement of the detected structures.

In this study we have investigated the potentialities of the joint use of images acquired in ascending and descending mode. The data have been analysed and processed individually and jointly and the results of the different processing steps are reported and discussed. Among the results, it has been proved that the joint use of the information extracted from the two different acquisition pass, leads to a more accurate and detailed representation of the urban environment descriptors.

REFERENCES

[1] M. Pesaresi, A. Gerhardinger, and F. Kayitakire, "A robust builtup area presence index by anisotropic rotation-invariant textural measure", IEEE Journal of Selected Topics in Applied Earth Observations and Remote Sensing, Vol. 1, No. 3, pp. 180-192, 2008.

[2] P. Gamba, M. Pesaresi, K. Molch, A. Gerhardinger, and G. Lisini, "Anisotropic rotation invariant built-up presence index: applications to SAR data", in Proc. IGARSS'08, Boston, MA, July 2008.

[3] F. Dell'Acqua, and P. Gamba: "Texture-based characterization of urban environments on satellite SAR images", IEEE Trans. on Geoscience and Remote Sensing, Vol. 41, n. 1, pp. 153-159, Jan. 2003.

8180-36, Session JS1

An experimental study on ship detection based on the fixed-point polarimetric whitening filter

D. Tao, Univ of Tromsø (Norway); C. Brekke, S. N. Anfinsen, Univ. of Tromsø (Norway)

This work investigates the behavior of the Fixed-Point Polarimetric Whitening Filter (FP-PWF) with respect to ship detection based on polarimetric Synthetic Aperture Radar (SAR) imagery. The purposes of this work are: (i) to investigate new distribution models for FP-



PWF output that incorporate texture, (ii) to examine Method of Log Cumulants (MoLC) for shape parameter estimation associated with texture, and (iii) to assess the impact of the improved modeling and estimation on the discrepancy between specified and observed false alarm rate. Experiments are performed on simulated data sets.

The Polarimetric Whitening Filter (PWF) algorithm [1] processes the quad polarimetric Single Look Complex (SLC) SAR data into full-resolution pixel intensities, and provides effective speckle reduction. In a previous study [2], the FP-PWF was proposed as a modification of the original PWF. In brief, the original PWF includes the complex multivariate Gaussian distributed scattering vector and the sample mean estimator for the covariance matrix which is Wishart distributed. The distribution of the original PWF output is then a linear transformation of the F-distribution. In the FP-PWF, the sample mean covariance matrix estimator is replaced with the fixed point (FP) estimator, which is asymptotically Wishart distributed also when the scattering vector has a non-Gaussian distribution [3]. The non-Gaussian scattering vector can be modeled as the product of a complex multivariate Gaussian vector representing the speckle and a texture variable representing spatial variability of the reflectivity, which is known to be an appropriate model for sea clutter. When texture variable is Gamma distributed or inverse Gamma distributed, the scattering vector becomes multivariate K-distributed or multivariate G0-distributed. Using Mellin Kind Statistics [4,5], new statistical models for the FP-PWF output can now be derived as a compound Gamma-F distribution and a compound inverse Gamma-F distribution, with the texture variable represented as Gamma and inverse Gamma distribution respectively. In this work, the goodness of fit of the compound F-distribution models are tested.

To the compound distribution models for the FP-PWF output, MoLC is applied to estimate the shape parameter [4,5]. The classical Method of Fractional Moments (MoFM) shape parameter estimator is involved as a reference in a comparison study. The MoLC shape parameter estimator is expected to provide better estimation accuracy (smaller bias and lower variance). The estimated parameters are applied by the cumulative distribution function of the FP-PWF output and affect the performance of the constant false alarm rate (CFAR) detector. In practice, there is an inevitable deviation between the specified false alarm rate and the observed false alarm rate, because of the inherent uncertainty in the parameter estimations. To compare the specified false alarm rate versus the observed false alarm rate, Monte Carlo simulations are performed with different statistical models and different shape parameter estimators. These simulations quantify the impact of the improved modeling and parameter estimation.

Reference:

[1] Novak, L. M., Burl, M. C., Irving, W. W., Optimal Polarimetric Processing for Enhanced Target Detection, IEEE Transactions on Aerospace and Electronic Systems, vol. 29, no. 1, 1993

[2] Anfinsen, S.N., Tao, D., and Brekke, C., Improved target detection in polarimetric SAR images by use of Mellin kind statistics, Proc. POLinSAR 2011, Frascati, Italy, 4 pp., 24-28 January, 2011

[3] Pascal, F., Forster, P., Ovarlez, J.-P., and Larzabal, P., Performance Analysis of Covariance Matrix Estimates in Impulsive Noise, IEEE Trans. Signal Proc., vol. 56, no. 6, 2206-2217, June 2008

[4] Nicolas, J.-M., Introduction aux statistiques de deuxi'eme esp'ece: applications des logs-moments et des logs-cumulants 'a l'analyse des lois d'images radar, Traitement du Signal, vol. 19, no. 3, pp. 139-167, 2002

[5] Anfinsen, S.N., On the supremacy of Logging, Proc. POLinSAR 2011, Frascati, Italy, 8 pp., 24-28 January, 2011

8180-37, Session JS1

A radar target DB construction method using 3D scattering centers

J. H. Yoo, C. H. Kim, D. Y. Chae, K. Kwon, Agency for Defense Development (Korea, Republic of)

There can be several types of radar target database (DB) depending on the purpose for using them and the technical levels the constructors have. The simplest form of databases would be the one composed of complex Radar Cross Section (RCS) over frequencies, polarizations, and angles. A one-step advanced DB could be made from 3-dimensional scattering centers of targets [1]. The database



of 3D scattering centers is obtained by signal processing the target RCSs over frequencies and angle apertures in azimuth and elevation directions via Matrix Pencil (MP), Estimation of Signal Parameters via Rotational Invariance Techniques (ESPRIT) or other superresolution techniques to get 3 dimensional positions and magnitudes of the scattering centers [2][3][4]. The scattering center database is different from the simple RCS value database in that it can be used to synthesize various radar signature datasets of a target such as High Resolution Range Profiles (HRRP) and Inverse Synthetic Aperture Radar (ISAR) images. It is also very useful from the point that changes of the received signal in a sensor can be modeled when the target is located within the near-field range, which happens when we do end game simulations.

Target RCS for scattering center extraction can be obtained not only by measurements but also by Computational Electromagnetics (CEM) using target Computer-Aided Design (CAD) models. In this paper, a method to obtain target CAD models from the real targets to be used for the construction of a scattering center database of radar targets is proposed and a consideration to decide the appropriate collection of RCS data sets is also described. 3D CAD models of the targets can be come by the modification of their design drawings which were used to build the targets, but those drawings are not available in many cases. Therefore, a method to make a geometric model from the real target is needed. A 3D measuring instrument by contact is a viable tool when the target size is around a meter. When the target is larger than that, target shapes can be measured by a laser scanner [5]. This shape data will be used as the basis to form a CAD model of the target. With the CAD model obtained as described above, RCS values of the target are predicted over a series of frequencies and angle apertures, which will be processed to be transformed into scattering centers.

When the database is constructed from those scattering centers, a criterion on how many sets of scattering centers are needed in azimuth and elevation angle directions should be determined. If one set of scattering centers is needed every 1 degree, then the size of database would be huge because it has to have 359 sets of scattering centers for one fixed elevation angle at one kind of frequency band and one polarization. On the other hand, if the sets of scattering centers are obtained coarsely like every 30 or 50 degrees, then the size of our database can be smaller but the database will not be able to provide the detailed characteristics of the target. Consequently, the CAD model of an air-target is utilized for the test to infer the criterion on the frequency of scattering center sets for the optimal database construction, where RCS data sets from every 5, 10, 15 and 20 degrees over the whole azimuth angles are calculated to be used for the scattering center extraction and then RCS values are reconstructed from those sets of scattering centers to compare with the original RCS values of the target which are calculated every 0.2 degrees. Correlation coefficient and maximum/average difference techniques were used as the analysis methods. As can be expected, the results show that the smaller the sampling distance or the higher the frequency of collecting scattering center sets we have, the better match between the original RCS and the reconstructed RCS of a target could be obtained. There were also a few cases where scattering center sets from 10 degrees gap or 15 degrees gap showed a better match depending on the analysis method being used, which requires more inspection on the accuracy of CAD models, CEM tool used, and scattering center extraction algorithm.

[1] S. H. W. Simpson, P. Galloway, M. Harman, "Applications of EpsilonTM: A Radar Signature Prediction and Analysis Tool", International Radar Symposium, IRS 1998, Munich Germany

[2] D. Andersh, J. Moore, S. Kosanovich, D. Kapp, R. Bhalla, R. Kipp, T. Courtney, A. Nolan, F. German, J. Cook, and J. Hughes, "Xpatch 4: The next generation in high frequency electromagnetic modeling and simulation software", International Radar Conference, IRS 2008

[3] Y. Hua, E. Baqai, Y. Zhu, D. Heilbronn, "Imaging of Point Scatterers from Step-Frequency ISAR Data", IEEE Transactions on AES, vol.29, no.1, pp195~205, 1993

[4] Andre Quinquis, Emanuel Radoi, Felix-Costinel Totir, "Some Radar Imagery Results Using Superresolution Techniques", IEEE Transactions on AP, vol.52, no.5, pp1230~1244, 2004

[5] Frank Chen, Gordon M. Brown, Mumin Song, "Overview of threedimensional shape measurement using optical methods," Optical Engineering, vol. 39, no. 1, pp. 10~22, 2000

8180-11, Session JS2

An unsupervised method for quality assessment of despeckling: an evaluation on COSMO-SkyMed data

B. Aiazzi, Istituto di Fisica Applicata Nello Carrara (Italy); L. Alparone, F. Argenti, Univ. degli Studi di Firenze (Italy); S. Baronti, Istituto di Fisica Applicata Nello Carrara (Italy); T. Bianchi, A. Lapini, Univ. degli Studi di Firenze (Italy)

The quality of despeckling is generally measured by corrupting a test image by means of synthetic noise with speckle statistics and computing a distance metrics between the original noise free and the filtered noisy image. Unfortunately this approach is correct only for scenes where speckle is fully developed, i.e. there is a large number of independent scattering elements within the smallest area that can be imaged by the instrument. In the presence of natural textures, e.g., forests, and of man-made structures, e.g., roads together with buildings, the fully developed speckle model no longer holds. As a limit case, a persistent scatterer produces an almost deterministic image, without any speckle.

Since despeckling filters should be optimized on true SAR images, the problem arises of how to evaluate the quality of despeckling; in other words, the fidelity of the despeckled image to a hypothetically noise free SAR observation. In the literature, this goal has been accomplished by taking the ratio of the original to the despeckled image, i.e. by extracting the noise that has been removed, and by matching its statistics (e.g. mean, variance, correlation, skewness) to the nominal ones of speckle on suitable manually chosen regions of interest (ROI), where speckle is assumed to be fully developed.

Goal of this paper is the development and evaluation of a fully automatic method for quality assessment of despeckled SAR images. The rationale of the new approach is that any structural perturbation introduced by despeckling, e.g. a local bias of mean or the blur of a sharp edge or the suppression of a point target, may be regarded as the introduction of a new structure, or the suppression of an existing one. Conversely, plain removal of random noise does not changes the structures in the image.

Implementation of the new approach is performed on the twodimensional scatterplot between estimators (e.g. 5x5 sliding averages) of the filtered and unfiltered image, or equivalently on the bivariate distribution obtained after binning. An ideally optimal filter would yield a scatterplot constituted by the superposition of several clusters, corresponding to classes encountered in the image. The ensemble of clusters is aligned along the diagonal of the first quadrant and spread across the plane far apart from the diagonal, where, however, all centers of clusters lie. The presence of filtering impairments produce secondary clusters that may be significantly far apart from the diagonal. Under this perspective, a measure of the accuracy of despeckling for each pixel may be formulated in the following way. For each point in the scatterplot, corresponding to one pixel in the original and in the filtered image, apply the mean shift algorithm to attract the scatterpoint towards its dominant cluster. II the final position of the point is on the diagonal, the corresponding pixel in the image has been perfectly filtered. If the scatterpoint is attracted by a secondary cluster not lying on the diagonal, filtering was inaccurate. A measure of such inaccuracy is given in terms of the position and population of the attracting cluster, by using information theoretic concepts. A fast implementation is obtained by preliminarily binning the scatterplot and by applying the mean shift algorithm to the central scatterpoint of each bin.

Results on true SAR images (COSMO-SkyMed) will be presented. Bayesian estimators (LMMSE, MAP) operating in the undecimated wavelet domain have been coupled with segment-based processing (Bianchi et al., IEEE TGARS, 2008). Quality measurements of despeckled SAR images carried out by means of the proposed method highlight the benefits of segmented MAP filtering.



8180-12, Session JS2

Basis for optronic ScanSAR processing

L. Marchese, P. Bourqui, S. Turgeon, INO (Canada); B. Harnish, M. Suess, European Space Research and Technology Ctr. (Netherlands); F. Châteauneuf, A. Bergeron, INO (Canada)

ScanSAR is an important imaging mode of operation for SAR systems. It allows extended range coverage albeit at the expense of azimuth resolution. Compared to stripmap, ScanSAR is used more for large swath coverage for mapping and monitoring over a wide area. Applications are numerous and include boreal forest mapping, wetland mapping and soil moisture monitoring.

From its very nature, ScanSAR produces large amounts of data, resulting in long processing times precluding instantaneous access to the images. In previous work, an optronic processor prototype designed for fast processing of stripmap-mode data from the ENVISAT/ASAR instrument was constructed and images were successfully processed in real-time. Given the ultra-fast processing and upsampling capabilities of the optronic SAR processor, it would make a perfect candidate for a real-time ScanSAR processor. ScanSAR processing however does significantly differ from stripmap SAR processing due to the multiple range-swath azimuth-burst format type of data generated. The main challenge for optronic implementation of ScanSAR lies scientifically, in the comprehension of the physical parameters substantiating the processor operation and technically, in proper handling, processing and combining each of the burst sections to produce the final image.

The goal of the present work was thus to explore the possibility of processing ScanSAR data optronicaly. Tests were performed with simulated and artificially bursted ASAR stripmap data demonstrating that reconstruction of ScanSAR data using the optronic SAR processor is feasible. This paper describes specifically how the data control and handling of ScanSAR data is performed to make it compatible with the optronic processor that was specifically designed for stripmap processing. As well, the ScanSAR images generated optronically are presented.

8180-38, Session JS2

Comparison of using single- or multipolarimetric TerraSAR-X images for segmentation and classification of manmade maritime objects

M. Teutsch, G. Saur, Fraunhofer-Institut für Optronik, Systemtechnik und Bildauswertung (Germany)

Spaceborne SAR imagery offers high capability for wide-ranging maritime surveillance. SAR image processing can be used especially in situations, where AIS (Automatic Identification System) data is not available such as for small ships, which don't need to send AIS, in case AIS sender dysfunction, or intentionally switched off AIS due to potential criminal activities. Therefore, maritime objects have to be detected and optional information such as size, orientation, or object/ ship class is desired. With StripMap (SM) mode of TerraSAR-X satellite, quite high resolution of 3x3 meters per pixel can be achieved while still covering an area of 30x100 kilometers per image. Thus, it is possible to go beyond object detection towards segmentation, structure analysis, size and orientation estimation, and classification.

In recent research work, we proposed a SAR processing chain consisting of preprocessing, detection, segmentation and classification for single-polarimetric (HH) TerraSAR-X StripMap images to finally assign detection hypotheses to class "clutter", "non-ship", "unstructured ship", or "ship of structure x" (paper accepted for IGARSS 2011). A basic CFAR-like algorithm is used for initial detection of object hypotheses tending to accept false positives rather than producing false negatives. Thus, true objects are unlikely to get lost in an early processing stage, but false positives can be rejected later after more information was extracted. Segmentation is done using Local Binary Pattern (LBP) to extract object contours on the one hand, and perform a statistical structural analysis of an object hypothesis on the other. Together with Histograms of Oriented Gradients (HOG), good estimation of object size and orientation is possible even for object hypotheses strongly affected by speckle noise and typical SAR data distortion. For classification, three cascaded Support Vector Machines (SVM) are used to separate between clutter and man-made objects in the first, non-ships and ships in the second, and unstructured ship and different ship structures in the third classification cascade-level. In training stage, an automatic feature selection module evaluates and selects features coming from a big feature database. This database includes several hundred features such as texture, gradient, structure or LBP features. For each SVM a specific feature vector is set up consisting of features with highest separability for the specific classification task. The processing and classification results are promising.

In this work, we extend the existing processing chain and are now able to handle dual- (HH, VV) and quad-polarimetric (HH, HV, VH, VV) TerraSAR-X data. With the possibility of better noise suppression using the different polarizations, we try to improve both the segmentation and the classification process. Automatic feature selection for the SVMs is applied to all polarizations to allow potentially mixed feature vectors in each classification cascade-level. In several experiments, we will investigate the potential benefit for both segmentation and classification. Precision of size and orientation estimation as well as correct classification rates will be calculated individually for single-, dual-, and quad-polarization and compared to each other. Furthermore, we will find out, if specific feature classes are suitable for specific polarizations.

8180-39, Session JS2

A new SAR image classification using compressive sensing on manifold

B. Hou, X. Cheng, S. Wang, L. Jiao, Xidian Univ. (China)

Compressive Sensing (CS) theory shows that we can reconstruct sparse or compressible signals from a small set of random-projection measurements. The utility of CS for signal reconstruction motivates the study of its latent capacity in other applications.

This paper proposes a new method for SAR image classification based on compressive sensing on manifold, which operates directly on the compressed random measurements of SAR images without reconstructing the images. The core idea of our method is that the compressive measurements of SAR images in one class can be modeled by a Mixture of Factor Analyzers (MFA) which fits to each class data very well by probabilistic formulation, and then SAR image classificaton is performed based on Bayes decision rule. We use the fact that the set of compressive measurements of SAR images in one class forms a nonlinear manifold and can be modeled as a finite mixture of Gaussians. We use nonparametric statistical methods to infer an appropriate number of mixture components for a given compressive measurements set, as well as the associated ranks of the covariance matrices.

The proposed compressive classification method have two parts including training and testing. First, the compressive measurements of each class are modeled so that the probability density function of compressive measurements of each class can be learned from the MFA as the prior distribution. Second, SAR image classification is performed based on the Bayes decision rule. Finally, we demonstrate the effectiveness of the proposed method in MSTAR dataset using limited random-projection measurements. The proposed method has reached a high classification rate with reasonable time cost even when the number of compressive measurements is far less than the dimensionality of the original images.

8180-40, Poster Session

Image segmentation by hierarchical Markov model

T. Mei, S. Zhong, Wuhan Univ. (China)

In this paper, we propose a novel image segmentation method based on hierarchical Markov Random Field(MRF) model. The segmentation method is carried out on multi-scale region adjacency graph(RAG). Specifically, we focused on how to introduce region based context information into multi-scale MRF model. This motivated by the fact that context information between regions can mitigate the appearance



ambiguity of image data. The method of how to incorporate context information into MRF model is detailed in this paper.

The hierarchical MRF model based segmentation method consists of two main components. The first is to build multi-scale RAG. Multi-scale RAG is built based on initial hierarchical segmentation. The hierarchical segmentation is carried out in wavelet domain, taking wavelet coefficients as image feature. At given scale, the watershed transform is performed to obtain segmentation results. A segmentation region at finer scale is a sub-space of the corresponding region at coarser scale due to the property of wavelet transform. If regional minima at finer scale fall within the region at coarser scale, the region at finer scale is a child of the region at coarser scale.

The second is to model the context information and inference the label on the Multi-scale RAG. The class label of the parent node and neighboring node of the parent node is regarded as the context of the corresponding child node. When multi-scale RAG and context model is established, the stand two sweep forward-backward algorithm is extended to multi-scale RAG. The upward sweep starts at the finest scale to compute the likelihood which depends on the interaction across scales and context model. The upward procession repeated until reaches the coarsest scale. Then the downward sweep starts at coarsest scale to get the label of each node. In this sweep, the label of each node is obtained by maximizing the posteriori probability. The process repeated until reaches the finest scale. The hierarchical MRF model parameters were estimated by EM algorithm.

Hierarchical MRF model is a powerful image segmentation tool. By introducing the context information into the MRF model, the performance of segmentation is improved, especially for remote sensing image. The proposed scheme was tested on remote sensing images, and the results show that the segment results are quite promising.

8180-41, Poster Session

Metrological performances of fiber Bragg grating sensors and comparison with electrical strain gages

M. Borotto, E. de Cais, M. Belloli, A. Bernasconi, S. Manzoni, Politecnico di Milano (Italy)

The fiber Bragg grating sensors (FBGs) have been recently introduced: they present a photorecord

grating on the fiber itself, which allows the reflection of a certain wavelength of the input light spectrum. The applied strain is estimated relying on changes of the reflected wavelength.

One of the possible applications that has prompted us to study this type of sensors is the possibility to create smart dynamometric structures based on carbon fiber by embedding FBGs: these kinds of structures are lightweight, strong and can be used for several ends.

Many papers are available in literature about some applications with smart structures but there is not yet an appropriate metrological characterization about these FBG sensors, their strengths and weaknesses: for these reasons it was deemed useful making several tests on FBG sensors in terms of measure quality, signal to noise ratio, ability to compensate for temperature variations and their behavior for dynamic applications. All these results have been compared to electrical strain gage ones, which represent the actual reference strain measurement systems.

The temperature variations have a huge influence on the measure: the most expensive FBGs on the market have shown metrological performances comparable to electrical strain gages from low to high temperatures (-20 °C,+50 °C). Otherwise low-cost FBGs pointed out worse performances with unexpected measurement errors at different temperatures. In addition these tests have given the possibility to better understand the FBGs sensitivity with temperature and its influence on thermal compensation.

The dynamic test has been realized bonding FBG strain gages on a steel beam imposing some sets of strains at different frequencies: the results, got by the ratio between the Fourier transform amplitudes of FBGs and the electrical strain gages, have shown how different supports and gluing methods cause light output variations. Nevertheless, good measurement performances and accuracy have been obtained.

Signal noise has been measured calculating the PSD (Power Spectral Density) and the standard deviation comparing to electrical strain gages and verifying that these quantities did not change with temperature.

The various solutions to compensate for thermal effects have offered several information for further analyses and the basis for a future use of these sensors for static or semi-static tests.

Being fully aware of FBGs characteristics and disadvantages allows to draw down guidelines about their integration in composite materials for the most different applications, understanding in a better way the sensor response.

8180-42, Poster Session

A visual attention model based on spectral residual and its application on ship detection

B. Hou, N. Fan, S. Wang, L. Jiao, Xidian Univ. (China)

Human visual system is very efficient and selective in scene analysis, so it has been widely used in image processing. Many visual attention models based on human visual system have been proposed, such as Itti's model, Saliency Toolbox and Graph-Based Visual Saliency etc. Recently, Hou et al. proposed a fast computational model called spectral residual based on Fourier transform, which is computationally simple, but when it is used for object detection, the erroneous results maybe exists.

Based on Hou's framework, a new visual attention model based on spectral residual used for ship detection is proposed in this paper. It is a bottom-up visual attention model driven by data rather than by task.

First, the input image is converted from RGB color space to HIS color space, which is suitable for human visual system, and channel H, I and S are treated as low-level features, where channel H and S are used to describe the color feature of the image and channel I is used to represent the intensity feature of the image.

Second, based on discrete cosine transform, the amplitude spectrum of feature is analyzed in frequency domain to obtain the spectral residual which is the difference between log amplitude spectrum and its smoothness. Then the conspicuity maps are obtained through inverse discrete cosine transform, during this stage, it makes the spectral residual as new amplitude spectrum and the unchanged phase spectrum as new one.

Third, the conspicuity maps are combined into the saliency map nonlinearly, which can be accomplished via a normalization operator and the weight coefficients. Different from Itti's method, the contribution rate of each conspicuity map to final saliency map is not equal. It is relevant to the difference between the level of the most active region and the average level of the other active regions in each conspicuity map.

Finally, the detection result of ships based on saliency map is got by region growing method. The seed is obtained from the saliency map and the growing process is implemented in intensity image.

Experiments on natural ship images show that our method is robust and efficient, compared with Itti's and Hou's method.

8180-43, Poster Session

Tracking moving objects by a series of Worldview-2 images

J. Tao, W. Yu, Shanghai Jiao Tong Univ. (China)

The author studied the position differences of moving objects in one set of images of different bands of Worldview-2, found that different bands had different imaging time for the same ground position. By calculating an airplane's moving characteristics, the author estimated the imaging time difference of different bands. The time difference can be used to estimate the instantaneous speed of moving objects in the image. With instant speed and the elapsed times between different sets of images, the traffic facility information (roads, bridges, street cross), the same vehicle can be distinguished in high possibility.



8180-44, Poster Session

Geometric superresolution using optical mask(OM) and subpixeling

M. Sohail, A. Mudassar, Pakistan Institute of Engineering and Applied Sciences (Pakistan)

Charged coupled devices (CCDs) are much common in use in different imaging modalities. In most cases, they mainly limit the resolution of imaging devices. The resolution may be limited by them in two different ways: one by the finite non-zero size of pixels and second by the spacing between the pixels or the pixel pitch. If the pixel spacings do not follow the Nyquist sampling theorem, the information obtained do not represent the true picture. The undersampling by CCD has been dealt before in literature by placing optical mask at the Fourier plane in a 4f system assuming pixels as point delta functions and reusing the same optical mask at the Fourier spectrum of the image captured by the CCD. If the pixels have non-zero width as in reality, the undersampling cannot be nullified using optical mask alone and a subpixeling in addition to optical mask is also required. To our knowledge, we for the first time are combining the optical mask at the Fourier plane in a 4f system and subpixeling at the CCD plane simultaneously for nullifying the effect of undersampling by the CCD.

8180-45, Poster Session

Cross-calibrating reflective bands of NOAA17/AVHRR using MODIS over a desert site

B. Zhong, Institute of Remote Sensing Applications (China); H. Huang, Institute of Remote Sensing Applications (China) and College of Geo-resources and Information (China); Y. Zhang, Institute of Remote Sensing Applications (China) and Shandong Univ. of Science and Technology (China); Q. Liu, Institute of Remote Sensing Applications (China)

With more and more satellites onboard different sensors with global observing capability launched, a lot of studies on land surface and global climate change through multi-sensors have been taking on. However, the radiometric calibration capability of different sensors has big difference, so the radiometric calibration should be unified before used simultaneously. NOAA/AVHRR series have the longest history of global observation and the MODIS is the state-of-art sensor with accurate onboard calibration system; in this paper, we therefore propose a new method using time series of MODIS imagery from both Terra and Aqua to cross-calibrate NOAA/AVHRR17 data over a desert calibration site. In this method, the BRDF characterization of the calibration site is firstly derived simultaneously with Aerosol Optical Depth (AOD) using time series of MODIS data. The BRDF is then used to simulate the surface reflectance under AVHRR's solar illumination and view geometries. Thirdly, the simulated surface reflectance of AVHRR is recalculated to the TOA reflectance using atmosphere radiative transfer model based on the retrieved AOD at the first step and the MODIS atmospheric water vapor content product (MOD05). At last, the cross-calibration of AVHRR is performed. In addition, since the spectral response functions of MODIS and AVHRR are different, the spectral translation between MODIS and AVHRR should be done at the first place; therefore, the surface reflectance of AVHRR can be accurately fitted.

In order to assess the performance of this cross-calibration method, we use the fitted BRDF from our research to simulate the surface reflectance of corresponding MODIS data, which are then compared with surface reflectance product of MODIS. The results show that the fitted BRDF in this study is more accurate than the MODIS BRDF product. In addition, the cross-calibration of AVHRR is performed and the comparison between the simulated TOA reflectance and the actual AVHRR TOA reflectance is also performed; the results show excellent agreement between the cross-calibration method and vicarious calibration published by NOAA.

8180-46, Poster Session

Identification the informal buildings using object-oriented analysis in Jazan, Saudi Arabia

H. A. Mashee, King Abdulaziz City for Science & Technology (Saudi Arabia)

At present time, more than half of the earth's population lives in random buildings in urban cities. These residential buildings were the result of many reasons, for example the lack of urban planning of cities for the future and the rapid and unusual growth and in some of the cities in the world. In this study, we have studied the development of slum areas in Abu Arish province related to Jazan region in the southwestern of Saudi Arabia. In this study, we have been using a satellite high resolution image IKONOS for the study area. The classification method used in this study was object-oriented classification by using Definiens Developer program, and since the objective of this study was to explore the informal buildings in the study area. Therefore, we concentrate on those two categories residential and roads areas. In this study, we found that there is a lack of urban planning in Abu Arish province, and a randomly distribution for the residential buildings, which led to existing informal buildings areas in the province and in a continuously way.

8180-47, Poster Session

A compressive sensing method for reconstruction of object in image based on measurement similarity

B. Hou, Q. Jiang, W. Shuang, L. Jiao, Xidian Univ. (China)

The recently developed theory of compressive sensing (CS) can reconstruct a sparse or compressible signal from a small number of linear measurements. The theory is first proposed by Candes, Romberg and Tao in 2004. Abhijit Mahalanobis, Robert Muise and Lockheed Matin proposed a scheme to reconstruct object specific image by minimizing a weighted L2-norm in 2009, which can reconstruct object of interest only and blur the background. The core idea is that a training image library is constructed and DCT coefficients of every image in image library are obtained, and then a mean value of DCT coefficients is got, finally, the detected image is divided into small blocks and each block is reconstructed by weighted L2-norm. A reconstructed image containing object only is thus obtained. But if DCT coefficients of those blocks are very similar, the object and background in final result are both well reconstructed, so it is hard to distinguish object from background.

To solve the above problem, a compressive sensing method for reconstruction of object in image based on measurment similarity is proposed in this paper, which improves the work of Abhijit Mahalanobis etc. The blocks of detected image are divided into two parts by comparing the similarity and reconstructed by two different strategies respectively. The details are as follows:

(1) Use 1000 vehicle images as training images and the measurement vector of each image is obtained, and then average vector of 1000 measurement ones is computed.

(2) Divide the detected image into small blocks whose size is the same as the training images, and then measurement vector of each block is obtained.

(3) Compute similarity between measurment vector and the average vector by normalized mean square error (NMSE), structural similarity (SSIM) and data similarity (DS) respectively.

(4) Select an empirical threshold. When the similarity is less than the threshold, the corresponding block is reconstructed by weighted L2-norm; otherwise, the block is reconstructed by conventional L2-norm.

(5) Output the reconstructed result of detected image.

Here, we use different reconstruction methods to reconstruct blocks containing object and the others, which can ensure that the object is reconstructed better than background. From experiments, we can find that DS is very suitable to compare measurement vectors, because it illustrates the accumulation tendency and distribution of information contained in two vectors. Experimental results show that the proposed

method can effectively extract object of interest in image better than the method proposed by Abhijit Mahalanobis.

8180-48, Poster Session

Characteristic analyses of the reflected components of IR signals due to multiple reflections on object surface

D. Kim, J. Choi, T. Kim, Chung-Ang Univ. (Korea, Republic of)

The major purpose of the present study is to develop a program that predicts infrared signals from 3D objects by considering spectral surface properties. Some preliminary observations have to be made first. The spectral radiance received by a remote sensor is consisted of the self-emitted component directly from the target surface, the reflected component of the solar irradiation and the sky irradiation at the object surface, and the scattered component by the atmosphere without reference to the object surface. In general, the self-emitted component and the reflected component account for the most of the spectral radiance.

In this study, infrared images from 3D objects in various environment conditions are created by calculating the reflected component of the spectral radiance received by a remote sensor. To achieve this calculation, the BRDF(Bi-Directional Reflectance Distribution Function) was introduced to explain reflection characteristics of object's surface. The BRDF provides a method of describing reflectance as a function of incident and reflected angles and wavelength. Analyzing the multiplereflection characteristics will be the next step. The multiple-reflection view factor was used to analyze influencing from some adjoining meshes. They will be applied to the methods for surface temperature calculation by considering 3-dimensional transient heat transfer including the conduction within the object, the convection on the object surface and the solar/sky irradiations. The multiple reflection of the surface radiation must be considered when we predict the infrared signal from objects in order to secure accuracy. The shadow effect is also included in this calculation. There are essential properties to create infrared images of 3D objects.

The infrared signals and images obtained by using the software developed in this study and a commercial software (RadThermIR) are computed and compared each other. Results obtained by using the software developed in this study show fairing good agreement with those obtained by a commercial software.

8180-49, Poster Session

131

Remote sensing image denoising based on partial difference equation and using auxiliary image as priors

P. Liu, D. Liu, Ctr. for Earth Observation and Digital Earth (China)

In recent years, several classes of denoising algorithms such as total variation, wavelet and non-local mean all achieve much success. Total variation method makes use of the geometry feature of the image, wavelet method makes use of the statistical feature of the coefficients and non-local method makes use the redundancy of the image texture feature. However, the priors that these methods make use of, all come from the denoised image itself. In fact, the features form other images of the same scene can also be used as priors in the denoising.

In many practical situations of remote sensing image, what we acquire are often multi-component images. Even an image in several bands is corrupted by noise, a single-component image of higher SNR is often available. So for multispectral or hyperspectral images there are often noise free images of other bands that can be used as priors in denoising.

In this paper, the new method of denoising of remote sensing images based on partial difference equation (PDE) is proposed. One of noise free image in multi-component remote sensing images as priors is introduced into PDE denoising. In order to make use the priors of noise free image in denoising, we construct the new smoothing term for the (PDE) when computing the total variation. The new smoothing term can refer to special smoothing direction and special smoothing intensity



of the reference image. In denoising, the direction of the smoothing is not only reference to the edge of observed image but also to the auxiliary image, and the strength of the smoothing is not only reference to the gradient of the observed noise image but also to the gradient of the auxiliary image. So when the auxiliary image is noise free or not as noisy as the observed image, the PDE based denoising could get better results. The proposed smoothing term is added into the PDE as a constraint. We also give the discrete form of the proposed smoothing term. Based on the proposed method, the similarity of the directions of the edges between the noisy image and the reference image make the promoted algorithm smooth out more noise and conserve more details in denoising.

To validate and compare the proposed method, we perform experiments on different data sets. These data sets contain both a noise image and a noise-free image. A higher quality image can be obtained from one of the sensors, or another part of the reflectance spectrum with higher SNR. The multispectral images come from the CEBERS satellite. There are five bands in the multispectral image of CEBERS, and we denoising the third band and use the fourth band as the reference image of the priors. For the hyperspectral images, the AVIRIS images over Cuprite, Nevada, is taken. The reference image is the twelfth band whose spectrum is near 472.7nm. A state-of-art wavelet based method that also introduces a noise-free image as priors will be compared with the proposed method, and this method is denoted as Wavelet-PNFI.

Better performance is achieved by the proposed method when comparing with other methods. Especially when the variance of the noise in multispectral image is large, the advantage of the proposed method is more obvious.

8180-50, Poster Session

Enhancing the actual operational performance of coaxial three-mirror anastigmatic optical system by wavefront coding

B. Zhang, B. Li, B. Hu, Y. Su, Beijing Institute of Space Mechanics and Electricity (China)

coaxial Three-Mirror Anastigmatic (TMA) optics has been well known in remote sensing for excellent anti-astigmatic, but space interfering factors such as thermal change, vibration, microgravity often caused deformation, tilt or position deviation of optical elements, the degree of structural stability became the key factor to influence the actual performance when coaial TMA run in orbit. This paper studied the influence mechanism of Wavefront Coding element on pupil function, derived the pupil phase distribution by which optical system became insensitive to misfocus and misfocus-related aberrations, the corresponding phase plate was designed and placed to pupil of coaxial TMA, optimized the modified optics in ZEMAX, a filter was developed based on wiener filter, the filter could effectively restore the blur produced by phase plate and misfocus, but magnify the image noise a little, finally, analyzed the actual performance of new imaging system by the simulation, and result showed that, for coaxial TMA optics, the requirement of structural stability was relaxed to 2 times, the depth of focus was extended to 20 times than before, and the imaging quality is almost invariant, actual performance in orbit was enhanced dramatically by Wavefront Coding.

8180-51, Poster Session

A new coastline extraction in remote sensing images

K. Xing, Beijing Institute of Space Mechanics and Electricity (China); Y. Fu, Harbin Institute of Technology (China)

Extraction of coastline from remote sensing image is of great significance for automatic navigation, marine rescue, ocean pollution monitoring, shoreline mapping, ship positioning, spacecraft position and attitude control, remote sensing image registration and cruise missile guidance. With the advent of ocean observing satellites, coastline detection technology from SAR image is rapidly becoming a hot field in remote sensing image processing, but research works

about optics image are few. There are two ways for SAR images to detect coastlines: one is low level image processing technique that smoothing, segmentation and tracking are applied, the other is high level image processing technique such as multi-resolution and wavelet transform. Unlike SAR images, visible images are formed with higher resolution, no speckle noises, large amounts of data and the gray level of water are closer to the gray level of land. So the above-mentioned methods are not strong reliability and accuracy for visible images. This paper presents a solution to the problem of extracting coastlines accurately and rapidly in high-resolution panchromatic remote sensing images. Active contour models, also called snakes, were proposed by Kass et al., and since then have been successfully applied in a variety of problems in computer vision and image analysis, such as edge and subjective contours detection, motion tracking and segmentation .There are several key difficulties with original snakes. Many works has been proposed to improve snake models: Balloon model, GVF Snake, greedy algorithm for snake, ACO Snake, Loop Snake and R-Snake. However, most of the methods proposed to address problems solve only one problem while creating new difficulties. The basic goal of this paper is to present the snake model as an effective coastline extraction technique. In order to improve motion performance, we develop better energy functions. Firstly, coastlines are detected by water segmentation and boundary tracking, which are considered initial contours to be optimized through active contour model. As better energy functions are developed, the power assist of snakes becomes effective. New internal energy has been done to reduce problems caused by convergence to local minima, and new external energy can greatly enlarge the capture region around features of interest. After normalization processing, energies are iterated using greedy algorithm to accelerate convergence rate. The experimental results encompassed examples in images and demonstrated the capabilities and efficiencies of the improvement.

8180-52, Poster Session

Lossless compression of images from China-Brazil Earth Resources Satellite

M. S. Pinho, Instituto Tecnologico de Aeronautica (Brazil)

The aim of this work is to evaluate the performance of different schemes of lossless compression when applied to compact images collected by the satellite CBERS-2B. This satellite is the third one constructed under the CBERS Program (China-Brazil Earth Resources Satellite) and it was launched in 2007. It has three imaging systems: a wild field imaging, a high resolution CCD camera, and a high resolution panchromatic camera. This work focuses in the compression of images from the CCD camera which has a resolution of \$20 times 20\$ meters and five bands: \$0.51-0.73\$ \$mu\$m (band 1), \$0.45-0.52\$ \$mu\$m (band 2), \$0.52-0.59\$ \$mu\$m (band 3), \$0.63-0.69\$ \$mu\$m (band 4), and \$0.77-0.89\$ \$mu\$m (band 5). CBERS-2B transmits the data from CCD in real time, with no compression and it does not storage even a small part of images. In fact, this satellite can work in this way because the bit rate produced by CCD is smaller than the transmitter bit rate. However, the resolution and the number of spectral bands of imaging systems are increasing and the constrains in power and bandwidth bound the communication capacity of a satellite channel. Therefore, in the future satellites the communication systems must be reviewed.

There are many algorithms for image compression described in the literature and some of them have already been used in remote sensing satellites. When the bit rate produced by the imaging system is much higher than the transmitter bit rate, a lossy encoder must be used. However, when the gap between the bit rates is not so high, a lossless procedure can be an interesting choice. Examples of lossless procedures used in some satellites are: JPEG-LS, CCSDS recommendation and lossless JPEG. In general, the algorithms with better performances are based on a predictive scheme or a discrete wavelet transform (or multiresolution transform). Examples of algorithms which uses prediction are JPEG-LS and CALIC. A discrete wavelet transform is used in SPIHT, JPEG2000 and the algorithm recommended by CCSDS. A little bit different scheme (which can be seen as a kind of multiresolution transform) is used in the new standard JPEG-XR. This work evaluates JPEG-LS, CALIC, SPIHT, JPEG2000, CCSDS recommendation, and JPEG-XR when they are used to compress images from the CCD camera of CBERS-2B with no loss. The algorithms are applied in a set of twenty images with \$5,812 times 5,812\$ pixels, running in blocks of \$128 times 128\$,



\$256 times 256\$, \$512 times 512\$ and \$1024 times 1024\$ pixels. The tests are done independently in each original band and also in five transformed bands, obtained by a procedure which decorrelates them. In general, the results have shown that algorithms based on predictive schemes (CALIC and JPEG-LS) applied in transformed decorrelated bands produces a better performance in the mean. Furthermore, as expected, the performance improves when the block length increases. However, the results with blocks of \$256 times 256\$ pixels are close to the better results. Since the compression rate is variable for each block, it is important to evaluate the distribution of this parameter. Preliminary results have shown that the distributions are quite similar for all algorithms.

8180-53, Poster Session

Improvement of appropriate training area selection method for texture classification based on advanced genetic algorithms

H. Okumura, M. Fukusaki, S. Takubo, K. Arai, Saga Univ. (Japan)

BACKGROUND:

As shown in IKONOS or GeoEve, remotely sensed images have had very high spatial resolution. It is difficult for the most of conventional classification methods to obtain land use maps by using such high resolution images, because these methods are too sensitive to variations of pixel intensity in the same land use area. The reasons are as follows: 1) these methods are only based on spectral (color) and spatial (shape) information; 2) these methods process the target images in pixel-by-pixel. Therefore, a new image classification method based on not only spectral and spatial information but also texture information is required to obtain land use maps similar to visual interpretation results. So, we have proposed a new rotation and translation invariant texture quantification method for remotely sensed images using the Normalized Zernike Moment Vector (NZMV) and has applied the method to supervised texture classification. We have also proposed an appropriate training area selection method based on the genetic algorithms (GA-ATAS)[1] for accurate supervised texture classification. In this article, we describe some improvements for GA-ATAS based on an advanced genetic algorithms to achieve relatively high accuracy in supervised texture classification.

METHODS:

GA-ATAS consists of the following procedures: 1) decision of the number of classification category and those content; 2) determination of searching area for each category; 3) each chromosome used in the GA consists of coordinates of center pixel of each training area and those size; 4) 50 chromosomes are generated using random number; 5) fitness of each chromosome is calculated; the fitness is the product of the Classification Reliability in the Mixed Texture Cases (CRMTC) and the Stability of NZMV against Scanning Field of View Size (SNSFS); 6) in the selection operation in the GA, the elite preservation strategy is employed; 7) in the crossover operation, multiple-point crossover is employed and two parent chromosomes are selected by the roulette strategy; 8) in mutation operation, the loci where the bit inverting occurs happens are decided by a mutation rate; 9) go to the procedure 5.To apply GA-ATAS for unsupervised texture classification, some improvements are employed. In the conventional GA-ATAS for supervised texture classification, searching areas for each category have to be determined in procedure 2.

In this article, advanced genetic algorithms, "island model" and "emergent system", are employed for selecting appropriate training areas in GA-ATAS to improve classification accuracy for supervised texture classification using selected training areas.

RESULTS AND DISCUSSION:

Some experiments are conducted to evaluate the capability of unsupervised texture classification of the proposed method by using images from Brodatz's photo album, actual airborne MSS and actual spaceborne sensor with high spatial resolution. The experimental results show that the proposed method can select appropriate training areas automatically which provide relatively high classification accuracy.

REFERENCES

[1] H. Okumura et al., Appropriate training area selection for supervised texture classification by using the genetic algorithms, The Proceeding

of the Conference on Image and Signal Processing for Remote Sensing 2002, SPIE, RS4885-51 (2002, in printing)

[2] P. Brodatz, Textures - A Photographic Album for Artists and Designers, Dover Publications Inc. (1966).

8180-54, Poster Session

Impact of informative band selection on target detection performance

H. Gholizadeh, M. J. Valadan Zoej, K.N. Toosi Univ. of Technology (Iran, Islamic Republic of); B. Mojaradi, Iran Univ. of Science and Technology (Iran, Islamic Republic of)

In this paper, the effect of dimensionality reduction of hyperspectral data on 10 subpixel target detectors is investigated. The genetic algorithm (GA) and wavelet feature extraction methods are used for dimensionality reduction as they maintain physically meaningful bands and physical structure of the spectra, respectively. In the former case, the wrapper method is used to improve subpixel target detectors' results in terms of the area under the curve (AUC) of the receiver operating characteristic (ROC) curve. Meanwhile, in the latter case, the AUC is used as a criterion to choose the optimum level of wavelet decomposition. Experimental results obtained from a real-world hyperspectral data and a challenging synthetic dataset approved that band selection methods without dimensionality reduction, especially in the presence of difficult targets at subpixel level.

8180-55, Poster Session

Comparison of supervised classification methods applied on high-resolution satellite images

A. Öztürk, Yalova Univ. (Turkey)

High resolution satellite images contain rich structural and spatial detail. The availability of high-resolution satellite images provides easy and cost-effective mapping of land features that was not previously available using medium resolution imagery. While unsupervised classification is easy to apply on satellite images, supervised classification methods give better results for accuracy and performance; thus, in this study, supervised classification methods are preferred. By increasing seperability of several land-use types, it is possible to group a satellite image into subparts which lead to solution to land cover mapping problem with application of supervised classification methods. Supervised classification methods use prior examples as a training to classify other unseen samples. In this study, a 'traditional' supervised classification method called Maximum Likelihood Classifier(MLC), Artificial Neural Networks(ANNs) and Support Vector Machines(SVM) are compared. No single classifier is proven yet to satisfactorily classify all the basic land cover classes that means there is no best classifier yet for both performance and accuracy. However, individual evaluations together with pros and cons of each method could give insight about applications of the methods compatible with the intent. MLC based on probability and gives good results. However, small dataset size causes some problems. ANNs certainly have good accuracy values, but training takes too much time. SVMs have less training time with comparable accuracy. Thus, SVM is a good candidate for satellite imagery classification works although its application on satellite image is a pretty new topic. By applying different coefficients and kernel functions, optimum settings could be achieved.

8180-56, Poster Session

Joint high dynamic range imaging and color demosaicing

J. Herwig, J. Pauli, Univ. of Duisburg-Essen (Germany)

Outline of the Approach: A non-parametric high dynamic range (HDR) fusion approach is



proposed that works on raw images of single-sensor color imaging devices which incorporate the Bayer pattern. Thereby the non-linear opto-electronic conversion function (OECF) is recovered before color demosaicing, so that interpolation artifacts do not affect the photometric calibration. Next, the 32-bit HDR radiance map is reconstructed by weighted summation from the differently exposed raw sensor images. Because the radiance map contains lower sensor noise than the individual images, it is finally demosaiced by weighted bilinear interpolation which prevents the interpolation across edges. Then, tone mapping is applied, whereby remaining demosaicing artifacts are further damped due to the coarser tonal quantization of the resulting image.

Photometric Calibration:

Graph-based segmentation greedily clusters the exposure set into regions of roughly constant radiance, whereby firstly for each spatial location pixels with high local contrast, that belong to properly exposed regions, are chosen from the time domain, but secondly the remaining pixels should have small variations in order to belong to the same region. The segmentation works on Gaussian-blurred sensor images, whereby the artificial gray value edges caused by the Bayer pattern are smoothed away.

The non-linear OECF resembles the law of film and is parametrized by its derivative. For every gray value the slope is robustly estimated by tracking the previously segmented regions throughout the exposure stack and relating them between successive exposures. A variation of the Debevec+Malik algorithm recovers the OECF per RGB plane from its first derivative.

Color Demosaicing of the Radiance Map:

A weighted bilinear demosaicing is implemented which utilizes the segmentation results from the photometric calibration in order to prevent the interpolation across regions of different radiance.

Evaluation of the Tone Mapped Results:

The results are evaluated on high-quality sequences of 3-CCD exposures with a simulated Bayer pattern and on real exposure brackets from single-sensor color cameras. The test data sets are processed under the proposed approach and also with the usual workflow, i.e. bilinear demosaicing comes before OECF calibration. Then the correlation of the red, green and blue image planes of each of the tone mapped results is measured by the conditional entropy, cross entropy and Pearson's correlation coefficient. Because natural images exhibit a high correlation between the color planes, these measures should indicate higher values when there are only minor processing errors but lower values if there are color interpolation artifacts and OECF calibration errors. This approach enables the indirect assessment of the image processing workflow even if no ground-truth data is available.

Contributions:

The photometric calibration of non-linear OECFs utilizes only raw sensor images. Gaussian smoothing of the sensor images approximates their luminance, so that these can be segmented before demosaicing. The unsupervised segmentation allows for automatic regularization of the OECF estimation. Demosaicing uses joint segmentation results from multiple exposures at once in order to robustly prevent the interpolation across edges. Tone mapped results are evaluated without ground-truth data but based on the degree of natural correlation between the color planes.

8180-57, Poster Session

Object-oriented high-resolution remote sensing image information extraction of urban green space based on support vector machine

X. Li, Q. Xing, P. Shi, Yantai Institute of Coastal Zone Research (China); C. Xu, South China Sea Institute of Oceanology (China)

Urban green space plays a very important role in urban planning, environmental protecting, sustainable development policy making and etc. High-resolution remote sensing images have detailed spectrum, texture and space structure information. Choose Laishan District, Yantai City as research region, and urban green space can be classified to production green space, protection green space, public green space, road green space and other objects. First,



precise geometric correction of high-resolution SPOT 5 image is performed. Then execute multi-level and multi-scale object or plaques segmentation to extract the object features such as spectral, texture, space and information. Implement support vector machine classifier based on LIBSVM and choose radial basis function as kernel and select the appropriate parameters. With object feature inputs, support vector machine training is executed. Finally, the trained SVM is used for image classification. The method is fully utilized the image spectrum, texture, color and space object information and can effectively improve the accuracy of the extraction of urban green space, relative to the traditional pixel-based extraction method.

8180-58, Poster Session

Fusion of hyperspectral and lidar data using morphological profiles

M. Pedergnana, Univ. of Iceland (Iceland) and Univ degli Studi di Trento (Italy); P. R. Marpu, Univ. of Iceland (Iceland); M. Dalla Mura, Univ. degli Studi di Trento (Italy); J. A. Benediktsson, Univ. of Iceland (Iceland); L. Bruzzone, Univ. degli Studi di Trento (Italy)

While hyperspectral data provides a wealth of spectral information, multireturn LIDAR data provides geometrical information on the elevation and the strcture of the objects on the ground as well as a measure of their laser cross section [1]. So, the data are complimentary in nature and can aid in improving the classification results. Morphological profiles (MPs) have been successfully used as tools to combine spectral and spatial information for classification of remote sensing data [2-6]. Morphological attribute profiles (MAPs) are an extension of MPs. They "provide a multilevel characterization of an image created by the sequential application of morphological attribute filters that can be used to model different kinds of the structural information. According to the type of the attributes considered in the morphological attribute transformation, different parametric features can be modeled [7]." MPs and MAPs can also be used with the LIDAR data to reduce the irregularities in the LIDAR measurements which can be caused due to sampling. In this work, we aim to fuse the LIDAR data and hyperspectral data by means of morphological profiles.

In the preliminary study, we used the subset of the dataset consisting of a hyperspectral image with 63 bands acquired over a rural area near Trento, Italy, and LIDAR data acquired over the same scene. MAPs for the hyperspectral data are built using the components derived with principal component analysis (PCA), which account for 99% of the total variance. MAPs for the LIDAR data are built on the altitude and intensity layers. All the classification results have been obtained by using a random forest classifier with 200 trees. In the first case, the classification was done by using the PCA components. In the second case, a MAP of the hyperspectral data has been built by choosing a standard deviation attribute and 7%, 12%, 18% as threshold values. The values for the thresholds are chosen based on the observations of standard deviations of the pixels in the ground truth classes. Finally, the same MAP combined with the LIDAR data has been chosen as input for the classification in the third case. The overall accuracy was increased from 96.7% to 98.75% and 99.3% for the second and third cases, respectively. In the latter case, it is worth to notice that the accuracy of the first three classes (Buildings, Woods and Apple trees) is much higher, and it is achieved by using the information of the altitude in the LIDAR data.

MPs and MAPs are very effective tools for fusing spectral and spatial information. In this work, we demonstrate that the hyerspectral and LIDAR data can be fused very effectively to provide better classification results by using MAPs. In the future, we aim to test the methods on multiple datasets to check for the consistency. The selection of the correct attribute and the corresponding threshold values to build a MAP is currently done by observing the values of the attributes at the pixels of the ground truth classes. There is a need to develop an adaptive methodology for the selection of the corresponding thresholds.

References:

1. A. P. Cracknell and L. Hayes (2007). Introduction to Remote Sensing (2 ed.). Taylor and Francis, London.

2. J. A. Benediktsson, M. Pesaresi, and K. Arnason, "Classification and feature extraction for remote sensing images from urban areas based

on morphological transformations," IEEE Trans. Geosci. Remote Sens., vol. 41, no. 9, pp. 1940-1949, September 2003.

3. J. A. Benediktsson, J. A. Palmason, and J. R. Sveinsson, "Classification of Hyperspectral Data From Urban Areas Based on Extended Morphological Profiles," IEEE Trans. Geosci. Remote Sens., vol. 43, no. 3, pp. 480-490, Mar. 2005.

4. M. Fauvel, J. Chanussot, J. A. Benediktsson, and J. R. Sveinsson, "Spectral and spatial classification of hyperspectral data using SVMs and morphological profiles," IEEE Trans. Geosci. Remote Sens., vol. 46, no. 10, pp. 3804-3814, Oct. 2008.

5. M. Pesaresi and J. A. Benediktsson, "A new approach for the morphological segmentation of high-resolution satellite imagery," IEEE Trans. Geosci. Remote Sens., vol. 39, no. 2, pp. 309-320, February 2001.

6. A. Plaza, P. Martinez, J. Plaza, and R. Perez, Dimensionality reduction and classification of hyperspectral image data using sequences of extended morphological transformations," IEEE Trans. Geosci. Remote Sens., vol. 43, no. 3, pp. 466-479, 2005.

7. M. Dalla Mura, J. A. Benediktsson, B. Waske, and L. Bruzzone, "Morphological Attribute Profiles for the Analysis of Very High Resolution Images," IEEE Trans. Geosci. Remote Sens., vol. 48, no. 10, pp. 3747-3762, Oct. 2010

8180-59, Poster Session

Spectral dimensionality reduction based on intergrated bispectrum phase for hyperspectral image analysis

D. Kim, K. M. Saipullah, Inha Univ. (Korea, Republic of)

The hyperspectral image (HSI) covers up to several hundreds of bands which results in more accurate and detailed information of each material than those of other remotely sensed data, as in the multispectral image. However, the large dimension of HSI requires extremely high computational complexity and also causes degradation in classification accuracy. In order to efficiently and effectively perform the spectral classification or target detection, this paper proposes a method to reduce the spectral dimension based on the phase of integrated bispectrum. The integrated bispectrum is computed by integrating radially along slices in one sector of the bi-frequency plane. This approach was motivated by the need to obtain certain invariant properties that are meaningful in pattern recognition. The result of the integrated bispectrum is a complex number which contains the magnitude and the phase. Based on the area size of the integrated bispectrum, the resulting phase can be split into a number of features and the resulting feature vectors are then used to represent the spectral of each pixel in the hyperspectral image. Because of the translation, dc-level, amplification, and scale invariant of the phase, it is selected to be the feature of the signal. The phase of the integrated bispectrum feature is tested on spectral classification and HIS segmentation. Because of the excellent and robust information extracted from the bispectrum, the proposed method can achieve high spectral classification accuracy even with low dimensional feature. The classification accuracies of bispectrum are consistent and high even for small dimensional feature size. This shows that bispectrum is able to optimizing the dimensionality reduction effectively compared to those of PCA and ICA, respectively. The classification accuracy of bispectrum with one dimensional feature is 98.8%, whereas those of principle component analysis (PCA) and independent component analysis (ICA) are 41.2% and 63.9%, respectively. For the segmentation experiment, we conducted an unsupervised segmentation of a HSI using the K-mean clustering algorithm with Euclidean distance. The HSI contains 288 bands including the noise and is divided into four regions which are the water, buildup, grass & trees and agricultural regions. 4-mean clustering is applied to cluster the pixels into those four regions. The unsupervised segmentation accuracy of bispectrum is also 20% and 40% greater than those of PCA and ICA, respectively.



Conference 8181: Earth Resources and Environmental Remote Sensing/GIS Applications

Tuesday-Thursday 20-22 September 2011

Part of Proceedings of SPIE Vol. 8181 Earth Resources and Environmental Remote Sensing/GIS Applications II

8181-01, Session 1

Accuracy analysis of DEM extraction over Japan using ALOS PRISM stereo images

Y. Kawata, T. Sasakawa, S. Yoshii, Y. Funatsu, K. Takemata, Kanazawa Institute of Technology (Japan)

The needs of the Digital Elevation Model (DEM) with a fine spatial resolution are nowadays increasing and the DEMs are used in a wide range of applications: mapping, risk management and disaster simulation, virtual 3D cities in game environment and web GIS applications such as Google Earth. This study is to make an accuracy assessment of the DEM extracted from a stereo pair of ALOS PRISM images of Kanazawa area, Japan. The altitude range of the study area is between 0 m and 1800m above sea level. In this study we assumed a 3D projection transformation model. We computed 12 unknown linear coefficients from a pseudo-inverse matrix using 18 triangular points. As for the tie points on stereo images, the point assignment errors were less than 1 pixel in both line and pixel directions. The accuracy analysis of the DEMs was performed at 45 triangular points which were given by Geospatial Information Authority of Japan. The generation of three DEMs were done using three sets of 15 tie points, namely, L, M, and H. They consist of 15 triangular points with low, middle and high elevations, respectively. We found the most accurate DEM was generated using the tie point set H. The overall accuracy of the DEM with 2.5m spatial resolution was computed to be RMSE=5.17m in the vertical direction.

8181-02, Session 1

Validation of ALOS DSM

K. G. Nikolakopoulos, Institute of Geology & Mineral Exploration (Greece); A. D. Vaiopoulos, Univ. of Athens (Greece)

One of the newest satellite sensors with stereo collection capability is ALOS. ALOS has a panchromatic radiometer with 2.5m spatial resolution at nadir. According to the specifications its extracted data will provide a highly accurate digital surface model (DSM). Panchromatic Remote-sensing Instrument for Stereo Mapping (PRISM) has three independent optical systems for viewing nadir, forward and backward producing a stereoscopic image along the satellite's track. Each telescope consists of three mirrors and several CCD detectors for push-broom scanning. The nadir-viewing telescope covers a width of 70km; forward and backward telescopes cover 35km each.

Four areas with different physiographic and geomorphologic features were selected for the ALOS DSM validation. The ALOS DSMs were compared to elevation data from different sources: 1/50.000 topographic maps and airphoto stereo-pairs. Points of known elevation have been used to estimate the accuracy of the DSMs. 2D RMSE, correlation and the percentile value were computed and the results are presented.

8181-03, Session 1

Positioning accuracy of GeoEye-1 RPC/ Ortho pan-sharpened color imagery

M. Tokunaga, M. Ichihara, Kanazawa Institute of Technology (Japan)

As a GeoEye-1 Pan-sharpened color imagery has the 0.5m ground resolution, it is expected that imagery will be utilized as a large scale map. In order to utilize a imagery as a large scale map, a positioning accuracy of a imagery should be made clear. GeoEye has announced

that the nominal positioning accuracy of GeoEye-1 imagery is 3 m in RMSE and 5m in Circular Error 90% (CE90).

This paper evaluated the positioning accuracy of a GeoEye-1 imagery using GCPs that were measured by VRS-GPS measurement. VRS(Virtual Reference Station)-GPS is a measurement method using GCP references installed by the Geographical Survey Institute of Japan, that look alike to RTK-GPS. The accuracy of GCP obtained 2-3 cm in horizontal level and 6 cm in vertical level. Since the ground resolution of a GeoEye-1 imagery is 0.5m, GCP has sufficient accuracy of position. Research area was selected 15km square in a central part of Kanazawa, Japan. A total of 91 GCPs were selected from road lines, zebra crossing, parking lines and so on.

As a result, positioning accuracy of GeoEye-1 RPC imagery obtained 7.79m in RMSE including mountainous area. This shows worse than nominal value. However error vectors were almost same direction. It means that only one point GCP is required to correct pointing error.

On the other hand, a positioning accuracy of Ortho imagery has influence on an accuracy of GPS when the imagery is produced. Usually, Japanese provider uses GCP derived from 5m or 10m grid DEM. Therefore the accuracy of GCP could be a few meters. In this case, a positioning accuracy of Ortho imagery obtained 1.78m in RMSE. This shows GeoEye-1 imagery has potential of 1:5000 scale map.

8181-05, Session 2

An integrated tool supporting volcanic activity monitoring

M. Musacchio, M. Silvestri, Istituto Nazionale di Geofisica e Vulcanologia (Italy); S. Zoffoli, Agenzia Spaziale Italiana (Italy); F. Buongiorno, Istituto Nazionale di Geofisica e Vulcanologia (Italy)

The Project called Sistema Rischio Vulcanico (SRV) is funded by the Italian Space Agency (ASI) in the frame of the National Space Plan 2003-2005 under the Earth Observations section for natural risks management. The SRV Project is coordinated by the Istituto Nazionale di Geofisica e Vulcanologia (INGV) which is responsible at national level for the volcanic monitoring. The project philosophy is to implement, by incremental versions, specific modules which allow to process, store and visualize through Web GIS tools. The ASI-SRV is devoted to the development of an integrated system based on EO data to respond to specific needs of the Italian Civil Protection Department (DPC) and improve the monitoring of Italian active volcanoes. The ASI-SRV provides support to the different volcanic activity phases risk management and its results are addressed by the Italian Civil Protection Department (DPC).

SRV provides the capability to manage the import many different EO data into the system, it maintains a repository where the acquired data have to be stored and generates selected products which will be functional to the phases described above.

The processing modules for EO Optical sensors data, are based on procedures mainly developed by INGV, University of Modena. This procedures allow to estimate a number of parameters which include: surface thermal proprieties, gas, aerosol and ash emissions and to characterize the volcanic products in terms of composition and geometry. For the analysis of the surface thermal characteristics, the available algorithms allow to extract information during the prevention phase and during the Warning and Crisis phase. In the prevention phase the thermal analysis is directed to the identification of temperature variation on volcanic structure which may indicate a change in the volcanic activity state. At the moment the only sensor that presents good technical characteristics for the prevention phase is the ASTER sensor (90 m pixel) on NASA satellite TERRA. The product regarding the Crisis phase is mainly finalized to the estimation of the effusion rate for active lava flows, the algorithms for this product are



well consolidated and could be applied to the low spatial resolution space sensors (eq. AVHRR, MODIS) and to high spatial resolution space sensors (eg. Hyperion, ASTER). A further class of products regards the analysis of degassing plumes and eruptive clouds. The analysis of the emitted gas species from degassing plume is usually performed trough ground networks of instruments based on the spectral behaviour of the gas species, although many volcanoes in the world do not have such permanent networks. The SRV system will produce information on the concentration and flux of sulphur dioxide (SO2) water vapour and volcanic aerosol optical thickness by means of ASTER, MODIS and HYPERION data on Etna test site. The analysis of ash clouds will be made by means of already consolidated procedures which uses low spatial resolution sensors with an high revisit time (eg. AVHRR, MSG, MODIS). For the Post Crisis phase the required products will be obtained through classification algorithms and spectral analysis operated by the scientific personnel of INGV and introduced in the system repository after the use of modules.

In this paper the first results obtained by means of modules developed within the ASI-SRV project and dedicated to the processing of EO historical series are presented.

8181-06, Session 2

Spectroscopy as a tool for geochemical modelling

V. Kopacková, Czech Geological Survey (Czech Republic); S. Chevrel, A. Bourguignon, BRGM (France)

In this study we used spectroscopy as a tool to determine metalic cation chemical form (speciation) and heavy metal concentrations. Field spectra of more than 250 surface samples, the representatives of anthropogenic sediments, collected at the Sokolov open-pit lignite mine, were systematically measured using an Analytical Spectral Device (ASD) spectroradiometer during 2007 -2009 field investigations. At the sampling points spectroradiometric measurements were collected in natural illumination conditions using an ASD FieldSpec 3® portable spectroradiometer. Furthermore, samples of the surface material (0-1 cm depth) were collected at selected points. They were dried and sieved to < 2 mm, and the abundance of trace elements was measured using a portable Innov-x Alpha RFA spectrometer. The samples were further subjected to X-Ray Diffraction analysis, whole-rock chemistry and determination of laboratory pH; sulphur (Stotal wt %) and Total Organic Carbon (TOC_%). The results coming from these analyses became basis for quantitative determination of mineral composition of the studied samples. Besides these laboratory analyses, laboratory spectra were obtained by measuring the analyzed samples in artificial illumination conditions.

Firstly, the effect of the diverse phases (e.g., organic matter containing mainly weather lignite - Clignite, iron oxides, clay minerals) on the reflectance property was studied and quantitative methods of image spectroscopy were used to derive parameters from variations in spectral signal (e.g., absorption depth, area, asymmetry, slope), secondly the relationship between geochemical properties (e.g., selected heavy metals (As, Hg) abundance and speciation, substrate pH) and derived spectral parameters were studied in detail and the prediction models for heavy metal abundance (As, Hg), pH and Clignite were constructed and applied to atmospherically corrected HyMap 2009 data. The prediction results were statistically evaluated using quantitative laboratory analysis of the ground truth data.

Furthermore, quantitative spectroscopy approach allowed us to answer the following key issues:

- The effect of spectral resolution on a model quality
- The effect of a mixing phenomena on a model quality
- Can we use spectroscopy as a tool to determine not only heavy metal concentrations but also a chemical form?

The present research is being undertaken within a framework of the grant No. 205/09/1989, funded by the Czech Science Foundation.

8181-07, Session 2

Time series geospatial data for seismic precursors assessment

M. A. Zoran, National Institute of Research & Development for Optoelectronics (Romania)

Rock microfracturing in the Earth's crust preceding a seismic rupture may cause local surface deformation fields, rock dislocations, charged particle generation and motion, electrical conductivity changes, gas emission, fluid diffusion, electrokinetic,

piezomagnetic and piezoelectric effects. These mechanisms have been considered as the main sources of the so-called seismoelectromagnetic emissions consisting of broad band electromagnetic (EM) fields observed at the Earth's surface and in the near-Earth space.

Space-time anomalies of Earth's emitted radiation (radon in underground water and soil , thermal infrared in spectral range measured from satellite months to weeks before the occurrence of earthquakes etc.), ionospheric and electromagnetic anomalies are considered as pre-seismic signals. Satellite remote sensing data provides a systematic, synoptic framework for advancing scientific knowledge of the Earth complex system of geophysical phenomena which often lead to seismic hazards.

The GPS data provides exciting prospects in seismology including detecting, imaging and analyzing signals in regions of seismo-active areas. Combined with ground-based seismological measurements and satellite remote sensing information, space-based geodetic measurements of the solid Earth are yielding the principal data for modeling lithospheric processes and for accurately estimating the distribution of potentially damaging strong ground motions which is critical for earthquake engineering applications. The mosaic pattern of the strain field in the epicentral zones creates a specific obstacle to the detection of precursory events and determination of the spatial scale of the earthquake preparation zone. Obviously, the size of the zone largely depends on the earthquake magnitude. Earthquake prediction has two potentially compatible but distinctly different objectives: (a) phenomena that provide information about the future earthquake hazard useful to those who live in earthquake-prone regions and (b) phenomena causally related to the physical processes governing failure on a fault that will improve our understanding of those processes. To understand the exact relationship of a precursor with an impending large earthquake, it is essential to know the geodynamical reason behind the occurrence of that precursor. A major challenge is to extract all available information contained in the system and to interpret it in terms of processes.

This paper aims at investigating the TEC ionospheric and geomagnetic precursors during some of the recent major earthquakes based on time series NOAA (http://www.swpc.noaa.gov) and WDC Australian (http:// www.ips.gov.au) databases as well as Land Surface Temperature in the epicentral areas from Landsat TM, ETM and MODIS data.

8181-08, Session 2

Discrimination of basement rocks in the Eastern Desert of Egypt based on spectral characterizations, ASTER TIR bands and data fusion of Egyptsat-1 and Landsat ETM

M. F. Sadek, S. M. Hassan Sayed, National Authority for Remote Sensing and Space Sciences (Egypt)

Application of different Remotely sensed data in rock discriminations and geological mapping.

These data are focused on the discrimination of the Precambrian basement rocks in the Eastern Desert of Egypt.

8181-09, Session 3

Simulation of operation of future Japanese spaceborne hyperspectral imager: HISUI

T. Matsunaga, S. Yamamoto, S. Kato, National Institute for Environmental Studies (Japan); O. Kashimura, T. Tachikawa, Earth Remote Sensing Data Analysis Ctr. (Japan); K. Ogawa, Rakuno Gakuen Univ. (Japan); A. Iwasaki, The Univ. of Tokyo (Japan); S. Tsuchida, National Institute of Advanced Industrial Science and Technology (Japan); N. Ohgi, Japan Resources Observation System and Space Utilization Organization (Japan); S. Rokugawa, The Univ. of Tokyo (Japan)

Japanese future spaceborne hyperspectral mission, Hyperspectral Imager Suite (HISUI), will be launched in 2015 or later as one of mission instruments onboard JAXA's Advanced Land Observation Satellite 3 (ALOS-3). HISUI will consist of a hyperspectral imager and a multispectral imager with 30 m and 5 m spatial resolution, 30 km and 90 km swath, and 185 and 4 spectral bands, respectively.

As the data rate of HISUI's hyperspectral and multispectral imagers are huge and ALOS-3's downlink capability is limited, detailed planning of HISUI observation and downlink will be necessary for efficient data acquisition by HISUI.

Especially for environmental and/or vegetation application, which require repeated observation of the same targets, the trade off between observation frequency and the area of the target will be critical.

To obtain necessary information for the discussion of HISUI operation and resource allocation, we have developed a software, which simulate HISUI operation in space. In the simulation, the global distribution of land and shallow coastal regions, solar elevation at the time of HISUI observation, the orbits of ALOS-3 satellite, maximum operation time of HISUI in one orbit, and maximum downlink amount allocated to HISUI hyperspectral imager are considered. Onboard lossless compression is assumed in the simulation. Cloud occurrence is also statistically considered.

Using this software, various operation scenarios of HISUI were simulated. The scenarios include : one-time emergency observation, one-time cloud-free data acquisition for large targets, repeated cloud-free data acquisition for medium-size targets, and one-time cloud-free global mapping.

If the ALOS-3's downlink capability of 300 Mbyte per day is allocatead to HISUI, the most of the mission objectives will be met in two - three years of operation. If the allocation is 30 Mbyte per day, however, only target observation will ve available.

These scenarios and the trade-off discussion will be introduced in the presentation.

8181-10, Session 3

Application of hyperspectral remote sensing at Edwards Air Force Base

R. Walmsley, Tetra Tech (United States); M. Frank, Galileo Group, Inc. (United States)

Edwards AFB requires remotely-sensed data to facilitate determining how plant communities change spatially over time, modeling ecosystem health and predicting sensitive species habitat. Tetra Tech and Galileo Group collected ground spectra and airborne hyperspectral imagery for over 400 square miles of Edwards AFB in order to map ecosystem health and habitat stability. Over 100 ground spectral measurements were collected with an ASD FieldSpec handheld spectrometer in tandem with the airborne collection. The spectral quality of the ground and airborne data as well as the spatial quality of the data was measured prior to mapping. Atmospherically corrected and continuum removed spectra were correlated over the Piute Ponds pilot-project area. The spectral quality of airborne pixels compared favorably with spectra collected on the ground at the same location. Spectra collected for known plant species on the ground are represented in the airborne data cubes. Therefore, each plant species has a much greater probably of being successfully identified in processing and mapping the airborne images. The results



show that the quality of the imagery enables excellent mapping of different vegetation types and habitat areas. A mapping pilot project was completed at Piute Ponds, a freshwater marsh area located in the southwestern portion of Edwards AFB, to evaluate the spectral richness and consistency of the airborne hyperspectral data. The reflectance georectified datacubes were used to facilitate integration with the may ground spectra training sites. The airborne VNIR data cubes contain enough spectral variation and depth to effectively map plant species and many different plant communities. Several plant species were successfully differentiated and identified using EVNI Image-processing algorithms. The ground spectral library matches the airborne spectra very well, making the ground spectra an invaluable resource for interrogating the airborne data cubes about specific targets. Superimposing the spectra demonstrates the importance of elevation and topographic relief to the geographical distribution of vegetation types. Superimposing the spectra demonstrates how existing maps can be correlated with and updated. The hyperspectral imagery collected will be used in future surveys to evaluate recovery of various habitats from mission related projects, activities and operations, as well as the implementation of environmental projects to benefit the Mohave Desert ecosystem.

8181-11, Session 3

Analysis of high-resolution remote sensing imagery with textures derived from single pixel objects

R. de Kok, K. Tasdemir, European Commission Joint Research Ctr. (Italy)

For image analysis, the textural features derived from a co-occurrence matrix, such as contrast, homogeneity and entropy, are commonly exploited. Due to information redundancy and practical implications, these textures are extracted from the panchromatic band or the first principal component of the multispectral bands. However, textural information obtained from different spectral bands might be crucial in the analysis. Yet, various alternatives on the parameters (such as window-size, direction) and selection of proper spectral bands lead to a rapid increment in additional image based information. For example, such additional textural imagery soon may require a disk space of 10 to 15 times larger than the original image size. When a huge amount of high-resolution remote-sensing imagery is required for analysis, for example for a study on national scale using HR data, the amount of additional textural imagery increases drastically.

Therefore, an alternative texture extraction approach is considered in this study. It is based upon textures derived from single-pixel objects in HR satellite imagery, by evaluating spatial and spectral feature attributes. The evaluation of single-pixel objects allows the analysis of a large variety of these spectral and spatial features such as contrast between neighboring objects or contrast between objects in a predefined radius. This type of textures are sensitive to nonhomogeneous areas in the image, particulary belonging to transition zones or infrastructure between larger homogeneous areas. This includes natural and man-made corridors. These are image objects with often a size/width smaller than or approaching the sensors instant field of view. After the evaluation, a small selection of essential contrast maps can be exported as GeoTiff files. Theoretically, the feature attributes for single-pixel objects can be simulated by a moving window technique. However, the speed and rapid evaluation possibilities of feature attribute for those single image objects is convenient in the practical applications.

The proposed textures of single-pixel objects will be compared to the commonly used texture features derived from co-occurrence matrix, in terms of classification accuracy for analysis of parcels in good agricultural condition in Hungary. Classification will be performed by self-organizing maps in an unsupervised manner. A dataset of high-resolution mosaic (5 meter resolution) of the country with 250 scenes (~approximately 120 gigabyte) will be considered. Creating additional textural imagery for such a dataset is already quite a challenge. Achieving accuracies-similar to the accuracies one can achieve with texture features derived from co-occurrence matrix-with the "on the fly" feature attributes of single-pixel objects can help for manageable classification of the total national coverage.

8181-12, Session 3

Developing Matlab scripts for image analysis and quality assessment

A. D. Vaiopoulos, Univ. of Athens (Greece)

It is clear that nowadays, nearly everybody is familiar with digital images. However, occasionally, we may want to subdue these images into a process, in order to get a second image, which will possibly contain more information than the original. Image processing is a vast field and has numerous applications. For example, we have to perform a satellite image fusion to enhance its spatial resolution. Then, we should find out which algorithm produces the best result (fused image).

There are many different algorithms which perform the fusion of the images and obviously producing different results. Of course, the resulting fused image must be visually examined to verify that the algorithm worked well and satisfies the purpose it was made for. Nevertheless, in many occasions, some of these algorithms produce images where it is very difficult or even impossible to recognize differences between fused image products or simply determine which fused image will correspond best to our needs, solely by their visual examination.

Exactly for this reason, researchers who work with processed images, often desire to use one or more mathematically based indices (such as bias, correlation coefficient, RMSE and others) which output a number that describes the quality of the process. For each of these indices, there is an ideal value, and the closer the number to the ideal value we have, the better the quality of the process is.

The scope of this paper is to present and describe scripts that were written in MATLAB code, in order to execute the indices calculations automatically. More specifically, the scripts calculate the below indices:

1) Bias, which is the difference between the means of the original and the processed image.

2) Correlation Coefficient, which defines the correlation between the original and the processed image. It is considered as a reliable index and is commonly used.

3) DIV (Difference In Variance), which is the difference between the variances of the original and the processed image. It indicates the quantity of information added or lost during the process.

4) ERGAS (Erreur Relative Globale Adimensionnelle de Synthèse)

5) Entropy, which involves more complex statistical and mathematical operations. Reflects the amount of information lost or added in the processed image.

6) Q (image quality index), which describes the quality of the image process. It is a robust index, as it uses the correlation coefficient and the standard deviation to produce the result.

7) RASE (Relative Average Spectral Error)

8) RMSE (Root Mean Squared Error)

Eight scripts were written and produce the respective index result. The image fusion example given above was not random. The development of the scripts was triggered by the need for calculation of these indices for processed hyperspectral satellite images in an automated and convenient way. The paper will feature demonstration of the scripts on multispectral and hyperspectral processed imagery, where they were tested and proved to be efficient (although they are estimated to work with most types of images).

8181-13, Session 3

Integrating remote sensing images on a contextual mobile GIS

E. López-Ornelas, R. Abascal-Mena, Univ. Autónoma Metropolitana (Mexico)

At the present time, the remote sensing community will have to deal with very different data type; having different resolution (spatial, temporal and spectral). Also the advance of mobile information systems is going in parallel with Geographical Information Systems where they both meet in providing location-based services (LBS). New systems are providing a new pervasive GIS dimension where access



to geographical attributes is being possible at "anytime, anyplace and anyhow".

Having this objective, one of the key problems in this article is the integration of remote sensing image information, which comes from multiple sources completely heterogeneous, with a Mobile GIS in order to deduce the user context. In this paper we consider context awareness to use remote sensing information with some user profile information to adapt the Mobile GIS application to the user's current situation and needs.

In this article, we propose an approach to integrate remote sensing data on a Mobile GIS application using XML descriptors to store all different information that the user will need when he is consulting his mobile device. Having this XML information has some advantages, for example it can be updated easily and it can be shared with other services and users. We also propose an approach that provides mobile users with a Mobile GIS that corresponds not only to their requests but also to their context.

To accomplish this task, two approaches must be taken into account; i) an image processing method has to be applied in order to segment the image; ii) the extraction using a XML modeling in order to extract the different cartographic elements; iii) integration of these cartographic elements on a Mobile GIS and; iv) the user profile integration in order to have a contextual application.

Image processing is considered an important step that provides a first isolation of the cartographic elements. At this point we use a morphological segmentation process.

The contribution of this work includes (1) the use of a segmentation approach based on morphological operations in order to obtain an elaborate knowledge of remote sensing images, (2) the use of XML tags to query and extract the desired cartographic elements and (3) the integration of cartographic elements from remote sensing images and the user profile on a Mobile GIS application.

8181-14, Session 4

Object-based detection of destroyed buildings based on remotely sensed data and GIS

N. Sofina, M. Ehlers, Univ. Osnabrück (Germany); U. Michel, Pädagogische Hochschule Heidelberg (Germany)

The remote sensing technology is widely used for obtaining information on a large area of the earth surface, especially for the change detection analysis. Conventional methods of image processing permit detection of changes by comparing remotely sensed multitemporal images. However, to perform a successful analysis it is desirable to take images at the same time of a season, at the same time of a day and in cloudless conditions. Thus, an application of the change detection analysis could be problematic especially for sudden catastrophic events. A promising alternative is an employment of vector-based maps containing information about the original urban state, which is related to a single image obtained after the catastrophe.

The paper describes a methodology of an object-based search of destroyed buildings as a consequence of an earthquake. The search is based on the analysis of remotely sensed and vector based data. The methodology includes three main steps: generation of features defining the states of buildings, classification of building state and data import in GIS. This paper concentrates on the first step of the three, the generation of features. The appropriately selected features are indispensable for the following successful classification.

One of the new proposed features is a detected part of a contour (DPC). To extract the feature, the edge detection algorithm is applied to a remotely sensed image. The algorithm yields a raster map, where pixels of a contour have a color corresponding to its direction. The pixels that do not belong to the counter have a "no data" value. At the same time test points are selected on the vector map of the considered building. For each test point a search area is defined where pixels with the appropriate contour direction are counted. The DPC value is calculated as a ratio of the pixel number found on the raster contour to that expected for the intact contour. Additionally several features based on the analysis of textural information corresponding to the investigated vector object are calculated.

Conference 8181: Earth Resources and Environmental Remote Sensing/GIS Applications

The described methodology is applied to remotely sensed images of areas that had been subject to an earthquake. Beside the discussion of the results, possible approaches for the following classification of the buildings state based on the generated features set are shortly discussed as well.

The change detection methodology has been developed solely with Open Source Software. GIS GRASS is involved for vector and raster data processing and presentation, Orange (data mining software) is applied for data classification. Programming languages Python and Bash are used to develop new GRASS-modules.

8181-15, Session 4

Building detection from single polarized TerraSAR-X data

M. Schmidt, T. Esch, Deutsches Zentrum für Luft- und Raumfahrt e.V. (Germany); M. Thiel, Julius-Maximilians-Univ. Würzburg (Germany); S. W. Dech, Deutsches Zentrum für Luftund Raumfahrt e.V. (Germany)

Urban areas undergo rapid and rigorous processes of change. The consequences of these developments are major challenges for urban management and planning. Conventional data sources often provide hardly enough information for adequate problem analyses and decision support. With the establishment of very high resolution (VHR) spaceborne remote sensing systems in the last decade, additional up-to-date and spatially detailed information has become available. This information - or the derived geodata - can support urban management and planning processes in an effective and cost-efficient manner. In particular the upcoming of operational VHR SAR systems such as the German TerraSAR-X (TSX) satellite provides interesting possibilities, because these systems record one-meter resolution information independently of atmospheric conditions and sun illumination.

In this study we aim at an area-wide detection of buildings from individual, single-polarized TSX intensity datasets recorded in stripmap mode. Due to SAR side-looking acquisition the building-related information is located in layover and shadow areas which do spatially not exactly correspond with the true location of the buildings. As a consequence the building backscatter information does not fit on the GIS-reference dataset which provides the buildings footprints with their respective height. To perform a supervised classification approach we at first create a mask of the layover and shadow areas based on the reference GIS-dataset by considering the viewing geometry of the TSX data. In order to classify the layover and shadow areas in the SAR data we utilize a random forest algorithm for classification. As input features for the classification we use various texture measures calculated from TSX data using a pixel based moving window approach. We randomly extract training samples by means of the generated mask of layover and shadow areas to determine the relationships between the texture features and the class membership. These relationships are used in the following to classify the entire TSX dataset.

To test which texture measure performs best in this context we calculate Grey Level Co-occurrence Matrix based features according to Haralick, Mathematical Morphology and Spatial Autocorrelation features. For each we consider several window sizes because of the multi scale nature of urban environments.

Trying different combinations of the texture features we get overall classification accuracies of the buildings layover and shadow areas up to 73%. Thereby producer and user accuracies almost reach this value as well. The most important influence factor for classification accuracy seems to be the simultaneous usage of input texture features calculated with different window sizes rather than the kind of texture measures per se.

8181-16, Session 4

Land use and land cover classification with evolutionary support vector machine (ESVM) and SPOT-5 images in Dalian, China

N. Chang, Univ. of Central Florida (United States); M. Han, W. Yao, S. Xu, Dalian Univ. of Technology (China)



Satellite remote sensing technology and the science associated with evaluation of land use and land cover (LULC) in urban region makes use of the wide range images and algorithms. Improved land management capacity is critically dependent on real-time or near realtime monitoring of land-use/land cover change (LUCC) to the extent to which solutions to a whole host of urban/rural interface development issues may be well managed promptly. Yet previous processing with LULC methods is often time-consuming, laborious, and tedious making the outputs unavailable within the required time window. In our study, a sophisticated image classification approach is used to identify the LULC patterns in a fast growing urban region with the aid of 2.5-meter resolution SPOT-5 image products. Since some different classes of LULC may be linked with similar spectral characteristics, texture features and vegetation indexes are extracted and included during the classification process to enhance the discernability. The classifier is constructed based on the evolutionary support vector machine (SVM), which is an advanced machine learning algorithm with remarkably high classification accuracy and outstanding generalization performance. A validation procedure based on ground truth data and comparisons with some other classic classifiers prove the credibility of the proposed SVM classification approach in terms of the classification accuracy, while the effectiveness of the classification strategies are also validated in a group of contrast tests. Case study in Dalian Development Area (DDA) based on the SPOT satellite images collected in the year of 2003 and 2007 fully support the monitoring needs and aid in the formulation of urban expansion and land reclamations.

8181-17, Session 4

Wireless sensors network innovative application for structural industrial works monitoring

D. Ulieru, SITEX 45 (Romania); F. N. Pistritu, National Institute for Research and Development in Microtechnologies (Romania)

Existing monitoring systems for engineering works structural health as wire based systems are expensive cost associated with laying out the wires and the maintenance costs. Use of wireless communications for the transfer of data between wireless sensing units can drastically reduce the cost of installation and maintenance of the monitoring system. The wireless transmission is more robust ,will remain operational. at an natural disaster than a wired one:

For structural monitoring could be considered the strain and acceleration measurement. Strain gauges provide the technical basis to measure strains for the health monitoring of industrial structures Dynamic measurements get information on the structural response of industrial works structures for the purpose of detecting changes which may indicate damage or degradation. The MEMS sensors by our monolithic integration concept allows the fabrication of the MEMS element on the same die with the signal conditioning circuitry

Both types of sensors that to be used in this work are packaged as chip devices. RFID tags offer the possibility of reading, writing, transmitting, storing and updating information and can hold up to 32 mega bytes . Information is communicated electronically via radio waves and does not require contact or line-of-sight to transmit stored data.

This idea of the paper is of RFID tags combination with micro-size sensors to be embedded or attached to engineering structural works to measure strain and acceleration for health monitoring applications of different industrial facilities and supply data on parameters to prevent damages or failure of the structure. Our proposed wireless system architecture ,technical characteristics and the RFID's system semi-active architecture are novel and will be detailed analyzed on the paper.

Another novelty is the multilayered stripline technology that will be used in the package by PCB rapid prototyping going in house the RFID and the antenna for wireless communication fabrications widely presented on the paper. The link between the RFID tag under interrogation and the microwave reader has been assumed the link distance to be 100m to 1000m. For operating frequency of 896MHz the path loss is ranging from 71dB to 91dB.

8181-18, Session 4

Using the SLEUTH urban growth model to simulate the impacts of future policy scenarios on urban land use in Tehran metropolitan area in Iran

S. Kargozar Nahavandy, M. R. Saradjian, Univ. of Tehran (Iran, Islamic Republic of)

The SLEUTH model, based on the Cellular Automata (CA), can be applied to city development simulation in metropolitan areas. Tehran as the biggest metropolitan in Iran, always faces uncontrolled urbanization through the past decades, thus in this study the SLEUTH model was used to model the urban expansion and predict the future possible behavior of the urban growth in order to control the unexpected growth and prevent undesirable consequences in the future. The fundamental data were five Landsat TM and ETM images of 1988, 1992, 1998, 2001 and 2010 which were utilized for generating maps of road networks, and urbanized area. The Calibration was performed in three steps: coarse, fine and final calibration, using the historical data to estimate the best set of parameters of the model. These parameters are breed factor, diffusion factor, spread coefficient, slope resistance and road gravity. As soon as the best fit parameters in calibration mode obtained, these parameters would be useful for the prediction phase to predict the future urban structure. In this study, the proposed method was applied on Tehran's data and the model effectiveness in Tehran is analyzed, then in order to investigate the impacts of future policy on urban growth, three scenarios were designed to simulate the spatial pattern under different conditions. The first scenario assumes historical urbanization mode would persist without any limitation. The second one is compact scenario which makes the growth mostly internal and limits the exterior expansion, especially the small patches are not allowed for further expansion in this scenario, and the last Scenario proposes a polycentric urban structure which let the little patches growth without any limitation and would not consider the areas beyond the specific buffer zone from the larger patches, for development. In the recent two scenarios, the nature resources are also protected from the new development. In the first scenario, results show that precious nature resources such as farmlands and open areas would not be preserved and the urban expansion would be beyond the government's urban policy. In the second and third scenarios the farmlands could be protected and the third scenario was more suitable for Tehran because it could avoid undesirable affects such as concestion and pollution and the results of this scenario were more agreeable to the urban policy.

8181-19, Session 4

Application of GIS for the modeling of spatial distribution of air pollutants in Tehran

S. Sargazi, H. Taheri Shahraiyni, Tarbiat Modares Univ. (Iran, Islamic Republic of); M. Habibi Nokhandan, Islamic Republic of Iran Meteorological Organization (Iran, Islamic Republic of); M. Sanaeifar, Islamic Azad Univ. (Iran, Islamic Republic of)

In Tehran (Capital city of Iran), the cars are the main factor of air pollution and the air pollution in Tehran is increasing continuously. Hence, it seems necessary to study on the air pollution in Tehran. Spatial modeling of pollutants is a useful method for the estimation and monitoring of the pollutants in the non-observed positions in Tehran. In addition, spatial modeling can determine the level of pollutants in different regions of Tehran. It is also useful for develop of an appropriate terrific program. There are some typical interpolation techniques (e.g., IDW (Inverse Distance Weighting), TPS (Thin Plate Splines), Kriging and Cokriging) for spatial modeling of air pollutants. In this study, these spatial modeling techniques were evaluated in the GIS environment for the modeling of spatial distribution of carbonmonoxide in Tehran.

The hourly data of carbon monoxide in 2008 have been extracted of 16 air pollution monitoring stations in Tehran. Then the hourly data was averaged and converted to the daily data. The hourly data of 3 selected days in 2008 (72 hours) and similarly, the daily data of 36 days in 2008 (3 days in each month) were utilized for spatial modeling in this study. Different typical interpolation techniques were implemented on different hourly and daily data using ArcGIS, respectively. The percent



of absolute error of each interpolation techniques for each hourly and daily interpolated data was calculated using cross validation techniques. Then the average of percent absolute errors of 72 hourly and 36 daily maps were calculated for each interpolation techniques. Then the methods were evaluated and compared according to their mean percent absolute errors in hourly and daily spatial modeling of carbon monoxide in Tehran.

The mean percent of absolute error of hourly spatial modeling of carbon monoxide using IDW, TPS, Kriging and Cokriging were 85.5, 110.5, 81.6 and 79.7%, respectively. Similarly, the mean percent of absolute error of daily spatial modeling of carbon monoxide using IDW, TPS, Kriging and Cokriging were 95.2, 109, 86.2 and 75.9%, respectively. The mentioned results demonstrated that Cokriging has better performance than other typical interpolation techniques in the hourly and daily modeling of carbon monoxide. Cokriging utilize three input variables (Latitude, Longitude and altitude) data for spatial modeling but the other methods use only two input variables (Latitude and Longitude). The three-hourly data of wind speed and direction was received from 5 meteorological stations in Tehran. In addition, the wind speed and direction map was generated using concurrent wind speed and direction data with the hourly carbon monoxide data. The wind map was overlapped with the map of spatial distribution of carbon monoxide, generated by Cokriging in ArcGIS environment. The visual interpretation of overlapped maps certified the appropriate modeling of Cokriging. Kriging was the appropriate method after Cokriging, and it shows better performance than IDW and TPS techniques. According to the appropriate results of Cokriging, it has merit to be introduced as an appropriate method for the spatial modeling of air pollutants.

8181-20, Session 5

High resolution remote sensing information identification for characterizing uranium mineralization setting in Namibia

J. Zhang, Beijing Research Institute of Uranium Geology (China)

The modern Earth Observe System (EOS) technology takes important role in the uranium geological exploration, and high resolution remote sensing as one of important parts of EOS is vital to character spectral and spatial information of uranium mineralization factors. Utilizing satellite high spatial resolution and hyperspectral remote sensing image (QuickBird, Radarsat2 and Hyperion), field spectral measurement (ASD spectrometer) and geological survey, this paper established the spectral identification pedigrees of uranium mineralization factors including six different types of alaskite, lower and upper marble of Rossing formation, dolerite, alkali metasomatism, hematitization, and chloritization, and so on in the central zone of the Damara Orogen, Namibia.

Moreover, adopted the texture information identification technology of QuickBird and Radarsat2 data, the geographical distribution zones of ore-controlling faults and boundaries between the different strata were delineated. Based on above approaches, the remote sensing geological anomaly information and image interpretation signs of uranium mineralization factors were extracted, the metallogenic conditions were evaluated, and the prospective areas have been predicted.

8181-21, Session 5

Hyperspectral remote sensing applied for hydrogeological mapping in a hard-rock terrain for water resource management

A. Singh, S. Mukherjee, Jawaharlal Nehru Univ. (India)

Out of several natural and anthropogenic factors influencing groundwater as well as surface water resources, hydrogeological characteristics of a landscape are vital in deciding and controlling the processes that lead to development of geo-ecosystem of in that landscape. This study aimed at studying the whole of geological environment associated with a semi-arid, hard-rock terrain utilizing hyperspectral satellite data, topographic analysis and 3D visualization techniques to infer hydrological regime in form of GIS outputs.

Conference 8181: Earth Resources and Environmental Remote Sensing/GIS Applications

The area selected for present study lies is in south of Delhi, the capital of India, with several industrial cum residential townships that have a rapidly changing landuse pattern with a high population density. Several pockets of the area have been subjected to mining activity to provide for construction material for these townships. It lies in vicinity of a fault that shows several surface manifestations. Pressures from changing landuse and mining have degraded the terrain and affected the ecosystem as well. Several natural lakes have dried up and few abandoned mining pits have turned up into lakes. There exists a wildlife sanctuary in the area and efforts are being made to restore the landscape and protect any further degradation. Availability of water (both surface as well as ground) is the prime decisive factor in all such efforts since the area itself is semi-arid in nature.

In this study, HYPERION data has been utilized in a unique and elaborated methodology designed to effectively isolate the intruding urban cover and extract maximum information in an unmixing approach involving SMACC, nD-Visualizer, SAM and MTMF. This has been coupled with ground surveys as well as collection and analysis of soil / sediment, rock and water samples. Geochemical characterization of samples was coupled with interpreted results of hyperspectral data analysis (matched with reflectance spectra of minerals). ASTER DEM has been used for topographic analysis using TauDEM to infer watershed characteristics and drainage pattern in the area. Apart from geological endmembers (quartzite, phyllite, montmorillonite and kaolinite), available pockets of vegetation have been identified as these are themselves an indicator of groundwater availability. This also resulted in identification of sites suitable for future geophysical surveys to determine the nature of sub-surface fractures (extent and connectivity) and associated influence on groundwater availability and surface water drainage.

This whole exercise in detail has been helpful in obtaining a synoptic view of water resource in the region and then subsequent planning for ecosystem regeneration. This will also be equally significant in long-term planning for integrated water resource management in the surrounding region to provide for the human consumption and reduce external pressures on the already fragile ecosystem.

8181-22, Session 5

Using satellite imagery and Geospatial Information Systems to make a better decision in geological interpretation

F. Beik, Z. Naseri, National Iranian Oil Co. (Iran, Islamic Republic of)

Abstract

In the high potential hydrocarbon area, different kinds of exploration studies have been done during the time. The scattered studies should be gathered. They can be used after complementation for future exploration programs. New techniques like Remote Sensing (RS) and Geospatial Information Systems (GIS) are some of the most useful methods to collect and improve data in a short time and by the least cost.

In this study a structural anticline with multiple prospects had been chosen to estimate the probability of hydrocarbons discovery in an exploration well [P (discovery)] based on the evaluation of a number of parameters which are recognized as being essential for the accumulation of hydrocarbons. All the available data of the structure was studied and no evidence of any erosion on the structure which could have cut deep enough to impair the seal was found at the first step. The only uncertainty was having no geological map with a scale larger than 1:100000. Thus, need to immediate interpretation on surface and subsurface formations of Shir Anticline, a geological structure located in South-East part of Zagros Mountain, made the necessity of old data management and using new methods to gain the proper accuracy information in a short time. Two types of data have been used in this study. The first group has been digital data involved LANDSAT Enhance Thematic Mapper (ETM+) images and Digital Elevation Models with spatial resolution of 10 m. The second group has been hard copy data involved available geological map with scale of 1:100000 and two old cross sections, using field data to draw and published by NIOC. Two old structural cross sections of the north anticline that had been passed on the intended structure show the outcrop of Asmari formation, which is one of the most important reservoir formations in the area. But the outcrops could not



be distinguished on an existing geological map by the 1:100000 scale. Therefore by data integration in GIS and their analysis in ARCGIS, especially satellite images and available geological data, a reliable map has been prepared. But as it was used as a new method in the office hence 5 check points have been collected by using GPS. The check points have confirmed the reliability of the results. Satellite images provide the advantage of large area or synoptic coverage and they provide the advantage of large area or synoptic coverage and they provide the ability to analyze multispectral band quantitatively in terms of numbers which permits the application of computer processing routine to enhance certain compositional properties of earth material. New techniques like GIS are very important and practical for integration of old and new data which exist in hydrocarbon areas. Consequently trying to approve the important outcrops in the office will prevent a new geological field trip, which would be taken time and cost in exploration programs.

8181-23, Session 5

Mineral detection in hyperspectral data using characteristics of spectral profiles

M. M. Oskouei, Sahand Univ. of Technology (Iran, Islamic Republic of)

Hyperspectral imaging has opened a new outlook for mineral detection in geological studies and mineral deposit explorations regarding to its spectral information. An exploration project is generally started by rationally fast and cheap studies and continued toward precise and of course expensive activities like bore holes drilling and tunnelling.

Mineral deposit exploration has highest risk in comparison to other industrial activities. Collecting and interpretation of any available information is therefore crucial before stepping on deep drilling stage. Remote sensing methods are one of the helpful techniques for this purpose. They are faster and cheaper than other prospecting methods. Developing of image processing methods for hyperspectral data on the other hand has made remote sensing more significant. One of the most interesting challenges in the ground of hyperspectral image processing is unmixing. This is performed by determination of the number and characteristics of endmembers and unmixing computations. Identifying of the endmembers is based on finding the pure pixels in the understudy scene and then comparing the spectral profile of them to reference spectral profiles (i.e. spectral library or field data). A great number of researches have been conducted to improve preprocessing and processing algorithms in this arena. Many researchers have tried to achieve realistic results by finding a reliable method for spectral matching (e.g. Spectral Feature Fitting (SFF), Spectral Angle Mapper (SAM)) that Tetracorder algorithm is referred as most robust one (e.g. Spectral Feature Fitting (SFF), Spectral Angle Mapper (SAM), Matched filtering method) that Tetracorder algorithm could be referred as most robust one.

According to Clark, the Tetracorder method makes a comparison between unknown spectral profile (endmember) and reference profiles (expert system). No match will be the answer if there is not significant similarity between them. The reference spectra include all possible surfaces (e.g. minerals, vegetation types, manmade, etc). The endmembers types inside the study scene on the other hand are usually limited due to the study scope. Therefore, the prior information about the possible surface types will decrease the number of the reference spectra that must be checked.

METHODOLOGY

This algorithm is implemented in two stages, preprocessing and determination of the unknown spectrum. Reliable and accurate results will be achieved if the distortions on the image are correctly rectified. These corrections are generally including topographic and atmospheric corrections, and some other preprocessing algorithms respected to the technical characteristic of sensors and data for instance, smile effect correction and polishing for Hyperion data. In addition to that, the reference mineral spectral library must be resampled regarding to the wavelengths of data bands as the reference spectra are collected usually by high spectral resolution spectrometers.

Since all minerals do not have explicit absorption features on their spectral profiles, in the current study, two libraries were formed consisting of minerals with and without absorption features. The unknown spectrum will then be compared to the minerals spectra in both libraries and the best matches from the libraries will be identified.

SPIE Remote Sensing

8181-24, Session 6

Object-based rapid change detection for disaster management

H. Thunig, U. Michel, Pädagogische Hochschule Heidelberg (Germany); M. Ehlers, Univ. Osnabrück (Germany); P. Reinartz, Deutsches Zentrum für Luft- und Raumfahrt e.V. (Germany)

Rapid change detection is used in cases of natural hazards and disasters. These analysis lead to quick information about areas of damage. In certain cases the lack of information after catastrophe events is obstructing supporting measures within disaster management. Earthquakes, tsunamis, civil war, volcanic eruption, droughts and floods have much in common: people are directly affected, landscapes and buildings are destroyed. In every case geospatial data is necessary to gain knowledge as basement for decision support. Where to go first? Which infrastructure is usable? How much area is affected? These are essential question which need to be answered before appropriate, eligible help can be established.

This study presents an innovative strategy to retrieve post event information by use of an object-based change detection approach. Within a transferable framework, the developed algorithms can be implemented for a set of remote sensing data among different investigation areas. Several case studies are the base for the retrieved results. Within a coarse dividing into statistical parts and the segmentation in meaningful objects, the framework is able to deal with different types of change. By means of an elaborated normalized temporal change index (NTCI) panchromatic datasets are used to extract areas which are destroyed, areas which were not affected and in addition areas which are developing new for cases where rebuilding has already started. The results of the study are also feasible for monitoring urban growth.

8181-25, Session 6

Object-Based vs. Per-Pixel Classification of Aster Imagery for Land Cover Mapping in Semi-Arid Areas

M. M. El Abbas, E. Csaplovics, Technische Univ. Dresden (Germany)

Effective management of fragile ecosystems requires flexible and reliable information. Pixel-based technique generally performs classification based on spectral values. While, the object-oriented image analysis approach uses textural and contextual information as well as the spectral information. Earth objects have different spectral information and can be specified easily. The ability of this approach is limited when objects have similar spectral information. Due to complexity and spectral similarity in semi-arid areas, land cover mapping with remotely sensed data encounters serious problems when applying methods based on spectral information and ignore spatial information. To cope with this issue, research was conducted in the Blue Nile area of Sudan to evaluate the effectiveness of innovative object-oriented analysis (OOA) approach versus pixel based approach to generate thematic land cover maps based on multi-spectral Advanced Spaceborne Thermal Emission and Reflection Radiometer (ASTER) imagery data acquired in March (2009). In the preprocessing phase geocoding was applied with a Root Mean Square (RMS) less than 0.5 of pixel size based on thirty four ground control points collected from the site, as well as atmospheric correction using Fast Line-of-sight Atmospheric Analysis of Spectral Hypercubes (FLAASH). Maximum likelihood classifier was performed in ERDAS imagine 9.3 software with random field points to examine if the spectral properties of the selected classes alone can be discriminated effectively. Nine land cover classes; agriculture (rain-fed), dense-forest, grassland, horticulture, irrigated croplands, bare-land, scattered-forest, settlements, and water body were generated with only about 64% overall classification accuracy. The segmentation algorithm applied is a bottom-up pair wise region merging technique, and different segmentation strategies were applied with the OOA paradigm that might be effective to separate similar spectral values into preliminary unclassified image objects of groups of relatively

homogeneous pixels based on shape and compactness criterion at different scales. The segmented objects assigned to different land cover classes with methods of membership functions and Nearest Neighbor classifiers implemented in Definiens Developer 8.1 (formerly known as eCognition) software with knowledge-based and randomized field Training and Test Areas (TTA) Mask respectively. The membership functions provided highly overall classification accuracy (98%), while Nearest Neighbor achieved about 76% accuracy. A confusion matrix of User's, producer's accuracies as well as kappa coefficient was also presented. A total of two hundreds and ten training samples were used for the classification and validation stage with approximately two third to one third respectively, in means of individual pixel samples in maximum likelihood classifier and an entire object in form of TTA Mask in Nearest Neighbor classifier derived from GPS testing samples shape file. This study emphasized that the OOA methods provides more accurate results than the classical per-pixel approach especially when user's expert knowledge is offered to develop the Rule sets. The study demonstrates the effectiveness of the combination of different parameters for segmentation, and of a set of optimal features used, as well as the flexibility of hierarchical data processing strategy. Main differences between methods applied are presented and also provides suggestions to reduce the weaknesses associated with the OOA approaches.

8181-26, Session 6

Estimating vegetation phenological trends using MODIS NDVI time series

M. Törmä, M. Kervinen, S. Anttila, SYKE Finnish Environment Institute (Finland)

Information concerning the start and end of vegetation growing season has its use in environmental monitoring like studying nutrient leaching or climate change. This paper presents methods to estimate phenological features of vegetation growing season using time series of MODIS vegetation index images. The methodology has been developed as backup method for SM-13 Vegetation Phenological Trends-product of European Union-funded Geoland2-project.

Product provides important dates of vegetation growing season, namely start, maximum and end of growing season in a form of text file and shapefile for different administrative areas and land cover types. Following features are computed:

1. Start of growing season A: Day of start of rapid increase in NDVI corresponding to the start of flux growing season (nutrient fluxes start to flow in plants).

2. Start of growing season B: Day when NDVI goes over defined threshold corresponding to birch bud-burst.

- 3. Day of maximum NDVI
- 4. End of growing season: Day when NDVI decreases below threshold.
- 5. Length of growing season A: feature 4 feature 1
- 6. Length of growing season B: feature 4 feature 2
- 7. Quality estimate for feature 1.
- 8. Quality estimate for feature 2.
- 9. Quality estimate for feature 4.

The product is based on Normalized Difference Vegetation Index time series computed from daily MODIS-images (years 2001-2008). Land cover types are agricultural areas, coniferous forest, deciduous forest, mixed forest and open wetland (open bogs). So far, hydrological drainage basins have been used as administrative units.

Quality estimates indicate how likely it is that corresponding feature has been estimated reliably. In-situ measurements have been provided by Finnish Meteorological Institute (plant flux measurements, 3 sites) and Finnish Forest Research Institute (plant phenological observations, 5 sites). Residuals of extracted features can be about 2 days in the best case but are typically around 7 days.



8181-27, Session 6

Change detection for Finnish CORINE land cover classification

M. Törmä, P. Härmä, S. Hatunen, R. Teiniranta, M. Kallio, E. Järvenpää, SYKE Finnish Environment Institute (Finland)

European Commission introduced the CORINE programme in order to gather information relating to the European environment. CORINE classifications have been produced using satellite images and visual interpretation with mapping scale of 1:100000 and 25 hectare minimum mapping unit. In Finland, CORINE classifications have been made differently in order to produce more detailed national land cover information at the same time, and have been based on automated interpretation of satellite images and data integration with existing digital map data. Map data has provided information describing land use and soils. Satellite images have been used in estimation of continuous variables describing vegetation type and coverage, as well as in updating map data. Generalization from national to European CORINE has been made using fully automated procedure. So far, CORINE classification has been produced for years 2000 and 2006 in Finland, and the next version is for year 2012. CORINE land cover mapping is nowadays part of operational GMES initial operations in which European land monitoring is implemented.

The aim of this paper is to document the semi-automatic change detection method used to produce changed areas between years 2000 and 2006, and present ideas to enhance change detection using e.g. image segmentation. Applied semi-automated approach enables detailed, high resolution change monitoring also for national and regional applications.

According to the specifications of EEA, changes in land cover should be based on visual image comparison of satellite images. Finnish approach is different and combines the detection of changed area using difference images of RED and NIR channels of satellite images and the type of changes is defined using CLC2000 and CLC2006 classifications. Some specific changes, like changes in artificial surfaces, arable lands and regrowth in forests, are based directly to comparison of CLC2000 and CLC2006 classifications, since they are difficult to detect using image-to-image comparison.

8181-28, Session 6

Hazards analysis and prediction from remote sensing and GIS using spatial data mining and knowledge discovery: a case study for landslide hazard mitigation

P. Hsu, National Taiwan Univ. (Taiwan); W. Su, National Science and Technology Ctr. for Disaster Reduction (Taiwan)

Due to the particular geographical location and geological condition, Taiwan suffers from many natural hazards, such as typhoons, flooding, landslides, land debris, and earthquakes, which often cause series property damages and even life losses. To reduce the damages and casualty, an effective real-time system for hazard prediction and mitigation is necessary. In the past decades, a large amount of hazard data and information have been collected during the hazard periods, such as the change detection of land use and land cover, the predicted results calculated from various physical hazard models in the pre-disaster period, the real-time monitoring hazard data during the hazard period, and the detection of hazardous areas and damage assessment from field survey and remote sensing technology in the post-disaster period. In addition, many different kinds of geo-spatial data are also collected ordinarily, including the multi-temporal aerial photos and satellite images, the digital elevation models (DEMs), topographic maps, vegetation maps, geology maps, land use and land cover maps, river and road systems, etc. How to integrate these data and promote the efficiency for hazard prediction will be an important issue. Recently, many methods of geospatial data mining and knowledge discovery have been proposed to extract useful information and discover knowledge from massive amounts of data in support of decision-making. The knowledge discovery form databases (KDD) process usually consists of several steps, namely, data selection, data preprocessing, data enrichment, data reduction and projection, data

mining, and pattern interpretation and reporting. The relationships between input/output data and the representation parameters can be revealed by KDD, and can be used for the design of related engineering systems, and sensitivity analysis concerns methods for analyzing these relationships.

In this study, a case study for Landslide Hazard Zonation (LHZ) is tested in accordance with the improved KDD process. Firstly, the locations of landslides caused by typhoon from 2006 through 2010 in the test area are detected from field survey and remote sensing technology. The results of landslides detection are used as the reference (output) data for learning and verifying in KDD. On the other hand, many different kinds of geospatial data including the terrain elevation, land cover types, the distance to roads and rivers, geology maps, NDVI from remotely sensed images, and monitoring rainfall data etc. are collected as the input data in the KDD process. The spatial data cleaning is essential to remove the noises, errors and outliers hiding in the input spatial data sets. The data defects, repetition and inconformity between different kinds of spatial data can also be removed by data cleaning. After the data cleaning, three different data mining methods, including logistic regression (LR), artificial neural networks (ANNs) and decision trees (DT) are applied to generate the LHZ map, and comparison between these methods are also illustrated in this paper. The experiment results show that the accuracy of LHZ is about 84% with the proposed KDD process and indicate the landslides induced by heavy-rainfall can be mapped efficiently from remotely sensed images and geospatial data using KDD technologies.

8181-29, Session 7

Structural analysis of forest areas in highresolution SAR images

M. Boldt, Fraunhofer-Institut für Optronik, Systemtechnik und Bildauswertung (Germany); A. Thiele, Karlsruher Institut für Technologie (Germany); K. Schulz, Fraunhofer-Institut für Optronik, Systemtechnik und Bildauswertung (Germany); S. Hinz, Karlsruher Institut für Technologie (Germany)

Nowadays, climatic and socioeconomic conditions require a change in thinking in the field of state forest management. A high demand for up to date and precise forest information is given - especially in regard to increasing forest damages by natural hazards. The increasing availability of high-resolution and fast-revisiting satellite systems (e.g., TerraSAR-X, Cosmo-SkyMed, RapidEye) allows to support such monitoring tasks. Furthermore, the combination of data of such different sensors allows the extraction of more forest parameters.

In comparison to data recorded in the visible spectral range, the acquisition date depends more on system workload than on weather conditions, due to the daylight independence and the nearly all-weather capability of radar sensors. At this stage of investigations, we focus on the recording and analyzing of SAR images. We analyze a TerraSAR-X image pair, which was recorded in 2010 in HH polarized Spotlight Mode with a wavelength of 31 mm (X-Band). The incidence angle is 49 degree and the geometric slant range resolution is about 1.2 m.

Focusing on the image analysis, we take advantage of the higher geometric resolution of the SAR imagery compared to the electrooptical RapidEye data. In particular, we focus on the extraction of structural forest parameters. First, the geocoding procedure is described - the most important step for fusion and assessment. We present geocoding results based on four different height models. Subsequently, several approaches for automatic extraction of forest parameters are described, whereby the processing software Definiens Developer7 and the programming environment MATLAB are used.

We discuss in detail an approach of forest boundary extraction based on image layers intensity and local coefficient of variation. Then, we focus on estimating tree and forest heights. Subsequently, the density of forest areas is analyzed by investigating intensity or/and GIS layer. Additionally, the classification of forest in three different types (deciduous, coniferous, and mixed forest) is investigated. Finally, all results are compared and validated with GIS data and field measurements.



8181-30, Session 7

Coastal water quality near to desalination project in Cyprus using Earth observation

D. G. Hadjimitsis, C. Papoutsa, Cyprus Univ. of Technology (Cyprus)

Remote sensing can become a very useful tool in order to monitor coastal water quality. Economically benefits of using remote sensing techniques are obviously comparatively to the field-based monitoring because water quality can be checked daily or weekly depended on satellite overpass frequency rather than monthly as done by traditional methods which involve expensive sampling campaigns. Moreover remote sensing allows the spatial and temporal assessment of various physical, biological and ecological parameters of water bodies giving the opportunity to examine a large area by applying the suitable algorithm. This paper describes the overall methodology in order to retrieve a coastal water monitoring tool for a high risk area in Cyprus. This project is funded by the Research Promotion Foundation of Cyprus and is been developed by the Department of Civil Engineering & Geomatics, Remote Sensing Laboratory, Cyprus University of Technology in corporation with the Department of fisheries and marine research in Cyprus. Firstly a time series of pigments will be done in order to determine the concentrations of the expedient parameters such as Chlorophyll, turbidity, total suspended solids (TSS), temperature etc at the same time of satellite overpass At the same time in situ spectroradiometric measurements will be taken in order to retrieve the best fitted algorithm. Statistical analysis of the data will be done for the correlation of each parameter to the in situ spectroradiometric measures. Several algorithms retrieved from the in situ data are then applied to the satellite images e.g. Landsat TM/ETM+, MODIS in order to verify the suitable algorithm for each parameter. In conclusion, the overall approach is to develop regression models in which each water quality parameter will be retrieved using image, field spectroscopy, and water quality data.

8181-31, Session 7

Land degradation monitoring in the Ocnele Mari salt mining area using satellite imagery

V. D. Poenaru, A. Badea, E. Savin, Romanian Space Agency (Romania); V. Poncos, D. Teleaga, Advanced Studies and Research Ctr. (Romania)

Mining is an important activity contributing to the economic development with long lasting environmental impacts. A major disaster took place in 2001 in the Ocnele Mari salt mining area located in the central-south part of Romania when the artificial lake brain was poured in rural areas, devastating homes and polluting the Olt River. Towards a sustainable and harmonious development of the Ocnele Mari area, the Romanian Authorities decided to ecology and rehabilitate it. This ongoing project is focused on land degradation monitoring from 2001 disasters until now. High Resolution Spotlight TerraSar-X synthetic aperture radar (SAR) data acquired within TerraSAR-X proposal LAN0778 are used to analyze terrain deformation by interferometric techniques knowing the mine subsidence is not constant; periods of relative stability are followed by quick deformation. The rocks forming in the region situated above the salt cushion have very low mechanical resistance and high intergranular fissured permeability so the hill's slopes are affected by landslides which are reactivated periodically. Additionally, analysis of the vegetation coverage (leaf area index - LAI and normalized difference vegetation index - NDVI) from the optical data gathered by different sensors such as SPOT and LANDSAT combined with the meteorological data (temperature, wind speed, humidity and solar radiation) provide indicators for the land degradation. The results will be validating on ancillary data. Satellite derived information in conjunction with in-situ measurements can provide valuable information for existing conservation development models for defining the essential elements of a planning process designed to maximize the values provided by salt ponds from Ocnele Mari.

8181-32, Session 7

Landslide detection and monitoring using remote sensing and spatial analysis in Taiwan

F. Tsai, T. Lin, L. Chen, National Central Univ. (Taiwan); W. W. Chen, National Taipei Univ. of Technology (Taiwan)

Taiwan is located in the edge of East Asia and is prone to natural hazards caused by extreme weathers and earthquakes. Conventional ground-based approaches for hazard investigation are usually expensive, time-consuming, and difficult to obtain comprehensive information for large areas. On the other hand, not only can remote sensing images provide abundant spectral and spatial information, they can also overcome difficult terrain and transportation conditions to cover large areas and to provide data in a short time. Therefore, remote sensing is an effective data source for investigating natural hazards. Combined with geographical information systems and spatial analysis, they can be used to map and analyse natural hazards such as flooding and landslides. The data produced are in turn helpful in developing effective strategies for hazard mitigation.

This paper presents a systematic approach to utilize multi-temporal remote sensing images and spatial analysis for the detection, investigation, and long-term monitoring of landslide hazards in Taiwan. Rigorous orthorectification of satellite images are achieved by correction of sensor orbits and backward projections with ground control points of digital elevation models. Individual images are also radiometrically corrected according to sensor calibration factors. In addition, multi-temporal images are further normalized based on pseudo-invariant features identified from the images. Probable landslides are automatically detected with a change-detection procedure that combines NDVI filtering and Change-Vector Analysis. A spatial analysis system is also developed to further edit and analyse detected landslides and to produce landslide maps and other helpful outputs such as field-investigation forms and statistical reports. The developed landslide detection and monitoring system was applied to a study of large-scale landslide mapping and analysis in southern Taiwan and to the long-term monitoring of landslides in the watershed of Shimen Reservoir in northern Taiwan. Both application examples indicate that the proposed approach is viable. It can detect landslides effectively and with high accuracy. The data produced with the developed spatial analysis system are also helpful for hazard investigation, reconstruction, and mitigation.

8181-35, Session 8

Coastal geomorphology changes of Quatre Bay of Iran using satellite data

A. Salehipour Milani, Geological Survey of Iran (Iran, Islamic Republic of); P. Akhgar, Ministry of Education (Iran, Islamic Republic of)

Geomorphologic changes of Quatre Bay coastal area at 61° 28'- 61° 47' Longitude in east and from 25° 01'- 25° 17' hotos and satellite data respectively. Initially. The data used in this study consisted of Landsat satellite images from Multispectral Scanner Landsat (MSS) (1976), Thematic Mapper (TM) (1989) , Enhanced Thematic Mapper plus (ETM+) (2000,2008) sensors. the boundary of water, changes of coast line, their evolution in various periods of time, and their effects on the lagoons caused by tides were investigated. Using satellite data, we were able to distinguish the direction of wakes currents and hence to determine the movement direction, transportation of sediments, investigate their role on evolution of coastal forms, and their effect on coastal construction. Extend, and changes in sand dunes and coastal barriers in four periods of time have been compared. Using the result obtained from the investigation on coastal barriers, sand dune, and their boundary, we could determine the late barrier on north of Quatre bay. The results from this research demonstrate severe changes in barriers.



8181-36, Session 8

Geoinformatics applications for flood mapping and management in Haryana State, India: key issues

B. S. Chaudhary, Kurukshetra Univ. (India)

The globe is suffering from one or the other type of disasters in recent years These are becoming more and more frequent in recent years. These include Earthquakes, Tsunamis, Floods, Landslides, Volcanic eruptions etc. In India, most common disaster in recent years is flood which is playing havoc. Haryana, one of the northern district, agriculturally dominated India is also suffering from floods time and again causing most of the damages. The present paper deals with key issues in flood mapping and management in the state by using the Geoinformatics technology in Haryana state, India. Haryana state covers a total area of 44,212 sq kms and lies between 270, 35' to 310, 55.5' N latitude and longitudes 740, 22.8' and 770 35.6' E longitudes. The state is bounded by natural features as Siwaliks in North, Aravallis in South, Yamuna River in East and Ghaggar in West. The area is covered by Survey of India toposheets Nos. 44K, 44O, 44P, 53C, 53D, 53F, 53G, 53H, 54E. Barring the Hilly portions, most of state lies between 200 to 300 meters above mean sea level. The average slope of the terrain is northeast to southwest however the slope in northern portion is towards south and in south it is towards north making it almost saucer shaped physiography. It mainly occupies Indo-Gangetic water divide and majority is covered by Indo-Gangetic alluvium. Ghaggar, Tangri, Markanda, Saraswati and Chautang originate in Siwaliks in the north, Yamuna is the only perennial river making its eastern boundary, Sahibi, Krishnawati and Dohan non-perennial rivers originate in the south in Aravalli hills of Rajasthan. Haryana is an agricultural state with 88% of the total geographical area under cultivation and cropping intensity of more than 150%. Dominant food crops in the state are wheat, paddy, maize and gram. The causative factors for flooding and the measures to mitigate floods have been discussed in detail. The major causes of floods in the area were heavy downpour, poor inland drainage, presence of localized depressions, breaching of canals and diminished carrying capacity of the water channels etc. The measures suggested for the mitigation are strong warning and communication network to help in effective evacuation; effective disaster management board with inputs from Geoinformatics studies; strengthening of vulnerable sites along the river courses/ canals; periodic de-silting and cleaning of water ways; proper drainage in poor inland drainage areas and construction of ring bunds around the settlement etc.

8181-37, Session 8

Soil erosion risk assessment using GIS and CORINE model: a case study from western Shiraz, Iran

M. Tayebi, A. Sameni, M. H. Tayebi, Shiraz Univ. (Iran, Islamic Republic of)

Soil erosion is a serious envirnomental problem and may have very significant impact on crop yields and human life. This study employs the CORINE model with Geographic Information System (GIS) to assess soil erosion risk for restoring and protecting areas within the Bonrod Zangane catchment in the Zagros mountain range, western Shiraz, Iran. Geographic Information System (GIS) technologies are valuable tools in developing environmental models through their advance features of data storage, management, analysis, and display. The CORINE model parameters including actual soil erosion risk (Ea) and potential soil erosion risk (EP) were determined using field surveying, laboratory analysis, Landsat TM imagery, and topographic map. Actual soil erosion risk was determined by combining two parameters including potential soil erosion risk and vegetation cover. Meanwhile, the potential soil erosion risk was generated by integrating soil erodibility, erosivity, and slope angle parameters. Soil texture, depth and stoniness layers were overlaid to form a soil erodibility map. Fournier and Bagnouls-Gaussen aridity indexes were calculated from the climatic data and consequently integrated to generating the erosivity layer. The slope angle classes also were generated from digital elevation model of the study area. The raster- based layers were then integrated to produce erosion risk map. The results showed that

about 56.01% and 31.8% of the study area has high and moderate soil erosion risk, respectively. Only 12.2% of the study area has low soil erosion risk. It is concluded that CORINE model with Geographic Information System (GIS) are effective for soil erosion risk assessment and produced actual soil erosion risk map could be used for protecting soil from land degradation phenomena

8181-72, Session 8

Remote sensing and GIS for the safety management of the interactions between natural and industrial hazard

M. Ciucci, A. Marino, Istituto Superiore per la Prevenzione e la Sicurezza del Lavoro (Italy)

In the Italian territory about 1/3 of municipalities are located in areas exposed to seismic hazard. At the same time most of the Italian territory is subject to hydrogeologic events (i.e. landslides and floods). The area object of this study, Sulmona Basin and upper Pescara Valley, is characterized by potential exposition to these hazards, with a particular attention to seismic hazard and landslide hazard. Furthermore the area is characterized by the presence of major hazard industrial plants.

For this paper a dedicated GIS database has been built in order to evaluate the interactions between specific natural hazards and industrial hazard and the related vulnerability of territory and population. For this research MIVIS hyperspectral (at a 1500 and 3000 m elevation) images have been used. The obtained images have been georeferenced. From the processing and classification of these images some information layer have been obtained: thematic maps of land-use (industrial areas identification), vegetation conditions, thermal pollution, quality parameters (temperature, organic matter, chlorophyll, sediments) for river waters. Thematic maps obtained from remote sensing have been inserted in a GIS, that means a system to insert, store, integrate, extract, retrieve, manipulate and analyze georeferenced data layers in order to produce interpretable information. Then the data base has been integrated with further information inserted as continuous layers; thematic layers; vector layers; punctual data; attributes. Among inserted layers: location and information regarding industrial plants, seismic classification, landslides and landsliding hazard maps. Some specific operators (overlaying, proximity analysis, recoding, matrix analysis) have been applied that allowed to integrate the information contents and therefore to obtain final thematic maps (hazard maps, vulnerability maps, events scenarios). The innovative technologies proposed facilitate and optimize the management of data and information obtained from different methodologies. Therefore it is useful to develop innovative methodologies in order to support industry and Competent Authorities in disaster management and land use planning.

8181-34, Poster Session

Study on the ecosystem health assessment for wetland of Lianyungang

H. Li, H. Peng, Huaihai Institute of Technology (China); J. Nie, Shouguang Modern School (China); Y. Wu, Cold and Arid Regions Environmental and Engineering Research Institute (China)

Coastal zone is important region because of its abundant natural resource and predominant geographical position. But it is unstable because of human activity and natural factors, such as coast erosion, silt deposition, inning, marine reclamation land, and so on. The changes of coastline are the most obvious symbol of instability of coastal zone. So, it is important for management and sustainable development of coastal zone to analysis and research on the changes of coastline. Measurements of the coastline are difficult to achieve in time by the traditional manner. Remote sensing has been an important technology for monitoring the changes because of its characteristics of rapid, extensiveness, real time, and so on.

Lianyungang is a prefecture-level city northeastern Jiangsu province, People's Republic of China. She is the eastern end of the New Eurasia Continental Land-bridge and the proposed Northern East West Freight

Conference 8181: Earth Resources and Environmental Remote Sensing/GIS Applications



Corridor. As one of the first 14 Chinese coastal cities opening to the outside world in 1984, She had developed more than 20 years, especially the harbor.

So, this paper aimed to monitor the changes of coastline in Lianyungang using TM and ETM+ data. The preprocessing include: calibration and geometric correction. Through the processing of three yeas images data of 1987, 2000 and 2007 and using automatic method to extract the coastline, the results showed that there are great changes of coastline in Lian Yungang. And length defined as the length of coastline and area defined as the area of region of ring composed of coastline changes. The length increased from about 131.4Km of 1987 to 168.8Km of 2007; and the area also increased greatly. But the results are need to be validated. And the erosion and human activity are the main reasons.

8181-43, Poster Session

Lightning hazard evaluation by integrating surface electromagnetic and physical properties

J. Baek, J. W. Kim, X. Wang, Univ. of Calgary (Canada); D. Lee, Sejong Univ. (Korea, Republic of)

To construct the potential lightning hazard map of northern Alberta, Canada, we adapted GIS data mining and Wavenumber Correlation Filter (WCF) to estimate potential lightning strikes by integrating physical properties of surface such as roughness, temperature and surface class with the non-hierarchical dielectric constant map. All six of surface classes were defined as a result of land classification, which are wetland, poplar and pine trees, fine and coarse artificial structures and water, respectively. The surface roughness and temperature were successfully derived from the SRTM (Shuttle Radar Topography Mission) 3 arc-second digital elevation model (DEM) and thermal band of Landsat-5 TM (Thematic Mapper) image. Non-hierarchical dielectric constant map was built up by applying the intrinsic weighting factors, which were computed from the Dubois (1995) model for less vegetated land areas and from the Ulaby (1986) model for open water areas, to the hierarchical dielectric constant proposed for the general use by Kim et al. (2004). We also downloaded the Albertan fire database (1959-1999) from Canadian Wildland Fire Information System (CWFIS) and extracted the fire events only caused by the lightning strikes.

GIS data mining technique was implemented to use association rule mining to find out the relationship between nature conditions of pixels (i.e., surface class, roughness, and temperature) and lighting records. We computed the relative frequencies of the rules containing three different nature conditions and sorted them in the descending order to identify which rule retains the highest possibility of lightning strike. Provided the rank of the rules, we generated lightning strike risk map with the normalized frequency ranging from 0 to 1.

Assuming that the dielectric constant of the surface is positively related with the lightning strike, we extracted the pixels satisfying the high dielectric constant and high frequency of a lightning strike. To identify such pixels, we carried out WCF with the dielectric constant and lightning strike risk maps. Sine the two maps were nearly independently made co-registered maps were initially correlated poorly showing the correlation coefficient (CC) of -0.001. To bring out the pixel correlations better, WCFs were applied to two maps. The correlation filtered maps were correlative at CC = 0.723, which corresponds to a total power reduction of about 52% and 44% for each map.

Positively correlated features can be mapped out by Summed LFI (SLFI) obtained by adding or stacking the normalized outputs pixel by pixel. The SLFI coefficients generally enhance the occurrence of directly correlative features, while suppressing the occurrence of inversely- (e.g., low risk-to-high risk correlations or high risk-to-low risk correlations) and non-correlative features in the two maps. By correlating the lightning strike risk map with the non-hierarchical dielectric constant map in the spectral domain using WCF and integrating them by the SLFI, we presented a new lightning hazard map of the study area.

8181-44, Poster Session

Oil seepage potential mapping using GIS: a case study from Zagros oil fields, SW Iran

M. H. Tayebi, M. Hosseinjani, M. H. Tangestani, Shiraz Univ. (Iran, Islamic Republic of)

Oil seepage is an important envirnomental hazard which can affect the water resources (ocean, sea, lake, river and groundwater), water quality and consequently, the ecological health. Oil seepage mapping is one of the most important endeavors in environmental impact assessment and defining targets with polluting potential. Geographic information Systems (GIS) are capable in producing and implementing spatial models in order to producing an oil seepage potential map. The study area is watershed of the Gotvand Dam, situated in the Zagros Fold and Thrust Belt (ZFTB), northern Ahwaz, and SW Iran. The ZFTB region is well known for its giant oil fields and also for oil seepages. Projection of area covered by Gotvand Dam lake on the topography map shows that this area locates on two giant Karoon and Lali oil fields. A conceptual model was created on the basis of expert knowledge on geotectonic and geological systems responsible for natural oil seepages in the Zagros as well as spatial distribution of known oil seepages. The evidential criteria including anticline axes, faults, lineaments, lithological units, lithological units boundary and oil wells were identified and used for producing predictor maps. The predictor maps and their internal classes were weighted and consequently integrated based on the multiple index overlay method to generating the oil seepage potential map. Field observations verified the results so that six new oil seepages were identified at high- to moderate-potential areas. The produced map could be efficiently used for decision making on the environmental impacts arising from oil seepages.

8181-45, Poster Session

Automatic dust storm detection in desert region based on supervised classification of multitemporal MODIS data

J. Gu, Cold and Arid Regions Environmental and Engineering Research Institute (China); G. S. Okin, Univ. of California, Los Angeles (United States); X. Li, C. Huang, Cold and Arid Regions Environmental and Engineering Research Institute (China)

During emission and the following atmospheric transport over the adjacent land, desert dust can be detected from space in the thermal infrared part of the spectrum. Several techniques based on multi-spectrum remote sensing data have been developed and show a good result. However, it is still difficult to be identified from bright surface like desert region since they have similar spectrum feature. The MODIS instruments are carried aboard the Earth Observing System (EOS) Terra and Aqua polar orbiting satellites. The high spatial and spectral resolution of MODIS enhances the visibility of airborne dust over land. Here, in this paper a new dust detection method in desert region based on the supervised classification of multi-temporal MODIS data has been developed in order to meet this problem.

In this algorithm, we follow the dust identification basis from the existed study first. For the elevated dust, it produces a depressed brightness temperature against the hot skin temperature of the desert background; For the cool layer of dust, it can be differentiated from water clouds having the same radiometric temperature based on its coloration properties.

Then the algorithm make full use of time-series MODIS data information by combining the temporal feature of the color information from multiple visible channels with near and far infrared measurements and the thermal information from thermal channels. To some extent, this temporal information can provide an improved ability to distinguish areas of dust from water/ice clouds and bright desert backgrounds.

In this study, the MODIS images of utah desert in the spring of 2009 have been collected to make further analysis in this study. And the band 1, 4,7,20,29, and 31 will be selected as the feature band in this experiment.

The construction of the algorithm mainly involves the processing of reference images generation, difference images generation and dust

Conference 8181: Earth Resources and Environmental Remote Sensing/GIS Applications



storm identification. The difference images are generated by the reference to extract the effect of background in clear sky condition. This idea is central to get a good reference image and cloud mask generation. In the following, we make a feature set based on the analysis of spectral bands reported in the literature. Then the dust storm is identified from the difference images by using Bayesian maximum likelihood classification.

At last, the Kappa analysis is used to evaluate our classification results compared with the visual interpretation. An initial comparison shows that our algorithm offers the potential to perform dust identification in desert region by time-series MODIS data. Results also indicate that the Bayesian maximum likelihood classifier based on time series MODIS data can provide improved dust classification performance.

8181-46, Poster Session

Land use/land cover changes and flooding surface estimation in Alqueva (Portugal) using 18 years of Landsat data

A. C. Teodoro, S. Rios, D. Ferreira, Univ. do Porto (Portugal)

Large dam construction in water deficient areas is a management decision often controversial. Alqueva dam was projected for the gorge of Guadiana River (Portugal). Its construction (1998-2000), resulted in the creation of the Europe's largest artificial lake with a flooding surface of 25,000 ha. Alqueva dam project includes a massive irrigation system across all southern Portugal, with irreversible changes in landscape and agricultural conversion. Landsat imagery can be used for detecting terrestrial land cover conditions, and tracking land vegetation, agricultural activity, urban growth, and surface hydrology and proved to be valuable in qualitative and quantitative terrestrial land cover changes.

In this work, 18 years of Landsat data, covering the period before dam construction (before 1998), during dam construction (1999-2001) and after floodgates of the Algueva dam were closed (February 2002) were used to estimate land use/land cover changes. The land use/ land cover rates and flooding surface estimation were based on image classification algorithms (pixel based and object-oriented approaches). In this study, we used one Landsat TM image from 1992 and eight Landsat ETM+ images between 2001 and 2010. The Landsat images (path 203; row 33) are all from April and were already geometrically corrected (UTM projection zone 29N and WGS84 datum). The image normalization process aims to remove radiometric differences between multitemporal images that are due to nonsurface factors. Linear regression using temporally invariant targets is a widely accepted method for normalization and was adopted in this work. After, a pixel based and objected-oriented approaches were employed in order to identify land cover classes and to estimate the flooding surface. Our classification schema comprises several land-use classes representing the dominant land cover types in the study area. The selection of landuse classes is based on the CORINE land cover nomenclature. Before classification, the spectral characteristics of each land cover class were explored.

In the pixel-based classification three supervised classification algorithms (parallelepiped, minimum distance and maximum likelihood) were applied to the dataset. In the object-oriented approach, we explored different algorithms (e.g., ClaTex) available in the open source software SPRING 5.1 (Camara et al., 1996). The performance of the algorithms employed was evaluated analysing the overall accuracy and the Kappa statistics. The classification algorithm presents a very good performance, demonstrated by the results of the overall accuracy and Kappa statistics (mostly higher than 95% and 0.95, respectively), for both approaches. The estimation of the flooding surface was also very accurate and is in agreement with the local authorities values published.

Lastly, land cover/land use maps were produced. GIS techniques were also used to quantify the land/use change rates and to compute the flooding surface increase.

The land cover and change detection information may help to explain local environmental modifications. This information is a critical requirement for the design and implementation of efficient and sustainable water resource management plans.

Camara G, Souza RCM, Freitas U M, Garrido, 1996, SPRING: Integrating remote sensing and GIS by object-oriented data modelling. J Computers & Graphics, 20: (3), pp. 395-403.

8181-47, Poster Session

Empirical model for salinity assessment on lacustrine and coastal waters by remote sensing

G. Bitelli, P. V. Curzi, E. Dinelli, E. Mandanici, Univ. degli Studi di Bologna (Italy)

The assessment of surface water salinity is a long standing feature request for water quality assessment by remote sensing. The recent Aquarius mission by NASA enables the assessment of ocean surface salinity on a global scale, based on the emission measurement in the microwave region. Unfortunately, the very coarse spatial resolution makes this approach unsuitable for inland water monitoring. The aim of the present work is to test an empirical method for surface water salinity retrieval by means of multispectral satellite images at medium resolution (30 m).

For this purpose, two case studies were selected. The first is lake Qarun, within the Fayyum Oasis (Egypt), a closed basin which is mainly fed by the discharge of an artificially regulated irrigation network. This very shallow lake is set in a hyper-arid environment and it suffers strong salinization and pollution problems, largely but not exclusively due to human pressure. The second case study is an on-shore tract of central Adriatic Sea, located between the mouths of Tronto and Salinello rivers (Italy). The Adriatic is a shallow epicontinental sea, which is characterized by a higher salinity (38) than the ocean average (34), despite it receives large quantities of fresh water. The selected case studies show some degrees of similarity, in the fact that they exhibit analogue total salinity values and both suffer nutrient pollution, causing widespread eutrophication phenomena.

For the experimentation, the ALI (Advanced Land Imager) imagery was acquired over Lake Qarun, while Landsat ETM imagery was used for the Adratic coast. Field data were acquired at both sites by means of in situ conductivity measurements, for calibration purpose. The model applied to convert atmospherically corrected reflectance value in practical salinity units (PSU) has been developed analysing the correlation between field data and an expressly defined salinity index, which involves three IR bands. First results show a promising overall correlation (R2 = 0.85), even if some difficulties arise for the inadequate radiometric resolution of Landsat data and for the striping effects on ALI images.

Further work and new data collection are in progress to provide a better validation of the obtained surface salinity maps and to produce also chlorophyll-a concentration maps on the same sites, which may assist the water quality monitoring process.

8181-48, Poster Session

Modeling of temporal-spatial dynamics of sediment supply in farms of a watershed, considering the annual variability of surface runoff

L. H. Pereira, S. dos Anjos Ferreira Pinto, Univ. Estadual Paulista (Brazil)

Adopting the watershed as a natural unit for territorial planning, one should consider wich in it is contained farms with different land uses and management technics, which may hamper the adoption of conservation practices appropriate for their integrated management, beyond intensify the erosive process. In this context, this paper had a goal to realise the modeling dynamics of sediment supply on farms based on temporal variability of surface runoff of rainwater, including the main inducers physical and anthropic laminar erosion, and also indicate priority areas for intervention erosion control along in a hydrological year. In methodological terms, this paper has developed based on systemic approach, in accord with a Modified Universal Soil Loss Equation (MUSLE). Initially, was structured an analytical segment, represented by the survey, treatment and description of the antropics parameters (C, P and mesh land) and physical environment parameters (L, S, K and Runoff) included in the equation. Owing to scale of detail (1:10000) used in this study, the antropics factors were extracted from remote sensing products with the aid of field survey, using colored aerial photography to determine the division between



farms and observation of land conservation practices (P), and support of satellite images (Alos, 10m, and CBERS-2b, 20m) for data acquisition of land use and landcover (C) over the years, including classifying the phenological development of crops. Aiming more accurate results of runoff, special attention was given to the calculation of slope length (L factor), obtained from the proposed Desmet and Govers (1996) for being a model capable of representing complex hillslope. Finally, we determined the values of runoff, whose acquisition depends indirectly of information as extension of hillslope, slope, landcover and use, crops management and soil characteristics, contemplated in Qrunoff and Qp (peak flow). The temporal variability of rainfall was determined by the historical average maximum observed for each month (Im). Each parameter, expressed as numerical models of the terrain, were integrated and analyzed in a GIS environment, in according to the logic of the model MUSLE. The results indicated that the relative loss of soil by farms is dynamic in time and space, being necessary to redirect every trimester approximately, the priority areas for intervention to the control erosion. The assessment of thematic products generated indicated that the variation of runoff does not present, for the same glebe, a linear constant over the months, contributing to the variability of soil loss between farms over year.

8181-49, Poster Session

Detection of ancient Egyptian archaeological sites using satellite remote sensing and digital image processing

R. Corrie, J. Baines, G. Lock, Univ. of Oxford (United Kingdom)

Satellite remote sensing and digital image processing are playing increasingly important roles in the detection and documentation of archaeological sites. Surveying an area from the ground using traditional methods often presents challenges due to the time and costs involved. In contrast, the multispectral synoptic approach afforded by the satellite sensor allows for the coverage of much larger areas in greater spectral detail and in a much more cost effective manner. This is especially the case when larger scale regional surveys are considered and these help to contribute to our understanding of ancient Egyptian settlement patterns. To date little work has been carried out on the design and development of methodologies and algorithms for archaeological site detection using optical and radar data obtained from orbit. This study presents an overview of remote sensing methodologies, data products, and image processing techniques for detecting lost or undiscovered archaeological sites in Egypt using satellite based remote sensing, exploiting channels in the optical, thermal, and microwave regions of the electromagnetic spectrum. A region in the western part of the Nile Delta was selected due to the large number of archaeological sites present. Spectral signatures were extracted from the imagery to differentiate ancient from modern building materials helping to define a more accurate method for archaeological feature classification and extraction. Results from the image processing were compared to the known archaeological base maps. Results from the imagery analysis correlate well with the known archaeology from the available maps. Imagery from a wide variety of sensors are examined including the Landsat Enhanced Thematic Mapper (ETM+), Advanced Thermal Emission and Reflection Radiometer (ASTER), declassified high resolution Corona imagery, and the Japanese PALSAR L-band imaging radar. Due to its increased spectral capabilities, especially in the shortwave infrared (SWIR) and thermal infrared (TIR), ASTER data was chosen as the data type of choice. Digital image processing techniques were applied to the imagery for enhancement purposes. These included simple band combinations and ratios, edge detection, unsupervised and supervised classification, log residuals, principal components analysis (PCA), decorrelation stretching (d-stretch), and radar analysis. The approach presented here is valid for any remote sensing study for archaeological site detection using multispectral imagery where an arid to semi-arid desert type environment is encountered.

8181-50, Poster Session

Sub-pixel method for analysis of optical data in determining the overburden dumps and open pit mines

D. Borisova, H. N. Nikolov, D. Petkov, Solar-Terrestrial Influences Lab. (Bulgaria); B. Banushev, Univ. of Mining and Geology (Bulgaria)

Mining plants are one of the factors having major negative impact on the area where they are situated. In our study this is the case of Mirkovo floatation plant, located in the outskirts of Stara Planina Mountain in the middle of Bulgaria. Delineation of overburden dumps and open pit mines by means of remotely sensed multispectral data with moderate spatial resolution (e.g. Landsat TM/ETM+ 30m) is a challenging task. The major difficulties begin from: 1) large period using the dump (introducing multitemporality); 2) the unknown proportions of vegetation, soil and embedding rock samples in the boundary areas; 3) relatively restricted access to places of interest. A variety of methods have been proposed to overcome the problems with pixels corresponding to 2 or more endmembers, but a promising one is the soft classification which assign single pixel to several land cover classes in proportion to the area of the pixel that each class covers. In this scenario for every pixel of the data the correct proportion of the end-members should be found and then co-registered with the corresponding original pixel. As a result this sub-pixel classification procedure generates a number of fraction images equal to the number of land cover classes (end-members). The sub-pixel mapping algorithms we have exploited so far have one property in common: accuracy assessment of sub-pixel mapping algorithms is impossible because of missing high resolution ground truth data. In this case one possible solution is to exploit additional ex-situ and in-situ measured data from field and laboratory spectrometers with bandwidth about 1 nm. This study presents a successful implementation of soft classification method with additional, precise spectrometric data for determination of dump area of the copper plant and open ore mine. The results are used for proving the in-situ gathered data and coincidence of 93.5% was achieved. The main advantage of the presented technique is that mixed pixels are used during the training phase. Compared to these other techniques, the present one is simple, cheap and objective. The results of the sub-pixel mapping exercise indicate that the technique can be useful to increase the resolution while keeping the classification accuracy high.

8181-52, Poster Session

Based on MODIS NDVI data to monitor the growing season of the deciduous forest in Beijing, China

K. Xu, X. Zhang, B. Chen, K. Hua, K. Zheng, T. Wu, Beijing Forestry Univ. (China)

Phenology is the important indicator of reflecting climate and environment change. Development of remote sensing provides a new method for mapping phenology. Normalized difference Vegetation Index (NDVI) derived from the Moderate Resolution Imaging Spectroradiometer (MODIS) is a key indicator to vegetation monitoring and phenology analysis. This paper uses time-series of MODIS NDVI 16 days vegetation indices of 250 meters, making use of Logistic model, extracting deciduous forest phenology of Beijing area. The results show that in most of Beijing area, trees growing begins between 115th and 120th day, but at downtown, trees growing season in most parts of trees is mainly between 110th and 140th day, but at downtown, growing season is 30 days longer than that in the mountain. Compared the results with phenology field observation, the results have a certain reliability.



8181-52, Poster Session

Generation of thematic maps using KOMPSAT-2 image data

K. Lee, Y. Kim, Korea Aerospace Research Institute (Korea, Republic of)

Earth Observation Satellite (EOS) with the very high resolution has been used for various civil applications. Especially, the mapping with the high resolution satellite image instead of aerial images is one of the most important applications in the field of remote sensing. The generation of high resolution imagery using previouslyproven defence technology provides an interesting source of data for digital topographic mapping as well as thematic applications such as agriculture, forestry, and emergency response. Traditionally, topographic maps have been created with analytical stereo plotters that can digitize the surface features and extract the elevation profiles manually from stereo aerial photograph pairs. Recently, with advancing technology, the Digital Photogrammetric Workstation (DPW) based on the high resolution satellite image is a relatively new technology that is currently being utilized by a cartographer with regard to the topographic mapping, land-use/cover mapping, and etc.

The second KOrea Multi-Purpose SATellite (KOMPSAT-2), which was successfully launched on July 28, 2006, has a capability to provide the pass-stereo images with 1m panchromatic image and 4m multi-spectral image from two different orbits. So it can be possible to use the topographic mapping as well as the thematic applications.

The purpose of this study is to investigate the possibility for generating the thematic maps such as digital map, ortho-rectified image, and DEM using the KOMPSAT-2 stereo images. The regulations with the related the mapping are defined by The National Geographic Information Institute (NGII) in Korea, with the consequence that mapping test using the KOMPSAT-2 stereo images should be performed under the related regulations.

The study areas were Daejeon, Damyang, and Pohang which are located in the middle, southern and eastern part of South Korea, respectively. Topographical characteristics of these areas are somewhat different. Daejeon is one of the metropolitan cities in Korea. Damyang, by contrast, is located in rural area. Pohang is a port city.

The requirement of GCP accuracy in this study is very strict for evaluating the mapping accuracy of KOMPSAT-2 stereo images. In order to use a control point and check point, 18 points were surveyed by Differential Accuracy of Global Positioning System (DGPS). An accuracy of GPS survey result is less than 5cm (CE90). The image coordinate accuracy is about one-third less than original pixel resolution. Bi-cubic interpolation resampling method in the ERDAS SW was used to extract directly a precise point from the KOMPSAT-2 PAN image. In this study, the function of Rational Function Refinement in the ERDAS LPS was utilized for determining a three-dimensional ground coordinates. The 1st order polynomial equation was used for the refinement. The results represent that the Root Mean Square Error (RMSE) of sensor modeling with control points and check points was less than 1m. However, vertical error in Damyang area was a little bit high than 1m.

In conclusion, the requirements of sensor modelling and digital stereo plotting for the scale of 1/5,000 were satisfied with the NGII's regulations. The accuracy of ortho-rectified image and extracted DEM was also less than the requirement of the NGII's regulations for the scale of 1/5,000. However, by interpretative measures, we realized that it is difficult to extract all layers which are needed to generate the digital map of 1/5,000 scale. Nevertheless, the results indicated that the KOMPSAT-2 would have a high potential for the mapping the new thematic map and improving the existing thematic map.

8181-53, Poster Session

Air pollution detection using MODIS data

J. Harbula, Palack? Univ. Olomouc (Czech Republic); V. Kopacková, Czech Geological Survey (Czech Republic)

The air quality and the quality of the environment has a great impact on public health. One of the most important negative indicators of environmental quality is environmental air purity, in which the individual occurs daily. The bad air quality influences very strongly the respiratory tract above all and it causes respiratory diseases. Particular matters smaller than 10 mirometters (PM10) in particle diameter are one of the most dangerous pollutants, which get to the lower respiratory tract and can cause serious health complications. In addition, people living in the areas influenced by surface coal mining are in much higher risk of these diseases. During mining gets into the air a lot of fine coal dust particles and health is more influenced.

Obtaining the air pollutant concentration values is limited by the number of ground measuring stations and their spatial location. Their network is often very sporadic and estimated or modeled situation of air quality can be highly inaccurate and unreliable on large scales, especially in areas without these stations. Therefore it is necessary to seek other sources of data to obtain air pollution. Images and data created by remote sensing methods can be one of these sources. Satellite and aerial multi-spectral data contain information about aerosol optical thickness values, for which there is evidence of correlation on the concentration of air pollution. Derivation of this correlation leads to the possibility of obtaining more accurate and better data about air pollution in areas where data from the ground measuring stations do not exist. To derive regression of the concentration of PM10 particles on the value of aerosol optical thickness MODIS satellite imagery, product MOD04, Level 2, and data from ground measuring stations were used. The study area was the Sokolov basin region.

Linear regression was found between measured concentrations of particular matter PM10 and detected aerosol optical thickness values. Time series show a same trend by both measured real data and detected data by remote sensing methods during time. Angstrom exponent values corresponding to the size of particular matter to 10 μ m were determined. Data from various type of measuring stations show different results of relationship retrieving between PM10 concentration from measured data and aerosol optical thickness from remote sensing imagery.

8181-54, Poster Session

An object-based multisensoral approach for the derivation of urban land use structures in the city of Rostock, Germany

M. Lindner, S. Hese, C. Berger, C. C. Schmullius, Friedrich-Schiller-Univ. Jena (Germany)

The present work is part of the Enviland-2 research project, which investigates the synergism between Radar- and optical satellite data for ENVIronment and LAND use applications. The urban work package of Enviland aims at the combined analysis of RapidEye and TerraSAR-X data for the parameterization of different urban land use structures.

This study focuses on the development of a transferable, objectbased rule set for the derivation of urban land use structures at block level. The data base consists of RapidEye and TerraSAR-X imagery, as well as height information of a LiDAR nDSM (normalized Digital Surface Model) and object boundaries of ATKIS (Official Topographic Cartographic Information System) vector data for a study area in the city of Rostock, Germany.

The classification of various land cover units forms the basis of the analysis. Therefore, an object-based land cover classification is implemented that uses feature level fusion to combine the information of all available input data. Besides spectral values also shape and context features are employed to characterize and extract specific land cover objects as indicators for the prevalent land use. The different land use structures are then determined by typical combinations and constellations of the extracted land use indicators and land cover proportions. Accuracy assessment is done by utilizing the available ATKIS information.

From this analysis the land use structure classes residential, industrial/ commercial, other built-up, allotments, sports facility, forest, grassland, other green spaces, squares/parking areas and water are distinguished with an overall accuracy of 63.2 %. Concerning the reference high classification accuracies of over 80 % are observed for residential, industrial/commercial, allotments, forest and water (producer accuracy). However residential, industrial/commercial and forest are distinctly overestimated in the classification result (user accuracy).



Most of these classification errors are due to the lack of appropriate land cover features to sufficiently describe the land use structure class other built-up.

8181-55, Poster Session

Analysis of cultivated land change by remote sensing data in Huangshui River watershed, northwestern China

X. Gao, S. Feng, J. Xie, J. Li, Qinghai Normal Univ. (China)

The Huangshui River Basin is located in a transitional zone between the Loess Plateau and Qinghai-Tibetan Plateau in northwest China. Rapid urbanization has resulted in loss of a large mount of cultivated land in valley region; at the same time, vast cultivated land which located in hilly-gully region and mountain region was returned back into forest land and grassland because of Grain-for-Green Policy since 1999. The objective of this study is to analyze and identify the spatial and temporal patterns of cultivated land in the Huangshui River watershed. Land use maps were derived from visual interpretation of Landsat TM images in 1996 and 2007, and transition matrix was obtained by overlaying two land use maps. Our results indicated that in 1996, the total cultivated land in the Huangshui River watershed was 255436.34ha whereas in 2007 it dropped to 229432.96 ha, with a net loss of 56550.86ha. Specially, during 1996-2007, the irrigated land in valley region decreased from 103608.94 ha to 97609.76 ha with a net loss of 5999.18ha, whereas built-up land increased by 5463ha mainly from the conversion of cultivated land. In hilly and gully region and mountain region, dry farmland rapidly decreased from 279938.33 ha and 157162.74ha in 1996 to 248090.48 and 138458.91ha in 2007, with a net decease of 31847.85ha and 18703.83ha, respectively. The decrease in cultivated land in hilly-gully region and mountain region was mainly converted to forest land and grassland. Our analysis suggested that the growth of population, rapid urbanization, economic development and land use policies are the primary driving forces of cultivated land change.

8181-56, Poster Session

Estimation of Leaf Area Index (LAI) using IRS-LISSIII Satellite data (Case study: Neishaboor plain, Iran)

A. Farid, A. Astaraei, S. H. Sanaei-Nejad, P. Mirhossieni Moosavi, Ferdowsi Univ. of Mashhad (Iran, Islamic Republic of)

Estimation of forest structural attributes, such as the Leaf Area Index (LAI), is an important step in identifying the amount of water use in forest areas. The goal of this study is to investigate the feasibility of using IRS LISS-III data to retrieve LAI. To get a LAI retrieval model based on reflectance and vegetation index, detailed field data were collected in the study area of eastern Iran. In this study, atmospheric corrected IRS LISS-III imagery was used to calculate Normalized Difference Vegetation Index (NDVI). Data of 50 samples of LAI were measured by Sun Scan System - SS1 in the study area. In situ measurements of LAI were related to widely use spectral vegetation indices (NDVI). The best model through analyzing the results was LAI = 19.305×NDVI+5.514 using the method of linear-regression analysis. The results showed that the correlation coefficient R2 was 0.534 and RMSE was 0.67. Thereby, suggesting that, when using remote sensing NDVI for LAI estimation, not only is the choice of NDVI of importance but also prior knowledge of plant architecture and soil background. Hence, some kind of landscape stratification is required before using multi- spectral imagery for large-scale mapping of vegetation biophysical variables.

8181-57, Poster Session

Object-based detection of LUCC with special regard to agricultural abandonment on Tenerife (Canary Islands)

S. Günthert, A. Siegmund, U. Michel, H. Thunig, Pädagogische Hochschule Heidelberg (Germany)

Since the beginning of the Spanish colonialism, the island Tenerife has always been used for intensive, mainly export-oriented agriculture, whereby the natural landscape was continuously altered. Especially mountainous areas with suitable climate conditions have been drastically transformed for agricultural use by building of large terraces to get flat surfaces. In recent decades political and economic developments on Tenerife lead to a transformation process (especially inducted by an expansive tourism), which caused concentrationand intensification-tendencies of agricultural land use in specific areas as well as agricultural set-aside and rural exodus. Due to these modifications in the economic sector the changes in land use and land cover increased. The trend leads recently to a spatial concentration of the population and settlements near to the coasts and increasing agricultural fallow land in higher and backward areas. This formerly cultivated land can generally be seen as major factor influencing natural reforestation and renaturation. It provides potential space where adjacent ecosystems can spread and hence a natural regeneration can come into effect.

In order to get information about the LULC patterns and especially the agricultural abandonment on Tenerife, a multi-scale, knowledgebased classification procedure for recent RapidEye data was developed with a main focus on the exact differentiation of the main ecosystems and their subsystems as well as settlements, different forms of agriculture and fallow land. Furthermore, a second detection technique was generated, which allows an exact identification of older agricultural fallow land or agricultural set-aside with a higher level of natural succession, under the assumption that long-term fallow areas can mainly be detected together with old agricultural terraces and its specific linear texture. These areas can hardly be acquired in the used satellite imagery. The method consists of an automatic texture-oriented detection and area-wide extraction of linear terraces structures in current orthophoto images of Tenerife. By integrating the outcome of the terrace detection algorithm into the existing LULC classification procedure, the total ever utilised agricultural area can be acquired. Within that zone potential resettlement trends on formerly abandoned agricultural land though the different adjacent ecosystems like pinewood (Pinar) and laurel forest (Laurisilva), as well as different influencing factors for renaturation will be identified.

8181-58, Poster Session

Object-based change detection: dimension of damage in residential areas of Abu Suruj, Sudan

T. Demharter, U. Michel, Pädagogische Hochschule Heidelberg (Germany); M. Ehlers, Univ. Osnabrück (Germany); P. Reinartz, Deutsches Zentrum für Luft- und Raumfahrt e.V. (Germany)

Object-based Change Detection: Dimension of damage in residential areas of Abu Suruj, Sudan.

Abstract

Given the importance of Change Detection, especially in the field of crisis management, this paper discusses the advantage of objectbased Change Detection. This project and the used methods give an opportunity to coordinate relief actions strategically. The principal objective of this project was to develop an algorithm which allows to detect rapidly damaged and de-stroyed buildings in the area of Abu Suruj. This Sudanese village is located in West-Darfur and has become the victim of civil war. The software eCognition Developer was used to per-form an object-based Change Detection on two panchromatic Quickbird images from two different time slots. The first image shows the area before, the second image shows the area after the massacres in this area. Seeking a classification for the huts of the Sudanese town Abu Suruj was reached by first segmenting the huts and then classifying them on the basis of geo-metrical and brightness-related



values. The huts were classified as "new", "destroyed" and "preserved" with the help of a self-developed algorithm. Finally the results were presented in the form of a map which displays the different conditions of the huts. The accuracy of the project is validated by an accuracy assessment resulting in an Overall Classification Accuracy of 90.50 percent. These change detection results allow aid organizations to provide quick and efficient help where it is needed the most.

8181-59, Poster Session

Development of a satellite-based multiscale land use classification system for land and water management in Uzbekistan and Kazakhstan

F. Löw, C. Conrad, Julius-Maximilians-Univ. Würzburg (Germany); S. W. Dech, Deutsches Zentrum für Luft- und Raumfahrt e.V. (Germany); U. Michel, Pädagogische Hochschule Heidelberg (Germany)

Satellite remote sensing is an invaluable tool to assess the status and changes of agricultural systems and to assure food security. Agricultural sites are among the most heterogeneous sites at the landscape level: spatial pattern of agricultural fields, within-field heterogeneity, crop phenology and crop management practices vary significantly. Highly dynamic objects (crops and crop rotations) result in large temporal variability of surface spatial heterogeneity. Technological advances have opened the possibility to monitor agricultural sites combining satellite images with both high spatial resolution and high revisit frequency, which could overcome these constraints. Yet depending on the field sizes and crop phenologies of the agricultural system observed, requisites in terms of the instrument's spatial resolution and optimal timing of crop observation will be different.

The overall goal is to quantitatively define region specific satellite observation support requirements in order to perform land use classification at the field basis. The main aspect studied here is the influence of spatial resolution on the accuracy of land use classification over a variety of different agricultural landscapes. This will guide in identifying an appropriate spatial resolution and input parameters for classification. The study will be performed over locations in irrigated agro-ecosystems in Central Asia, where reliable information on agricultural crops and crop rotations is needed for sustainable land and water management. Geostatistics were used to quantify the differences in spatial structure across the studied agricultural landscapes. Experimental variograms were computed for the NDVI over distinct sites in Karakalpakstan, Uzbekistan and Kyzl-Orda, Kazakhstan. First results show large differences in spatial heterogeneity, field size and pattern and indicate different needs for satellite observation support in terms of spatial resolution. A comprehensive set of features will be derived from geostatistical measures, in particular the variogram, and texture measures at the field basis in order to perform object oriented image classification. Emphasize is put on quantitatively analyzing the effect of increasingly coarser pixel size using simulated images on the performance and robustness of these features. Basis for the simulations will be a data set consisting of multitemporal RapidEye, Landsat, and SPOT data.

8181-60, Poster Session

Improvement of the spatial resolution of MODIS coastal waters thermal mapping

S. Teggi, F. Despini, M. Serafini, Univ. degli Studi di Modena e Reggio Emilia (Italy)

Thermal mapping of water bodies is an highly relevant tool for the study of thermal pollution, an issue to which increasing attention is paid.

Spaceborne and airborne remote sensing play a key role in monitoring the thermal pollution of water bodies, since it allows to monitor in near real time large water surfaces. The remote sensing of surface water temperature using measurements of emitted thermal-infrared (TIR) radiation can provide spatially distributed values of radiant temperature in the skin layer (top 100 μ m). of the water . The main limiting

factor of remotely sensed data is the spatial resolution. Airborne sensors acquire images at high spatial resolution nevertheless their employment is limited by cost and organization of airborne campaigns. Satellite images have been used extensively to estimate sea surface temperatures (SST), but streams, small lakes and coastal areas are often not resolved at the spatial resolution of TIR imagery.

MODIS satellite sensor offers 16 bands in the thermal infrared with a spatial resolution of 1 km. MODIS images are available multiple times per day at any given location and are distributed free of charge. These features make the MODIS sensor an useful tool for the monitoring of large water surfaces, but the spatial resolution does not allow an accurate study of coastal areas.

In this work it is shown the spatial improvement of MODIS thermal imagery on coastal water obtained with the SWTI (Sharpening Water Thermal Imagery) algorithm.

SWTI is applied to two MODIS images, acquired on the lagoon of Venice and on the delta of the Po River. The spatial resolution of the images is improved from 1 km to 250 m using information from the MODIS VNIR bands.

The performances of the algorithm have been evaluated using as a reference a couple of ASTER images acquired simultaneously to the MODIS images and on the same areas. This analysis mainly consisted in the comparison of the temperature of costal waters retrieved from the ASTER images and these computed by SWTI. The root mean square errors computed excluding outliers (< 5% of the cases) are lower than 1.5 K that can be considered satisfactory when compared with the ASTER and MODIS temperature accuracies.

Moreover, to reinforce the effectiveness of the spatial improvement produced by SWTI, the reference ASTER images have been also compared with the coastal waters temperature maps obtained by simple bilinear interpolation of the MODIS images.

8181-61, Poster Session

A oceanic satellite data service system based on web

Y. Kang, D. Pan, X. He, D. Wang, J. Chen, X. Chen, The Second Institute of Oceanography, SOA (China)

The ocean satellite observation is more and more important to study the global change, protect ocean resource and implement ocean engineering for their large area cover and high frequency observation, which have already given us a global view of ocean environment parameters, including the sea surface temperature, ocean color, wind, wave, sea level and sea ice, etc.. China has made great progress in ocean environment remote sensing over the last couple of years. The successful launching of the Shenzhou spacecraft series (SZ series), the ocean satellite series Hai Yang-1 (HY-1 series) is the concrete witness of such progress. The State Key Laboratory of Satellite Ocean Environment Dynamics (SOED) of the Second Institute of Oceanography (SIO) produces the ocean color and temperature data products, which include sea surface temperature (SST), chlorophyll concentration (CHL), suspended sediment concentration (SSC), water transparency (SDD), diffuse attenuation coefficient at 490nm (KD3), normalized water-leaving radiance at 490nm (LW3) and aerosol optical thickness at 865nm (TAU), etc.. We involve the grid data files (Level-3B) and the contour files (Level-4A) of these data products in this paper. Level-3B data which have the spatial resolution of 1.825km and Level-4A range from 14°N to 42°N for latitude, and from 105°E to 130°E for longitude. These data are widely used for a variety of applications in ocean environment studies, coastal water quality monitoring environmental, fishery resources protection, development and utilization of fishery resources, coastal engineering and oceanography. But the data are no online information access and dissemination, no online visualization & browsing, no online query and analyze capability. To facilitate the application of the data and to help disseminating the data, a web-service system has developed. The system provides capabilities of online oceanic satellite information access, query, visualize and analyze. It disseminates oceanic satellite data to the users via real time retrieval, processing and publishing through standards-based geospatial web services. A region of interest can also be exported directly to Google Earth for displaying or downloaded. This web service system greatly improves accessibility, interoperability, usability, and visualization of oceanic satellite data without any clientside software installation.

8181-62, Poster Session

Research trend analysis of Qinghai-Tibet Plateau based on the spatial information mining from scientific literature

X. Wang, M. Ma, Cold and Arid Regions Environmental and Engineering Research Institute (China)

The global climatic change due to the increasing CO2 concentration and temperature is noticeable in the worldwide range. A lot of climate indicators indicate a warming of our earth. Average temperatures are 0.4 to 0.8 °C higher than a century ago (Hansen et al., 1997; Konstantin et al., 2003). The Qinghai-Tibet Plateau is so important for research of global climatic change, which is considered as one of the drivers and ampilfers of the global climatic change (Pan et al., 1996). Therefore, the researches on the Qinghai-Tibet Plateau have been a hotspot of geosciences for several decades. A lot of papers were published in these research field. The regular methods of Bibliometrics mainly include information gathering, publication enumeration and statistical analysis. Normally the research status and trends could be quantificationally analyzed based on Bibliometrics methods (Nourbala et al., 2008).

The subject intersection becomes one of the hot research topics recently. Wang et al. (2009) had ever analyzed the spatial information of the author's countries. The spatial distribution was presented by the format of maps based on the GIS technologies. This paper tried to couple the Bibliometrics and Geographical Information System (GIS) technologies for studying on the spatial information mining and visualization for the Qinghai-Tibet Plateau's literature.

The literature is mainly research papers indexed from the Science Citation Index Expanded (SCIE) and Chinese Science Citation Database (CSCD) database. The spatial information was extracted from these research papers by manual work, which mainly include study areas, sampling points, frozen boreholes, and so on. The time information is also collected for each spatial element. Figure 1 shows partial sampling points extracted from CSCD database's research papers. The distribution characteristics indicate that most of the field investigation works are performed mainly in east Tibet and south Tibet. They are mainly distributed along the Qinghai-Tibet Highway (from Xining to Lhasa), Sichuan-Tibet Highway (from Chengdu to Lhasa), and Qing Kang Highway Road (from Xining to Mangkang). It is chiefly because most of the regions in Qinghai-Tibet Plateau are no mans land and have poor transport facilities. The other reason is because a lot of studies focus on these important construction projects. The time dimension information can also be considered in this analysis. The investigation regions changing with time can reveal the research trends of hotspot study areas and fields. The geostatistical method is also used to analysis the spatial variability of the investigation points. As a result, this paper aims to afford some reference information for the researchers who are interesting in Qinghai-Tibet Plateau.

8181-63, Poster Session

Image fusion to extract land use information from moderate resolution image

H. Lu, G. Liu, Henan Univ. (China)

Image fusion is a popular method to integrate different sensors data for obtaining a more suitable image for a variety of applications, such as visual interpretation, image classification, etc. Thus, the merged image provides faster interpretation, and can help in extracting more features. The resulting merged image is a product that synergistically integrates the information provided by various sensors or by the same sensor. Various image fusion techniques are available in published literature.

The most significant problem for image fusion is color distortion. This problem could lead to poor accuracy in image classification. For example, a particular vegetation type may have a consistent spectral signature in the original, unfused image. However, due to color distortion in the fusion process, such type may have several different spectral signatures in the fused image. So the impact of color distortion from different data fusion methods on classification accuracy was an imperative question that cannot be ignored. In this paper, a comparative study was conducted on image fusion methods based on



moderate resolution images of MODIS and TM data. First land types of forest, paddy field, dry land, water and building was selected through field survey. Then supervised classification and non-supervised classification were used upon original image and two fusion images (PCA and IHS) respectively. Finally Land change area, change rate and classification accuracy were calculated and impact of color distortion from different data fusion methods on classification accuracy was presented.

The result showed:

(1) Only one sensor data from MODIS or TM does not work well in extracting land use information because of the limitation of spatial resolution or spectral information. Compared with the single TM or MODIS image, the fusion result can preserve the color information from multispectral image and the spatial details of TM. Residential texture, water, the relative position between roads, industrial and dry land, etc, was identified easily.

(2) Effects from IHS and PCA technique were different. IHS method improves feature identification without significant distortion of color, which is quite useful for classification purposes. On the contrast PCA image has abundance spatial information but with big color distortion. There were less phenomena of "same object with different spectral and same spectral with different object" on HIS image. This proves HIS technique to be an excellent tool for distinguishing the small spectral differences on the image. Selected samples on the IHS image showed a 91.69% Kappa value.

8181-64, Poster Session

Modelling the backscattering coefficient of salt-affected soils using AIEM model

Y. Wu, W. Wang, Cold and Arid Regions Environmental and Engineering Research Institute (China)

One of the most principal environmental problem affecting developing countries is soil salinity, especially in arid and semi-arid regions, where precipitations are insufficient to drain the soluble salts contained in the soil profile. Soil salinity also influences soil properties and cause land degradation and the reduction of productivity of agricultural areas. Its detection can use radar imaging system to distinguish from non-affected saline soils based on their dielectric properties.

Currently, no inversion algorithms exist for directly determining soil salinity from microwave remote sensing data. However, a number of soil moisture inversion algorithms have been developed and applied over the last two decades. The theory of soil moisture measurement is based on large difference in dielectric constant between dry soil and water. As the water content of a dry soil increase the dielectric constant rises consequently, which directly affects the backscattering coefficient. The dielectric constant is comprised of the permittivity or real part and the loss factor or imaginary part. The presence of soluble salt in the soil solution also has a direct effect on the value of the dielectric constant. When comparing the complex dielectric constant of pure water with saline (sea) water (≈49.69), minimal difference in the real part, but significant difference in the imaginary part is observed less than 7GHz. In contrast to the non-affected soils, the imaginary part of the dielectric constant of affected wet soils is higher than or comparable to the real part. Studies that evaluate the relationship between dielectric constant, soil salinity and the backscattering coefficient are rare, but we can draw on the soil moisture retrieval algorithms to retrieve soil salinity, which emphasize the imaginary part of dielectric constant.

Considering the complexity of the relationship among soil moisture, soil salinity, backscattering coefficient and dielectric constant, we plan to simulate this relation and the salinity effect on the backscattering coefficient of soils using theoretical model: AIEM. So, we can offer some scientific basin for retrieving soil salinity content using microwave remote sensing data. During the simulation, the properties of the studied soil will be taken account by the Dobson mixing model, and their related changes in the outputs of the models



8181-65, Poster Session

A first reference dataset for the evaluation of geometric correction methods under the scope of remote sensing applications

H. Gonçalves, A. C. Teodoro, J. A. Gonçalves, L. Corte-Real, Univ. do Porto (Portugal)

The geometric correction of images under the scope of remote sensing applications is still mostly a manual work. This time and effort consuming task is associated to an intra- and inter-operator subjectivity, beyond not bringing any scientific value to the research work.

Although several automatic image registration (AIR) methods have been proposed in the last years, there are several reasons for the lack of a wide use of any of these methods. One of the main reasons may be the lack of a proper evaluation of the different available methods, since some methods are only adequate for certain type of applications/ data.

In order to fulfil a gap in this context, we have created the first reference dataset of pairs of images comprising some types of geometric distortions, which are commonly found under the scope of remote sensing applications. Moreover, it is divided according to the Level 1 of CORINE Land Cover nomenclature (European Environment Agency). It is composed by pairs of a corrected and an uncorrected image, covering different sensors, spatial resolutions and geometric distortions. The pair of images includes areas of artificial structures (mostly urban), agricultural areas (agriculture and natural vegetation), forest and semi-natural areas and coastal wetlands. This dataset will allow for gaining perception of the abilities and limitations of some AIR methods. Some AIR methods were evaluated in this work, including the traditional correlation-based method and the SIFT approach, in order to illustrate the importance of the reference dataset.

A set of measures for an objective evaluation of the geometric correction process quality was computed for every combination of pair of images/AIR method. This was followed by a statistical analysis of the performance of each AIR method, taking into account the appropriateness of each sensor for a particular class, as well as the performance of each sensor for the several land cover classes.

The reference dataset will be available from an internet address, being expected that it becomes a channel of interaction among the remote sensing community interested in this field.

8181-66, Poster Session

Study on urban heat island of Lian Yungang based on remote sensing

H. Li, H. Peng, Huaihai Institute of Technology (China); Y. Wu, Cold and Arid Regions Environmental and Engineering Research Institute (China); J. Nie, Shouguang Modern School (China)

An area of higher temperatures in an urban setting compared to the temperatures of the suburban and rural surroundings. It appears as an 'island' in the pattern of isotherms on a surface map. With the development of Lian Yungang, the climate changes of the city have more and more drawn people's attention. Heat island is a negative effect resulted from the development of the city and an expression of urbanization. From opening to the outside world in 1984, the city is developing fast and the phenomena that city's temperature is higher than that of suburban is more obvious.

This paper aimed to study the urban heat island of Lian Yungang based on MODIS LST product and TM images. The LST were estimated from band 6 of TM images. And then compare the results derived from TM with that of MODIS, and discuss the relationship between urban heat island and its ground, vegetation, illumination and man-made features, specifically analyze the influences of these factors to urban heat island in Lianyungang.

This article classified the ground objects into 3 classes, water, vegetation and land for construction. The result showed that land for construction was the main contributor of the urban heat island effect, and that vegetation and water lessened the effect. In comparison

with four counties, the temperature and increment of temperature of Lian Yungang were always higher than them. From 2000 to 2010, the temperature range had been increasing, especially from 2005 to 2010. And the urban heat island intensity is strongest at autumn and winter, weakest at summer.

This article related the analysis results with urban sprawl and planning. The study showed that with the development and urbanization of city, urban heat island effect appeared gradually. The level of the effect was related with the speed of urbanization. In the future, the heat island effect will be increasing and influence the urban environment. Finally, we give some suggestions about heat island and building a technical system for Lianyungang's future developing.

8181-67, Poster Session

Fuzzy logic for North-Western Black Sea coastal zone land cover change quantifying

L. F. V. Zoran, C. C. Ionescu Golovanov, Polytechnical Univ. of Bucharest (Romania); M. A. Zoran, National Institute of Research & Development for Optoelectronics (Romania)

Satellite imagery offers great potential of marine coastal areas mapping, being used as an important tool for spatiotemporal dynamics assessment. Due to climate and anthropogenic -induced changes on coastal zone morphology as well as on stocks of plankton and fish, climate-sea interactions and their response on marine ecosystems have recently been focus of

considerable attention. Fuzzy theory applied for the analysis of coastal areas changes, for which each pixel on the map is assigned a membership grade in all classes, represent reasonable alternatives to traditional fixed classifications. Mixture modeling and subpixel spectral analysis is used for the percent cover of individual cover types within a pixel assessment. These

methods require a definition of spectral endmembers, which is difficult (and perhaps impossible) for complex and highly variable land cover units. Fuzzy classifications and mixture/subpixel models provide information on variations in spectral signature between pixels and not on differences in the on-the-ground content of mapped land cover. The coastal zone units are recognized on a ground truth map of an area using Landsat Thematic Mapper (TM) and Enhanced Thematic Mapper (ETM) as well as IKONOS and Quickbird imagery for North-Western Black Sea coastal zone, Romania, over 1990-2010 period.

The application of fuzzy logic to quantifying magnitudes of coastal zone land cover change is highly appealing because of its capability to deal with uncertainties such as in the case when one cannot accurately identify a threshold value to separate areas of change from areas of no-change.

Anthropogenic eutrophication coastal erosion affect the North-Western Black Sea to various extents.

The land cover/land use information, properly classified, can provide a spatially and temporally explicit view of societal and environmental attributes for Black Sea coastal area and can be an important complement to in-situ measurements.

The analysis of an ever longer time series of satellite data, and the derivation of bio-optical algorithms with sounder statistical foundations will allow the exploration of such features in more detail, and in particular the definition of their evolution in both the spatial and temporal domains.

8181-68, Poster Session

Comprehensive high-speed simulation software for ladar systems

S. Kim, S. Hwang, I. Lee, The Univ. of Seoul (Korea, Republic of)

LADAR can produce range and intensity images as well as point clouds by measuring the flight time and the return power of laser pulses being transmitted toward the targets. During the development of such a LADAR system, the system simulation is significantly important especially for the verification of the system design through the performance assessment. Difficulties in implementing an accurate

Conference 8181: Earth Resources and Environmental Remote Sensing/GIS Applications



and efficient simulator mainly originate from the need to understand multidisciplinary knowledge ranging from electronics, optics, physics, and geoinformatics in conjunction with high speed operation to generate tens of thousands of laser pulses per second. Although many researchers have attempted to develop various kinds of LADAR simulators for their own purposes, most of them have some limitations in being practically used for the general design of diverse types of LADAR system. To overcome these limitations, we thus attempt to develop high-speed simulation software that is applicable for a variety of LADAR systems.

In this comprehensive study, we analyzed the previous research works related to LADAR simulation, and employed their principles to perform the sensor modeling in various aspects. For example, as the input targets, we utilized a realistic sophisticated 3D city models in conjunction with a 3D spatial database system. We also employed sub-beam processing to generate realistic return waveforms mainly generated from the targets of complex surfaces (i.e. objects under trees). Furthermore we performed modeling of FPA (focal plane array) detectors to implement the simulation of Imaging (or Flash) LADAR that can acquire numerous points for each laser beam shot.

For the high-speed operation, we incorporated time-efficient incremental coherent ray-tracing algorithms, 3D spatial database systems for efficient spatial query, and parallel computing based CUDA with GPU. LADAR simulation executes a tremendous amount of spatial computations to search for the intersections of beams with target surfaces. This computation time can be significantly reduced using the incremental algorithms and parallel processing together with 3D spatial database.

The simulator is mainly composed of three modules: geometry, radiometry, and visualization modules. In the geometry module, the rays of laser beams are defined and then the locations, where the rays intersect with the target surfaces, are calculated. In the radiometry module, the simulator computes the powers of the return pulses and generates the waveforms. The visualization module presents, to the users, the outputs of the simulation which are 3D point cloud, range and intensity images, and waveforms.

Our simulation software could successfully generate the simulated data based on the pre-defined system parameters. The validation of simulation results is performed by comparing with the real LADAR data, and the intermediate results are promising.

We believe that the developed simulator can be widely used for various activities, for example, to introduce the principles of LADAR systems, to predict the performance of future LADAR systems, and to provide test data for the development of application algorithms.

8181-69, Poster Session

Satellite remote sensing for assessment of environment quality and impacts of nuclear power plants

M. A. Zoran, National Institute of Research & Development for Optoelectronics (Romania)

The main environmental issues affecting the broad acceptability of nuclear power plant environment are the emission of radioactive materials, the generation of radioactive waste, and the potential for nuclear accidents. All nuclear fission reactors, regardless of design, location, operator or regulator, have the potential to undergo catastrophic accidents involving loss of control of the reactor core, failure of safety systems and subsequent widespread fallout of hazardous fission products. Risk is the mathematical product of probability and consequences, so low probability and high-consequence accidents, by definition, have a high risk. NPP environment surveillance is a very important task in frame of risk assessment. Satellite remote sensing data had been applied for dosimeter levels first time for Chernobyl NPP accident in 1986. Just for a normal functioning of a nuclear power plant, multitemporal and multispectral satellite data in synergy with field data are very useful tools for NPP environment surveillance and risk

assessment. This is helpful for analysis of spatio-temporal changes of environmental features (water, near field soil, vegetation and air) nearby nuclear facilities.

The aim of this paper was to demonstrate that the combination of multisensor satellite and in situ monitoring data allows for an improved

monitoring potential, in particular for applications to nuclear power plants zone management.

As a test case the methodology was chosen Nuclear Power Plant (NPP) Cernavoda, Romania, where are in function two CANDU reactors (Unit 1 of 705.6 MW of electricity - is operating starting from 1996 year and Unit 2 of 706MW is operating starting from 2007 year). Such analysis have been done based on LANDSAT TM, LANDSAT ETM, MODIS and QuickBird data acquired during 1989 -2009 period in synergy with in-situ data. Thermal discharge from nuclear reactors cooling is dissipated as waste heat in Danube-Black -Sea Canal and Danube River. Water temperatures captured in thermal IR imagery have been correlated with meteorological parameters. If during the winter thermal plume is localized to an area of a few km of NPP, the temperature difference between the plume and non-plume areas being about 1.5 oC, during summer and fall, is a larger thermal plume up to 5-6 km far along Danube Black Sea Canal ,the temperature change is about 1.0 oC. A variety of biogeophysical and ecological parameters extracted from Visible and Infra Red satellite data have been analyzed. This paper examines also, the effectiveness of the environmental impact assessment process for nuclear power plant in Cernavoda area, Romania. Seismic safety issues at nuclear power plant site must be reconsidered through implementing comprehensive hazard reevaluation programmes for these facilities.

8181-70, Poster Session

Research on LC-based spectral imaging system for visible band

Z. Shen, China Academy of Engineering Physics (China)

LC-based spectral imaging is a novel spectral imaging technology using the liquid crystal tunable filter(LCTF), which is a miniaturized device based on the electrically controlled birefringence of nematic liquid crystal. Continuously tuning electrically controlled through a spectral coverage is realized using LCTF under low voltages. Spectral imaging system based on LCTF is a miniaturized, multi-functional and real-time system with high spatial resolution and spectral resolution, which means that more and further information about the Earth and its resources can be acquired for new applications in large-scale mapping and monitoring.

LC-based tunable filter with large aperture has been developed utilizing the effect of electric controlled birefringence. Spectral test indicates that this filter can operate on the visible band with average 20 nm FWHM. A small scale spectral imaging system is established based on this tunable filter. Spectral imaging experiments on certain number of samples show that this system can provide continuously, and random-access selection of any wavelength, and has a higher level of resolving power in respect of both imaging and spectral tuning in the visible band , which indicates a brilliant application potentiality in environmental protection, resource detection.

Key words: LC-based spectral imaging , electric controlled birefringence, operating spectral coverage, spectral resolution,

8181-73, Poster Session

The use of high resolution satellite and GIS modelling for epidemic diseases (malaria) in Part Saudi Arabia

K. M. Sheikho, King Abdulaziz City for Science & Technology (Saudi Arabia); A. M. Al-Rabeah, Ministry of Health (Saudi Arabia)

The main objective of this paper is the use the of remote sensing technology and geographic information system (GIS) to find the relationship between natural environments in some parts of the Kingdom of Saudi Arabia and the spread of malaria diseases. Remote sensing technology used to give an overview of the factors and elements that help in spread of the disease (weather data, vegetation , swamp types mosquitoes types and numbers. All statistical information and image maps extracted from satellites/ remote sensing images transformed into GIS format. New geodatabase has been created in order to compare and analysis the information and maps (in terms of geography and environment) . There are difficulties in building an

environmental Model axes between the environment and the spread of the disease).

8181-38, Session 9

Satellite data applications for monitoring Arabian Sea tropical cyclone

L. Rafiq, T. Blaschke, Univ. Salzburg (Austria); K. R. F. Ul-Haq, The National Space Agency of Pakistan (Pakistan)

From last two decades advances in earth observation technology resulted in improved forecasting of various hydrometeorological related disasters. Particularly multiple observations by various satellites now able to provide detailed information about the major features of tropical cyclones including development from initial tropical depressions, intensification, and their tracks, landfall, and associated rainfall and wind fields. Two tropical cyclones are taken as the example for the present study and therefore an attempt has made to explore the applications of TRMM and NCEP-NCAR reanalysis data sets for monitoring the total rainfall amount, positions, intensities and motion of two Arabian Sea tropical cyclones June (1-7), and June (21-26)' 2007. By analyzing the results it is found that the role of warm-core anomaly (at 200 hPa and above) with respect to the minimum sea surface pressure in central core in influencing the development pattern of the tropical cyclone. Low vertical wind shear over Arabian Sea found one of several environmental factors that provide suitable conditions for formation of tropical cyclones. High middle troposphere relative humidity, high winds (above 60 m/s) and closed pressure contours were observed during intensification stage. Outgoing long wave radiation (OLR) parameter in terms of watts/sq.meters found useful to monitor structure of the developing disturbance and least values were observed at the central region of the systems with respect to the outer core, indicating an increase of deep cumulonimbus convection and inner core intensification. The contour analysis of OLR also indicates the direction of the movement of the cyclones. By using the surface pressure (central core) the translational movement and velocities (ground speed) of the tropical cyclone were calculated. Such study is expected to shed light on the formation, their intensification, structure and tracks etc as well as disaster mitigation measures and would play a major role in cyclone warning strategies.

8181-39, Session 9

SOLDEO: an innovative solution for environmental monitoring using a low cost lidar mobile system

M. Piras, A. Lingua, Politecnico di Torino (Italy)

The analysis and prevention of natural hazards is one of the main aims of scientific researchers and those who manage the environment and territory. Terrestrial LiDAR and photogrammetric techniques are effective methods of acquiring environmental data and of integrating their in digital products (i.e. solid images and solid true orthophotos). These techniques have shown remarkable effectiveness in many case studies or when the area of interest is limited.

This integration is powerful, but it is not available for large area because a lot of time for the acquisition is required.

A possible solution is to use a mobile system where LiDAR, GPS and camera sensors are contained. Different commercial solutions are available, but the cost (>300k), the requirement of high skill and the low flexibility of the system reduce the number of potential application fields.

The Geomatic group of the Politecnico di Torino has realized a mobile metallic platform that can be installed on any vehicle, where several sensors could be installed (i.e. GPS antenna, webcams, IMU, etc.).

In this paper, the authors explain their attempts to use a mobile vehicle that was instrumented only with low cost sensors (i.e. LiDAR, GPS receivers and webcams) in order to have extensive use the LiDAR-photogrammetric integrated techniques for environmental monitoring.

This kind of system requires dedicated procedures, in particular devoted to calibrating the system(absolute reference system), to elaborate the raw data with dedicated algorithms. A novel produce



was realized to be able to make a deeper analysis: the SOLid viDEO (SOLDEO).

The SOLDEO was born from the solid image experience (i.e. solid image), but in this case a continuous sequences of images were three-dimensional spatial informations are contained and some measurements as distance between two points or related angle are available.

The used procedures and the significant results obtained during the conducted survey campaign, are described, focusing the attention to the practical aspects.

8181-40, Session 9

Towards an open geospatial service architecture supporting heterogeneous Earth observation missions

T. Usländer, Fraunhofer-Institut für Optronik, Systemtechnik und Bildauswertung (Germany)

Heterogeneous Earth Observation (EO) missions pose the problem that each of them offers its own way and technology of how to search for and access to mission results in terms of software products, i.e. series of EO datasets, or images derived from these source products. Typically, these tasks are provided by ground segment software services which may be called through corresponding interfaces by client applications, e.g. Web portal applications, or other software components such as GIS applications.

However, without a coordinated strategy and harmonized development, these ground segment services all have different interfaces following the needs and the business requirements of the individual stakeholders. While this may not be a problem when accessing EO products just from one mission, it gets difficult and tedious when EO products are required from multiple missions, or even worse, when the EO products from multiple missions shall be combined or processed together in order to provide higher-level services or to deliver fused EO datasets. A client application of one mission cannot call ground segment services of another mission if their interfaces are not agreed upon.

Hence, there is a need to find and define a common technological foundation in order to harmonize the ground segment interfaces, or in the speak of software architects, to ensure interoperability between the ground segments.

Consequently, the main project identified by the European Ground Segment Coordination Body, that coordinates the missions of ESA, CNES, ASI, DLR, CSA and EUMETSAT, was "related to interoperability from the point of view of inter-accessibility across heterogeneous missions". The resulting collaborative project was called Heterogeneous Mission Accessibility (HMA). The final objective of HMA, at least on but not limited to the technical level, is to leverage the idea of a service-oriented architectural style. This means, that the individual ground segment systems shall be loosely-coupled by means of an HMA Service Network.

This paper presents the design and the architecture of HMA. HMA follows the thinking of the ISO 19100 series of geomatics standards combined with the industry- and research-driven standardization work of the Open Geospatial Consortium (OGC). It defines an architectural profile of the OGC Reference Model following an interpretation of the ISO Reference Model of Open Distributed Processing tailored to geospatial service-oriented architectures (SOA).

The paper describes how the functional requirements of user authentication and authorization are mapped to standard Web services of the World Wide Web Consortium and how the discovery of, the access to and the presentation of EO datasets may be realized by OGC services. It is outlined how the feasibility analysis of sensor observation tasks and the ordering of EO products may be expressed by the service and information models of the OGC Sensor Web Enablement initiative.

Finally, this paper discusses the follow-on research topic of serviceoriented design of Earth Observation/GIS applications : How shall they be designed such that, on the one hand, they fulfill the user requirements, and, on the other hand, make a maximum use of the capabilities of geospatial service networks such as HMA?



8181-41, Session 9

GMES services for irrigation water management: SIRIUS project

C. De Michele, F. Vuolo, Ariespace s.r.l. (Italy); F. Altobelli, P. Nino, Istituto Nazionale di Economia Agraria (Italy)

The combined use of Earth Observation (EO) data, Geographic Information Systems (GIS) and Information Technologies (IT) has been proven to be useful in many operative tools to repetitively gather and deliver information at spatial and temporal resolution suitable for environmental applications. In this work, we present an operational procedure for improving the efficiency of irrigation at farm and river basin levels. We describe the implementation of the service in a regional case study (Southern Italy) and the current integration of this regional service into a larger framework that will allow local solutions to spread out to other areas within the context of the Global Monitoring for Environment and Security (GMES) programme.

In the last years, the gap between the EO processing chain and data users (farmers, irrigation water managers and local administrators) was filled by providing real-time mapping products from high-resolution EO satellites and distribution of these products to the users in nearly real time from satellite overpass. Such results were achieved within several EU FP5-6 projects (DEMETER, PLEIADeS). Currently, GMES is offering the global infrastructural (both Spatial Data Infrastructure and EO) framework to further stimulate the development of new services for irrigation water management. The work is carried out in the context of the VII F.P. funded SIRIUS project (Sustainable Irrigation water management and River-basin governance: Implementing User-driven Services) (for details: http://www.sirius-gmes.es/). A description of the service concept is presented and preliminary results from the 2010-2011 irrigation seasons are reported for the pilot area located in Southern Italy.

8181-42, Session 9

Wetland landscape pattern analysis with remote sensing images in Ximen Island special marine protected area

H. Zhang, The Second Institute of Oceanography, SOA (China)

Ximen Island sites in the north of Yueqing Bay, and its area is about 7 square kilometer. The large shallow beach around of the island provides rich coastal wetland resources, such as mangrove plants, a variety of birds and the coastal beach wetland. So this area is a typical coastal wetland ecosystem, which has great value of ecological protection and scientific research. In order to protect its biological resources, coastal wetlands and marine ecosystems, Ximen Island special marine protected areas (XISMPA) is established in 2005.

In this paper, four scenes remote sensing images from Landsat-7, SPOT-4, SPOT-5 and WorldView-2 satellites are collected. These images are used for wetland investigation and analysis in Ximen Island special marine protected area. Land wetland and tidal wetland are derived from the remote sensing images. Land wetland includes aquaculture water, pond water, paddy fields and reservoirs. Tidal wetland includes vegetation areas, breeding areas, beaches and waterways. The results showed as following:

(1) The area of land wetland is 1,281,973.04 square meters, accounting for 18.09% of the island area. The area of largest wetland type, aquaculture water, is 644,533.41 square meters. Aquaculture water are widely distributed around the island. Paddy field is accounting for the total area of wetland land 42.49%, mainly distributed in northeast and southwest of the island. Pond water mainly sites between paddy fields and aquaculture water used to guide water. The island has only one reservoir located in the northwest, the area of 910.11 square meters.

(2) The whole tidal region is wetland. According to the remote sensing survey result, vegetation areas are mainly distributed in the southwest of tidal flats, with a total area of 2,918,605.42 square meters. Breeding areas site throughout the inter-tidal zone, especially around Ximen Island and southeastern regions of tidal flats, with a total area of 7,839,263.17 square meters, which is about one-third of the total beach area. Therefore, culture is very developed in XISMPA.
(3) Mangrove plants communities along the coast of Ximen Island.

According to the situation of mangrove forest, mangrove plants will be divided into four classes, such as old-forest, adults-forest, mid-forest and seedlings. The total area of mangrove is 59,741.23 square meters, and the areas of old-forest, adults-forest, mid-forest and seedlings are 2,027.88 square meters, 14,794.81 square meters, 27,223.91 square meters and 15,694.63 square meters, respectively.



Monday-Tuesday 19-20 September 2011

Part of Proceedings of SPIE Vol. 8182 Lidar Technologies, Techniques, and Measurements for Atmospheric Remote Sensing VII

8182-02, Session 1

Development and infusion of lidar technologies for NASA science missions

S. P. Sandford, W. C. Edwards, U. N. Singh, NASA Langley Research Ctr. (United States)

Lidar systems often provide the best measurements for advancing our understanding of atmospheric science. The progress over the past several decades in developing laser and lidar technology offers significant opportunities now for improving our knowledge of global winds, aerosols, and carbon dioxide. This paper will discuss the enabling advances and current status of the lidar systems developed to provide global measurements of these important atmospheric properties. Next steps leading to other lidar system development will provide a roadmap for future space-based remote sensing capabilities.

8182-03, Session 1

Spaceborne lasers development for future remote sensing applications

A. W. Yu, NASA Goddard Space Flight Ctr. (United States)

At NASA's Goddard Space Flight Center, we are working with several industry partners to develop laser technology for the second Ice Cloud and Land Elevation Satellite (ICESat-2) mission, scheduled to launch in 2016. ICESat-2 will fly a single, multi-beam instrument, the Advanced Technology Laser Altimeter System (ATLAS), which will use the time-offlight of laser pulses to make topographic measurements of the Earth's surface. The ATLAS laser will be a 1064 nm MOPA (master oscillator power amplifier) system that is frequency-doubled to the green. We have been focusing on advancing the technology readiness of these technologies for a space environment. The 1.0 µm, high repetitionrate (~10 kHz) and short pulse width (~1 ns) MOPA technology developed can be used for several future infrared NASA laser missions including LIST and ASCENDS. In this paper, we will discuss the laser technology developed thus far for ICESat-2 and how this technology can be applied to meet future needs. The ATLAS laser technology that is being advanced differs from conventional laser altimeter systems in which high repetition rate at tens of kHz, pulse energies of hundreds of microjoules and sub-nanosecond pulses are use for the science measurements. This represents a new era in space-based instrumentation for the space agency. We will discuss scientific goals and likely instrument requirements for these missions.

8182-04, Session 2

The MERLIN Mission: a space-based IPDA lidar for methane monitoring

P. H. Flamant, Lab. de Météorologie Dynamique (France); G. Ehret, Deutsches Zentrum für Luft- und Raumfahrt e.V. (Germany)

Methane is the second anthropogenic GHG with Warming Potential of 23 years relative to carbon dioxide time scale of about 100 years. To understand the complex global Methane surface source-sink cycle, it is necessary to apply space-based measurements techniques in order to obtain global coverage. The Methane Remote Sensing Lidar Mission (MERLIN) is a joint French-German cooperation to develop a micro satellite mission for space-based measurement of spatial and temporal gradients of atmospheric Methane columns on a global scale. MERLIN is is intended for a launch in 2015. MERLIN will be the first Integrated Path Differential Absorption (IPDA) Lidar in space. In contrast to

passive missions, the lidar instrument allows to monitoring Methane OD, dry mixing ratio XCH4 and so CH4 fluxes at all-latitudes, allseasons and during night. Range-gated signal detection of the surface echo ensures that possible biases from unknown aerosol scattering or scattering from thin cirrus clouds are avoided. First scientific studies show a substantial reduction of the prior Methane flux uncertainties in key observational regions when using synthetic MERLIN observations in the flux inversion experiments. The presentation gives an overview on the mission concept with the German IPDA Lidar on the French micro satellite platform MYRIADE, its present status and briefly reports on results from scientific impact studies.

8182-05, Session 2

Optical parametric oscillators and amplifiers for airborne and spaceborne active remote sensing of CO₂ and CH₄

A. Fix, C. Büdenbender, M. Wirth, M. Quatrevalet, A. Amediek, C. Kiemle, G. Ehret, Deutsches Zentrum für Luft- und Raumfahrt e.V. (Germany)

Carbon dioxide (CO2) and methane (CH4) are the most important of the greenhouse gases that are influenced directly by human activities. For a detailed understanding of their sources and sinks remote sensing instruments are required that can measure those gases on a global or regional scale from spaceborne or airborne platforms. In particular, the Integrated Path Differential Absorption (IPDA) lidar technique using hard target reflection in the near IR (1.57 μ m and 1.64 μ m) to measure the column-averaged dry air mixing ratio of CO2 and CH4 with high precision and low bias has been found potentially suited for fulfilling the target observational requirements.

A basic prerequisite for an airborne or spaceborne IPDA instrument is the availability of adequate tunable laser sources in these wavelength regions that fulfill the challenging requirements in terms of pulse energy for high SNR together with high frequency stability (< 300 kHz for CO2 and < 100 MHz for CH4) and spectral purity. Since not many well characterized and mature laser materials are available for the generation of high power radiation in this wavelength region, nonlinear frequency conversion techniques such as optical parametric oscillators (OPOs) and optical parametric amplifiers (OPAs) appear favorable.

Within this study the radiation of a nanosecond injection-seeded OPO system pumped at 100 Hz could be amplified to generate average powers of more than 5 W and pulse energies of more than 50 mJ in the near infrared spectral range coincident with appropriate absorption lines. Emphasis was put on the spatial and spectral characterization of the device. Using the technique of injection seeding bandwidths of less than 100 MHz have been achieved. The M2-factor was better than 2.3.

The OPO when seeded and stabilized by means of a heterodyne technique showed an Allan deviation of < 70 kHz relative to the seed source for averaging times of more than 3 s. At the same time its spectral purity was measured to be better than 99.97%. Using a DFB fiber laser as the seed and an optical frequency comb for stabilization, an absolute frequency stability of the seed of the order of 500 Hz was achieved.

Owing to these outstanding properties optical parametric devices are currently under investigation for the lidar instrument to be deployed on the joint French-German satellite MERLIN to measure methane from a small satellite platform. A similar device is under development at DLR for the lidar demonstrator CHARM-F which will enable the simultaneous measurement of CO2 and CH4 from an airborne platform.



8182-06, Session 2

Development effort of the airborne lidar simulator for the lidar surface topography (LIST) mission

A. W. Yu, NASA Goddard Space Flight Ctr. (United States)

In 2009 we started a three-year Instrument Incubator Program (IIP) project, funded by NASA's Earth Science Technology Office (ESTO), for early technology development for the Lidar Surface Topography (LIST) mission. The purpose is to develop and demonstrate technologies for a next-generation, efficient, swath-mapping space laser altimeter. Our approach allows simultaneous measurements of 5-m spatial resolution topography and vegetation vertical structure with decimeter vertical precision in an elevation-imaging swath several km wide from a 400 km altitude Earth orbit. This capability meets the goals of the LIST mission recommended in the Earth Science Decadal Survey by the NRC Committee on Earth Science and Applications from Space. To advance and demonstrate needed technologies for the LIST mission, we are developing the Airborne LIST Simulator (A-LISTS) pathfinder instrument. A-LISTS is a micropulse, photon-sensitive waveform recording system that is based on a new, highly efficient laser measurement approach utilizing emerging laser transmitter and detector technologies.

The A-LISTS instrument uses a single laser to generate sixteen beams for high-resolution mapping. Backscatter from the surface is collected with a telescope and the spots from the swath are imaged onto a photon sensitive detector array. The output from each detector element is histogrammed and analyzed to determine ranges to the surface and derive echo waveforms that characterize the vertical structure of the surface. This signal processing technique allows for throughfoliage interrogation in order to observe the ground surface beneath vegetation cover and to characterize vegetation vertical structure.

In this paper we will discuss the development effort of the A-LISTS instrument and discuss the results from the airborne experiment.

8182-07, Session 2

In space performance of the lunar orbiter laser altimeter (LOLA) laser transmitter

A. W. Yu, NASA Goddard Space Flight Ctr. (United States)

The LOLA instrument was turned on 4 July, 2009 and has been in essentially constant operation since then. The LOLA laser oscillator is a cross-Porro resonator with an effective output reflectivity of ~18% to produce a specified output energy of 2.7 ± 0.3 mJ per pulse (prior to transmit beam expander and DOE) at a rate of 28 Hz, with a minimum pulse width of 6 ± 2 ns.

The receive telescope is a refractor design in a beryllium structure with a sapphire objective. The received light is imaged onto fiber optic bundle placed at the focal plane of the telescope and coupled to the aft optics. The return light is detected by silicon APDs that have heritage from previous missions. The range measurement unit is similar in design to the MLA which uses high resolution time-of-flight ASICs. A DOE fabricated in etched fused silica with anti-reflective (AR) coating at 1064 nm is used to split a single laser beam five ways into the required five ground spots. The far field divergence of each of the five spots is 100 µrad. At 50 km orbit, this will produce five-5 m diameter spots with center-to-center separation of 25 m on the lunar surface.

The LOLA laser transmitter successfully produced approximately 800 million combined shots during the Exploration Phase of the LRO mission. This provided an ample quantity of lunar elevation measurements that allowed the LOLA instrument to meet all high-level data requirements in delivering the most detailed three-dimensional map of the lunar surface to date.

Since it was first turned-on, the LOLA laser transmitter has a combined shots fired of over 1.3 Billion, with ~700 Million shots for L1 and ~600 Million shots for L2. Both lasers continue to operate nominally with energies the same as delivered and the orbit-averaged switch-out times for L1 and L2 are currently 158 μ s and 178 μ s, respectively.

The LOLA instrument is designed to map the lunar surface and provide unprecedented data products in anticipation of future manned flight missions. The laser transmitter has been operating on orbit at the Moon continuously since July 2009. The LOLA laser transmitter design has heritage dated back to the MOLA laser transmitter launched more than 10 years ago and incorporates lessons learned from previous laser altimeter missions at NASA Goddard Space Flight Center.

8182-08, Session 3

Examination of possible synergy between lidar and ceilometer for the monitoring of atmospheric aerosols

I. Binietoglou, A. Amodeo, G. D'Amico, A. Giunta, F. Madonna, L. Mona, G. Pappalardo, CNR Istituto di Metodologie per l'Analisi Ambientale (Italy)

In this paper the advanced measurement capabilities of the multiwavelenght raman lidar are used to investigate the possibility of using ceilometers for atmospheric aerosol monitoring. In the CNR - IMAA Atmospheric Observatory (C.I.A.O), located in southern Italy, the possible synergies of diverse ground based techniques for atmospheric aerosol monitoring are actively investigated. To this end, a CHM15k ceilometer of Jenoptik Laser Optik Systeme is operated since September 2009 providing vertical profiles of atmospheric backscatter at 1064nm up to 15km. In the same location, the Potenza EArlinet Raman Lidar (PEARL), a quality-assured, multi wavelength raman lidar (elastic chanels 355, 532, 1064, raman channels 386, 407, 608, depolarization: 532) operates in the framework of EARLINET lidar network and performs regular measurements plus measurements of special events (Sahara dust outbreaks, volcanic eruptions etc.). Using the PEARL optical products as a reference, the long term capability of commercially available ceilometers to provide useful information about the atmospheric aerosols load and their limitations in this task are investigated. The regular performance of collocated measurements by the two systems permits the quantitative characterization of the ceilometer's performance. The fact that both systems use the 1064nm wavelength for elastic backscatter measurements allows for a comparison procedure that minimizes external assumptions. The long-term stability of the calibration of ceilometer systems is examined. The variation of ceilometers' performance for different atmospheric conditions is analyzed while favorable scenarios for the ceilometer to provide reliable atmospheric data are identified. The possible synergies with other ground based instruments, such as sun photometers, for improving the reliability of the ceilometer's products are also investigated.

8182-09, Session 3

Preliminary measurements of tropospheric water vapor using Raman lidar system in the Great Lakes area

W. Al-Basheer, K. B. Strawbridge, B. J. Firanski, Environment Canada (Canada)

Raman lidar technique is widely recognized as the most effective tool to study water vapor and aerosols profiles in the lower atmosphere. The Great lakes area is one of the ideal areas to study the environmental impact of water vapor and aerosols profiles on air quality due to its dynamic ecological system, and proximity to most North American industrial centers. Latest results of a newly developed lidar instrument at the Environment Canada's Centre for Atmospheric Research Experiments (CARE) will be presented. In this study, the instrument is described and its capabilities are illustrated along with preliminary measurements. The CARE Raman lidar setup, second (532 nm), third (355 nm), and forth (266 nm) harmonic outputs of three simultaneously employed YAG lasers, were utilized to probe aerosols, water vapor and ozone profiles, respectively. By manipulating inelastic backscattering lidar signals of the Raman nitrogen channel (386.7 nm) and Raman water vapor channel (407.5 nm), the water vapor mixing ratio, which is defined as the mass of water vapor divided by the mass of dry air in a given volume, is deduced. Furthermore, environmental parameters such as, temperature, humidity, pressure, and wind direction, will provide valuable ancillary data. Details of the setup design, modifications, calibration tools, and their contribution to water vapor lidar system sensitivity will be presented.



8182-10, Session 3

Validation of COSMIC water vapor profiles using Raman lidar measurements performed at CIAO

F. Madonna, CNR Istituto di Metodologie per l'Analisi Ambientale (Italy); P. Burlizzi, Univ. del Salento (Italy); A. Giunta, CNR Istituto di Metodologie per l'Analisi Ambientale (Italy); M. R. Perrone, Univ. del Salento (Italy); G. Pappalardo, CNR Istituto di Metodologie per l'Analisi Ambientale (Italy)

Water vapor is one the most important greenhouse gases. Water vapor is considered one of the Essential Climate Variables (ECV) and its role in the Earth's radiative balance represents a key uncertainty for understanding the climate change. Difficulties over their representation within numerical models are responsible for much of the uncertainty of future climatic trends. Therefore, there is a strong need for evaluating model capabilities to reproduce the behaviour of these key parameters in the atmosphere using satellite and ground based remote sensing profiling measurements.

The development of the Global Position System (GPS) satellite network has provided new opportunities to characterize atmospheric parameters using innovative techniques. The GPS Radio Occultation Technique (GPS RO) is one of the most recent and promising atmospheric remote sensing technique applied to GPS measurements. The GPS RO technique allows obtaining profiles of refractivity, temperature, pressure and water vapor in the neutral atmosphere and electron density in the ionosphere. The GPS RO technique is based on the inversion of excess-phase measurements related to the signal transmitted by a GPS setting or rising satellite and detected by a GPS receiver placed on a low earth orbit (LEO). The GPS Meteorology was the first experiment which has provided an evidence of the radiooccultation (RO) limb-sounding technique efficiency in 1995-97. In the last years, other missions confirmed the RO efficiency, like GPS/ MET, COSMIC (Constellation Observing System for Meteorology, Ionosphere, and Climate), Formosa Satellite Mission 3 and the last Radio Occultation Sounder Antenna for the Atmosphere.

In this work, water vapor mixing ratio profiles retrieved from COSMIC observations are presented and validated using ground based water vapor Raman lidar profiles. Raman lidar represents one of the most powerful techniques for measuring water vapor with high accuracy as well as high temporal and spatial resolution. This makes Raman lidar measurements a very good reference measurements for satellite validation.

COSMIC water vapor profiles used in this study are based on 1D variational analysis using ECMWF low resolution analysis data, while Raman lidar measurements of the water vapor mixing ratio profiles are provided by PEARL (Potenza EArlinet Raman Lidar) system running at CIAO (CNR-IMAA Atmospheric Observatory - 40.60N, 15.72E), located in Tito Scalo, Potenza, Italy.

COSMIC performances are studied over a two years period (2007-2008) of systematic water vapor Raman lidar measurements and the sensitivity of GPS RO to the structure of water vapor field at different altitude ranges is discussed. Co-location mismatch between satellite footprint and the lidar station are discussed as well as the problem of the vertical resolution of COSMIC profiles respect to Raman lidar.

8182-12, Session 3

One year of regular aerosol observations with a multi-wavelength Raman lidar in Portugal

J. Preissler, F. Wagner, J. L. Guerrero-Rascado, A. M. Silva, Univ. de Évora (Portugal)

The multi-wavelength Raman lidar PAOLI (Portable Aerosol and Cloud Lidar) of the type PollyXT is operated in Évora, Portugal (38.57°N, 7.91°W, 290 m asl) since September 2009. The Évora Geophysics Centre (CGE) is member of EARLINET. Night time measurements analysed for the presented study were performed according to the EARLINET schedule, on Mondays and Thursdays after sunset. Such

regular measurements assure statistical results unbiased by so-called special events, i.e. periods of high aerosol load caused, for example, by desert dust outbreaks, volcanic eruptions or forest fires. Those special events often lead to more intense observation periods and consequently to more data.

For the presented work, data of one year (January to December 2010) has been analysed regarding aerosol layers in the free troposphere. In total, 122 layers were observed during 56 out of 78 performed measurements. For each layer, three 10-day back-trajectories were calculated by means of the HYSPLIT model [http://ready.arl. noaa.gov/HYSPLIT.php] for the top, the base and the centre of the layer, respectively. The main aerosol types observed over Évora in 2010 are Saharan dust (17% of all layers), European anthropogenic aerosol (11%), forest fire and anthropogenic aerosol from North America (17%) and aerosol transported close to the surface of, and therefore influenced by, the Atlantic Ocean (18%). Additionally, layers of Portuguese forest fire smoke (8 layers), volcanic ash from Eyjafjallajökull (5), aged aerosol from polar regions (10) and long range transported layers from the Pacific Ocean or Asia (9) were observed.

The seasonal variability of the layer origin and the geometrical properties of the layers have been investigated. Resulting from different prevailing circulation patterns there is specific seasonal behaviour of the occurrence of layers from the different source regions. In general, more and higher layers could be observed in spring and summer.

A clear correlation between the layer height and the transport distance has been found with increasing height at longer distances. However, exceptionally high are the aerosol layers from the Saharan desert and from the volcano, considering their comparatively short distance from the measurement site. This can be explained firstly by the generally high dust layer height over the Sahara and secondly by the explosiveness of volcanic eruptions, which leads to an intrusion of volcanic aerosol into high altitudes of the troposphere.

The conference contribution will also include optical properties of the aerosol layers and a comparison of those in dependence of their origin.

8182-13, Session 4

Analysis of pulsed airborne lidar measurements of atmospheric CO₂ column absorption from 3-13 km altitudes

J. B. Abshire, C. J. Weaver, H. Riris, J. Mao, X. Sun, NASA Goddard Space Flight Ctr. (United States); G. Allan, W. E. Hasselbrack, Sigma Space Corp. (United States); E. V. Browell, NASA Langley Research Ctr. (United States)

We have developed a pulsed lidar technique for measuring the tropospheric CO2 concentrations as a candidate for NASA's ASCENDS space mission [1]. It uses two pulsed laser transmitters allowing simultaneous measurement of a CO2 absorption line in the 1575 nm band, O2 extinction in the Oxygen A-band, surface height and backscatter profile. The lasers are precisely stepped in wavelength across the CO2 line and an O2 line region during the measurement. The direct detection receiver measures the energies of the laser echoes from the surface along with the range profile of scattering in the path. The column densities for the CO2 and O2 gases are estimated from the ratio of the on- and off- line signals via the integrated path differential absorption (IPDA) technique. The time of flight of the laser pulses is used to estimate the height of the scattering surface and to reject laser photons scattered in the atmosphere.

We developed an airborne lidar to demonstrate an early version of the CO2 measurement from aircraft. The lidar stepped the pulsed laser's wavelength across the selected CO2 line with 20 wavelength steps per scan. The line scan rate is 450 Hz, the laser pulse widths are 1 usec, and laser pulse energy is 24 uJ. The time resolved laser backscatter is collected by a 20 cm telescope, detected by a NIR photomultiplier and is recorded on every other reading by a photon counting system [2].

During August 2009 we made a series of 2.5 hour long flights and measured the atmospheric CO2 absorption and line shapes using the 1572.33 nm CO2 line. Measurements were made at stepped altitudes from 3-13 km over locations in the US, including the SGP ARM site in Oklahoma, central Illinois, north-eastern North Carolina, and over the Chesapeake Bay and the eastern shore of Virginia. Although the received signal energies were weaker than expected for ASCENDS,

clear CO2 line shapes were observed at all altitudes, and some measurements were made through thin clouds. The Oklahoma and east coast flights were coordinated with a LaRC/ITT CO2 lidar on the LaRC UC-12 aircraft, and in-situ measurements were made using its CO2 sensor and radiosondes.

We have conducted an analysis of the ranging and IPDA lidar measurements from these flights. Most flights had 5-6 altitude steps with 200-300 seconds of recorded measurements per step. We used a cross-correlation approach to process the laser echo records. This was used to estimate the range to the scattering surface, to define the edges of the laser pulses and to determine echo pulse energy at each wavelength. We used a minimum mean square approach to fit an instrument response function and to solve for the best-fit CO2 absorption line shape. We then calculated the differential optical depth (DOD) of the fitted CO2 line. We computed its statistics at the various altitude steps, and compare them to the DODs calculated from spectroscopy based on HITRAN 2008 and the column conditions calculated from the airborne in-situ readings. The results show the lidar and in-situ measurements have very similar DOD change with altitude and > 10 segments per flight where the scatter in the lidar measurements are \leq 1ppm. We also present the results from subsequent CO2 column absorption measurements, which were made with stronger detected signals during three flights on the NASA DC-8 over the southwestern US in during July 2010.

References:

1. Abshire, J.B., Riris, H., Allan, G.R., Weaver, C.J., Mao, J., Sun, X., Hasselbrack, W.E., Yu, A., Amediek, A., Choi, Y., Browell, E.V. (2010), "A lidar approach to measure CO2 concentrations from space for the ASCENDS Mission," SPIE Proceedings Vol. 7832, DOI: 10.1117/12.868567

2. Abshire, J.B., Riris, H., Allan, G.R., Weaver, C.J., Mao, J., Sun, X., Hasselbrack, W.E., Kawa. S.R. and Biraud, S. (2010), "Pulsed airborne lidar measurements of atmospheric CO2 column absorption," Tellus B, 62: 770-783. doi: 10.1111/j.1600-0889.2010.00502.x

8182-14, Session 4

Improvement of the 1.57-micron laser absorption sensor with chirp modulation to evaluate spatial averaging carbon dioxide density

D. Sakaizawa, S. Kawakami, T. Tanaka, M. Nakajima, Japan Aerospace Exploration Agency (Japan)

A 1.57-µm laser remote sensor using differential absorption is being developed as a candidate for the next space-based mission to observe atmospheric CO2 and/or other trace gases. In previous study, the performance of the proto-type with a sinusoidal modulation has been evaluated on the ground and airborne measurements. The system can suppress an impact of aerosol layer on the differential absorption measurement over the high surface reflectivity, although the elevated layer in the observation path disturbs an accurate differential absorption measurement. In order to improve the measurement of the column averaged CO2, we employed a chirp modulation scheme to prevent the impact of elevated layer on the differential absorption measurement. Results of the ground-based measurements will be shown in this meeting.

8182-15, Session 4

Pulsed laser transmitter development for direct detection of CO_2 from space

U. N. Singh, J. Yu, NASA Langley Research Ctr. (United States)

The development of a high pulse energy 2-µm laser transmitter for high-precision CO2 measurements from space leverages years of NASA investment in solid-state laser technology. Under NASA Laser Risk Reduction Program, funded by Earth Science Technology Office, researchers at NASA Langley Research Center developed an injection seeded, high repetition rate, Q-switched Ho:YLF laser transmitter for differential absorption lidar/integrated path differential absorption CO2 measurements from ground and airborne platforms. The planned laser



transmitter development will lead to a Tm:Fiber pumped Ho:YLF laser transmitter capable of delivering 65 mJ at 50 Hz at on-line wavelength and 50 mJ at 50 Hz at off-line wavelength.

8182-16, Session 4

Direct detection 1.6 μ m DIAL for measurements of CO₂ concentration profiles in the troposphere

C. Nagasawa, M. Abo, Y. Shibata, Tokyo Metropolitan Univ. (Japan); T. Nagai, Meteorological Research Institute (Japan); M. Tsukamoto, Eko Instruments Co., Ltd. (Japan)

Inverse techniques using atmospheric transport models are developed to estimate the CO2 sources and sinks based on the observed data. In comparison with the ground-based monitoring network, CO2 measurements for vertical profiles in the troposphere have been due to the limited observations by using campaign-style aircrafts and the commercial airlines with limited spatial and temporal coverage. The differential absorption lidar (DIAL) with the range resolution is expected to bring several advantages over passive measurements, for example, daytime coverage and neglecting influences of aerosol and cirrus layers. We have succeeded to develop the 1.6 µm DIAL technique using direct detection method for measurement of CO2 concentration profiles in the atmosphere. This paper describes the advanced CO2 1.6 µm DIAL technique consisting of the optical parametric generator (OPG) transmitter (10mJ/pulse) that excited by the LD pumped Nd:YAG laser with high repetition rate (500Hz) and the receiving optics that included the large telescope with 60cm diameter and the photomultiplier tube with high quantum efficiency (~8%) operating at the photon counting mode and the narrowband interference filter (0.5nm bandwidth) for daytime observations. The CO2 concentration profiles from ground to an altitude of 12km are conducted to measure with better than 1% standard deviation using 500m bins by this CO2 DIAL.

Reference

D. Sakaizawa, C. Nagasawa, T. Nagai, M. Abo, Y. Shibata, M. Nakazato, T. Sakai, Development of a 1.6µm differential absorption lidar with a quasi-phase-matching optical parametric oscillator and photon-counting detector for the vertical CO2 profile, Appl. Opt., Vol.40, No.4, pp.748-757, 2009.

8182-17, Session 4

New broadband lidar for greenhouse carbon dioxide gas sensing in the Earth's atmosphere

E. M. Georgieva, W. S. Heaps, NASA Goddard Space Flight Ctr. (United States); W. Huang, Science Systems and Applications, Inc. (United States)

250 Word Summary:

We present demonstration of a novel broadband lidar technique capable of dealing with the atmospherically induced variations in CO2 absorption using a Fabry-Perot based detector and a broadband laser. The Fabry-Perot solid etalon in the receiver part is tuned to match the wavelength of several CO2 absorption lines simultaneously. Same approach is used for the laser photons in the transmitter part using a different air gapped etalon. The receiver itself has been in development over the last few years at GSFC as a passive sensor to measure atmospheric CO2 column. It was tested during two successful flight campaigns. This new active approach reduces the number of individual different wavelength lasers required from three or more to only one, considerably reducing the risk of failure associated with multiple laser systems. The broadband technique also tremendously reduces the requirement for source wavelength stability, instead putting this responsibility on the Fabry- Perot based receiver. Laboratory, ground based and airborne results of the lidar system will be discussed. For the laboratory experiments we were using the OPA based system for 1.57 µm that has demonstrated pulse energies as high as 14.6 mJ per pulse, rep. rate of 15 Hz, 4 ns pulse duration over 2 nm spectral range. The fielded laser will operate with ~100 mJ pulse energy in 5

ns pulses over a 0.5 nm spectral range. The instrument technology we are developing has a clear pathway to space and realistic potential to become a robust, low risk space measurement system.

8182-18, Session 5

Airborne direct-detection and coherent wind lidar measurements along the east coast of Greenland in 2009 supporting ESA's Aeolus mission

U. Marksteiner, O. Reitebuch, S. Rahm, Deutsches Zentrum für Luft- und Raumfahrt e.V. (Germany); I. Nikolaus, Physics Solutions (Germany); C. Lemmerz, B. Witschas, Deutsches Zentrum für Luft- und Raumfahrt e.V. (Germany)

The measurement of wind is considered to be a preferential objective by the World Meteorological Organisation (WMO) since it is crucial for numerical weather prediction (NWP) and climate studies.

The Aeolus mission of the European Space Agency ESA will send the first wind lidar to space to fulfil the utmost need for global wind profile observations.

Before the scheduled launch in late 2013, pre-launch campaigns to validate the measurement principle and optimize algorithms were performed.

Therefore, an airborne prototype instrument has been developed, the ALADIN Airborne Demonstrator (A2D), a direct-detection wind lidar working in the ultraviolet region at 355 nm.

It comprises two interferometers dedicated to narrowband Mie backscatter from aerosol and clouds and broadband Rayleigh backscatter from molecules, respectively.

In September 2009 an airborne campaign over Greenland, Iceland and the Atlantic Ocean was conducted using two instruments: the A2D and a well established coherent 2- μ m lidar for aerosol and cloud backscatter.

Thus, two wind lidar instruments measuring Mie and Rayleigh backscatter in parallel were successfully flown for the first time worldwide.

The A2D and the 2- μ m lidar retrieve wind information from the Doppler shift of the collected backscatter signal with respect to the initially transmit laser pulse frequency.

If operated in a fixed viewing geometry, i.e. pointing direction of laser and telescope, both lidars are restricted to the detection of so called line of sight (LOS) wind components.

Additionally, the 2-µm lidar can be operated in scanning mode, enabling it to measure the 3-dimensional wind vector profile.

LOS-wind fields from the A2D Rayleigh and Mie channel as well as from the 2-µm wind lidar will be presented from a flight track along the east coast of Greenland from September 2009. It is the first time that wind profiles from an airborne direct-detection Doppler lidar were obtained. The systematic and random error of the direct-detection wind lidar A2D was assessed with a statistical comparison to the 2-µm LOS winds yielding values of -0.5 m/s and 2 m/s, respectively.

8182-19, Session 5

Field programmable gate array processing of eye-safe all-fiber coherent wind Doppler lidar return signals

S. Abdelazim, D. Santoro, M. Arend, F. Moshary, S. Ahmed, The City College of New York (United States)

A field deployable all-fiber eye-safe Coherent Doppler LIDAR is being developed at the Optical Remote Sensing Lab at the City College of New York (CCNY) and is being designed to monitor wind fields autonomously and continuously in urban settings. The transmitter wavelength of 1.5 μ m is chosen to leverage affordable and readily available components from the telecommunication industry. Data acquisition is accomplished by sampling lidar return signals at 400



MHz and performing on-board processing using field programmable gate arrays (FPGAs). The FPGA is being programmed to accumulate signal information that will be used to calculate the power spectrum of back scattered signal. An experimental setup was conducted in which wind speed was measured up to 1.5 km range. Laser pulses are transmitted and backscatter signals received from the atmosphere using a collinear refractive optical antenna and with the return signal then routed through an optical circulator. The received signal is time gated and processed. Each gate represents scattered signal throughout a range distance in the atmosphere. In order to increase the resolution of wind speed, we curve fitted the power spectrum to a Gaussian curve. This permits detection of wind speed within a frequency bin i.e. increases the velocity estimate resolution (verified to be within an accuracy of better than 0.2 m/s using of a hard target.) The advantage of using FPGA is that signal processing is performed at the hardware level, reducing the load on the host computer and allowing for nearly 100% return signal processing.

8182-20, Session 5

Estimation of radial wind velocity for the non-Gaussian statistics of the Doppler lidar signal in the turbulent atmosphere

E. A. Shelekhova, Institute of Monitoring of Climatic and Ecological Systems and V.E. Zuev Inst. of Atmospheric Optics (Russian Federation); A. P. Shelekhov, V.E. Zuev Institute of Atmospheric Optics (Russian Federation)

The statistical analysis of the signal is the first stage of investigations of random process and it is complete if absolute and conditional statistical characteristics are studied in detail. The investigations of absolute and conditional statistical characteristics allow us to understand the major cause of non-Gaussian properties of the Doppler lidar signal in the turbulent atmosphere and use method of mathematical physics correctly.

In this paper the calculation results of correlation functions of the Doppler lidar signal of second and fourth orders in the turbulent atmosphere are presented. The absolute statistical characteristics are defined as averaging over all random parameters: coordinates and number of particles and wind velocity fluctuations of the atmospheric turbulent flow. The conditional statistical characteristics are defined as averaging over random parameters excepting wind velocity fluctuations of the atmospheric turbulent flow.

The problem statement is based on the single scattering approximation for the Doppler lidar signal: it is sum of random oscillating functions. The oscillation frequencies are defined by radial wind velocities of the atmospheric turbulent flow. Also we assume that coordinates, velocity and number of particles are independent in terms of statistics. At initial time the particles are distributed uniformly and independently in scattering volume. The number of particles obeys Poisson distribution, and a distribution law of wind velocity fluctuations of the atmospheric turbulent flow obeys a low of normal probability distribution.

The analysis of correlation functions of second and fourth orders shows that absolute statistical characteristics are not factorable according to the law of Gaussian statistics. It means that the Doppler lidar signal is the non-Gaussian random process. It follows from analysis of absolute and conditional statistical characteristics of the Doppler lidar signal, that the major cause of non-Gaussian properties of Doppler lidar signal is wind velocity fluctuations of the atmospheric turbulent flow.

We obtain the form of the estimation of radial wind velocity for the non-Gaussian statistics of the Doppler lidar signal in the turbulent atmosphere. It shows that the estimation of radial wind velocity is sum of regular part and two fluctuations parts. The regular part of the estimation is mean radial wind velocity, two fluctuations parts are conditional Gaussian and non-Gaussian fluctuations of the Doppler lidar frequency.



8182-21, Session 6

The Canadian observational research aerosol lidar network (CORALNet)

K. B. Strawbridge, Environment Canada (Canada)

The Canadian Operational Research Aerosol Lidar Network (CORALNet) was established in 2008 with the deployment of the first lidar system to Canada's West Coast. The network of lidars have been chosen at strategic places across Canada where the main function of the network is to look at the degree of long-range transported aerosols to study and monitor their impact on air quality on local, regional and national scales. Some occur naturally (biogenic), coming from volcanoes, dust storms, forest and grassland fires, living vegetation and sea spray while others result from human activities (anthropogenic), such as burning fossil fuels and altering natural surface cover. The establishment of CORALNet is critical for understanding the roles of man-made, locally-produced air pollutants as well as those which move into the area via meteorological "highways" and their impacts on air quality. Every 10 seconds the system provides vertical aerosol profiles from near ground to 20 km into the sky. It operates 24 hours a day, seven days a week except during precipitation events and when aircraft fly over the site. The system is operated remotely and the data, which are updated every hour, are publicly available on the website www.coralnet.ca.

8182-22, Session 6

Ineractive aerosol lidar monitor for multiple displays and users via a network multicast

J. P. Herron, Utah State Univ. (United States); G. W. Lemire, J. T. Pearson, M. S. Marshall, U.S. Army Dugway Proving Ground (United States)

Dugway Proving Ground is a major range test facility charged with testing chemical and biological defense systems and materials. The facilities at DPG include state-of-the-art laboratories and extensive field test grids. A suite of mobile elastic backscatter lidar systems are used as referee systems to track and quantify biological and interferent aerosol releases on the test range. While each lidar has its own display software, it typically is only intended for and available to the system operator. The display is typically not adequate for every test scenario and requires the data to be post-processed into an acceptable format for presentation to a test client. The lidar systems are typically positioned several kilometers from any release point or the command post. This geographic separation caused major limitations in certain test scenarios, as the data output from the lidar system was only available to other test personnel via verbal comments from the lidar operator until post test. To increase the utility and impact of the lidar systems on field testing, a real-time data visualization software package was developed for the DPG lidar systems. Multiple display types are included in the software to accommodate various testing and calibration scenarios. Data from a fielded system is uploaded to the local test network via either a direct or wireless connection. The data is sent via a UDP multicast which allows for multiple end users to receive the data without increasing the load on the server or network as there is minimal error checking, and duplication of the data is done at the router level. The software is designed for test personnel and clients of DPG to operate without significant training and only a passing familiarity with lidar systems. In addition to providing a realtime display the software can capture the data locally making a test event available for immediate review. A software description and the display philosophy for various field test scenarios are included in this presentation.

8182-23, Session 6

A high-energy, eye-safe, injection seeded, KTA ring-cavity optical parametric oscillator

R. Foltynowicz, M. Wojcik, Utah State Univ. (United States)

We have demonstrated a 243mJ, eye-safe, injection seeded, noncritically phase-matched (NCPM), singly resonant oscillator (SRO), KTA ring-cavity optical parametric oscillator (OPO). The OPO was pumped with a single mode 7ns FWHM, 30Hz, Q-switched, Nd:YAG at a wavelength of 1064.162nm. The OPO was injection-seeded utilizing a single longitudinal (SLM) distributed feedback (DFB) diode laser. As a result, the KTA OPO generated an eye-safe signal wavelength of 1535.200nm with a maximum energy of 243mJ, a conversion efficiency of 27%, a cavity mode seed range of 853MHz FWHM, and a maximum M2=30. This high energy, eye-safe OPO could potentially increase the sensitivity and range capabilities of elastic LIDAR and DIAL systems which are used for remote sensing applications.

8182-24, Session 6

Long term observation of low altitude atmosphere by high precision polarization lidar

T. Shiina, Chiba Univ. (Japan); K. Noguchi, Chiba Institute of Technology (Japan); T. Fukuchi, Central Research Institute of Electric Power Industry (Japan)

Prediction of weather disaster such as heavy rain and light strike is an earnest desire. Successive monitoring of the low altitude atmosphere is important to predict it. The weather disaster often befalls with a steep change in a local area. It is hard for usual meteorological equipments to capture and alert it speedily.

We have been developed the near range lidar to capture and analyze the low altitude atmosphere. In this study, high precision polarization lidar was developed to observe the low altitude atmosphere. This lidar has the high extinction ratio of polarization of >30dB to detect the small polarization change of the atmosphere. The change of the polarization in the atmosphere leads to the detection of the depolarization effect and the Faraday effect, which are caused by ice-crystals and lightning discharge, respectively. As the lidar optics is "inline" type, which means common use of optics for transmitter and receiver, it can observe the near range echo with the narrow field of view.

The long-term observation was accomplished at low elevation angle. It aims to monitor the low altitude atmosphere under the cloud base and capture its spatial distribution and convection process. In the viewpoint of polarization, the ice-crystals' flow and concentration change of the aerosols are monitored. The observation has been continued in the cloudy and rainy days. The thunder cloud is also a target.

In this report, the system specification is explained to clear the potential and the aims. The several observation data including the long-term observation will be shown with the consideration of polarization analysis.

8182-25, Session 6

Application of lidar and ceilometers to probe the vertical structure of the urban boundary layer and assess anomalies in air quality model PM2.5 forecasts

B. Gross, C. Gaan, F. Moshary, S. Ahmed, The City College of New York (United States)

In this paper, the predictions of the Weather Research and Forecast (WRF) and Community Multiscale Air Quality (CMAQ) Models using a variety of different Planetary Boundary Layer Height Parameterizations including the Modified Blackadar scheme, ACM2 and MYJ applied to the urban New York City area are assessed with the aid of vertical profiling and column integrated remote sensing measurements. In particular, we find that during mid-day when the boundary layer is well mixed, all WRF MLH's retrievals show excellent correlation to lidar derived convective boundary layer (CBL) height with correlation coefficients in summer of R~.85 although an over-bias ~ 300 meters is seem in some of the PBL parameterizations. Best results occur when the meteorological fields are nudged with surface meteorological fields but even in forecast mode, strong correlations are found although dispersion is somewhat higher. In achieving these strong correlations, we found it necessary to extract PBL height from lidar measurements using a Wavelet Covariance Transform (WCT) based analysis which is



modified using climatology based constraints to limit the domain of the search algorithm to better isolate the convective layer from the residual layer. Further restrictions on the matchup include absence of weather fronts to reduce mechanical shear and the absence of haze formation. Without these constraints, the matchups between the WRF and lidar retrievals are severely distorted in early morning during the growth phase of the CBL growth. The WCT method is also compared to the maximum variance technique which is shown to result in much poor correlations R \sim .45 and high dispersion.

In addition, we apply vertical ceilometer measurements to assess observed anomalies in WRF driven CMAQ models. In particular, strong overestimations in the surface PM2.5 mass in comparison to the Tapered Element Oscillating Microbalance (TEOM) measurements, which are most strongly observed during summer for pre-dawn and post-sunset, are found to be the result in underestimations of the Planetary Boundary Layer (PBL) heights which result in increased pollutant mass compressed near the surface and less to enhanced emissions during these periods. This interpretation is consistent with observations that the TEOM PM2.5 measurements are better correlated to path integrated CMAQ PM2.5 mass than near surface during these periods.

8182-26, Session 7

Depolarization lidar profiling during volcanic ash intrusion. Comparison between software and hardware techniques.

D. N. Nicolae, L. Belegante, E. Carstea, C. Talianu, National Institute of Research & Development for Optoelectronics (Romania)

Vertical profiles of linear particle depolarization ratio for volcanic ash were measured during the Eyjafjallajökull eruption in April 2010 using a multi-wavelength Raman Lidar system (Light Detection and Ranging) with three elastic channels (1064, 532 and 355nm - with depolarization on 532 - cross and parallel), two Raman channels (387 and 607nm) and a water vapor (408nm) channel. This paper presents results of linear particle depolarization ratio obtained in the vicinity of Bucharest, using the 532nm cross and parallel channels, for several case studies during the Eyjafjallajökull volcanic eruption.

The study is based on the investigation of linear particle depolarization ratio for specific layers measured by the lidar system and predicted by models to have volcanic origins. The data analysis is accompanied by a discussion of different depolarization calibration methods: software calibration and two hardware calibration methods. Advantages and drawbacks of these techniques are discussed and analyzed.

The hardware depolarization calibration involves the determination of the relative amplification factor V* obtained using either the +45° or the ±45° calibration methods. Both the volume particle depolarization ratio and linear particle depolarization ratio can be retrieved using the amplification factor V*. This type of calibration involves the implementation of a hardware module capable of rotating both the parallel and cross depolarization channels at ±45° in respect to the incident plane of the polarized light.

The software calibration involves normalization of the linear particle depolarization ratio to the value of the molecular depolarization ratio at an altitude with clean air, where we can assume that particle scattering can be neglected. The software calibration method is an appropriate tool in cases of clean atmosphere. The uncertainty is minimal because the particle scattering is very low at the calibration height.

The linear particle depolarization ratios from measurements performed during the Eyjafjallajökull volcanic eruption using both methods show some similarities. The uncertainty for the software method is considerable grater than in the case of hardware calibration either using the +45° or ±45° method. The observed differences in the results are mainly explained by aged volcanic ash arriving above Bucharest. The aged volcanic ash had a large vertical distribution, reaching up to the calibration height. The presence of ash up to that height had a negative impact on the software calibration, leading to an underestimation for the depolarization factor. This underestimation is not an issue in clean air, with linear particle depolarization close to zero.

8182-27, Session 7

Planetary boundary layer height retrieval at UMBC in the frame of NOAA/ARL campaign

S. Lolli, Leosphere France (France); R. Delgado, J. Compton, R. Hoff, Univ. of Maryland, Baltimore County (United States)

The determination of the depth of daytime and nighttime Planetary Boundary Layer Height (PBLH) must be known very accurately to relate boundary layer concentrations of gases or particles to upstream fluxes. Moreover, the air quality forecasts rely upon semi-empirical parameterizations within numerical models for the description of dispersion, formation and fate of pollutants influenced by the spatial and temporal distribution of emissions in cities, topography, and weather. The particulate matter (PM) mass measured at the ground level is a common way to quantify the amount of aerosol particles in the atmosphere and is the standard used to evaluate air quality. Remote sensing of atmospheric aerosols in the lower troposphere that affect air quality is done at UMBC by the Atmospheric Lidar Group, that supported the joint NOAA/ARL and NCEP ad hoc field study. These campaigns launched radiosondes from Howard University(HU) (26.6km south of UMBC) and RFK Stadium (29.15 km south of UMBC) during September 14-22, 2009 to developed a database to investigate the evolution and spatial variability of the PBLH. In this paper, we examined the potential for continual observation of PBLH by performing a statistical comparison of the spatial and temporal resolution of PBLH from lidar, wind profiler, and radiosonde measurements.

8182-28, Session 7

Tropospheric ozone investigations based on ozone DIAL measurements and photochemical regional modeling in Bucharest area

L. Belegante, R. Radulescu, C. Radu, National Institute of Research & Development for Optoelectronics (Romania); I. Balin, EnviroScopY SA (Switzerland)

Tropospheric ozone investigations are commonly used for assessing the photochemical potential of the lower troposphere i.e. PBL (Planetary Boundary Layer) altitudes. The presence of high quantities of ozone in the lower troposphere, due to certain meteorological conditions (summer, absence of clouds, high concentration of NOX due to anthropogenic activities) can have a negative impact on the quality of life.

Ozone concentration forecast is generally made using mesoscale models. One important particularity of mesoscale models is the possibility of generating not only ground forecasts, but vertical profiles of ozone concentration, a key feature needed for exchange studies in the troposphere.

One of the models capable of providing ozone vertical profiles is the Mesoscale Air Pollution 3D Modeling - Map3D. This tool is a permanent modeling system which provides daily forecast of the local meteorology and the air pollutant (gases and particles such as ozone) concentrations. The data provided by this model is mainly based on the existing air pollution point monitor stations at the ground level, but still not sufficient for an accurate input for ozone profiling. Taking into account that the uncertainty of the models is directly linked with the input data, measurement techniques that give reliable and complete information regarding vertical ozone profiles must be considered.

On the other hand, measurements can be used to validate model's output. The DIAL (Differential Absorption Lidar) technique is a widely used method for remote tropospheric and stratospheric ozone investigations. Remote sensing DIAL systems are appropriate tools for retrieving data used as input for different mesoscale models that use ozone cycles for pollutant modeling.

For the retrieval of tropospheric ozone profiles near Bucharest (lat 44.25N, long 27.6E), a four channels dial system, OLI (Ozone lidar) was used in the UV frequency range (266nm, 289nm, 299nm and 316nm). These four channels are split in "on"-"off" pairs according with the corresponding ozone absorption cross section, for different height intervals. Using three "on"-"off" pairs, the dial system can perform



measurements from 2 km reaching up to 12 km during night time, over a period of several hours with a spatial resolution of hundred meters.

The paper presents a comparison between measured ozone vertical profiles and the ones forecasted by MAP3D. This comparison highlights the limitation of the model in assessing ozone concentration especially in the vicinity of a complex city such as Bucharest. Also, extended analysis of advantages/outputs and drawbacks when using remote sensing investigations as a validation tool for a mesoscale model is discussed and analyzed.

8182-29, Session 7

Vertical resolved separation of aerosol types using CALIPSO level-2 products

E. Giannakaki, D. S. Balis, Aristotle Univ. of Thessaloniki (Greece); V. Amiridis, National Observatory of Athens (Greece)

A lidar-based method was used to separate profiles of optical parameters due to different aerosol types over different European Aerosol Research Lldar NETwork (EARLINET) stations. The method makes uses of particle backscatter profiles at 532nm and vertically resolved linear particle depolarization ratio measurements at the same wavelength. Values of particle depolarization ratio of 'pure' aerosol types (Saharan dust, biomass burning aerosols, anthropogenic aerosols, Volcanic ash aerosols) were taken from literature. Cases of CALIPSO space-borne lidar system were selected on the basis of different mixing state of the atmosphere over EARLINET stations. To identify the origin of air-masses four-day air mass back trajectories were computed using HYbrid Single-Particle Langrangian Integrated Trajectory (HYSPLIT) model, for different arrival heights, for the location and time under study was used. Also, the Dust REgional Atmospheric Modeling (DREAM) model was used to identify cases where dust from Saharan region was affecting the place under study. For our analysis we have used Atmospheric Volume Description (AVD) array to screen out everything that is not an aerosol. Also, the cloud-aerosol discrimination (CAD) score, which provides a numerical confidence level for the classification of layers by the CALIOP cloudaerosol discrimination algorithm was set between -80 and -100. CALIPSO extinction QC flags, which summarize the final state of the extinction retrieval, was also used. In our analysis we have used those measurements where the lidar ratio is unchanged (extinction QC = 0) during the extinction retrieval or it the retrieval is constrained (extinction QC = 1). The method was applied for different horizontal resolution of 5, 25, 45 and 105 km. The height-resolved lidar results were finally compared with column-integrated products obtained with Aerosol Robotic Network Sun photometer (AERONET) in order to see to what extent Sun photometer columnar data are representative when different aerosol layers are present in the atmosphere.

8182-30, Session 7

Indirect aerosol hygroscopic growth observations with a backscattering lidar, part II: six day breeze onset data analyses

E. Landulfo, P. F. Rodrigues, R. F. da Costa, F. J. da Silva Lopes, W. M. Nakaema, Instituto de Pesquisas Energéticas e Nucleares (Brazil)

Atmospheric aerosol particles have received much attention in recent years due to their importance in climate change. The influence of these particles on Earth's radiative budget depends on a number of factors, including their size distribution and chemical composition.

This work addresses a particular property of aerosols, namely, the extent to which they have affinity for water vapor. The size increase of aerosol particles resulting from water vapor uptake has important implications for the direct scattering of radiation and cloud droplets formation.

We used a single-wavelength backscatter LIDAR (532 nm), and relative humidity profiles obtained from radiosounding, to assess the hygroscopic growing factor of aerosols over Sao Paulo metropolitan region, for six days altogether on March and September 2007 and August 2009. In these days we had a breeze onset over the metropolitan area, potentially bringing marine aerosols and humidity

from the Atlantic Ocean. In this way we were able to detect a change in the boundary layer aerosol optical properties during these onsets using range corrected backscattering signal from LIDAR and a detailed analysis on the changes in backscattering coefficient profiles by a Klett analysis.

In order to infer the hygroscopic growing factor, we developed a fitting model algorithm, already proposed in the literature, calculating the backscattering coefficient at 532 nm for thirty minutes periods after and during the breeze onset and comparing backscattering at various altitude levels with a reference backscattering at the lowest relative humidity level inside the breeze, i.e., below the top of the mixing layer. In addition, we performed a comparison between the thirty minutes backscattering profiles inside the breeze with a reference thirty minutes backscattering profile before the breeze.

We present here the results for theses analyses and discuss the sensibility of the method applied to determine the hygroscopic growing under these conditions.

8182-31, Session 7

Supercontinuum laser absorption spectroscopy in the mid-infrared range for remote identification and concentration estimation of a multi-component atmospheric gas mixture

N. Cezard, A. Dobroc, G. Canat, M. Duhant, S. Lefebvre, ONERA (France); J. Fade, Institut de Physique de Rennes (France)

We report on our recent achievement of a mid-infrared supercontinuum fiber laser source in laboratory, and we address the potential applications of this new kind of source for broadband remote sensing of multiple gas species in the atmosphere. This sensing technique is referred here as Supercontinuum Laser Absorption Spectroscopy (SLAS). In fiber technology, supercontinuum radiation refers to a spectrally broad but spatially coherent light, obtained by spectral broadening of short pulses in specially-designed, highly non-linear fibers. Using fluoride fibers in the nanosecond regime, we have generated a wavelength supercontinuum covering the whole 2-3.5µm range, with an expected upcoming extension above 4µm. Experimental results are presented. Such a source can open great opportunities for remote sensing of multiple gas species in the atmosphere. Indeed, many important gases exhibit strong absorption lines in the mid-infrared, and the high spatial coherence of the laser beam favours long-range applications (>some hundreds of meters). By using a spectral library and realistic instrument parameters, we first simulate gas mixtures and the corresponding SLAS signals, including noise. Then we apply to these signals a processing method that performs unsupervised identification and concentration estimation of the constituent of the gas mixture. The algorithm uses complexity penalization principles so as to select the best compromise between model likelihood and model complexity. This method allows avoiding over-fitting the noise features by improbable gas components. Numerical results allow to assess the system's potential performance for identification/estimation tasks. Finally, we describe the status of our experimental SLAS breadboard, and first experimental results, obtained in the near infrared range (0.7-1.8 µm) with a commercial supercontinuum source, are shown to illustrate the SLAS method.

8182-11, Poster Session

Six-channel polychromator design and implementation for the UPC elastic/Raman lidar

D. Kumar, F. Rocadenbosch, S. Tomás, M. Sicard, A. Comeron, C. Muñoz, D. Lange, Univ. Politècnica de Catalunya (Spain)

A 6-channel dichroic-based polychromator is presented as the spectrally selective unit for the U.P.C. elastic/Raman lidar. The light emission is made at 355-nm (ultraviolet, UV), 532-nm (visible, VIS) and 1064-nm (near infrared, NIR) wavelength while in reception, the polychromator works as the beam separation unit and separates the



laser backscattered composite return into 3 elastic (355, 532, 1064nm wavelengths) and 3 Raman channels (386.7, 607.4 and 407.5-nm (water-vapor) wavelengths). The polychromator houses photo-multiplier tubes (PMT) for all the channels except for the NIR one, which is avalanche photodiode (APD) based.

The optomechanical design uses 1-inch optics and Eurorack standards. The APD-based receiver uses a XY-axis translation/ elevation micro-positioning stage due to its comparatively small active area and motorised neutral density filters are used in all the PMT-based channels to avoid detector saturation. The design has been specially optimized to provide homogeneous spatial light distribution onto the photodetectors and good mechanical repeatability in all the channels. They are acquired in mixed analogue and photon counting mode using Licel® transient recorders and controlled by means of a user friendly LabVIEWTM interface.

The paper focuses on the main polychromatic optical design parameters, that is, light collimation trade-offs, end-to-end transmissivity, net channel responsivity, light distribution and spot size onto the photodetectors.

The polychromator along with the rest of the U.P.C. lidar system has successfully been tested during a recent lidar system intercomparison campaign carried out in Madrid during Oct. 2010.

Keywords: lidar, multi-spectral, spot size, spatial distribution, end-toend transmissivity.

8182-32, Poster Session

Numerical simulation of laser Doppler anemometer

C. Gavrila, Univ. Tehnica de Constructii Bucuresti (Romania); I. Lancranjan, National Institute for Aerospace Research (Romania); S. I. Miclos, D. M. Savastru, National Institute of Research & Development for Optoelectronics (Romania)

Laser anemometers based on application of Doppler Effect have been developed and are used in-flight, on aircrafts for measurement of air flow parameters, mainly its speed versus the airplane. The air speed measurements are vital for safe flights. The main basic idea of Doppler techniques consists in measuring the frequency of scattered light. In this paper, we propose a numerical simulation of a laser Doppler Anemometer using finite element method. The main purpose of this study is to provide essential data for an improved design of this type of laser devices. The use of Laser Doppler Anemometer simulations is under continuous development by using more and more realistic values of input constructive laser device parameters. The considered development includes comparison with experimental results.

8182-33, Poster Session

Numerical modeling of fiber Bragg grating optical sensor

I. Lancranjan, National Institute for Aerospace Research (Romania); C. Gavrila, Univ. Tehnica de Constructii Bucuresti (Romania); S. I. Miclos, D. M. Savastru, National Institute of Research & Development for Optoelectronics (Romania)

Fiber optic sensors provide measurements in applications where the conventional electrical based sensors cannot be used, due to measurement requirements such as extreme temperature, small size, high sensor count, or high electromagnetic energy or radiation environments. In this paper, we propose a numerical modeling of an optical sensor based on a Fiber Bragg Grating (FBG) setup arrangement using finite element method. The effect of environmental parameters on the composite material machine part is observed by the modification of the length (L) of the Fabry-Perot interferometer formed by two Bragg grating mirrors. This variation can be studied by a transmission spectroscopy measurement. The developed sensor model takes into account the interaction of Fiber Bragg Grating (FBG) with composite material.

8182-34, Poster Session

Development of white light polarization lidar system

T. Somekawa, Osaka Univ. (Japan); K. Oka, Hokkaido Univ. (Japan); M. Fujita, Osaka Univ. (Japan)

We have been developing white light lidar using a terawatt laser system, which uses a coherent white light continuum in the wavelength range from 300 nm to more than 2200 nm as a lidar light source. The coherent white light continuum was generated by focusing an intense femtosecond laser pulse at 800 nm in atmospheric pressure Kr gas. The white light lidar has the advantage of performing the simultaneous multi-wavelength measurements at preferred spectral lines for various applications. In addition, the white light generated in Kr gas keeps the linear polarization of the original laser. The white light lidar can be applied to sensing the polarization of multi-wavelength backscattered light. Depolarization lidar measurements provide a promising method for distinguishing water and ice clouds and detecting nonspherical particles, because the depolarization ratio is known to depend on the degree of nonsphericity of the particles. The white light depolarization system was developed to permit simultaneous measurement of depolarization ratio at 450, 550, and 800 nm. Linearly polarized white light was transmitted to the atmosphere, and backscattered light was collected with a telescope of about 30 cm in a diameter and the light was separated into photomultiplier tubes using dichroic mirrors, polarizing beamsplitters, and interference filters. The results presented here provided the wavelength dependence to enable the 3-wavelength depolarization ratio to be used as a method to evaluate the size and shape of clouds without using conventional inversion algorithms. Also, a new approach, called channeled spectropolarimetry, is developed that provides a complete polarization description of clouds and aerosols. The complete set of Stokes parameters from 450 to 700 nm are reconstructed from one spectral measurement. We demonstrated this approach capable of characterizing the spectrally resolved polarization state of a linearly polarized beam transmitted by a birefringent sample. Current research is focused on detecting the Stokes parameters from a remote target.

8182-35, Poster Session

Lidar real time mapping of industrial flares in an industrial site in Cubatão/Brazil

J. Steffens, R. Guardani, Escola Politécnica da Univ. de São Paulo (Brazil); E. Landulfo, Instituto de Pesquisas Energéticas e Nucleares (Brazil); P. Firmino Moreira Junior, Escola Politécnica da Univ. de São Paulo (Brazil); F. J. da Silva Lopes, Instituto Nacional de Pesquisas Espaciais (Brazil); R. F. da Costa, Instituto de Pesquisas Energéticas e Nucleares (Brazil)

The industrial complex of Cubatão, in the state of São Paulo, Brazil, is one of the largest petrochemical and industrial sites in Brazil and has been subject of severe damage caused by continuous emissions of pollutants, as a result of the progressive industrialization in the area. Therefore it is necessary to monitor the area to be able to control and to prevent environmental issues. In a partnership with the University of São Paulo (USP) the Brazilian oil company PETROBRAS has started off an Environmental Research Center - CEPEMA- located in the industrial site, in which the development of fieldwork has been carried out.

Elevated flare stacks present a difficult measurement challenge, because it is extremely difficult to determine concentrations in the post-combustion gas of operational flares by sampling techniques. A laser remote sensing measurement system has been developed for the continuous real-time monitoring of industrial atmospheric emissions from industrial flares in an oil refinery site located in Cubatão. The system is able to perform 3 D scanning and profiling around the emission point.

Tests were carried out using a scanning system pointed to the petrochemical flare. The mapping was obtained from a sequence of measurements at different altitudes and azimuthal and elevation angles, resulting in a 3 D image of the flare shape plus the flame itself. The measurements have generated estimates of the aerosol size distribution based on the backscattering ratio at three distinct wavelengths, namely: 1064/532 nm, 1064/355 nm, and 532/355 nm.

The system can be used in the real time monitoring of industrial aerosol emissions and in the control of industrial processes.

8182-36, Poster Session

Remote sensing detection of atmospheric pollutants using lidar, sodar and correlation with air quality data in an industrial area

J. Steffens, R. Guardani, Escola Politécnica da Univ. de São Paulo (Brazil); E. Landulfo, Instituto de Pesquisas Energéticas e Nucleares (Brazil); P. Firmino Moreira Junior, Escola Politécnica da Univ. de São Paulo (Brazil); R. F. da Costa, F. J. da Silva Lopes, Instituto de Pesquisas Energéticas e Nucleares (Brazil)

Monitoring of atmospheric industrial emissions is a relatively difficult task due to the adverse conditions that prevail in most industrial stacks, like access difficulties, high temperature, and corrosive gases. A practical monitoring sensor for industrial atmospheric emissions should allow for on site, continuous, and unattended operation over a long period of time preferably achieved by an instrument with a simple and robust design. Optical remote sensing techniques have obvious advantages for gas and aerosol emissions monitoring, since they enable the operation over large distances, far from hostile environments, and fast processing of the measured signal.

In this study two remote sensing devices, namely a LIDAR (Light Detection and Ranging) for monitoring the vertical profile of backscattered light intensity, and a SODAR (Accoustic Radar) for monitoring the vertical profile of the wind vector were operated during specific periods. The collected and processed data were compared with data on air quality collected by ground level monitoring stations, in order to verify the possibility of using the remote sensing techniques to monitor atmospheric emissions. The campaigns were carried out in the area of the Environmental Research Center (CEPEMA) of the University of São Paulo, in the city of Cubatão, Brazil, a large industrial site where a number of different industries are located, including an oil refinery, a steel plant, plus fertilizer, cement and chemical/petrochemical plants. The local environmental problems caused by the industrial activities are aggravated by the climate and topography of the site, unfavorable to pollutant dispersion.

Results of campaigns under different atmospheric conditions are presented, showing results correlations of LIDAR and SODAR vertical profiles with the air quality data using multivariate techniques, aimed at identifying in a quantitative basis the similarities in the behavior of groups of the variables considered in the study.

8182-37, Poster Session

Experimental evaluation of a model for the influence of coherent wind lidars on their remote measurements of atmospheric boundary-layer turbulence

M. Sjöholm, T. Mikkelsen, L. Kristensen, Risø National Lab. (Denmark); S. Kapp, Robert Bosch GmbH (Germany)

Affordable coherent wind lidars based on modern telecom components have recently emerged on the wind energy market spurred by high demand of the wind energy industry for compact and accurate remote sensing wind and turbulence profilers.

Today, hundreds of ground based wind lidars that achieve the range resolution by either focusing a continuous-wave laser beam or by gating a pulsed laser beam are used for measuring mean wind and turbulence profiles in the lower atmospheric boundary-layer. However, detailed understanding of the influence of the spatial filtering of the lidars on their precise assessment of turbulence is still a challenge.

For assessment of the fine structure turbulence, and in particular for the easy and fast assessment of the dissipation rate of turbulent kinetic energy within the Kolmogorov inertial subrange, we have modeled the atmospheric velocity structure functions and spectra obtainable from fixed-orientation along-beam wind measurements by these lidars.

From knowledge about the spatial sampling functions of the two types of lidars, we derive useful and simple analytical expressions and



compare their filtering effects of the along-beam turbulent velocity. In particular, we have established a practical and simple method for determination of the turbulence fine-structure (and spectra) in terms of the rate of dissipation of specific kinetic energy in the atmospheric boundary layer and the lidars pointing angle relative to the mean wind direction.

The model is experimentally evaluated with data obtained with a pulsed lidar pointing horizontally into horizontally homogeneous turbulence encountered at the top level of a 125 m tall meteorological tower, equipped with an in-situ turbulence measurement device (a three-dimensional sonic anemometer) for intercomparison.

Our experimental study has revealed that the simple analytical model (Risø-R-1762: http://www.risoe.dtu.dk/Knowledge_base/publications/ Reports/ris-r-1762.aspx) accounts well for the observed fine structure turbulent spectra and their dependence on the pointing direction of the lidar beam relative to the mean wind direction. The results demonstrate that turbulence dissipation rates, and hence boundary-layer turbulence, can easily be obtained from simple wind lidar-based fine structure measurements.

8182-38, Poster Session

Retrieval of aerosol optical thickness from synergy of ceilometer, aethalometer and nephelometer observations during nights

K. M. Markowicz, O. Zawadzka, Univ. of Warsaw (Poland)

The aerosol optical thickness is usually measured by sun photometers during clear sky conditions. Observation can be performed only during daytime, which significant limited diurnal cycle of the aerosol optical thickness and study longwave aerosol radiative forcing during night. Active remote sensing provided opportunity to estimate this quantity also during the night. For this purpose we use the CHM-15K Jenoptik ceilometer together with aethalometer and nephelometer. We developed two method to estimate aerosol optical thickness at 1064 nm to provide its diurnal cycle. First method is based on the ceilometer range and overlap corrected signal only. The overlap correction was estimated by a horizontal observation during homogenous conditions. It allowed reduce the overlap from original 650 m to 250 m. In the second method the aerosol optical properties measured by the aethalometer and nephelometer at the surface and are used as boundary conditions to solve lidar equation. For this purpose a forward method are used. This method required estimation of the lidar calibration coefficient. This quantity is obtained using the ceilometer auto-calibration technique applied for low level stratocumulus cloud. Calculated profile of the aerosol extinction coefficient from forward method is used for the aerosol optical thickness estimation. The aethalometer and nehelpmeter instruments are use to determine of the aerosol extinction coefficient and lidar ratio. The last parameter is retrieval from spectral variability of the aerosol absorption, scattering and hemispheric backscatter coefficients.

8182-39, Poster Session

Uncertainty computation in aerosol size distribution retrieval in multiwavelength lidar extended to IR wavelengths above 1.5µm

B. R. Herman, Finnish Meteorological Institute (Finland)

Multiwavelength lidar is a well established method of retrieving high vertical resolution profiles of aerosol properties. Traditionally such lidars have implemented Nd:YAG lasers generating pulses of light at 1064, 532, and 355nm. There have been few if any studies of the possibility of improving retrievals of aerosol properties by incorporating measurements of backscatter at wavelengths at longer wavelengths. A lidar operating at such a wavelength could potentially be used in unattended operation since there are less strict requirements on eye safety.

Therefore the work presented shows the results of simulated retrievals of aerosol properties from inversion of standard lidar measured optical coefficients combined with backscatter and depolarization coefficients at infrared wavelengths of 3.3, 2.2, and 1.5um. In particular, configurations of combining one or more wavelength > 1064nm



along with 532nm backscatter and depolarization is analyzed. Such a configuration could potentially be implemented in conjunction with a commercial off-the-shelf 532nm micro-pulse lidar.

The inversion of optical coefficients to retrieve the parameters of the multiple modes of an aerosol size distribution uses an algorithm that is within the general class of Metropolis-Hastings Markov chain Monte Carlo algorithms. The Metropolis-Hastings method is a way of generating random samples congruent with an arbitrary probability density function.

This capability is critical in the case of using a parameterized definition of an aerosol size distribution, e.g. multiple gamma-distributions each with their own effective radii, volume concentrations, and distribution width. In such cases Gaussian-distributed measurement errors translate into grossly non-Gaussian likelihood functions. The specific implementation of the Metropolis-Hastings algorithm was designed to be efficient in handling such likelihood functions with complicated structures. In using this Monte Carlo technique uncertainty of the inverse is given automatically since an ensemble of solutions is produced in a way that is directly related to the posterior probability density function that describes uncertainty of the aerosol size distribution.

Initial results using this analysis have shown that including infra-red backscatter at wavelengths longer than the standard 1064nm greatly reduces uncertainty of coarse mode volume concentration.

8182-40, Poster Session

First open field measurements with a portable CO_2 Lidar dial system for early forest fires detection

P. Gaudio, M. Gelfusa, I. Lupelli, A. Malizia, C. Serafini, M. Richetta, Univ. degli Studi di Roma Tor Vergata (Italy); C. Bellecci, CRATI S.c.r.I. (Italy)

Lidar and dial techniques are very well established technologies to explore the atmosphere and different groups have already shown experimentally the possibility to measure the density variation in the atmosphere due to plumes emitted in forest fire events with this kind of systems. The aim of the present work is to demonstrate the capabilities of our mobile lidar/dial system, based on a CO2 laser, for detecting forest fires and minimizing false alarm events. For this purpose, our system can be operated in both lidar and dial measurements configurations in sequence. The first lidar measurement is performed to evaluate the variation of the local density in atmosphere, using a non-absorption water wavelength 10R18 (10.571 µm). If the returned signal reports a backscattering peak, the presence of a fire is probable. To confirm this hypothesis, a second dial measurement is carried out to reveal a second component emitted during the combustion process. The chosen second component is water vapour, which is, as it is well-known, largely produced at the first combustion stage. Measuring the water concentration peak after the detection of the aerosol density increment (referred to the standard mean atmospheric value) represents a good method to reduce false alarms with a dial system. In order to test this methodology, a first set of measurements has been performed in a field near the Engineering Faculty of the University of Rome "Tor Vergata". A quite small controlled-fire has been lighted into a box at different distances from the system. The data acquired at the two wavelengths (10R18 and 10R20) have been averaged on 100 elastic backscattered lidar signals. The first results confirm the effectiveness of the measurement strategy for reducing the number of false alarm preserving the early detection.

The first measurements with our mobile lidar system in open field in both configurations will be presented and discussed in detail.

8182-41, Poster Session

Initial analysis from a lidar observation campaign of sugar cane fires in the Central and Western portion of the São Paulo State, Brazil

F. J. da Silva Lopes, P. F. Rodrigues, Instituto de Pesquisas Energéticas e Nucleares (Brazil); J. M. Bassan, Instituto de Pesquisas Meteorológicas (Brazil); G. Held, Univ. Estadual de São Paulo (Brazil); E. Landulfo, Instituto de Pesquisas Energéticas e Nucleares (Brazil)

The Central and Western portion of the São Paulo State has large areas of sugar cane plantations, and due to the growing demand for biofuels, the production is increasing ever year. During the harvest period some plantation areas are burnt few hours before the manual cutting, causing significant quantities of biomass burning aerosol to be injected into the atmosphere. During August 2010, a field campaign has been carried out in the town of Ourinhos, situated in the south-western region of São Paulo State. A 2-channels Raman Lidar system, two meteorological Radars, a Sodar and some aerosol samplers had been deployed. CALIPSO Satellite observation will be used to compare with the biomass burning aerosols detected in that regional atmosphere. Although the campaign yielded 30 days of measurements, this paper will be focusing only on one case study, when aerosols, released from nearby sugar cane fires, were detected by the Lidar during a CALIPSO overpass. The meteorological radar, installed in the central region of São Paulo, had recorded "echoes" (dense smoke comprising aerosols) from several fires close to the Raman Lidar system, which also detected an intense load of aerosol in the atmosphere. The Sodar data provided half-hourly wind speed and direction up to 800 m above ground level, in order to track the dispersion of the aerosols. Since the plumes can extend to 6 km or more, wind and temperature profiles from the Meso-Eta Model Analysis (00 and 12 UT) will also be added. Preliminary Lidar Ratio values from the 532 nm elastic and 607 nm Raman channel analyses have indicated the predominance of aerosol from biomass burning sources. Such results are correlated with the products from the onboard Lidar system of the CALIPSO satellite.

8182-42, Poster Session

Validation of CALIPSO level-2 products using a ground-based lidar in Thessaloniki, Greece

E. Giannakaki, E. Vraimaki, D. S. Balis, Aristotle Univ. of Thessaloniki (Greece)

We present initial aerosol validation results of the space-borne lidar CALIOP -onboard the CALIPSO satellite - Level 2 extinction coefficient profiles, using coincident observations performed with a ground-based lidar in Thessaloniki, Greece (40.5° N, 22.9° E, 50m above sea level). A ground-based backscatter/Raman lidar system is operating since 2000 at the Laboratory of Atmospheric Physics (LAP) in the framework of the European Aerosol Research Lldar NETwork (EARLINET), the first lidar network for tropospheric aerosol studies on a continental scale. Since July 2006, a total of 150 coincidental aerosol ground-based lidar measurements were performed over Thessaloniki during CALIPSO overpasses. The ground-based measurements were performed each time CALIPSO overpasses the station location within a maximum distance of 100 km. The duration of the ground-based lidar measurements was approximately two hours, centred on the satellite overpass time. The analysis was performed for 4 different horizontal resolutions of 5, 25, 45 and 105 km. For our analysis we have used Atmospheric Volume Description (AVD) array to screen out everything that is not an aerosol. Also, the cloud-aerosol discrimination (CAD) score, which provides a numerical confidence level for the classification of layers by the CALIOP cloud-aerosol discrimination algorithm was set between -80 and -100. CALIPSO extinction QC flags, which summarize the final state of the extinction retrieval, was also used. In our analysis we have used those measurements where the lidar ratio is unchanged (extinction QC = 0) during the extinction retrieval or it the retrieval is constrained (extinction QC = 1). The comparison was performed both for extinction and backscater



coefficient profiles. For clear sky conditions, the comparison shows good performances of the CALIPSO on-board lidar.

8182-43, Poster Session

The usage of multiwavelength micropulse lidar in atmospheric aerosols study

M. Posyniak, S. P. Malinowski, T. Stacewicz, K. M. Markowicz, Univ. of Warsaw (Poland); T. Zielinski, T. Petelski, P. Makuch, Institute of Oceanology (Poland)

We present selected results of investigation of atmospheric aerosols with Multiwavelength Micropulse Lidar (MML) [1]. Pulsed diode pumped Nd:YAG laser (DPSS) is used to generate light at three wavelengths (1064, 532 and 355 nm). Energies of pulses are 30, 15 and 7 μ J respectively, while their repetition rate is 1,5 kHz. Cassegrain telescope with the mirror of 170 mm in diameter collects return signals, which are then separated by a polichromator and detected with photomultipliers and photon counters. Application of DPSS laser makes MML suitable for permanent observation.

The instrument was used in following measurement campaigns:

- 2009 COAST campaign on Baltic Sea during which marine aerosol was investigated from research vessel "Oceania";

- 2010 RFP IOP campaign in southern Poland, aimed at studies of aerosol direct effect in the rural conditions.

Example lidar profiles will be presented and discussed. In particular the profiles of backscatter coefficient of marine and rural aerosol will be shown to demonstrate advantages and drawbacks of MML. Various techniques improving signal to noise ratio and methods of retrieval of aerosol optical properties will be discussed. In particular, we will present application of techniques based on additional information about aerosol optical thickness from hand-held sun-photometer Microtops (e.g. Welton et all [2]) which allow to improve estimation of extinction profiles retrieved with Klett - Fernald method.

[1] M. Posyniak, T. Stacewicz, M. Miernecki, A K. Jagodnicka, S. P. Malinowski, Multiwavelength micropulse lidar for atmospheric aerosol investigation, Optica Applicata vol 40, 2010

[2] Welton, E.J., K.J. Voss, H.R. Gordon, H. Maring, A. Smirnov,
B. Holben, B. Schmid, J.M. Livingston, P.B. Russell, P.A. Durkee,
P. Formenti, M.O. Andreae, "Ground-based Lidar Measurements of Aerosols During ACE-2: Instrument Description, Results, and Comparisons with other Ground-based and Airborne Measurements", Tellus B, 52, 635-650, 2000.

8182-44, Poster Session

Estimating the relationship between aerosol optical thickness and PM10 using lidar and meteorological data in Limassol, Cyprus

D. G. Hadjimitsis, A. Nisantzi, Cyprus Univ. of Technology (Cyprus)

Daily Aerosol Optical Thickness (AOT) values from MODIS satellite instrument may be useful to predict Particulate Matter (PM) values in local scale in accordance with vertical profile of the atmosphere and meteorological data. In the frame of 'AIRSPACE' project, correlations between the AOT retrieved from MODIS to sun photometer data from both hand-held MICROTOPS II and ground-based CIMEL from the AERONET network were applied with good correlation coefficients. This permits to use MODIS retrievals as a reliable tool for assessing PM whereas the relationship between these two quantities is not lucid. The main study area is the centre of Limassol in Cyprus. Results concerning the relation between AOT and PM are presented. In cases where high AOT values corresponded to low PM surface values, the vertical distribution of aerosols from lidar allows the AOT to be quantifies within the boundary layer as this fraction best represents the PM measurements in a well-mixed layer. The results are part of the 'AIRSPACE' project funded by the Cyprus Research Promotion Foundation and EC regional Funds.

8182-45, Poster Session

Mathematical modeling on synthetic aperture ladar imaging

J. Wu, M. Zhao, Z. Zhao, F. Li, D. Wang, Institute of Electronics (China)

Mathematical models are set up by means of diffraction optics theory to simulating imaging performance of Synthetic Aperture Ladar (SAL) whether operating in stripmap mode or spotlight mode. Detailed image forming data equations are given, providing a useful and helpful tool in developing experimental SAL imaging system. Several simulating results with vivid pictures are given as examples.

8182-46, Poster Session

The equation of optical location for supergaussian fan ladar

G. M. Krekov, G. G. Matvienko, A. A. Lisenko, V.E. Zuev Institute of Atmospheric Optics (Russian Federation)

New modification of the ladar equation is proposed for the special case of supergaussian fan beams with superior uniformity and efficiency in remote sensing. Results of the system analysis have been incorporated into computer simulation that is used to optimize ladar parameters. Finally, a method of implementing a practical thresholding circuit is presented.

Laser detection and ranging formed into an independent research field by the early 1980s. Significant progress in quantum electronics has allowed not only the development and manufacture of unique LADAR (Laser Detection And Ranging) systems, but also their efficient use in various technological fields. An advantage of active optical LADAR systems is the possibility of giving information color to a LADAR signal, and this facilitates considerably the solution of problems of detection and identification of remote objects in the atmosphere, the space, and on the Earth's surface under conditions of noise of both instrumental and radiative origin. The field of ladar application is very wide: from the remote monitoring of the state of the atmosphere to high-accuracy measurements of coordinates and dynamic characteristics of smallsized objects. In the last time, the interest to the new application of the technique and technology of ladar sensing to the urgent problem of on-line monitoring of traffic increased. This report is concentrated at particular features of this problem. Among few papers devoted to this problem, the most promising, in our opinion, is the idea to use two stationary (in space) fan laser beams acting as a speed trap. The ideology of time-of-flight (TOF) ladars remains, but in place of mechanic scanning within a traffic lane it is proposed to use a plane or fan laser beam with the intensity close to the so-called supergaussian profile, because it allows one to avoid difficulties connected with the recording of edge parts of a laser illumination spot. The direct increase of the laser power leads to overrange of laser safety limits or of the detector dynamic range. When deriving the optical ladar equation for the supergaussian fan ladar, we proceed from the fact that the canonic form of the main ladar equation is not applicable to the interpretation of signals of modern imaging lidars, which form 3D images of sensed objects allowing their identification. Within the linear systems approach, we have corrected the lidar equation in order to take into account the complex spatiotemporal source function and to use suitable BRDF models for the more adequate description of sensed objects.

The simulation based on the derived optical ladar equation for the fan supergaussian beam yielded temporal profiles for an ensemble of reflected pulses at an entrance of the receiving system as functions of the size and shape of the illumination spot, shape and dimensions of the reflecting surface, reflection coefficients of transport vehicles and road surface, pulse duration, and geometry of the transceiving system.



8182-47, Poster Session

Multiwave lidar sensing of atmospherical aerosol based on a genetic algorithm

G. M. Krekov, G. G. Matvienko, A. J. Sukhanov, V.E. Zuev Institute of Atmospheric Optics (Russian Federation)

The advent of broadband laser radiation sources allows us to find their new application in problems of remote sensing of the atmosphere, in particular, in problems of determination of microphysical atmospheric parameters such as cloudiness. The effect of filamentation gives rise to a beam with a narrow divergence angle and a wide spectrum from 0.4 to 2 µm, which covers a lot of absorption lines of atmospheric gases and bands falling within atmospheric windows. This opens a way for the selection of wavelength for the sensing of atmospheric aerosols. In this paper, we have analyzed the absorption spectra of atmospheric gases and selected four spectral ranges near 1.28, 1.56, 1.61, and 2.13 µm, which are free from the effect of absorption and most informative with respect to the spectrum of cloud droplets. A numerical experiment on the multiwave lidar sensing of stratified inhomogeneous cloudiness has been conducted within the framework of the Monte Carlo technique. Then the inverse problem on the reconstruction of optical and microphysical characteristics of cloudiness, such as vertical profiles of the extinction and backscattering coefficients, as well as the particle number density and the size spectrum as functions of the depth of penetration into the cloud layer, has been solved. For the solution of this inverse problem, a new method of genetic search has been proposed. This method combines the procedure of reconstruction of optical and microphysical characteristics of clouds and aerosol formations from signals received at several optimally selected wavelengths in a single algorithm. The genetic algorithm is a heuristic algorithm simulating the process of natural evolution for the solution of optimization problems. It allows one to find a global optimum. The general principle of the genetic algorithm consists in the formation of a set of solutions referred to as a population. Then two solutions are selected from the population, and the recombinationcrossing-over operation is performed with them. This usually corresponds to an exchange of bit sequences in elements of the solution vector or the following operation , where is a random value from 0 to 1, are elements of the new solution vector and parent pairs. Then the mutation operation is performed with the new solution. This operation is a change of the bit representation or a change of the element of the solution vector. The obtained solution is included into the population of solutions. The operation of selection of parent pairs and creation of a new unit can consist of a certain number of steps. After a certain number of iterations, the unit or units corresponding to the worst solutions or to the maximal probability are removed from the population. The worst solution is determined with the use of the socalled fitness function. Usually, the role of the fitness function is played by an optimizable functional. In the canonic form, this algorithm often leads to the situation that a local minimum is treated as a global one, which corresponds to the degeneration of the solution population, and the convergence in this case is rather slow. We decided to modify the fitness function and the genetic algorithm for the faster convergence to the sought solution. The report discusses peculiarities of the algorithm of reconstruction of microphysical characteristics of cloudiness and aerosol formations with the use of white-light lidars based on lasers with the femtosecond pulse duration and presents numerical estimates confirming the efficiency of this algorithm under conditions of increased multiple scattering background.



Monday-Tuesday 19-20 September 2011

Part of Proceedings of SPIE Vol. 8183 High-Performance Computing in Remote Sensing

8183-01, Session 1

Fuzzy clustering of large satellite images using high performance computing

D. Petcu, D. Zaharie, S. Panica, Univ. de Vest din Timisoara (Romania); A. S. Hussein, Ain Shams Univ. (Egypt); A. T. Sayed, H. E. El-Shishiny, IBM Ctr. for Advanced Studies in Cairo (Egypt)

Unsupervised classification, also called clustering, plays an important role in the analysis of satellite images. It aims to identify spatially continuous regions of pixels characterized by similar features, which most likely, corresponds to similar ground cover types, e.g. generate vegetation maps of an area of interest.

There are several challenges related to the unsupervised classification of satellite images. The first one is related to the fact that the images are usually large with respect to the number of pixels and the number of spectral bands. This leads to the necessity of developing parallel and/or distributed variants of the clustering algorithms. On the other hand, the pixels of a satellite image may contain spectral information corresponding to different ground components, accordingly it's difficult to classify a pixel in just one class. One way of dealing with this problem is to allow a pixel to belong to different classes with corresponding membership values as is specific to fuzzy clustering. Another issue, caused by the limited sensors sensitivity, is the noise, which can mislead the clustering process. A possibility of limiting the negative impact of noise on the clustering results is to take into account, besides the pixel features (corresponding to spectral information), the spatial information, i.e. the relationship between neighboring pixels. The inclusion of the spatial information in the clustering process leads to some extra computational costs. All these motivate the interest in developing parallel implementations of algorithms for fuzzy clustering involving spatial information. Currently there are parallel variants of traditional fuzzy clustering algorithms but, at our updated knowledge, their extension to the case of algorithms involving spatial information has not been investigated.

The aim of the work presented in this paper is to extend the existing approaches of parallelizing the Fuzzy C-Means (FCM) algorithm to the case of spatial variants (e.g. FCM with spatial information and Gaussian kernel based FCM). The proposed parallelization is based on dividing the images in spatial slices. Several slicing strategies are analyzed with respect to their ability to ensure a balanced load of processors and to limit the size of data transferred between different processors. There are also proposed parallel variants for the computation of cluster validity indices useful in the context of semi-automatic identification of the number of classes. The parallelization approach is mainly based on the idea to exploit, as much as possible, the collective computations and to reduce the volume of the communication between processors.

The parallel version of the classical FCM, the variants proposed for the FCM using spatial information and the Gaussian Kernel-based FCM were implemented, in C using MPICH2, and tested on a cluster of PCs and on a IBM BlueGene supercomputer. The scalability analysis on the later involved up to 1024 processors and illustrated that once the spatial slicing of the image is appropriate, the speed-up is close to the ideal one.

8183-02, Session 1

3D-processor arrays accelerators for highpPerformance computing in remote sensing applications

A. Castillo Atoche, Univ. Autónoma de Yucatán (Mexico); J. Vazquez Castillo, Univ. de Quinatana Roo (Mexico)

In the real-world Geospatial intelligence and resource management, the electronic images provided with modern remote sensing (RS) sensors suffer drastically from different sources of errors due to limited system resolution, observation noise, speckle effects and propagation channel perturbations. Geospatial applications for the RS image enhancement/ reconstruction is now a mature and well developed research field, presented and detailed in many works. The understanding of the Geospatial imagery is an important intelligent procedure that substantially improves the enhancement of the real-world noised low resolution RS scenes. Now, although the existing theory offers a manifold of statistical and descriptive regularization techniques for reconstructive imaging, in many application areas there still remain some unresolved crucial theoretical-level and computational-level problems related to large scale sensor array or synthesized array real-time enhancement image processing. Thus, the predominant practice-motivated challenge is to solve the RS image enhancement/ reconstruction tasks in a high-performance computational fashion that admits the real time implementation.

In this paper, we address a new approach for such real-time enhancement of the large-scale Geospatial imagery with the robust Bayesian regularization (RBR) method, for solving the RS image enhancement/reconstruction of inverse problems adapted for an efficient HW/SW co-design-based paradigm using the conceptualized 3D-PAs as accelerators units.

The initial problem of enhancement/reconstruction of the Geospatial RS imagery at the software level stage consist in to solve the illconditioned inverse spatial spectrum pattern (SSP) estimation problem with model uncertainties via the fusion of the Bayesian minimum risk (BMR) estimation strategy.

Next, the real time implementation of the algorithmic tasks is approached via Hardware-Software (HW/SW) co-design oriented at the Field Programmable Gate Array (FPGA) digital implementation of the RBR method with the efficient implementation of the 3D-PAs as accelerators units.

Alternatives HW/SW co-design propositions which use PAs structures as accelerators units have been developed in other works, in order to achieve the near real time implementation of the regularization-based procedures for the reconstruction of RS Geospatial applications. However, the addressed here approach develops a new paradigm for the integration of 3D-PAs-based architectures as specialized hardware modules integrated in the HW/SW co-design scheme that results in a considerably decreased computational complexity and required processing time for implementing the RBR method in a Virtex-5 FPGA platform.

8183-03, Session 1

A GPU accelerated extended Kalman filter

S. Wei, Tamkang Univ. (Taiwan); B. Huang, Univ. of Wisconsin-Madison (United States)

The extended Kalman filter is one of the most widely used techniques for state estimation of nonlinear systems. In its forecast and data assimilation steps, many matrix multiplication and inverse operations are involved. As recent graphic processor units (GPU) have shown to provide much speedup in matrix operations, we will explore in this work a GPU-based implementation of the extended Kalman filter. The Compute Unified Device Architecture (CUDA) on the Nvidia Tesla GPU hardware will be used for comparision with a single threaded CPU counterpart.

8183-04, Session 1

Efficient data storage of astronomical data using HDF5 and PEC compression

C. Estepa, Institute for Space Studies of Catalonia (Spain); J. Portell de Mora, Institut d'Estudis Espacials de Catalunya (Spain) and Institute for Cosmos Sciences (ICCUB) (Spain); E. García-Berro, Univ. Politècnica de Catalunya (Spain); J. Castañeda, Univ. de Barcelona (Spain); M. Clotet, Institute for Space Studies of Catalonia (Spain)

Future space missions are based on a new generation of instruments that often generate vast amounts of data. Transferring this data to ground, and once there, between different computing facilities is not an easy task whatsoever. A leading example of these missions is Gaia, a space astrometry mission of ESA. To carry out the data reduction tasks on ground, an international consortium, the so-called Data Processing and Analysis Consortium (DPAC), has been set up. Among the tasks of DPAC perhaps the most demanding one is the Intermediate Data Updating (IDU), which will have to repeatedly re-process nearly 100TB of raw data received from the satellite using the latest instrument calibrations available. One of the best data compression solutions is PEC (Prediction Error Coder). PEC is a highly optimized entropy coder that performs very well with data following realitic statistics. On the other hand, the HDF5 file format provides a completely indexed, easily customizable file with a quick and parallel access. Moreover, HDF5 has a friendly presentation format and multi -platform compatibility. Thus, it is a powerful environment to store data compressed using PEC. Here we show the integration of both systems for the storage of Gaia raw data. Here we show that the file sizes obtained using HDF5 and PEC on realistic Gaia data are often smaller than those obtained using other compression algorithms that require more computing load.

8183-05, Session 1

An efficient framework for Java data processing systems in HPC environments

A. D. Fries, J. Portell de Mora, Univ. de Barcelona (Spain) and Institute for Cosmos Sciences (ICCUB) (Spain); R. Sirvent, Ctr. Nacional de Supercomputación (Spain); G. L. Taboada, Univ. of A Coruña (Spain); J. Castañeda, Y. Isasi, Univ. de Barcelona (Spain) and Institute for Cosmos Sciences (ICCUB) (Spain)

Java is a commonly used programming language, although its use in High Performance Computing (HPC) remains relatively low. In this work we investigate the current status of Java in HPC, including the libraries available to support the execution of Java applications in such environments. The analysis of the currently available Java communication libraries for HPC revealed a number of projects that target the support of low latency networks although their efficiency is relatively low due to the use of TCP/IP-based protocols (socketsbased projects) or a significant buffering overhead for JNI-based MPI wrapper projects.

Significantly for this work, we identify F-MPJ communication support as a highly efficient solution for data tranfers on low latency networks due to its direct access to the NIC and the reduction of the buffering and serialization overhead. In this paper we present a Java-based library, called DpcbTools, designed to provide a set of functions useful to Java applications running in HPC environments. It includes a set of communication routines, which make use of an underlying implementation of Message Passing Interface (MPI), yet providing a higher level of abstraction. DpcbTools also includes a framework that allows for the launching, monitoring and management of Java applications in HPC environments, making use of JMX (Java Management Extensions) to communicate with remote Java Virtual Machines. The Gaia Data Processing and Analysis Consortium (DPAC) is the data processing pipeline that will process the scientific data returned by the Gaia astrometry satellite of the European Space Agency. In this paper we briefly describe the DPAC, how DPAC makes



use of DpcbTools, and how the DpcbTools framework can be used to manage and monitor the execution of DPAC systems. In order to assess the usefulness and performance of DpcbTools, we describe some tests which compare the performance of specific parts of DPAC operating without the use of DpcbTools, against the performance obtained when using DpcbTools. For these tests we have used up to 512 processor cores of the MareNostrum supercomputer.

8183-06, Session 2

Geostatistical analysis of Landsat-TM lossy compression images in a high performance computing environment

L. Pesquer, A. Cortés, I. Serral, X. Pons, Univ. Autònoma de Barcelona (Spain)

Lossy data compression provides many benefits that facilitate accessing, sharing and transmitting huge spatial datasets in environments with limited storage. Despite this, lossy data compression procedures modify the original information, and therefore rigorous studies are needed to understand the effects and consequences of this manipulation. This work aims to explore the differences in the spatial pattern domain between the original and compressed images, and, in particular, the impact on the geostatistical use of remote sensing images. This comparison of spatial patterns adds more detailed information than merely comparing the global parameter peak signal with the noise ratio (PSNR).

Geostatistical analysis, specifically variogram analysis, is a powerful tool for spatial pattern comparison purposes, but it is an especially slow procedure for processing large amounts of remotely sensed data. Indeed, this computational constraint makes it necessary to use distributed environments. High Performance Computing (HPC) provides methods for distributing computation with the aim of reducing the total execution time. The proposed parallel solution is based on a master/worker scheme and using MPI as the message-passing library and obtains an efficient computing performance.

For this work purposes, radiometrically and geometrically corrected Landsat-5 TM images from April, July, August and September 2006, corresponding to two areas of about 22500 ha of the 197-031 and 198-31 path-rows, were compressed using the JPEG 2000 standard at a wide range of compression ratios (2.5:1, 5:1, 10:1, 50:1, 100:1, 200:1 and 400:1, from soft to hard compression). The exhaustive geostatitical analysis exploring all spectral bands on several scene dates, on different study regions, for non-compressed images and all detailed compression ratio, need executed on an HPC environment. IBM cluster, in a research laboratory was a suitable computing environment. It is formed by 32 nodes, each with two Dual Core Intel(R) Xeon (R) 3.0 GHz processors with 12 Gb of RAM, which communicate with Integrated dual Gigabit Ethernet.

The study concludes that geostatitical analyses in all compression ratios maintain the variogram shapes and on the higher ratios (more than 100:1) reduce variance in the sill parameter by about 20 to 25%. Moreover, the proposed MPI parallel solution demonstrates that HPC offers a suitable scientific test bed for demanding time execution processes, such as geostatistical analyses applied to remote sensing images.

8183-07, Session 2

Accelerating the CCSDS rice coding on graphics processing units

X. Wu, Y. Li, Xidian Univ. (China); B. Huang, Univ. of Wisconsin-Madison (United States)

The Rice coding is the Consultative Committee for Space Data Systems (CCSDS) recommendation for lossless data compression on several different types of data. The CCSDS Rice coding is an adaptive entropy coder with a preprocessor, applied to each block of J samples. The default preprocessor uses a unit-delay predictor with positive mapping. The adaptive entropy coder concurrently applies a set of variable-length codes to a block of J consecutive preprocessed samples. The code option that yields the shortest codeword sequence for the current block of samples is selected for transmission. A unique



identifier bit sequence is attached to the code block to indicate to the decoder which decoding option to use. The CCSDS Rice coding is suitable for parallel implementation where all codeword blocks can be encoded independently and simultaneously. In addition to satellite onboard compression, the CCSDS Rice coding also has other applications such as lossless compression of medical images as well as earth science data via the Hierarchical Data Format (HDF) software. In order to perform high-performance Rice encoding on earth science data by the CCSDS Rice coding, we propose to accelerate the Rice coding on the Graphics Processing Units (GPUs) using Compute Unified Device Architecture (CUDA). The GPU-based Rice coder will process many codeword blocks in a massively parallel fashion by different GPU multiprocessors. It is expected to achieve a remarkable speedup over its single-threaded CPU counterpart.

8183-08, Session 2

Heterogeneous computing system with GPU-based IDWT and CPU-based SPIHT and Reed-Solomon decoding for satellite image decompression

C. Song, Y. Li, Xidian Univ. (China); B. Huang, Univ. of Wisconsin-Madison (United States)

The discrete wavelet transform (DWT)-based Set Partitioning in Hierarchical Trees (SPIHT) algorithm is widely used in many image compression systems. In order to perform real-time Reed-Solomon channel decoding and SPIHT+DWT source decoding on a massive bit stream of compressed images continuously down-linked from the satellite, we propose a novel graphics processing unit (GPU)accelerated decoding system. In this system the GPU is used to compute the time-consuming inverse DWT, while multiple CPU threads are run in parallel for the remaining part of the system. Both CPU and GPU parts were carefully designed to have approximately the same processing speed to obtain the maximum throughput via a novel pipeline structure for processing continuous satellite images. Through the pipelined CPU and GPU heterogeneous computing, the entire decoding system approaches a speedup of 84x as compared to its single-threaded CPU counterpart.

8183-09, Session 2

Parallel design of JPEG-LS encoder on graphics processing units

Y. Fang, Northwest A&F Univ. (China)

Lossless JPEG (JPEG-LS) is a lossless/near-lossless image compression standard with low complexity, which consists of three independent and distinct stages called prediction, residual modeling, and context-based coding of the residuals. To parallelize the prediction and modeling stages, each thread processes each row of pixels. Then parallelized AC is run to do entropy coding of the residuals, which can be modeled as a discrete Laplace process.

8183-10, Session 2

Accelerating arithmetic coding on GPUs

Y. Fang, Northwest A&F Univ. (China)

Arithmetic Coding (AC) is widely used in lossless data compression. However, compared to Huffman coding, its computational complexity is much higher due to multiplication and branching operations. This paper researches the implementation of AC encoder on GPUs. The main idea is to use block AC. Each thread processes one block, so that data blocks can encoded in parallel. We will use the well-known FastAC as a benchmark to verify the acceleration efficiency of our work.

8183-11, Session 2

High-performance computing in the remote sensing image data compression

A. Lin, National Space Program Office of Taiwan (Taiwan); C. F. Chang, National Space Organization (Taiwan); M. C. Lin, L. J. Jan, Chung-Shan Institute of Science and Technology (Taiwan)

The high-performance computing is necessary for remote sensing image compression to achieve real time output. There are one Panchromatic (PAN) band and four Multi-Spectrum (MS) bands with total 970Mbps data rate in the FORMOSAT-5 Remote Sensing Instrument(RSI. Three Xilinx Virtex 5 FPGAs with external memory are used to perform real time image data compression based on CCSDS 122.0-B-1. Parallel and concurrent handling strategies are used to achieve high-performance computing in the process.

8183-12, Session 3

Parallel implementation of linear and nonlinear spectral unmixing of remotely sensed hyperspectral images

A. J. Plaza, J. Plaza, Univ. de Extremadura (Spain)

Hyperspectral unmixing is a very important task for remotely sensed hyperspectral data exploitation. It addresses the (possibly) mixed nature of pixels collected by instruments for Earth observation, which are due to several phenomena including limited spatial resolution, presence of mixing effects at different scales, etc. Spectral unmixing involves the separation of a mixed pixel spectrum into its pure component spectra (called endmembers) and the estimation of the proportion (abundance) of endmember in the pixel. Two models have been widely used in the literature in order to address the mixture problem in hyperspectral data. The linear model assumes that the endmember substances are sitting side-by-side within the field of view of the imaging instrument. On the other hand, the nonlinear mixture model assumes nonlinear interactions between endmember substances. Both techniques can be computationally expensive, in particular, for high-dimensional hyperspectral data sets.

In this paper, we develop and compare parallel implementations of linear and nonlinear unmixing techniques for remotely sensed hyperspectral data. For the linear model, we adopt a parallel unsupervised processing chain made up of three steps: i) estimation of the number of pure spectral materials or endmembers, ii) automatic identification of endmembers, and iii) estimation of the abundance of each endmember in each pixel of the scene. For the nonlinear model, we adopt a supervised procedure based on the training of a parallel multi-layer perceptron neural network using intelligently selected training samples also derived in parallel fashion. The compared techniques are experimentally validated using hyperspectral data collected at different altitudes over a so-called Dehesa (semiarid environment) in Extremadura, Spain, and evaluated in terms of computational performance using high performance computing systems such as commodity Beowulf clusters.

8183-13, Session 3

A comparative analysis of GPU implementations of spectral unmixing algorithms

S. Sanchez, A. J. Plaza, Univ. de Extremadura (Spain)

Spectral unmixing is a very important task for remotely sensed hyperspectral data exploitation. It involves the separation of a mixed pixel spectrum into its pure component spectra (called endmembers) and the estimation of the proportion (abundance) of each endmember in the pixel. Over the last years, several algorithms have been proposed for: i) automatic extraction of endmembers, and ii) estimation of the abundance of endmembers in each pixel of the hyperspectral image. The latter step usually imposes two constraints in abundance estimation: the non-negativity constraint (meaning that the estimated abundances cannot be negative) and the sum-to-one constraint

(meaning that the sum of endmember fractional abundances for a given pixel must be unity). These two steps comprise a hyperspectral unmixing chain, which can be very time-consuming (particularly for high-dimensional hyperspectral images). Parallel computing architectures have offered an attractive solution for fast unmixing of hyperspectral data sets, but these systems are expensive and difficult to adapt to on-board data processing scenarios, in which low-weight and low-power integrated components are essential to reduce mission payload and obtain analysis results in (near) real-time. In this paper, we perform an inter-comparison of parallel algorithms for automatic extraction of pure spectral signatures or endmembers and for estimation of the abundance of endmembers in each pixel of the scene. The compared techniques are implemented in graphics processing units (GPUs). These hardware accelerators can bridge the gap towards on-board processing of this kind of data. The considered algorithms comprise the orthogonal subspace projection (OSP), iterative error analysis (IEA) and N-FINDR algorithms for endmember extraction, as well as unconstrained, partially constrained and fully constrained abundance estimation. The considered implementations are inter-compared using different GPU architectures and hyperspectral data sets collected by the NASA's Airborne Visible Infra-Red Imaging Spectrometer (AVIRIS).

8183-14, Session 3

FPGA implementation of endmember extraction algorithms from hyperspectral imagery: pixel purity index versus N-FINDR

C. Gonzalez, D. Mozos, Univ. Complutense de Madrid (Spain); J. Resano, Univ. de Zaragoza (Spain); A. J. Plaza, Univ. de Extremadura (Spain)

Endmember extraction is an important task for remotely sensed hyperspectral data exploitation. It comprises the identification of spectral signatures corresponding to macroscopically pure components in the scene, so that mixed pixels (resulting from limited spatial resolution, mixing phenomena happening at different scales, etc.) can be decomposed into combinations of pure component spectra weighted by an estimation of the proportion (abundance) of each endmember in the pixel. Over the last years, several algorithms have been proposed for automatic extraction of endmembers from hyperspectral images. These algorithms can be time-consuming (particularly for high-dimensional hyperspectral images). Parallel computing architectures have offered an attractive solution for fast endmember extraction from hyperspectral data sets, but these systems are expensive and difficult to adapt to on-board data processing scenarios, in which low-weight and low-power hardware components are essential to reduce mission payload, overcome downlink bandwidth limitations in the transmission of the hyperspectral data to ground stations on Earth, and obtain analysis results in (near) real-time. In this paper, we perform an inter-comparison of the hardware implementations of two widely used techniques for automatic endmember extraction from remotely sensed hyperspectral images: the pixel purity index (PPI) and the N-FINDR. The hardware versions have been developed in field programmable gate arrays (FPGAs). Our study reveals that these reconfigurable hardware devices can bridge the gap towards on-board processing of remotely sensed hyperspectral data and provide implementations that can significantly outperform the (optimized) equivalent software versions of the considered endmember extraction algorithms.

8183-15, Session 3

Lossy hyperspectral image compression with state-of-the-art video encoder

L. Santos Falcon, S. López Suarez, G. Marrero Callicó, J. F. López, R. Sarmiento Rodriguez, Univ. de Las Palmas de Gran Canaria (Spain)

One of the main drawbacks encountered when dealing with hyperspectral images is the vast amount of data to process. This is especially dramatic when data are acquired by a satellite or an aircraft due to the limited bandwidth channel needed to transmit



data to a ground station. Several solutions are being explored by the scientific community. Software approaches have limited throughput performance, are power hungry and most of the times do not match the expectations needed for real time applications. Under the hardware point of view, FPGAs, GPUs and even the Cell Processor, represent attractive options, although they present complex solutions and potential problems for their on-board inclusion. However, sometimes there is an impetus for developing new architectural and technological solutions while there is plenty of work done in the past that can be exploited for solving drawbacks in the present. In this scenario, H.264/AVC arises as the state-of-the-art standard in video coding, showing increased compression efficiency with respect to any previous standard, and although mainly used for processing hyperspectral imaginery.

In this work, an inductive exercise of compressing hyperspectral cubes with H.264/AVC is carried out. An exhaustive set of simulations have been performed, applying this standard locally to each spectral band and evaluating globally the effect of the quantization factor, QP, in order to determine an optimum configuration of the baseline encoder for INTRA prediction modes. Results are presented in terms of spectral angle as a metric for determining the feasibility of the endmember extraction. These results demonstrate that under certain assumptions, the use of standard video codecs represent a good compromise solution in terms of complexity, flexibility and performance.

8183-16, Session 4

GPU implementation of JPEG2000 for hyperspectral image compression

M. Ciznicki, K. Kurowski, Poznan Supercomputing and Networking Ctr. (Poland); A. J. Plaza, Univ. de Extremadura (Spain)

Hyperspectral image compression has received considerable interest in recent years due to the enormous data volumes collected by imaging spectrometers for Earth Observation. JPEG2000 is an important technique for data compression which has been successfully used in the context of hyperspectral image compression, either in lossless and lossy fashion. Due to the increasing spatial, spectral and temporal resolution of remotely sensed hyperspectral data sets, fast (onboard) compression of hyperspectral data is becoming a very important and challenging objective, with the potential to reduce the limitations in the downlink connection between the Earth Observation platform and the receiving ground stations on Earth. For this purpose, implementation of hyperspectral image compression algorithms on specialized hardware devices are currently being investigated. In this paper, we develop an implementation of the JPEG2000 compression standard in commodity graphics processing units (GPUs). These hardware accelerators are characterized by their low cost and weight, and can bridge the gap towards on-board processing of remotely sensed hyperspectral data. Specifically, we develop GPU implementations of the lossless and lossy modes of JPEG2000. For the lossy mode, we investigate the utility of the compressed hyperspectral images for different compression ratios, using standard techniques for hyperspectral data exploitation such as classification and unmixing. In all cases, we investigate the speedups that can be gained by using the GPU implementations with regards to the serial implementations. Our study reveals that GPUs represent a source of computational power that is both accessible and applicable to obtaining compression results in valid response times in information extraction applications from remotely sensed hyperspectral imagery.

8183-17, Session 4

Parallel implementation of RX anomaly detection on multi-core processors: impact of data partitioning strategies

J. M. Molero, E. Martin, I. Garcia, Univ. de Almería (Spain); A. J. Plaza, Univ. de Extremadura (Spain)

Anomaly detection is an important task for remotely sensed hyperspectral data exploitation. One of the most widely used and

successful algorithms for anomaly detection in hyperspectral images is the Reed-Xiaoli (RX) algorithm. Despite its wide acceptance and high computational complexity when applied to real hyperspectral scenes, few documented parallel implementations of this algorithm exist, in particular for multi-core processors. The advantage of multi-core platforms over other specialized parallel architectures is that they are a low-power, inexpensive, widely available and well-known technology. A critical issue in the parallel implementation of RX is the sample covariance matrix calculation, which can be approached in global or local fashion. This aspect is crucial for the RX implementation since the consideration of a local or global strategy for the computation of the sample covariance matrix is expected to affect both the scalability of the parallel solution and the anomaly detection results. In this paper, we develop new parallel implementations of the RX in clusters of multicore processors and specifically investigate the impact of different data partitioning strategies when parallelizing its computations. For this purpose, we consider both global and local (with and without overlapping) data partitioning strategies in the spatial domain of the scene, and further analyze their scalability in different multi-core platforms. The numerical effectiveness of the considered solutions is evaluated using receiver operating characteristics (ROC) curves, analyzing their capacity to detect thermal hot spots (anomalies) in hyperspectral data collected by the NASA's Airborne Visible Infra-Red Imaging Spectrometer system over the World Trade Center in New York, five days after the terrorist attacks of September 11th, 2011.

8183-18, Session 4

Real time orthorectification of high resolution airborne pushbroom imagery

J. Reguera-Salgado, Univ. de Vigo (Spain) and Sound of Numbers, S.L. (Spain); J. Martin-Herrero, Univ. de Vigo (Spain)

Advanced hardware and software architectures have been proposed for efficient orthorectification of digital airborne camera images. Recently [1], a system based on GPU processing and distributed computing was able to geocorrect three digital still aerial photographs per second.

Here, we address the computationally harder problem of geocorrecting image data from airborne pushbroom sensors, where a whole scene is not captured from a single position with a single camera attitude, but each individual image line has its own camera attitude parameters and associated camera position. In pushbroom imagers, scenes are built line per line while the aircraft flies along track.

We use the parallel computing and hardware acceleration characteristics of modern GPUs by means of OpenGL and CUDA, integrated in standard computer hardware (PC), to address real time geocorrection of aerial pushbroom imagery.

Using projective texture techniques [2], originally developed for fast shadow rendering, image data is projected onto a Digital Terrain Model (DTM) as if by a slide projector placed and rotated in accordance with GPS position and inertial navigation (IMU) data, in order to generate a geometrically corrected georeferenced orthoimage. Each line is sequentially projected onto the DTM to generate an intermediate frame, consisting of a unique projected line shaped by the DTM relief. All the intermediate frames thus generated are mixed into a final orthoimage.

In order to target higher order multiband systems, such as hyperspectral systems, avoiding the overhead of highly dimensional data, our method deals with an orthoimage of pixel identifiers or placeholders pointing to the raw image data, which can then be combined as needed to generate visual representations of the multichannel data or whenever the multichannel data needs to be processed taking into account the geocorrected spatial positions and/ or structures.

Real time geocorrection of aerial pushbroom imagery can be important for specific real time applications that must take into account the spatial structures present in the images, but specially for coverage of wide areas where the terrain is combed through repeated parallel passes. Having a real time geocorrection of the acquired passes allows a better coverage, optimizing flight time and minimizing or totally avoiding blind gaps in the resulting mosaic.

Our method running on standard hardware over a DTM with 1 m grid achieved real time performance, allowing in-flight inspection of the resulting geocorrected image during acquisition. We tested the method



with a hyperspectral pushbroom system working at a line rate of 30 Hz with 200 bands and 1280 pixel wide swath, achieving a minimum processing speed of 245 lines per second (up to 341 lps), more than eight (up to eleven) times the acquisition line rate. Our method also allows the correction of systematic GPS and/or IMU biases by means of 3D interactive navigation.

[1] U. Thomas, F. Kurz, D. Rosembaum, R. Mueller, P. Reinartz (2008) GPU-Based Orthorectification of Digital Airborne Camera Images in Real Time. The International Archives of the Photogrammetry, Remote Sensing and Spatial Information Sciences, XXXVII(B1):589-594.

[2] C. Everitt (2001) Projective Texture Mapping. NVIDIA.

 $\label{eq:url:http://developer.nvidia.com/object/Projective_Texture_Mapping. html \\$

8183-19, Session 4

Design and analysis of algorithms for enhancing the quality and the resolution of Dubai Sat-1 images

S. H. AL-Mansoori, Emirates Institution for Advanced Science and Technology (United Arab Emirates)

DubaiSat-1 (DS1) captures multispectral images with 5-meter resolution using three visible bands red (420 to 510 nm), green (510 to 580 nm), blue (600 to 720 nm) and one near-IR band (760 to 890 nm). It will also have a panchromatic channel with 2.5-meter resolution (420 to 720 nm). [1] Under certain conditions, degradation in quality might occur over DS1 captured images. The aim of this project is to enhance the quality of the image in terms of resolution, sharpness and color quality. It is well known that the enhancement procedure is a very difficult task due to the significant noise increase resulted from any sharpening action. Moreover, sometimes the color of the captured images might become saturated, thus some areas will be given false coloring (i.e., some colors will be presented as gray instead of their original colors).

Dubai Sat-1 was launched on the 29th of July 2009 and the current earth station located in Dubai, UAE is still receiving images of different parts around the world on a daily basis. These images will be processed and distributed to customers including government agencies, universities, research centers, etc. The value of these images can be increased if the quality and the resolution of these images are improved. Interpolation in image processing is a well-known method to increase the resolution of a digital image. The aim of this project is to develop algorithms to improve the quality and the resolution of DS1 images. As an example, captured image by DS1 was compared by another image taken by GeoEye-1 for the same location. GeoEye-1 is a high commercial satellite, which provides images at 0.41m for the panchromatic mode and 1.65m for the multispectral mode.

This research is centered on enhancing the quality and the resolution of Dubai Sat-1 images. Different interpolation techniques will be used including spatial and transformed domain techniques. Both polynomial and Fourier interpolation will be used to improve the resolution of the images. Sharpening techniques will be used followed by noise reduction techniques. The algorithms will utilize the multispectral images captured by the different sensors on-board Dubai Sat-1. The color of the resultant images will be assessed by using PSNR and Structure Similarity Index Measure (SSIM).

There are different challenges facing this study. The use of the interpolation techniques to increase the resolution of the images will result in degrading the edges in the images. Also, the sharpening of the images will result in increasing the level of the noise. The output of this project will be an added value to DS-1 images; the UAE's first earth observation satellite.

8183-20, Session 5

Development of the GPU-based Hilbert-Huang transform

J. Wang, B. Huang, Univ. of Wisconsin-Madison (United States)

The Hilbert-Huang Transform (HHT) is an empirical algorithm for analysis of nonlinear and nonstationary data. It consists of the



empirical mode decomposition (EMD) and the Hilbert spectral analysis (HSA). The EMD method is to decompose a signal into a collection of the intrinsic mode functions (IMFs), while the HSA method is to obtain the instantaneous frequencies. The HHT has been widely used in various science and engineering applications, including remote sensing data processing. The process of extracting an IMF is to connect all the local maxima by a cubic spline line as the upper envelope and all the local minima as the lower envelope. This sifting procedure is suitable for parallel implementation. In recent years graphics processing units (GPUs) with hundreds of compute cores have become an affordable alternative to a CPU cluster for high performance computing. In this study we exploit the GPU massively parallel capabilities to accelerate the HHT with an expected significant speedup.

8183-21, Session 5

GPU acceleration of the solution to the polarized atmospheric radiative transfer model

C. Song, Y. Li, Xidian Univ. (China); B. Huang, Univ. of Wisconsin-Madison (United States)

The plane-parallel polarized radiative transfer model developed in a seminal paper by Evans and Stephens (1991) has been widely used for passive atmospheric remote sensing of the planets in the solar system. The model considers both solar and thermal energy sources and computes the monochromatic polarized radiance emerging from a vertically inhomogeneous atmosphere with multiple scattering and randomly-oriented particles of arbitrary shapes. The diffuse radiance field is expressed as a four-vector of Stokes parameters. The solution method converts the single-scattering information into a form suitable for applying the doubling and adding method to compute the optical properties of the whole atmosphere from the local properties of each infinitesimal layer. The computation for a more accurate solution could be time-consuming in many applications involving Rayleigh or Mie atmospheres in sunlight or microwave transfer through a precipitating atmosphere. In recent years the NVidia GPUs provide affordable supercomputing power with Compute Unified Device Architecture (CUDA) as the GPU programming tool. In this paper we take advantage of GPU massively parallel capabilities to speed up the computation of the solution to the polarized radiative transfer problem.

8183-22, Session 5

Massively parallelizing the CIMSS IASI radiative transfer model on GPUs

J. Mielikainen, B. Huang, H. A. Huang, Univ. of Wisconsin-Madison (United States)

Radiative transfer model (RTM) computes radiance as a nonlinear functional of surface properties and atmospheric temperature and absorbing gas profiles. Limited by the computing power, the current operational numerical weather prediction systems can assimilate only a few hundred spectral channels of an ultraspectral sounder with thousands of spectral measurements. In recent years the programmable commodity graphics processing unit (GPU) has evolved into a highly parallel, multi-threaded, many-core processor with tremendous computational speed and very high memory bandwidth. The radiative transfer model is very suitable for the GPU implementation to take advantage of the hardware's efficiency and parallelism where radiances of many channels can be calculated in parallel in GPUs. In this paper, we demonstrate the Graphics Processing Unit (GPU)-based RTM for the Infrared Atmospheric Sounding Interferometer (IASI) launched in 2006 onboard the first European meteorological polar-orbiting satellites (METOP-A). The original CPU-based IASI RTM was developed in the Cooperative Institute for Meteorological Satellite Studies (CIMSS) at the University of Wisconsin-Madison. Our GPU-based CIMSS IASI RTM is developed to run on a low-cost personal supercomputer with 4 NVIDIA Tesla C1060 GPUs with total 960 cores, delivering near 4 TFlops theoretical peak performance. We show two different GPU-based RTM implementations. The first one computes one IASI spectrum at a time, whereas the second one computes multiple IASI spectra simultaneously. The CIMSS IASI radiative transfer

model consists of three modules. The first module for computing the regression predictors takes less than 0.004% of CPU time, while the second module for transmittance computation and the third module for radiance computation take approximately 92.5% and 7.5%, respectively. By massively parallelizing the second and third modules on GPUs, we reached 364× speedup for 1 GPU and 1455× speedup for all 4 GPUs for computing one IASI radiance spectrum at a time, whereas 763x speedup for 1 GPU and 3024x speedup for all 4 GPUs for computing 10 IASI radiance spectra simultaneously, all with respect to the original CPU-based single-threaded Fortran code. The significant 3024x speedup means that the proposed GPU-based highperformance CIMSS IASI RTM is able to compute one day's amount of 1,296,000 IASI spectra within 6 minutes while the original CPU code will take more than 10 days.

8183-23, Session 5

An efficient GPU-based implementation of Kalman filter

Y. Chang, M. Huang, T. Hsieh, National Taipei Univ. of Technology (Taiwan)

The Kalman filter has been widely used in many nature science and engineering research, to estimate the states of a linear system that can only be observed indirectly or inaccurately in a way that minimizes the mean of the squared error. The Kalman filter equations involve a set of matrix manipulations which include matrix inversion and transpose. State-of-the-art airborne and satellite sensors with higher spatial, temporal and spectral resolutions often result in significant usage of large-scale data matrices for Earth remote sensing observations. Accordingly, this present a challenge to the necessity for these computationally intensive tasks and the usage of a cost-effective highperformance computing device is desired. In this paper we propose an efficient graphic-processing-units (GPU) based implementation of Kalman Filter. The GPU code to run on NVIDIA GPUs uses the compute unified device architecture (CUDA) language. The GPU-based Kalman filter is expected to achieve a significant speedup over its CPU-based single-threaded counterpart.

8183-24, Session 5

GPU implementation of orthogonal matching pursuit for compressive sensing

Y. Fang, Northwest A&F Univ. (China)

Compressive sensing (CS) is useful in image compression. Recovery algorithms play an important role in CS. Among those CS recovery algorithms, the orthogonal matching pursuit (OMP) algorithm achieves good performance at low complexity. The complexity of OMP comes mainly from matrix operations, e.g. matrix multiplication, matrix inverse, etc., which makes it very suited to parallelized implementation. This paper considers the GPU implementation of OMP algorithm for the CS application.

8183-25, Session 6

Efficient GPU Implementation of Tsunami Simulation Based on the MacCormack Scheme

S. Wei, Tamkang Univ. (Taiwan); B. Huang, Univ. of Wisconsin-Madison (United States); T. Hsieh, W. Liang, Y. Chang, National Taipei Univ. of Technology (Taiwan)

Tsunami simulation involves fluid dynamics, numerical computations, and visualization techniques. The tsunami propagation is often modeled by the nonlinear shallow water equations which can be numerically solved by the MacCormack method, a variation of the two-step Lax-Wendroff scheme. By adding the friction slope to the momentum equations, the phenomena of tsunami inundation can be modeled. The MacCormack method is a two-step second-order finite difference method which is suitable for parallel computing. In



this paper, we develop an efficient tsunami simulation code to run on graphics processing units (GPUs) using the NVidia Compute Unified Device Architecture (CUDA). The GPU-based tsunami simulation is expected to achieve a significant speedup over its CPU-based single-threaded counterpart.

8183-26, Session 6

Accelerating the Weather Research and Forecast (WRF) Purdue Lin microphysics scheme on NVidia graphics processing units

J. Wang, B. Huang, Univ. of Wisconsin-Madison (United States); J. Mielikainen, Univ. of Eastern Finland (Finland); H. A. Huang, Univ. of Wisconsin-Madison (United States); M. D. Goldberg, National Oceanic and Atmospheric Administration (United States)

The Weather Research and Forecasting (WRF) model is a numerical weather prediction and atmospheric simulation system. It has been designed for both research and operational applications. WRF code can be run in different computing environments ranging from laptops to massively-parallel supercomputers. Purdue Lin scheme is a relatively sophisticated microphysics scheme in WRF. The scheme includes six classes of hydro meteors: water vapor, cloud water, raid, cloud ice, snow and graupel. In this paper, we will presents our results in accelerating Purdue Lin scheme on many-core NVIDIA graphics processing units (GPUs). GPUs have evolved into a highly parallel, multi-threaded, many-core processors with tremendous computational speed and a high memory bandwidth. We will discuss how our GPU implementation is able to take advantage of the hardware's massive parallelism, which results on a highly efficient GPU acceleration. Enabling the Purdue Lin microphysics scheme to be executed at a very high speed on a low-cost personal supercomputer with over 2000 CUDA cores on four GPUs.

8183-27, Session 6

GPU acceleration of WRF WSM5 microphysics

J. Mielikainen, Univ. of Eastern Finland (Finland); B. Huang, H. A. Huang, Univ. of Wisconsin-Madison (United States); M. D. Goldberg, National Oceanic and Atmospheric Administration (United States)

The Weather Research and Forecast (WRF) model is the most widely used community weather forecast and research model in the world. There are several single moment ice microphysics models in WRF. A mixed phase for WRF Single Moment (WSM) represents the condensation, precipitation, and thermodynamic effects of latent heat release. Earlier, WSM5 has been ported to NVIDIA graphics processing units (GPUs) using two different approaches. First, WSM5 was programmed manually for NVIDIA GPUs using CUDA. Later on, it was ported using directives on PGI Accelerator Programming Model. In this paper, we will show our optimization efforts on WSM5 and compare the results to the earlier GPU acceleration efforts. Our preliminary result shows more than 100x speedup.

8183-28, Session 6

High-performance visual analytics of terrestrial LIDAR data for cliff erosion assessment on large displays

T. Hsieh, Y. Chang, National Taipei Univ. of Technology (Taiwan); B. Huang, Univ. of Wisconsin-Madison (United States)

Heavy development on cliffs places a heavy emphasis on maintaining a healthy natural environment. The ability to explore, conceptualize and correlate spatial and temporal changes of topographical records is required for the development of new analytical models that capture the mechanisms contributing towards cliff erosion. This paper presents a visualization based approach using large displays in a digital immersive environment. Visual analytics are performed for cliff erosion assessment from a terrestrial LIDAR (LIght Detection And Ranging) data, including visualization techniques for the delineation, segmentation, and classification of features, change detection and annotation. Research findings are described in the context of a cliff failure observed in Solana Beach in California. The visualization system presented in this paper demonstrates the insights that can be gained by observing the temporal change of a failure mass using frequent site monitoring.

8183-29, Session 6

Efficient GPU implementation of the weather research and forecasting (WRF) Kesler Microphysics Scheme

J. Wang, B. Huang, Univ. of Wisconsin-Madison (United States); J. Mielikainen, Univ. of Eastern Finland (Finland); H. A. Huang, Univ. of Wisconsin-Madison (United States); M. D. Goldberg, National Oceanic and Atmospheric Administration (United States)

The Weather Research and Forecasting (WRF) Model is a nextgeneration mesoscale numerical weather prediction system designed to serve both operational forecasting and atmospheric research needs for a broad spectrum of applications across scales ranging from meters to thousands of kilometers. Kessler microphysics module in WRF is a simple warm cloud scheme that includes water vapor, cloud water and rain. The modeled microphysics processes are rain production, fall and evaporation. The accretion and auto-conversion of cloud water processes are also included as is the production of cloud water from condensation. In this paper, we develop an efficient WRF Kessler scheme to run on graphics processing units (GPUs) using the NVidia Compute Unified Device Architecture (CUDA). The GPU-based Kessler scheme is expected to achieve a significant speedup over its CPU-based single-threaded counterpart.

8183-30, Session 6

Development of the GPU-based Stony-Brook University 5-class microphysics scheme in the Weather Research and Forecasting (WRF) Model

J. Mielikainen, Univ. of Eastern Finland (Finland); B. Huang, H. A. Huang, Univ. of Wisconsin-Madison (United States); M. D. Goldberg, National Oceanic and Atmospheric Administration (United States)

Several bulk water microphysics schemes are available within the Weather Research and Forecasting (WRF) model, with different numbers of simulated hydrometeor classes and methods for estimating their size fall speeds, distributions and densities. The Stony-Brook University scheme is a 5-class scheme with riming intensity predicted to account for mixed-phase processes. In this paper, we develop an efficient graphics processing unit (GPU) based Stony-Brook



University scheme. The GPU-based Stony-Brook University scheme will be compared to a CPU-based single-threaded counterpart and is expected to show a promising speedup.

8183-31, Session 6

Calculating the electromagnetic scattering of vegetation model by Monte Carlo and CUDA

Z. Wu, X. Su, J. Wu, Xidian Univ. (China)

Research on the electromagnetic scattering of random rough surface, the foundation of remote sensing and target detection, is very important to improve the performance of the radar. This paper describes one-dimensional and two-dimensional rough surface respectively simulated by Monte Carlo and finite impulse response filter including fast Fourier transform (FFT) and then introduces Kirchhoff Approximation (KA) method to study the scattering characteristics of the rough surface, analyze the actual dielectric properties of the soil surface and solve the actual ground scattering coefficient, which is compared with the results computed by small perturbation method (SPM). Based on these, the double layers random medium model with vegetation layer and ground layer is established. The back scattering characteristics of this model is investigated by vector radiative transfer theory (VRT) and the actual rough surface scattering effect of this model is solved by Monte-Carlo Method. Due to the randomness of rough surface, a large number of sample data should be calculated that limits the application of this model. To overcome this bottleneck, the compute unified device architecture (CUDA), which provides fine-grained data parallelism and thread parallelism, is introduced to accelerate the calculation. Full use of tens of thousands of threads in CUDA program, we make every thread compute a sample data and then collect these results. Comparing this parallel algorithm with the traditional sequential algorithm, it can be found that computational efficiency has been improved significantly.